A Molecular Building Block Approach Toward Nanoscale Molecular Scaffolds

by

Christopher G. Levins

B.S., University of Pittsburgh, 2000

Submitted to the Graduate Faculty of

Arts and Sciences in partial fulfillment

of the requirements for the degree of

Doctor of Philosophy

University of Pittsburgh

2006

UNIVERSITY OF PITTSBURGH

FACULTY OF ARTS AND SCIENCES

This dissertation was presented

by

Christopher G. Levins

It was defended on

September 22, 2006

and approved by

Kay Brummond, Ph.D., Associate Professor, Department of Chemistry, Faculty of Arts and Sciences

Paul Floreancig, Ph.D., Associate Professor, Department of Chemistry, Faculty of Arts and Sciences

Catalina Achim, Ph.D., Assistant Professor, Department of Chemistry, Carnegie Mellon University

Dissertation Advisor: Christian E. Schafmeister, Ph.D., Assistant Professor, Department of Chemistry, Faculty of Arts and Sciences

A Building Block Approach Toward Nanoscale Molecular Scaffolds

Christopher G. Levins, Ph.D.

University of Pittsburgh, 2006

We are developing a systematic method for the design and synthesis of rigid macromolecular scaffolds capable of displaying chemical functionality in three dimensional space. These scaffolds will enable the study of structure-function relationships in designed receptors, and to examine factors governing biological catalysis. The scaffolds might also be used as tools for the construction of nanoscale devices. The monomers used to synthesize the oligomeric scaffolds are orthogonally protected bis-amino acids. These heterocyclic monomers are coupled through diketopiperazines to neighboring monomers. The formation of two peptide bonds between adjacent monomers eliminates the rotational flexibility in the scaffold backbone, and results in unique spirocyclic fused ring structures that we have christened bis-peptides.

We discuss the synthesis of the four stereoisomers of a bis-amino acid monomer derived from 4-hydroxyproline, as well as the development of procedures for fabricating bis-peptides from these monomers. Combinations of all four "pro4" monomers were incorporated into oligomers of different lengths. The solution conformation of six oligomers was determined by analysis of their 2D-NMR spectra and using computational modeling. Based upon the conformational preferences of the monomers, two pentamer scaffold oligomers were designed to form distinguishable shapes: a molecular rod, and a curved shape. We confirmed the design hypothesis by labeling the ends of these scaffolds with dansyl and naphthyl fluorophores; this allowed us to determine the approximate end to end distances by measuring the efficiency of fluorescence resonance energy transfer. This result suggests that we can rationally design the physical properties of bis-peptides based upon the stereochemistry of their constituent monomers.

We also discuss progress toward the synthesis of chiral molecular cavities from bis-peptides and from assemblies of bis-peptides. The resulting macrocyclic cavities may ultimately serve as receptors for designed sensors of small chiral organic molecules.

TABLE OF CONTENTS

LIST OF TABLES

LIST OF FIGURES

LIST OF SCHEMES

PREFACE

I am very proud to have worked with Dr. Schafmeister; his enthusiasm for science and technology is inspiring, and being a part of his group from nearly the beginning has been an adventure. During my apprenticeship in his lab, Chris has proved himself an excellent mentor and advisor, and has helped me to grow as a scientist. I thank the members of my dissertation committee, Dr. Floreancig, Dr. Brummond, and Dr. Achim, for their valuable assistance and patience. I would also like to thank Dr. David Waldeck and Dr. Stephane Petoud for helpful discussions about the FRET experiments, and the support staff of the chemistry department for helping to keep my career on course and on schedule.

I am grateful to all of my peers in the Schafmeister group (past and present) for their friendship and support. I feel indebted to Sharad Gupta, who has been my desk-mate for nearly four years. He has been a gracious sounding board for my ideas and proof-reader of my first drafts. I will miss deliberating with Sharad about strategy in the lab, chemistry, life, the universe, and everything else.

We have been privileged to have several excellent undergraduates in the lab, and I've had the good fortune to have worked with several of them. Jacob Smith showed enthusiasm and creativity throughout a very difficult project. Sam Getchell helped me with some remarkable cyclization chemistry; I envy his technical skill in the lab. Both are excellent scientists, and I wish them the best in their future careers.

George Bandik has played a role in my education and career for over a decade; I am going to sorely miss being able to visit George's office for a chat, for consolation, or for advice. He is an inspirational teacher, an excellent mentor and wonderful person, and I owe him an incredible debt of gratitude.

I have had many teachers and mentors that have driven me toward a career in science, and I would like to thank them for their time and support: Dr. Elizabeth A. Rosvold and Dr.

Kenneth A. Buetow (FCCC, Philadelphia), Dennis Erlick, William Brooks, and Dr. Joel Simon (Central High School, Philadelphia), Steve Winowich (Artificial Heart Program, UPMC), Dr. William Wagner (Chemical Engineering, University of Pittsburgh), Dr. Chris Deible (UPMC); Corey Brown (Bend Research, Bend, Oregon).

My family has given be immeasurable love and encouragement, and I would have never reached this point without them; thank you Mom, Beth, Kim and Steve. I've tried hard to follow my mom's advice; that science should be explained "so that your mother can understand it." I hope that most of what I've written satisfies this mandate. I would also like to thank my Pittsburgh family for making me feel at home for so many years; $Mom_{(2)}$, Kristina, Mike, and Nate. Mariah Hout, my wife and my best friend, has given me all possible love and support during my long wander through graduate education.

The research described herein is thanks to financial support from the University of Pittsburgh, the Camille and Henry Dreyfus Foundation, the Research Corporation, and the National Institutes of Health/NIGMS (GM067866).

"…there are rules that determine the reaction of most life forms to emerging technologies:

1. Anything that is in your world when you're born is normal and ordinary and is just a natural part of the way things work.
2. Anything that's invented in the first third of your life-span is new and exciting and revolutionary and you can probably get a career in it.
3. Anything invented once you are middle aged is against the natural order of things."

— Douglas Adams

1.0 INTRODUCTION

Proteins are complex molecular machines that position functional groups within three dimensional space.[1] In part, this is how proteins achieve a remarkable variety of tasks; they are molecular motors, they process and transmit information, and catalyze chemical reactions. A goal within molecular nanotechnology is to develop methods that allow rational design of molecules that begin to approach the capabilities of proteins. A way to achieve this goal is to design synthetic molecular scaffolds as a framework for positioning functional groups with optical, magnetic, or chemical properties.[2] The challenge is to develop efficient methods to prepare macromolecular scaffolds that are asymmetric and that have well-defined conformation and connectivity.[3] The ability to fashion non-natural macromolecules that have designed tertiary structure and that precisely align chemical functionality in three dimensional space would be valuable for bio-mimetic and nanotechnology applications.[4,5]

Synthetic chemistry provides the means to construct remarkably complex structures from covalent bonds.[6] There are a number of natural products, such as brevetoxin B (Figure 1-1),[7] that are rigid, covalent, scaffold-like macromolecules.[2] Brevetoxin B is a relatively large molecule. It is nearly 1 kilodalton, nearly 2 nm from end to end, and has well-defined stereochemistry and structure. Though it is possible to achieve the synthesis of molecules the size and complexity of brevetoxin, this represents neither a general nor an efficient approach toward the development of complex nanoscale systems. The total synthesis of brevetoxin B required monumental effort over nearly a decade.[8-10] Using the current array of traditional covalent bond forming tools, the synthesis of very large and complex molecules is costly, inefficient, and time consuming.[11] A more straightforward approach for fabrication of non-natural molecular scaffolds would be to assemble the desired structure from similar repeating units (building blocks). This modular approach is more efficient, and diverse structures can be generated by simply incorporating different monomers.[12]

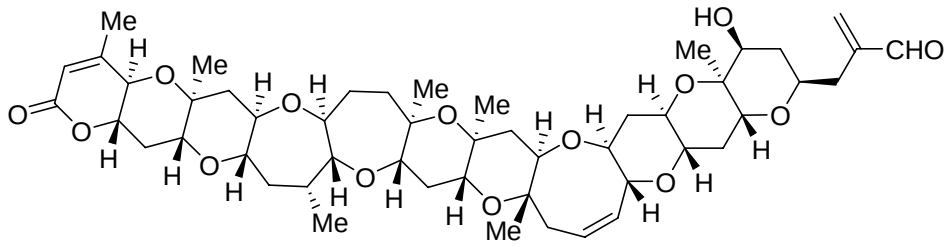

Figure 1-1: Brevetoxin B, a natural molecular scaffold

We are developing a unique method to synthesize well-defined asymmetric macromolecules as molecular scaffolds to display chemical functionality.[13-15] These scaffolds are oligomers assembled in a modular and efficient way from a modest library of monomers. The synthesis of macromolecules with well-defined shapes has been attempted using a host of oligomeric molecules and monomers; in most cases, the monomers are connected by a single covalent bond. Our strategy is unique because each building block in the oligomer is coupled to neighboring building blocks through multiple covalent bonds.[4] This increases the rigidity of the scaffold, allowing us to change the scaffold shape in predictable ways by changing the stereochemistry and sequence of the constituent monomers. As this method uses simple building blocks to construct complex structures in a predictable way,[16] it might ultimately provide a means to approach the functional capabilities of proteins.

1.1 OLIGOMERIC APPROACHES TOWARD NANOSCALE STRUCTURES

Nature assembles its wide assortment of nanoscale machinery using a small collection of simple building blocks. Proteins are oligomers of the 20 naturally occurring amino acids; the α-amino acids in peptides or proteins are connected to each neighboring residue by a single amide bonds. A potential route to nanoscale devices and machines is the design of new proteins, or the redesign of existing proteins to perform new functions.[17] The remarkable properties of proteins inspires us to design proteins.[5] Also, protein synthesis relies on a relatively small library of interchangeable monomers, and there are existing chemical and biochemical ways to synthesize homogeneous proteins quickly and reliably to scale.[18] The design of new proteins, unfortunately, is non-trivial because of the complexities associated with protein folding.[19]

For a protein to perform its required function, random-coil polypeptide oligomers must fold into compact, functional forms (Figure 1-2). Protein folding is an incredibly complex process of self-assembly driven by non-covalent interactions such as Van der Waals forces, hydrogen bonding, and the hydrophobic effect.[20] Although the primary sequence of amino acids in a protein contains the information required for a protein to fold into its functional, three-dimensional form,[21] the complexity of the folding process impedes prediction of the folded tertiary structure of a protein based upon the primary sequence.[19,20,22,23]

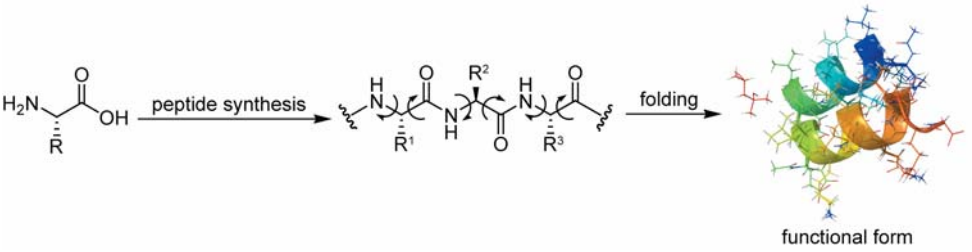

Figure 1-2: Proteins must fold to assume a functional form

There have been significant advances in experimental and computational methods used to redesign proteins to perform new functions,[17,24,25] and some examples of novel protein design from first principles.[26,27] Nonetheless, most proteins created by *de novo* design do not behave as "natural" proteins and enzymes. Many of these structures are designed around general structural motifs, without consideration or prediction of the atomic-level positioning of individual atoms, which may be required for the construction of effective catalysts.[28]

An alternative approach which tries to circumvent some of the complexity of folding α-amino acid polypeptides is to design peptide-like molecules with simplified folding rules.[29] Like peptides and proteins, foldamers are oligomers constructed from monomers; the monomers are connected through single bonds, and the oligomers fold into secondary structural motifs, driven by non-covalent interactions.[30] Foldamers mimic some aspects of the folding and organization of peptides and proteins.[1,30] While short peptides tend to be conformationally mobile, short foldamer oligomers adopt well-defined conformations in solution. The literature on foldamers is vast, and an extraordinary number of foldamer-type oligomers have been reported.[30] Several foldamer backbones are illustrated in Figure 1-3. The study of β-peptides has been particularly intense.[31,32] In solution, β-peptides form secondary structures, such as helices, that are considerably more stable than analogous α-peptide secondary structure.[33]

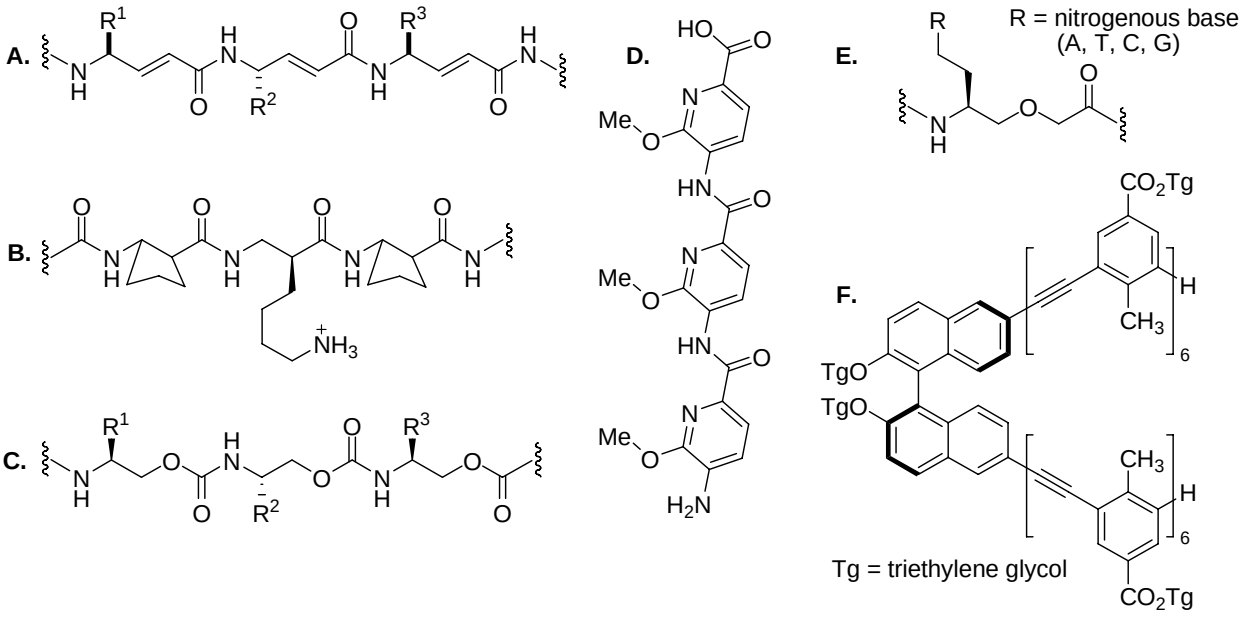

A. vinylogous polypeptides: β-sheet and hairpin turn mimics (Schreiber, 1992);[29] **B.** β-peptides: helical secondary structure (Gellman, Seebach);[31,33-39] **C.** oligocarbamates (Schultz, 1993);[40] **D.** trispyridylamide α-helix mimics (Hamilton, 2003);[41,42] **E.** peptide nucleic acids (Nielsen);[43,44] **F.** oligo(*m*-phenylene ethynylene) (Moore, 2002)[12,45,46]

Figure 1-3: A few representative examples of foldamer backbones

The objective of current foldamer research is to identify oligomer backbones that fold into persistent secondary structures, such as helices and pleated sheets. The ultimate goal, however, is to combine the secondary structural motifs into macromolecules with compact tertiary structures.[1] Both foldamers and proteins form three-dimensional structures through self-organization driven by weak, non-covalent interactions; in general, it is difficult to design shaped, asymmetric macromolecules using non-covalent interactions.[12] Foldamers do not entirely avoid the "folding problem," and there still is no way to predictably design foldamers with compact tertiary structures.

To avoid folding altogether, numerous modular oligomers with limited rotational flexibility have been designed.[2] Molecular "rods" might be useful as construction elements for the fabrication of large macromolecular assemblies.[4] Michl's molecular "Tinkertoys" are a representative example.[47-49] The scaffold arms are rigid molecular rods composed of geometrically constrained building blocks, such as [1.1.1]propellane and bipyrimidine. The arms are typically connected to halogenated aromatic rings using palladium mediated cross-coupling reactions. The resulting macromolecules are nanometer scale, but symmetrical. This approach is intended to provide synthetic access to "designer solids": three-dimensional matrices

of molecular rods, functionalized at lattice points with functional groups that produce unique optical, magnetic or materials properties.

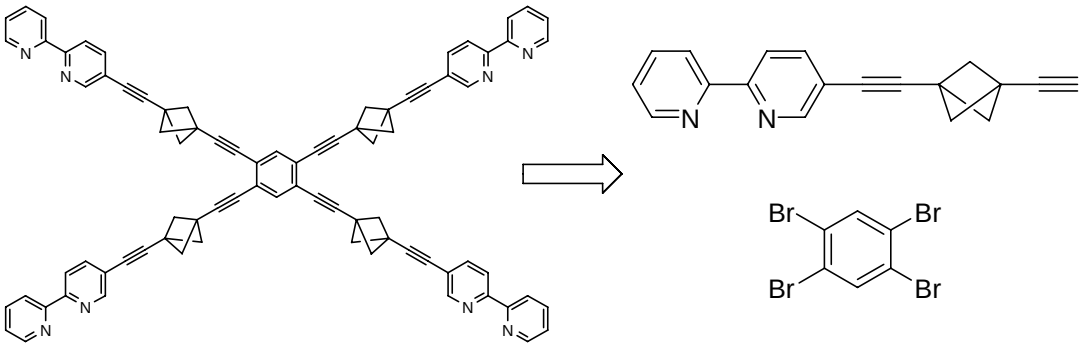

Figure 1-4: Michl's "Tinkertoy" construction set

Moore has also described molecular scaffolds using a similar design strategy. Oligomers constructed from phenylacetylene based monomers are assembled by sequential palladium cross-coupling coupling reactions.[12] This methodology has been used to synthesize a variety of macrocycles, dendrimers, and other three-dimensional structures (Figure 1-5).[12,46,50] The solubility of the resulting symmetrical scaffolds tends to be limited. In some cases, it has been possible to overcome this issue by decorating the structures with linear alkane and t-butyl groups.

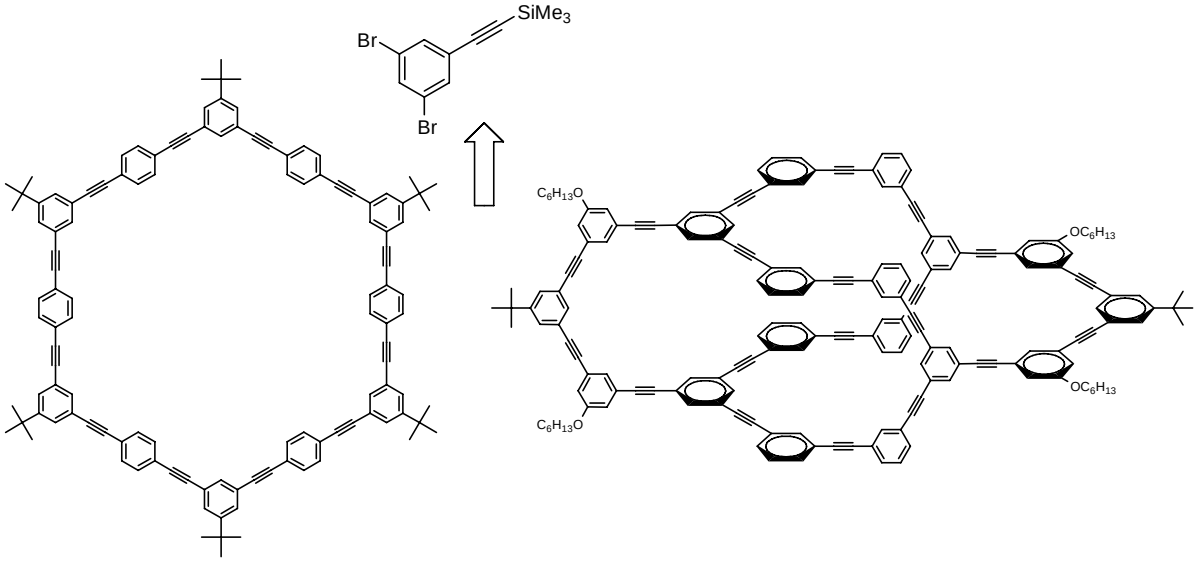

Figure 1-5: Moore's phenylacetylene based molecular architectures

There are a number of biological applications for rigid-rod oligomers. These applications require that the molecular rods be water-soluble, which precludes the use of many rigid

oligomers.[41] There are relatively few designed molecular scaffolds for biological applications. Oligoproline is the best known example of a water-soluble molecular rod. Proline oligomers form stable helices in water (the polyproline II helix, Figure 1-6).[51] By changing the number of proline residues in the oligomer, the length of the helix can be changed in a predictable way; polyproline has been used as a molecular "ruler".[52] It is not an ideal molecular rod to incorporate into macromolecular architectures, however, because the rigidity of this peptide is a function of solvent and temperature.[53] Double stranded DNA has also been used as a rigid spacer for certain biological applications.[54]

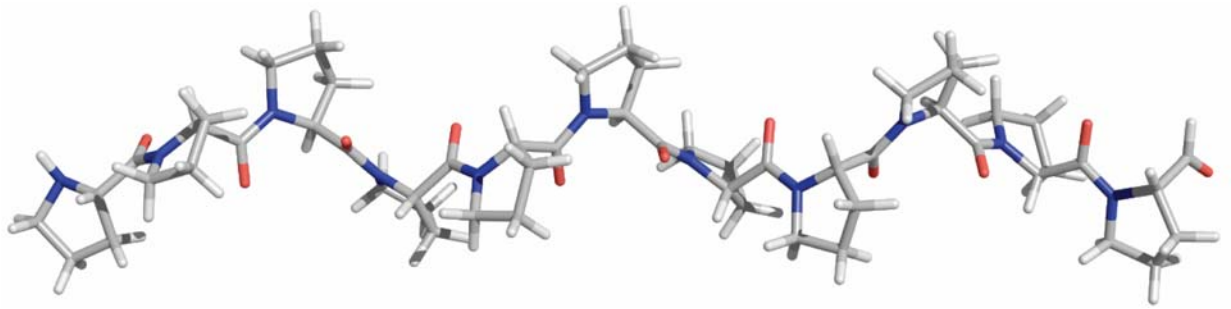

Figure 1-6: Oligo-L-proline, the standard molecular spacer for biological applications

Whitesides recently reported a water-soluble oligomer based on oligopiperidine (Figure 1-7),[41] intended for use as a spacer for multi-valent ligand display.[55] Construction of the oligomer is achieved by iterative reductive aminations with 4,4-piperidinediol. Highly substituted *p*-oligophenyls have also received attention as molecular rods for trans-membrane ion-transport model systems.[56] For most water-soluble molecular rods, it is possible to change the length of the scaffold. These structures cannot, however, position functional groups arbitrarily in two or three dimensions.

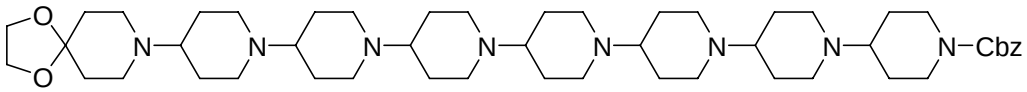

Figure 1-7: Oligo-piperidine spacer for biological applications

1.2 A NOVEL APPROACH TOWARD THE SYNTHESIS OF MOLECULAR SCAFFOLDS

The approach we have described for the synthesis of macromolecular scaffolds is to create oligomers without rotatable bonds.[15] The oligomers do not fold to achieve their functional form; predicting the shape of the oligomer does not require determining the outcome of a complex folding process. The shapes of the oligomers are directly related to the stereochemistry and structure of their constituent monomers.

The monomers in our approach are orthogonally protected *bis*-amino acids; the oligomers created using these monomers are called *bis*-peptides. The *bis*-amino acids that have already been synthesized are illustrated in Figure 1-8. Each monomer is a small heterocycle functionalized with two α-amino acids. The protecting groups, P^1 and P^2 are orthogonal; either may be removed selectively. The selection of P1 and P2 also depends upon the linker used to tether the oligomer to solid phase. R is usually a small alkyl group; this ester must survive the conditions used for the removal of P^1 and P^2, as well as the conditions used to cleave the oligomer from the solid support (see below).

We are more concerned about isolating stereochemically pure monomers than about the stereoselectivity in the reactions used to generate the chiral centers in a monomer. *bis*-Peptide shape is a function of the stereochemistry and conformational preferences of its monomer constituents; each monomer stereoisomer will affect *bis*-peptide shape in a different way. Using 4 monomers (e.g., the 4 possible stereoisomers of the *pro4* monomer), 1024 non-equivalent pentamer *bis*-peptides could be synthesized. The *bis*-amino acid stereoisomers provide access to structural diversity, so synthetic routes that provide access to all stereoisomers of a *bis*-amino acid are ideal.

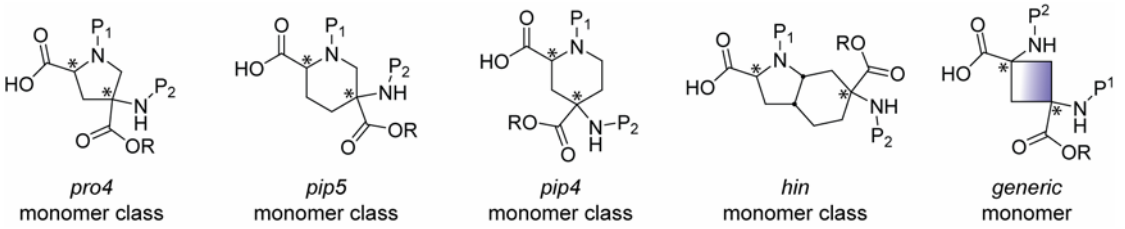

Figure 1-8: *bis*-Amino acid monomers that have been synthesized in our laboratory. Asterisks represent stereocenters that are set during synthesis. The generic monomer (right) is used for the discussion of *bis*-peptide oligomer assembly.

We assemble *bis*-peptide oligomers from *bis*-amino acids in two phases: chain elongation, and rigidification (annealing). During elongation, the sequence of monomers in an oligomer is set by connecting the desired *bis*-amino acid monomers sequentially on solid support through single amide bonds. For this process, we have elected to use the reliable method of solid-phase peptide synthesis (SPPS).[57-59]

After attaching the first *bis*-amino acid to solid phase, protecting group P^1 is removed (Figure 1-9). The next monomer is coupled to the first, and the process is repeated until all of the desired monomers have been incorporated into the oligomer. The oligomer is then cleaved from the resin; with our current protecting group strategy, this usually removes the P^2 protecting groups as well. The product is the "open-form" oligomer, because only one amide bond connects each monomer to neighboring monomer residues.

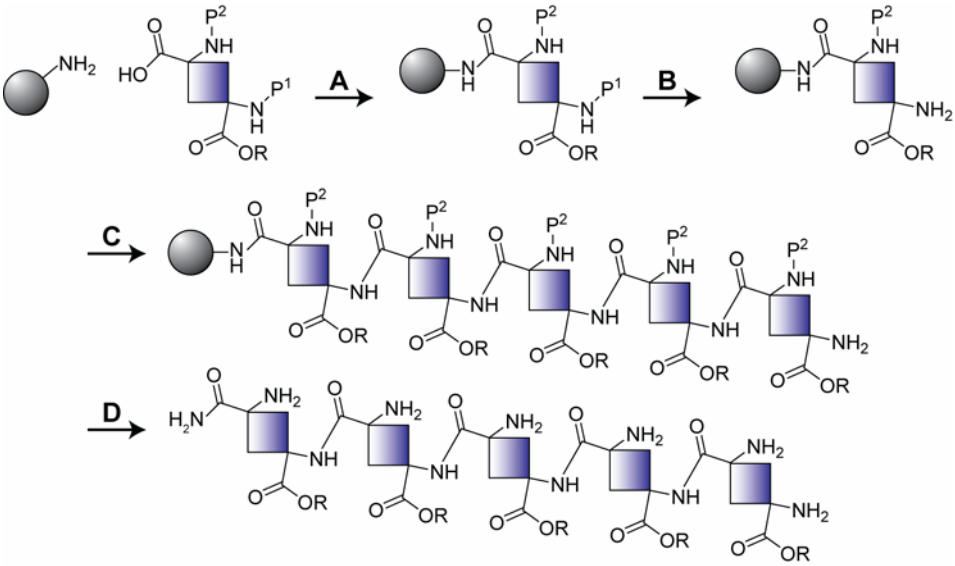

A. Attachment of the first monomer to the solid phase resin; **B.** Removal of N-protecting group, P^1; **C.** Sequence of deprotection and coupling reactions that elongate the chain; **D.** Cleavage from the solid support (can occur with or without cleavage of P^2)

Figure 1-9: Chain elongation by solid-phase peptide synthesis

The second phase of *bis*-peptide synthesis is rigidification of the open-form oligomer. After cleavage and removal of the P^2 protecting groups, the free amine of each monomer attacks the alkyl ester of the preceding monomer, forming a diketopiperazine ring between all adjacent monomers. This process usually occurs within 24 hours under mild conditions (20% piperidine/DMF at room temperature). Forming the second amide bond between adjacent monomers eliminates all rotational flexibility in the oligomer backbone. The resulting *bis*-

peptides are typically water soluble, and are usually stable under neutral or acidic aqueous conditions for weeks.

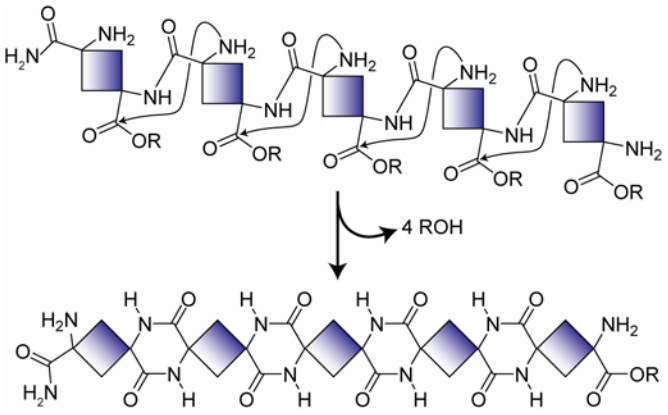

Figure 1-10: Rigidification of the open-form oligomer to the *bis*-peptide

To generate the second amide bond between adjacent monomers, the process of rigidification exploits a well-known side reaction that occurs during solid-phase peptide synthesis (Figure 1-11).[60] This reaction is frequently observed when performing Fmoc solid-phase peptide synthesis with benzyl ester resin linkers (Figure 1-11).[61-63] After removing the N^{α}-Fmoc group from the second α-amino acid residue, the primary amine will attack the ester linkage, causing premature release of a cyclic dipeptide from the solid support. Diketopiperazines occur in natural products,[64] and are produced when peptides and proteins decompose under certain conditions.[65,66]

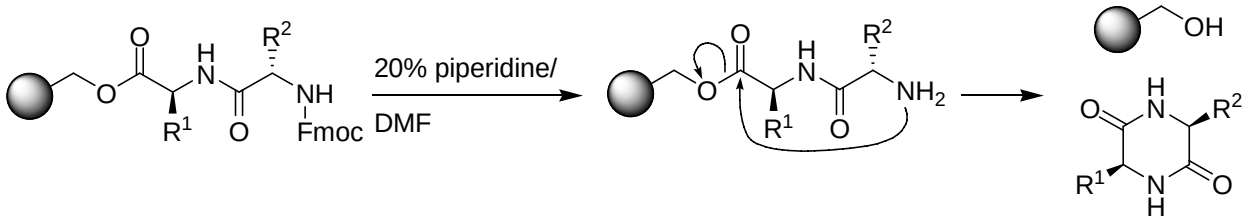

Figure 1-11. Spontaneous DKP formation after removal of the N^{α}-Fmoc group from the second α-amino acid residue during Fmoc-SPPS generates a cyclic dipeptide that is released from the resin.

Chain elongation uses the same chemistry employed for the synthesis of α-amino acids and β-peptides. This process is rapid, and oligomers containing several *bis*-amino acids can be prepared in less than one day. As elongation is a modular process, a modest library of *bis*-amino acids enables the synthesis of a large variety of molecular scaffolds. Our primary hypothesis is that the shape of *bis*-peptides can be controlled in predictable ways because their shape is a function of the stereochemistry and conformational preferences of the constituent monomers.

2.0 *PRO4* MONOMER SYNTHESIS

To pursue *bis*-peptide oligomer development, suitable *bis*-amino acid monomers are required. The *bis*-amino acids monomers must be stereochemically pure, and synthetic routes toward the monomers should be relatively short, reproducible, and scalable. In this chapter, we discuss the synthesis and development of the *pro4 bis*-amino acid monomers (Figure 2-1).

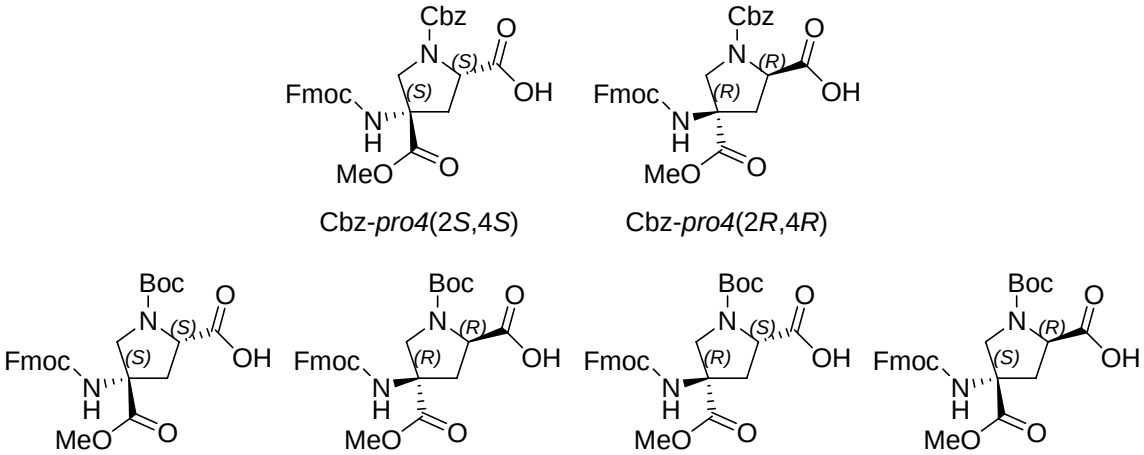

Cbz-*pro4*(2*S*,4*S*) Cbz-*pro4*(2*R*,4*R*)

Boc-*pro4*(2*S*,4*S*) Boc-*pro4*(2*R*,4*R*) Boc-*pro4*(2*S*,4*R*) Boc-*pro4*(2*S*,4*R*)

Figure 2-1: The *pro4 bis*-amino acid monomers

2.1 SYNTHESIS OF THE CBZ-*PRO4*(2*S*,4*S*) MONOMER

The first monomer intended for *bis*-peptide synthesis was orthogonally protected piperizine *bis*-amino acid **1** (Figure 2-2).[67] The synthesis of **1** is short, convergent, and provides access to all four stereoisomers of the piperazine monomer. **1** has all of the components required by the definition of a *bis*-amino acid monomer.

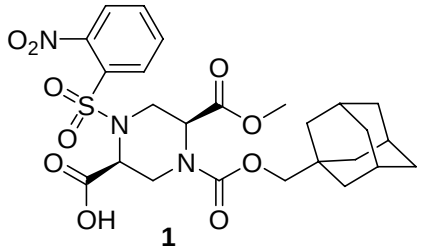

1

Figure 2-2: Piperazine *bis*-amino acid monomer **1**

During solid-phase peptide synthesis, it became evident that the piperazine monomers were far from ideal. It was possible to couple the monomer to the N-terminus of a peptide anchored to a solid-phase resin, and to remove the terminal adamantyloxycarbonyl (Adoc)[68] protecting group using TFA. Nonetheless, coupling a second piperazine monomer to the first was extremely difficult; even when **1** was activated as an acid chloride, yields were unacceptably low (usually less than 50%). The nucleophilicity of the leading secondary amine appeared to be compromised, possibly by inductive effects from the other piperazine nitrogen atom.

The synthesis of new types of *bis*-amino acid monomers was driven by the difficulties encountered with the piperazine monomer. Developing methods for *bis*-peptide oligomer assembly was contingent on being able to couple monomers on solid support, preferably with well-established peptide synthesis protocols. These factors were considered when designing the next generation of *bis*-amino acid monomers.

The *pro4* bis-amino acid monomer was based on the template illustrated in Figure 2-3. After removing protecting group P^1, the monomer would be coupled to a resin bound amine by activating the revealed carboxylic acid. Protecting group P^2 would then be removed, and a second *pro4* monomer would be activated and coupled to the primary amine on the quaternary carbon of the resin bound monomer. This reaction is analogous to coupling proline to α-aminoisobutyric acid (Aib), which can be achieved using reasonable conditions on solid phase.[69] Group P^3 would be removed immediately before diketopiperazine formation between adjacent monomers.

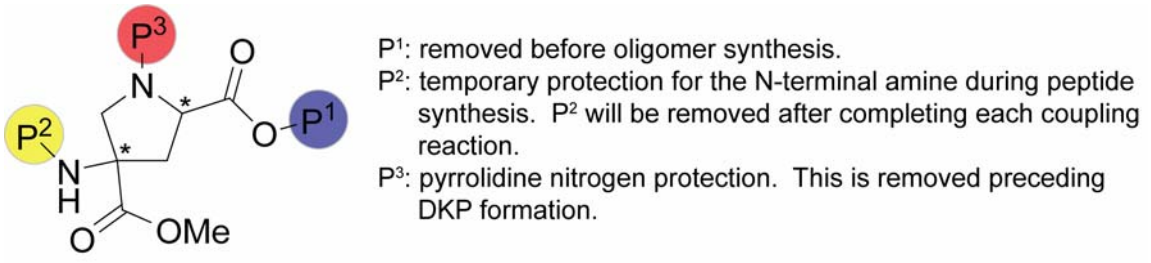

Figure 2-3: Template for the *pro4* monomer class: asterisks indicate chiral centers.

2.1.1 First approach: attempted synthesis of *o*-Ns-*pro4*(2*S*,4*S*) monomer

The original vision for the structure and retrosynthesis of the *pro4* monomer is illustrated in Figure 2-4. Monomer **5** was to be derived from *trans*-4-hydroxy-L-proline, **2**, which is relatively inexpensive[70] and has been used extensively as a building block for the synthesis of functionalized pyrrolidine rings.[71] We named **5** *o*-Ns-*pro4*(2*S*,4*S*); *pro4* refers to the starting material, 4-hydroxyproline, *o*-Ns designates the protecting group for the pyrrolidine N-atom, and (2*S*,4*S*) indicates the stereochemistry at C2 and C4 (as shown in Figure 2-4). The key transformation is installation of the second amino acid at C4. We planned to achieve this by hydrolysis of the hydantoin derived from ketone **3** using the Bucherer-Bergs reaction.[72,73]

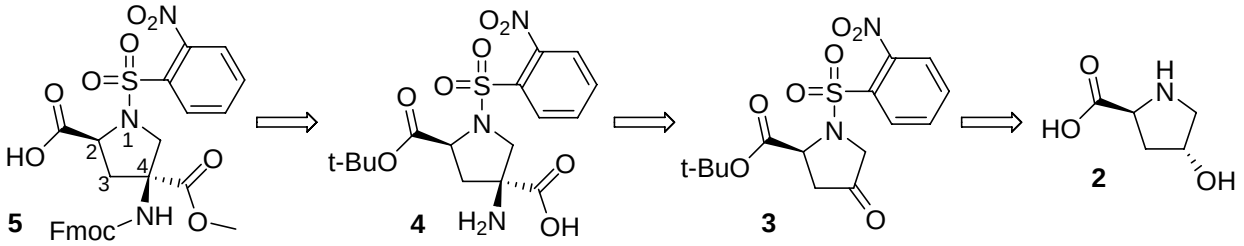

Figure 2-4: Retrosynthesis for proposed *o*-Ns-*pro4*(2*S*,4*S*) monomer **5**

The 9-fluorenylmethoxycarbonyl (Fmoc) group[74] was selected for protecting the primary amine on the quaternary carbon; it can be removed by exposure to secondary amines. Fmoc-based solid-phase peptide synthesis[58] can be performed with resin linkers that are more acid-labile than those used for Boc peptide synthesis;[75] resin cleavage conditions are less aggressive than in Boc peptide synthesis.[58] The *o*-nitrobenzenesulfonyl (*o*-Ns) group[76,77] is stable to the conditions used to cleave the *t*-butyl ester and for removing the Fmoc group. There has been some interest in the *o*-Ns group for use in peptide synthesis because *o*-Ns-protected α-amino acid chlorides cannot form oxazolones.[78] During solid-phase peptide synthesis, tertiary amine

bases can promote the rapid conversion of Fmoc-protected amino acid chlorides to oxazolones,[79] attenuating the activity of the acid chlorides, and providing a route to epimerization at the α-carbon; oxazolone formation is illustrated in Figure 2-5.

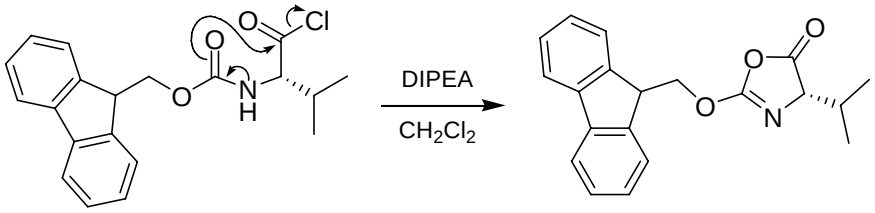

Figure 2-5: Fmoc-Val-Cl conversion to corresponding oxazolone[79]

Another advantage of the *o*-Ns protecting group was that it could be removed without cleaving the oligomer from the resin, enabling oligomer rigidification on solid support. Deprotection can be monitored visually, because removing the *o*-Ns group releases a bright yellow chromophore into solution; when 2-mercaptoethanol and DBU are used to remove the *o*-Ns group, 2-(2-nitrophenylthio)ethanol is liberated, as shown in Figure 2-6.

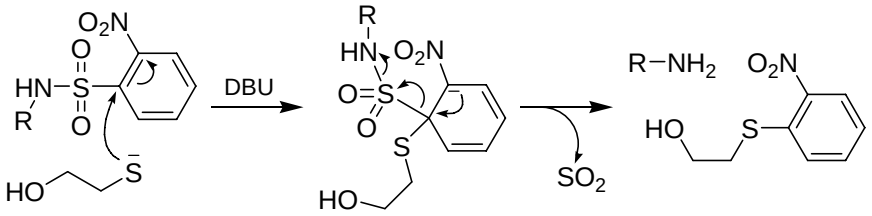

Figure 2-6: Deprotection of *o*-Ns group by means of the Meisenheimer[80] complex

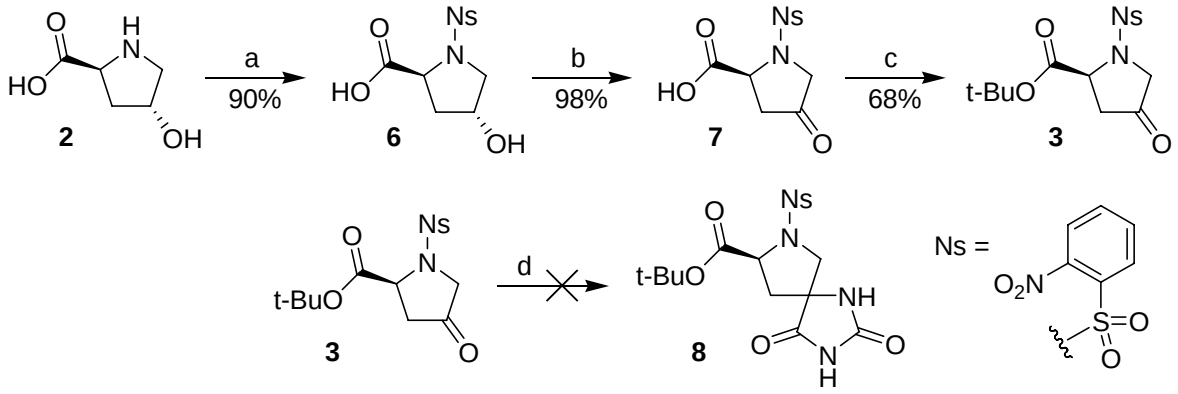

Reagents and Reaction Conditions
(a) i. TMS-Cl, DIPEA, CH_2Cl_2, reflux. ii. *o*-NsCl, 0 °C to rt. (b) Jones reagent, acetone, 20 °C. (c) Isobutylene, H_2SO_4 (cat.), CH_2Cl_2, rt. (d) $(NH_4)_2CO_3$, KCN, 1:1 DMF/H_2O, 60 °C.

Scheme 2-1: First steps in the synthesis of *o*-Ns-*pro4*(2*S*,4*S*) monomer **5**

Steps that were achieved in the synthesis of the *o*-Ns-*pro4*(2*S*,4*S*) monomer are shown in Scheme 2-1. The first step of the synthesis was to generate the sulfonamide **6**. We attempted to protect the secondary amine of *trans*-4-hydroxy-L-proline methyl ester using *o*-NsCl under Schotten-Baumann conditions[81] based on the procedure described by Natchus.[82] The yield of **6** by this method was poor: TLC analysis of the reaction mixture suggested incomplete conversion of the starting material even after 16 hours at room temperature.

We decided to employ a procedure described by Bolin for the synthesis of N^{α}-urethane amino acids,[83] a method based upon earlier work by Theodoropoulos.[84] *trans*-4-Hydroxy-L-proline, **2**, was suspended in dichloromethane with DIPEA and TMS-Cl, and was converted under reflux to the *N*,*O*,*O*'-*tri*-TMS intermediate (not isolated), as shown in Figure 2-7. The TMS groups increase the solubility of the amino acid in organic solvent, making the reaction setup and workup more convenient. Bolin noted that this procedure suppresses the formation of peptide oligomers; under Schotten-Baumann conditions, a reaction between amino acids and Fmoc-Cl can result in the formation of dipeptide and tripeptide side products that have similar polarity as the desired product. Furthermore, the TMS group increases the nucleophilicity of the nitrogen toward sp^2 carbon centers; this effect has been described elsewhere[85] and has been exploited to increase yields when coupling sterically hindered amino acids during SPPS.[86,87] Using Bolin's procedure, crystalline **6** was obtained with excellent yield.

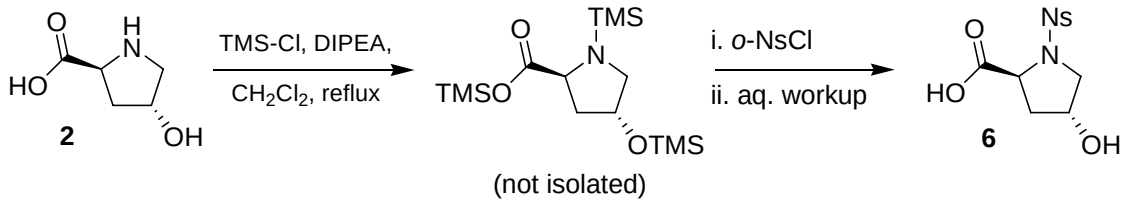

Figure 2-7: One-pot, 2-step procedure for the synthesis of *N*-Ns hydroxyproline

Compound **6** was oxidized in acetone to **7** in high yield using the Jones reagent.[82,88] *t*-Butyl esterification of **7** proved more difficult than the oxidation of **6**. Exposing **7** to the esterification reagent *t*-butyl 2,2,2-trichloroacetimidate in the presence of the Lewis acid catalyst $BF_3{\cdot}Et_2O$[89] yielded no isolable product. It was reported that Cbz-proline was converted to the corresponding *t*-butyl ester in quantitative yield using di-*t*-butyl dicarbonate (Boc_2O) and catalytic DMAP in *t*-butyl alcohol;[90] using these conditions, we observed only starting material **7** by TLC.

The traditional conditions for *t*-butyl esterification provided the desired product.[91] Isobutylene was bubbled into a solution of **7** in dichloromethane containing a catalytic amount of sulfuric acid. Following aqueous workup, the desired product **3** was obtained with 68% yield. This is the most atom economical[92] method of generating a *t*-butyl ester (an excess of isobutylene is used, but it could be recovered from the solution by distillation).

To synthesize amino acid **4**, we planned to transform ketone **3** to the hydantoin **8** using the Bucherer-Bergs reaction,[72,73] as shown in Scheme 2-1. Hydantoins are convenient intermediates in the synthesis of amino acids from ketones and aldehydes.[93] Unfortunately, we were not able to isolate the desired product from the reaction mixture; by TLC, it appeared that starting material **3** decomposed under the Bucherer-Bergs reaction conditions. It is possible that cyanide, a soft nucleophile, was able to attack and cleave the *o*-Ns protecting group.

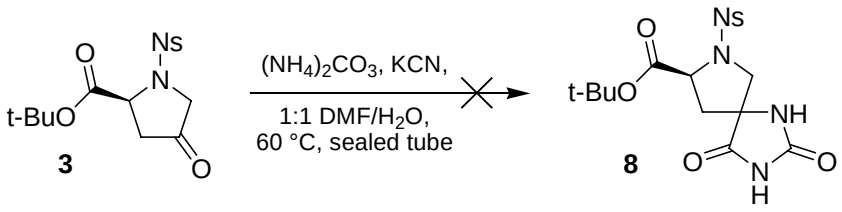

Figure 2-8: Failed Bucherer-Bergs reaction of the *o*-Ns protected ketone

2.1.2 Second approach: Cbz-*pro4*(2*S*,4*S*) monomer

The *o*-Ns protecting group was incompatible with the planned synthetic route for the *pro4*(2*S*,4*S*) monomer. Rather than change the synthetic strategy, we decided to protect the pyrrolidine nitrogen as the benzyl carbamate (Cbz group).[94] The Cbz protecting group can be removed by catalytic hydrogenolysis[94] or using strong acid, such as HBr in acetic acid[57] or triflic acid.[95] Changing the protecting group proved to be a good choice. The Cbz-*pro4*(2*S*,4*S*) monomer, **18**, was synthesized in 9 steps with 23% overall yield on multi-gram scale, as shown in Scheme 2-2.

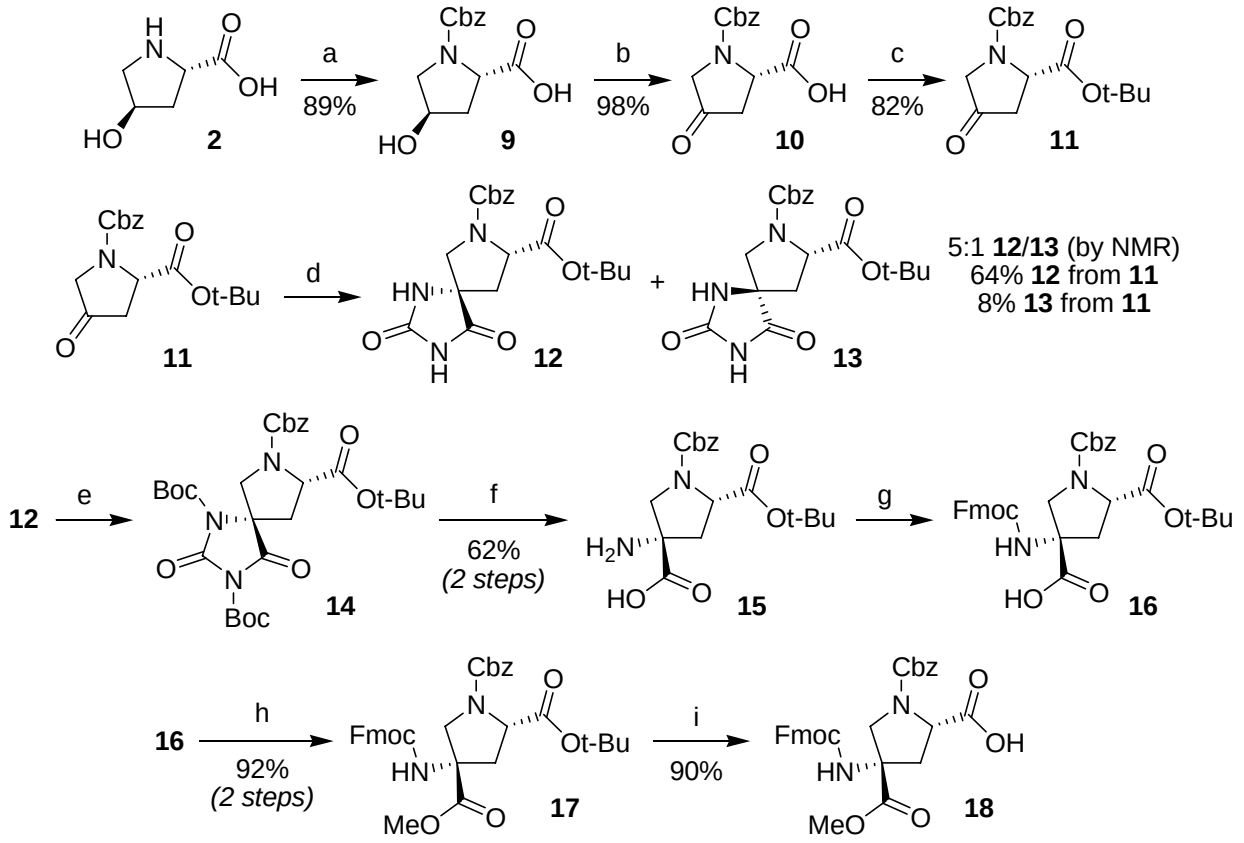

Reagents and Reaction Conditions
(a) i. TMS–Cl, NEt(*i*-Pr)$_2$, CH_2Cl_2, reflux; ii. Cbz-Cl, 0 °C to room temperature. (b) Jones reagent, acetone, 20 °C. (c) Isobutylene, H_2SO_4 (cat.), CH_2Cl_2, room temperature. (d) $(NH_4)_2CO_3$, KCN, 1:1 DMF/H_2O, 60 °C, sealed tube. (e) $(Boc)_2O$, DMAP, THF, 0 °C to room temperature. (f) KOH, 1:1 H_2O/THF. (g) i. TMS–Cl, NEt(*i*-Pr)$_2$, CH_2Cl_2, reflux; ii. Fmoc–Cl, 0 °C to room temperature. (h) TMS–CHN_2, MeOH, Et_2O. (i) CF_3COOH, CH_2Cl_2.

Scheme 2-2: Synthesis of the Cbz-*pro4*(2*S*,4*S*) monomer **18**

Compound **9** was prepared from *trans*-4-hydroxy-L-proline using Bolin's procedure.[83] The secondary alcohol of **9** was oxidized to the ketone in excellent yield using the Jones reagent, affording **10**. Removal of chromium during the workup was facilitated by performing the reaction in a large volume of acetone. Residual Cr^{VI} is converted to Cr^{IV} by the addition of methanol. The Cr^{IV} salts are insoluble in acetone, and precipitate from the reaction mixture during the methanol quench; the majority of the chromium salts can then be removed by filtration. Although CrO_3 is quite toxic, it is inexpensive. The Jones reagent has been used for the oxidation of hydroxyproline previously.[71,82,96] A recent review[97] contrasts the atom-economy and environmental impact of the Jones oxidation with other oxidation methods, including the Swern[98] and Dess-Martin[99] oxidation protocols. Following the oxidation, **10** was converted to the *t*-butyl ester **11** with isobutylene and catalytic sulfuric acid.[91]

t-Butyl ester **11** was then subjected to Bucherer-Bergs reaction conditions (ammonium carbonate and potassium cyanide) at 60 °C for 4 hours, affording a 5:1 mixture of diasteromeric hydantoins, **12** and **13**. These hydantoins were originally separated using flash chromatography over silica using a step gradient.[15] The separation procedure was tedious. The crude mixture of hydantoins was loaded onto silica, and eluted with 99:1 CH_2Cl_2/MeOH; this resulted in a large number of dilute fractions containing **12**. Later fractions containing **12** were contaminated with hydantoin **13**. The methanol concentration was then increased by one percent, usually affording several mixed fractions of **12** and **13**, and finally some fractions containing only **13**. This procedure required multiple purifications, and it was difficult to isolate large quantities of the less-polar diastereomer **13**. Continuous gradient elution methods have since enabled the separation of much larger batches of hydantoin.[100] Using less than 2 equivalents of KCN in the Bucherer-Bergs reaction has improved the yield of the reaction slightly (see experimental details, below); excess cyanide ion promotes unproductive formation of the cyanohydrin.[101]

The stereochemistry of the major and minor products, **12** and **13**, was confirmed by 2D-NMR experiments. The stereochemical assignment of **13** is supported by NOESY correlations H1-H9a, H1-H6a, and H1-H8 (Figure 2-9). The NOESY correlations for **12** do not provide positive evidence for its relative stereochemistry, but the absence of the H1-H8 correlation is consistent with the proposed structure.

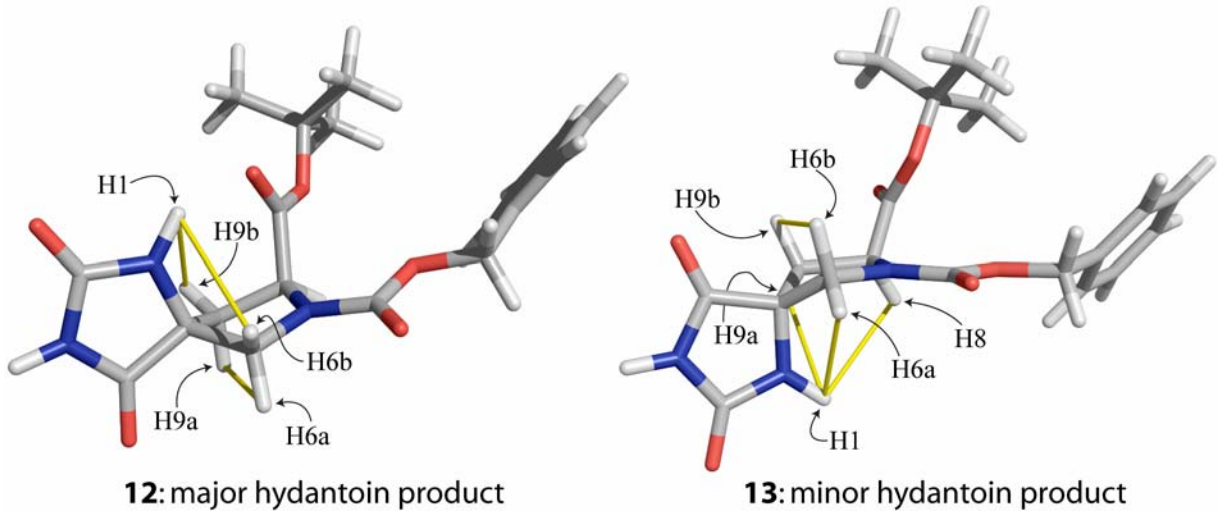

Figure 2-9: The NOESY correlations used to assign the stereochemistry of the major and minor hydantoins (**12**, left; **13**, right). NOESY correlations are represented by gold cylinders. The structures were generated by a stochastic search using the MMFF94x forcefield within MOE.[102]

Hydantoin **12** is the major product of the Bucherer-Bergs reaction (Scheme 2-2). We predicted the stereochemistry of the major and minor hydantoin products based upon Tanaka's results with a similar substrate (**A**, Scheme 2-3).[103] The selectivity (**B** over **C**, Scheme 2-3) is driven by an unfavorable steric interaction between the ester and the C=NH group of the imino-oxazolidinone intermediate (Figure 2-10). The diastereoselectivity of the reaction in Scheme 2-3 increases in proportion to the steric bulk of the ester.

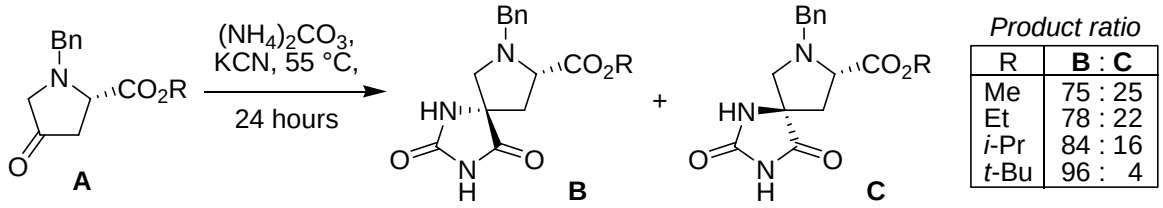

Product ratio

R	**B** : **C**
Me	75 : 25
Et	78 : 22
i-Pr	84 : 16
t-Bu	96 : 4

Scheme 2-3: Diastereoselectivity of the Bucherer-Bergs reaction reported by Tanaka[103]

Our results[15] and Tanaka's results[103] are consistent with the mechanism proposed by Edward and Jitrangsri (Figure 2-10),[104] an elaboration of the mechanism first proposed by Bucherer and Steiner.[73] Edward's mechanism is based upon studies of hydantoin formation from 4-*tert*-butylcyclohexanone; the α-hydantoin (**E**, Figure 2-10) is the predominant product. The transformation from **B** to **C** and from **G** to **H** (Figure 2-10) is the rate limiting step;[104] it is an endothermic transformation, suggesting a product-like transition state.[105] There is an unfavorable steric interaction in **H** between the 3,5 axial hydrogen atoms and the C=NH group of the imino-oxazolidinone; this interaction is avoided in **C**. Under the reaction conditions, there is rapid equilibrium between aminonitriles **A** and **F**, and the barrier of the rate limiting step from **B** to **C** is less than that from **G** to **H**. Accordingly, the route from **A** to **E** is kinetically favored.[106]

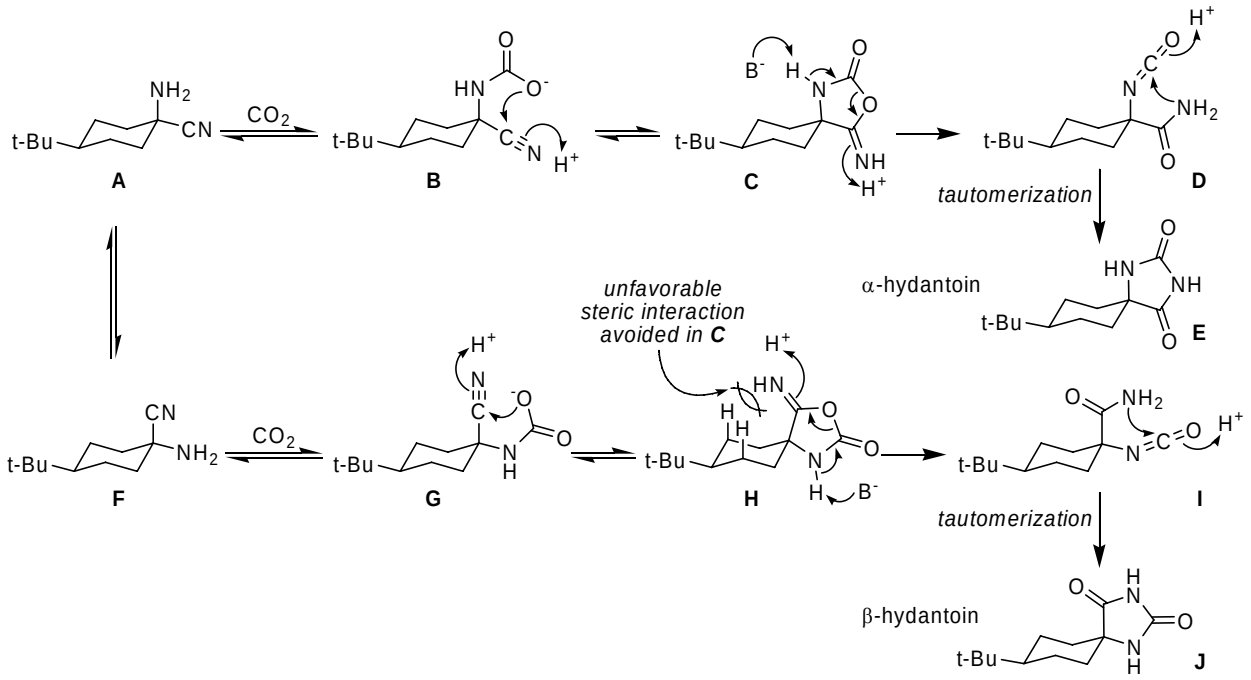

Figure 2-10: Edward and Jitrangsri's proposed mechanism of the Bucherer-Bergs reaction of 4-*tert*-butylcyclohexanone that accounts for the observed product selectivity.

Harsh conditions are usually required to hydrolyze a hydantoin to the corresponding amino acid, such as long exposure to concentrated aqueous HCl or $Ba(OH)_2$ in a sealed tube at temperatures greater than 100 °C.[93] These methods were incompatible with the protecting groups we had selected; neither the *tert*-butyl ester or Cbz group of **12** would survive exposure to these conditions. There are enzymatic methods for hydantoin hydrolysis,[107,108] but poor substrate scope limits their application. We chose to employ a relatively mild method for hydantoin hydrolysis reported by Rebek.[109] The amide and imide nitrogen atoms of the hydantoin are both converted to *tert*-butyl carbamates; the *bis*-Boc hydantoin is more susceptible to nucleophilic attack, and can be hydrolyzed to the amino acid using 1 M aqueous lithium hydroxide. The increased nucleophilic sensitivity of the hydantoin is likely due to increased steric strain, and because the Boc protected nitrogen atom is a better leaving group.[109] A similar method was first described by Grieco for the regioselective hydrolysis and alcoholysis of secondary amides.[110]

Using Boc_2O and catalytic DMAP, hydantoin **12** was converted efficiently to *bis*-Boc hydantoin **14**. TLC analysis of the reaction revealed that the starting material was almost entirely consumed within 30 minutes. DMAP was removed from the reaction by filtration

through a silica plug, and the *bis*-Boc hydantoin **14** was hydrolyzed without further purification. Conversion of the hydantoin **12** to *bis*-Boc hydantoin **14** was achieved with nearly quantitative yield.

Hydrolysis of **14** using aqueous lithium hydroxide and THF as co-solvent[109] gave poor yields of **15**. When the reaction was neutralized and concentrated, the amino acid was contaminated with a significant amount of salt (lithium chloride) and di-*tert*-butyl imidodicarbonate (Boc_2NH). Boc_2NH is a product of *bis*-Boc hydantoin hydrolysis; it was identified by comparison with an authentic sample by TLC. Additionally, the *tert*-butyl ester of some amino acid had been hydrolyzed to the carboxylic acid. Isolating pure **15** from this intractable mixture proved difficult.

In order to improve the yield and simplify recovery of the amino acid, we attempted a variation of the procedure reported by McLaughlin.[111] Aqueous potassium hydroxide was added to a solution of the *bis*-Boc hydantoin **14** in THF; the aqueous and organic solutions were stirred vigorously, generating a milky-white suspension. When allowed to stand, the suspension broke into two layers that could be analyzed separately by TLC. The progress of the reaction was monitored by TLC of the aqueous and organic layers. The starting material **14** was soluble only in the THF layer, and was consumed within 30 minutes. The desired product **15** migrated to the aqueous layer. Boc_2NH was predominantly confined to the THF. Adding diethyl ether to reaction mixture (after all of the starting material had been consumed) promoted migration of Boc_2NH to into the organic layer, and **15** into the aqueous layer. The aqueous solution was separated from the ethereal solution; and the organic solution was washed with small portions of water to recover additional amino acid. The aqueous layer and water washes were combined, chilled, and then acidified to pH 6.5 with an aqueous HCl solution with mechanical stirring. The resulting white precipitate was filtered from the solution and dried in a vacuum oven. ^{1}H and ^{13}C NMR analysis of the precipitate verified that it was the desired product **15.** The amorphous precipitate can be crystallized using hot $EtOH/H_2O$ solution.[100]

The primary amine of **15** was protected with an Fmoc group using a similar procedure as that described for the Cbz protection of **2**.[83] The product, Fmoc protected amino acid **16**, was converted to the methyl ester **17**. This was originally achieved using DCC, DMAP and methanol in CH_2Cl_2,[15] affording only a modest yield of the methyl ester (71%). Considerably better yields of the methyl ester have been achieved by dissolving **16** in a mixture of anhydrous methanol and

ether, and then slowly adding ethereal TMS-CHN_2 to the solution. This generates the methyl ester **17** in high yield (typically, > 90%), and TMS-CHN_2 is safer than the explosive and toxic reagent diazomethane.[112] Finally, the *tert*-butyl ester was cleaved from **17**, affording the Cbz-*pro4*(2*S*,4*S*) monomer **18** as a shelf-stable solid that has been used for solid-phase oligomer synthesis without further purification.

2.2 BOC-*PRO4*(2*S*,4*S*) MONOMER AND *PRO4* DIASTEREOMERS

2.2.1 Boc to Cbz exchange

The Cbz-*pro4*(2*S*,4*S*) monomer **18** was used successfully in the synthesis of *bis*-peptide oligomers.[15,100] The Cbz group is stable to the conditions used for the removal of the Fmoc group during solid phase synthesis. This protecting group is usually removed by catalytic hydrogenation with heterogeneous Pd/C and H_2, or by using very strong acid.[94] For the synthesis of the first *bis*-peptide (page 59), the Cbz groups were removed after the oligomer was cleaved from the solid phase resin using hydrogen gas and Pd/C.[15] Because the polarity of the open-form oligomers increases dramatically when the Cbz groups are removed, it was difficult to find appropriate solvent conditions for the hydrogenation reaction, especially for longer oligomers. Although the Cbz groups could be removed using triflic acid in TFA without solubility problems, these aggressive conditions were not compatible with some functional groups (i.e., dansyl) that we wanted to attach to the oligomers.[100] Accordingly, we exchanged the Cbz protecting group with a Boc group, which can be cleaved by treatment with TFA. The Boc groups could be removed simultaneously with cleavage of the oligomer from the resin.

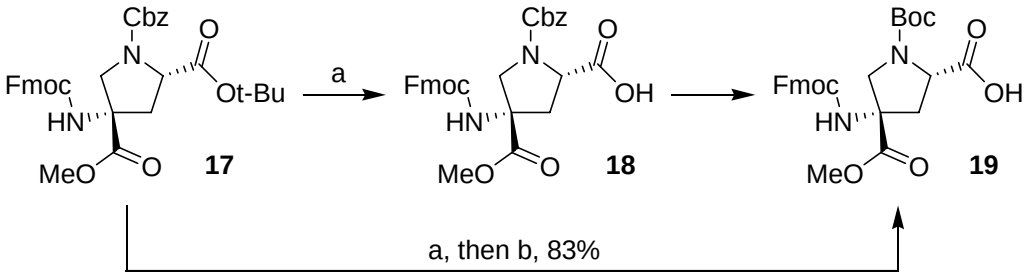

Reagents and Reaction Conditions
(a) CF_3COOH, CH_2Cl_2. (b) Boc_2O, Pd/C, H_2, THF.

Scheme 2-4: Cbz to Boc exchange reaction

Following a one-pot procedure described by Sakaitani,[113] the Cbz group of **18** was converted to a Boc group with good yield (Scheme 2-4). The *tert*-butyl ester of **17** was cleaved using TFA in dichloromethane. After removing the reaction solvent, the residue (crude **18**) was dissolved in THF. Pd/C and Boc_2O were added to this solution; and the reaction mixture was stirred under a hydrogen atmosphere for approximately 24 hours, providing Boc-*pro4*(2*S*,4*S*) monomer **19** in 83% yield from **17**.

2.2.2 Cbz and Boc-*pro4*(2*R*,4*R*) monomers

The Cbz- and Boc-*pro4*(2*R*,4*R*) monomers (**29** and **30**, respectively) were prepared using the same methods described for the synthesis of the *pro4*(2*S*,4*S*) monomers (Scheme 2-5).[100]

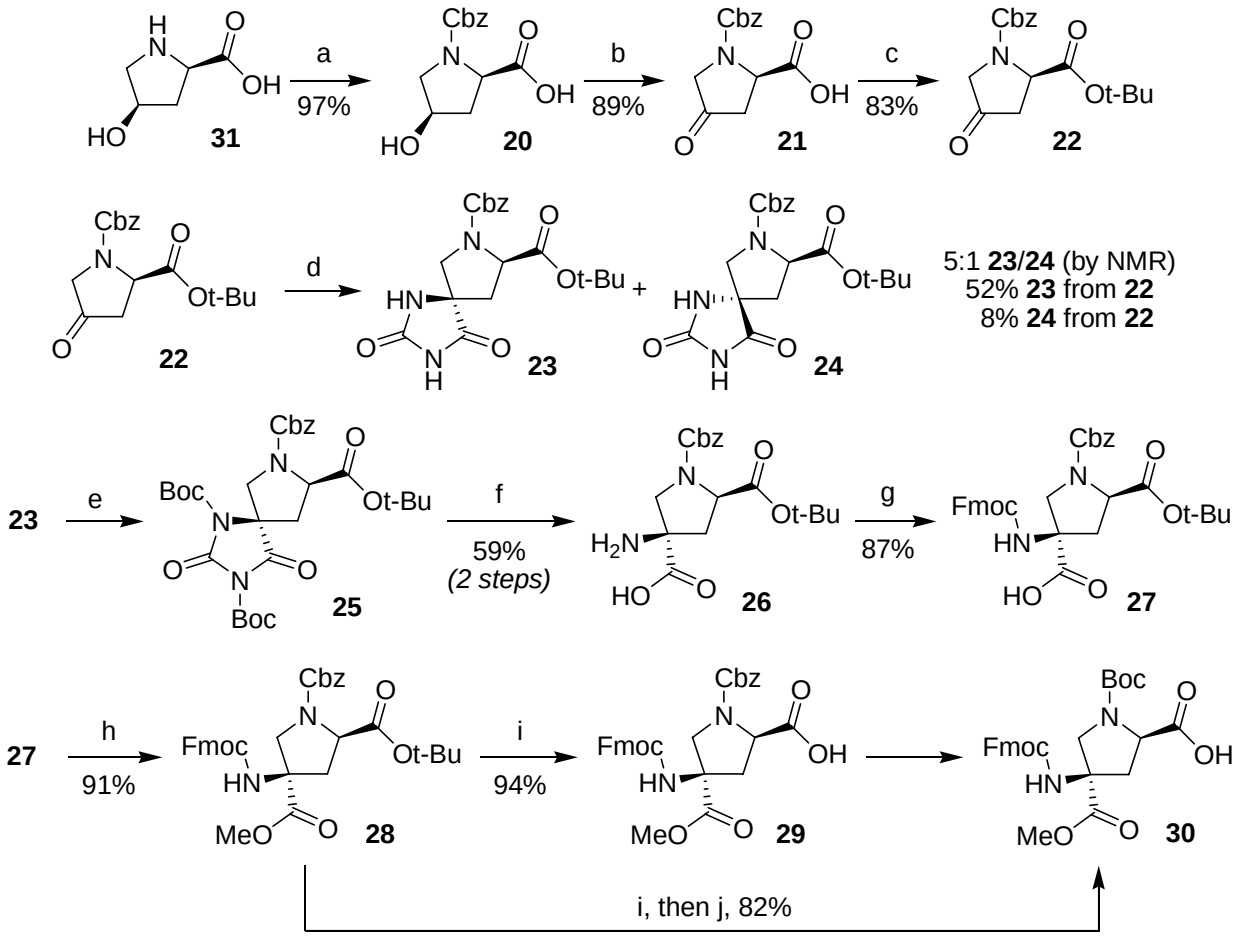

Reagents and Reaction Conditions
(a) i. TMS–Cl, NEt(*i*-Pr)$_2$, CH_2Cl_2, reflux; ii. Cbz-Cl, 0 °C to room temperature. (b) Jones reagent, acetone, 20 °C. (c) Isobutylene, H_2SO_4 (cat.), CH_2Cl_2, room temperature. (d) $(NH_4)_2CO_3$, KCN, 1:1 DMF/H_2O, 60 °C, sealed tube. (e) $(Boc)_2O$, DMAP, THF, 0 °C to room temperature. (f) KOH, 1:1 H_2O/THF. (g) i. TMS–Cl, NEt(*i*-Pr)$_2$, CH_2Cl_2, reflux; ii. Fmoc–Cl, 0 °C to room temperature. (h) TMS–CHN_2, MeOH, Et_2O. (i) CF_3COOH, CH_2Cl_2. (j) Boc_2O, Pd/C, H_2, THF.

Scheme 2-5: Synthesis of the Cbz-*pro4*(2*R*,4*R*) (**29**) and Boc-*pro4*(2R,4R) (**30**) monomers.

Although *cis*-4-hydroxy-D-proline (**31**) is commercially available, it is fairly expensive ($47.60 / gram from Acros 2006/2007; compare with $1.59 / gram for *trans*-4-hydroxy-L-proline (**2**)). Fortunately, **31** can be prepared from **2** (the starting material for the synthesis of the Cbz-*pro4*(2*S*,4*S*) monomer). A method for epimerization of **2** with acetic acid and acetic anhydride was described in 1951;[114] we used a variation of this procedure described by Lowe.[115] Epimerization of **2** proceeds through an azalactone (**B**, Figure 2-11).[116] Under the epimerization reaction conditions, there is equilibrium between the cis and trans forms of the acetylated hydroxyproline (**A** and **C**, Figure 2-11). The hydroxyl group of the cis form (**C**) can attack the

mixed anhydride, trapping the epimerized product as a bicyclic lactone (**B**). Acidic hydrolysis with aqueous HCl converts the lactone to the hydrochloride salt of **31**. From 20 grams of *trans*-4-hydroxy-L-proline, we typically obtain *cis*-4-hydroxy-D-proline in ~ 40% yield. Though this recovery is not ideal, epimerization of the trans isomer is far less expensive than purchasing similar quantities of the cis isomer.

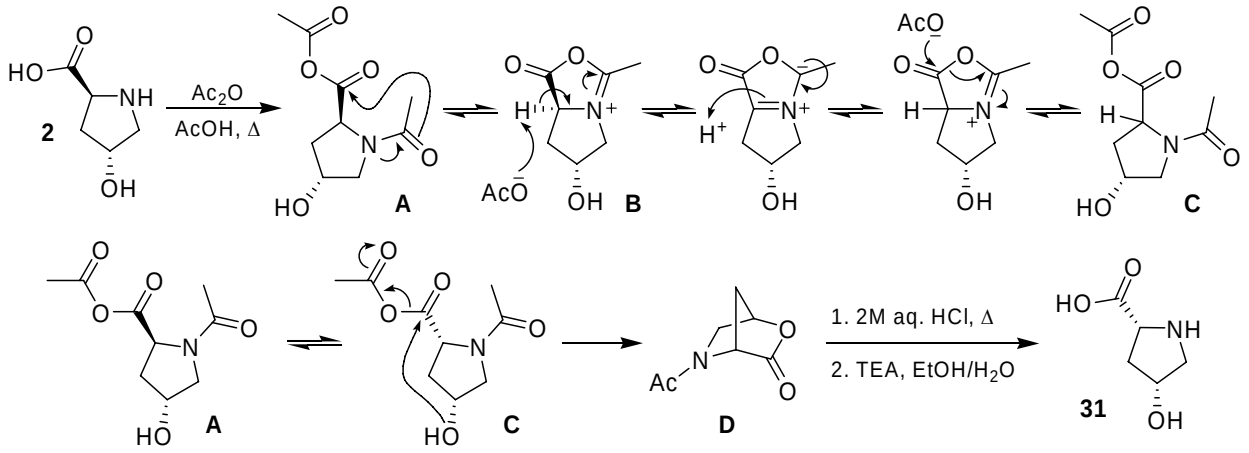

Figure 2-11: Proposed mechanism for the epimerization of *trans*-4-hydroxy-L-proline with acetic acid and acetic anhydride

2.2.3 Measuring the enantiopurity of the *pro4*(2*S*,4*S*) and *pro4*(2*R*,4*R*) monomers

^{1}H NMR, ^{13}C NMR and reverse phase HPLC chromatography suggested that monomers **18**, **19**, **29**, and **30** were single diastereomers, but these methods cannot be used (directly) to detect the presence of enantiomers. Epimerization at the α-carbon (from hydroxyproline) during synthesis would have resulted in mixtures of enantiomers. We determined the enantiopurity of the monomers by coupling them to both enantiomers of a chiral amine, as shown for **19** in Scheme 2-6. The L-(–)-α-methylbenzylamine and D-(+)-α-methylbenzylamine derivatives of the monomers were prepared on analytical scale and analyzed by HPLC-MS.

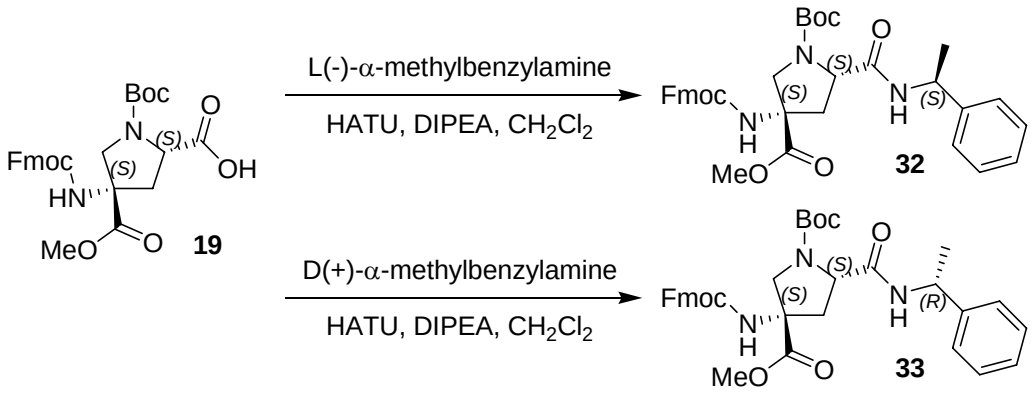

Scheme 2-6: Coupling of monomer **19** to both enantiomers of methylbenzylamine for a test of enantiopurity

Monomer derivatives **32** and **33** are baseline separable by HPLC (Figure 2-12). The sample of **32** contained less than 3% of an UV-active compound with a retention time equivalent to that of **33**; **33** contained less than 1% of an impurity with the retention time of **32** (the enantiopurity of the amine used to make **33** was greater than that used to make **32**). Similar results were obtained for the derivatives of monomers **18**, **29**, and **30**. This result confirms that there is insignificant epimerization at the α-carbon along the synthetic routes described in Scheme 2-2 and Scheme 2-5.

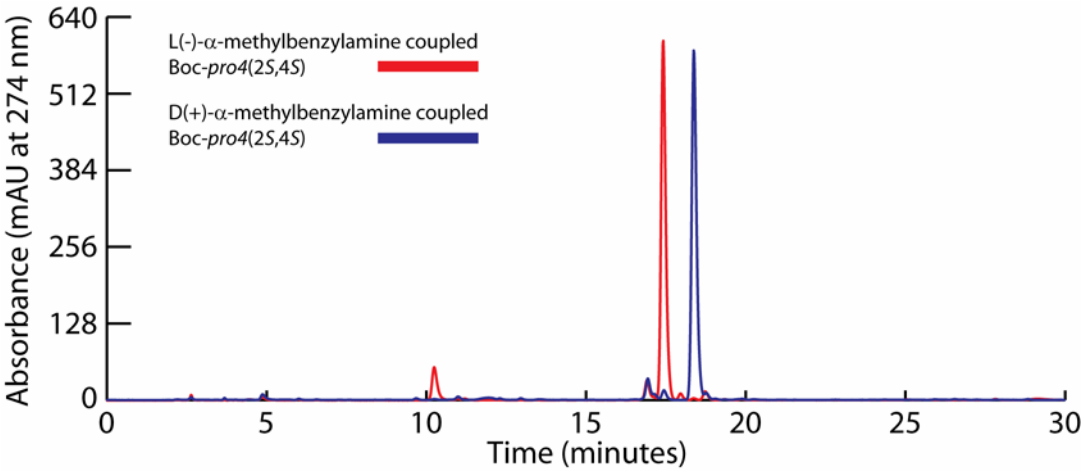

HPLC: column, Microsorb 100 C_{18}, 4.6 mm × 250 mm; mobile phase, CH_3CN (0.05% TFA) / water (0.1% TFA), 50% to 95% CH_3CN over 30 minutes; flow rate, 1.00 mL / min; UV detection at 274 nm; t_R for **32**, 17.4 min: t_R for **33**, 18.4 min.

Figure 2-12: HPLC chromatograms (overlaid) of chiral amine derivatives of Boc-*pro4*(2*S*,4*S*) monomer. The two derivatives are baseline separable.

2.2.4 Boc-*pro4*(2*S*,4*R*) and Boc-*pro4*(2*R*,4*S*) monomers

Monomers **37**, named Boc-*pro4*(2*S*,4*R*), and **41**, named Boc-*pro4*(2*R*,4*S*), are the final stereoisomers of the *pro4* monomer class. Their synthesis was achieved on gram scale using procedures similar to those described for the *pro4*(2*S*,4*S*) and *pro4*(2*R*,4*R*) monomers, as shown in Scheme 2-7. The synthesis of **37** and **41** begins with hydantoins **13** and **24**, respectively. These hydantoins are the minor products of the Bucherer-Bergs reaction; they are isolated during the synthesis of Boc-*pro4*(2*S*,4*S*) **19** and Boc-*pro4*(2*R*,4*R*) **30**.

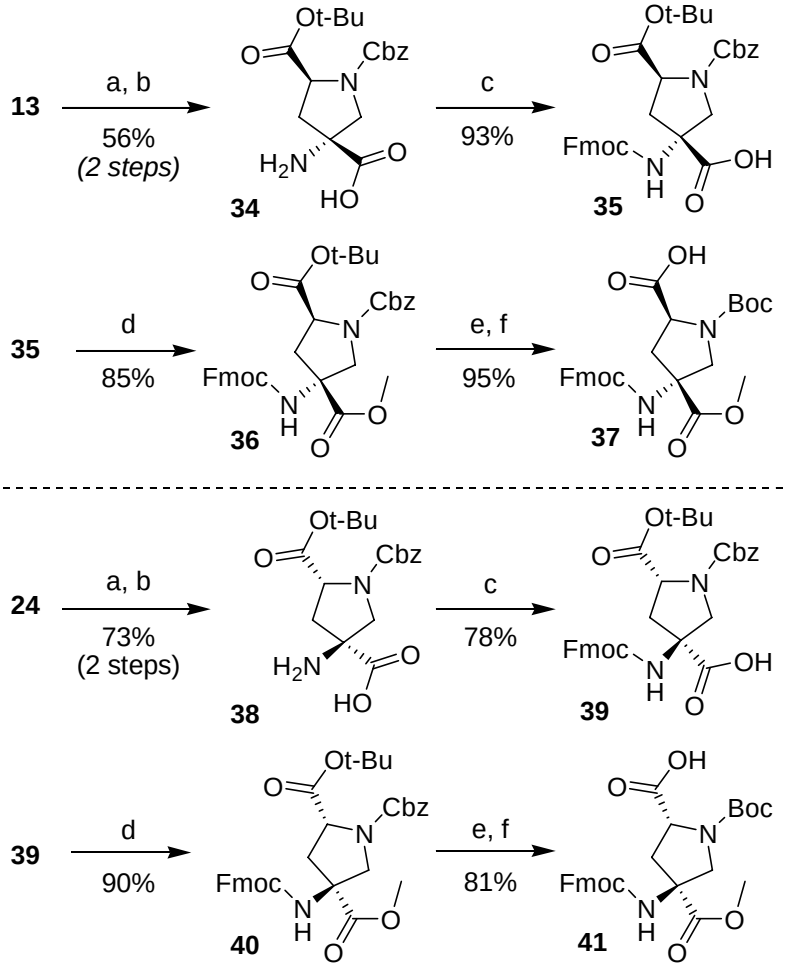

Reagents and Reaction Conditions
(a) $(Boc)_2O$, DMAP, THF, 0 °C to room temperature. (b) KOH, 1:1 H_2O/THF. (c) i. TMS–Cl, NEt(*i*-Pr)$_2$, CH_2Cl_2, reflux; ii. Fmoc–Cl, 0 °C to room temperature. (d) TMS–CHN_2, MeOH, Et_2O. (e) CF_3COOH, CH_2Cl_2. (f) Boc_2O, Pd/C, H_2, THF.

Scheme 2-7: Synthesis of monomers Boc-*pro4*(2*S*,4*S*) (**37**) and Boc-pro4(2R,4R) (**41**)

Product yields were similar to those achieved during the synthesis of **19** and **30**. While amino acids **15** and **26** were soluble in methanol, their respective diastereomers, **34** and **38**, were almost entirely insoluble in room temperature methanol or ethanol. **34** and **38** were crystallized by dissolving them in hot methanol and then allowing the solution to cool.[117]

2.3 DISCUSSION

The synthesis of all four stereoisomers of the *pro4* monomer class has been achieved from a common starting material.[15,100,117] These monomers have been used extensively for the synthesis of *bis*-peptide oligomers,[13-15,100,117,118] some of which are described in the following chapters.

The methods developed for *pro4* monomer synthesis are scalable; the Boc-*pro4*(2*S*,4*S*) and Boc-*pro4*(2*R*,4*R*) monomers have been prepared in > 10 gram batches without a significant change in yield for each step. In practice, silica chromatography of intermediates is only required following the Bucherer-Bergs reaction and the methyl esterification.[15] Nonetheless, gradient elution flash chromatography has enabled rapid and easy purification of the Fmoc protected amino acid intermediates (**16**, **27**, **35**, and **39**), as well as the final Boc-*pro4* or Cbz-*pro4* monomers.[100,117]

Typically, the *pro4* monomers are prepared starting with 20 to 25 grams of hydroxyproline; beyond this, the workups become unwieldy. Furthermore, separating greater than ~ 30 gram batches of the diasteromeric hydantoins (**12** from **13**, and **23** from **24**) is time consuming. Fmoc protection of the amino acids remains the most difficult and least reproducible reaction; it seems to be sensitive the purity of the starting material. Crystallization of the amino acids prior to Fmoc protection has improved the consistency in yield from batch to batch, but the crystallization procedure is somewhat difficult. The synthesis would be improved considerably by developing a more reproducible method for de-salting and purification of the amino acid (e.g., ion exchange chromatography).

The *pro4* monomer has been described as “complicated”.[41] Monomer synthesis requires 9 (Cbz-*pro4*) or 10 (Boc-*pro4*) linear steps, but several of these steps are straightforward, high-yield protecting group manipulations. Moreover, a number of asymmetric building blocks for

foldamers and other oligomers have been reported that require syntheses of comparable length.[29,31,35,39]

Others in our laboratory have expanded upon the synthesis of the *pro4* monomer. Starting from hydroxyproline, they have synthesized the structurally similar pipecolic acid based monomers, *pip4* and *pip5* (Figure 2-1); these also have been incorporated into *bis*-peptide oligomers.[13,119] All of the transformations described for the synthesis of the *pro4* monomer class have been translated successfully for the synthesis of the *pip4* and *pip5* monomers.

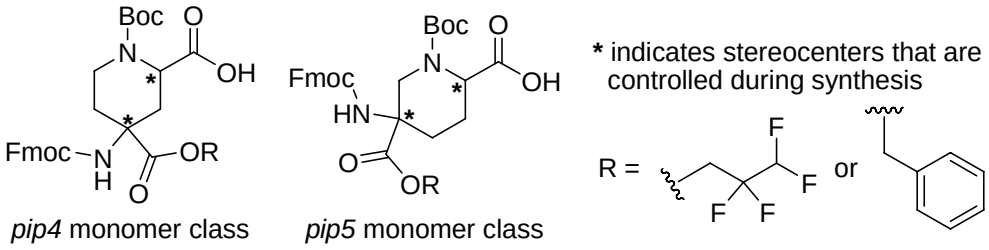

Figure 2-13: The pipecolic acid based monomer class

2.4 EXPERIMENTAL DETAILS

2.4.1 General procedures

THF was dried by distillation from sodium/benzophenone ketyl under nitrogen. CH_2Cl_2 was dried by distillation over CaH_2 under nitrogen. *trans*-4-hydroxy-L-proline was obtained from Acros Chemical Company. Reactions were carried out under a nitrogen atmosphere using oven dried glassware, unless otherwise noted. Column chromatography was performed using ICN Silitech 32 – 63 D (60 Å) grade silica gel and TLC analyses were performed on EM Science Silica Gel 60 F254 plates (250 μm thickness). Flash chromatography was either performed by hand or using the ISCO CombiFlash Companion, with cartridges filled with Silitech 32 – 63 D (60 Å) grade silica gel. NMR experiments were performed on Bruker Avance 300 MHz, 500 MHz, or 600 MHz instruments. Chemical shifts are reported in parts per million (ppm) on the δ scale, and were referenced to residual protonated solvent peaks (unless otherwise noted): spectra obtained in DMSO-d_6 were referenced to (C*H*D_2)(CD_3)SO at δ_H 2.50 and (*C*D_3)$_2$SO at δ_C 39.5; spectra obtained in acetic acid-d_4 were referenced to (C*H*D_2)COOD at δ_H 2.07 and (*C*D_3)COOD

at δ_C 20.0. If possible, rotational isomers were resolved by obtaining spectra at 75 °C in DMSO-d_6. IR spectra were obtained using a Nicolet Avatar E.S.P. 360 FT-IR. Optical rotations were measured at 25 °C (± 2 °C) in chloroform, unless otherwise noted, using a Perkin-Elmer 241 Polarimeter with a 1 mL cell (10 cm path length).

Mass spectrometry was performed either on a Micromass Autospec high resolution mass spectrometer (CEBE geometry) with an electron impact ion source (HRMS-EI), or on a Waters Micromass LC/Q-Tof Premier mass spectrometer using an electrospray ion source (HRESIQTOFMS). HPLC analysis was performed on a Hewlett-Packard Series 1050 instrument with a diode array detector, using a Varian Chrompack Microsorb 100 C_{18} column (5 μm packing, 4.6 mm x 250 mm). HPLC-MS analysis was performed on a Hewlett-Packard Series 1050 instrument with diode array detector, Agilent 1100 series LC-MSD detector (ES ion source) using a Waters XTerra MS C_{18} column (3.5 μm packing, 4.6 mm x 100 mm)

2.4.2 Synthetic procedures and analytical data

(2*S*,4*R*)-4-hydroxy-1-(2-nitrobenzenesulfonyl)-pyrrolidine-2-carboxylic acid (6)

trans-4-hydroxy-L-proline (15.2 g, 116 mmol) and a magnetic stir bar were transferred into a 500 mL three-neck round bottom flask equipped with a Friedrichs condenser and nitrogen inlet adaptor. DCM (250 mL) was added to the flask. DIPEA (66.5 mL, 383 mmol) was added by syringe; TMS-Cl (66.5 mL, 522 mmol) was added carefully to the stirred mixture by syringe. The solution was heated to reflux for 1.5 hours, and the flask was then immersed in an ice bath. *o*-Ns-Cl (23.1 g, 104 mL) was added to the solution in one portion, and the reaction mixture was stirred while it slowly warmed to room temperature. The solution was concentrated to an oil, which was dissolved in 2.5% aqueous $NaHCO_3$ solution (~ 250 mL). The aqueous solution was washed with 2 portions of Et_2O. The organic layers were combined and washed with water; all aqueous portions were then combined and acidified to pH 2 with 1M aq. HCl. The desired product was extracted from the aqueous layers with EtOAc (3 × 100 mL). The EtOAc solution was concentrated by rotary evaporation, and the resulting oil was recrystallized from hot water yielding **6** (29.7 g, 93.9 mmol, 90%) as off-white crystals. ^{1}H NMR (300 MHz, DMSO-d_6): δ 12.90 (br s, 1H), 8.11 (m, 1H), 7.93 (m, 1H), 7.88 – 7.79 (m, 2H), 5.11 (br s, 1H, –O*H*), 4.44 (t, *J*

= 7.8 Hz, 1H), 4.30 (m, 1H), 3.51 (dd, *J* = 10.7, 3.9 Hz, 1H), 3.36 (dt, *J* = 10.7, 1.7 Hz, 1H), 2.19 (m, 1H), 2.03 (ddd, *J* = 12.6, 7.9, 4.6 Hz,. 1H); ^{13}C NMR (75.4 MHz, DMSO-d_6): δ 173.0, 147.9, 134.4 (CH), 132.2 (CH), 131.1, 130.3 (CH), 124.1 (CH), 68.5 (CH), 59.9 (CH), 56.4 (CH_2), 39.1 (CH_2); EI-MS *m/z* (relative intensity): 317 (<1%, M + H^+), 271 (82%, [M – COOH]$^+$), 186 (100%); HRMS-EI calcd for $C_{11}H_{13}N_2O_7S$ (M + H^+) 317.0438, found 317.0459.

(*S*)-1-(2-Nitrobenzenesulfonyl)-4-oxopyrrolidine-2-carboxylic acid (7)

Compound **6** (10 g, 32 mmol) was dissolved in acetone (86 mL) that had been distilled from $KMnO_4$; this solution was transferred to a round bottom flask containing a magnetic stir bar. Freshly prepared Jones Reagent[88] (8 M, 34 mL) was added slowly to the stirred solution of **6**. After 4 hours, the reaction mixture was diluted with water (~ 300 mL) and the product was extracted from the aqueous solution with EtOAc (3 ×). The organic layers were washed with water (2 ×) and brine (2 ×), dried over Na_2SO_4, and concentrated by rotary evaporation. Residual solvent was removed from the resulting clear oil under reduced pressure overnight yielding **7** (9.7 g, 31 mmol, 98%) as a white foam, used without further purification. ^{1}H NMR (300 MHz, DMSO-d_6): δ 8.11 (dd, *J* = 7.5, 1.8 Hz, 1H), 8.00 (dd, *J* = 7.7, 1.5 Hz, 1H), 7.88 (m, 2H), 4.76 (dd, *J* = 10.0, 2.2 Hz, 1H), 3.94 (d, *J* = 16.9, 1H), 3.85 (d, *J* = 16.9 Hz, 1H), 3.17 (dd, *J* = 18.2, 9.9 Hz, 1H), 2.62 (dd, *J* = 18.2, 2.2 Hz, 1H); ^{13}C NMR (75.4 MHz, DMSO-d_6): δ 206.7, 172.1, 147.5, 134.9, 132.7, 130.4, 130.4, 124.4, 58.0, 52.5, 41.5; EI-MS *m/z* (relative intensity): 297 (<1%, [M – OH]$^+$), 269 (<1%, [M – COOH]$^+$), 186 (100%); HRMS-EI calcd for $C_{10}H_9N_2O_5S$ (M – COOH) 269.0232, found 269.0235.

(*S*)-1-(2-Nitrobenzenesulfonyl)-4-oxopyrrolidine-2-carboxylic acid *tert*-butyl ester (3)

Compound **7** (8.0 g, 25 mmol) and a magnetic stir bar were transferred to a 200 mL round bottom flask. DCM (51 mL) was added to the flask. Concentrated sulfuric acid (254 μL) was added to the resulting solution by syringe. While stirring the mixture, isobutylene gas was gently bubbled into the solution through a glass pipette until the volume of the reaction mixture had increased by 50%. The reaction mixture was allowed to stir for 2 hours, at which time the reaction mixture was washed with an aqueous $NaHCO_3$ solution (saturated) to neutralize residual sulfuric acid. The organic layer was separated, washed with water, dried over $MgSO_4$, filtered, and then concentrated by rotary evaporation. Residual solvent was removed under reduced

pressure yielding **3** (6.4 g, 17 mmol, 68%) as a pale yellow foam. An analytical sample was prepared by recrystallizing a portion of the product from hot water:
^{1}H NMR (300 MHz, DMSO-d_6): δ 8.14 (dd, J = 7.1, 2.1 Hz, 1H), 8.00 (dd, J = 7.4, 1.9 Hz, 1H), 7.90 (m, 2H), 4.77 (dd, J = 9.8, 1.9 Hz, 1H), 4.00 (d, J = 16.8 Hz, 1H), 3.90 (d, J = 16.9 Hz, 1H), 3.23 (dd, J = 18.1, 9.9 Hz, 1H), 2.60 (dd, J = 18.2, 1.8 Hz, 1H), 1.31 (s, 9H); ^{13}C NMR (75.4 MHz, DMSO-d_6): δ 206.4, 169.4, 147.5, 134.9 (CH), 132.7 (CH), 130.9, 130.4 (CH), 124.4 (CH), 82.3, 58.6 (CH), 52.5 (CH_2), 41.6 (CH_2), 27.4 (CH_3); EI-MS m/z (relative intensity): 314 (1.8%, $[M - C_4H_9 + H]^+$), 269 (29%, $[M - CO_2C(CH_3)_3]^+$), 186 (100%); HRMS-EI calcd for $C_{11}H_{10}N_2O_7S$ (M – C_4H_9 + H) 314.0203, found 314.0211.

(2*S*,4*R*)-4-Hydroxypyrrolidine-1,2-dicarboxylic acid 1-benzyl ester (9)

An oven-dried 1000 mL three-neck flask containing a magnetic stir bar was charged with *trans*-4-hydroxy-L-proline (**2**, 25 g, 190 mmol). Dichloromethane (406 mL) was transferred into the flask. The flask was fitted with a reflux condenser with nitrogen inlet adapter, a glass stopper and rubber septum. DIPEA (96.8 mL, 557 mmol, 2.92 equivalents) was added to the stirred suspension via syringe through the rubber septum; this was followed by slow addition of TMS-Cl (72.8 mL, 572 mmol, 3 equivalents), also by syringe. The flask was thoroughly flushed with nitrogen, the rubber septum was replaced with a glass stopper, and the reaction mixture was heated to reflux for 1.5 hours. The three-neck flask was submerged in an ice bath, and benzyl chloroformate (Cbz-Cl, 26 mL, 181 mmol, 2 equivalents) was added to the reaction mixture which was stirred overnight while warming to room temperature. The solution was concentrated by rotary evaporation to a dark red oil which was distributed between 2.5% aqueous $NaHCO_3$ (1250 mL) and Et_2O (750 mL), then transferred to a 2 L separatory funnel. The ether layer was removed, and the aqueous solution was washed with additional portions of Et_2O (2 × 200 mL). The combined ether layers were washed with water (2 × 100 mL). All aqueous layers were then combined and acidified to pH 2 with 1 M aqueous HCl; the desired product was then extracted from the acidified solution with EtOAc (3 × 350 mL). The EtOAc solution was dried over Na_2SO_4, filtered, and concentrated by rotary evaporation. Residual solvent was removed overnight under reduced pressure yielding **9** (42.9 g, 161 mmol, 89%) as an off-white foam that was used without further purification. ^{1}H NMR (300 MHz, 75 °C, DMSO-d_6): δ 12.2 – 12.4 (br s, 1H), 7.31 – 7.35 (m, 5H), 5.08 (s, 2H), 4.30 – 4.35 (m, 2H), 3.51 (dd, J = 11.0, 4.7 Hz, 1H),

3.41 (ddd, *J* = 11.0, 2.8, 1.4 Hz, 1H), 2.19 (dddd, *J* = 12.0, 8.3, 4.1, 1.2 Hz, 1H), 2.02 (ddd, *J* = 12.0, 6.7, 5.2 Hz, 1H); ^{13}C NMR (75.4 MHz, 75 °C, DMSO-d_6): δ 172.8, 153.7, 136.5, 127.7 (2C), 127.0, 126.7 (2C), 67.8, 65.6, 57.4, 54.2, 38.0; IR (neat film): 3407, 2951, 1684, 1499, 1430, 1359, 1211, 1173, 1127, 1081, 992, 965 cm^{-1}; $[\alpha]_D$ -70.2° (*c* 6.2, CH_2Cl_2); EI-MS *m/z* (relative intensity) 265 (1.7%), 221 (0.9%), 176 (21%), 130 (36%), 108 (16%), 91 (100%); HRMS-EI calcd for $C_{13}H_{15}NO_5$ ($M^{\bullet+}$) 265.0950, found 265.0959.

(2*S*)-4-Oxopyrrolidine-1,2-dicarboxylic acid 1-benzyl ester (10)

An 8 M solution of Jones reagent was prepared as described elsewhere.[88] Compound **9** (39.0 g, 147 mmol) was dissolved in reagent grade acetone (3 L) and transferred into a 5 L round bottom flask. A Teflon paddle was submersed into the solution and attached to a mechanical stirring apparatus. The Jones reagent (158 mL, 1265 mmol) was added dropwise to the stirred acetone solution from a graduated cylinder through a Teflon canula over ~ 20 minutes. As the reagent was added to the reaction mixture, the color of the reaction mixture changed from clear to bright red, and finally to dark brown. Following the addition, the reaction mixture was stirred for an additional 2 hours. Methanol (119 mL, 2942 mmol) was then added dropwise to the reaction mixture with vigorous stirring in order to consume the residual Jones reagent; the color of the solution changed from dark brown to light green, and a large amount of fine, green precipitate was evolved. The entire mixture was filtered through paper to remove the precipitated chromium salts, and then concentrated by rotary evaporation to an oil (a clear oil with a suspension of green droplets). This oil was dissolved in 1 L of EtOAc, transferred to a 2 L separatory funnel, and washed with water (5 × 100 mL); the combined aqueous layers were then backwashed with EtOAc (1 × 200 mL). The EtOAc layers were combined, washed with saturated brine, dried over Na_2SO_4, and concentrated by rotary evaporation. Residual solvent was removed overnight under reduced pressure yielding **10** (38.2 g, 145 mmol, 98%) as slightly yellow foam, used without further purification. ^{1}H NMR (300 MHz, 75 °C, DMSO-d_6): δ 13.2 – 13.8 (br s, 1H), 7.56 – 7.51 (m, 5H), 5.35 (s, 2H), 4.95 (dd, *J* = 10.4, 2.8 Hz, 1H), 4.14 (d, *J* = 18.2 Hz, 1H), 3.98 (d, *J* = 18.2 Hz, 1H), 3.29 (ddd, *J* = 18.7, 10.4, 0.9 Hz, 1H), 2.72 (dd, *J* = 18.5, 2.8 Hz, 1H); ^{13}C NMR (75.4 MHz, 75 °C, DMSO-d_6): δ 207.5, 172.4, 153.9, 136.3, 128.0 (2C), 127.5, 127.1 (2C), 66.4, 56.0, 52.1, 41.2; IR (neat film): 3035, 2627, 1765, 1709, 1587, 1431, 1360, 1263, 1195, 1163, 1028, 957, 874, 769, 752, 698 cm^{-1}; EI-MS *m/z* (relative

intensity) 263 (1.2%), 218 (1.4%), 174 (2.4%), 128 (31%), 108 (23%), 91 (100%); HRMS-EI calcd for $C_{13}H_{13}NO_5$ ($M^{\bullet+}$) 263.0794, found 263.0783.

(2*S*)-4-Oxopyrrolidine-1,2-dicarboxylic acid 1-benzyl ester 2-*tert*-butyl ester (11)

Compound **10** (38.9 g, 148 mmol) was transferred to a heavy-walled 1000 mL round bottom flask containing a magnetic stir bar and dissolved in dichloromethane (295 mL). The flask was submersed in an ice bath, concentrated sulfuric acid (1.5 mL) was added to the mixture, and the solution was stirred gently. Isobutylene gas was bubbled into the reaction mixture until the volume of the solution had increased by about 50%. The flask was sealed with a rubber septum secured by a plastic strap and placed behind a blast shield. The reaction mixture was stirred overnight, slowly warming to room temperature. The following day, the septum was pieced by a needle in order to release accumulated pressure. When the bubbling of the solution subsided, the septum was removed and solid $NaHCO_3$ was added in order to neutralize residual sulfuric acid. This suspension was filtered through paper and concentrated by rotary evaporation. The resulting oil was dissolved in EtOAc (1 L) and transferred to a 2 L separatory funnel, wherein it was washed with water (2 × 200 mL); the combined aqueous washes were backwashed with EtOAc (1 × 100 mL). The organic layers were combined, dried over Na_2SO_4, filtered, then concentrated by rotary evaporation. Residual solvent was removed under reduced pressure affording **11** (39.8 g, 124 mmol, 82%) as a yellow oil that was used without further purification. An analytical sample was prepared by silica column chromatography (3:7 EtOAc/hexanes, R_f = 0.27). ^{1}H NMR (300 MHz, 75 °C, DMSO-d_6): δ 7.42 – 7.38 (m, 5H), 5.22 (s, 2H), 4.72 (dd, J = 10.3, 2.5 Hz, 1H), 3.99 (d, J = 18.1 Hz, 1H), 3.81 (d, J = 18.1 Hz, 1H), 3.17 (dd, J = 18.5, 10.3 Hz, 1H), 2.52 (dd, J = 18.5, 2.2 Hz, 1H), 1.44 (s, 9H); ^{13}C NMR (75.4 MHz, 75 °C, DMSO-d_6): δ 207.9, 171.0, 154.6, 137.1, 128.8, 128.3, 128.0, 82.3, 67.2, 57.5, 52.9, 40.8, 28.0; IR (neat film): 3065, 3034, 2979, 2934, 1767, 1716, 1499, 1455, 1415, 1368, 1298, 1259, 1233, 1211, 1152, 1115, 1027, 968, 913, 834, 769, 699 cm^{-1}; EI-MS *m/z* (relative intensity) 319 (0.28%), 263 (12%), 218 (11%), 174 (10%), 128 (7.0%), 91 (100%); HRMS-EI calcd for $C_{17}H_{21}NO_5$ ($M^{\bullet+}$) 319.1420, found 319.1412.

(5*S*,8*S*)-2,4-Dioxo-1,3,7-triaza-spiro[4.4]nonane-7,8-dicarboxylic acid 7-benzyl ester 8-*tert*-butyl ester (12)

(5*S*,8*R*)-2,4-Dioxo-1,3,7-triaza-spiro[4.4]nonane-7,8-dicarboxylic acid 7-benzyl ester 8-*tert*-butyl ester (13)

A solution of **11** (42.3 g, 132.5 mmol) in DMF (330 mL) was transferred to a pressure vessel containing a magnetic stir bar. Potassium cyanide (12.9 g, 198 mmol, 1.5 equivalents) was carefully transferred into an Erlenmeyer flask in a fume hood. Ammonium carbonate (63.7 g, 663 mmol, 5 equivalents) was then measured into the same Erlenmeyer flask. The salts were transferred into the pressure vessel with deionized water (330 mL), and then the vessel was sealed and immersed in a 60 °C oil bath behind a blast shield. The reaction mixture was stirred vigorously for 6 hours. The flask was removed from the oil bath, allowed to cool, and cautiously opened behind the blast shield. The solution was transferred from the pressure vessel into a 2 L Erlenmeyer flask containing a large magnetic stir bar, and acidified with efficient stirring to pH 6 with 1 M aqueous HCl (this must be done in an efficient fume hood because the excess KCN generates HCN gas); as a result of the acidification, amorphous crude **12** and **13** crash out of the aqueous solution. A portion of EtOAc (~ 250 mL) was added to the stirred solution in the Erlenmeyer flask, causing the insoluble products to dissolve in the organic phase. The entire biphasic mixture was transferred to a 2 L separatory funnel. The EtOAc layer was set aside, and the aqueous solution was extracted with EtOAc (5 × 200 mL). The combined organic layers were washed with brine, dried over Na_2SO_4, and concentrated by rotary evaporation to a yellow oil containing a crude mixture of **12** and **13** in a ratio of 5:1. The crude products were dissolved in dichloromethane, concentrated by rotary evaporation onto Celite, and then purified by chromatography on silica (gradient elution from CH_2Cl_2 to 95:5 CH_2Cl_2/MeOH). Each fraction was tested by TLC. The developed TLC plates were briefly immersed in the bromophenol blue solution and then heated, causing the hydantoin spots to stain bright yellow against a dark blue background. Similar fractions were combined, concentrated by rotary evaporation, and placed under reduced pressure affording **12** (33.1 g, 85.1 mmol, 64% recovered yield from **11**) and **13** (4.0 g, 10 mmol, 7.8% recovered yield from **11**), both as off-white foams. The overall recovered yield of hydantoin from **11** was 72%, and the ratio of **12** to **13** based upon purified, recovered material was 8:1.

Less polar **12**:

^{1}H NMR (300 MHz, 25 °C, DMSO-d_6): δ 10.82 (s, 1H), 7.89 (s, 1H), 7.34 – 7.29 (m, 5H), 5.09 – 5.04 (m, 2H), 4.33 – 4.23 (m, 1H), 3.89 – 3.82 (m, 1H), 3.43 – 3.36 (m, 1H), 2.70 – 2.63 (m, 1H), 2.06 – 1.97 (m, 1H), 1.39 and 1.30 (s, rotameric, 9H); ^{1}H NMR (300 MHz, 75 °C, DMSO-d_6): δ 7.32 (m, 5H), 5.10 (s, 2H), 4.36 (dd, J = 8.2, 7.4 Hz, 1H), 3.84 (d, J = 11.2 Hz, 1H), 3.50 (d, J = 11.9 Hz, 1H), 2.63 (dd, J = 13.3, 8.6 Hz, 1H), 2.11 (dd, J = 13.3, 7.2 Hz, 1H), 1.40 (s, 9H); ^{13}C NMR (75.4 MHz, DMSO-d_6): mixture of rotamers δ 176.7, 170.8 and 170.4, 156.0, 153.6 and 153.3, 136.6 and 136.3, 128.4 and 128.2, 127.8 and 127.7, 127.3, 81.4 and 81.2, 66.5 and 66.3, 64.5 and 63.8, 58.7 and 58.2, 52.3 and 51.8, 37.9 and 37.0, 27.5 and 27.4; IR (neat film): 3247, 2067, 2979, 2751, 1782, 1720, 1587, 1537, 1499, 1417, 1355, 1293, 1232, 1155, 1114, 1084, 1050, 1013, 971, 833, 768, 738, 698, 641 cm^{-1}; $[\alpha]_D$ -11.7° (*c* 8.0, $CHCl_3$); EI-MS m/z (relative intensity) 333 (3.8%), 288 (2.8%), 276 (0.7%), 244 (0.6%), 108 (17%), 91 (100%), 84 (29%), 65 (7.7%), 57 (26.5%); HRMS-EI calcd for $C_{15}H_{15}N_3O_6$ ($M^{\bullet+}$ - *t*-Bu + H) 333.0961, found 333.0963.

More polar **13**:

^{1}H NMR (300 MHz, 25 °C, DMSO-d_6): δ 10.93 (s, 1H), 8.62 (s, 1H), 7.35 – 7.31 (m, 5H), 5.09 – 4.99 (m, 2H), 4.36 – 4.32 (m, 1H), 3.78 – 3.69 (m, 1H), 3.55 – 3.40 (m, 1H), 2.57 – 2.37 (m, 1H), 2.20 – 2.12 (m, 1H), 1.37 and 1.29 (s, rotameric, 9H); ^{1}H NMR (300 MHz, 75 °C, DMSO-d_6): δ 7.34 (m, 5H), 5.08 (s, 2H), 4.42 (apparent t, J = 8.3 Hz, 1H), 3.72 (dd, J = 11.2, 1.6 Hz, 1H), 3.61 (d, J = 11.2 Hz, 1H), 2.43 (ddd, J = 13.4, 8.1, 1.5 Hz, 1H), 2.30 (dd, J = 13.4, 8.5 Hz, 1H), 1.39 (s, 9H); ^{13}C NMR (75.4 MHz, DMSO-d_6): mixture of rotamers δ 174.1 and 174.0, 170.5 and 170.1, 156.2 and 156.1, 153.6 and 153.5, 136.7 and 136.4, 128.4 and 128.3 (CH), 127.9 (CH), 127.55 and 127.48 (CH), 81.3 and 81.1, 66.7 and 66.0, 66.5 and 66.3 (CH_2), 59.0 and 58.4 (CH), 56.1 and 55.6 (CH_2), 40.4 and 39.4 (CH_2), 27.6 and 27.4 (CH_3); IR (neat film): 3253, 3067, 2979, 2750, 1779, 1735, 1499, 1420, 1357, 1312, 1232, 1191, 1158, 1139, 1060, 1016, 975, 836, 736, 698 cm^{-1}; $[\alpha]_D$ -18.9° (*c* 2.7, $CHCl_3$); EI-MS *m/z* (relative intensity) 346 (0.3%), 333 (0.8%), 244 (8.0%), 154 (8.0%), 91 (100%), 65 (15.0%), 57 (35.0%); HRMS-EI calcd for $C_{18}H_{22}N_2O_5$ ($M^{\bullet+}$ – CONH) 346.1529, found 346.1519.

(5*S*,8*S*)-2,4-Dioxo-1,3,7-triazaspiro[4.4]nonane-1,3,7,8-tetracarboxylic acid 7-benzyl ester 1,3,8-tri-*tert*-butyl ester (14)

Hydantoin **12** (24.8 g, 63.7 mmol) was transferred into a 2 L round bottom flask containing a magnetic stir bar. THF (1309 mL) was added to the flask followed by DMAP (299 mg, 2.44 mmol). The flask was sealed with a septum; a nitrogen inlet line was inserted into the septum and the flask was flushed with nitrogen, then immersed in an ice bath. Boc_2O (32.0 g, 147 mmol) was added as a solid in one portion to the cold reaction mixture. The solution was stirred under nitrogen while warming to room temperature. The reaction was complete after 30 minutes, as determined by TLC (1:2 EtOAc/hexanes, DMAP R_f = 0.0, **12** R_f = 0.08, **14** R_f = 0.41, Boc_2O R_f = 0.67). The reaction mixture was concentrated by rotary evaporation and filtered through silica using 1:1 EtOAc/hexanes in order to remove DMAP. The filtrate was concentrated to an oil and used immediately in the next reaction without further purification. An analytical sample of **14** was prepared by silica column chromatography (1:2 EtOAc/hexanes). ^{1}H NMR (300 MHz, DMSO-d_6) mixture of rotamers δ 7.34 (m, 5H), 5.10 (m, 2H), 4.35 (m, 1H), 4.04 (apparent dd, J = 11.5, 4.1 Hz, 1H), 3.81 (apparent dd, J = 11.5, 8.7 Hz, 1H), 2.76 (m, 1H), 2.64 (m, 1H), 1.54 – 1.25 (m, 27H); ^{13}C NMR (75.4 MHz, DMSO-d_6) mixture of rotamers δ 169.9, 169.6, 169.5, 153.7, 153.4, 147.5, 146.6, 146.5, 144.8, 136.5, 136.4, 128.4, 128.3, 127.8, 127.44, 127.36, 85.5, 85.3, 84.2, 81.2, 81.0, 66.4, 65.8, 65.1, 58.5, 58.0, 50.2, 49.6, 35.4, 34.4, 27.6, 27.3, 26.8; IR (neat film): 2981, 2937, 1830, 1784, 1751, 1717, 1498, 1475, 1456, 1395, 1419, 1370, 1356, 1255, 1213, 1145, 1071, 1029, 1003, 950, 843, 773, 698 cm^{-1}; $[\alpha]_D$ -7.0° (*c* 1.0, $CHCl_3$); EI-MS *m/z* (relative intensity) 433 (0.3%), 388 (0.8%), 368 (0.3%), 360 (0.2%), 333 (7.8%), 288 (13.2%), 244 (23.5%), 198 (10.5%), 154 (10.8%), 107 (10.5%), 91 (100%), 69 (11%), 65 (20%); HRMS-EI calcd for $C_{15}H_{15}N_3O_6$ (M – *t*-Bu – 2 $COOC(CH_3)_3$ + H) 333.0961, found 333.0962.

(2*S*,4*S*)-4-Aminopyrrolidine-1,2,4-tricarboxylic acid 1-benzyl ester 2-*tert*-butyl ester (15)

Crude **14** (37.5 g, 63.7 mmole, assuming quantitative conversion of **12** to **14**) was transferred into a 1 L round bottom flask containing a magnetic stir bar and dissolved in THF (254 mL). A 2.0 M aqueous solution of potassium hydroxide (254 mL) was then added to the flask. The reaction mixture was stirred vigorously for 30 minutes. The solution and a portion of Et_2O (250 mL) were transferred into a 1 L separatory funnel and agitated; the aqueous and organic layers

were then allowed to separate completely. The aqueous layer was removed and poured into large beaker which was immediately submerged into an ice bath. The organic layer was washed with water (1 × 100 mL); the water wash was added to the aqueous solution in the beaker. With mechanical stirring, the solution was acidified to pH 6.5 by slow addition of 2.0 M aqueous HCl, resulting in the precipitation of a fine, white solid. We continued to stir the cold, aqueous slurry for another hour; during this time, the pH of the slurry tended to rise, and HCl solution was added to maintain the pH at 6.5. The slurry was filtered through a fine-fritted sintered glass funnel, and the precipitate was washed with ice cold water. Hot water (~ 70 mL) was added to the solid in a 500 mL Erlenmeyer flask containing a large magnetic stir bar; this was just enough water to barely cover the precipitate, and generated a wet slurry. The stirred suspension was brought to near boiling on a hot plate, and hot ethanol was added in small portions until the solid had dissolved. The hot solution was filtered through paper into a clean flask and allowed to cool to room temperature; the flask was covered and placed in the 4 °C refrigerator overnight. The crystalline material that formed was filtered and then dried at 50 °C in a vacuum oven affording **15** (14.4 g, 39.5 mmol, 62% from **12**) as white crystals. ^{1}H NMR (300 MHz, 25 °C, CD_3OD): δ 7.20 (m, 5H), 5.01 – 4.95 (m, 2H), 4.37 – 4.32 (m, 1H), 3.89 (d, J = 11.6 Hz, 1H), 3.63 (d, J = 11.7 Hz, 1H), 2.84 – 2.73 (m, 1H), 2.06 – 2.00 (m, 1H), 1.35 and 1.18 (s, rotameric, 9H); ^{13}C NMR (75.4 MHz, 25 °C, CD_3OD): mixture of rotamers δ 174.8, 173.2, 156.0 and 155.8, 137.7 and 137.4, 129.5 (CH), 129.2 (CH), 129.1 (CH), 84.2, 68.8 and 68.6 (CH_2), 65.4 and 64.5, 61.1 and 60.6 (CH), 56.0 and 55.6 (CH_2), 39.8 and 38.8 (CH_2), 28.1 and 28.0 (CH_3); IR (neat film): 3416, 2978, 1712, 1643, 1499, 1421, 1393, 1354, 1296, 1232, 1153, 976, 851, 829, 768, 733, 697 cm^{-1}; $[\alpha]_D$ -23.5° (*c* 3.0, methanol); EI-MS *m/z* (relative intensity) 308 (8.0%), 263 (8.0%), 217 (23.5%), 173 (7.9%), 155 (9.5%), 127 (9.0%), 100 (8.8%), 91 (100%), 65 (17.5%); HRMS-EI calcd for $C_{14}H_{16}N_2O_6$ (M – *t*-Bu + H) 308.1008, found 308.1004.

(2*S*,4*S*)-4-(9*H*-Fluoren-9-ylmethoxycarbonylamino)-pyrrolidine-1,2,4-tricarboxylic acid 1-benzyl ester 2-*tert*-butyl ester (16)

Finely divided **15** (13.2 g, 36.3 mmol) was transferred to a three-neck round bottom flask containing a stir bar. The flask was evacuated on a vacuum line and backfilled with nitrogen three times. Dichloromethane (727 mL) was then added to the flask. The flask was fitted with a reflux condenser equipped with a nitrogen inlet adapter, a rubber septum with a needle (allowing

nitrogen to flow freely through and out of the flask), and a glass stopper. Distilled DIPEA (15.8 mL, 90.8 mmol) was added by syringe through the septum to the stirred solution, followed by TMS-Cl (9.3 mL, 73.0 mmol). After flushing the flask briefly with nitrogen, the septum was removed and replaced with a glass stopper, and the solution was refluxed for 1.5 hours. The flask was then immersed in an ice bath, and Fmoc-Cl (8.9 g, 34.5 mmol) was added to the reaction mixture. The solution was stirred for 5 hours while warming to room temperature, and then concentrated by rotary evaporation. The resulting oil was dissolved in EtOAc (1 L), transferred to a 2 L separatory funnel, then washed with 1 M aqueous HCl (1 × 200 mL), and with brine (2 × 200 mL). The organic layer was dried over $MgSO_4$, filtered, and concentrated by rotary evaporation; residual solvent was removed under reduced pressure affording crude **16** as a white foam that was used in the next reaction without further purification. An analytical sample was prepared by chromatography on silica (gradient elution from $CHCl_3$ with 0.1% AcOH to 90:10 $CHCl_3$/MeOH with 0.1% AcOH). ^{1}H NMR (300 MHz, 75 °C, DMSO-d_6) δ 12.12 (br s, 1H), 7.84 (d, *J* = 7.1 Hz, 2H), 7.74 (br s, Fmoc-N*H*, 1H), 7.69 (d, *J* = 7.2 Hz, 2H), 7.42 – 7.29 (m, 9H), 5.10 (s, 2H), 4.39 – 4.20 (br m, 4H), 4.06 (d, *J* = 11.3 Hz, 1H), 3.68 (d, *J* = 11.3 Hz, 1H), 2.87 (br m, 1H), 2.36 (dd, *J* = 13.1, 5.14 Hz, 1H), 1.31 (s, 9H); ^{13}C NMR (75.4 MHz, DMSO-d_6): mixture of rotamers δ 172.6, 169.9, 155.4, 153.3, 143.4, 140.5, 136.4, 127.9 (CH), 127.4 (CH), 127.3 (CH), 127.0 (CH), 126.7 (CH), 124.8 (CH), 119.6 (CH), 80.6, 65.9 (CH_2), 65.5 (CH_2), 62.4 and 61.8, 58.5 (CH), 54.7 and 54.6 (CH_2), 46.5 (CH), 39.4 and 38.3 (CH_2), 28.0 (CH_3); IR (neat film): 3319, 3066, 2978, 1721, 1531, 1450, 1423, 1357, 1259, 1157, 1118, 1087, 1044, 957, 911, 841, 760, 739, 698, 648 cm^{-1}; $[\alpha]_D$ 3.6° (*c* 9.9, $CHCl_3$); ESI-MS *m/*z (ion): 586.2 (M^+), 609.2 ($M + Na^+$), 625.2 ($M + K^+$).

(2*S*,4*S*)-4-(9*H*-Fluoren-9-ylmethoxycarbonylamino)-pyrrolidine-1,2,4-tricarboxylic acid 1-benzyl ester 2-*tert*-butyl ester 4-methyl ester (17)

Unpurified **16** (20.5 g, 35.0 mmol, assuming quantitative conversion of **15** to **16**) was transferred to a 500 mL round bottom flask containing a stir bar. Anhydrous Et_2O (208 mL) was added to the flask, followed by anhydrous methanol (142 mL). The flask was fitted with a pressure-equalizing dropping funnel that was charged with a 2 M solution of TMS-CHN_2 in Et_2O. The dropping funnel was capped with a rubber septum containing two needles: one for a nitrogen line, and another for pressure release. The TMS-CHN_2 solution was added very slowly to the

stirred solution of **16** causing the reaction mixture to bubble gently. When the reaction mixture had developed a persistent yellow color (after addition of approximately 30 mL of the TMS-CHN_2 solution), TLC analysis revealed complete consumption of the starting material (1:1 EtOAc/hexanes, **16** R_f = 0.05, **17** R_f = 0.49). Residual TMS-CHN_2 was quenched by extremely slow addition of a 9:1 MeOH/AcOH solution. The reaction mixture was concentrated by rotary evaporation and purified by chromatography on silica (gradient elution from hexanes to 1:1 EtOAc/hexanes). Fractions containing the desired product were pooled and concentrated, then residual solvent was removed under reduced pressure affording **17** (19.5 g, 32.5 mmol, 92% from **15**) as a white foam. ^{1}H NMR (300 MHz, 75 °C, DMSO-d_6): δ 7.83 (d, J = 7.5 Hz, 2H), 7.66 (d, J = 7.5 Hz, 2H), 7.59 (br s, Fmoc-N*H*, 1H), 7.42 – 7.31 (m, 9H), 5.09 (s, 2H), 4.43 – 4.18 (m, 4H), 4.01 (d, J = 11.4 Hz, 1H), 3.61 (s, 3H), 3.59 (d, overlap with –CO_2CH_3, 1H), 2.80 (dd, J = 13.6, 8.9 Hz, 1H), 2.27 (dd, J = 13.6, 5.9 Hz, 1H), 1.37 (s, 9H); ^{13}C NMR (75.4 MHz, DMSO-d_6): δ 171.7, 170.2 and 169.9, 155.7, 153.5 and 153.3, 143.6, 140.7, 136.6 and 136.4, 128.3 (CH), 128.2 (CH), 127.6 (CH), 127.5 (CH), 127.3 (CH), 127.0 (CH), 125.2 (CH), 125.1 (CH), 120.0 (CH), 81.0, 66.2 (CH_2), 65.6 (CH_2), 63.0 and 62.1, 58.3 and 58.0 (CH), 54.7 and 54.3 (CH_2), 52.7 (CH_3), 46.5 (CH), 38.4 and 37.3 (CH_2), 27.3 (CH_3); IR (neat film): 2932, 2852, 1743, 1716, 1653, 1557, 1540, 1450, 1418, 1356, 1297, 1249, 1157, 1108, 1084, 1049, 976, 750, 741, 698 cm^{-1}; $[\alpha]_D$ 4.3° (*c* 4.4, $CHCl_3$); EI-MS *m/z* (relative intensity) 600 (0.1%), 499 (0.5%), 455 (1.05), 409 (0.1%), 393 (0.2%), 361 (0.2%), 322 (5.3%), 303 (3.0%), 277 (4.0%), 259 (6.6%), 233 (8.2%), 216 (14.5%), 196 (6.0%), 178 (77.0%), 165 (24.0%), 126 (7.5%), 91 (100%); ESI-MS m/z (ion): 623.2 (M + Na^+), 639.2 (M + K^+); HRMS-EI calcd for $C_{34}H_{36}N_2O_8$ ($M^{\bullet+}$) 600.2472, found 600.2523.

(2*S*,4*S*)-4-(9*H*-Fluoren-9-yloxycarbonylamino)-pyrrolidine-1,2,4-tricarboxylic acid 1-benzyl ester 4-methyl ester (18)

A solution of **17** (2.25 g, 3.75 mmol) in dichloromethane (1.0 mL) was added to a 100 mL round bottom flask equipped with a stir bar. TFA (~25 mL) was added to the reaction flask, and the solution was stirred for 1 hour. The mixture was concentrated, and residual TFA was removed by dissolving the residue in toluene, then re-concentrating the solution using the rotary evaporator at 50 °C 2 times. The resulting yellow oil was dissolved in EtOAc (50 mL), transferred to a separatory funnel, and was washed with 2.5% aqueous $NaHCO_3$ (25 mL), dilute aqueous HCl,

pH ~2 (25 mL), and brine (2 x 50 mL). The EtOAc layer was dried over Na_2SO_4, the solution was concentrated, and residual solvent was removed under reduced pressure yielding **18** (1.8 g, 3.4 mmol, 90%) as a foamy white solid, used without further purification. ^{1}H NMR (300 MHz, 75 °C, DMSO-d_6): δ 7.83 (d, J = 7.3 Hz, 2H), 7.66 (d, J = 7.5 Hz, 2H), 7.62 (s, Fmoc-N*H,* 1H), 7.39 – 7.29 (m, 9H), 5.11 (s, 2H), 4.39 – 4.35 (m, 3H), 4.21 (t, J = 6.5 Hz, 1H), 4.10 (d, J = 11.5 Hz, 1H), 3.61 (s, 3H), 3.59 (d, overlap with -CO_2CH_3, 1H), 2.84 (dd, J = 13.6, 8.9 Hz, 1H), 2.29 (dd, J = 13.6, 6.4 Hz, 1H); ^{13}C NMR (75.4 MHz, DMSO-d_6): mixture of rotamers δ 172.1, 171.8, 155.4, 153.4, 143.5 and 143.4, 140.5, 139.2, 136.5, 128.0 (CH), 127.4 (CH), 127.3 (CH), 126.9 (CH), 126.7 (CH), 124.3 (CH), 119.7 (CH), 66.0 (CH_2), 65.6 (CH_2), 62.6 and 61.9, 57.6 (CH), 54.7 (CH_2), 52.3 (CH_3), 46.5 (CH), 38.3 and 37.3 (CH_2); IR (neat film): 3314, 3037, 2952, 1710, 1529, 1450, 1422, 1356, 1297, 1250, 1215, 1109, 1085, 1051, 973, 769, 741, 697 cm^{-1}; $[\alpha]_D$ -31.6° (*c* 9.7, $CHCl_3$); EI-MS *m/z* (relative intensity) 544 (0.4%), 439 (0.6%), 365 (0.5%), 259 (1.3%), 231 (3.5%), 217 (2.1%), 178 (100%), 165 (22.3%), 152 (5.0%), 126 (14.5%), 114 (6.7%), 91 (57.4%); HRMS-EI calcd for $C_{30}H_{28}N_2O_8$ ($M^{\bullet+}$) 544.1846, found 544.1833.

(2*S*,4*S*)-4-(9*H*-Fluoren-9-ylmethoxycarbonylamino)-pyrrolidine-1,2,4-tricarboxylic acid 1-*tert*-butyl ester 4-methyl ester (19)

Compound **17** (6.30 g, 11.5 mmol) was transferred to a 500 mL round bottom flask containing a magnetic stir bar, then dissolved in 1:1 CH_2Cl_2/TFA (210 mL). The reaction mixture was stirred at room temperature and monitored by TLC (5:1 $CHCl_3$/MeOH, **17** R_f = 0.7, **18** R_f = 0.4). When all of the starting material was consumed (approximately 4 h), the solution was concentrated by rotary evaporation. Residual solvent was removed under reduced pressure overnight. Pd/C (10 wt. %, 1.1 g), THF (300 mL), and Boc_2O (7.2 mL, 32 mmol) were added to the flask, and the solution was degassed under reduced pressure, then back-filled with H_2 gas. The reaction mixture was stirred overnight under a H_2 atmosphere (~ 1 atm). The reaction mixture was filtered, and the filtrate was concentrated by rotary evaporation to an oil, which was purified by chromatography on silica (gradient elution over 10 column volumes from $CHCl_3$ to 10% MeOH/$CHCl_3$). Fractions containing the desired product were concentrated, and residual solvent was removed under reduced pressure giving **19** (4.5 g, 8.8 mmol, 83% from **17**) as a white foam. ^{1}H NMR (300 MHz, DMSO-d_6): mixture of rotamers δ 8.32 (s, Fmoc–N*H*, 1H), 7.93 (d, J = 7.4 Hz, 2H), 7.75 (d, J = 7.1 Hz, 2H), 7.48 – 7.35 (m, 4H), 4.29 – 3.94 (m, 5H), 3.58 (s, 3H), 3.41 –

3.32 (m, 1H), 2.76 – 2.59 (m, 1H), 2.18 – 2.08 (m, 1H), 1.39 and 1.34 (s, 9H, rotameric); ^{13}C NMR (75.4 MHz, DMSO-d_6): mixture of rotamers δ 174.9, 172.4, 155.6, 153.4 and 153.3, 143.6 and 143.5, 140.6, 127.5 (CH), 127.0 (CH), 125.1 (CH), 120.0 (CH), 78.7 and 78.5, 65.6 (CH_2), 62.6 and 61.9, 59.1 and 58.9 (CH), 55.0 and 54.5 (CH_2), 52.3 (CH_3), 46.5 (CH), 39.3 and 38.4 (CH_2), 28.0 and 27.9 (CH_3, 3C); IR (neat film): 3307, 3016, 2979, 1744, 1529, 1477, 1450, 1408, 1369, 1254, 1156, 1088, 1050, 972, 913, 858, 759, 667 cm^{-1}; $[\alpha]_D$ -61.8° (*c* 1.42, $CHCl_3$); ESI-MS *m/z* (relative intensity): 533.2 (100%, M + Na^+), 477.1 (35%), 433.1 (90%), 411.2 (20%); HRESIQTOFMS calcd for $C_{27}H_{30}N_2NaO_8$ (M + Na^+) 533.1900, found 533.1887.

(2*R*,4*R*)-4-Hydroxypyrrolidine-1,2-dicarboxylic acid 1-benzyl ester (20)

Commercially available *trans*-4-hydroxy-L-proline (**2**) was converted in modest yield to *cis*-4-hydroxy-D-proline (**31**) using a method described elsewhere.[115] *cis*-4-Hydroxy-D-proline (**31**, 9.50 g, 72.4 mmol) and a magnetic stir bar were added to a 250 mL three neck round bottom flask fitted with a reflux condenser, rubber septum and nitrogen inlet adapter. The flask was flushed with nitrogen, and then the amino acid was suspended in CH_2Cl_2 (155 mL). DIPEA (36.8 mL, 212 mmol) was added to the suspension followed by TMS-Cl (27.7 mL, 217 mmol), which was added slowly via syringe through the rubber septum. The reaction mixture was heated to reflux and stirred vigorously for 1.5 hours. The resulting red-orange solution was cooled to 0 °C using an ice bath. Cbz-Cl (9.8 mL, 69 mmol) was added to the solution in one portion while nitrogen was flushed through the flask. The solution was allowed to warm to room temperature overnight with stirring, and was then concentrated by rotary evaporation. The resulting paste was dissolved in 2.5% aqueous $NaHCO_3$ (700 mL) and diethyl ether (600 mL) and transferred to a 2000 mL separatory funnel. The aqueous layer was separated and washed with ether (2 × 150 mL). The ether layers were combined and backwashed with water (2 × 60 mL). All of the aqueous layers were combined and acidified to pH 2 with 1 M aqueous HCl. The aqueous solution was transferred to another separatory funnel, and the product was extracted with ethyl acetate (3 × 250 mL). The ethyl acetate layers were combined, dried over Na_2SO_4, and filtered. The solvent was removed by rotary evaporation and then under reduced pressure overnight yielding the desired product **20** (17.8 g, 67.5 mmol, 97.6%) as a straw-colored foam used without further purification. ^{1}H NMR (300 MHz, 75 °C, DMSO-d_6): δ 7.29 – 7.35 (m, 5H), 5.07 (s, 2H), 4.24 – 4.30 (m, 2H), 3.63 (dd, *J* = 10.8, 5.7 Hz, 1H), 3.24 (dd, *J* = 10.8, 3.9 Hz, 1H), 2.38 (ddd, *J*

= 13.7, 9.1, 5.7 Hz, 1H), 1.92 (m, 1H); ^{13}C NMR (75.4 MHz, DMSO-d_6): mixture of rotamers δ 173.4 and 173.1, 154.1 and 153.9, 137.0, 128.4 and 128.3 (2C), 127.8 and 127.6, 127.5 and 127.1 (2C), 68.6 and 67.7, 65.9, 57.7 and 57.3, 54.6 and 54.1, 37.7; IR (neat film): 3419, 2953, 1685, 1498, 1428, 1358, 1210, 1123, 1084, 1003, 969 cm^{-1}; $[\alpha]_D$ 28.1° (*c* 9.71, $CHCl_3$); EI-MS m/z (relative intensity) 265 (20%), 220 (83%), 176 (34%), 130 (35%), 108 (5.5%), 91 (100%); HRMS-EI calcd for $C_{13}H_{15}NO_5$ ($M^{\bullet+}$) 265.0950, found 265.0954.

(*R*)-4-Oxopyrrolidine-1,2-dicarboxylic acid 1-benzyl ester (21)

An 8 molar solution of Jones reagent was prepared as described elsewhere. Compound **20** (17.8 g, 67.1 mmol) was dissolved in acetone (1350 mL) and transferred to a 2 L Erlenmeyer flask. The solution was mixed with an overhead mechanical stirrer while adding the Jones reagent (72.2 mL, 577 mmol) slowly (over approximately 10 minutes). As the reaction mixture was stirred, the color of the solution changed from bright red to dark brown. This solution was stirred for an additional 3 hours, and then the excess oxidant was consumed by slow addition of MeOH (~ 50 mL). The solution was filtered through a Celite packed chromatography column in order to remove precipitated chromium salts, concentrated by rotary evaporation, and diluted with EtOAc (1000 mL). The resulting solution was transferred to a 2 L separatory funnel, washed with brine (6 × 250 mL), dried over Na_2SO_4, filtered, and concentrated by rotary evaporation. Residual solvent was evaporated under reduced pressure, yielding the product **21** (15.7 g, 59.9 mmol, 89.3%) as a pale yellow oil, which was used without further purification. ^{1}H NMR (300 MHz, 75 °C, DMSO-d_6): δ 12.42 (br s, 1H), 7.13 – 7.05 (m, 5H), 4.90 (s, 2H), 4.47 (dd, *J* = 10.5, 2.4 Hz, 1H), 3.69 (d, *J* = 18.3 Hz, 1H), 3.52 (d, *J* = 18.3 Hz, 1H), 2.89 (dd, *J* = 18.6, 10.5 Hz, 1H), 2.28 (dd, *J* = 18.6, 2.4 Hz, 1H); ^{13}C NMR (75.4 MHz, 75 °C, DMSO-d_6): δ 207.6, 172.3, 153.7, 136.1, 127.9 (CH, 2C), 127.3 (CH), 126.9 (CH, 2C), 66.1 (CH_2), 55.7 (CH), 52.0 (CH_2), 40.3 (CH_2); IR (neat film): 3035, 1766, 1713, 1587, 1499, 1433, 1360, 1264, 1163, 1028, 959, 874, 699 cm^{-1}; EI-MS *m/z* (relative intensity) 263 (6.5%), 218 (9.5%), 174 (12%), 128 (58%), 108 (31%), 91 (100%); HRMS-EI calcd for $C_{13}H_{13}NO_5$ ($M^{\bullet+}$) 263.0794, found 263.0803.

(*R*)-4-Oxopyrrolidine-1,2-dicarboxylic acid 1-benzyl ester 2-*tert*-butyl ester (22)

A 500 mL round bottom flask containing a stir bar was charged with a solution of **21** (17.0 g, 64.6 mmol) in CH_2Cl_2 (130 mL). The solution was cooled to 0 °C using an ice bath, and concentrated sulfuric acid (645 μl) was added with stirring. Isobutylene was bubbled into the solution until the volume of the mixture had increased by ~ 50%. The flask was sealed with a rubber septum secured with a plastic strap, and the reaction mixture was stirred overnight while warming to room temperature. The septum was then carefully punctured, allowing the isobutylene to evaporate. The remaining solution was concentrated by rotary evaporation, and the resulting residue was distributed between EtOAc (500 mL) and 2.5% aqueous $NaHCO_3$ (125 mL). The EtOAc was washed with additional $NaHCO_3$ solution (2 × 125 mL), and the aqueous layers were combined and backwashed with EtOAc (250 mL). The combined organic layers were washed with brine, dried over Na_2SO_4, filtered, and concentrated by rotary evaporation. Residual solvent was evaporated under reduced pressure overnight, yielding the desired product **22** (17.2 g, 53.9 mmol, 83.4%) as a yellow oil that was used without further purification. An analytical sample was prepared by silica column chromatography (1:2 EtOAc/hexanes, R_f = 0.33). ^{1}H NMR (300 MHz, 75 °C, DMSO-d_6): δ 7.33 – 7.36 (m, 5H), 5.14 (s, 2H), 4.63 (d, J = 10.3 Hz, 1H), 3.93 (d, J = 18.1 Hz, 1H), 3.73 (d, J = 18.1 Hz, 1H), 3.13 (dd, J = 18.5, 10.3 Hz, 1H), 2.46 (d, J = 18.5 Hz, 1H), 1.35 (s, 9H); ^{13}C NMR (75.4 MHz, DMSO-d_6): mixture of rotamers δ 208.6, 208.0, 170.8, 170.6, 154.3, 153.7, 136.5, 136.3, 128.4, 128.3, 127.9, 127.5, 81.7, 81.6, 66.5, 56.8, 56.6, 52.6, 52.3, 40.8, 27.4, 27.3; IR (neat film): 3066, 3034, 2979, 2934, 1767, 1713, 1499, 1414, 1368, 1297, 1258, 1211, 1152, 1114, 1027, 967, 912, 836, 768, 699 cm^{-1}; EI-MS *m/z* (relative intensity) 263 (11%), 218 (27%), 174 (39%), 128 (53%), 91 (100%); HRMS-EI calcd for $C_{13}H_{13}NO_5$ ($M - C_4H_9^{\bullet} + H^+$) 263.0794, found 263.0789.

(5*R*,8*R*)-2,4-Dioxo-1,3,7-triaza-spiro[4.4]nonane-7,8-dicarboxylic acid 7-benzyl ester 8-*tert*-butyl ester (23)

(5*R*,8*S*)-2,4-Dioxo-1,3,7-triaza-spiro[4.4]nonane-7,8-dicarboxylic acid 7-benzyl ester 8-*tert*-butyl ester (24)

A 350 mL pressure vessel was charged with ammonium carbonate (10.3 g, 107.2 mmol), potassium cyanide (2.10 g, 32.2 mmol) deionized water (54 mL) and a magnetic stir bar. Compound **22** (6.9 g, 22 mmol) was dissolved in DMF (54 mL) and added to the pressure vessel.

After sealing the vessel, the flask was warmed to 60 °C in an oil bath and the solution stirred for 4 hours. The pressure vessel was then cooled to room temperature, opened cautiously, and the solution and stir bar were transferred to a 250 mL Erlenmeyer flask. The solution was adjusted to pH 6.5 by slow addition of 1M aqueous HCl, and diluted with EtOAc (200 mL) and water (~ 600 mL). The aqueous layer was removed and extracted with additional EtOAc (2 × 200 mL). The organic layers were combined, washed with brine (2 × 100 mL), dried over $MgSO_4$, and concentrated by rotary evaporation yielding a crude mixture of the products **23** and **24** in a ratio of 5:1 (determined by ^{1}H NMR by integration of the hydantoin amide proton). The crude mixture of products was purified by flash chromatography on silica (gradient elution from CH_2Cl_2 to 95:5 CH_2Cl_2/MeOH). Fractions containing the less polar diastereomer (determined by TLC, 95:5 CH_2Cl_2/MeOH, R_f = 0.21) were concentrated by rotary evaporation and then under reduced pressure overnight yielding **23 (**4.3 g, 11 mmol, 52% recovered yield). The fractions containing the more polar diastereomer (determined by TLC, 95:5 CH_2Cl_2/MeOH, R_f = 0.10) were similarly treated yielding **24** (1.0 g, 2.6 mmol, 12% recovered yield). The stereochemical assignment of **23** and **24** was based upon the 2D-NMR analysis of their respective enantiomers.[15]

Less polar **23**:

^{1}H NMR (300 MHz, 75 °C, DMSO-d_6): δ 10.64 (s, 1H), 7.64 (s, 1H), 7.34 (m, 5H), 5.10 (s, 2H), 4.35 (apparent t, J = 7.8 Hz, 1H), 3.86 (d, J = 11.1 Hz, 1H), 3.49 (d, J = 11.1 Hz, 1H), 2.65 (dd, J = 13.1, 8.3 Hz, 1H), 2.09 (dd, J = 13.1, 7.7 Hz, 1H), 1.38 (s, 9H); ^{13}C NMR (75.4 MHz, 75 °C, DMSO-d_6): δ 176.1, 170.3, 155.5, 153.2, 136.2, 127.9 (2C), 127.4, 127.0 (2C), 81.0, 66.1, 64.1, 58.4, 52.3, 37.6, 27.2 (3C); IR (neat film): 3242, 3068, 2979, 1783, 1724, 1499, 1417, 1356, 1293, 1233, 1156, 1113, 1014, 833, 767, 698 cm^{-1}; $[\alpha]_D$ +11.9° (*c* 3.9, $CHCl_3$); EI-MS *m/z* (relative intensity) 333 (13%), 288 (11%), 244 (16%), 198 (7.0%), 154 (9.5%), 91 (100%); HRMS-EI calcd for $C_{15}H_{15}N_3O_6$ ($M - C_4H_9^{\bullet} + H^+$) 333.0955, found 333.0967.

More polar **24**:

^{1}H NMR (300 MHz, 75 °C, DMSO-d_6): δ 10.68 (s, 1H), 8.40 (s, 1H), 7.36 (m, 5H), 5.10 (s, 2H), 4.40 (apparent t, J = 8.4 Hz, 1H), 3.75 (dd, J = 11.2, 1.7 Hz, 1H), 3.58 (d, J = 11.2 Hz, 1H), 2.44 (ddd, J = 13.2, 8.0, 1.7 Hz, 1H), 2.25 (dd, J = 13.2, 8.9, 1H), 1.37 (s, 9H); ^{13}C NMR (75.4 MHz,

DMSO-d_6): mixture of rotamers δ 173.9 and 173.8, 170.4 and 170.0, 156.0 and 155.9, 153.4 and 153.3, 136.5 and 136.3, 128.3 and 128.2 (CH), 127.8 (CH), 127.4 and 127.3 (CH), 81.2 and 81.0, 66.6 and 65.8, 66.4 and 66.2 (CH_2), 58.9 and 58.3 (CH), 55.9 and 55.5 (CH_2), 40.3 and 39.3 (CH_2), 27.5 and 27.3 (CH_3, 3C); IR (neat film) 3246, 2980, 1781, 1733, 1498, 1418, 1367, 1312, 1217, 1192, 1159, 1138, 1060, 1014, 977, 836, 755, 698 cm^{-1}; $[\alpha]_D$ +23.9° (*c* 2.5, $CHCl_3$); EI-MS *m/z* (relative intensity) 333 (0.5%), 288 (3.0%), 244 (5.2%), 198 (1.5%), 154 (5.2%), 121 (6.2), 91 (100%); HRMS-EI calcd for $C_{15}H_{15}N_3O_6$ ($M - C_4H_9^{\bullet} + H^+$) 333.0955, found 333.0963.

(2*R*,4*R*)-4-Aminopyrrolidine-1,2,4-tricarboxylic acid 1-benzyl ester 2-*tert*-butyl ester (26)

Compound **23** (16.8 g, 43.1 mmol) was dissolved in THF (647 mL) and transferred to a 1 L round bottom flask containing a magnetic stir bar. The solution was cooled to 0 °C, and DMAP (263 mg, 2.16 mmol) was added to the flask followed by di-*tert*-butyl dicarbonate (28.2 g, 129 mmol). The reaction mixture was stirred under nitrogen while warming to room temperature. After three hours, the starting material **23** had been completely consumed (by TLC). The solution was concentrated by rotary evaporation, and then filtered through a plug of silica with 1:2 EtOAc/hexanes to remove DMAP from crude product **25**. The filtrate was concentrated and the resulting yellow oily residue was dissolved in THF (172 mL) and transferred to a 500 mL round bottom flask containing a magnetic stir bar. To this solution was added a 2.0 M aqueous solution of potassium hydroxide (172 mL). The reaction mixture was stirred vigorously for 30 minutes. The solution was then transferred to a 1 L separatory funnel with an additional volume of ether (172 mL) and agitated. After the aqueous and organic layers had completely separated, the aqueous layer was transferred to a 250 mL beaker and cooled to 0 °C using an ice bath. With mechanical stirring, this solution was acidified to pH 6.5 by slow addition of 2.0 M aqueous HCl, causing the precipitation of a fine, white solid. The solution was filtered and the precipitate was washed with cold water (~ 100 mL). The precipitate was crystallized from ~ 150 mL of a hot 2:1 water/ethanol solution, yielding white needle-like crystals. These were dried in a vacuum oven at 60 °C yielding **26** (mp 187 °C dec) (9.32 g, 25.6 mmol, 59.4% recovered yield from **23**). ^{1}H NMR (300 MHz, CD_3COOD): mixture of rotamers δ 7.41 – 7.38 (m, 5H), 5.25 – 5.20 (m, 2H), 4.56 – 4.52 (m, 1H), 4.14 (br s, 2H), 3.25 – 3.10 (m, 1H), 2.47 – 2.42 (m, 1H), 1.55 and 1.36 (s, 9H, rotameric); ^{13}C NMR (75.4 MHz, CD_3COOD): mixture of rotamers δ 176.0, 172.7, 156.0 and 155.8, 137.0, 129.5, 129.2, 129.1, 85.0, 69.2, 67.2 and 66.2 (CH_2), 60.5 and 60.0 (CH), 55.8

and 55.4 (CH_2), 39.1 and 38.1 (CH_2), 28.0 (CH_3, 3C); IR (crushed powder): 3500, 2977, 1707, 1659, 1656, 1500, 1464, 1421, 1392, 1354, 1311, 1261, 1238, 1170, 1150, 1150, 1131, 1100, 730; $[\alpha]_D$ +25.8° (*c* 1.0, methanol); ESI-MS *m/z* (relative intensity, ion) 387 (19%, M + Na^+), 331 (100%, M – $C_4H_9^+$ + H^+ + Na^+), 309 (11%, M – $C_4H_9^+$ + H^+), 265 (34%); HRESIQTOFMS calcd for $C_{14}H_{16}N_2O_6$ (M – $C_4H_9^+$ + H^+ + Na^+) 331.0906, found 331.0894.

(2*R*,4*R*)-4-(9*H*-Fluoren-9-ylmethoxycarbonylamino)-pyrrolidine-1,2,4-tricarboxylic acid 1-benzyl ester 2-*tert*-butyl ester (27)

Finely divided **26** (3.90 g, 10.7 mmol) was transferred to an oven dried 500 mL three neck flask with a magnetic stir bar. This flask was placed in a vacuum oven for 4 hours under reduced pressure (50 °C, ~ 0.5 mm Hg) to remove any residual moisture. After backfilling with nitrogen, the flask was fitted with a reflux condenser, nitrogen inlet adapter, glass stopper, and rubber septum. After suspending the solid in CH_2Cl_2 (215 mL), DIPEA (4.50 mL, 25.8 mmol) was added to the suspension via syringe through the rubber septum. This was followed by similar addition of TMS-Cl (2.73 mL, 21.5 mmol). The flask was flushed with nitrogen, and the solution was refluxed for 1.5 hours. The solution was cooled to 0 °C in an ice bath and 9-fluorenylmethyl chloroformate (Fmoc-Cl, 2.5 g, 9.7 mmol) was added in one portion. The reaction mixture was allowed to stir overnight while warming to room temperature. The reaction mixture was concentrated by rotary evaporation to an oil which was dissolved in EtOAc (500 mL) and transferred to a 1 L separatory funnel. This solution was washed with 1M aqueous HCl (2 × 250 mL), then brine (250 mL). The organic layer was dried over Na_2SO_4, filtered, and concentrated by rotary evaporation. Residual solvent was removed under reduced pressure to give the desired product **27** (5.0 g, 8.5 mmol, 87%) as a white foamy solid which was used without further purification. An analytical sample was prepared by chromatography on silica (gradient elution from $CHCl_3$ to 95:5 $CHCl_3$/MeOH). ^{1}H NMR (300 MHz, 75 °C, DMSO-d_6): δ 12.46 (br s, 1H), 7.85 (d, *J* = 7.5 Hz, 2H), 7.74 (br s, Fmoc-N*H*, 1H), 7.69 (d, *J* = 7.4 Hz, 2H), 7.42-7.29 (m, 9H), 5.09 (s, 2H), 4.50 – 4.20 (m, 4H), 4.02 (d, *J* = 11.2 Hz, 1H), 3.64 (d, *J* = 11.2 Hz, 1H), 2.84 (m, 1H), 2.32 (dd, *J* = 13.4, 5.5 Hz, 1H), 1.37 (s, 9H); ^{13}C NMR (75.4 MHz, DMSO-d_6): mixture of rotamers δ 172.9, 170.2 and 169.9, 155.6, 153.5 and 153.3, 143.5, 140.7, 136.6 and 136.4, 128.2 (CH), 128.1 (CH), 127.8 (CH), 127.6 (CH), 127.5 (CH), 127.2 (CH), 127.1 (CH), 126.9 (CH), 125.1 (CH), 119.9 (CH), 80.8 and 80.7, 66.1 (CH_2), 65.6 (CH_2), 62.7

and 61.9, 58.6 and 58.3 (CH), 54.9 and 54.5 (CH_2), 46.5 (CH), 41.5 (CH_2), 37.5 and 37.5 (CH_2), 27.4 and 27.3 (CH_3, 3C); IR (neat film): 3319, 2978, 1713, 1530, 1450, 1423, 1357, 1257, 1188, 1157, 1119, 1087, 1045, 957, 911, 877, 841, 760, 739, 698 cm^{-1}; $[\alpha]_D$ -3.3° (c 2.4, $CHCl_3$); ESI-MS *m/z* (relative intensity): 767.2 (7.5%), 699.2 (12%), 631.2 (33%), 609.2 (100%), 553.2 (70%), 487.2 (17%); HRESIQTOFMS calcd for $C_{33}H_{34}N_2NaO_8$ ($M + Na^+$) 609.2213, found 609.2225.

(2*R*,4*R*)-4-(9*H*-Fluoren-9-ylmethoxycarbonylamino)-pyrrolidine-1,2,4-tricarboxylic acid 1-benzyl ester 2-*tert*-butyl ester 4-methyl ester (28)

A solution of **27** (14.2 g, 24.3 mmol) in anhydrous diethyl ether (150 mL) was transferred into a 500 mL three neck flask containing a magnetic stir bar and equipped with a pressure equalizing dropping funnel. Anhydrous methanol (98 mL, 2.4 mol) was added to the solution by syringe. A 2 M ethereal solution of TMS-CHN_2 (~ 20 mL, 40 mmol) was loaded into the dropping funnel under a N_2 atmosphere. The TMS-CHN_2 solution was added to the reaction mixture dropwise until the solution developed a persistent yellow color, at which time the starting material had been completely consumed (determined by TLC, 1:2 EtOAc/hexanes, R_f = 0.2). The flask was immersed in an ice bath and a 9:1 MeOH/AcOH solution (48 mL) was slowly added to quench residual TMS-CHN_2. The reaction mixture was concentrated by rotary evaporation to a yellow oil which was purified by chromatography on silica (gradient elution from hexanes to 1:1 EtOAc/hexanes). Fractions containing the desired product were concentrated by rotary evaporation. Residual solvent was removed under reduced pressure overnight giving the product **28** as a white foam (13.4 g, 22.2 mmol, 91%). ^{1}H NMR (300 MHz, 75 °C, DMSO-d_6): δ 7.86 (d, *J* = 7.4 Hz, 3H, overlap with Fmoc-N*H*), 7.66 (d, *J* = 7.5 Hz, 2H), 7.41 – 7.32 (m, 9H), 5.09 (s, 2H), 4.40 – 4.20 (m, 4H), 3.97 (d, *J* = 11.3 Hz, 1H), 3.60 (m, 4H), 2.80 (br m, 1H), 2.27 (br m, 1H), 1.36 (s, 9H); ^{13}C NMR (75.4 MHz, DMSO-d_6): mixture of rotamers δ 171.8 and 171.7, 170.2 and 169.8, 155.7, 153.5 and 153.3, 143.5, 140.6, 136.6 and 136.4, 128.3 (CH), 128.1 (CH), 127.8 (CH), 127.7 (CH), 127.5 (CH), 127.4 (CH), 127.2 (CH), 126.9 (CH), 125.1 (CH), 125.0 (CH), 120.0 (CH), 80.9 and 80.8, 66.2 (CH_2), 65.6 (CH_2), 63.0 and 62.1, 58.4 and 58.0 (CH), 54.7 and 54.3 (CH_2), 52.6 (CH_3), 46.5 (CH), 38.4 and 37.4 (CH_2), 27.4 and 27.3 (CH_3, 3C); IR (neat film): 3320, 2977, 1743, 1711, 1526, 1450, 1417, 1356, 1296, 1246, 1157, 1114, 1084, 979, 918, 843, 760, 740, 698 cm^{-1}; $[\alpha]_D$ -3.6° (*c* 2.0, $CHCl_3$); ESI-MS *m/z* (relative intensity):

681.5 (4.5%), 623.4 (100%), 567.4 (45%), 501.4 (13%); HRESITOFMS calcd for $C_{34}H_{36}N_2NaO_8$ (M + Na^+) 623.2369, found 623.2360.

(2*R*,4*R*)-4-(9*H*-Fluoren-9-ylmethoxycarbonylamino)-pyrrolidine-1,2,4-tricarboxylic acid 1-benzyl ester 4-methyl ester (29)

Compound **28** (4.1 g, 6.8 mmol) was transferred to a 200 mL round bottom flask with a magnetic stir bar and dissolved in a solution of 1:1 TFA/CH_2Cl_2 (70 mL). The reaction mixture was stirred for 4 h and then concentrated by rotary evaporation; the resulting oily residue was dissolved in toluene and concentrated again. Solvent was removed under vacuum overnight, yielding **29** (3.4 g, 6.4 mmol, 94%) as a foam, used without further purification. An analytical sample was purified by chromatography on silica (gradient elution over 14 column volumes from $CHCl_3$ (0.1% AcOH) to 95:5 $CHCl_3$/MeOH (0.1% AcOH)). ^{1}H NMR (300 MHz, 75 °C, DMSO-d_6): δ 7.96 (br s, Fmoc-N*H*, 1H), 7.86 (d, *J* = 9.3 Hz, 2H), 7.68 (d, *J* = 7.5 Hz, 2H), 7.43 – 7.31 (m, 9H), 5.11 (s, 2H), 4.36 (m, 3H), 4.22 (apparent t, *J* = 6.3 Hz, 1H), 4.08 (d, *J* = 9.0 Hz, 1H), 3.61 (s, 3H), 3.58 (overlap with –CO_2CH_3, 1H), 2.84 (m, 1H), 2.28 (dd, *J* = 12.8, 5.6 Hz, 1H); ^{13}C NMR (75.4 MHz, DMSO-d_6): mixture of rotamers δ 172.5, 172.2, 171.9, 155.6, 153.6 and 153.3, 143.5 and 143.4, 140.6, 136.5, 128.2 (CH), 128.1 (CH), 127.7 (CH), 127.4 (CH), 127.3 (CH), 126.9 (CH), 125.0 (CH), 119.9 (CH), 66.1 (CH_2), 65.6 (CH_2), 62.7 and 61.9, 57.7 and 57.4 (CH), 54.8 and 54.4 (CH_2), 52.5 (CH), 46.5 (CH_3), 37.6 and 37.5 (CH_2); IR (neat film): 3308, 3065, 2953, 1715, 1529, 1450, 1423, 1357, 1251, 1110, 1085, 1051, 973, 826, 760, 740, 699 cm^{-1}; $[\alpha]_D$ +31.3° (*c* 1.4, $CHCl_3$); HPLC: C_{18} column, mobile phase, CH_3CN (0.05% TFA)/water (0.1% TFA), 5% to 95% CH_3CN over 30 min, 1.00 mL/min, UV detection at 274 nm; t_R for **29**, 23.80 min; ESI-MS *m/z* (relative intensity): 567.2 (100%), 501.2 (11%); HRESIQTOFMS calcd for $C_{30}H_{28}N_2NaO_8$ (M + Na^+) 567.1743, found 567.1743.

(2*R*,4*R*)-4-(9*H*-Fluoren-9-ylmethoxycarbonylamino)-pyrrolidine-1,2,4-tricarboxylic acid 1-*tert*-butyl ester 4-methyl ester (30)

Compound **28** (13.4 g, 22.2 mmol) was transferred to a 500 mL round bottom flask containing a magnetic stir bar, then dissolved in 1:1 CH_2Cl_2/TFA (222 mL). The reaction mixture was stirred at room temperature and monitored by TLC (1:2 EtOAc/hexanes, **28** R_f = 0.24, **29** R_f = 0.07). When all of the starting material was consumed, the solution was concentrated by rotary

evaporation. A portion of toluene was added to the flask, and the solution was concentrated again. Residual solvent was removed under reduced pressure overnight. Pd/C (10 wt. %, 1.1 g), THF (635 mL), and Boc_2O (12.1 g, 55.6 mmol) were added to the flask, and the solution was degassed under reduced pressure, then back-filled with H_2 gas. The reaction mixture was stirred overnight under a H_2 atmosphere (~ 1 atm). The reaction mixture was filtered, and the filtrate was concentrated by rotary evaporation to an oil, which was purified by chromatography on silica (gradient elution from $CHCl_3$ to 10% MeOH/$CHCl_3$). Fractions containing the desired product were concentrated, and residual solvent was removed under reduced pressure giving **30** (9.3 g, 18.2 mmol, 82% from **30**) as a white foam. ^{1}H NMR (300 MHz, DMSO-d_6): mixture of rotamers δ 8.29 (s, Fmoc-N*H*, 1H), 7.88 (d, J = 7.4 Hz, 2H), 7.71 (d, J = 7.1 Hz, 2H), 7.44 – 7.31 (m, 4H), 4.31 – 4.20 (m, 4H, rotameric), 3.98 (apparent dd, J = 24.3, 11.2 Hz, 1H), 3.60 (s, 3H), 3.48 (apparent t, J = 10.4 Hz, 1H), 2.89 – 2.76 (m, 1H), 2.29 – 2.20 (m, 1H), 1.41 and 1.36 (s, 9H, rotameric); ^{13}C NMR (75.4 MHz, DMSO-d_6): mixture of rotamers δ 173.5, 172.2, 155.7, 153.3, 152.9, 143.6 and 143.5, 140.7, 127.6 (CH), 127.0 (CH), 125.2 (CH), 120.0 (CH), 79.0, 65.6 (CH_2), 62.7 and 61.9, 58.1 and 57.7 (CH), 54.8 and 54.4 (CH_2), 52.5 (CH_3), 46.6 (CH), 38.8 and 37.9 (CH_2), 28.0 and 27.8 (CH_3, 3C); IR (neat film): 3307, 3016, 2979, 1744, 1530, 1477, 1450, 1409, 1368, 1297, 1253, 1217, 1160, 1088, 1050, 972, 913, 858, 759, 667 cm^{-1}; $[\alpha]_D$ +61.8° (*c* 1.9, $CHCl_3$); HPLC: C_{18} column, mobile phase, CH_3CN (0.05% TFA)/water (0.1% TFA), 5% to 95% CH_3CN over 30 min, 1.00 mL/min, UV detection at 274 nm, t_R for **30**, 23.20 min; ESI-MS *m/z* (relative intensity): 533.2 (100%, M + Na^+), 477.1 (30%), 433.1 (90%); HRESIQTOFMS calcd for $C_{27}H_{30}N_2NaO_8$ (M + Na^+) 533.1900, found 533.1904.

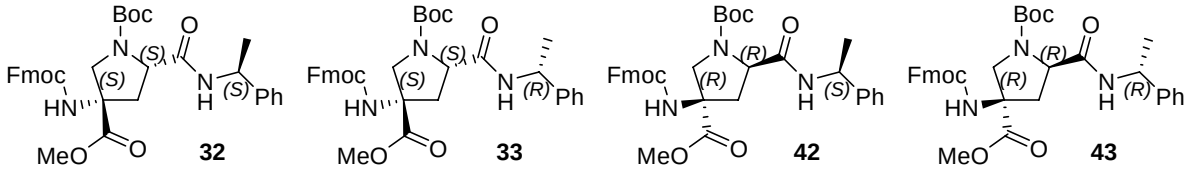

Figure 2-14: Phenethylamine derivatives of the Boc-*pro4*(2*S*,4*S*) and Boc-*pro4*(2*R*,4*R*)

(3S,5S)-3-(9*H*-Fluoren-9-ylmethoxycarbonylamino)-5-((*S*)-1-phenylethylcarbamoyl)-pyrrolidine-1,3-dicarboxylic acid 1-*tert*-butyl ester 3-methyl ester (32)

(3S,5S)-3-(9*H*-Fluoren-9-ylmethoxycarbonylamino)-5-((*R*)-1-phenylethylcarbamoyl)-pyrrolidine-1,3-dicarboxylic acid 1-*tert*-butyl ester 3-methyl ester (33)

(3R,5R)-3-(9*H*-Fluoren-9-ylmethoxycarbonylamino)-5-((*S*)-1-phenylethylcarbamoyl)-pyrrolidine-1,3-dicarboxylic acid 1-*tert*-butyl ester 3-methyl ester (42)

(3R,5R)-3-(9*H*-Fluoren-9-ylmethoxycarbonylamino)-5-((*R*)-1-phenylethylcarbamoyl)-pyrrolidine-1,3-dicarboxylic acid 1-*tert*-butyl ester 3-methyl ester (43)

General procedure for the preparation of the methylbenzylamine derivatives of monomers **30** and **19**:

Two 4 mL conical vials with magnetic spin vanes were dried in an oven. To each vial was added the monomer (~ 5 mg), HATU (3.7 mg, 9.8 μmol), DIPEA (3.2 μL, 19.6 μmol) and CH_2Cl_2 (~ 100 μL). L(-)-α-methylbenzylamine (2 μL, 9.8 μmol) was added to the solution in the first vial, and D(+)-α-methylbenzylamine (2 μL, 9.8 μmol) was added to the second. The addition of the amine to the solution caused an immediate color change from pale to bright yellow. The vials were sealed with a rubber septum, and the solutions were stirred for an additional 30 minutes at room temperature. pH 4 aqueous HCl (2 mL) was added to each vial, and the mixture was extracted with $CHCl_3$ (2 mL). The $CHCl_3$ extracts were washed with brine, dried over Na_2SO_4, filtered, and then concentrated by centrifugal evaporation. The residues were dissolved in CH_3CN (~ 2 mL), filtered through 0.2 μm nylon filters into vials, and analyzed by HPLC using appropriate gradient elution methods.

Compound 32, Compound 33

HPLC: column, Microsorb 100 C_{18}, 4.6 mm × 250 mm; mobile phase, CH_3CN (0.05% TFA) / water (0.1% TFA), 50% to 95% CH_3CN over 30 minutes; flow rate, 1.00 mL / min; UV detection at 274 nm; t_R for **32**, 17.4 min: t_R for **33**, 18.4 min.

Compound 42, Compound 43

HPLC: column, Microsorb 100 C_{18}, 4.6 mm × 250 mm; mobile phase, CH_3CN (0.05% TFA) / water (0.1% TFA), 5% to 95% CH_3CN over 30 minutes; flow rate, 1.00 mL / min; UV detection at 274 nm; t_R for **42**, 27.4 min: t_R for **43**, 27.9 min.

(2*S*,4*R*)-4-Amino-pyrrolidine-1,2,4-tricarboxylic acid 1-benzyl ester 2-*tert*-butyl ester (34)

13 (3.7 g, 9.6 mmol) was dissolved in THF (144 mL) and transferred to a round bottom flask containing a magnetic stir bar. DMAP (59 mg, 0.48 mmol) was added to the solution, and the flask was sealed with a rubber septum and flushed with nitrogen. The flask was then submerged in an ice bath. Boc_2O (6.3 grams, 29 mmol) was added to the solution in one portion. This

mixture was stirred under nitrogen and the reaction progress was monitored by TLC (1:2 EtOAc/hexanes, **13** R_f = 0.1, product R_f = 0.5). When the starting material was entirely consumed (about 4 hours) the solution was concentrated by rotary evaporation, and the residue was dissolved in 1:2 EtOAc/hexanes. This solution was filtered through a short silica plug to remove DMAP. All fractions containing the desired product (determined by TLC) were pooled and concentrated by rotary evaporation; residual solvent was removed under reduced pressure overnight. The resulting white foam was dissolved in THF (38 mL). 2 M aqueous KOH (38 mL) was added to this solution. This biphasic mixture was stirred vigorously for 40 minutes. Et_2O (~ 60 mL) was added to the reaction mixture, and the entire solution was transferred to a 250 mL separatory funnel. The solution was agitated then allowed to separate entirely. The aqueous layer was removed and the organic layer washed with water (1 × 15 mL); the aqueous layers were combined in a beaker. This beaker was submerged in an ice bath. The solution was adjusted to pH ≈ 6.5 by slow addition of 2 M aqueous HCl under mechanical stirring. The resulting precipitate was filtered from the solution, dried under reduced pressure overnight at 50 °C then crystallized from hot methanol affording the desired product **34** (2.0 g, 5.4 mmol, 56% yield over two steps) as white needle-like crystals (mp 255 °C dec). ^{1}H NMR (300 MHz, CD_3COOD): mixture of rotamers δ 7.40 (m, 5H), 5.20 (m, 2H), 4.57 (apparent ddd, *J* = 8.5, 8.4, 5.4 Hz, 1H), 4.21 (apparent dd, *J* = 12.3, 6.5 Hz, 1H), 4.05 (apparent t, *J* = 12.8 Hz, 1H), 2.87 (m, 1H), 2.75 (m, 1H), 1.47 and 1.39 (s, 9H, rotameric); ^{13}C NMR (75.4 MHz, CD_3COOD): mixture of rotamers δ 172.8, 171.8 and 171.6, 156.3 and 156.0, 137.4 and 137.1, 129.5 (CH), 129.3 (CH), 129.1 (CH), 128.8 (CH), 83.7, 69.0 and 68.8 (CH_2), 67.4 and 66.6, 59.9 and 59.5 (CH), 55.7 and 55.4 (CH_2), 39.9 and 39.0 (CH_2), 28.2 (3C, CH_3); IR (crushed powder): 2981, 1743, 1705, 1641, 1498, 1453, 1426, 1369, 1283, 1231, 1158, 1116, 1030, 984, 955, 919, 853, 819, 759 cm^{-1}; $[\alpha]_D$ -36.2° (*c* 0.66, AcOH); ESI-MS *m/z* (relative intensity): 365.2 (100%, M + H^+), 387.2 (45%, M + Na^+), 403.1 (3%, M + K^+); HRESIQTOFMS calcd for $C_{18}H_{25}N_2O_6$ (M + H^+) 365.1713, found 365.1704.

(2*S*,4*R*)-4-(9*H*-Fluoren-9-ylmethoxycarbonylamino)-pyrrolidine-1,2,4-tricarboxylic acid 1-benzyl ester 2-*tert*-butyl ester (35)

Finely divided **34** (2.9 g, 7.9 mmol) and a magnetic stir bar were added to a 250 mL 3-neck round bottom flask equipped with a nitrogen inlet adapter and a reflux condenser. CH_2Cl_2 (160

mL) was added to the flask, and the suspension was stirred vigorously. DIPEA (3.5 mL, 20 mmol) was added to the suspension by syringe, followed by TMS-Cl (2.0 mL, 16 mmol). The flask was flushed with nitrogen, and then the solution was refluxed for 1 hour. The reaction mixture was cooled to 0 °C in an ice bath, and Fmoc-Cl (2.0 g, 7.6 mmol) was added to the flask in one portion. The mixture was allowed to warm to room temperature overnight with stirring. The solution was concentrated by rotary evaporation, and the residue dissolved in EtOAc (500 mL). This solution was transferred to a separatory funnel and washed with 1 M aqueous HCl (2 × 100 mL) then brine (1 × 100 mL), dried over $MgSO_4$, filtered, and concentrated by rotary evaporation. The resulting white foam was purified by chromatography on silica (gradient elution over 14 column volumes from $CHCl_3$ (0.1% AcOH) to 95:5 $CHCl_3$/MeOH (0.1% AcOH)). Desired fractions were pooled and concentrated, and residual solvent was removed under reduced pressure overnight yielding **35** (4.1 g, 7.0 mmol, 93%) as a white foam. ^{1}H NMR (300 MHz, 350 K, DMSO-d_6): δ 12.60 (br s, 1H), 7.86 (d, J = 7.5 Hz, 2H), 7.81 (s, 1H, Fmoc-N*H*), 7.68 (d, J = 7.4 Hz, 2H) 7.41 (t, J = 7.2 Hz, 2H), 7.32 (m, 7H), 5.08 (m, 2H), 4.32 (m, 3H), 4.22 (t, J = 6.8 Hz, 1H), 4.07 (apparent dd, J = 11.3, 1.3 Hz, 1H), 3.73 (d, J = 11.3 Hz, 1H), 2.69 (dd, J = 12.7, 8.2 Hz, 1H), 2.26 (dd, J = 13.0, 8.9 Hz, 1H), 1.92 (s, 9H); ^{13}C NMR (75.4 MHz, DMSO-d_6): mixture of rotamers δ 171.5 and 171.4, 170.4 and 170.0, 155.3, 153.8 and 153.7, 143.6 and 143.5, 140.6, 136.5 and 136.2, 128.1 (CH), 127.9 (CH), 127.6 (CH), 127.4 (CH), 127.2 (CH), 127.1 (CH), 126.9 (CH), 125.0 (CH), 119.9 (CH), 80.9 and 80.8, 66.2 and 66.0 (CH_2), 65.4 (CH_2), 63.4 and 62.6, 58.5 and 58.0 (CH), 54.3 and 53.8 (CH_2), 46.5 (CH), 38.7 and 37.8 (CH_2), 27.4 and 27.3 (CH_3); IR (thin film): 3317, 2979, 2613, 1709, 1586, 1529, 1450, 1358, 1259, 1193, 1150, 1084, 1046, 987, 846, 758, 698, 667 cm^{-1}; $[\alpha]_D$ -35.4° (*c* 0.99, $CHCl_3$); ESI-MS *m/z* (relative intensity): 553.2 (45%), 587.2 (30%), 604.3 (40%), 609.2 (100%); HRESIQTOFMS calcd for $C_{33}H_{34}N_2O_8Na$ (M + Na$^+$) 609.2207, found 609.2227.

(2*S*,4*R*)-4-(9*H*-Fluoren-9-ylmethoxycarbonylamino)-pyrrolidine-1,2,4-tricarboxylic acid 1-benzyl ester 2-*tert*-butyl ester 4-methyl ester (36)

35 (5.2 g, 8.9 mmol) and a magnetic stir bar were transferred to a 200 mL round bottom flask. Anhydrous Et_2O (53 mL) was added to the flask, which was then sealed with a rubber septum. A needle connected to a nitrogen line was inserted into the septum, as well as a needle open to the air. Anhydrous methanol (36.2 mL, 900 mmol) was added to the flask by syringe. The solution

was stirred, and TMS-CHN_2 (2 M in ether) was added dropwise from a syringe until there was a persistent yellow color in the solution (~ 10 to 15 mL of the TMS-CHN_2 solution). The reaction endpoint was confirmed by analytical TLC (5:1 $CHCl_3$/MeOH, **35** R_f = 0.2, **36** R_f = 0.8). Excess TMS-CHN_2 was quenched by careful, slow addition of a 10% AcOH/MeOH solution to the reaction mixture (CAUTION: quenching the excess TMS-CHN_2 generates a significant amount of nitrogen gas). The solution was concentrated by rotary evaporation and the desired product was isolated through chromatography on silica (gradient elution over 14 column volumes from hexanes to 1:1 EtOAc/hexanes) giving **36** (4.6 g, 7.6 mmol, 85%) as a white foam. ^{1}H NMR (300 MHz, 350 K, DMSO-d_6): δ 7.94 (s, 1H, Fmoc-N*H*), 7.86 (d, *J* = 7.5 Hz, 2H), 7.67 (d, *J* = 7.4 Hz, 2H), 7.41 (t, *J* = 7.2 Hz, 2H), 7.33 (m, 7H), 5.08 (m, 2H), 4.38 (m, 2H), 4.29 (m, 1H), 4.22 (t, *J* = 6.6 Hz, 1H), 4.00 (d, *J* = 11.3 Hz, 1H), 3.72 (d, *J* = 11.4 Hz, 1H), 3.62 (s, 3H), 2.65 (dd, *J* = 12.0, 8.2 Hz, 1H), 2.24 (dd, *J* = 12.4, 9.2 Hz, 1H), 1.38 (s, 9H); ^{13}C NMR (75.4 MHz, DMSO-d_6): mixture of rotamers δ 170.4 and 170.3, 169.9, 155.3, 153.7 and 153.3, 143.6 and 143.4, 140.6, 136.4 and 136.2, 128.1 (CH), 127.7 (CH), 127.5 (CH), 127.3 (CH), 126.9 (CH), 124.9 (CH), 119.9 (CH), 81.1 and 80.9, 66.3 and 66.1 (CH_2), 65.3 (CH_2), 63.3 and 62.6, 58.3 and 57.8 (CH), 54.2 and 53.7 (CH_2), 52.5 (CH_3), 46.5 (CH), 38.5 and 37.6 (CH_2), 27.4 and 27.3 (CH_3); IR (thin film): 3319, 2979, 1702, 1529, 1421, 1358, 1244, 1192, 1150, 1081, 979, 847, 741, 698, 667 cm^{-1}; $[\alpha]_D$ -34.6° (*c* 0.94, $CHCl_3$); ESI-MS *m/z* (relative intensity): 501.2 (95%), 623.2 (100%); HRESIQTOFMS calcd for $C_{34}H_{36}N_2O_8Na$ (M + Na$^+$) 623.2364, found 623.2357.

(2*S*,4*R*)-4-(9*H*-Fluoren-9-ylmethoxycarbonylamino)-pyrrolidine-1,2,4-tricarboxylic acid 1-benzyl ester 4-methyl ester (37)

36 (5.3 g, 8.7 mmol) was dissolved in CH_2Cl_2 (43 mL) and transferred to a 200 mL round bottom flask containing a magnetic stir bar. TFA (43 mL) was added to this solution. The reaction mixture was stirred for 5 hours, and then concentrated by rotary evaporation; residual solvent was removed overnight under reduced pressure. 10 wt. % Pd/C (876 mg) was added to the resulting yellow-brown foam, which was then dissolved in THF (250 mL). Melted Boc_2O (6.0 mL, 26 mmol) was added to the solution, and the reaction mixture was degassed by purging the flask under reduced pressure and backfilling with H_2 gas several times. The reaction mixture was then stirred vigorously under H_2 (balloon) overnight. The reaction was monitored by HPLC (C_{18} column; mobile phase, CH_3CN (0.05% TFA)/water (0.1% TFA), 5% to 95% CH_3CN over

30 min; flow rate, 1.00 mL/min; UV detection at 220 nm; Cbz-*pro4*(2*S*,4*R*) t_R = 23.8 min, **37** t_R = 23.0). The catalyst was removed by filtration, and the solution was concentrated by rotary evaporation. The product was purified by chromatography on silica (gradient elution over 14 column volumes from $CHCl_3$ to 10% MeOH/$CHCl_3$). The desired fractions were pooled and concentrated by rotary evaporation; residual solvent was removed under reduced pressure yielding **1** (4.3 g, 8.4 mmol, 95%) as a white foam. ^{1}H NMR (300 MHz, DMSO-d_6): mixture of rotamers δ 12.83 (br s, 1H), 8.18 (apparent d, *J* = 5.6, 1H, Fmoc-N*H*), 7.89 (d, *J* = 7.4 Hz, 2H), 7.69 (t, *J* = 5.4 Hz, 2H), 7.42 (t, *J* = 7.3 Hz, 2H), 7.33 (t, *J* = 7.3 Hz, 2H), 4.38 (m, 2H), 4.20 (m, 2H), 3.88 (apparent dd, *J* = 10.8, 6.5 Hz, 1H), 3.65 (apparent s, 1H, overlap with –COOC*H*$_3$), 3.61 (s, 3H), 2.59 (m, 1H), 2.19 (m, 1H), 1.35 (s, 9H); ^{13}C NMR (75.4 MHz, DMSO-d_6): mixture of rotamers δ 173.3 and 172.8, 170.7, 155.5, 153.5 and 152.8, 143.6 and 143.5, 140.7, 127.6 (CH), 127.0 (CH), 125.1 (CH), 120.1 (CH), 79.4 and 79.3, 65.5 and 65.3 (CH_2), 63.5 and 62.7, 57.6 and 57.4 (CH), 54.0 and 53.6 (CH_2), 52.6 (CH_3), 46.6 (CH), 38.4 and 37.8 (CH_2), 27.9 and 27.8 (CH_3); IR (thin film): 3323, 3015, 2979, 1725, 1529, 1477, 1450, 1415, 1369, 1321, 1247, 1153, 1107, 1084, 931, 862, 758, 667 cm^{-1}; $[\alpha]_D$ -39.5° (*c* 1.41, $CHCl_3$); ESI-MS *m/z* (relative intensity): 411.1 (100%), 533.2 (28%), 1043.4 (28%, 2M + Na^+); HRESIQTOFMS calcd for $C_{27}H_{30}N_2O_8Na$ (M + Na^+) 533.1894, found 533.1917.

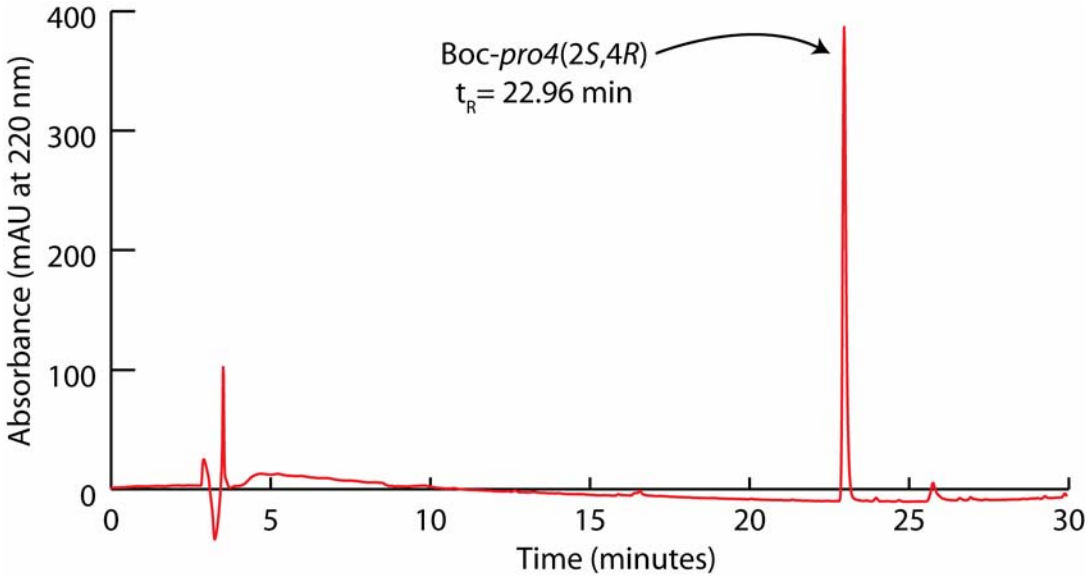

HPLC: C_{18} column; mobile phase, CH_3CN (0.05% TFA) / water (0.1% TFA), 5% to 95% CH_3CN over 30 min; flow rate, 1.00 mL/min; UV detection at 220 nm; t_R for **37**, 23.0 min

Figure 2-15: HPLC chromatogram of purified **37**

(2*R*,4*S*)-4-Amino-pyrrolidine-1,2,4-tricarboxylic acid 1-benzyl ester 2-*tert*-butyl ester (38)

24 (2.6 g, 6.7 mmol) was dissolved in THF (100 mL) and transferred to a round bottom flask containing a magnetic stir bar. DMAP (41 mg, 0.33 mmol) was added to the solution, and the flask was sealed with a rubber septum and flushed with nitrogen. The flask was then submerged in an ice bath. Boc_2O (4.4 g, 20 mmol) was added to the solution, and the mixture was stirred under nitrogen and monitored by TLC (1:2 EtOAc/hexanes, **24** R_f = 0.2, product R_f = 0.6) until the starting material was entirely consumed (about 4 hours). The reaction mixture was concentrated by rotary evaporation, and the residue was dissolved in 1:2 EtOAc/hexanes; this solution was filtered through a silica plug to remove DMAP. Fractions containing the desired product were pooled and concentrated by rotary evaporation; residual solvent was removed under reduced pressure overnight. The resulting white foam was dissolved in THF (85 mL). 2 M aq. KOH (85 mL) was added to this solution. This biphasic mixture was stirred vigorously for 35 minutes. Et_2O (~ 85 mL) was added to the mixture, and the entire solution was transferred to a 500 mL separatory funnel. The solution was agitated and then allowed to separate entirely. The aqueous layer was removed and transferred to a beaker. This beaker was submerged in an ice bath. The solution was adjusted to pH ≈ 6.5 by slow addition of 2 M aqueous HCl under mechanical stirring. The resulting precipitate was filtered from the solution, dried under reduced pressure overnight at 50 °C, and crystallized from hot methanol producing the desired product **38** (1.7 g, 4.7 mmol, 73% yield over two steps) as white needle-like crystals (mp 253 °C dec). ^{1}H NMR (300 MHz, CD_3COOD): mixture of rotamers δ 7.37 (m, 5H), 5.20 (m, 2H), 4.61 (apparent t, *J* = 8.3 Hz, 1H), 4.25 (apparent dd, *J* = 12.4, 4.2 Hz, 1H), 4.04 (apparent t, *J* = 11.9 Hz, 1H), 2.91 (m, 1H), 2.75 (m, 1H), 1.46 and 1.38 (s, 9H, rotameric); ^{13}C NMR (75.4 MHz, CD_3COOD): mixture of rotamers δ 172.4, 171.8 and 171.6, 156.2 and 156.0, 137.4 and 137.1, 129.5 (CH), 129.2 (CH), 129.1 (CH), 128.8 (CH), 83.7, 69.0 and 68.8 (CH_2), 67.0 and 66.2, 59.8 and 59.4 (CH), 55.6 and 55.3 (CH_2), 39.8 and 38.9 (CH_2), 28.2 (CH_3, 3C); IR (crushed powder): 2980, 1742, 1606, 1454, 1427, 1368, 1283, 1229, 1156, 1116, 984, 853, 756 cm^{-1}; $[\alpha]_D$ +37.2° (c 0.50, AcOH); ESI-MS *m/z* (relative intensity): 365.2 (100%, M + H^+), 387.2 (45%, M + Na^+), 403.1 (3%, M + K^+); HRESIQTOFMS calcd for $C_{18}H_{25}N_2O_6$ (M + H^+) 365.1713, found 365.1717.

(2*R*,4*S*)-4-(9*H*-Fluoren-9-ylmethoxycarbonylamino)-pyrrolidine-1,2,4-tricarboxylic acid 1-benzyl ester 2-*tert*-butyl ester (39)

Finely divided **38** (1.5 g, 4.1 mmol) and a magnetic stir bar were added to a 250 mL 3-neck round bottom flask equipped with a nitrogen inlet adapter and a reflux condenser. CH_2Cl_2 (160 mL) was added to the flask, and the suspension was stirred vigorously. DIPEA (1.7 mL, 10 mmol) was added to the suspension by syringe, followed by TMS-Cl (1.1 mL, 8.3 mmol). The flask was flushed with nitrogen, and then the solution was refluxed for ~ 2 hours. The reaction mixture was cooled to 0 °C in an ice bath, and Fmoc-Cl (1.0 g, 3.9 mmol) was added to the flask in one portion. The mixture was allowed to warm to room temperature overnight with stirring. The solution was concentrated by rotary evaporation and immediately purified by chromatography on silica (gradient elution over 14 column volumes from $CHCl_3$ (0.1% AcOH) to 95:5 $CHCl_3$/MeOH (0.1% AcOH)). Desired fractions were pooled and concentrated, and residual solvent was removed under reduced pressure providing **39** (1.8 g, 3.1 mmol, 78%) as a white foam. ^{1}H NMR (300 MHz, 350 K, DMSO-d_6): δ 12.41 (br s, 1H), 7.86 (d, J = 7.5 Hz, 2H), 7.81 (s, 1H, Fmoc-N*H*), 7.68 (d, J = 7.4 Hz, 2H), 7.41 (t, J = 7.2 Hz, 2H), 7.32 (m, 7H), 5.08 (m, 2H), 4.33 (m, 3H), 4.22 (t, J = 6.8 Hz, 1H), 4.07 (apparent dd, J = 11.3, 1.4 Hz, 1H), 3.74 (d, J = 11.3 Hz, 1H), 2.70 (dd, J = 12.7, 8.0 Hz, 1H), 2.26 (dd, J = 13.1, 8.9 Hz, 1H), 1.38 (s, 9H); ^{13}C NMR (75.4 MHz, DMSO-d_6): mixture of rotamers δ 171.5 and 171.4, 170.4 and 170.0, 155.3, 153.8 and 153.4, 143.6 and 143.5, 140.6, 136.5 and 136.2, 128.1 (CH), 127.6 (CH), 127.5 (CH), 127.3 (CH), 127.1 (CH), 126.9 (CH), 125.0 (CH), 119.9 (CH), 81.0 and 80.8, 66.2 and 66.0 (CH_2), 65.4 (CH_2), 63.4 and 62.6, 58.5 and 58.0 (CH), 54.3 and 53.8 (CH_2), 46.5 (CH), 38.7 and 37.8 (CH_2), 27.4 and 27.3 (CH_3); IR (thin film): 3322, 3018, 2979, 1713, 1531, 1450, 1359, 1260, 1193, 1150, 1084, 1046, 987, 758, 698, 667, 621 cm^{-1}; $[\alpha]_D$ +39.1° (*c* 0.70, $CHCl_3$); ESI-MS *m/z* (relative intensity): 569.1 (10%), 587.2 (30%), 604.3 (33%), 609.2 (100%); HRESIQTOFMS calcd for $C_{33}H_{34}N_2O_8Na$ (M + Na$^+$) 609.2207, found 609.2266.

(2*R*,4*S*)-4-(9*H*-Fluoren-9-ylmethoxycarbonylamino)-pyrrolidine-1,2,4-tricarboxylic acid 1-benzyl ester 2-*tert*-butyl ester 4-methyl ester (40)

39 (1.8 g, 3.0 mmol) and a magnetic stir bar were transferred to a 100 mL round bottom flask. Anhydrous Et_2O (15 mL) was added to the flask, which was then sealed with a rubber septum. A needle connected to a nitrogen line was inserted into the septum, as well as a needle open to the

air. Anhydrous methanol (15 mL) was added to the flask by syringe. The solution was stirred, and TMS-CHN_2 (2M in ether) was added dropwise from a syringe until there was a persistent yellow color in the solution. The color change indicated the completion of the reaction, and was confirmed by analytical TLC (5:1 $CHCl_3$/MeOH, **39** R_f = 0.2, **40** R_f = 0.8). Excess TMS-CHN_2 was quenched by careful, slow addition of a 10% AcOH/MeOH solution to the reaction mixture. The solution was concentrated by rotary evaporation and the desired product purified by chromatography on silica (gradient elution over 14 column volumes from hexanes to 1:1 EtOAc/hexanes) giving **40** (1.6 g, 2.7 mmol, 90%) as a white foam. ^{1}H NMR (300 MHz, 350K, DMSO-d_6): δ 7.93 (s, 1H, Fmoc-N*H*), 7.86 (d, *J* = 7.4 Hz, 2H), 7.66 (d, *J* = 7.4 Hz, 2H), 7.41 (t, *J* = 7.2 Hz, 2H), 7.32 (m, 7H), 5.08 (m, 2H), 4.38 (m, 2H), 4.29 (m, 1H), 4.22 (t, *J* = 6.6 Hz, 1H), 3.99 (d, *J* = 11.3 Hz, 1H), 3.71 (d, *J* = 11.4 Hz, 1H), 3.61 (s, 3H), 2.64 (dd, *J* = 12.0, 8.2 Hz, 1H), 2.23 (dd, *J* = 12.6, 9.1 Hz, 1H), 1.38 (s, 9H); ^{13}C NMR (75.4 MHz, DMSO-d_6): mixture of rotamers δ 170.4 and 170.3, 169.9, 155.3, 153.7 and 153.3, 143.6 and 143.4, 140.6, 136.4 and 136.2, 128.1 (CH), 127.7 (CH), 127.4 (CH), 127.3 (CH), 126.8 (CH), 124.9 (CH), 119.9 (CH), 81.1 and 80.9, 66.3 and 66.1 (CH_2), 65.3 (CH_2), 63.3 and 62.6, 58.3 and 57.8 (CH), 54.2 and 53.7 (CH_2), 52.5 (CH_3), 46.5 (CH), 38.6 and 37.6 (CH_2), 27.4 and 27.3 (CH_3); IR (thin film): 3319, 3011, 2979, 2953, 1713, 1528, 1450, 1422, 1359, 1243, 1192, 1150, 1081, 978, 847, 758, 698, 667 cm^{-1}; $[\alpha]_D$ +40.3° (c 1.00, $CHCl_3$); ESI-MS *m/z* (relative intensity): 567.2 (27%), 583.1 (6%), 601.3 (8%), 618.3 (10%), 623.2 (100%); HRESIQTOFMS calcd for $C_{34}H_{36}N_2O_8Na$ (M + Na^+) 623.2364, found 623.2354.

(2*R*,4*S*)-4-(9*H*-Fluoren-9-ylmethoxycarbonylamino)-pyrrolidine-1,2,4-tricarboxylic acid 1-benzyl ester 4-methyl ester (41)

40 (1.6 g, 2.7 mmol) was dissolved in CH_2Cl_2 (14 mL) and transferred to a 50 mL round bottom flask containing a magnetic stir bar. Trifluoroacetic acid (14 mL) was added to the solution, the flask was sealed with a rubber septum, and the reaction mixture was stirred for approximately 4 hours. The reaction mixture was concentrated by rotary evaporation and residual solvent was removed under reduced pressure overnight. The resulting yellow foam was dissolved in THF (77 mL) and transferred to a 200 mL round bottom flask containing a magnetic stir bar and 10 wt. % Pd/C (270 mg). Melted Boc_2O (1.9 mL, 8.1 mmol) was added to the reaction mixture by syringe. The solution was degassed by purging the flask under reduced pressure and backfilling

with H_2 gas several times. The solution was stirred overnight under an H_2 atmosphere (balloon). The catalyst was removed by filtration, and the solution was concentrated by rotary evaporation. The product was isolated by chromatography on silica (gradient elution over 14 column volumes from $CHCl_3$ to 10% MeOH/$CHCl_3$). Desired fractions were pooled and concentrated by rotary evaporation; residual solvent was removed under reduced pressure overnight affording **41** (1.1 g, 2.2 mmol, 81%) as a white foam. ^{1}H NMR (300 MHz, DMSO-d_6): mixture of rotamers δ 12.69 (br s, 1H), 8.19 (apparent d, J = 5.9 Hz, 1H, Fmoc-N*H*), 7.89 (d, J = 7.4 Hz, 2H), 7.69 (t, J = 5.1 Hz, 2H), 7.42 (t, J = 7.3 Hz, 2H), 7.33 (t, J = 7.3 Hz, 2H), 4.35 (m, 2H), 4.20 (m, 2H), 3.89 (apparent dd, J = 10.6, 6.2 Hz, 1H), 3.66 (apparent s, 1H, overlap with –COOC*H*$_3$), 3.61 (s, 3H), 2.59 (m, 1H), 2.21 (m, 1H), 1.36 (s, 9H); ^{13}C NMR (75.4 MHz, DMSO-d_6): mixture of rotamers δ 173.3 and 172.8, 170.7, 155.5, 153.5 and 152.8, 143.6, 140.7, 127.6 (CH), 127.0 (CH), 125.1 (CH), 120.1 (CH), 79.4 and 79.3, 65.5 and 65.4 (CH_2), 63.5 and 62.8, 57.6 and 57.4 (CH), 54.0 and 53.7 (CH_2), 52.6 (CH_3), 46.6 (CH), 38.4 and 37.8 (CH_2), 27.9 and 27.8 (CH_3); IR (thin film): 3318, 3016, 2978, 1725, 1529, 1477, 1450, 1415, 1369, 1321, 1247, 1152, 1106, 1084, 931, 862, 758, 667 cm^{-1}; $[\alpha]_D$ +39.9° (c 1.06, $CHCl_3$); ESI-MS *m/z* (relative intensity): 411.1 (100%), 533.2 (65%), 1043.4 (85%, 2M + Na^+); HRESIQTOFMS calcd for $C_{27}H_{30}N_2O_8Na$ (M + Na^+) 533.1894, found 533.1912.

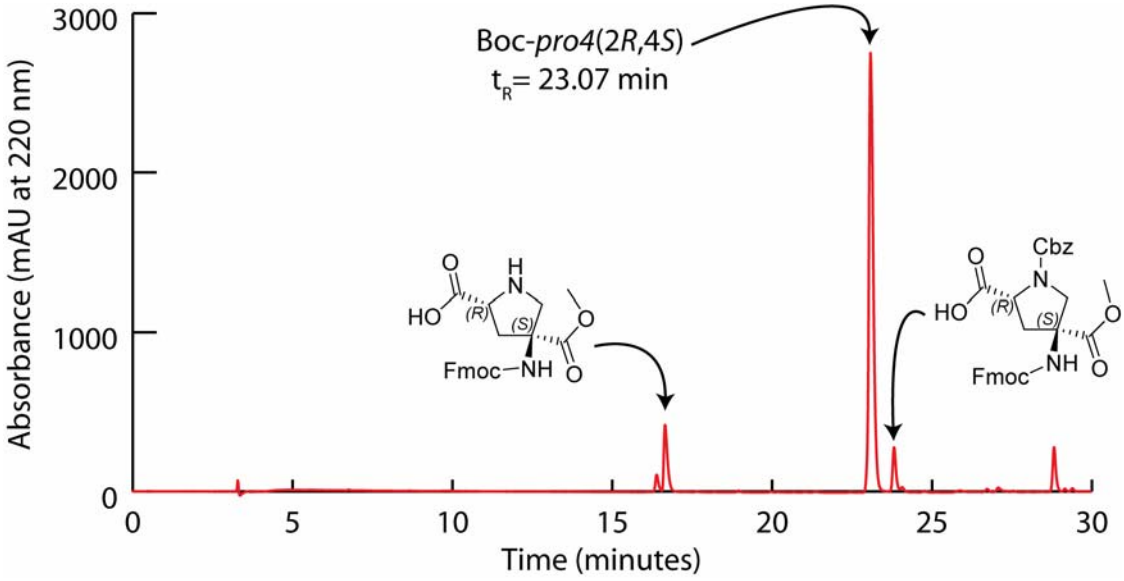

HPLC: C_{18} column; mobile phase, CH_3CN (0.05% TFA) / water (0.1% TFA), 5% to 95% CH_3CN over 30 min; flow rate, 1.00 mL/min; UV detection at 220 nm; t_R for **41,** 23.0 min.

Figure 2-16: HPLC chromatogram of Cbz to Boc exchange reaction (**40** to **41**) before the reaction was complete

3.0 OLIOGOMER SYNTHESIS AND NMR STUDIES

Ultimately, functional *bis*-peptide oligomers will be designed *in silico* and then rapidly synthesized in the laboratory. After measuring the properties of the oligomers, second-generation oligomers could be tailored *in silico* to optimize their structure and function. To realize this strategy, reliable and scalable methods must be developed for the synthesis of *bis*-peptide oligomers.

Three Cbz-*pro4*(2*S*,4*S*) monomers were coupled using Fmoc solid phase peptide synthesis. After removing the Cbz groups, simultaneous formation of the DKP rings between each of the monomer residues was achieved by basic catalysis. The connectivity and stereochemistry of the resulting trimer *bis*-peptide oligomer was confirmed by NMR; the conformation of the trimer in aqueous solution was determined based upon the 2D-NMR data and molecular mechanics calculations. A pentamer *bis*-peptide was synthesized in a similar manner to demonstrate the generality of the approach, and a model dimer oligomer was prepared to measure the rate of DKP formation under various basic conditions.

The possibility of achieving productive iterative cycles of *bis*-peptide design, synthesis, testing and redesign is based upon the hypothesis that the shape of *bis*-peptide oligomers can be modified in predictable ways by changing the sequence and stereochemistry of the constituent monomers. To start examining the relationship between *bis*-peptide shape and the stereochemistry and sequence of its constituent monomers, five tetramer oligomers were prepared. Each tetramer was assembled using various combinations of the four stereoisomers of the *pro4* monomer. The conformation of each tetramer in aqueous solution was determined by analysis of their respective 2D-NMR spectra and by molecular mechanics calculations.

3.1 SYNTHESIS OF A TRIMER BIS-PEPTIDE

Having developed a reproducible procedure for synthesizing the *pro4 bis*-amino acid monomers, we wanted to demonstrate the feasibility of *bis*-peptide synthesis. The structure of the first *bis*-peptide oligomer, **44**, is shown in Figure 3-1. The connectivity and stereochemistry of **44** were confirmed by interpretation of its 2D-NMR spectra. L-tyrosine was attached to the C-terminus of the oligomer as a UV-active chromophore to simplify HPLC analysis of intermediates. Tyrosine also increased the lipophilicity of the molecule; unlabeled *bis*-peptides are extremely polar, and are difficult to purify using C_{18} reverse phase HPLC.

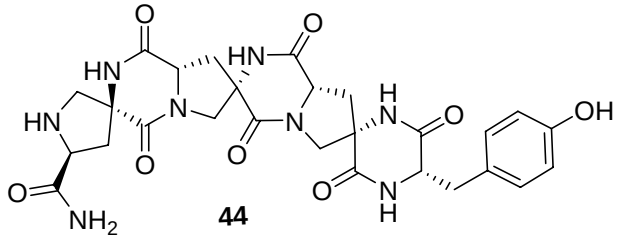

44

Figure 3-1: Structure of the first *bis*-peptide, **44**

3.1.1 Synthesis of trimer *bis*-peptide 44, part 1: chain elongation and resin cleavage.

The first part of *bis*-peptide synthesis is chain elongation. During this phase, the monomers are connected to one another sequentially on solid phase through amide bonds. The product of chain elongation is the "open-form" of the *bis*-peptide oligomer (the open-form of *pro4* monomer oligomers are γ-peptides).[120]

We selected Rink Amide AM resin (Scheme 3-1) as the solid support for the synthesis of **44**. Rink Amide AM resin is aminomethylpolystyrene (1% divinylbenzene cross linker) resin, functionalized with the Rink amide linker.[121] This resin is typically used for peptide synthesis using Fmoc-SPPS protocols.[58] Peptides are cleaved from the linker using 95% TFA with appropriate cation scavengers[122] affording C-terminal peptide amides.

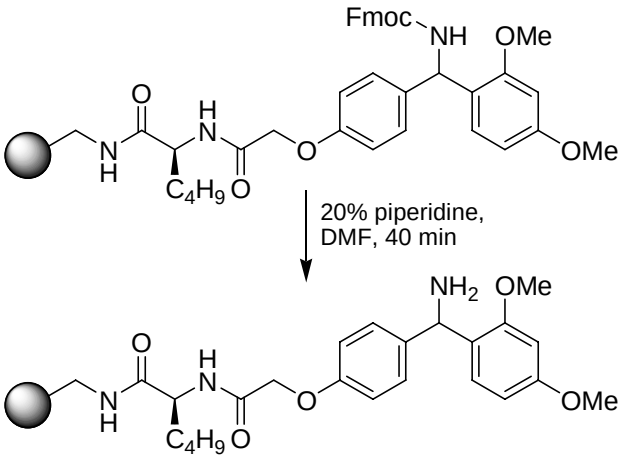

Scheme 3-1: The structure of the Rink Amide AM linker is shown (top). Removal of the terminal Fmoc protecting group from Rink Amide AM resin is achieved using 20% piperidine/DMF.

The Fmoc protecting group was removed from the resin linker using 20% piperidine in DMF (Scheme 3-1). The reported resin loading was confirmed by measuring the concentration of the dibenzofulvene-piperidine adduct (Figure 3-2) in the 20% piperidine/DMF solution.[123] This chromophore has a characteristic UV-absorption spectrum with a maxima at 301 nm (ε = 7800 M^{-1} cm^{-1}) and is used to quantify coupling yields during Fmoc-SPPS.

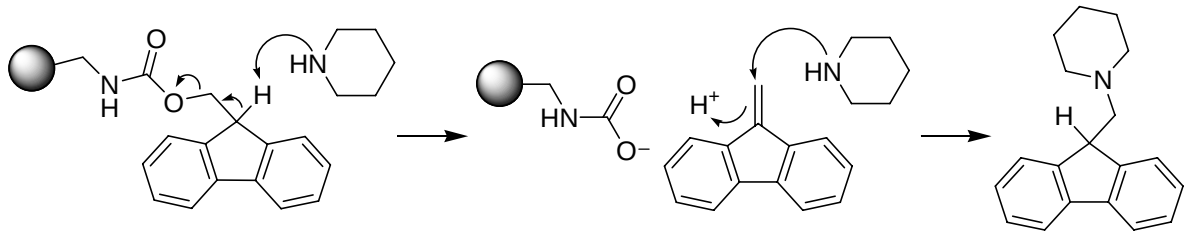

Figure 3-2: Removing the Fmoc carbamate with piperidine generates a dibenzofulvene-piperidine adduct with a characteristic UV-absorbance spectrum that may be used to quantify coupling yields.

After the Fmoc group was removed from the resin linker, the Cbz-*pro4*(2*S*,4*S*) monomer **18** was coupled to the resin (Scheme 3-2). We achieved quantitative coupling of **18** to the primary amine of the linker using coupling reagent HATU with DIPEA base in 20% CH_2Cl_2/DMF. Quantitative coupling was confirmed by performing the ninhydrin resin test[124] and by measuring the release of the piperidine-dibenzofulvene adduct during subsequent Fmoc removal.

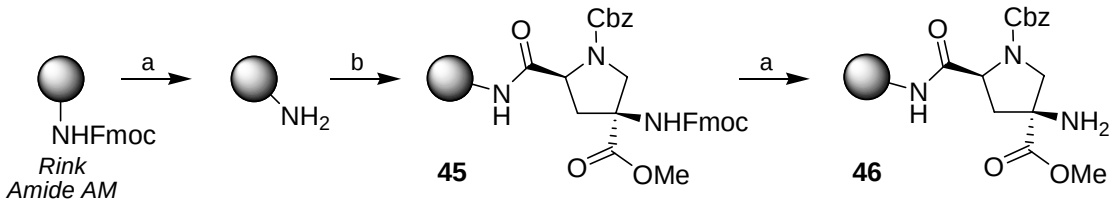

Reagents and Reaction Conditions:
(a) 20% piperidine/DMF, 40 min. (b) **18**, HATU, DIPEA, 20% CH_2Cl_2/DMF.

Scheme 3-2: The first Cbz-*pro4*(2*S*,4*S*) monomer was coupled quantitatively to the solid support using HATU.

The uronium salt HATU is a superior peptide coupling reagent[125,126] that is used extensively for activating sterically hindered amino acids.[127] Peptide fragments activated with HATU are less prone to racemization than fragments activated with analogous reagents, such as HBTU;[128] adding less-polar solvents (i.e., dichloromethane) to the DMF during coupling has been shown to further suppress racemization. The mechanism of amide bond formation with HATU is illustrated in Figure 3-3;[129] the increased reactivity of HOAt esters relative to analogous HOBt esters is hypothesized to be due to the neighboring group effect illustrated in Figure 3-3.[130] When used for the coupling of severely hindered amino acids, uronium reagents can generate guanidino side-products by reacting with the resin bound amine.[127] We have avoided this side reaction by mixing the monomer, base, and HATU before adding these reagents to the resin, and have not observed guanidinium formation during Cbz-*pro4*(2*S*,4*S*) monomer coupling. TFFH,[69,131,132] a uronium coupling reagent that generates acid fluorides, was also a suitable coupling reagent for the *pro4* monomer.

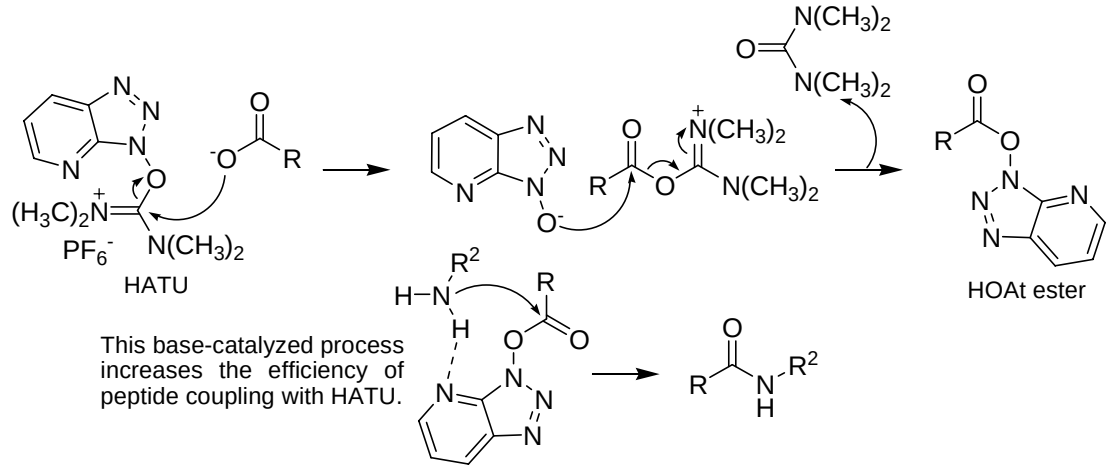

Figure 3-3: The mechanism of amide bond formation with HATU.

After removing the Fmoc group from the resin-bound monomer (affording **46**, Scheme 3-2) two additional monomers were coupled sequentially to the resin, followed by *N*-α-Fmoc-*O*-*tert*-butyl-L-tyrosine (Scheme 3-3). Removal of the Fmoc group also caused DKP formation between the tyrosine and the preceding Cbz-*pro4*(2*S*,4*S*) monomer residue, as expected (**48**, Scheme 3-3).[60,62,133] DKP formation was confirmed by analysis of the resin cleavage products by HPLC-MS (see below).

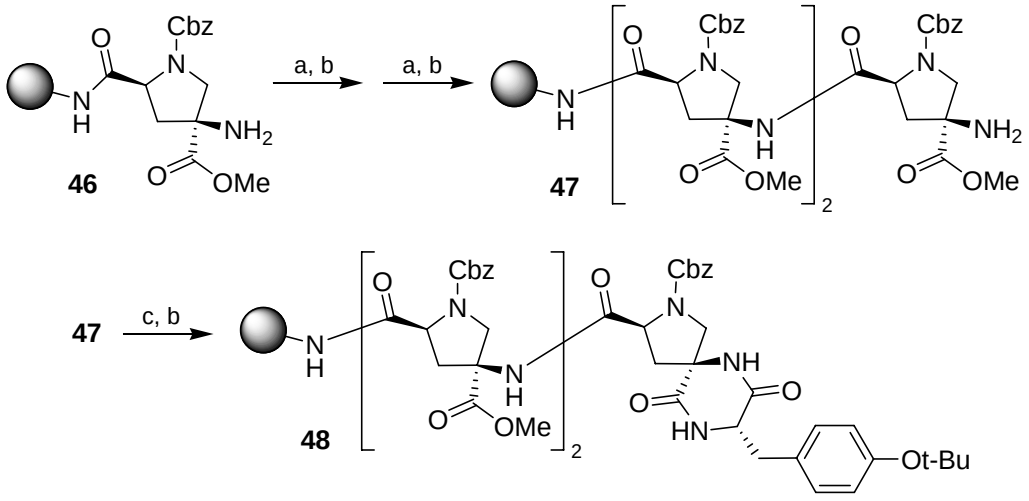

Reagents and Reaction Conditions:
(a) **18**, HATU, DIPEA, 20% CH_2Cl_2/DMF. (b) 20% piperidine/DMF. (c) *N*-α-Fmoc-O-*tert*-butyl-L-tyrosine, HATU, DIPEA, 20% CH_2Cl_2/DMF.

Scheme 3-3: Chain elongation of the oligomer on solid phase was achieved by sequential coupling and deprotection reactions.

Product **49** was obtained upon cleavage of resin **48** with 95% TFA containing triisopropylsilane[134] and water as cation scavengers. The expected mass of **49** was confirmed by HPLC-MS; the HLPC chromatogram of the crude resin cleavage product is illustrated in Figure 3-4. DKP formation between the tyrosine and preceding monomer residues was quantitative. Crude **49** was taken into subsequent reactions without further purification.

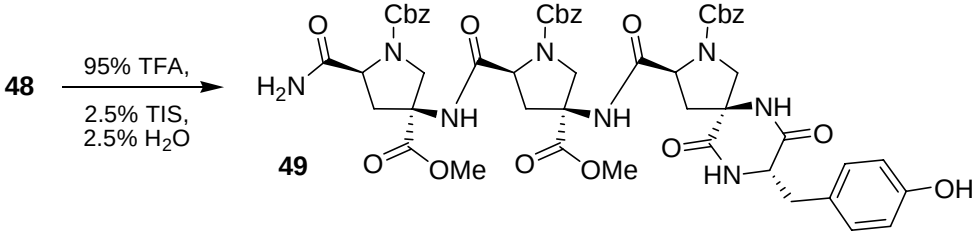

Scheme 3-4: 49 was obtained by cleaving resin **48** with 95% TFA containing cation scavengers.

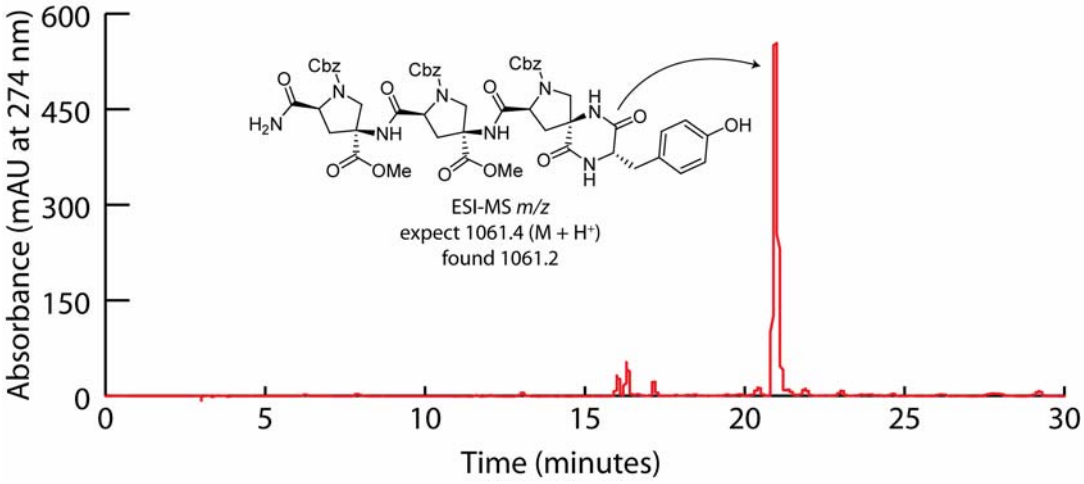

HPLC-MS: column, Waters XTerra MS C_{18}, 4.6 × 100 mm; mobile phase, H_2O (0.1% TFA) / CH_3CN, 5% to 95% CH_3CN over 30 min; flow rate, 0.40 mL/min; UV detection at 274 nm; t_R for **49**, 21.0 min; ESI-MS *m/z* (ion) 1061.2 ($M + H^+$).

Figure 3-4: HPLC chromatogram of crude **49** following resin cleavage

3.1.2 Synthesis of trimer *bis*-peptide 44, part 2: Cbz group removal and DKP formation.

Crude **49** was subjected to catalytic hydrogenation to remove the Cbz groups, affording the open-form oligomer **50** (Scheme 3-5). Methanol was not a good solvent for this reaction. When hydrogenation was performed in methanol, the starting material **49** was consumed, but very little of the desired product **50** could be recovered. The Cbz or Boc protected open-form *bis*-peptides (e.g., **49**) are non-polar, whereas the unprotected open-form *bis*-peptides (e.g., **50**) are polar. When the Cbz groups were removed, the product **52** either precipitated from the methanol solution and was filtered away with the catalyst, or was absorbed by the charcoal. Both **49** and **50** are soluble in mixtures of acetonitrile and water. Catalytic hydrogenation in this solvent mixture did remove all of the Cbz groups, but the free amines were quantitatively ethylated, presumably by reduced acetonitrile playing the role of an aldehyde.[135] 7:2:1 methanol/water/acetic acid proved to be an excellent solvent for this reaction (Scheme 3-5). Both the starting material and the product were soluble in this solvent mixture, and the reaction was complete in less than one hour. These solvent conditions suppress the formation of alkylated side-products; alkylation of the amines can occur when methanol alone is used as the

solvent.[136,137] An HPLC chromatogram of the reaction mixture following hydrogenolysis is illustrated in Figure 3-5.

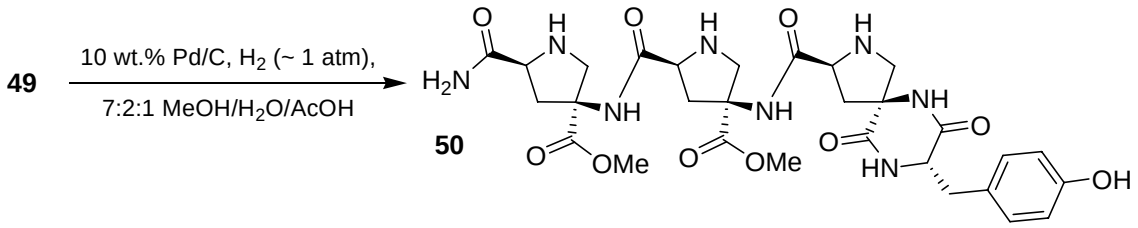

Scheme 3-5: Removal of Cbz groups from **49** by catalytic hydrogenation was achieved in less than one hour with 10 wt. % Pd/C in 7:2:1 MeOH/H_2O/AcOH under H_2, affording the Cbz-deprotected open-form oligomer **50**.

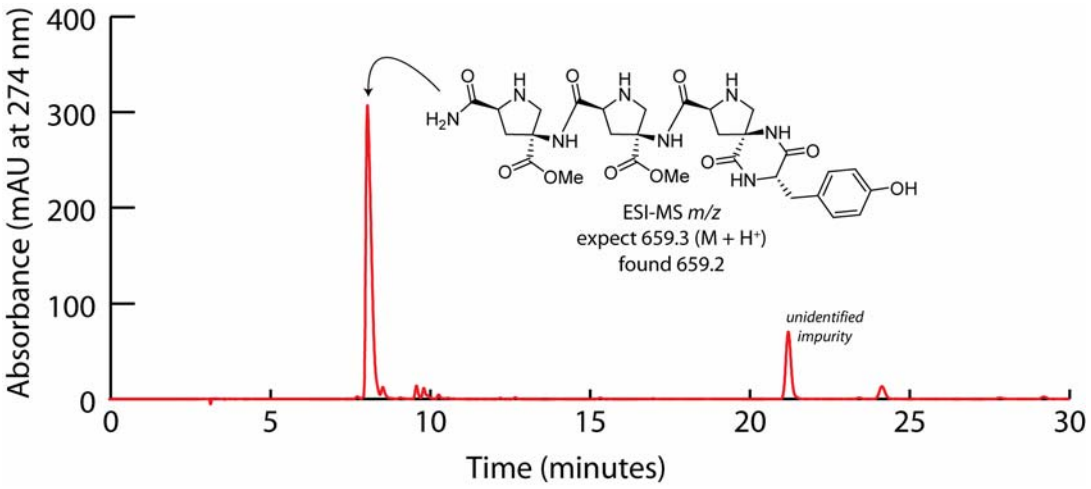

HPLC-MS: column, Waters XTerra MS C_{18}, 4.6 × 100 mm; mobile phase, H_2O (0.1% TFA) / CH_3CN, 5% to 95% CH_3CN over 30 min; flow rate, 0.40 mL/min; UV detection at 274 nm; t_R for **50**, 8.03 min; ESI-MS *m/z* (ion) 659.2 ($M + H^+$).

Figure 3-5: HPLC chromatogram of crude **50**, the product of catalytic hydrogenolysis of **49**

Closure of the remaining DKPs was not spontaneous in the 7:2:1 MeOH/H_2O/AcOH solution used for catalytic hydrogenation. At low concentrations, acetic acid can behave as a bifunctional catalyst for DKP formation;[60] in concentrated AcOH solutions, the pyrrolidine nitrogen atoms are protonated and non-nucleophilic. After concentrating the filtered hydrogenation solution, we found that it was possible to accelerate DKP formation by dissolving **50** in 20% piperidine/DMF (Scheme 3-6); these conditions accelerate unwanted DKP formation during Fmoc SPPS of α-peptides connected to the resin linker by a C-terminal ester (see Figure 1-11, page 9).[133]

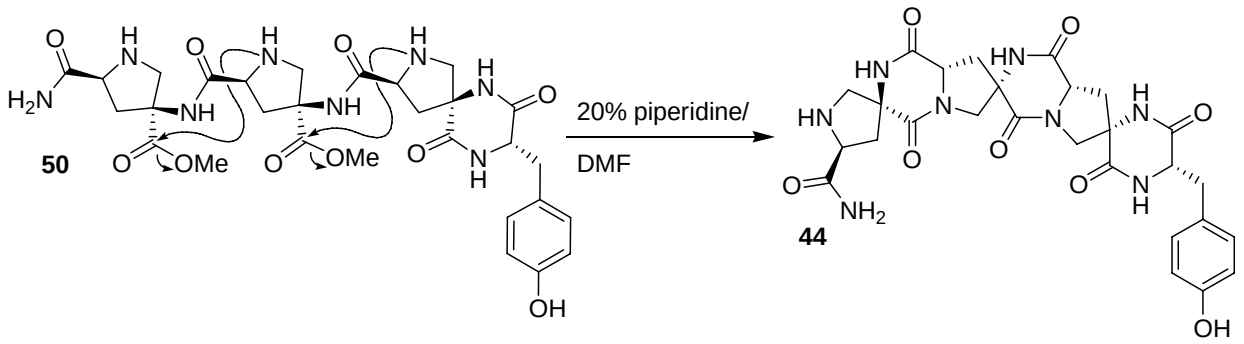

Scheme 3-6: The rigidified oligomer **44** was generated by dissolving **50** in 20% piperidine/DMF

The conversion of open-form oligomer **50** to *bis*-peptide **44** was difficult to monitor by HPLC. Although the starting material **50** was consumed, there appeared to be no corresponding evolution of the desired product **44**. Careful inspection of the reaction solution revealed a fine precipitate, as well as needle-like crystals. The amorphous precipitate was filtered from the solution and found to be pure **44** by HPLC-MS; X-ray crystallography indicated that the needle-like crystals were piperidine·HCl (the formation of piperidine salts during *bis*-peptide rigidification has since been avoided by using high-purity DMF and piperidine). The precipitation of **44** from the 20% piperidine/DMF solution accounts for why this product was not detected using HPLC analysis, and also provided a convenient way to purify the product.

A second batch of **50** was dissolved in 20% piperidine/DMF in a sealed HPLC vial and incubated for 48 hours at 2 °C (to facilitate product precipitation). The precipitate **44** was filtered, and found to be soluble in D_2O to more than 5 mg/mL. **44** was stable under neutral and acidic aqueous solutions at room temperature for weeks. The recovered yield of **44**, based upon the initial resin loading, was 17%. An HPLC chromatogram of *bis*-peptide **44** in D_2O solution is shown in Figure 3-6; this illustrating the exceptional purity of this *bis*-peptide oligomer, isolated without preparative HPLC purification.

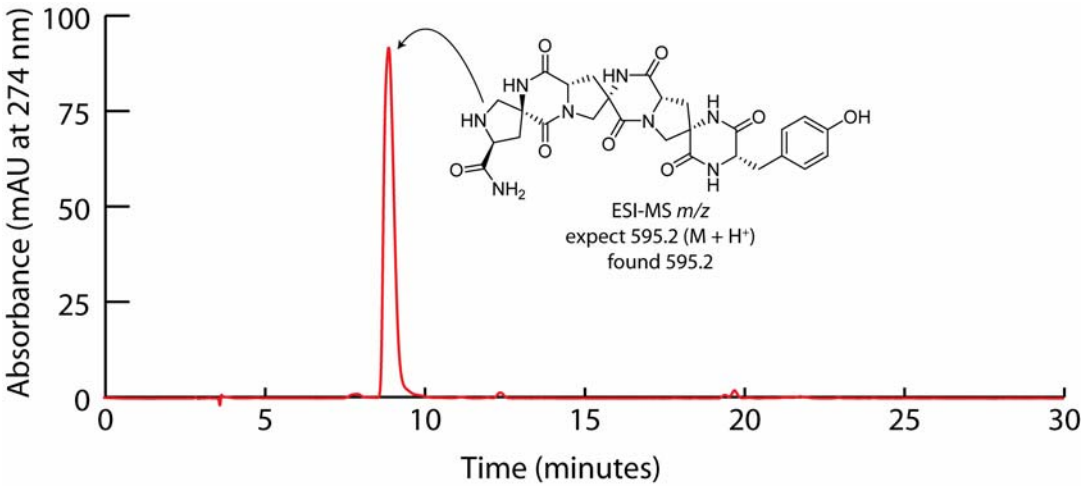

HPLC-MS: column, Waters XTerra MS C_{18}, 4.6 × 100 mm; mobile phase, H_2O (0.1% TFA) / CH_3CN, 5% to 20% CH_3CN over 30 min; flow rate, 0.40 mL/min; UV detection at 274 nm; t_R for **44**, 8.84 min; ESI-MS *m/z* (ion) 595.2 ($M + H^+$).

Figure 3-6: HPLC chromatogram of **44**, the first trimer *bis*-peptide oligomer

3.1.3 Structural analysis of trimer oligomer 44

To simplify discussion of the NMR results, we have adopted the naming system for *pro4 bis*-peptide oligomers illustrated in Figure 3-7 (right); the numbering of atoms and heterocycles in **44** is shown as well (left). The diastereotopic Cβ and Cδ hydrogen atoms on the same face as Hα of that pyrrolidine ring are called Hβa and Hδa, respectively. The pyrrolidine ring hydrogen atoms on the opposite face as Hα are called Hβb and Hδb.

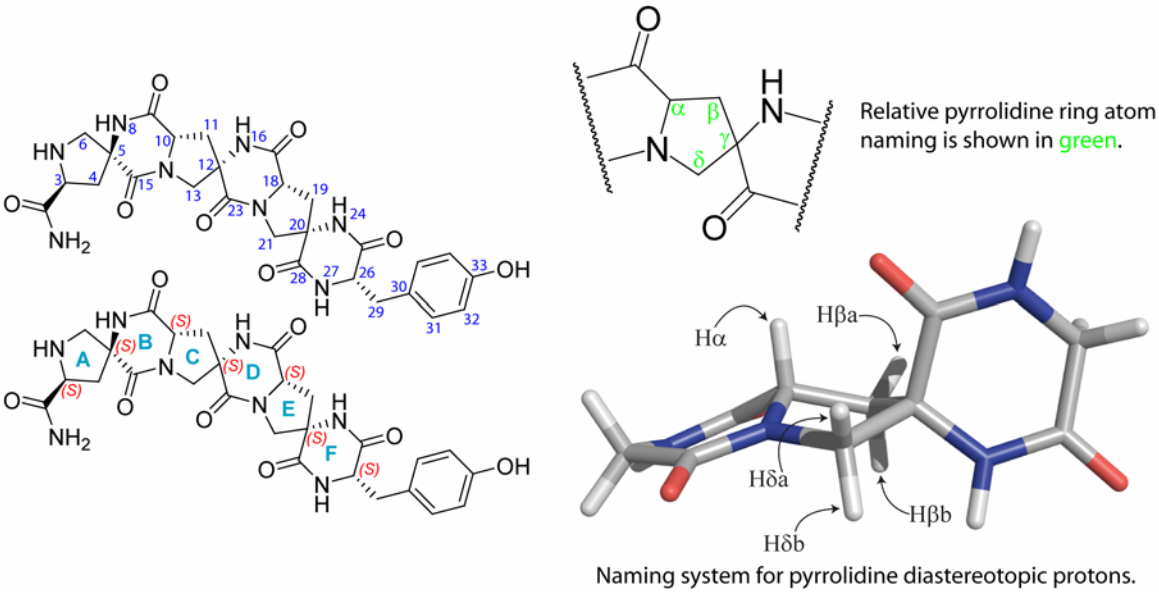

Figure 3-7: The naming system for trimer *bis*-peptide **44**. C–H–N atom number is labeled on the top structure in blue. Stereochemistry at each chiral center is labeled on the bottom structure in red. The names of the diastereotopic protons on the pyrrolidine rings are shown on the three-dimensional model.

To construct a model of oligomer **44**, we carried out an *in vacuo* conformational search using the Amber94 force field[138] within the molecular mechanics package MOE.[102] This search revealed a cluster of six lowest energy conformations (the blue markers on the plot in Figure 3-8). The mean energy of this cluster of six conformations is separated from the next highest energy cluster of conformations (yellow markers on the plot in Figure 3-8) by a gap of approximately 2.0 kcal/mole. This suggests that collectively, the molecule spends roughly 96% of its time in one of the six lowest energy conformations at room temperature. A superposition of these predicted lowest energy conformations (inset structures, Figure 3-8) reveals that rings B, C, D, E, F and the folded tyrosine conformation are nearly identical. The differences between these six calculated conformations involve combinations of rotamers around the C2-C3 bond, rotamers around the tyrosine –OH bond, and two envelope conformations of N-terminal pyrrolidine ring A.

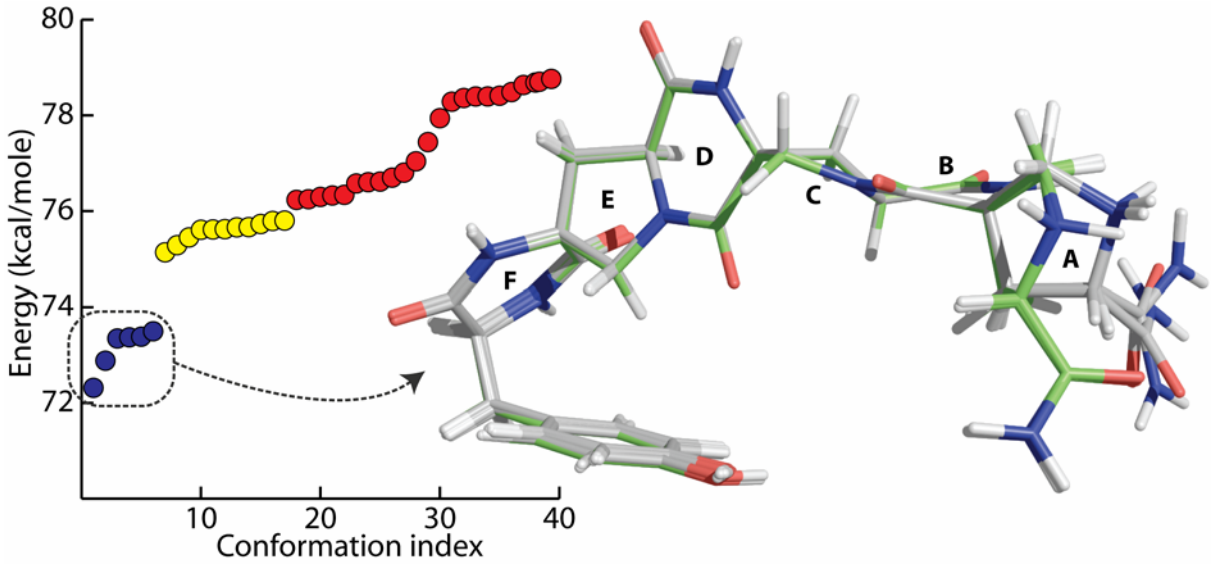

Figure 3-8: Plot of the Amber94 calculated energies for conformations of **44** generated by the *in vacuo* stochastic search (left). The six lowest energy conformations (blue markers) are superimposed (right). Carbon atom coloring in the pyrrolidine ring A flipped conformations has been changed to green for contrast. The names of the pyrrolidine and diketopiperazine rings are labeled.

In the modeled conformers, the diketopiperazine rings are shallow boats, and the α-protons are oriented in the axial position. This is consistent with NMR and X-ray crystallographic studies on the conformations of cyclic dipeptides.[63,139-141] For cyclic dipeptides containing proline, the preferred DKP conformation is boat-like, with axial α-protons (this conformation is referred to as "bowsprit boat"). The bowsprit boat DKP conformation maintains the planarity of the amide bonds, and avoids steric interference between the amino acid side chains.

The Amber94 molecular mechanics calculations also suggest that in the lowest energy oligomer conformations, the pyrrolidine rings assume an envelope conformation where atom Cβ is positioned out of the plane defined by Cα, Cγ, Cδ, and the pyrrolidine N-atom. In this conformation (the "Cβ displaced conformation"), Hβb and Hδb are closer to one another than Hβa to Hδa. This results in a unique pattern of transannular ROESY interactions characteristic of this pyrrolidine conformation. The Cβ displaced conformation appears to avoid a 1,3-interaction (a syn-pentane like interaction) between the quasiequatorial substituent on Cα and the substituents on Cγ.

Trimer *bis*-peptide **44** was readily soluble in water, so for the NMR studies we dissolved approximately 5 mg of the *bis*-peptide in 0.7 mL of D_2O. The ^1H NMR spectra indicated that the

sample was contaminated with piperidine trifluoroacetate; we used this as an internal standard for the NMR experiments. At room temperature, the HOD peak in the NMR spectrum completely overlapped the peak corresponding to α-proton H18. Accordingly, the NMR spectra were obtained with the sample at 10 °C; this shifted the HOD peak downfield by 0.16 ppm, allowing clear visualization of the signals from H18.

Although the NMR spectra obtained in D_2O (COSY, ROESY, HMQC, HMBC, ^1H and ^{13}C) were consistent with the proposed structure of **44**, deuterium exchange had silenced the signals from the amide protons. To compliment the analysis in D_2O, the sample was concentrated and dissolved in 90% H_2O/D_2O; 5 μL of TFA were added to the solution (final pH ~ 0). A similar set of NMR experiments were performed, but with pulse programs implementing presaturation of the solvent signal for the ROESY, COSY, and ^1H spectra. The amide protons produced interpretable signals under these conditions. Cooling the sample slows amide proton exchange with the solvent; performing the experiments with solvent suppression at low temperature increased amide proton signal intensity relative to the intensities observed at room temperature. Under acidic conditions, there were slight changes in the chemical shifts of some of the aliphatic protons (especially for α-protons H3, H10, and H26).

The cross-peaks in the ROESY spectra of the sample in D_2O and in H_2O/D_2O (pH ~ 0) were integrated, and designated as strong, medium, or weak. The Amber94 minimized conformation that we judged most consistent with the ROESY data is depicted in Figure 3-9.

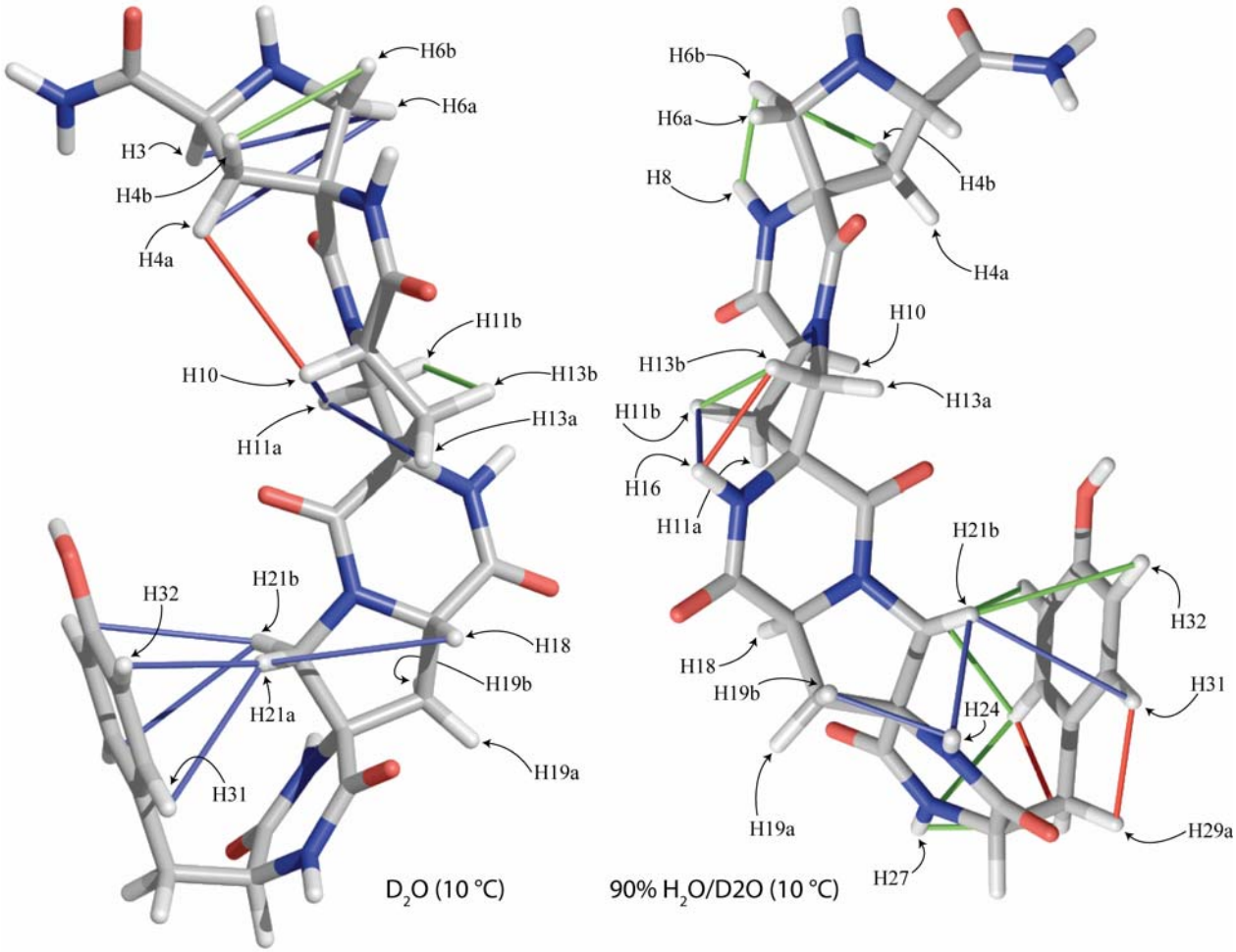

Figure 3-9: Both structures are illustrations of the modeled conformer of **44** found to be most consistent with the observed ROESY correlations. ROESY correlations from the spectrum obtained in D_2O are superimposed upon the left structure; ROESY correlations from the spectrum obtained in 90% H_2O/D_2O are superimposed upon the right structure. The thin red, green and blue cylinders represent strong, medium, and weak ROESY correlations.

The medium-intensity ROESY correlations between Hβb and Hδb for pyrrolidine rings A and C (H4b-H6b, H11b-H13b) contrast the weaker correlations between Hβa and Hδa (H4a-H6a, H11a-H13a, D_2O spectrum) supporting the Cβ displaced envelope conformation for these pyrrolidine rings. The strong trans-DKP H10-H4a correlation (which is visible in both ROESY spectra, but overlapped in the H_2O/D_2O spectrum) is also consistent with the ring A conformation illustrated. Furthermore, it supports the predicted boat conformation of DKP ring B. We had also anticipated a ROESY correlation across DKP ring D from α-proton H18 to β-proton H13a. Unfortunately, this region of the ROESY spectrum is overlapped by the interaction between H18-H19a.

The ROESY correlations between the Hβ and Hδ protons of pyrrolidine ring E are overlapped. Nonetheless, the weak H21a-H18, H24-H19b and H24-H21b correlations are not inconsistent with the modeled structure. DKP ring F is calculated to be boat-like, positioning the aromatic ring of the tyrosine residue aside the δ-protons of pyrrolidine ring E. This is supported by correlations between the aromatic ring protons and pyrrolidine ring E δ-protons (H31-H21a, H32-H21a) as well as by correlation H27-H31. The chemical shift of δ-protons H21a and H21b is about 1 ppm upfield from the analogous δ-protons on pyrrolidine rings A and C; this might be an effect caused by their proximity to the face of the aromatic ring.

Cyclic dipeptides containing tyrosine or phenylalanine have been studied by NMR and X-ray crystallography. The DKP rings in these structures are boats, and the aromatic substituent is oriented in the axial position,[139,141] in a manner similar to that proposed for **44**. Similar aromatic shielding NMR effects, like those observed for H21a and H21b, are described for the cyclic dipeptides. If DKP ring F were to flip to the other boat conformation, H26 would be positioned closer to H19a; in the D_2O ROESY spectrum, there is a very weak correlation between these protons. This suggests that ring F may have some conformational mobility, and spend some time in the opposite boat conformation. When modeled using the Amber94 force field without the Van der Waals energy term, the tyrosine aromatic ring tends not to fold back upon the scaffold, suggesting that these interactions may be responsible for the folded tyrosine conformation in solution. In water, this may also be due to the hydrophobic effect.

3.2 OLIGOMER PENTAMER SYNTHESIS

To demonstrate the generality of the approach used for the synthesis of trimer *bis*-peptide **44**, we prepared pentamer *bis*-peptide **53**, as illustrated in Scheme 3-7. Rink Amide AM resin was charged with *N*-Fmoc protected tyrosine. Five Cbz-*pro4*(2*S*,4*S*) monomers (**18**) were coupled sequentially to the tyrosine; **51** was then cleaved from the resin with TFA. The Cbz groups were stripped from the pyrrolidine nitrogen atoms by catalytic hydrogenolysis in 7:2:1 MeOH/H_2O/AcOH, yielding **52**. Finally, the open-form oligomer **52** was rigidified in 20% piperidine/DMF for 24 hours. The desired product, pentamer *bis*-peptide **53**, was isolated by

precipitation from ether. The overall yield of pentamer **53** was approximately 33%, based on the initial resin loading.

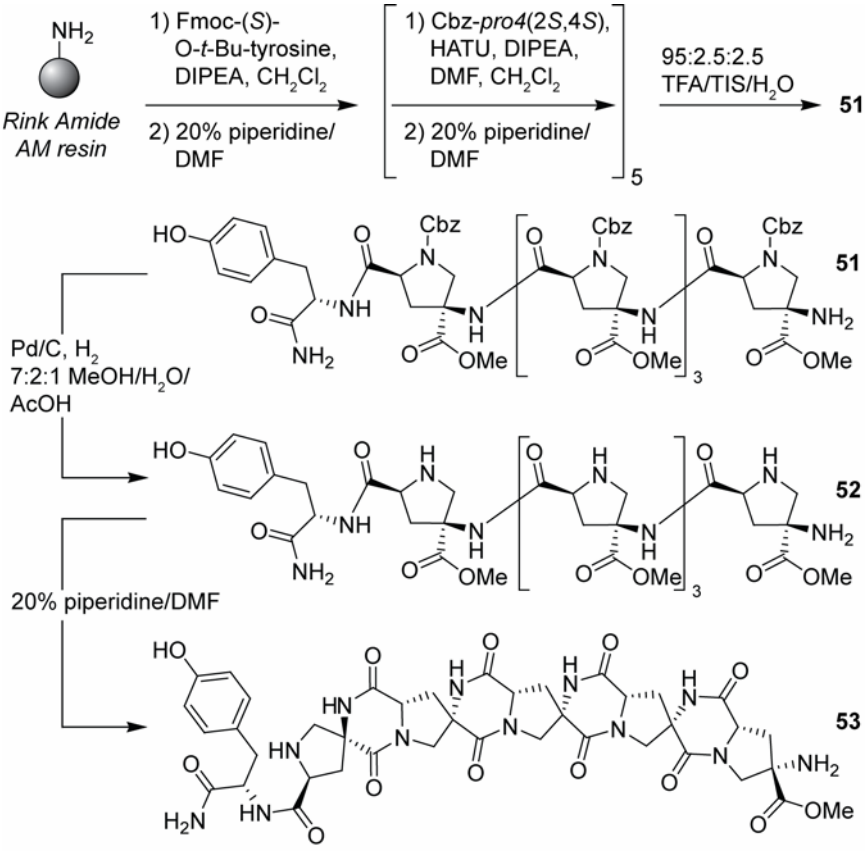

Scheme 3-7: The synthesis of pentamer *bis*-peptide **53**. The Cbz-protected open-form oligomer **51** is converted to open-form oligomer **52** by catalytic hydrogenolysis; the oligomer is rigidified with base, yielding *bis*-peptide **53**.

HPLC analysis of precipitated **53** shows that the product was remarkably homogeneous (Figure 3-10), despite the fact that intermediates **51** and **52** were not purified by chromatography. HPLC-MS analysis confirms that the major product has the same *m/z* ratio as the desired product, **53**. The crude pentamer material was soluble in 10% D_2O/H_2O to at least 5 mg/mL. We did not attempt to analyze the structure of **53** in solution using 2D NMR experiments because of extensive overlap in its ^1H NMR spectrum.

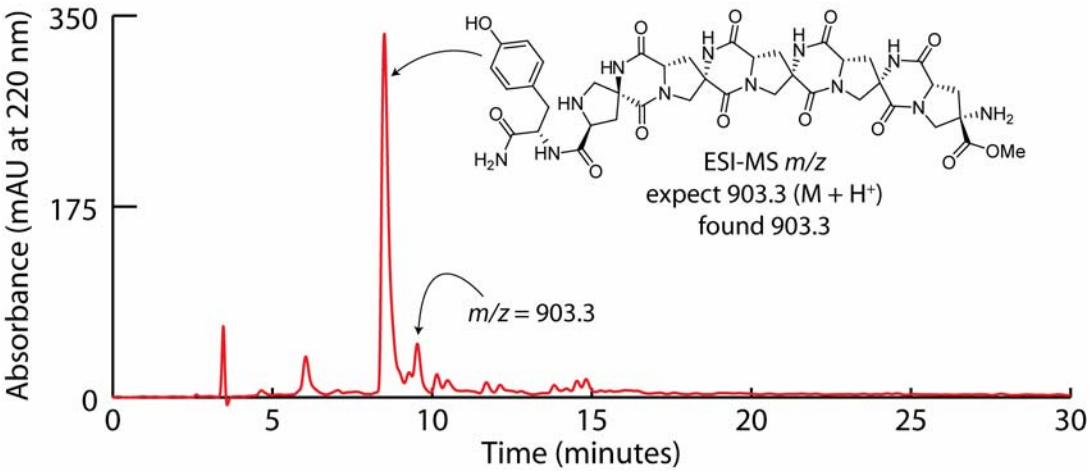

HPLC: column, Microsorb 100 C_{18}, 4.6 × 250 mm; mobile phase, CH_3CN (0.05% TFA) / water (0.1% TFA), 5% to 95% CH_3CN over 30 min; flow rate, 1.00 mL/min; UV detection at 220 nm; t_R for **53**, 8.50 min; ESI-MS *m/z* (ion) 903.3 ($M + H^+$).

Figure 3-10: HPLC chromatogram of crude pentamer *bis*-peptide oligomer **53**

The small peak indicated in the HPLC chromatogram of crude **53** (Figure 3-10) has the same ESI mass spectrum as the major product; it is probably an epimer of **53**. Epimerization proceeds through the carbanion (enolate) resulting from deprotonation at the chiral α-carbon atoms of the DKP.[65] N-methylated peptides and DKPs are prone to epimerization under basic conditions;[63,65,142,143] Gund and Veber accounted for the ease of N-methyl peptide and DKP epimerization computationally.[143] They calculated the energy required to deprotonate the α-proton from the cis and trans conformers of N-acetylglycinamide (Figure 3-11, box **A**) and N-methyl-N-acetylglycinamide (Figure 3-11, box **B**). The results of this computational study indicate that removing the α-proton is facilitated by N-alkylation and by enforcing the *cis*-peptide bond conformation.

The conjugate bases of the cis conformers (the "transoid" amino carbanions, Figure 3-11, box **E**) are more stable than the conjugate bases of the trans conformers (the "cisoid" amino carbanions, Figure 3-11, box **D**). One contributing factor is the dipole moment of the transoid amino carbanion, which is favorably opposed to the dipole moment of the amide C=O bond.

N-alkylation has both a direct and indirect effect upon deprotonation. The difference in energy between the cis and trans conformers of secondary amides (ΔE = 1.55 kcal for trans-cis isomerization shown in Figure 3-11, box **A**) is greater than the difference in energy between the cis and trans conformers of tertiary amides (0.20 kcal for the analogous isomerization shown in

Figure 3-7, box **B**). N-methyl amides and proline residues increase the population of cis-amide bonds in peptides.[144,145] N-alkylation thus indirectly promotes peptide epimerization by increasing the proportion of the cis conformation, which is easier to deprotonate. N-alkylation also has a direct effect upon deprotonation by stabilizing the amino carbanion through hyperconjugation.[146] Proline containing DKPs (Figure 3-11, box **C**), structurally similar to the DKP rings in the *bis*-peptides, are especially prone to epimerization because the amide bond is locked in the cis conformation, and because the amide nitrogen adjacent to the α-proton is alkylated.

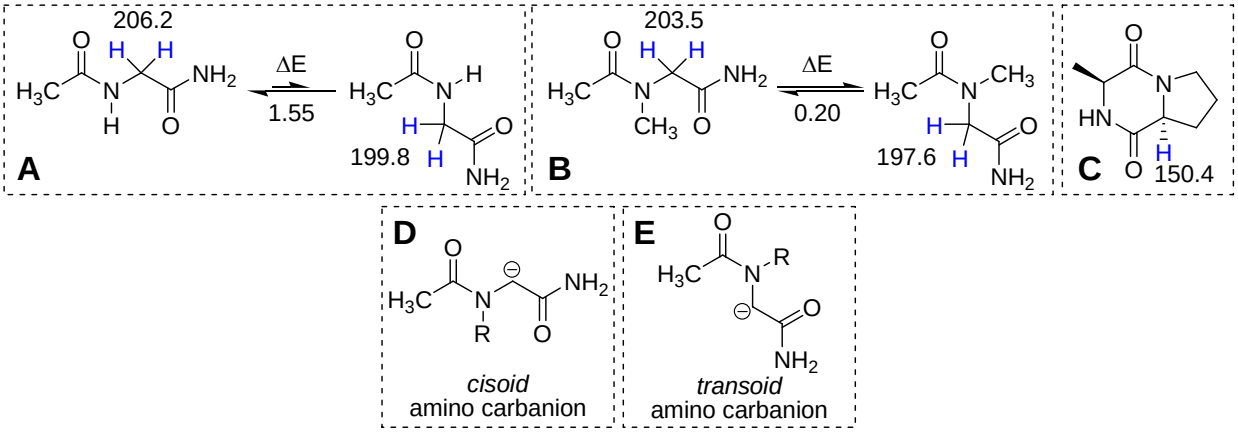

Figure 3-11: Energies (in kcal) required to remove protons adjacent to amides (blue protons in figure), as calculated by Gund and Veber.[143] The ΔE for the cis-trans isomerizations shown (from left to right) is given in kcal. Box **A**: cis and trans conformers of N-acetylglycinamide. Box **B**: cis and trans conformers of N-methyl-N-acetylglycinamide. Box **C**: *cyclo*-L-alanine-L-proline. Box **D**: a *cisoid* amino carbanion. Box E: a *transoid* amino carbanion.

3.3 MEASURING THE RATE OF DKP CLOSURE: EXPLORING DKP CLOSING CONDITIONS

Rigidification of trimer **44** and pentamer **53** by DKP formation was complete within 24 hours.[117] The small amount of epimerization that occurred during rigidification of pentamer *bis*-peptide **53** was probably due to the basic annealing conditions (20% piperidine/DMF) and the susceptibility of DKPs to epimerization. It was unclear at the time whether DKP formation would compete with epimerization during rigidification of very long *bis*-peptides. Because *bis*-peptide shape is related to its stereochemistry, analyzing the relationship between *bis*-peptide

structure and function requires that the oligomers retain the relative stereochemistry of their monomer constituents. We typically assume that the major product of rigidification with the desired *m/z* ratio has the expected stereochemistry; this has been proven the case for every *bis*-peptide that we have studied by NMR.[13-15,100,117] Unfortunately, NMR analysis of the oligomers is non-trivial, and cannot be used to test the stereochemical fidelity of every *bis*-peptide synthesized.

To start addressing the issue of the relative rates of epimerization and DKP formation, the rate of DKP formation was determined in a model *bis*-peptide. Compound **54** (Scheme 3-8) was synthesized by coupling tyrosine, two Cbz-*pro4*(2*S*,4*S*) monomers, then 4-nitrobenzoic acid sequentially to Rink Amide resin using HATU. To avoid reduction of the nitro group, the product was cleaved from the resin using triflic acid, which simultaneously removed the Cbz protecting groups from the monomer residues.[95] **54** is baseline separable from the product of DKP closure, **55** (Scheme 3-8, inset HPLC chromatogram). The desired product was **55**; under certain conditions, the methyl ester of **55** would hydrolyze, causing gradual formation of **56**.

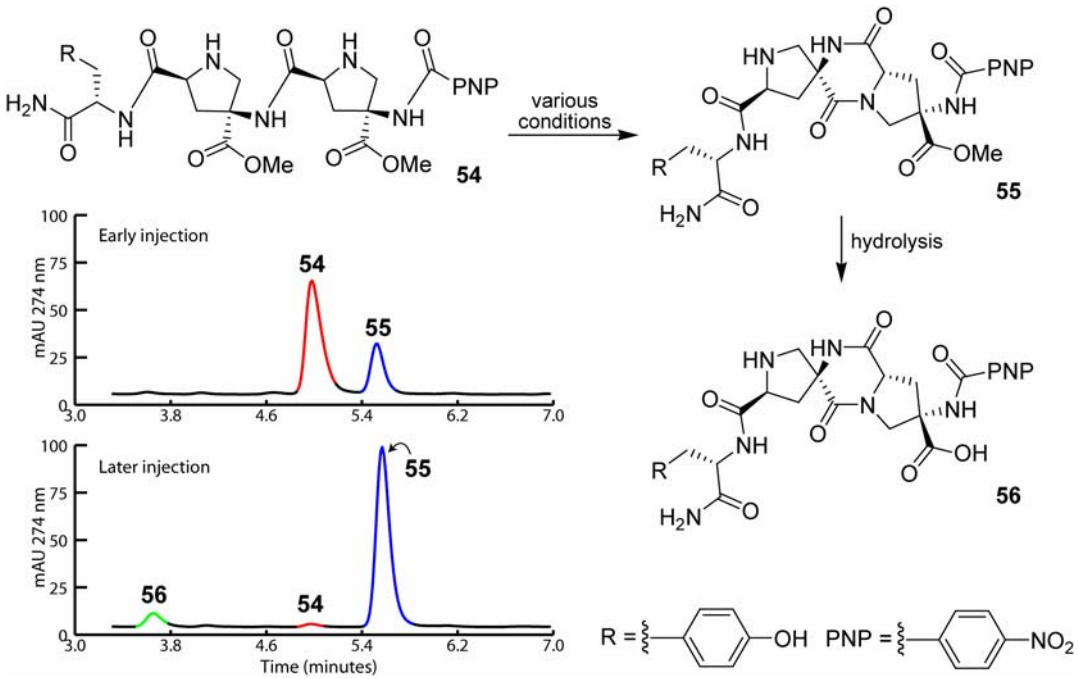

HPLC (inset): column, Microsorb 100 C_{18}, 4.6 × 250 mm; mobile phase, CH_3CN (0.05% TFA) / water (0.1% TFA), 28% to 35% CH_3CN over 5 min; flow rate, 1.00 mL/min.

Scheme 3-8: Compounds used or observed in the initial DKP closure study. The inset HPLC chromatogram (top) is representative of analysis of a sample from the DKP closure reaction early in the reaction; the second chromatogram is a later injection in the same trial.

The model dimer was dissolved in various solvents; the reaction was monitored by HPLC until complete. For each HPLC chromatogram, the UV-absorbance peaks corresponding to **54**, **55**, and **56** (Scheme 3-8, inset) were integrated, and the data was normalized. The progress of the DKP closing reaction for model compound **54** under each set of conditions is plotted with respect to reaction time in Figure 3-12.

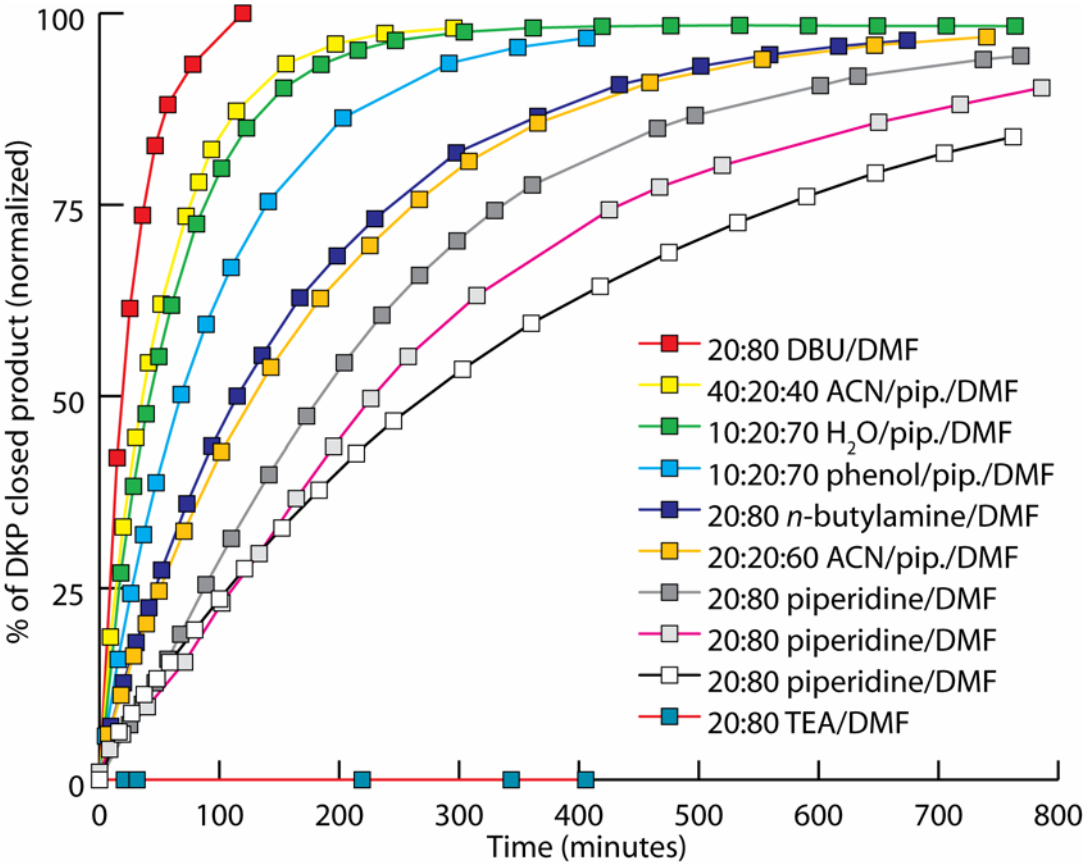

Figure 3-12: Plot of reaction progress during the conversion of **54** to **55** under various conditions

The rate of change in the concentration of the starting material **54** with respect to time was consistent with first order reaction kinetics, described by differential equation 3.1 (where [A] = [**54**]):

$$-\frac{d[\mathrm{A}]}{dt} = k[\mathrm{A}] \qquad \textbf{(3-1)}$$

The rate of the reaction, *k*, was determined for each set of conditions by plotting *ln*[**54**] with respect to elapsed reaction time and deriving the slope. These results from the DKP closure study are summarized in Table 3-1.

Table 3-1: Summary of the reaction rate data for the DKP closure model study

	Conditions	$k \times 10^3$ (min^{-1})	R^2 [a]	N [b]	$t_{½}$ (min) [c]	Notes
A	20:80 TEA/DMF	N/A			N/A	no DKP formation
B	20:80 pip.[d]/DMF (1)	2.4	0.9998	21	293	
C	20:80 pip./DMF (2)	3.0	0.9966	17	228	
D	20:80 pip./DMF (3)	4.0	0.9966	21	176	
					232	average, 3 trials
E	20:20:60 ACN/pip./DMF	4.9	0.9963	17	143	
F	20:80 *n*-butylamine/DMF	5.1	0.9965	19	137	
G	10:20:70 phenol[e]/pip./DMF	9.9	0.9999	9	70	slight hydrolysis
H	10:20:70 H_2O/pip./DMF	14.9	0.9995	9	47	13% hydrolysis at 12 hours
I	40:20:40 ACN/pip./DMF	17.7	0.9997	9	39	
J	20:80 DBU/DMF	34.7	0.9950	6	20	26% hydrolysis at 2 hours

(a) R^2 value for the linear curve used to calculate the rate constant (b) number of data points used for analysis (c) half-life of the reaction in minutes (d) piperidine (e) liquefied phenol

The average half-life of DKP closure using 20% piperidine/DMF at room temperature (the standard conditions for rigidifying *pro4* oligomers thus far)[15,100,117,118] is 232 minutes (~ 4 hours), but there was considerable variation between the 20% piperidine/DMF trials **A**, **B** and **C**. This may have been caused by variable water content in the samples prior to adding the piperidine and DMF. When water was added directly to the piperidine/DMF solution (trial **H**), the rate of DKP closure was much greater than the rate of trials **A**, **B** and **C**; hydrolysis of the methyl ester also occurred under these conditions. Although TEA did not accelerate DKP formation, piperidine and *n*-butylamine were both effective. DBU increased the rate of DKP formation significantly, but also the rate of methyl ester hydrolysis by adventitious water. Adding acetonitrile to the solvent mixture increased the rate of DKP formation (**E** and **I**); the $t_{½}$ for trial **I** was less than the average for piperidine alone by nearly a factor of six. Acetonitrile, and other aprotic dipolar protophobic solvents,[61,147] were reported to accelerate the rate of DKP closure.[61]

Based on the half-life of DKP closure between two *pro4* monomers, we can extrapolate the time that it might take to rigidify longer *bis*-peptides. For an oligomer containing (n + 1)

monomers, *n* DKPs must close during rigidification. Assuming that closing each DKP ring is an independent event (that closing any DKP ring in an oligomer does not affect the rate of closure for other DKP rings in the molecule) the probability that *n* DKPs have closed at time *t* is given by a derivation of the Poisson distribution (equation 3-2)

$$\mathrm{P}_n(t) = e^{-nkt}(e^{kt} - 1)^n \qquad \textbf{(3-2)}$$

where *k* is the rate of DKP closure. Using the average rate for DKP closure between two *pro4* monomers in 20% piperidine/DMF (~ 4 hours), rigidification of a pentamer would be 95% complete in around 25 hours; rigidification of a 25-mer would be 95% complete at 34 hours. The *bis*-peptides prepared for NMR studies were rigidified for greater than 24 hours; the major product of rigidification was the desired stereoisomer in each case. This suggests that the rate of epimerization is considerably slower than the rate of DKP formation between adjacent *pro4* monomers in 20% piperidine/DMF. While the addition of acetonitrile increased the rate of DKP formation for the model system, this is not generally applicable to solution phase rigidification because of problems with solubility. DKP formation with DBU was rapid, but seems ill-advised because this might also increase the rate of epimerization.

DKP formation between adjacent *pro4*(2*S*,4*S*) monomer residues has a half-life of ~ 4 hours in 20% piperidine/DMF. Unfortunately, these conditions are not effective for all of the *bis*-amino acid monomers that have been synthesized in our laboratory.[13,14,119] In 20% piperidine/DMF, DKP formation between adjacent *pip5*(2*S*,4*S*) monomer residues cannot be detected (Figure 3-13). For the *pip5* monomer class, Sharad Gupta has addressed this issue by several approaches: using coupling reagents to generate the second amide bond in the DKP,[13] closing the DKPs on solid support at high temperature with acetic acid as a catalyst,[60,61,119] and by changing the methyl ester to a better leaving group.[119]

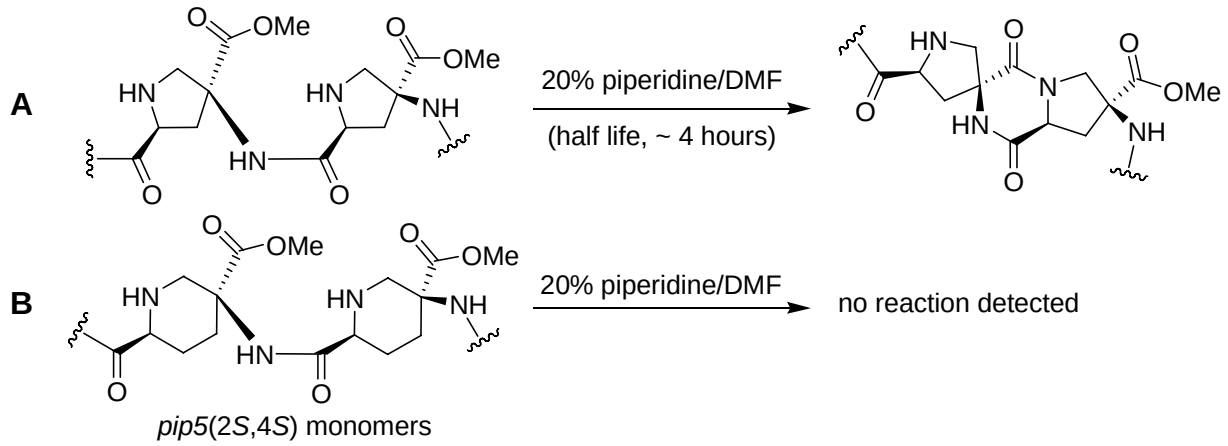

Figure 3-13: DKP formation between adjacent *pro4*(2*S*,4*S*) monomer residues with 20% piperidine/DMF (**A**, top) occurs at a reasonable rate. The analogous reaction between adjacent *pip5*(2*S*,4*S*) monomers (**B**, bottom) is immeasurably slow.

3.4 MONOMER STEREOCHEMISTRY AND *BIS*-PEPTIDE SHAPE: 1. *PRO4*(2*R*,4*R*) MONOMER

The trimer oligomer **44** is a linear, rod-like structure. The Amber94 minimized model of pentamer oligomer **43** is also a linear rod. Modeling suggests that every *pro4*(2*S*,4*S*) monomer increases the length of a *bis*-peptide by about 5 Å. Increasing the number of *pro4*(2*S*,4*S*) monomers increases the length of a *bis*-peptide; this effect has been measured qualitatively by FRET,[100] and quantitatively by ESR experiments.[118] *bis*-Peptides containing only the *pro4*(2*S*,4*S*) monomer may prove ideal for biological applications that require rigid, rod-like, water-soluble molecules.[42,51,54,148] To extend the scope of potential applications, access to a wider variety of oligomer shapes is required. We wanted to demonstrate that this was possible by simply incorporating different monomer stereoisomers.

Two *bis*-peptide tetramer oligomers containing combinations of the Cbz-*pro4*(2*S*,4*S*) monomer **18**, and its enantiomer, Cbz-*pro4*(2*R*,4*R*) monomer **29** were synthesized.[100] Structural analysis by NMR confirmed that it is possible to change the shape of a *bis*-peptide by changing the stereochemistry of its constituent monomers.

3.4.1 Oligomer synthesis

Our goal is to accurately predict the structures of large oligomers. Models of large bis-peptides will be based on the conformational preferences of each monomer in the context of its immediate neighbors. If we call the *pro4*(2*S*,4*S*) "A" and the *pro4*(2*R*,4*R*) monomer "B", then all possible sequences of three monomers are: AAA, AAB, BAA, BAB (and their respective enantiomers BBB, BBA, ABB, and ABA). The conformation of the central monomer of an AAA sequence was determined using trimer **44**.

To determine the conformation of the central monomer in the context of sequences AAB, BAA, and BAB, we synthesized *bis*-peptides **57** (sequence AABB) and **58** (sequence ABAB). The structure and naming of each of these tetramers is illustrated in Figure 3-14.

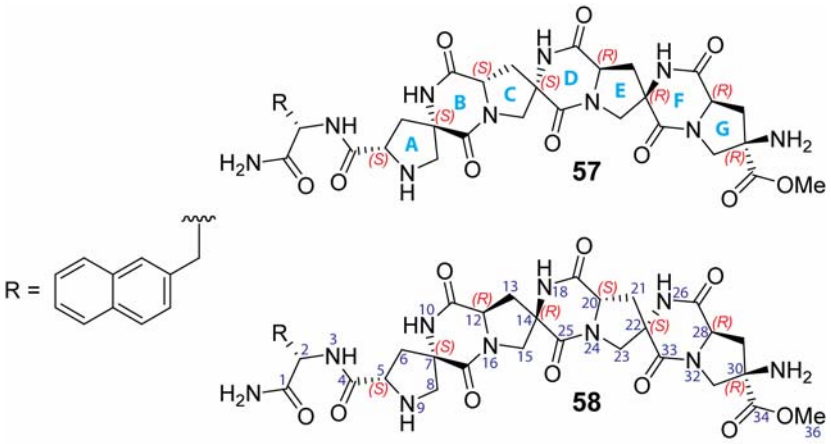

Figure 3-14: Tetramer *bis*-peptide oligomers incorporating different sequences of the *pro4*(2*S*,4*S*) and *pro4*(2*R*,4*R*) monomers: **57** (top), **58** (bottom). C–H–N atom number is labeled on structure **57** in blue. The stereochemistry at each chiral center is labeled in red. Heterocycle naming is indicated on **57** in cyan.

The synthesis of oligomers **57** and **58** is summarized in Scheme 3-9. Fmoc-(*S*)-2-naphthylalanine was coupled to Rink Amide AM resin using HATU. For **57**, Cbz-*pro4* monomers **18**, **18**, **29**, and **29** were coupled in sequence to the resin-bound naphthylalanine. For **58**, the sequence for monomer coupling was **18**, **29**, **18**, and **29**. The coupling reactions were performed for 30 minutes each with HATU as described for the synthesis of trimer **44** and pentamer **53**. Resin cleavage was affected by treatment with TFA. As there was no acid-sensitive functionality on either oligomer, we chose to remove the Cbz protecting groups using 8% triflic acid in TFA, affording open-form oligomers **59** and **60**. This procedure was fast,

relatively clean, and avoided the use of heterogeneous Pd/C catalyst, which tended to complicate recovery of the highly polar open-form oligomers.

The open-form oligomers **59** and **60** were dissolved in 20% piperidine/DMF. DKP closure was complete within 2 days at room temperature, affording the desired *bis*-peptides **57** (from **59**) and **58** (from **60**).

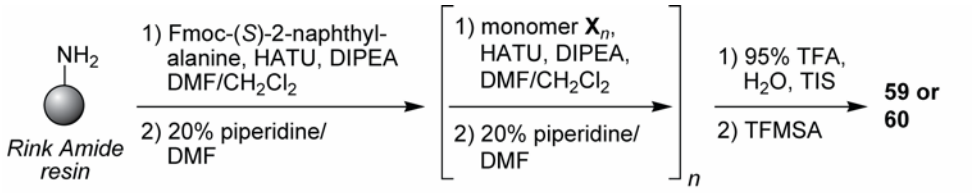

Oligomer	Cbz-*pro4* monomer $\mathbf{X}_n$ for coupling *n*			
	n = 1	*n* = 2	*n* = 3	*n* = 4
57 (from **59**)	**18** (2*S*,4*S*)	**18** (2*S*,4*S*)	**29** (2*R*,4*R*)	**29** (2*R*,4*R*)
58 (from **60**)	**18** (2*S*,4*S*)	**29** (2*R*,4*R*)	**18** (2*S*,4*S*)	**29** (2*R*,4*R*)

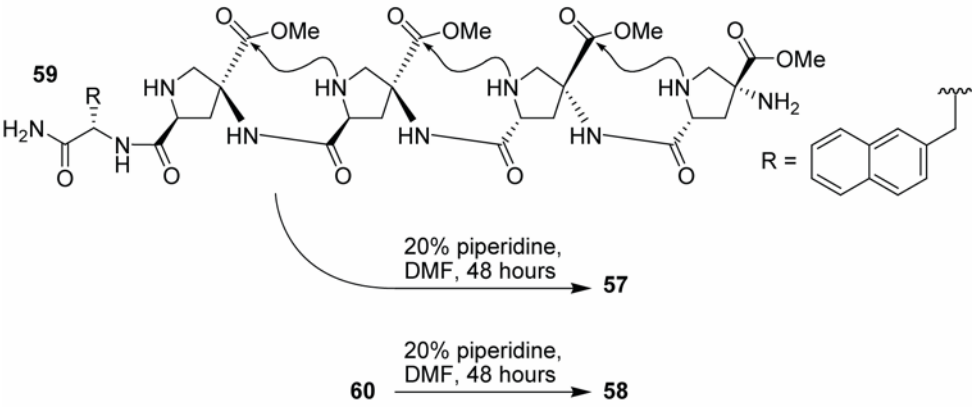

Scheme 3-9: Synthesis of oligomers **57** and **58**

3.4.2 Modeling and NMR analysis of tetramers 57 and 58

Tetramers **57** and **58** were both soluble in water, so the NMR experiments were performed in 9:1 H_2O/D_2O at a pH between 4 and 5. Amide proton exchange was suppressed by cooling the sample to 2 °C. The expected stereochemistry and connectivity of each tetramer was verified by analysis of their ROESY, HMBC, and COSY spectra; the composition of each was confirmed by high resolution mass spectroscopy.

As with the trimer *bis*-peptide, **44**, we generated working models of **57** and **58** by an *in vacuo* conformational search with the Amber94 force field[138] within MOE.[102] In the minimum

energy conformations, the diketopiperazine rings are, once again, shallow boats, with the Cα protons in the axial orientation. As with the proposed structure of the trimer oligomer, the pyrrolidine rings assume the Cβ displaced envelope conformation, avoiding the potential 1,3-interaction between the substituents on Cα and Cγ. The ROESY correlations between non-*J*-coupled protons were sorted by integrated intensity, classified as strong, medium and weak, and superimposed upon the modeled structures.

For **57**, the ROESY correlations were most consistent with the minimum energy Amber94 structure illustrated in Figure 3-15. The H8b-H6b, H15b-H13b, and H21b-H23b medium intensity correlations support the Cβ displaced conformations for pyrrolidine rings A, C and E. With the exception of the weak H23a-H21a correlation across pyrrolidine ring E, correlations across the opposite face of each pyrrolidine ring (Hβa-Hδa) are absent or overlapped.

The boat-like conformations of the DKP rings are supported by a number of strong trans-DKP correlations: H12-H6a, H20-H15a, and H28-H21a. The strong H20-H15a, medium H20-H15b, and weak H20-H15b correlations fit extremely well with the illustrated conformations of DKP ring D and pyrrolidine ring C. There is a similar patterns of ROESY correlations across DKP rings B and F consistent with the Cβ displaced conformation of pyrrolidine rings A and E. There are relatively few ROESY correlations for pyrrolidine ring G, which may be conformationally mobile.

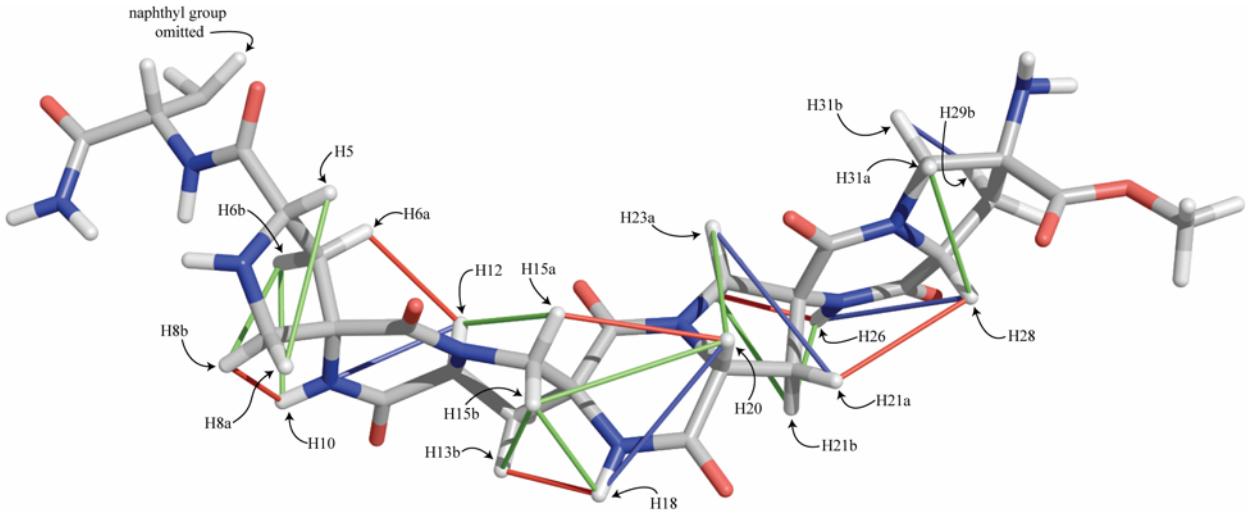

Figure 3-15: Illustration of the Amber94 minimized conformer of **57** most consistent with the observed ROESY correlations. The thin red, green and blue cylinders represent strong, medium, and weak ROESY correlations, respectively.

The minimized structure most consistent with the ROESY correlations for **58** is illustrated in Figure 3-16. The medium intensity correlations H6b-H8b and H13b-H15b suggest the Cβ displaced conformation for pyrrolidine rings A and C. The boat conformation of DKP B and Cβ displaced conformation of pyrrolidine A are consistent with correlations H12-H8a (strong), H12-H8b (medium), and H12-H10 (weak). There was a considerable amount of overlap in the ROESY spectrum of **58**. For instance, the trans-DKP ring D correlations from Hα proton H20 to H15b and H15a (Hδ protons on pyrrolidine ring C) were overlapped. Although it was not possible to integrate these peaks directly, by taking one-dimensional slices through the ROESY spectrum, the relative strengths of these correlations could be inferred.

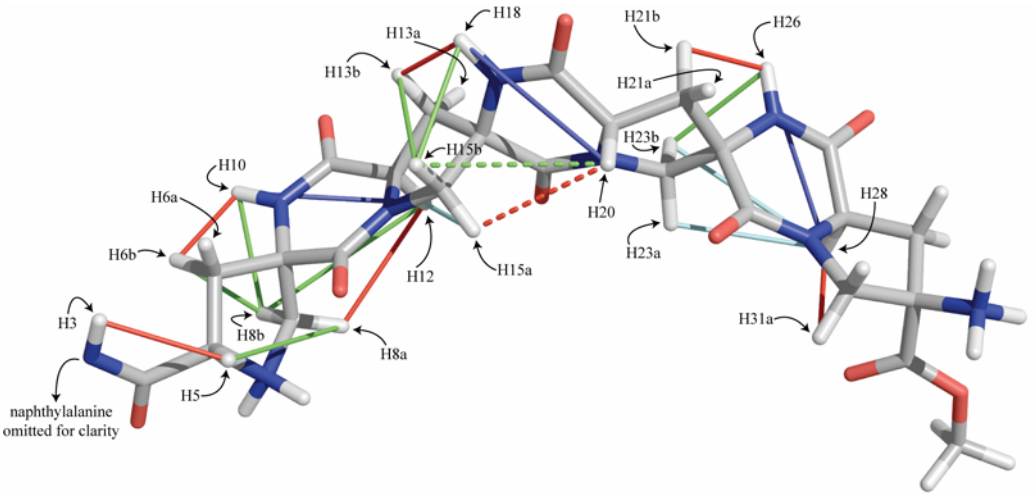

Figure 3-16: Illustration of the Amber94 minimized conformer of **58** most consistent with the observed ROESY correlations. The thin red, green, blue and cyan cylinders represent strong, medium, weak, and undefined ROESY correlations, respectively. The broken (dashed) cylinders correspond to ROESY correlations whose intensities were evaluated visually by examining 1D slices of the ROESY spectrum.

Both **57** and **58** have an alternating sequence of *pro4*(2*S*,4*S*) and *pro4*(2*R*,4*R*) monomer residues. The Amber94 minimized conformers for these structures are gently curved; the curvature of **58** is slightly greater than that for **57**. The shape imparted by this sequence motif was used to design a curved pentamer *bis*-peptide. The design hypothesis was tested by comparing the end-to-end distance of the curved structure with that of a linear structure by fluorescence resonance energy transfer (Chapter 4, page 111).

3.5 MONOMER STEREOCHEMISTRY AND BIS-PEPTIDE SHAPE: 2. INCORPORATING ALL MONOMER STEREOISOMERS

The library of four Boc-*pro4* monomers allows an arbitrary stereochemical configuration at any chiral center within a *bis*-peptide, and the means to direct hydrogen bonding groups in three-dimensional space along the length of the molecule. We synthesized three additional tetramers; each sequence was a permutation of all four members of the *pro4* monomer class. As for the previous structural studies, the ROESY data were used to select oligomer conformations generated by an *in vacuo* stochastic search with the Amber94 force field within MOE.

3.5.1 Oligomer synthesis

The structure and naming for each of the three *bis*-peptides is shown in Figure 3-17. Each tetramer contains a different permutation of all four stereoisomers of the *pro4* monomer. As with trimer **44**, tyrosine was incorporated into each as a UV tag and to ease purification.

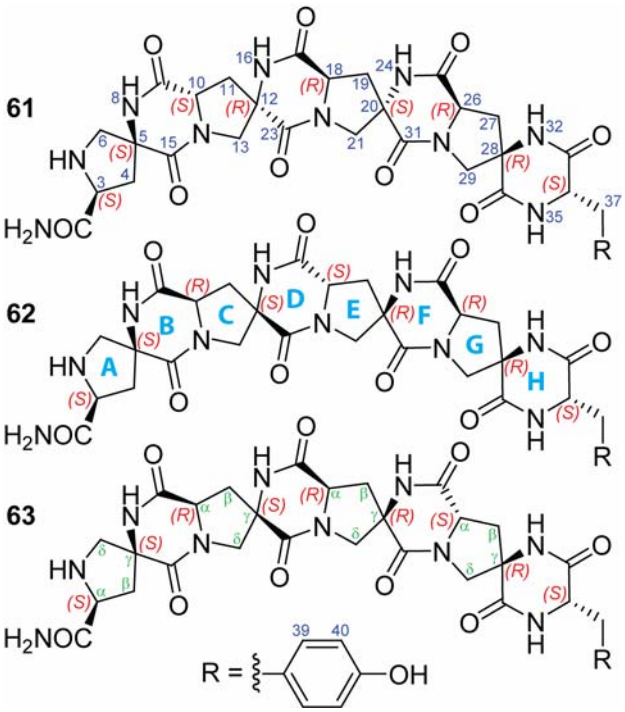

Figure 3-17: Tetramer *bis*-peptide oligomers incorporating permutations of all four stereoisomers of the *pro4* monomer: **61** (top), **62** (middle), **63** (bottom). C–H–N atom number is labeled on **61** in blue. Stereochemistry at each chiral center is labeled on each structure in red. Heterocycle naming is labeled on **62** in cyan. Relative pyrrolidine atom naming is illustrated in green on **63**.

For oligomer **61**, monomers **19**, **37**, **41**, and **30** were coupled sequentially to solid support, followed by Fmoc-L-tyrosine (Scheme 3-10). The synthesis was carried out on 100 mg of Rink Amide AM resin (0.64 mmol/g loading) using similar methods as those described for the synthesis of the previous tetramers (above). The product was cleaved from the resin by treatment with 8% triflic acid in TFA for 1.5 hours in an ice bath. The crude, open-form oligomer **64** was precipitated from diethyl ether to remove triflic acid. The precipitate was dissolved in a solution of 20% piperidine/NMP to rigidify the oligomer; after ~ 48 hours, the desired *bis*-peptide **61** was precipitated from ether, and purified by preparative HPLC. Oligomers **62** and **63** were prepared in similar fashion, as described in Scheme 3-10.

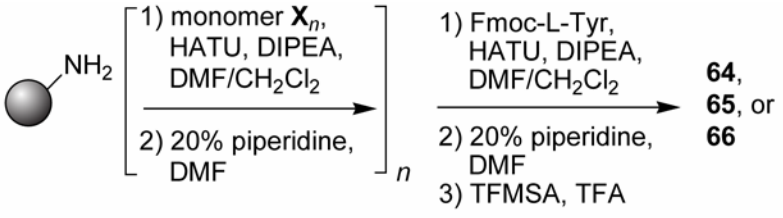

Oligomer	Boc-*pro4* monomer $\mathbf{X}_n$ for coupling *n*			
	n = 1	*n* = 2	*n* = 3	*n* = 4
61 (from **64**)	**19** (2*S*,4*S*)	**37** (2*S*,4*R*)	**41** (2*R*,4*S*)	**30** (2*R*,4*R*)
62 (from **65**)	**19** (2*S*,4*S*)	**41** (2*R*,4*S*)	**37** (2*S*,4*R*)	**30** (2*R*,4*R*)
63 (from **66**)	**19** (2*S*,4*S*)	**41** (2*R*,4*S*)	**30** (2*R*,4*R*)	**37** (2*S*,4*R*)

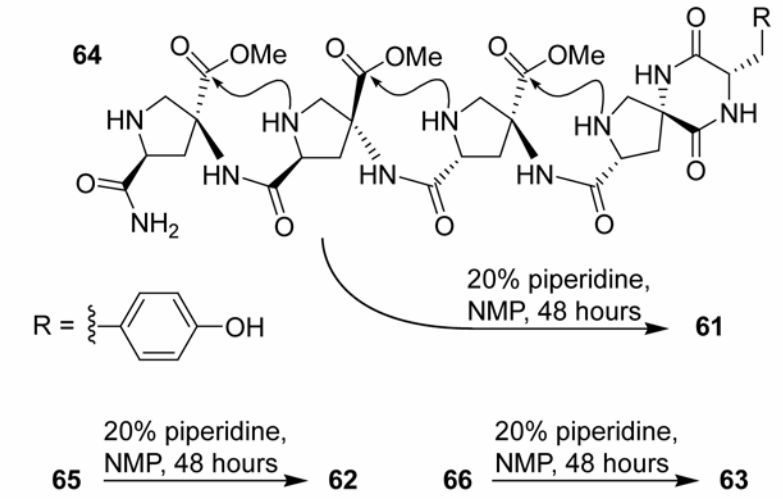

Scheme 3-10: Synthesis of oligomers **61**, **62**, and **63**

3.5.2 Modeling and NMR analysis of tetramers 61, 62, and 63

The structure shown for **61** in Figure 3-18 is identical to the Amber94 minimum energy conformation except for pyrrolidine ring E. The integrated intensities of the Hβb-Hδb correlations across pyrrolidine rings A, C and G (H4b-H6b, H11b-H13b, H19b-H21b, H28b-H29b) are four to five times greater than those for the corresponding Hβa-Hδa correlations, supporting the Cβ displaced conformation. The expected ROESY correlations across DKP ring D of **61** are occluded due to overlap, but the H10-H4a correlation suggests the predicted boat conformation of DKP ring B, and provides additional evidence for the Cβ displaced conformation of pyrrolidine A. Correlations between H27a and H27b with H39 and H40 evince the predicted boat conformation of DKP ring H, and suggest that the aromatic ring of the tyrosine residue is folded back against the backbone of the oligomer.

The conformation of pyrrolidine ring E of **61** (Cδ displaced rather than Cβ displaced, with Hβa closer to Hδa than Hβb is to Hδb) is unexpected. The integrated intensity of the H19a-H21a correlation is two times greater than the intensity of correlation H19b-H21b correlation, and the H26-H21b correlation across DKP ring F is four times the integrated intensity of the H26-H21a correlation.

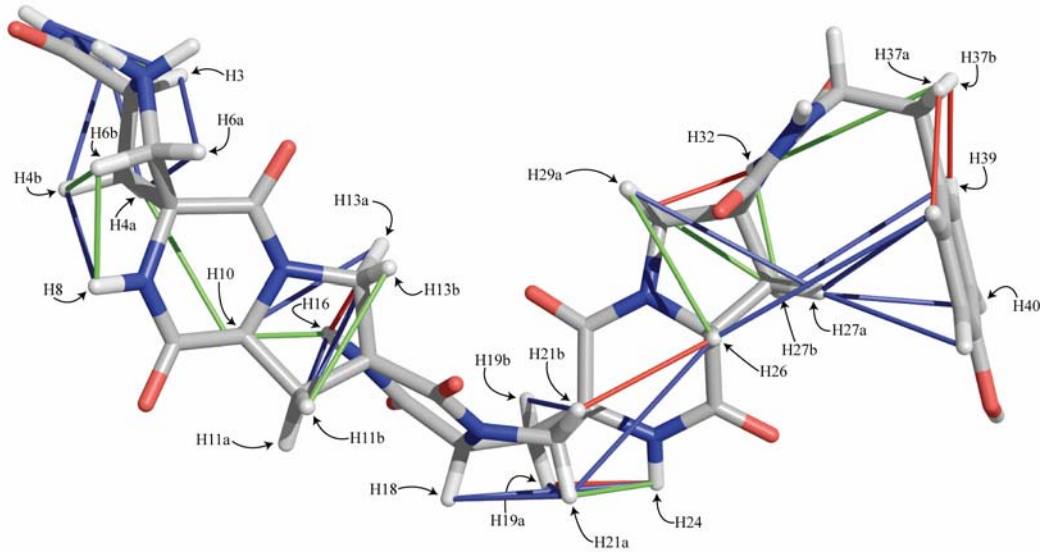

Figure 3-18: Illustration of the modeled conformer of **61** most consistent with the observed ROESY correlations. The thin red, green, and blue cylinders represent strong, medium, and weak ROESY correlations, respectively.

For compound **62**, the ROESY correlations were consistent with the minimum energy Amber94 structure shown in Figure 3-19. The four Hβb-Hδb correlations (H4b-H6b, H11b-H13b, H19b-H21b, H27b-H29b,) are three to five times greater in integrated intensity than the corresponding Hβa-Hδa correlations, suggesting the Cβ displaced conformation for every pyrrolidine ring. As with **61**, correlations across DKP ring D are overlapped. Nevertheless, the strong H10-H6a correlation supports the illustrated conformation of DKP ring B, while the strength of this correlation relative to H10-H6b (visibly weaker, but overlapped, preventing integration) supports the depicted conformation of pyrrolidine ring A. Furthermore, correlation H26-H19a, across DKP ring F, is ten times the intensity of the correlation H26-H19b, which lends support to the conformation of DKP ring F and the envelope conformation of E shown in Figure 3-19.

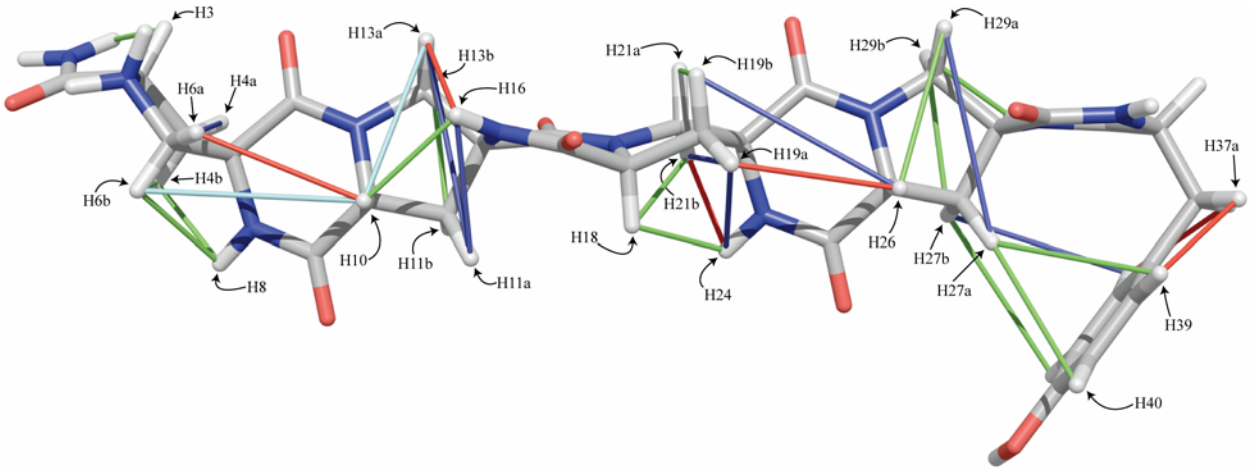

Figure 3-19: Illustration of the modeled conformer of **62** most consistent with the observed ROESY correlations. The thin red, green, blue and cyan cylinders represent strong, medium, weak, and undefined ROESY correlations, respectively.

The structure of **63** shown in Figure 3-20 is consistent with its Amber94 predicted minimum energy structure, except for pyrrolidine ring C. The Hβb-Hδb correlations across rings A, E, and G (H4b-H6b, H19b-H21b, H27b-H29b) are visibly stronger than the corresponding Hβa-Hδa interactions (though the integrated intensities are greater only by factors of 1.2 to 2.1) supporting the predicted Cβ displaced conformations. For pyrrolidine ring C, correlation H11a-H13a is slightly more intense (1.1 times) than H11b-H13b, suggesting the unexpected Cδ displaced conformation. The integrated intensities of the Hβa-Hδa correlations in **63** were similar to those between Hβb-Hδb, contrasting with the results for **61** and **62**, and providing only

weak support for the conformation of **63** shown. There are very clear ROESY correlations across all of the DKP rings of **63** (H10-H6a, H18-H13b, and H26-H21a which are five, nine and two times the intensity of H10-6Hb, H18-H13b, and H26-H21b, respectively) supporting the illustrated conformation of DKP rings B, D, and F, and for pyrrolidine rings A, C, and E.

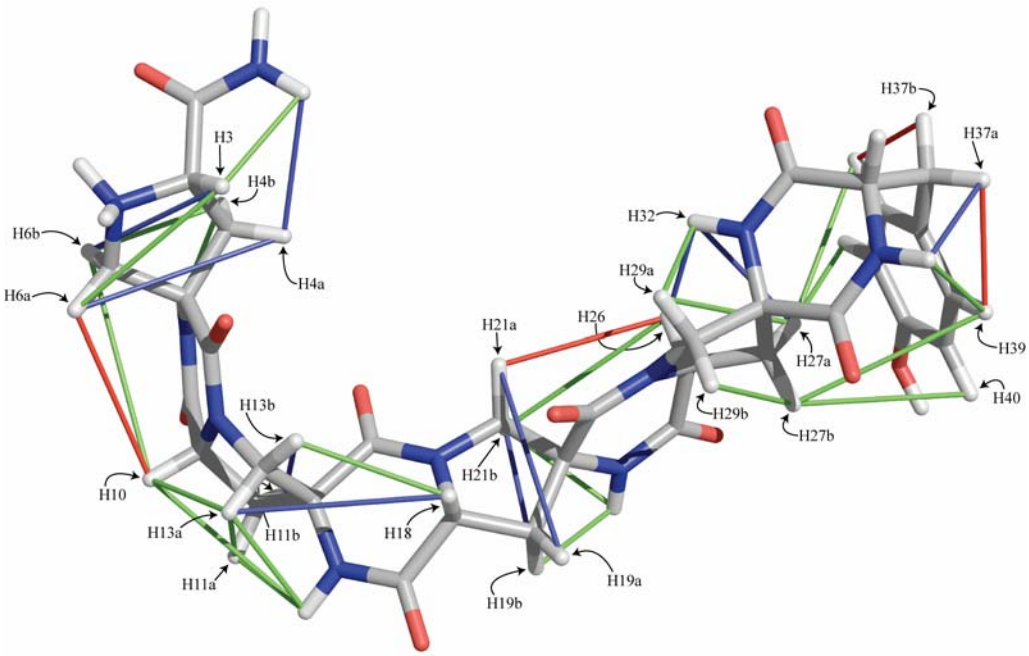

Figure 3-20: Illustration of the modeled conformer of **63** most consistent with the observed ROESY correlations. The thin red, green, and blue cylinders represent strong, medium, and weak ROESY correlations, respectively.

In **62**, the *pro4*(2*R*,4*S*) residue is clearly in the Cβ displaced conformation; it precedes a *pro4*(2*S*,4*R*) residue in this oligomer. In both **61** and **63**, where *pro4*(2*R*,4*S*) precedes a *pro4*(2*R*,4*R*) residue, there is strong evidence that its pyrrolidine ring prefers the Cδ displaced conformation. This suggests that the preferred envelope conformation of a particular residue may be context dependant.

DFT calculations suggest small energy differences between the Cβ displaced and Cδ displaced pyrrolidine conformations (<1 kcal/mol), with no strong preference for one ring conformation over the other.[117] Yet the NMR experiments suggest that the *bis*-peptides do have conformational preferences; the difference between experiment and theory may be due to solvent stabilization of one conformation over the other.

3.6 CONCLUSIONS

We have demonstrated the synthesis of a number of *bis*-peptide oligomers. The synthesis of *bis*-peptides occurs in two phases: assembly of the flexible oligomer by Fmoc-SPPS, and rigidification of the oligomer by forming a second amide bond between adjacent monomer residues. Among the numerous examples of molecular rods and scaffolds[2] these *bis*-peptides exhibit the rare property of water solubility, making them suitable for biological applications.[41,51,54,56,148] *bis*-Peptides containing the *pro4* monomer have rod-like three dimensional structures. All four stereoisomers of the *pro4* monomer have been incorporated into *bis*-peptides; NMR evidence suggests that curvature may be controlled by changing the stereochemistry of the constituent monomers.

The half-life of DKP formation between *pro4* monomer residues in 20% piperidine/DMF is around 4 hours; this is faster than the rate of DKP epimerization under the same conditions. Rigidification of *bis*-peptides in solution has been achieved numerous times. The method is reliable, and reaction progress can be monitored by HPLC-MS. On occasion, the product or intermediates of DKP closure have precipitated from the 20% piperidine/DMF solution; this proved beneficial in one case (for trimer **44**).

The method described for comparing the ROESY data to Amber94 minimized conformations is rather crude.[149] At best, comparing the relative intensities of the ROESY correlations may support or refute the modeled conformation; it does not necessarily rule out similar conformations. For example, calculations with the Amber94 force-field suggest that pyrrolidine ring C of **63** prefers the Cδ-displaced conformation (Figure 3-21, **A**). This conformer should have a particular pattern of trans-pyrrolidine ROESY correlations. Minimization of the same structure with a different force field (Amber89,[150] for instance) generates the Cγ displaced conformation (Figure 3-21, **B**). The pattern of ROESY correlations that result from the Cγ displaced conformation would be nearly indistinguishable from those arising from the Cδ displaced conformation. In fact, the energy difference between conformers **A** and **B** (Figure 3-21) is likely very small; the ROESY correlations may actually reflect the dynamic equilibrium between the two. Better modeling of the *bis*-peptides will require a more quantitative analysis of pyrrolidine conformation and dynamics.

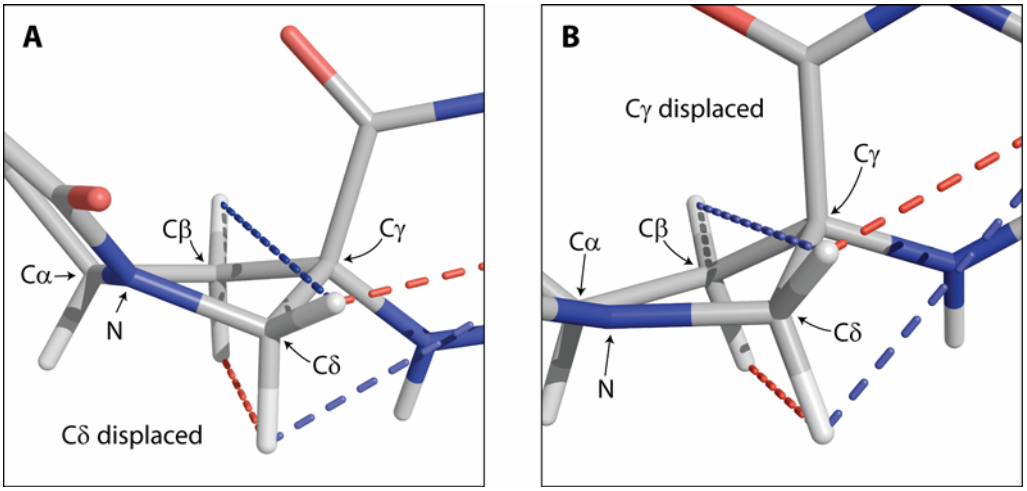

Figure 3-21: Comparison of the Cδ and Cγ displaced pyrrolidine conformations of an internal *pro4*(2*R*,4*S*) monomer residue in the context of a bis-peptide. Structure **A** (left) was minimized with the Amber94 force field, structure **B** (right) with Amber89. The dotted lines represent the expected ROESY correlation intensities for each conformation: red is strong, blue is weak.

3.7 EXPERIMENTAL DETAILS

3.7.1 General methods and procedures

High resolution mass spectrometry was performed on a Waters Micromass LC/Q-Tof Premier mass spectrometer using an electrospray ion source (HRESIQTOFMS). HPLC analysis was performed on a Hewlett-Packard Series 1050 instrument with a diode array detector, using a Varian Chrompack Microsorb 100 C_{18} column (5 µm packing, 4.6 mm × 250 mm) or Waters XTerra C_{18} column (3.5 µm packing, 4.6 mm × 150 mm). Preparative HPLC was performed on a Varian ProStar 500 HPLC system with a Varian Chrompack Microsorb 100 C_{18} column (8 µm packing, 21.5 mm x 50 mm). HPLC-MS analysis was performed on a Hewlett-Packard Series 1050 instrument with diode array detector, Agilent 1100 series LC-MSD detector (ES ion source) using a Waters XTerra MS C_{18} column (3.5 µm packing, 4.6 mm × 100 mm). UV-visible absorbance spectra were obtained using a Cary Bio-50 UV-visible spectrophotometer. ^{1}H, ^{13}C, and 2D NMR experiments were performed on a Bruker 500 MHz or 600 MHz instrument.

General Procedure A: reagents and equipment for solid-phase peptide synthesis (SPPS)

There is extensive literature explaining the techniques and best-practices for Fmoc solid-phase peptide synthesis.[18,59,123] SPPS was performed manually in fritted polypropylene reaction vessels using a homemade peptide synthesis apparatus (Supplemental Figure 96, page 292). Small reaction vessels (Note 1) were used for solid-phase synthesis on batches of resin between 5 and 15 mg. The tip of a glass pipette was heated in a flame and used to spot weld the frits to the bottom of the reaction vessels; this prevented the frits from dislodging during SPPS. Medium reaction vessels (Note 2) were used for batches of resin between 10 mg and 50 mg. Large reaction vessels (Note 3) were typically used for batches of resin exceeding 50 mg.

CH_2Cl_2 used in coupling reactions was distilled from CaH_2. Anhydrous DMF for coupling reactions and diketopiperazine formation was purchased from Aldrich; it was used as received. DIPEA was distilled from ninhydrin, and then under a nitrogen atmosphere from potassium hydroxide. After distillation, it was stored in amber bottles over activated 4 Å molecular sieves. HATU was obtained from Aldrich, Acros, or GenScript, and was used as received (Note 4). All solid-phase reactions were performed at ambient room temperature unless otherwise noted.

Notes on General Procedure A:

1. 1.5 mL polypropylene solid-phase extraction reservoirs were purchased from Alltech (part number 210001, frit part number 211401).
2. 10 mL polypropylene fritted PolyPrep columns were purchased from Bio-Rad (part number 731-1550), and did not require spot welding.
3. 20 mL polypropylene fritted EconoPac columns were purchased from Bio-Rad (part number 732-1010). The frits of the 20 mL reaction vessels were spot welded into place.
4. At the time of publication, HATU from GenScript was considerably less expensive than that purchased from Acros or Aldrich, and performed similarly in coupling reactions.

General Procedure B: resin mixing/agitation (argon bubbling)

To mix a suspension of solid-phase resin, argon gas was bubbled into the SPPS reaction vessel. Argon (Note 1) was passed through a drying tube containing granular calcium sulfate with indicator (Drierite, 10 to 20 mesh) into the argon pressure reservoir (Supplemental Figure

96). Argon flow to each SPPS reaction vessel from the pressure reservoir was limited using a needle valve (Note 2). The gas was bubbled through the frit of the solid-phase reaction vessel through the solution in which the solid-phase resin was suspended. The gas flow rate through the reaction vessel was carefully adjusted to gently churn and mix the resin suspension (Note 3).

Notes on General Procedure B:

1. Argon was purchased from Valley National Gases: catalog listing AR336, "industrial" grade.
2. The 1/4-28 threaded needle valves were purchased from Upchurch: catalog listing P-721.
3. If gas flow rate was too great, the solvents would evaporate (i.e., CH_2Cl_2 and DIPEA) or the suspension would become frothy.

General Procedure C: resin mixing/agitation (argon bubbling with stirring)

For reactions involving larger batches of resin (typically, greater than 50 mg of resin), argon bubbling did not provide adequate mixing of the resin suspension; the resin would clump and stick to the sides of the reaction vessel. To augment mixing by argon bubbling, a magnetic stir bar (7 mm × 2 mm) was placed into the solid-phase reaction vessel. The stir bar was actuated by a custom-built stir plate mounted near the outside of the solid-phase reaction vessel (Supplemental Figure 96). Larger stir bars (e.g., 10 mm × 3 mm) would grind the solid-phase resin, generating fine particles that clogged the frit of the reaction vessel.

General Procedure D: preparation of the solvent for coupling N^{α}-protected amino acids or *pro4* monomers using HATU

A 25 mL round bottom flask was removed from the oven (125 °C) (Note 1) and capped with a rubber septum. A needle connected to a positive pressure nitrogen line was inserted into the septum. A second needle open to air was then inserted into the septum. The flask was allowed to cool to room temperature while flushing with nitrogen. Anhydrous DMF (16 mL) and CH_2Cl_2 (4 mL) (Note 2) were transferred into the flask through the septum by syringe. The solution was mixed by swirling the flask. The needle open to air was removed from the rubber septum (Note 3).

Notes on General Procedure D:

1. The round bottom flask was kept in the oven for at least 4 h.
2. CH_2Cl_2 was distilled as described in General Procedure A.
3. Each batch of 20% CH_2Cl_2/DMF was used to prepare coupling reaction mixtures for 2 days. After 2 days, remaining solution was discarded, and a fresh batch of 20% CH_2Cl_2/DMF solution was prepared.

General Procedure E: resin washing

Residual solvent or reaction mixture was filtered from the resin by vacuum-assisted filtration. The appropriate reagent-grade solvent was transferred into the solid-phase reaction vessel using a squirt bottle. The volume of solvent was typically greater than 5 times the volume of solvent used for the coupling reactions (see General Procedure F). Care was taken to wash the inside walls of the reaction vessel using the squirt bottle. The resin was mixed in the solvent (using either General Procedure B, argon bubbling, or General Procedure C, argon bubbling augmented with magnetic stirring, depending on the amount of resin) from 1 to 3 min. The wash solvent was then removed from the resin using vacuum assisted filtration.

General Procedure F: coupling N^{α}-protected amino acids or *pro4* monomers using HATU

The amino acid or *pro4* monomer (2 equiv) (Note 1) was added to a 2 mL microcentrifuge tube (Notes 2, 3, 4), followed by HATU (2 equiv) (Notes 1, 5). Freshly prepared 20% CH_2Cl_2/DMF solution (see General Procedure D) was added to the microcentrifuge tube by syringe (0.2 M) (Note 6). Diisopropylethylamine (DIPEA, 4 equiv) (Notes 1, 7) was added to the mixture using an adjustable volume pipette (Notes 8, 9).

The microcentrifuge tube was capped, and the solution was mixed using a bench-top vortex mixer for ~ 3 s. The tube was centrifuged in a bench-top microcentrifuge (~ 5 to 10 s) (Note 10). The coupling solution was transferred from the microcentrifuge tube to the resin in the fritted solid-phase reaction vessel (see General SPPS methods, above) using an adjustable volume pipette (Note 8). The resin-solution suspension was mixed either by General Procedure B (argon bubbling) or General Procedure C (argon bubbling with magnetic stirring) for 30 min. The coupling solution was removed from the solid-phase reaction vessel by vacuum-assisted

filtration. The resin was washed with DMF, *i*-PrOH and DMF sequentially as described in General Procedure E.

After the resin wash, this procedure for the coupling reaction was usually repeated one time using exactly the same reagents and methods (Notes 11, 12).

Notes on General Procedure F:

1. Equivalents relative to resin loading
2. Microcentrifuge tubes were made of polypropylene.
3. The *pro4* monomers are shelf stable, and could be transferred into the microcentrifuge tubes days in advance of coupling. This decreased the time required to prepare for each coupling reaction during the course of SPPS.
4. No special care was taken to dry the polypropylene tubes.
5. HATU is relatively stable.[127] As a precaution, HATU was stored in a dessicator at room temperature and added to the microcentrifuge tube containing the amino acid or *pro4* monomer within 1 h prior to the coupling reaction.
6. 0.2 M in amino acid or *pro4* monomer.
7. Distilled DIPEA was used for the coupling reactions
8. Eppendorf "Research" adjustable volume micropipettor with Molecular BioProducts Aerosol Resistant Tips; no special care was taken to dry the pipette tips.
9. Upon the addition of DIPEA, the color of the solution would usually change from pale yellow to darker yellow.
10. After using the vortex mixer, the solution adheres to the sides and top of the microcentrifuge tube. Centrifugation forces all of the coupling solution to the bottom of the microcentrifuge tube so that it can be recovered easily.
11. Repeating a coupling reaction is known as "double coupling"; this is performed to ensure quantitative coupling. Resin beads adhere to the walls of the solid-phase reaction vessel and are potentially underexposed to the coupling solution during the first coupling cycle.
12. The resin wash between the first and second cycle of doubling coupling can be abbreviated by eliminating the intermittent *i*-PrOH washing step; this does not seem to affect the yield of the coupling reaction.

General Procedure G: resin "capping" with acetic anhydride

Reagent grade DMF (8 mL), acetic anhydride (2 mL) and distilled DIPEA (160 μL) were added to a 15 mL polypropylene Falcon® tube. The tube was capped and the solution was mixed using a bench-top vortex shaker. A portion of this solution was applied to the resin after it had been washed in DMF (see General Procedure D). After capping, the resin was usually washed with DMF, *i*-PrOH, and then DMF in the manner described in General Procedure D.

General Procedure H: Fmoc group deprotection on solid-phase

Reagent grade DMF (80 mL) was transferred into a 125 mL Erlenmeyer flask. Piperidine (20 mL) was added to the flask. The solution was mixed by gentle swirling, and the flask was capped with a polypropylene stopper (Note 1).

To remove the Fmoc group from a resin-bound amine, freshly prepared 20% piperidine/DMF solution was measured into the reaction vessel containing the resin using an adjustable volume Eppendorf pipette (Note 2). The resin-solution suspension was mixed using General Procedure B (mixing by argon bubbling) or General Procedure C (mixing by argon bubbling and magnetic stirring) for 40 minutes (Note 3). After 40 minutes, the mixing was stopped, and the resin settled to the bottom of the solid-phase reaction vessel.

An aliquot of the deprotection reaction mixture was taken from the top of the solution and added to 20% piperidine/DMF in a 1 cm UV-absorbance cell (Note 4). The sample was mixed by pipetting the solution up and down several times using a 2 mL glass pipette with a rubber bulb. The UV-absorbance spectrum of this solution was measured between 250 nm and 350 nm. The absorbance spectrum of the 20% piperidine/DMF solution was subtracted from the UV-absorbance spectrum of the sample. The absorbance of the processed spectrum at 301 nm was recorded (Note 5).

Following Fmoc deprotection, the resin was washed with DMF (~ 3 ×), i-PrOH (~ 3 ×) and DMF (~ 3 ×) using General Procedure E (Notes 6, 7).

Notes on General Procedure H:

1. The 20% piperidine/DMF solution was used for the removal of Fmoc groups during SPPS, and to dilute samples from the deprotection reaction solution (for quantifying coupling reaction yields by measuring the UV-absorbance of the released dibenzofulvene-piperidine

chromophore). After 2 days, residual solution was discarded, and a fresh batch of 20% piperidine/DMF was prepared.

2. 1 mL of 20% piperidine/DMF was typically used for small batches of resin (25 mg of resin or less). 2 mL to 5 mL of the 20% piperidine/DMF solution was typically used for larger batches of resin. The volume was chosen such that the resin could tumble freely within the solution during the deprotection reaction.
3. The reaction time for Fmoc deprotection has been abbreviated to 30 minutes without an appreciable effect on the reaction yields.
4. Aliquot size was chosen based upon the theoretical loading of the resin, and upon the volume of 20% piperidine/DMF in the UV cell. The dilution factor was chosen so that the absorbance of the solution in a 1 cm cell was roughly 1 AU (within the linear range of the spectrophotometer).
5. $\varepsilon = 7800\ M^{-1}\ cm^{-1}$ for the dibenzofulvene-piperidine adduct in 20% piperidine/DMF at room temperature.
6. Special care was taken to wash the inner walls of the solid-phase reaction vessel after Fmoc deprotection to remove all traces of residual piperidine solution.
7. The resin was washed with either DMF or 20% CH_2Cl_2/DMF prior to the next coupling reaction.

General Procedure I: resin washing and treatment prior to linker cleavage

After completing SPPS, the solid-phase resin was generally washed with DMF, *i*-PrOH, DMF, CH_2Cl_2, MeOH, and finally CH_2Cl_2 as described in General Procedure E. After the final wash with CH_2Cl_2, the reaction vessel was removed from the SPPS apparatus and the top was sealed with a polypropylene cap. Residual solvent was removed from the resin under reduced pressure.

3.7.2 Details for synthesis of trimer bis-peptide 44 and intermediates

Compound 49

Rink Amide AM Resin (72 mg resin, 46.1 μmol loading) was transferred into a 10 mL fritted polypropylene SPPS reaction vessel. DMF (~ 5 mL) was added to the reaction vessel; the resin

was swollen in the DMF solution with argon bubbling (General Procedure B). The Fmoc group was removed from the Rink Amide linker using 20% piperidine/DMF (General Procedure H). The resin was then washed with DMF, *i*-PrOH and 20% CH_2Cl_2/DMF (General Procedure E). Cbz-*pro4*(2*S*,4*S*) monomer **18** (50.2 mg, 92.2 μmol) and HATU (35.1 mg, 92.2 μmol) were measured into a 2.2 mL polypropylene microcentrifuge tube and dissolved in 20% CH_2Cl_2/DMF (460 μL). DIPEA (32 μL, 184.4 μmol) was added to the tube, and the coupling solution was mixed briefly and transferred to the resin. This coupling reaction was allowed to proceed for 60 minutes at room temperature; the coupling solution was then removed from the resin by vacuum assisted filtration. The resin was washed with DMF (General Procedure B), and coupling with **18** was repeated a second time (see General Procedure F). The resin was washed with DMF (General Procedure E). The Fmoc group of the Cbz-*pro4*(2*S*,4*S*) monomer residue was removed with 20% piperidine/DMF (General Procedure H). UV-visible spectroscopic analysis of the dibenzofulvene-piperidine adduct in the solvent at 301 nm suggested nearly quantitative coupling, relative to the initial resin loading. The resin was washed with DMF, *i*-PrOH, and then 20% CH_2Cl_2/DMF (General Procedure E). Two additional Cbz-*pro4*(2*S*,4*S*) monomers (**18**) were coupled to the resin using the same sequence of procedures.

N-α-Fmoc-O-*tert*-butyl-L-tyrosine (63.6 mg, 138.3 μmol) and HATU (52.6 mg, 138.3 μmol) were added to a 2.2 mL polypropylene microcentrifuge tube then dissolved in 20% CH_2Cl_2/DMF (690 μL). DIPEA (48.1 μL) was added, and the solution was mixed then quickly transferred to the resin (General Procedure F). After 60 minutes of mixing (General Procedure B), the coupling solution was removed by vacuum filtration and washed with DMF (General Procedure E). The *N*-terminal Fmoc group of tyrosine was removed by treatment with 20% piperidine/DMF over 120 minutes. The resin was thoroughly washed with DMF, methanol, and CH_2Cl_2 (General Procedure I). Solvent was removed from the resin under reduced pressure. Cleavage of the product from the resin was affected by treatment with 3 mL of 95:2.5:2.5 TFA/TIS/H_2O for 120 minutes. The resin was filtered from the cleavage solution, and then washed with additional TFA. The TFA washes were combined with the cleavage solution, and the solvent was evaporated at room temperature under a stream of dry nitrogen. Residual solvent was removed under reduced pressure, affording **49** as a yellow residue.

HPLC-MS: column, Waters XTerra MS C_{18}, 4.6 × 100 mm; mobile phase, CH_3CN / water (0.1% TFA), 5% to 95% CH_3CN over 30 min; flow rate, 0.40 mL/min; UV detection at 274 nm; t_R for **49**, 21.0 min; ESI-MS *m/z* (extracted ion) 1061.2 ($M + H^+$).

Compound 50

49 was dissolved in 7:2:1 methanol/water/acetic acid (4 mL). A small volume of this solution (50 μL) was removed for HPLC-MS analysis. The remaining solution was transferred into a 10 mL round bottom flask containing 10 wt. % Pd on activated carbon (~ 5 mg) and a magnetic stir bar. The flask was evacuated under reduced pressure and backfilled with H_2 gas. The reaction mixture was stirred under H_2 gas (balloon) for 60 minutes. The reaction mixture was filtered through a centrifugal spin filter (0.2 μm nylon frit), and the activated carbon was washed with an additional portion of the reaction solvent (3 × 333 μL). The filtered reaction mixture and washes were combined, and the solvent was removed at 40 °C for 5 hours under centrifugal evaporation. Residual solvent was removed under reduced pressure at room temperature overnight yielding **50** as a foamy white solid.

HPLC-MS: column, Waters XTerra MS C_{18}, 4.6 × 100 mm; mobile phase, CH_3CN / water (0.1% TFA), 5% to 95% CH_3CN over 30 min; flow rate, 0.40 mL/min; UV detection at 274 nm; t_R for **50**, 8.03 min; ESI-MS *m/z* (ion) 659.2 (100%, $M + H^+$).

Compound 44

50 was dissolved in 1400 μL of 20% piperidine/DMF (anhydrous) and transferred to a 2.2 mL polypropylene microcentrifuge tube. The tube was placed in a 4 °C refrigerator and stored for 24 hours, then transferred to a 2 °C refrigerator where it was stored for an additional 24 hours. An irregular, straw colored precipitate formed in the solution during this time. The supernatant was filtered from the precipitate using a centrifugal spin filter (0.2 μm nylon frit). The precipitate was washed with $CHCl_3$ 500 μL), dissolved in 60:40 MeCN/D_2O with 0.1% TFA (5 mL); the resulting solution was transferred into a Falcon® tube. The solution was frozen by immersing the tube into liquid nitrogen and rotating the tube so that a thin shell of frozen solvent covered the walls of the tube. The frozen solution was lyophilized, yielding **44** (~ 5 mg, 8 μmol, 17% from

initial resin loading), as a fine white powder, analyzed by NMR without further purification. This product was contaminated with piperidine salt (~ 5.6 μmol, determined by NMR). A small sample of **44** was dissolved in 0.1% TFA/H_2O for HPLC-MS analysis. ^1H chemical shifts are reported in ppm (δ) relative to the piperidine salt, which was calibrated under identical experimental conditions to the sodium salt of 3-(trimethylsilyl)propionic-2,2,3,3-d_4 acid. ^{13}C chemical shifts are reported in ppm (δ) relative to the piperidine salt, which was calibrated under identical experimental conditions to dioxane.

^1H NMR (500 MHz, 10 °C, D_2O): δ 7.05 (d, *J* = 4.9 Hz, 2H), 6.90 (d, *J* = 4.9 Hz, 2H), 4.84 (dd, *J* = 10.1, 7.9 Hz, 1H), 4.60 (dd, *J* = 10.0, 8.0 Hz, 1H), 4.53 (dd, *J* = 10.6, 6.9 Hz, 1H), 4.48 (t, *J* = 3.2 Hz, 1H), 4.08 (d, *J* = 12.5 Hz, 1H), 4.06 (d, *J* = 12.4 Hz, 1H), 3.67 (d, *J* = 12.6 Hz, 1H), 3.53 (d, *J* = 12.5 Hz, 1H), 3.22 (dd, *J* = 14.1, 1.9 Hz, 1H), 3.07 (dd, *J* = 13.7, 7.6 Hz, 1H), 2.95 (dd, *J* = 14.1, 4.5 Hz, 1H), 2.78 – 2.69 (m, 3H), 2.44 – 2.35 (m, 3H), 2.17 (dd, *J* = 13.0, 11.0 Hz, 1H); ^{13}C NMR (125 MHz, 10 °C, D2O) δ 171.3, 170.7, 170.5, 169.7, 167.2, 166.7, 156.2, 132.7 (2C), 126.7, 118.2, 116.5 (2C), 115.9, 65.0, 62.4, 60.5, 59.4, 58.7, 57.7, 56.4, 55.2, 52.8, 51.2, 40.8, 40.1, 38.6.

^1H NMR (500 MHz, 10 °C, 10% D_2O/H_2O, pH ≈ 0) δ 8.81 (s, 1H), 8.80 (s, 1H), 8.78 (s, 1H), 8.71 (s, 1H), 7.99 (s, 1H), 7.54 (s, 1H), 7.05 (d, *J* = 8.04 Hz, 2H), 6.90 (d, *J* = 6.1 Hz, 2H), 4.81 (t, *J* = 8.7 Hz, 1H), 4.60 (dd, *J* = 17.1, 8.3 Hz, 1H), 4.47 (br s, 1H), 4.08 (d, *J* = 12.2 Hz, 1H), .07 (d, *J* = 12.1 Hz, 1H), 3.68 (d, *J* = 12.5 Hz, 1H), 3.54 (d, *J* = 12.5 Hz, 1H), 3.21 (d, *J* = 14.0 Hz, 1H), 3.09 (dd, *J* = 13.7, 7.8 Hz, 1H), 2.94 (dd, *J* = 14.0, 3.5 Hz, 1H), 2.79 – 2.72 (m, 3H), 2.45 – 2.36 (m, 3H), 2.16 (t, *J* = 12.0 Hz, 1H); ^{13}C NMR (125 MHz, 10 °C, 10% D_2O/H_2O, pH ≈ 0) δ 170.7, 170.2, 170.0, 169.1, 166.6, 166.1, 155.7, 132.2 (2C), 126.2, 117.7, 116.2 (2C), 115.4, 64.8, 62.3, 60.4, 59.3, 58.5, 57.5, 56.2, 55.0, 39.9, 38.5.

HPLC-MS: column, Waters XTerra MS C_{18}, 4.6 × 100 mm; mobile phase, CH_3CN / water (0.1% TFA), 5% to 20% CH_3CN over 30 min; flow rate, 0.40 mL/min; UV detection at 274 nm; t_R for **44**, 8.84 min; ESI-MS *m/z* (ion) 595.2 (100%, $M + H^+$).

3.7.3 Details for synthesis of pentamer *bis*-peptide 53

Compound 51

Rink Amide AM Resin (49 mg resin, 31.4 μmol loading) was added to a 10 mL polypropylene SPPS reaction vessel and swollen overnight in DMF under argon. The *N*-terminal Fmoc group was removed with 20% piperidine/DMF (General Procedure H). The resin was washed with DMF, *i*-PrOH, and 20% CH_2Cl_2/DMF (General Procedure E). *N*-α-Fmoc-O-*tert*-butyl-L-tyrosine (46.5 mg, 101.2 μmol), HATU (38.5 mg, 101.2 μmol), and 20% CH_2Cl_2/DMF (690 μL) were added to a 2.2 mL polypropylene microcentrifuge tube. DIPEA (48.1 μL) was added to the tube; the solution was mixed briefly, and was then transferred to the resin (General Procedure F). The coupling reaction was mixed for 60 minutes at room temperature. The coupling solution was removed by vacuum filtration, and the resin was washed (General Procedure E). The *N*-Fmoc group was removed with 20% piperidine/DMF (General Procedure H)

18 (34.2 mg, 62.8 μmol), HATU (23.9 mg, 62.8 μmol) and 20% CH_2Cl_2/DMF (314 μL) were added to a 2.2 mL polypropylene tube. DIPEA (22 μL, 126 μmol) was added; the coupling solution was mixed briefly then added to the resin (General Procedure F). The coupling reaction was mixed for 60 minutes at room temperature, and then the reaction mixture was removed from the resin by vacuum assisted filtration. The resin was washed with DMF (General Procedure F). The coupling reaction was repeated a second time using identical conditions for an additional 60 minutes. The resin was washed, and the terminal *N*-Fmoc group was removed using 20% piperidine/DMF (General Procedure H). The UV-visible absorption spectrum of the piperidine-dibenzofulvene adduct in the deprotection solution suggested nearly quantitative coupling, relative to the initial resin loading. The resin was washed with DMF, *i*-PrOH, and 20% CH_2Cl_2/DMF (General Procedure E). Double coupling and deprotection of **18** was repeated sequentially four additional times. The resin was washed with DMF, methanol, and then CH_2Cl_2; residual solvent was removed from the resin over 4 hours under reduced pressure (General Procedure I). Product cleavage was affected by treating ~ 13 mg of the resin with 95:2.5:2.5 TFA/H_2O/TIS (2 mL) for 120 minutes. The resin was filtered from the cleavage solution, and was washed with additional TFA (3 × 1 mL). The TFA washes were combined with the cleavage solution, and the solvent was evaporated at room temperature under a stream of dry

N_2 gas. Residual solvent was removed under reduced pressure affording crude **51** as a slightly yellow residue.

HPLC-MS: column, Waters XTerra MS C_{18}, 4.6 × 100 mm; mobile phase, CH_3CN / water (0.1% TFA), 5% to 95% CH_3CN over 30 min; flow rate, 0.40 mL/min; UV detection at 220 nm; t_R for **51**, 22.90 min; ESI-MS *m/z* (relative intensity) 1701.4 (25%, $M + H^+$).

Compound 52

Crude **51** was dissolved in 7:2:1 MeOH/H_2O/AcOH (2 mL). A small volume of this solution (50 μL) was removed for HPLC-MS analysis. The remaining solution was transferred to a 10 mL round bottom flask containing 10 wt. % Pd/C (~ 5 mg) and a magnetic stir bar. The flask was evacuated under reduced pressure, and backfilled with H_2 gas. The reaction mixture was stirred under H_2 gas (balloon) for 60 minutes. The reaction mixture was filtered through a centrifugal spin filter (0.2 μm nylon frit), and the activated carbon was washed with 7:2:1 MeOH/H_2O/AcOH (3 × 333 μL). The solvent was removed by centrifugal evaporation at 40 °C, then under reduced pressure overnight yielding a yellow residue. HPLC-MS analysis indicated that the major component of this crude product was the compound **52** with one DKP closed.

HPLC-MS: column, Waters XTerra MS C_{18}, 4.6 × 100 mm; mobile phase, CH_3CN / water (0.1% TFA), 5% to 20% CH_3CN over 30 min; flow rate, 0.40 mL/min; UV detection at 274 nm; t_R for major component, 15.3 min; ESI-MS *m/z* (relative intensity) 999.3 (13%, $M_{\mathbf{52}}$ – MeOH + H^+), 500.2 (80%).

Compound 53

The products of the catalytic hydrogenolysis of **51** were dissolved in 20% piperidine/DMF (1 mL) and transferred to a 2.2 mL polypropylene tube. After 24 hours at room temperature, the solution was added dropwise to ether (50 mL); the resulting fine, white precipitate was pelleted by centrifugation. The pellet was dried overnight affording crude **53** (~ 3 mg, 3 μmol, 33% from initial resin loading) as a white solid. Crude **53** was dissolved in 60:40:1 MeCN/H_2O/TFA (200 μL), and a portion of this solution (20 μL) was added to an additional volume of 60:40:1 MeCN/H_2O/TFA (180 μL) for HPLC analysis.

HPLC-MS: column, Waters XTerra MS C_{18}, 4.6 × 100 mm; mobile phase, CH_3CN / water (0.1% TFA), 5% to 20% CH_3CN over 30 min; flow rate, 0.40 mL/min; UV detection at 274 nm; t_R for **53**, 8.84 min; ESI-MS *m/z* (ion extracted) 903.3 ($M + H^+$).

3.7.4 Details for synthesis of compounds in model DKP closure study

Compound 54, **Compound 55**, **Compound 56**

Rink Amide AM Resin (20 mg, 12.8 μmol loading) was added to a 10 mL polypropylene SPPS reaction vessel and swollen in DMF. *N*-α-Fmoc-O-*tert*-butyl-L-tyrosine, **18**, **18**, and 4-nitrobenzoic acid were coupled sequentially to the resin using HATU with DIPEA in 20% CH_2Cl_2/DMF (coupling by General Procedure F, Fmoc deprotection by General Procedure H, and washing by General Procedure E). The resin was washed with CH_2Cl_2, MeOH, and CH_2Cl_2, then dried under reduced pressure overnight (General Procedure I). Thioanisole (50 μL), ethanedithiol (EDT, 25 μL), and TFA (500 μL) were added to the resin. Triflic acid (50 μL) was added carefully to the solution; the cleavage cocktail and resin were agitated occasionally over 90 minutes. The cleavage solution was filtered from the resin, and added dropwise into ether (~ 40 mL). The resulting precipitate was formed into a pellet by centrifugation; the ether was decanted, and an additional portion of ether (40 mL) was added to the pellet. The pellet was broken up, suspended in the ether, then reformed by centrifugation; the ether wash was decanted, affording the product **54** as a white solid. This was dissolved in 1:1 H_2O/ACN (0.1% TFA) and lyophilized, yielding a fluffy white solid that was dissolved in another portion of H_2O/ACN and divided evenly into 1 mL polypropylene tubes. The solvent was removed by centrifugal evaporation. To analyze DKP formation, solvents (100 μL portions) were added to the tubes containing **54**, mixed quickly with a pipette. Each reaction was monitored by HPLC.

HPLC: column, Microsorb 100 C_{18}, 4.6 mm × 250 mm; mobile phase, CH_3CN (0.05% TFA) / water (0.1% TFA), 28% to 35% CH_3CN over 5 minutes; flow rate, 1.00 mL / min; UV detection at 274 nm; t_R for **54**, 4.88 min; t_R for **55**, 5.41 min; t_R for **56**, 3.51 min. For **54**: ESI-MS *m/z* (ion) 670.2 ($M + H^+$). For **55**: ESI-MS *m/z* (ion) 638.3 ($M + H^+$). For **56**: ESI-MS *m/z* (ion) 624 ($M + H^+$)

3.7.5 Details for the synthesis of 57 and 58, and preparation of NMR samples

Compound 57, Compound 59

100 mg of Rink Amide AM resin (0.63 mmol/gram substitution) were transferred to a solid phase reaction vessel and swollen in DMF for several hours. The *N*-Fmoc protecting group of the resin was removed by treatment with a solution of 20% piperidine/DMF for 40 minutes (General Procedure H). The resin was washed sequentially with DMF, CH_2Cl_2, *i*-PrOH, and DMF (General Procedure E). (*S*)-*N*-Fmoc-2-naphthylalanine (56.4 mg, 128 μmol) and HATU (48.6 mg, 128 μmol) were added to a polypropylene microcentrifuge tube. The protected amino acid and coupling reagent were dissolved in 640 μL of 20% CH_2Cl_2/DMF. DIPEA (45.0 μL, 256 μmol) was added to the coupling solution; the solution was mixed and added to the resin immediately (General Procedure F). The resin and coupling solution were agitated for 1 hour and then washed. The coupling reaction was repeated one additional time. The resin was capped with a solution of 400:100:8 DMF/Ac_2O/DIPEA (General Procedure G). The naphthylalanine *N*-terminal Fmoc protecting group was removed using a solution of 20% piperidine/DMF over 40 minutes (General Procedure H), and the resin was washed sequentially with DMF, CH_2Cl_2, *i*-PrOH, and DMF (General Procedure E).

Monomer **18** (70.0 mg, 128 μmol) was coupled to the resin using HATU in a similar fashion (General Procedure F). Following coupling of the first monomer to the solid phase, the resin was capped (General Procedure G), the *N*-terminal Fmoc protecting group was removed (General Procedure H), and the resin was washed (General Procedure E). Three additional monomers were coupled sequentially to the resin using similar procedures (monomers **18**, **29**, then **29**). The *N*-terminal Fmoc protecting group was removed (General Procedure H). The resin was washed with CH_2Cl_2, MeOH, and CH_2Cl_2 then dried under reduced pressure overnight (General Procedure I).

The resin was transferred to a 4 mL conical vial containing a magnetic spin vane. Triisopropylsilane (86 μL), water (86 μL), and trifluoroacetic acid (TFA, 3.25 mL) were added sequentially. This cleavage solution was stirred for 2 hours, and then the resin was filtered from the solution and washed with an additional volume of TFA. The filtrates were combined and

concentrated by centrifugal evaporation at room temperature. Thioanisole (25 μL) and ethanedithiol (10 μl) were added to the resulting oily residue, followed by TFA (250 μL) and triflic acid (25 μL). This solution was stirred for 15 minutes, then added slowly to diethyl ether (~ 80 mL); the precipitate (crude **59**) was pelleted by centrifugation. The ether was decanted from the pellet, and the pellet was dissolved in 20% piperidine/DMF (1.25 mL). After approximately 48 hours at room temperature, the crude product was precipitated from ether. The precipitate was dissolved in a 90:10:1 H_2O/MeCN/TFA solution, and the product (**57**) was purified by preparative HPLC (C_{18} column; 30 mm × 300 mm; mobile phase, CH_3CN (0.05% TFA) / water (0.1% TFA), 10% to 35% CH_3CN over 30 min; flow rate, 43 mL/min). The fractions containing the desired product were concentrated by lyophilization yielding **57** (10.3 mg, 12.9 μmol, ~ 20% overall yield, based upon initial resin loading): HRESIQTOFMS calcd for $C_{38}H_{43}N_{10}O_{10}$ ($M + H^+$) 799.3158, found 799.3251.

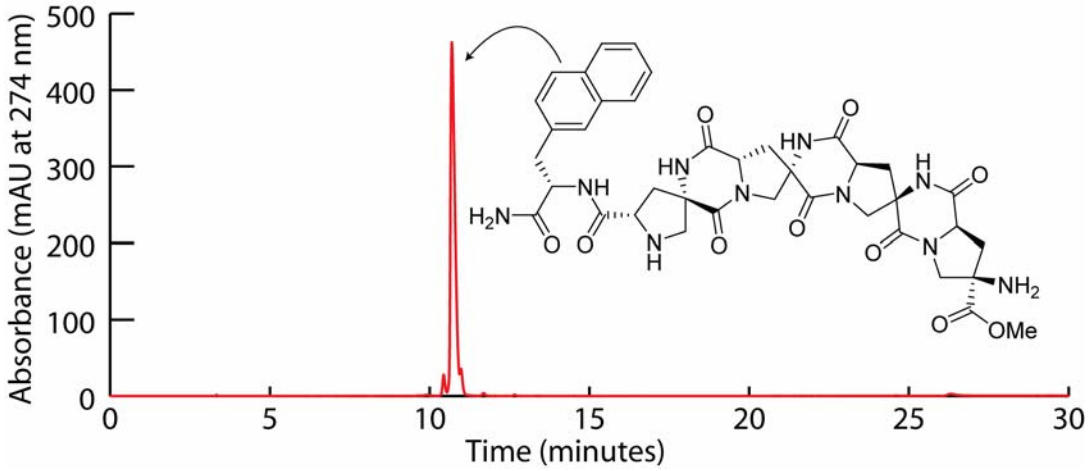

HPLC: column, Microsorb 100 C_{18}, 4.6 × 250 mm; mobile phase, CH_3CN (0.05% TFA) / water (0.1% TFA), 5% to 95% CH_3CN over 30 min; flow rate, 1.00 mL/min; UV detection at 274 nm; t_R for **57**, 11.67 min.

Figure 3-22: HPLC chromatogram of purified **57**

Compound 58, Compound 60

58 was prepared using a procedure similar to the one described for the synthesis of **57**. (*S*)-*N*-Fmoc-2-naphthylalanine, **18**, **29**, **18**, and **29** were coupled sequentially to 100 mg of Rink Amide AM resin (coupling using General Procedure F, capping using General Procedure G, washing as described for **57**, Fmoc deprotection using General Procedure H, and final resin wash using General Procedure I). The resin was cleaved using TFA, and the Cbz groups of the crude

product were removed with exposure to triflic acid, affording compound **60**. This was treated with 20% piperidine/DMF for 48 hours, precipitated from ether, and purified by preparative HPLC. Fractions containing the desired product were concentrated by lyophilization yielding **58** (10.4 mg, 13.0 μmol, ~ 20% overall yield, based upon initial resin loading): HRESIQTOFMS calcd for $C_{38}H_{43}N_{10}O_{10}$ ($M + H^+$) 799.3158, found 799.3190.

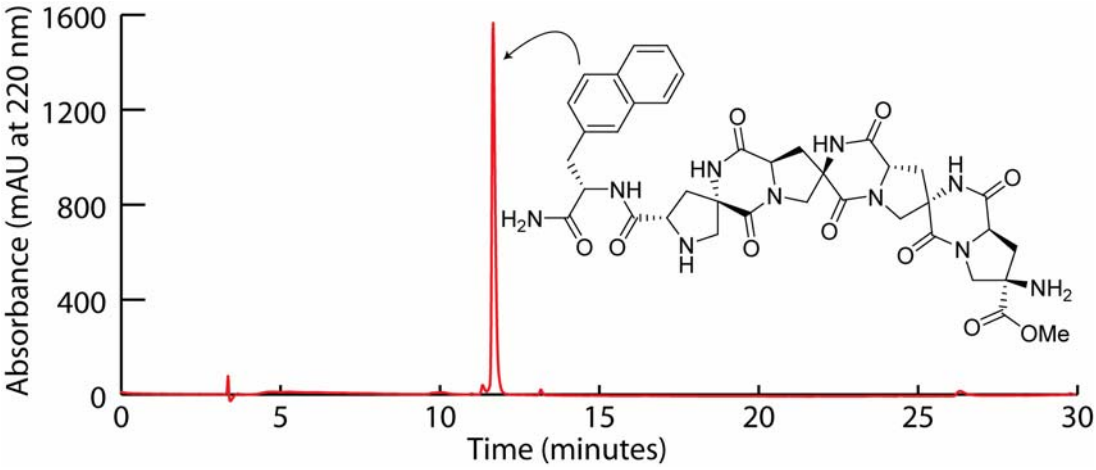

HPLC: column, Microsorb 100 C_{18}, 4.6 × 250 mm; mobile phase, CH_3CN (0.05% TFA) / water (0.1% TFA), 5% to 95% CH_3CN over 30 min; flow rate, 1.00 mL/min; UV detection at 274 nm; t_R for **58,** 10.69 min.

Figure 3-23: HPLC chromatogram of **58**

NMR Analysis of 57 and 58

The NMR samples of **57** and **58** were prepared by dissolving each in approximately 450 μL of degassed 9:1 H_2O/D_2O with 0.025 M ND_4COOD:CD_3COOD buffer (pH 4-5). The samples were filtered through 0.2 μm Nylon frit centrifugal filters and transferred to a D_2O matched Shigemi NMR tube. Experiments were acquired on a 500 MHz spectrometer at 2 °C. COSY, ROESY (mixing time of 300 ms), HMQC and HMBC experiments were performed. Processed data sets were analyzed using Sparky.[151] The chemical shift assignments are based upon the COSY, HMBC, and ROESY cross-peaks.

3.7.6 Details for the synthesis of 61, 62, and 63, and preparation of NMR samples

Compound 61, Compound 62, Compound 63

A 100 mg batch of Rink Amide AM resin (0.64 mmol/g loading) was transferred to a solid-phase reaction vessel containing a small magnetic stir bar. The resin was swollen in DMF for several hours with gentle argon bubbling (General Procedure B). The *N*-Fmoc group of the resin linker was removed using 20% piperidine/DMF for 40 minutes; the resin was washed sequentially with DMF, CH_2Cl_2, *i*-PrOH, and DMF (General Procedure E). The desired monomer was coupled to the resin. The coupling reaction mixture was prepared by measuring the desired monomer (193 mg, 378 μmole) and HATU (143 mg, 378 μmole) into a 15 mL polypropylene centrifuge tube. Freshly prepared anhydrous 4:1 DMF/CH_2Cl_2 (1800 μL, 0.2 M in monomer) was added to the tube followed by DIPEA (131 μL, 756 μmole). The coupling solution was mixed for about one minute, and then transferred to the resin. The resin and coupling solution were mixed by slowly bubbling argon through the solution and by using a small magnetic stir bar (General Procedure C). Coupling was allowed to proceed for 30 minutes, and the coupling solution was drained from the resin. The resin was washed with DMF, *i*-PrOH, and DMF (General Procedure E). The coupling and washing procedure was repeated one additional time with the same monomer. Unreacted amines were then capped with a solution of 50:12.5:1 DMF/Ac_2O/DIPEA for 20 minutes (General Procedure G). The *N*-Fmoc group of the terminal amine was removed using 20% piperidine/DMF solution for 40 minutes (General Procedure H), and the coupling yield was determined by measuring the concentration of the piperidine/dibenzofulvene adduct in the deprotection reaction solution.

The coupling, capping, and deprotection sequence was repeated for each of the desired monomers on each batches of resin. The sequence of monomers coupled to each batch of resin is shown in the following table (Table 3-2). After the final monomer was coupled to the resin (General Procedure F) and the Fmoc group removed (General Procedure H), (*S*)-*N*-Fmoc-tyrosine was coupled in a similar fashion using HATU and DIPEA. The *N*-Fmoc group of the tyrosine residue was removed (General Procedure H), and the resin was washed sequentially

with DMF, CH_2Cl_2, MeOH, and CH_2Cl_2 (General Procedure I). Residual solvent was removed from the resin under reduced pressure.

Table 3-2: The coupling sequence for the solid phase synthesis of oligomers **61**, **62**, and **63**

	Sequence of monomers used for compounds:		
	61	**62**	**63**
Coupling 1	*pro4*(2*S*4*S*)	*pro4*(2*S*4*S*)	*pro4*(2*S*4*S*)
Coupling 2	*pro4*(2*S*4*R*)	*pro4*(2*R*4*S*)	*pro4*(2*R*4*S*)
Coupling 3	*pro4*(2*R*4*S*)	*pro4*(2*S*4*R*)	*pro4*(2*R*4*R*)
Coupling 4	*pro4*(2*R*4*R*)	*pro4*(2*R*4*R*)	*pro4*(2*S*4*R*)

70 mg of the resin was removed from each batch and transferred into a fritted polypropylene reaction vessel containing a small stir bar. Ethanedithiol (100 μL) and thioanisole (200 μL) were added to the resin, and the reaction vessels were submerged in an ice bath. TFA (2 mL) was added to the resin, followed by triflic acid (100 μL). The cleavage solution was stirred for 2 hours and then added dropwise to a stirred, room temperature Et_2O (100 mL). The resins were washed with TFA (1 mL); this was filtered into the ether as well. The resulting precipitates were pelleted by centrifugation. The pellets were washed with an additional volume of ether and then dried to a yellowish residue. The product of each cleavage was dissolved in 20% piperidine/NMP (1.25 mL) and sealed in an HPLC vial for 48 hours. Each solution was then slowly added to ether, the precipitate was isolated by centrifugation. The products were purified by preparative HPLC (C_{18} column; mobile phase, CH_3CN (0.05% TFA) / water (0.1% TFA), 0% to 20% CH_3CN over 30 min; flow rate, 15 mL/min). Desired fractions were concentrated by centrifugal evaporation.

Preparing the NMR Samples of 61, 62, and 63

Samples were each dissolved in 420 μL of a degassed 90:10 H_2O/D_2O solution buffered with 10 mM $CD_3COOD/CD_3COO^-ND_4^+$, pH 1.5. The final solution was around pH 3.0. A trace amount of the sodium salt of 3-(trimethylsilyl)propionic acid-d_4 (TSP-d_4) was added to the solution as an internal standard. The solutions were filtered through 0.2 μm Nylon centrifugal filters. 50 μL of each sample was used for HPLC and for high resolution mass spec analysis; the remainder was transferred into the Shigemi NMR tubes for analysis by NMR. Based upon the maximum tyrosine absorbance at 274 nm, it was determined by HPLC that the overall isolated yield (based on initial resin loading) was between 25% and 30%, and that the concentration of the NMR

samples was on the order of 10 mM. The NMR samples of **61** and **62** were contaminated with a trace amount of NMP.

Analytical data for *bis*-peptide **61**:

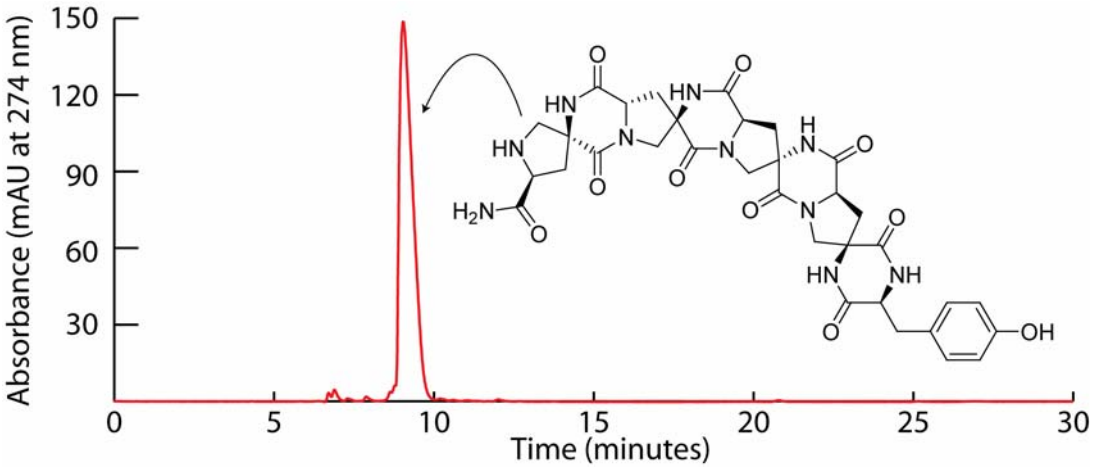

HPLC: C_{18} column; mobile phase, CH_3CN (0.05% HCOOH) / water (0.1% HCOOH), 0% to 25% CH_3CN over 30 min; flow rate, 0.80 mL/min; UV detection at 274 nm; t_R for **61**, 9.03 min; HRESIQTOFMS calcd for $C_{33}H_{37}N_{10}O_{10}$ ($M + H^+$) 733.2689, found 733.2675.

Figure 3-24: HPLC chromatogram and HRMS analysis of the NMR sample containing compound **61**

Analytical data for *bis*-peptide **62**:

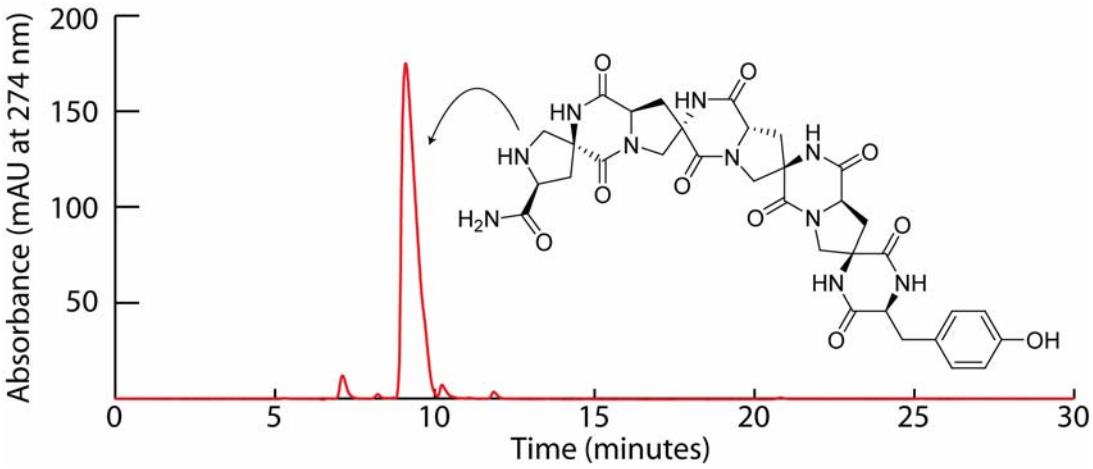

HPLC: C_{18} column; mobile phase, CH_3CN (0.05% HCOOH) / water (0.1% HCOOH), 0% to 25% CH_3CN over 30 min; flow rate, 0.80 mL/min; UV detection at 274 nm; t_R for **62**, 9.09 min; HRESIQTOFMS calcd for $C_{33}H_{37}N_{10}O_{10}$ ($M + H^+$) 733.2689, found 733.2653.

Figure 3-25: HPLC chromatogram and HRMS analysis of the NMR sample containing compound **62**

Analytical data for oligomer **63**:

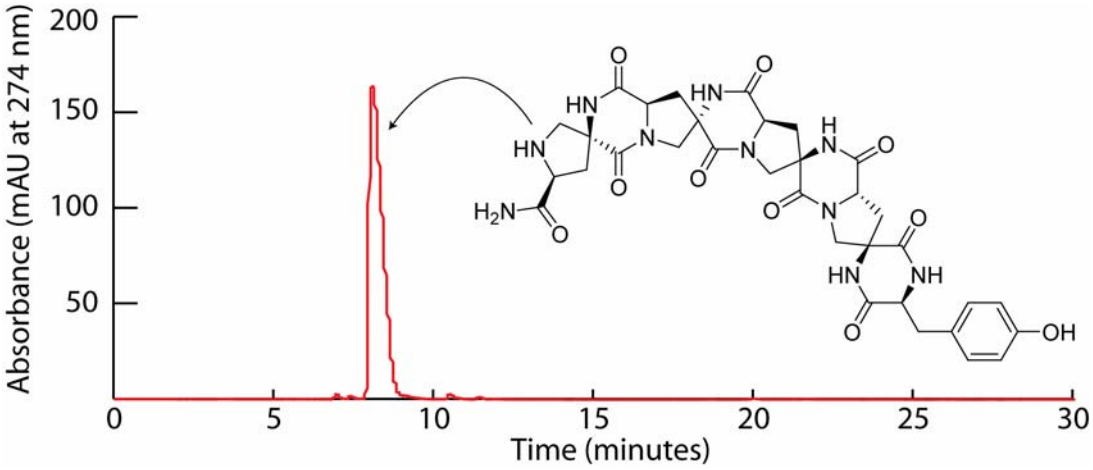

HPLC: C_{18} column; mobile phase, CH_3CN (0.05% HCOOH) / water (0.1% HCOOH), 0% to 25% CH_3CN over 30 min; flow rate, 0.80 mL/min; UV detection at 274 nm; t_R for **63**, 8.06 min; HRESIQTOFMS calcd for $C_{33}H_{37}N_{10}O_{10}$ $(M + H^+)$ 733.2689, found 733.2719.

Figure 3-26: HPLC chromatogram and HRMS analysis of the NMR sample containing compound **63**

4.0 FRET STUDY

2D-NMR experiments have been used to determine the conformation and shape of *bis*-peptide oligomers in solution. Oligomers were modeled using molecular mechanics calculations, and the resulting conformers were evaluated by measuring the relative intensity of ROESY correlations across the pyrrolidine and DKP rings. Measurable ROESY correlations can be detected between protons that are within 3 to 4 Å of one another. Modeling suggests that **44**, containing three *pro4*(2*S*,4*S*) monomer residues, is around 15 Å in length. The ROESY correlations provided insight into the conformation of heterocycles within the oligomer, but predicting global structure from the sum of local interactions is error prone.

Analysis of oligomer structure by 2D-NMR is non-trivial and time consuming. Although multiple *bis*-peptide oligomers can be designed and synthesized in parallel within days, NMR structure determination requires weeks. We envision a rapid cycle of design, synthesis, testing, and re-design; faster and more convenient methods for analyzing oligomer structure and function could enable this approach. There is need to explore other methods for measuring the shape and structure of *bis*-peptide oligomers.

We have attempted structure determination by X-ray diffraction, but growing suitable crystals is an extremely slow process. Crystal-packing forces can elicit changes in molecular conformation;[152] this effect has been observed in molecules containing DKPs.[139] The conformation of an oligomer in solution is arguably more relevant than its crystal structure because the applications for the oligomers are primarily solution-based. Although the size of larger oligomer structures might be determined using viscosity measurements, light scattering, and ultracentrifugal sedimentation, these methods are inappropriate for smaller oligomers.[153] Our first approach was to synthesize fluorophore end-labeled oligomers, and to evaluate the relative length of these oligomers by fluorescence resonance energy transfer (FRET).

FRET is technique used to measure the distance between a "donor" and an "acceptor" fluorophore.[154] FRET is only possible when the fluorescence emission spectrum of the donor overlaps with the absorption spectrum of the acceptor (Figure 4-1). Light energy excites the donor fluorophore; when the acceptor is absent, the donor fluoresces at a particular wavelength, λ_1.[155] If the acceptor is positioned near the donor, energy is transferred from the donor into the acceptor; the acceptor will then emit light at λ_2 (a longer wavelength than λ_1). The energy transfer between the donor and acceptor (Förster energy transfer) is caused by resonance between the dipoles of the excited state of the donor and the excited state of the acceptor, and not by emission of a photon from the donor.[156]

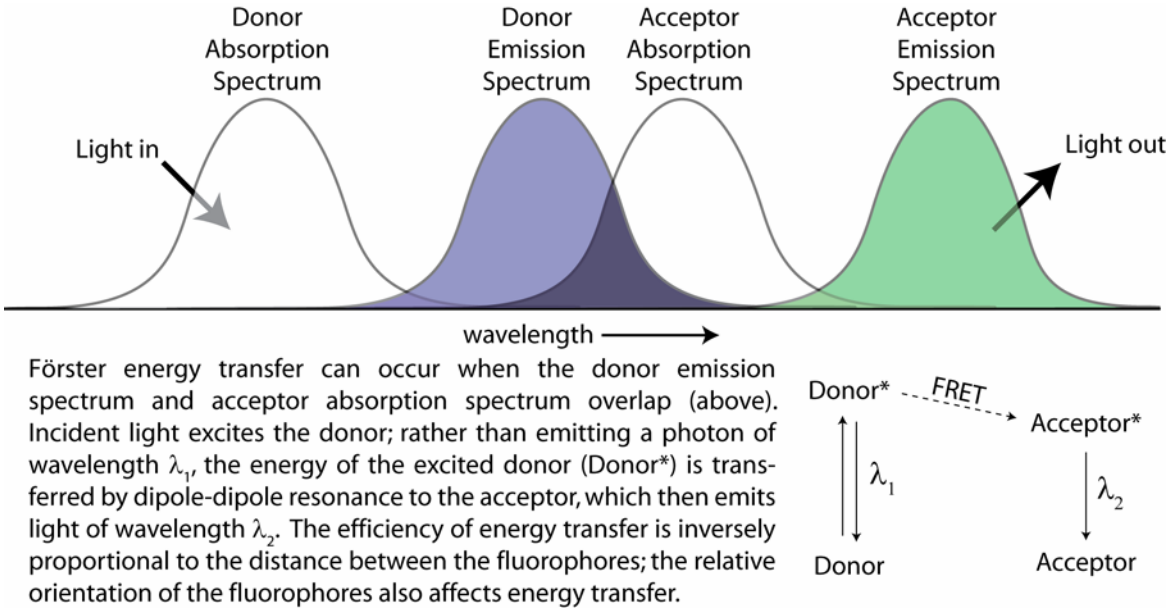

Figure 4-1: A schematic representation of fluorescence resonance energy transfer (illustration adapted from "Modern Physical Organic Chemistry")[155]

The efficiency of Förster energy transfer is proportional to $(1 / r^6)$, where r is the distance between the donor and acceptor. The relationship between donor-acceptor distance and energy transfer efficiency was first exploited as a "spectroscopic ruler" by Stryer and Haugland;[52] they measured the lengths of poly-L-proline oligomers by labeling the C-terminus of each oligomer with a naphthyl group and the N-terminus of each oligomer with a dansyl group. FRET has since been used extensively to measure dimensions and dynamics of biological macromolecules and peptides.[53,153,154,157]

We designed two pentamer oligomers based upon the conformational preferences described in the previous chapter. The first (pentamer **69**) was designed to be a helical rod,

whereas the second (pentamer **70**) was designed to have a curved shape. The pentamers were end-labeled with naphthyl (fluorescence donor) and dansyl (fluorescence acceptor) groups. The design hypothesis was confirmed by measuring the efficiency of fluorescence resonance energy transfer between the naphthyl and dansyl pair.

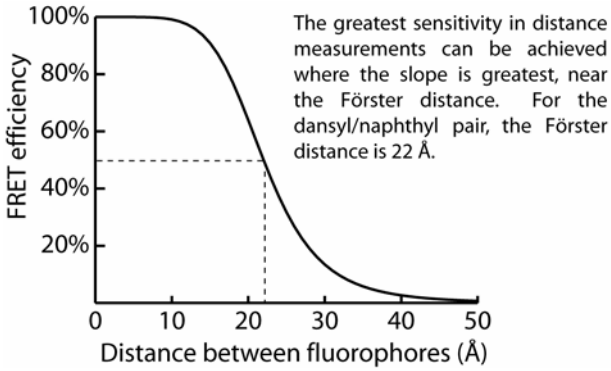

Figure 4-2: Theoretical FRET efficiency plotted as a function of the distance between a pair of fluorophores with a Förster distance of 22 Å.

Modeling suggests that **69** and **70** are around 20 Å long; the dansyl-naphthyl pair was an appropriate choice for this system because their Förster distance is 22 Å.[158] FRET active fluorophore pairs each have a characteristic Förster distance, where Förster energy transfer is 50% efficient. The greatest sensitivity for FRET distance measurements is achieved when the donor-acceptor pair is positioned at or near their characteristic Förster distance (Figure 4-2).

The fluorescence excitation spectra and absorption spectra of the dansyl and naphthyl groups are illustrated in Figure 4-3. The naphthyl chromophore absorbs strongly around 290 nm (Figure 4-3, solid line), and fluoresces at 350 nm (Figure 4-3, inset spectrum, solid line). The dansyl group absorbs light at the frequency of dansyl emission (around 350 nm) and fluoresces at 520 nm (Figure 4-3, inset, dashed line). With this pair of fluorophores, the naphthyl group behaves as the energy donor, while the dansyl group behaves as the energy acceptor. We planned to model our analysis of the fluorescence data based upon Stryer and Haugland's original experiments with oligoproline.[52]

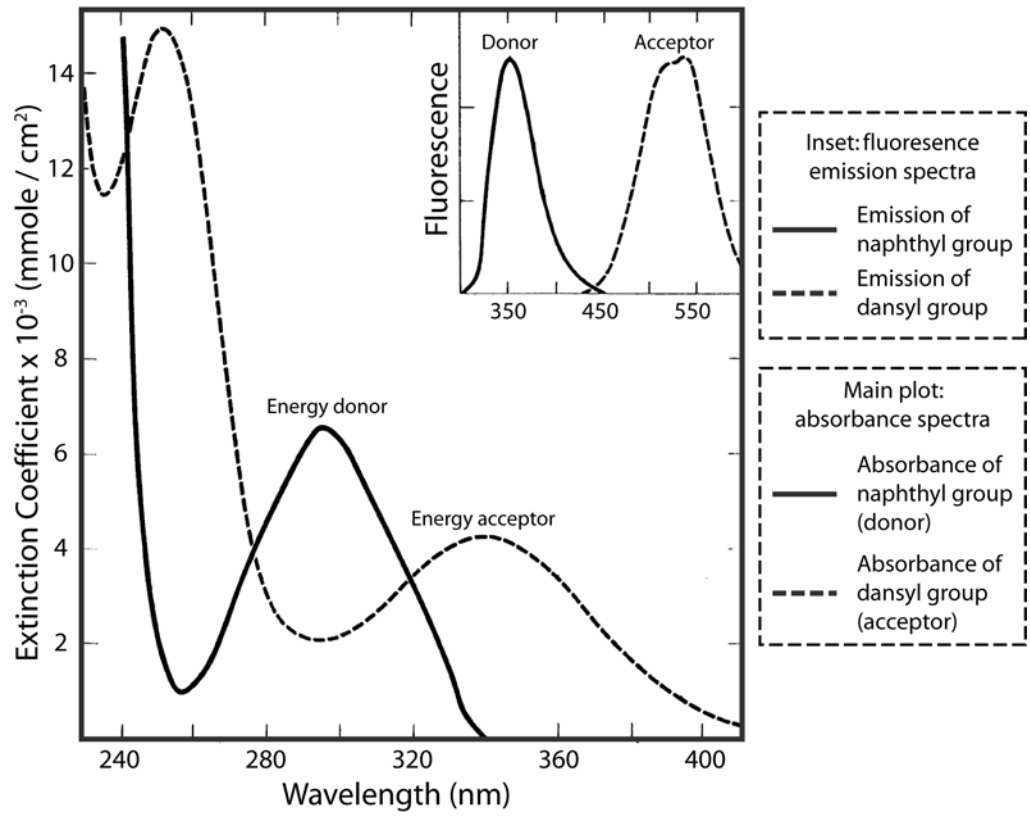

Figure 4-3: The fluorescence excitation and absorption spectra (inset spectra) of the naphthyl (donor) and dansyl (acceptor) groups. The spectra were obtained in ethanol. This illustration was adapted from Stryer and Haugland.[52]

4.1 SYNTHESIS OF FLUOROPHORE LABELED SCAFFOLDS

The structures of the compounds designed for the FRET study are illustrated in Figure 4-4. **69** contains a sequence of 5 *pro4*(2*S*,4*S*) monomers. On the basis of the conformational preferences determined for linear trimer *bis*-peptide **44** (3 *pro4*(2*S*,4*S*) monomers), **69** was expected to be a linear molecular rod. **70** is a pentamer *bis*-peptide of alternating *pro4*(2*R*,4*R*) and *pro4*(2*S*,4*S*) monomer residues. On the basis of the conformational preferences determined for tetramer *bis*-peptide **58** (alternating *pro4*(2*S*,4*S*) and *pro4*(2*R*,4*R*) monomers), it was anticipated that **70** would adopt a curved shape. We also synthesized **71**, wherein the dansyl group is coupled through a short linker to naphthylalanine, and **72**, labeled only with the dansyl group; these were used as controls for the FRET measurements.

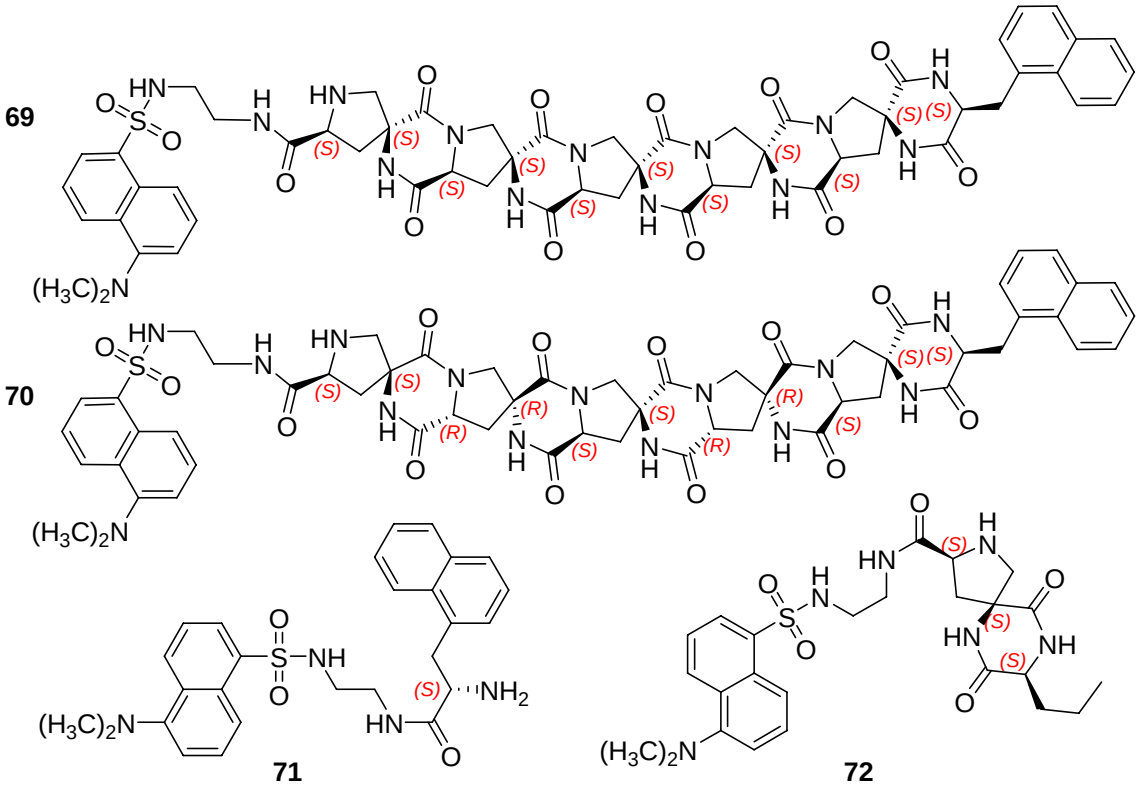

Figure 4-4: Structure of the molecules used in the FRET study. The stereochemistry has been labeled in red to highlight the differences between **69** and **70**.

The dansyl fluorophore was installed at the C-terminus of **69**, **70**, **71**, and **72** by performing solid-phase synthesis on Dansyl NovaTag™ resin (Figure 4-5).[159] This is polystyrene resin functionalized with a variation of the "PAL" linker used for the Fmoc-SPPS of C-terminal peptide amides.[160] When the NovaTag linker is cleaved with TFA, the C-terminus of the peptide remains connected by a short linker to the dansyl sulfonamide.

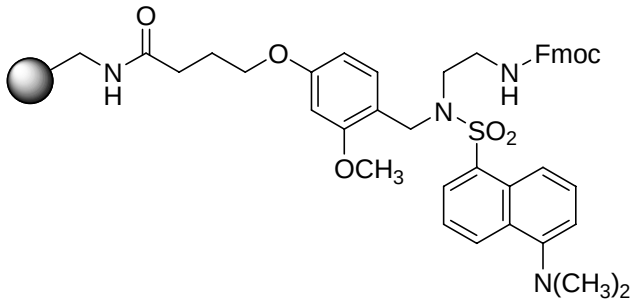

Figure 4-5: Dansyl NovaTag resin

We attempted to synthesize the oligomers for the FRET study using the Cbz-*pro4* monomers **18** and **29**, but abandoned this approach because the dansyl labeled oligomers

decomposed when exposed to the conditions used for Cbz group removal (8% triflic acid in TFA). Boc-*pro4* monomers **19** and **30** were used instead. The Boc groups are removed concurrently with resin cleavage, eliminating one post-cleavage transformation required when using the Cbz-*pro4* monomers.

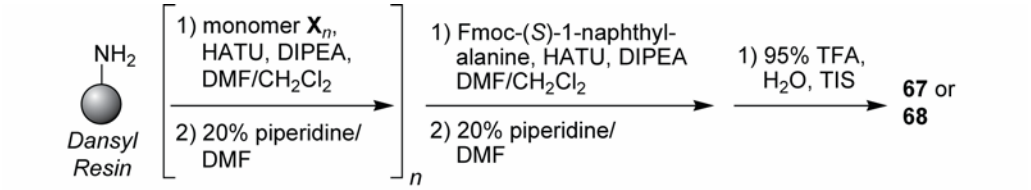

Oligomer	Boc-*pro4* monomer $\mathbf{X}_n$ for coupling *n*				
	n = 1	*n* = 2	*n* = 3	*n* = 4	*n* = 5
69 (from **67**)	**19** (2*S*,4*S*)	**19** (2*S*,4*S*)	**19** (2*S*,4*S*)	**19** (2*S*,4*S*)	**19** (2*S*,4*S*)
70 (from **68**)	**19** (2*S*,4*S*)	**30** (2*R*,4*R*)	**19** (2*S*,4*S*)	**30** (2*R*,4*R*)	**19** (2*S*,4*S*)

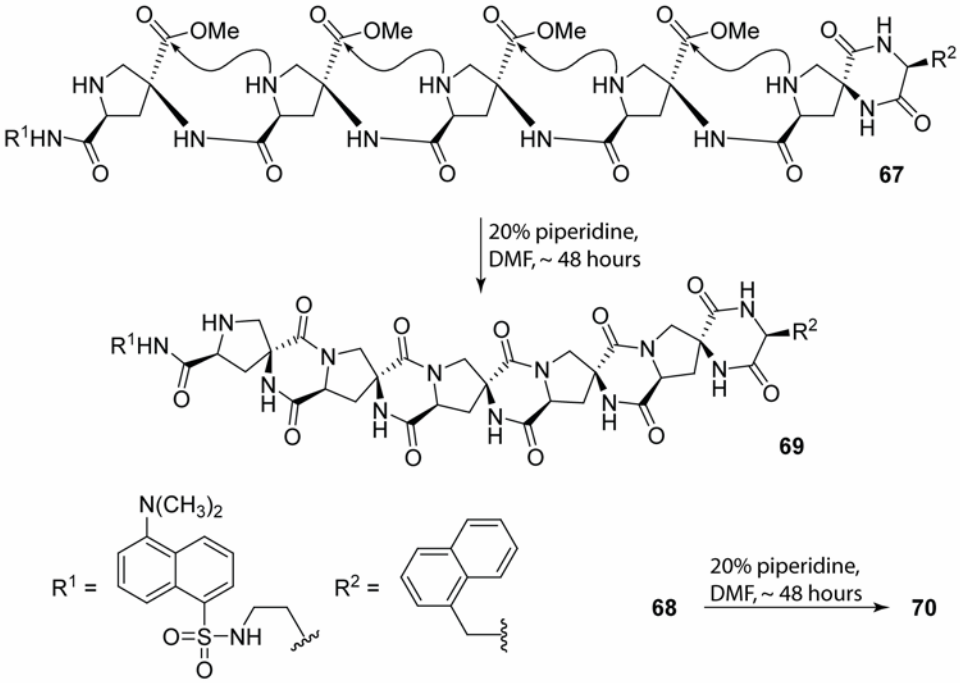

Scheme 4-1: Synthesis of pentamer oligomers **69** and **70**

Synthesis of the labeled pentamer oligomers **69** and **70** is illustrated in Scheme 4-1. Five Boc-*pro4* monomers were coupled sequentially to Dansyl NovaTag™ resin, followed by Fmoc-(*S*)-1-naphthylalanine. The open-form oligomers **67** and **68** were obtained upon resin cleavage. DKP ring closure (rigidification) was achieved by dissolving the open-form oligomers in 20%

piperidine/DMF. The rigidification reaction was complete after approximately 2 days, affording the desired products **69** (from **67**) and **70** (from **68**).

The purpose of executing this experiment was to demonstrate that the shape of a *bis*-peptide oligomer could be designed in a rational way by changing the stereochemistry of its monomers. To draw legitimate conclusions from the FRET data regarding the relationship between monomer stereochemistry and oligomer shape, it was essential to avoid epimerization during DKP closure.

Proving the stereochemical fidelity of **69** and **70** would require NMR experiments, but the oligomers were prepared on small scale, and overlap in the ^{1}H spectra would likely prevent analysis. The trimer **44**, and tetramers **57**, **58**, **61**, **62**, and **63**, were each the sole or major product of DKP closure; the stereochemistry of each was confirmed by NMR. Experience with these compounds suggests that the rate of *bis*-peptide epimerization is considerably slower than the rate of DKP closure. We partially addressed the epimerization issue by monitoring the DKP closing reactions as a function of time by HPLC-MS. The progress of the DKP closing reaction of **67** (to **69**) is illustrated in Figure 4-6. After 3 hours, a large number of intermediates containing less than 5 DKP rings were observed (Figure 4-1, chromatogram **B**). After 32 hours, however, the reaction is nearly complete (Figure 4-1, chromatogram **C**). The intermediate compounds disappear and converge into a single major product, **69**. Two small peaks with longer retention times than **69** are visible in the HPLC chromatogram of the crude product (Figure 4-1, **C**). These minor impurities are likely epimers of **69**. **69** was purified easily by preparative HPLC. Similar results were observed during the conversion of **68** to **70**.

There is mass spectral evidence that the intermediates are partially rigidified. In Figure 4-7, **D** is the HPLC chromatogram of the rigidification of **67** to **69** after 3 hours (identical to **B**, Figure 4-6). **E** (Figure 4-7, right of **D**), is the total ion count from analysis of the effluent during the HPLC analysis at 3 hours. The signal peaks in the total ion count chromatogram coincide with the UV-absorbance peaks in chromatogram **D**. The *m*/*z* ratios of each partially closed intermediate were extracted from the total ion count; these ion extractions are illustrated in chromatograms **F1** through **J1**. The ion extractions confirm that DKP closure is taking place, but that at 3 hours, there is little of the desired product **69** (note the small ion signal in **J1**). Averaged ESI-MS spectra for each ion extraction are shown (**F2** through **I2**): these are consistent with the mixtures of intermediates. The ESI-MS of purified **69** is shown (**J2**, Figure 4-7).

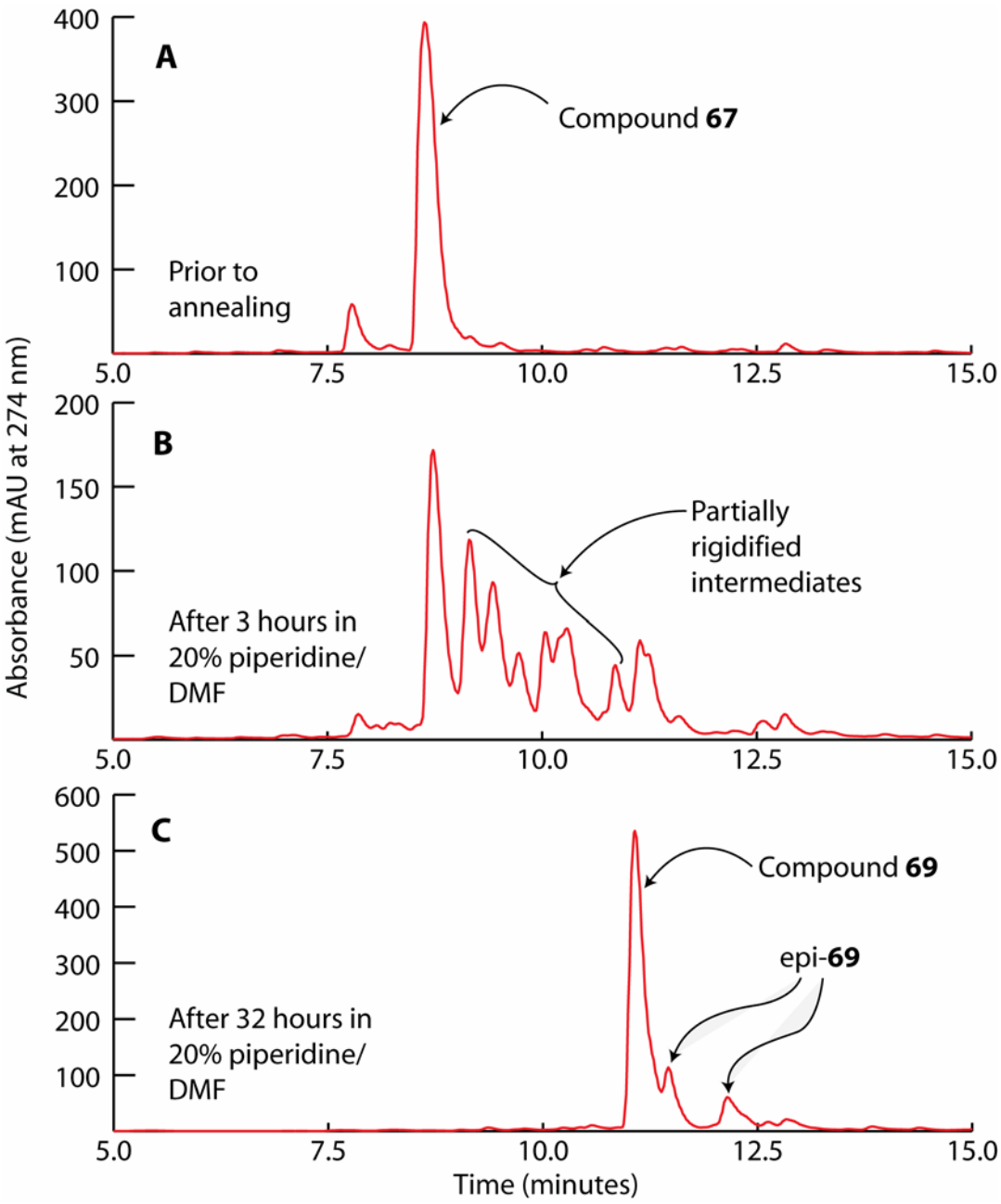

HPLC: column, Microsorb 100 C_{18}, 4.6 × 250 mm; mobile phase, CH_3CN (0.05% TFA) / water (0.1% TFA), 5% to 95% CH_3CN over 30 min; flow rate, 1.00 mL/min; UV detection at 274 nm.

Figure 4-6: Progress of diketopiperazine formation as monitored by C_{18} reverse-phase HPLC. **A** (top): crude resin cleavage product **67**. **B** (middle): after three hours dissolved in 20% piperidine/DMF. **C** (bottom): after 32 hours in 20% piperidine/DMF.

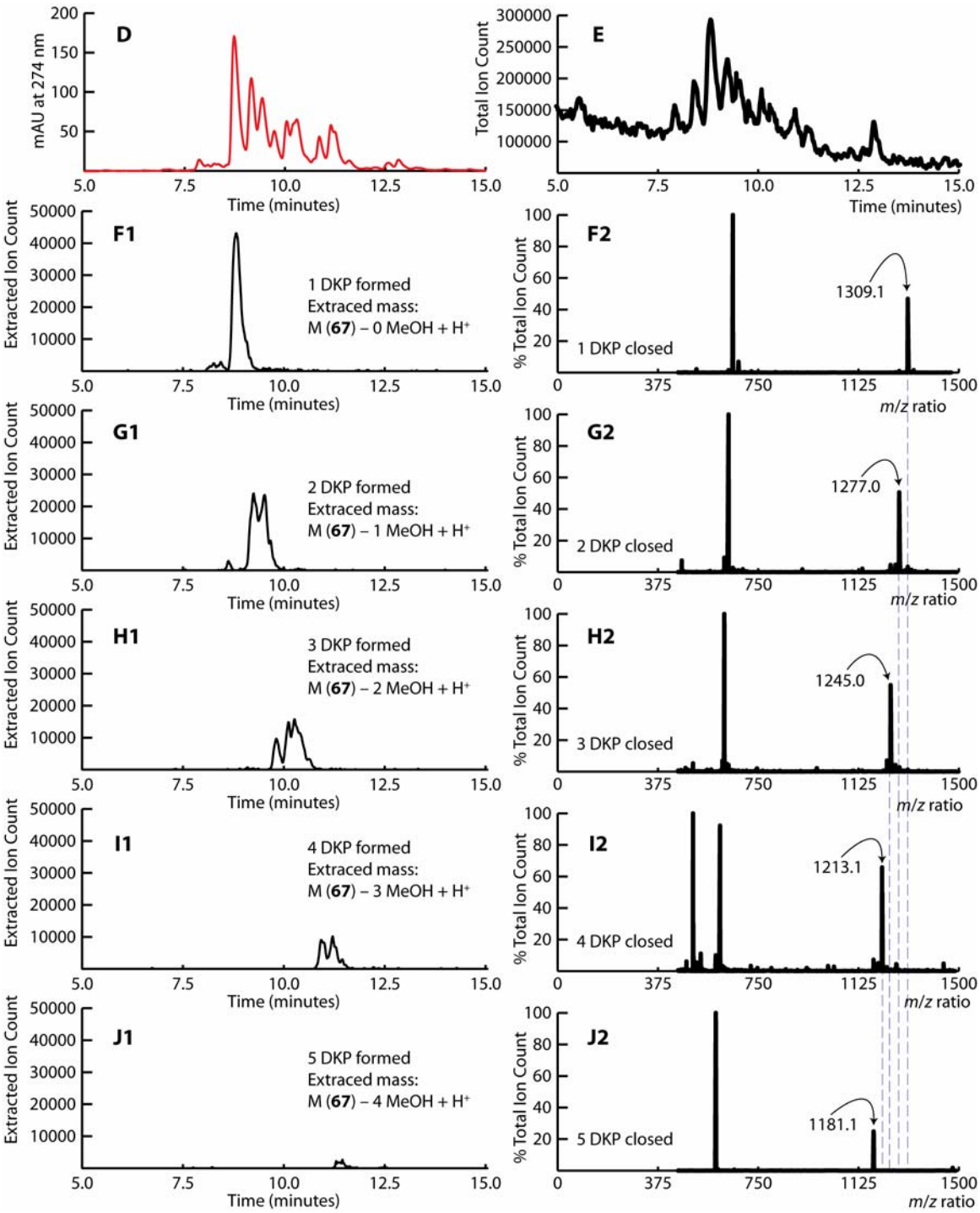

Figure 4-7: ESI-MS analysis of the intermediate products during rigidification of open-form oligomer **67**. **D** (5% to 95% CH_3CN): HPLC of rigidification of **67** after 3 hours. **E**: total ion count during ESI-MS analysis of effluent during analysis shown in **D**. **F1** through **J1**: computational extraction of the ions (from signal **E**) of the partially-closed intermediates. **F2** through **J2**: ESI-MS averaged over the signal obtained from **F2** through **I2**. **J2**: ESI-MS of purified **69**.

Synthesis of controls **71** and **72** was straightforward (Scheme 4-2). Fmoc-(*S*)-1-naphthylalanine was coupled to the NovaTag™ resin using HATU. The terminal Fmoc group was removed, and the resin was cleaved with TFA affording **71**. **72** was prepared by coupling one Boc-*pro4*(2*S*,4*S*) monomer then Fmoc-(*S*)-leucine to the Dansyl NovaTag resin; extended exposure to 20% piperidine/DMF quantitatively closed the terminal DKP, and the desired product was cleaved from the resin with TFA.

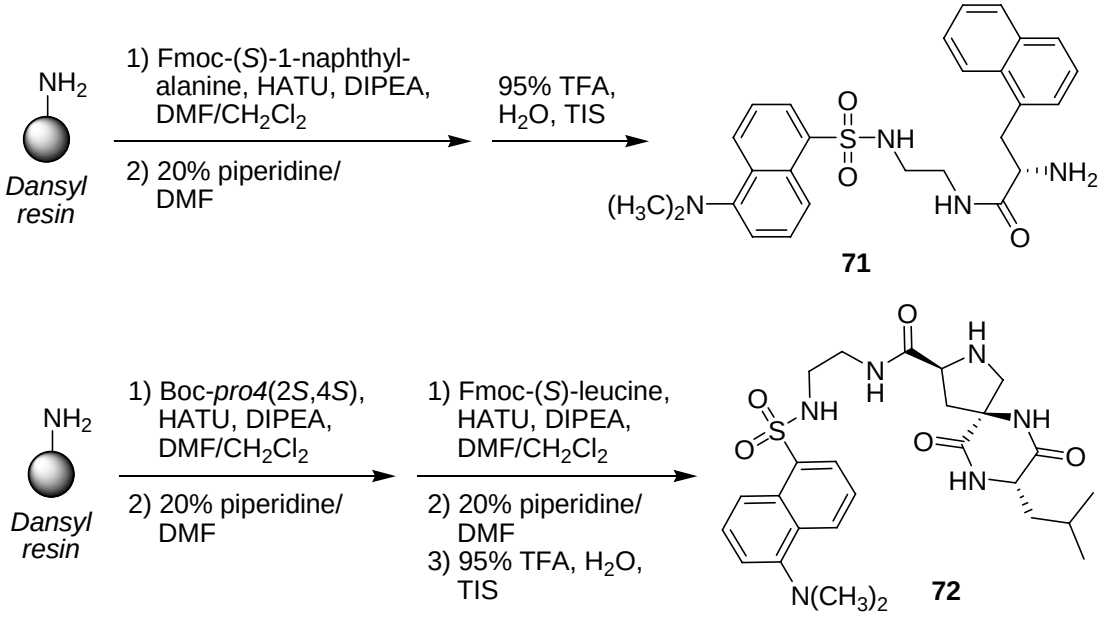

Scheme 4-2: Synthesis of **71** and **72**, controls for the FRET study

4.2 FLUORESCENCE MEASUREMENTS

bis-Peptide **69** was designed to form a molecular rod about 20 Å long, while *bis*-peptide **70** was designed to be curved, holding its two ends closer together. Models of compound **69**, calculated by molecular mechanics using the Amber89[150] and Amber94[138] force fields within MOE, predict that the distance from the pyrrolidine nitrogen of the first monomer to the quaternary center of the last monomer will be 19 Å and 21 Å, respectively. Modeling compound **70** using the Amber89 and Amber94 force fields predicts that the distance from the pyrrolidine nitrogen of the first monomer to the quaternary center of the last monomer will be 12 Å and 16 Å, respectively.

The excitation spectra of all four molecules are shown in Figure 4-8. Excitation at 293 nm causes strong emission at 520 nm when the dansyl and naphthyl groups are in close proximity, as resonance energy transfer increases with decreasing donor-acceptor distance.[52] The excitation spectrum of **72** (black curve, Figure 4-8) is that of a dansyl group infinitely far away from a naphthyl donor. The excitation spectrum of **72** represents the case of minimum energy transfer between donor and acceptor (0% energy transfer efficiency). The excitation spectrum of **71** (green curve, Figure 4-8) indicates highly efficient resonance energy transfer from the naphthyl group to the dansyl group, as they are coupled through a short linker. The excitation spectrum of **71** approaches the maximum possible energy transfer efficiency (100% energy transfer efficiency). We assumed that the excitation spectra of **71** and **72** represented 100% and 0% efficient energy transfer, respectively, based upon Stryer and Haugland's original experiments using FRET as a molecular ruler.[52] Relative to the excitation spectra of **71** and **72**, the spectrum of **69** (blue curve, Figure 4-8), the oligomer designed to form the molecular rod, demonstrates resonance energy transfer that is approximately 50% efficient (at 293 nm). This is reasonable, considering that the Förster distance of the dansyl/naphthyl pair is 22 Å.[158] The excitation spectrum of the curved oligomer **70** (red curve, Figure 4-8) shows resonance energy transfer (at 293 nm excitation) that is about 72% efficient, suggesting that **70** has a curved shape, as designed.

Interestingly, the excitation spectra of the open-form flexible precursors **67** and **68** (Figure 4-8, purple dotted line and yellow dotted line, respectively) are indistinguishable from one another, and nearly identical to the excitation spectrum of curved compound **70** An explanation for this is that prior to rigidification, the open-form flexible oligomers **67** and **68** exist as an ensemble of conformations where the dansyl and naphthyl groups are close enough to one another on average to permit efficient resonance energy transfer. It is only after the molecules are rigidified that they exhibit the behavior inherent to their design.

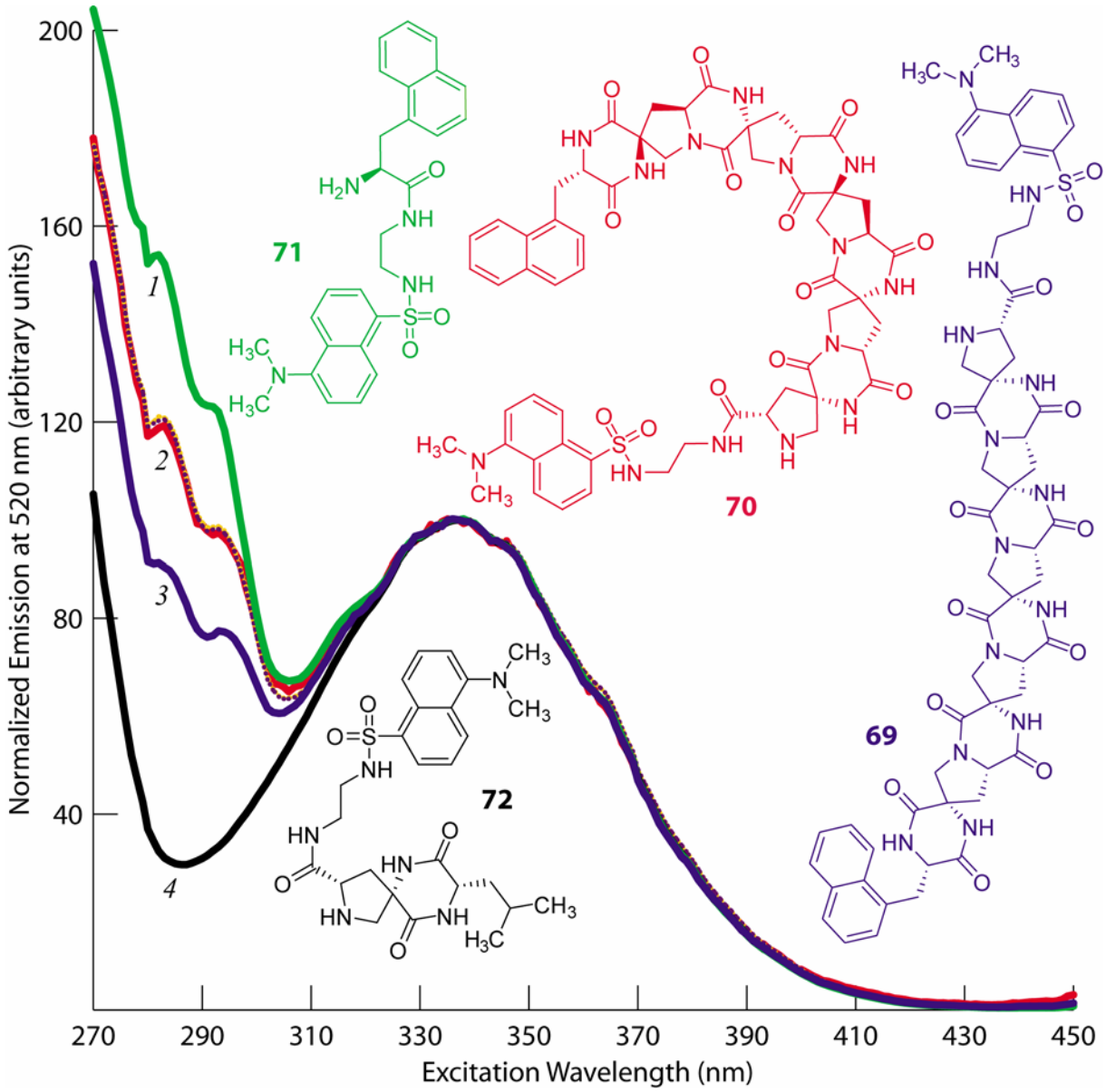

Figure 4-8: Excitation spectra of the FRET oligomers: **71** (green, *1*); **69** (red, *2*); **70** (blue, *3*); **72** (black, *4*); **67** (broken purple line); **68** (broken yellow line).

The fractional efficiency of Förster energy transfer (E) is described by the following expression (equation 4-1)[161]

$$E = \frac{1}{1 + \left(\frac{r}{R_o}\right)^6} \qquad \textbf{(4-1)}$$

where r is the distance between the donor and acceptor, and R_o is the Förster distance. The Förster distance for a donor/acceptor pair depends on the spectral characteristics of the

fluorophores, the refractive index of the medium, and κ^2, a function of the relative angular orientations of the donor and acceptor dipoles.[154] κ^2 averages to 2/3 when the donor and acceptor undergo sufficient re-orientation over the fluorescence lifetime.

Calculating the distance between the naphthyl and dansyl groups with equation **4-1** requires a number of assumptions. For the Förster distance, R_o, we used a literature value of 22 Å.[158] This choice is legitimate only if the angular relationship between the dansyl and naphthyl groups is substantially randomized, such that the value κ^2 is equal to 2/3.[52] The values for *E* (percent energy transfer efficiency) for the excitation spectra of **69** and **70** were calculated relative to the normalized excitation spectra of controls **71** and **72**, as described above (the efficiency of energy transfer was 50% for **69** and 72% for **70**, relative to the assumed energy transfer efficiencies of 0% for **72** and 100% for **71**). Based on the preceding assumptions, the calculated distances between the donor acceptor pair are 22 Å for the rod-shaped compound **69**, and 18.5 Å for the curved compound **70**. These values are more consistent with the predictions of the Amber94 force field. Nonetheless, recent single-molecule fluorescence measurements reveal that distances measured using FRET tend to be overestimated when the donor and acceptor are closer to each other than the Förster distance.[162] This suggests that the curved oligomer **70** may hold its donor-acceptor pair closer together than 18.5 Å. It must also be considered that in **69** and **70**, the naphthyl group might fold back across the neighboring DKP ring.[15,117,139] This would impede dipole rotational averaging in this fluorophore, and might invalidate any quantitative analysis of end-to-end distance.

4.3 EXPERIMENTAL DETAILS

General procedures used for solid-phase peptide synthesis are described above (section 3.7, page 91). Fluorescence excitation spectra were obtained using a fluorescence spectrophotometer (Cary Eclipse). The excitation and emission slits were both set to 5 nm. Excitation was monitored at 520 nm and samples were irradiated between 270 and 450 nm at a scan rate of 120 nm/min. Samples were measured in a 1 cm quartz cell. Fluorescence samples were prepared such that their concentrations were approximately 2 μM; this was determined

based upon theoretical yields from the solid phase resin. Each sample was scanned ten times sequentially, and the ten scans were averaged. The excitation spectra were normalized such that the emission maximum of the dansyl group (337 nm) was 100 arbitrary units for all samples.

Compound 67

10 mg of Dansyl NovaTag resin (Novabiochem, 0.51 mmol/gram substitution) were transferred to a solid phase reactor and swollen in DMF. The *N*-terminal Fmoc protecting group was removed by mixing the resin with 20% piperidine/DMF for 40 minutes (General Procedure H). The resin was then washed with DMF, CH_2Cl_2, *i*-PrOH, CH_2Cl_2, and DMF. **19**, **19**, **19**, **19**, **19** and (*S*)-*N*-Fmoc-1-naphthylalanine were coupled sequentially to the resin (2 equiv. of *N*-Fmoc protected amino acid, 2 equiv. of HATU, 4 equiv. of DIPEA, 0.2 M in 20% CH_2Cl_2/DMF, 30 minutes reaction time) Each coupling reaction was repeated an additional time (see General Procedure F), and was followed by washing (General Procedure E), resin capping with a 400:100:8 DMF/Ac_2O/DIPEA solution (General Procedure G), and deprotection of the terminal *N*-Fmoc group with 20% piperidine/DMF (General Procedure H). After careful washing, residual solvent was removed from the resin overnight under reduced pressure (General Procedure I). The resin was cleaved using 95% TFA, 2.5% triisopropylsilane, 2.5% water over two hours with stirring. The cleavage solution was filtered, the resin washed with an additional volume of TFA, and the filtrates were combined and concentrated by centrifugal evaporation. One quarter of the resulting residue was purified by preparative HPLC (C_{18} column; mobile phase, CH_3CN (0.05% TFA) / H_2O (0.1% TFA), 5% to 95% CH_3CN over 30 min; flow rate, 15 mL/min, herein, the "standard method" for the purification of the oligomers in the FRET study). Fractions containing the desired product were pooled and concentrated to dryness by centrifugal evaporation yielding compound **67**. HRESIQTOFMS calcd for $C_{61}H_{77}N_{14}O_{17}S$ ($M + H^+$) 1309.5312, found 1309.5281.

This sample of **67** was dissolved in UV/VIS grade MeOH (1.5 mL) and filtered through a 0.2 μm Nylon frit. A sample for fluorescence spectroscopy was prepared by diluting an aliquot (22.6 μL) of this stock solution into MeOH (3 mL).

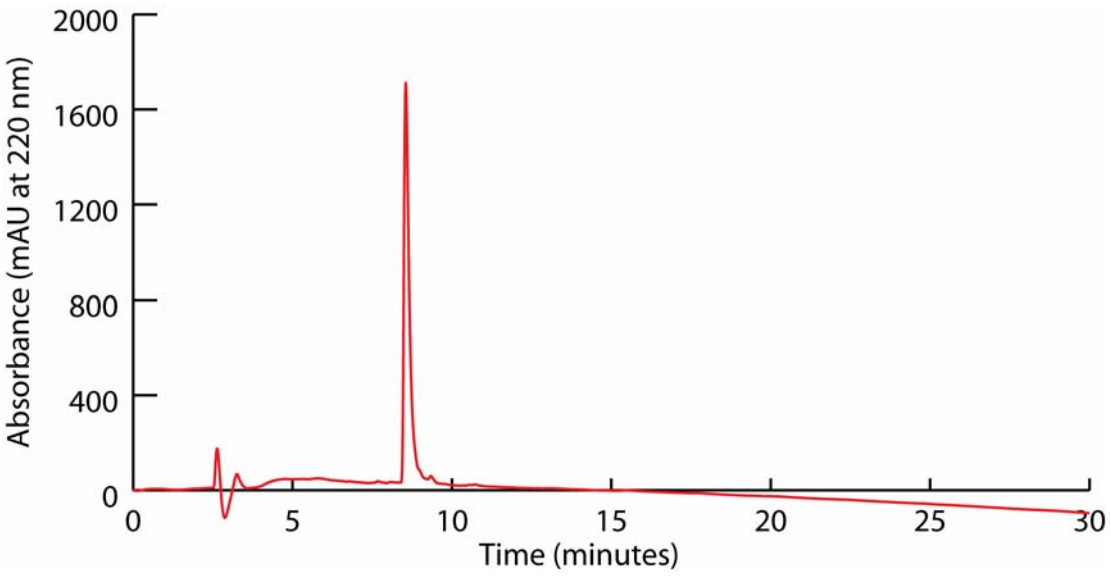

HPLC-MS: C_{18} column; mobile phase, CH_3CN (0.05% HCOOH) / water (0.1% HCOOH), 5% to 95% CH_3CN over 30 min; flow rate, 0.80 mL/min; UV detection at 220 nm; t_R for **67**, 8.55 min; ESI-MS *m/z* (ion): 1309.0 ($M + H^+$).

Figure 4-9: HPLC chromatogram and ESI-MS analysis of the methanol stock solution of purified **67**

Compound 68

19, 30, 19, **30**, **19**, and (*S*)-*N*-Fmoc-1-naphthylalanine were coupled sequentially to 10 mg of Dansyl NovaTag resin using the methods described for the synthesis of compound **67**. Following removal of the terminal *N*-Fmoc group, the product was cleaved from the resin; the cleavage solution was filtered from the resin, and then concentrated by centrifugal evaporation. One quarter of the resulting residue was purified by preparative HPLC using the standard method. Fractions containing the desired product were pooled and concentrated to dryness by centrifugal evaporation yielding compound **68**. HRESIQTOFMS calcd for $C_{61}H_{77}N_{14}O_{17}S$ ($M + H^+$) 1309.5312, found 1309.5237.

This sample of **68** was dissolved in UV/VIS grade MeOH (1.5 mL) and filtered through a 0.2 μm Nylon frit. A sample for fluorescence spectroscopy was prepared by diluting an aliquot (7.4 μL) of this stock solution into MeOH (3 mL).

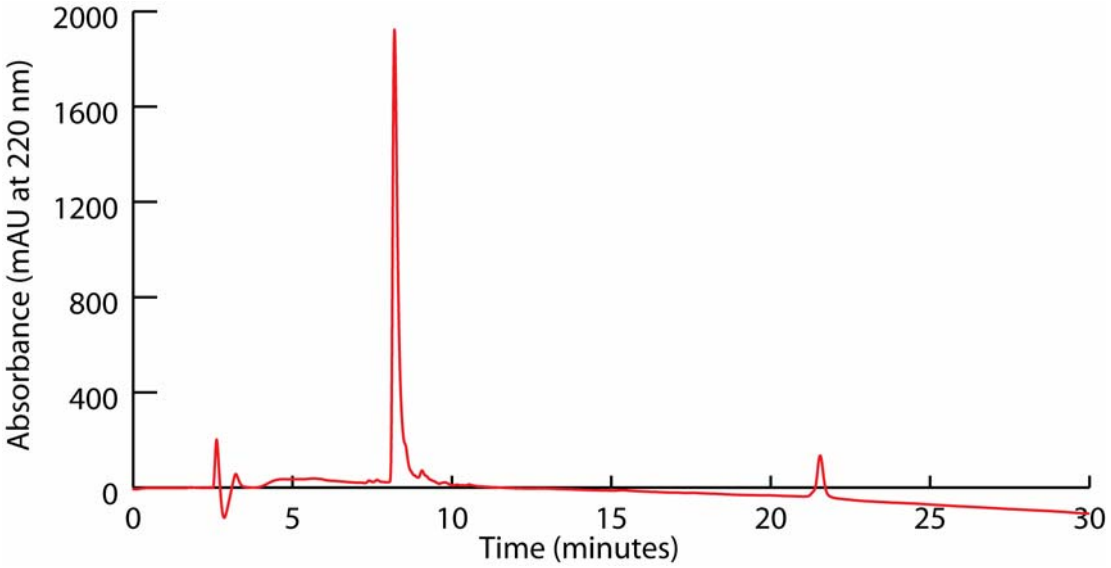

HPLC-MS: C_{18} column; mobile phase, CH_3CN (0.05% HCOOH) / water (0.1% HCOOH), 5% to 95% CH_3CN over 30 min; flow rate, 0.80 mL/min; UV detection at 220 nm; t_R for **68**, 8.19 min; ESI-MS *m/z* (ion): 1309.0 ($M + H^+$).

Figure 4-10: HPLC chromatogram and ESI-MS analysis of the methanol stock solution of purified **68**

Compound 69

The larger portion of the residue containing crude **67** was dissolved in 20% piperidine/DMF (1.25 mL) and transferred to a sealed, amber HPLC vial. Diketopiperazine closure was monitored by analytical HPLC-MS. After ~ 48 hours, the solution was added slowly to diethyl ether (45 mL); the resulting precipitate was pelleted by centrifugation. After decanting the ether, the pellet was dissolved in a 50:50:1 H_2O/MeCN/TFA, and the desired product was purified by preparative HPLC using the standard method. The desired fractions were pooled and concentrated to dryness by centrifugal evaporation affording compound **69**. HRESIQTOFMS calcd for $C_{57}H_{61}N_{14}O_{13}S$ ($M + H^+$) 1181.4263, found 1181.4136.

This sample of **69** was dissolved in UV/VIS grade MeOH (1.5 mL) and filtered through a 0.2 μm Nylon frit. A sample for fluorescence spectroscopy was prepared by diluting an aliquot (10.0 μL) of this stock solution into MeOH (3 mL).

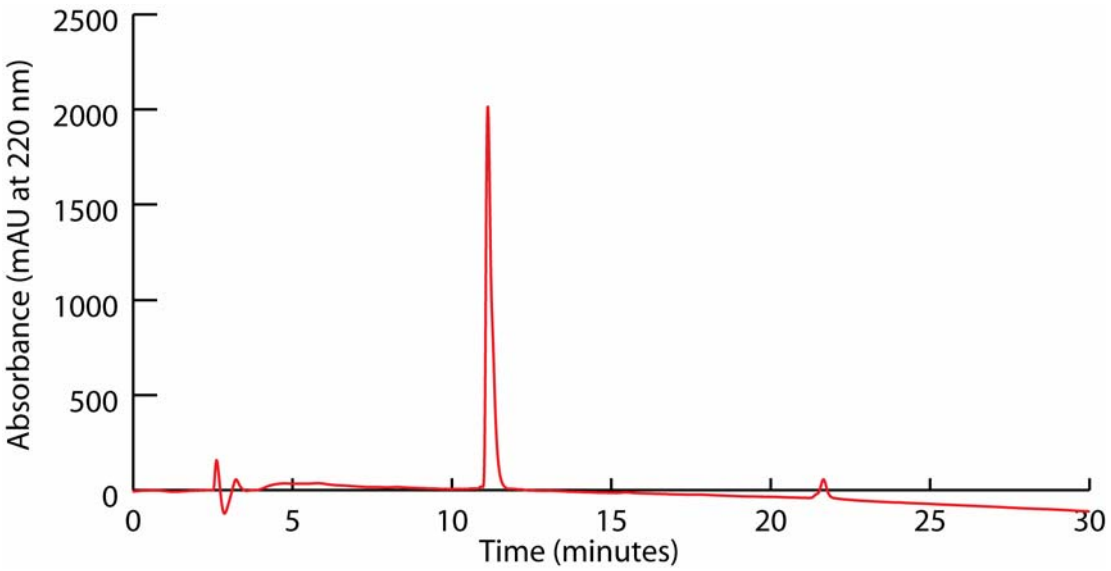

HPLC-MS: C_{18} column; mobile phase, CH_3CN (0.05% HCOOH) / water (0.1% HCOOH), 5% to 95% CH_3CN over 30 min; flow rate, 0.80 mL/min; UV detection at 220 nm; t_R for **69**, 11.13 min; ESI-MS *m/z* (ion): 1181.0 ($M + H^+$).

Figure 4-11: HPLC chromatogram and ESI-MS analysis of the methanol stock solution of purified **69**

Compound 70

The larger portion of the residue containing crude **68** was dissolved in 20% piperidine/DMF (1.25 mL) and transferred to a sealed amber HPLC vial. After ~ 48 hours, the solution was added slowly to diethyl ether (45 mL); the resulting precipitate was pelleted by centrifugation. After decanting the ether, the pellet was dissolved in a 50:50:1 H_2O/MeCN/TFA, and the desired product was purified by preparative HPLC using the standard method. The desired fractions were pooled and concentrated to dryness by centrifugal evaporation affording compound **70**. HRESIQTOFMS calcd for $C_{57}H_{61}N_{14}O_{13}S$ ($M + H^+$) 1181.4263, found 1181.4182.

This sample of **70** was dissolved in UV/VIS grade MeOH (1.5 mL) and filtered through a 0.2 μm Nylon frit. A sample for fluorescence spectroscopy was prepared by diluting an aliquot (150 μL) of this stock solution into MeOH (3 mL).

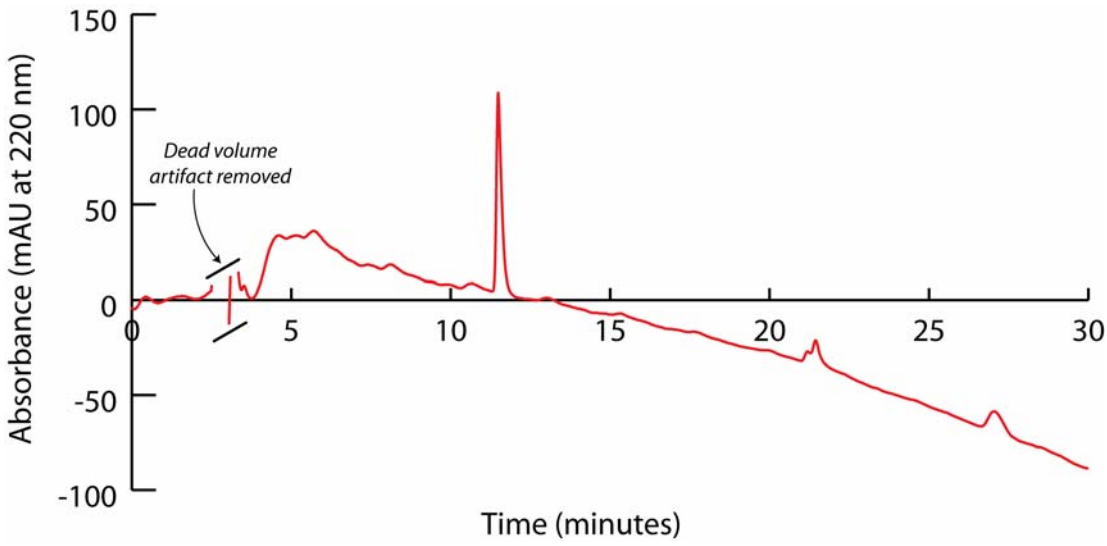

HPLC-MS: C_{18} column; mobile phase, CH_3CN (0.05% HCOOH) / water (0.1% HCOOH), 5% to 95% CH_3CN over 30 min; flow rate, 0.80 mL/min; UV detection at 220 nm; t_R for **70**, 11.49 min; ESI-MS *m/z* (ion): 1181.0 ($M + H^+$).

Figure 4-12: HPLC chromatogram and ESI-MS analysis of the methanol stock solution of purified **70**

Compound 71

(*S*)-*N*-Fmoc-1-naphthylalanine was coupled to Dansyl NovaTag resin (10 mg) with HATU using the method described above. Following removal of the *N*-Fmoc group of the naphthylalanine, resin cleavage and filtration of the resin, the cleavage solution was concentrated by centrifugal evaporation. The resulting residue was dissolved in 40:60:0.1 MeCN/H_2O/TFA (1 mL) and purified by preparative HPLC by the standard method. The desired fractions were pooled and concentrated to dryness by centrifugal evaporation giving compound **71**. HRESIQTOFMS calcd for $C_{27}H_{31}N_4O_3S$ ($M + H^+$) 491.2117, found 491.2092.

This sample of **71** was dissolved in UV/VIS grade MeOH (1.5 mL) and filtered through a 0.2 μm Nylon frit. A sample for fluorescence spectroscopy was prepared by diluting an aliquot (2.5 μL) of the stock solution into MeOH (3 mL).

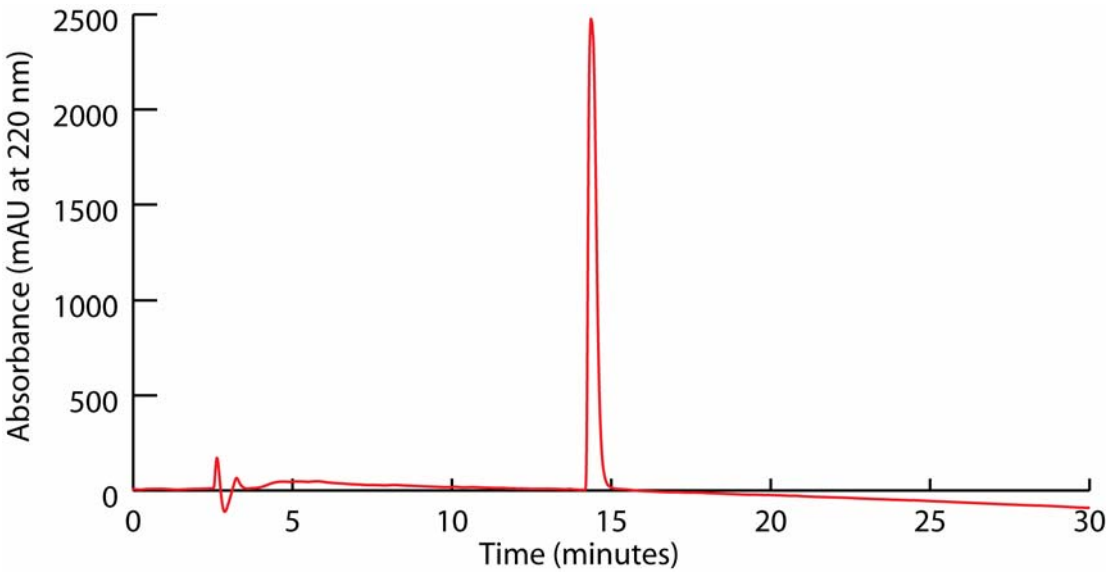

HPLC-MS: C_{18} column; mobile phase, CH_3CN (0.05% TFA) / water (0.1% TFA), 5% to 95% CH_3CN over 30 min; flow rate, 0.80 mL/min; UV detection at 220 nm; t_R for **71**, 14.36 min; ESI-MS *m/z* (ion): 491.0 ($M + H^+$).

Figure 4-13: HPLC chromatogram and ESI-MS analysis of the methanol stock solution of purified **71**

Compound 72

19 and then (*S*)-*N*-Fmoc-leucine were coupled to Dansyl NovaTag resin (10 mg) using the method described above. The *N*-Fmoc group of leucine was removed using 20% piperidine/DMF; the resin was treated an additional time with the same solution to ensure that the diketopiperazine between the monomer residue and the leucine had completely formed. After resin cleavage, the cleavage solution was removed from the resin by filtration and concentrated by centrifugal evaporation. The resulting residue was dissolved in 40:60:0.1 MeCN/H_2O/TFA (1 mL) and purified by preparative HPLC by the standard method. The desired fractions were pooled and concentrated to dryness by centrifugal evaporation giving compound **72**. HRESIQTOFMS calcd for $C_{26}H_{37}N_6O_5S$ ($M + H^+$) 545.2546, found 545.2516.

This sample of **72** was dissolved in UV/VIS grade MeOH (1.5 mL) and filtered through a 0.2 μm Nylon frit. A sample for fluorescence spectroscopy was prepared by diluting an aliquot (15 μL) of this stock solution into MeOH (3 mL).

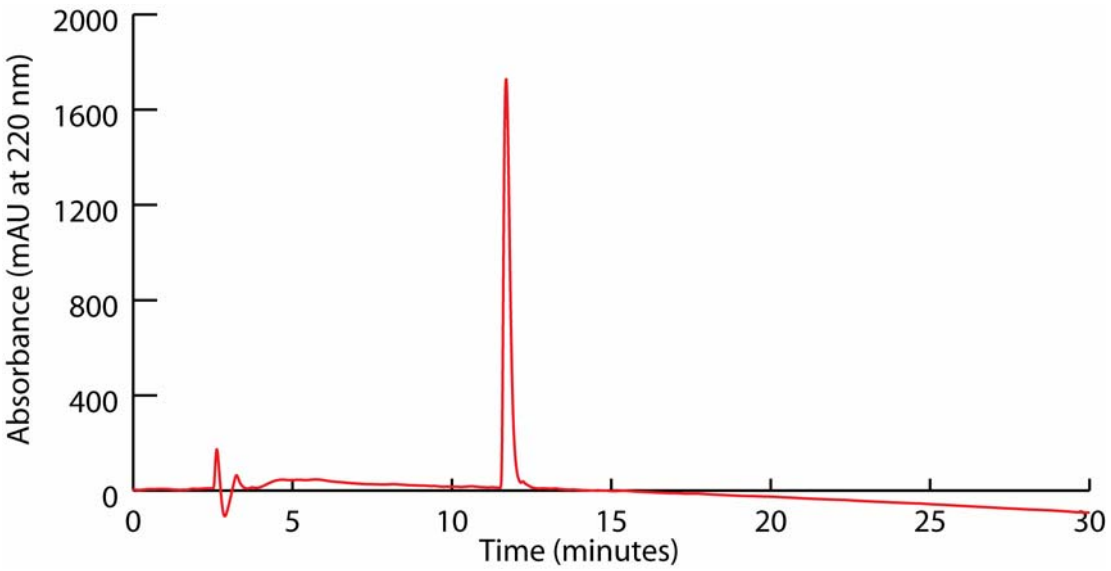

HPLC-MS: C_{18} column; mobile phase, CH_3CN (0.05% TFA) / water (0.1% TFA), 5% to 95% CH_3CN over 30 min; flow rate, 0.80 mL/min; UV detection at 220 nm; t_R for **72**, 11.70 min; ESI-MS *m/z* (ion): 545.2 ($M + H^+$).

Figure 4-14: HPLC chromatogram and ESI-MS analysis of the methanol stock solution of purified **72**

5.0 PROGRESS IN OLIGOMER LIGATION

Many biologically active natural products are macrocycles.[163,164] The activity of a compound is related to how efficiently it can bind to a receptor; macrocyclization is believed to lower the entropic penalty of binding by providing some conformational pre-organization, but allows enough flexibility in the compound to achieve the best fit.[164] A modular approach to the synthesis of non-natural macrocycles would enable convergent synthesis of diverse structures for nanotechnology and bio-mimetic applications, and allow fine-tuning of the structures to optimize their properties.[165] A number of modular approaches toward non-natural cyclic macromolecules have been reported; many generate symmetrical macrocycles.[166-168]

From the outset, we have been interested in using *bis*-peptide oligomers to construct cavity-like receptors for sensors[169,170] and catalysts.[34,171] All four *pro4* monomers have been incorporated into oligomers of varying length. Data from NMR,[15,100,117] ESR,[118] and FRET[100] experiments suggest that the *bis*-peptides made exclusively from *pro4* monomers have linear or slightly curved topology; they resemble "twisted sticks". It is not likely that a small pocket or cavity could be fashioned from a single *bis*-peptide oligomer containing only the *pro4* monomers.

This has led us to consider a different strategy for assembling nanoscale cavities: using individual *bis*-peptide oligomers as construction elements for large macrocyclic structures (Figure 5-1).[4] This is a modular approach toward the design of macrocycles. The macromolecules would be composed of interchangeable *bis*-peptide oligomers; the rigid *bis*-peptide oligomers are composed of interchangeable monomers. The resulting macrocycles would have large, extended structures with hydrogen bonding groups around the perimeter. Probes that have been designed to investigate protein-protein interactions share these characteristics.[165]

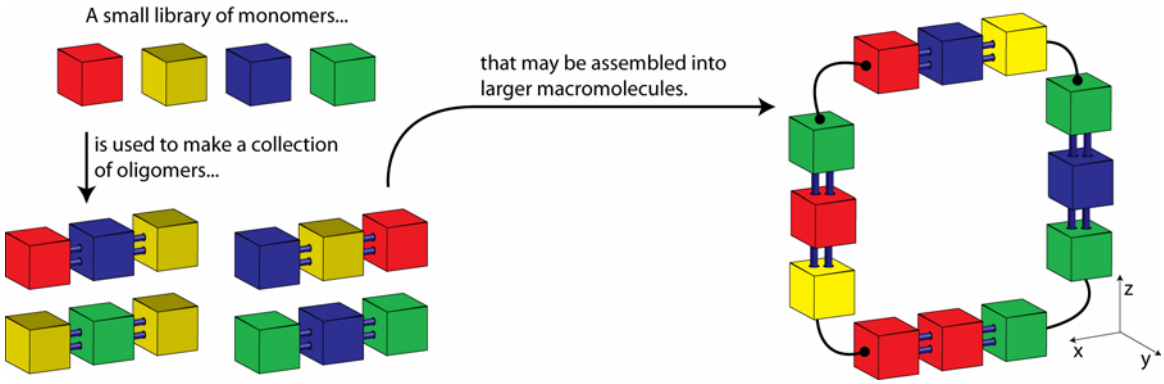

Figure 5-1: Figurative representation of modular, asymmetric macrocycle synthesis using *bis*-peptide oligomers as construction elements

The crux of this approach is selecting the methods used to connect the ends of the *bis*-peptide oligomers. Many types of chemistry have been used to cyclize peptides, including amidation, esterification, and olefin methathesis.[163] All of these might be considered for oligomer macrocyclization; the *bis*-peptide oligomers are peptide-like, and tolerate similar conditions as peptides.[13-15,100,117-119] For a preliminary study of oligomer macrocyclization, we selected the copper-assisted alkyne/azide cycloaddition (CuAAC) reaction. This reaction is high-yielding, regioselective, and is performed under mild conditions. It provides considerable latitude for designing a strategy for cyclization, as it is compatible with aqueous and organic solvents. Adding additional functional groups to *bis*-amino acid oligomers requires careful consideration of protecting group chemistry; one benefit of the CuAAC reaction is that alkynes and azides do not require protecting groups during Fmoc-SPPS.

The thermal 1,3-dipolar cycloaddition reaction between alkynes and azides (Huisgen's cyclization) is relatively slow; it requires high temperatures and long reaction times, and generates two triazole regioisomers (Scheme 5-1, reaction **A**).[169,172,173] 1,4-triazoles are very stable; they resist hydrolysis, oxidation, and reduction, and have been used as restrained analogues of amide bonds.[174,175] The copper-assisted variation of Huisgen's cycloaddition was reported independently by the Sharpless[176] and Meldal[177] groups (Scheme 5-1, reaction **B**). Cu^{I} salts dramatically increase the rate of the reaction between terminal alkynes and azides at room temperature. The 1,4-triazole is generated exclusively with the copper-assisted cyclization.

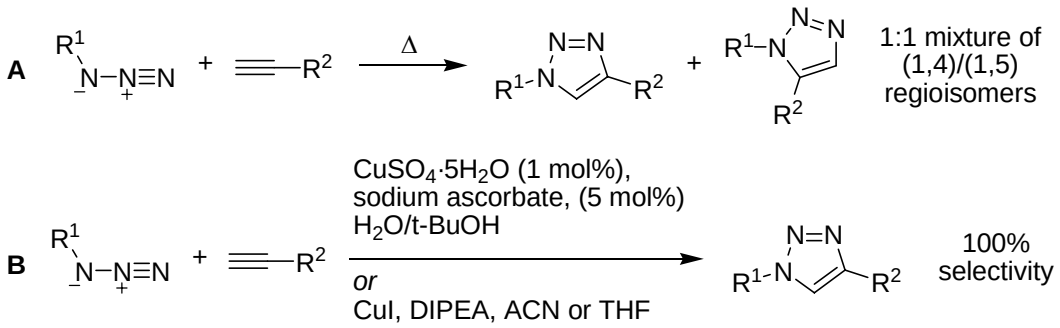

Scheme 5-1: Huisgen's thermal, 1,3-dipolar cycloaddition (**A**) and the copper catalyzed alkyne-azide cycloaddition reaction (**B**)

CuAAC has been used for diverse applications, including bioconjugation,[178] for generating libraries of compounds during drug discovery,[174] in materials chemistry,[179] dendrimer synthesis,[180] and for the conjugation of peptides[181] and carbohydrates.[182] CuAAC has been used primarily in an intermolecular fashion,[173] but there are increasingly more examples of the CuAAC reaction being used for intramolecular macrocyclization.

Gin reported the synthesis of the C_2 symmetric β-cyclodextrin analogue **74** (Scheme 5-2) using CuAAC to perform tandem dimerization/macrocylization.[179] An alkyne/azide functionalized, benzyl ether protected mannose trisaccharide (**73**, Scheme 5-2) was subjected to CuAAC conditions for 16 hours in toluene. The major product of the cycloaddition reaction was the cyclic dimer **74**; the reaction also generated trace amounts of cyclic trimer and higher order oligomers. Like β-cyclodextrin, **74** formed inclusion complexes with small, hydrophobic molecules.

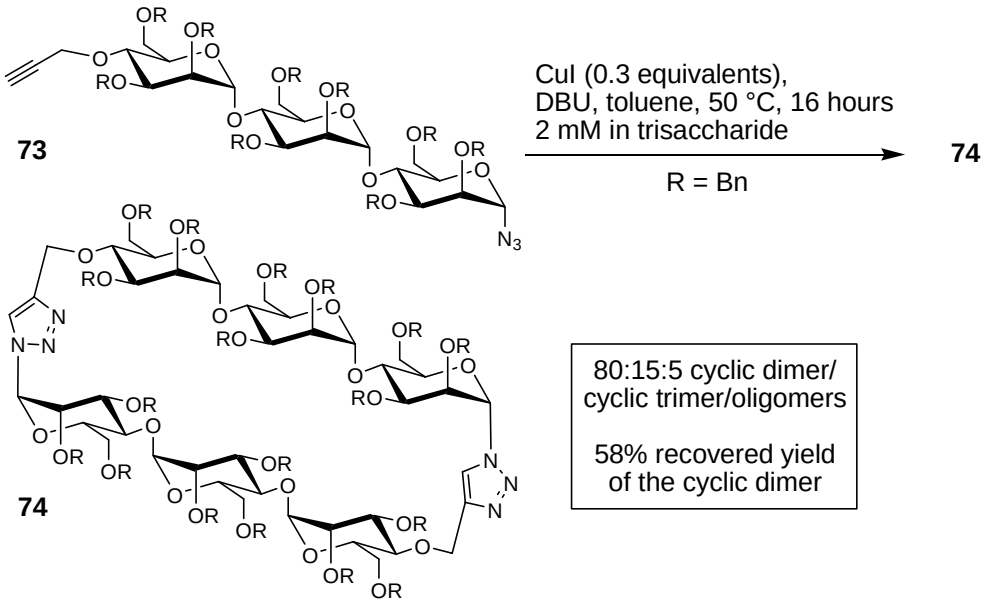

Scheme 5-2: Synthesis of cyclodextrin analogue **74** by CuAAC

Billing used a similar method to synthesize a C_2 symmetric dimer from a carbohydrate/peptide conjugate (Scheme 5-3).[183] The alkyne/azide functionalized monomer **75** (Scheme 5-3) polymerized unless the CuAAC reaction was performed under very dilute conditions. Dynamics simulations suggest that the product, macrocycle **76,** forms a relatively rigid cavity in water.

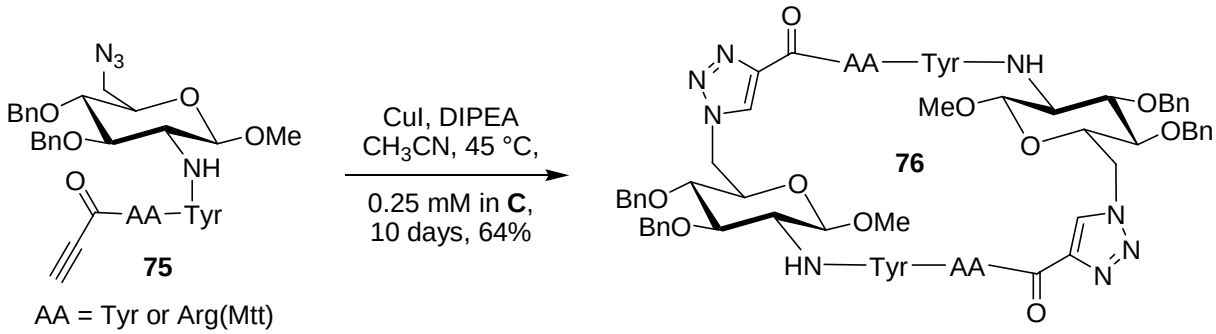

Scheme 5-3: Synthesis of a peptide/carbohydrate cyclic dimer by CuAAC

Several examples of peptide cyclization with CuAAC have been reported.[184-187] Ghadiri reported cyclodimerizaton of the short peptide **77** (Scheme 5-4)[186] in 12 hours to **78** with 80% recovered yield at room temperature using excess CuI in CH_3CN. van Maarseveen reported the cyclization of short peptide **79** (Scheme 5-4),[185] which could only be achieved under reflux in

toluene; the cyclic monomer **80** was the exclusive product. These examples illustrate the potential difficulties in anticipating the cyclic monomer / cyclic dimer product distribution.

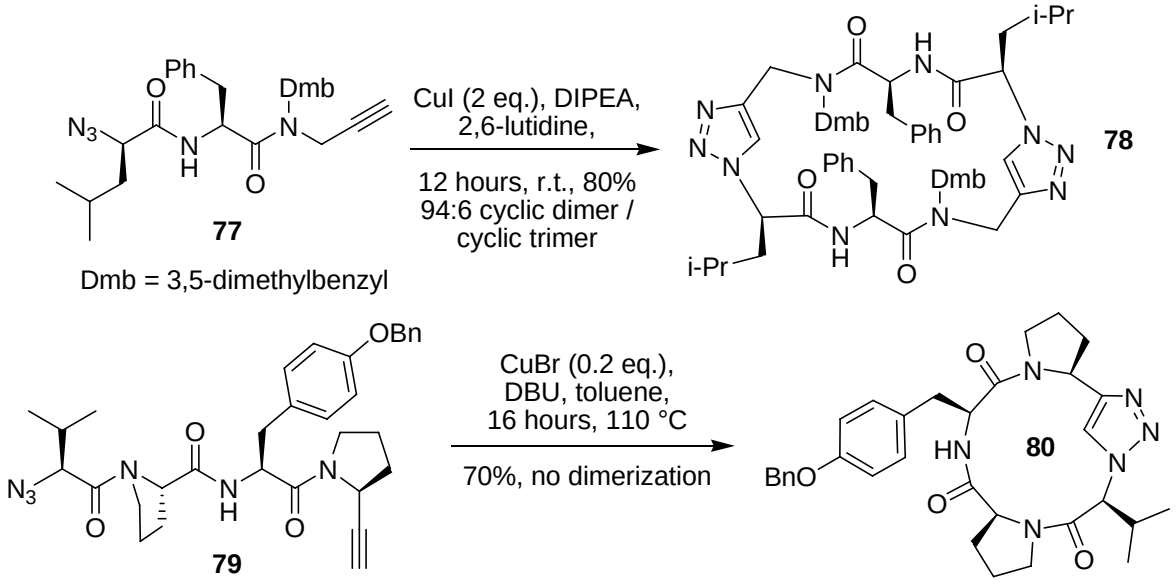

Scheme 5-4: Examples of short-peptide cyclization by CuAAC

5.1 CHOOSING A MACROCYCLIZATION STRATEGY

Having selected CuAAC as the vehicle for macrocyclization, we needed to design a synthetic strategy for oligomer ligation. Four possible cyclization strategies are illustrated in Figure 5-2; each route has certain advantages and disadvantages. For route **B** and route **C**, the cyclic dimer is the expected product; the rigidified oligomer between the terminal alkyne and azide would likely prevent self-cyclization. For routes **A** and **D**, where the CuAAC reaction is performed before DKP formation, it was difficult to predict the cyclic monomer / cyclic dimer distribution. We were concerned that macrocyclization would preclude complete DKP formation by preventing the inter-monomer amide bonds from making the required *trans-cis* isomerization for DKP formation. Cyclization is performed on solid phase for routes **C** and **D**, which would allow easy removal of the copper salts from the reaction. It is more complicated to monitor the reaction progress on solid support, however. The CuAAC substrates for **A** and **D** are non-polar, and the reaction could be tested in acetonitrile.[177] The substrates for **B** and **C** are very polar, so the reaction would need to be performed under aqueous or mixed solvent conditions.[176]

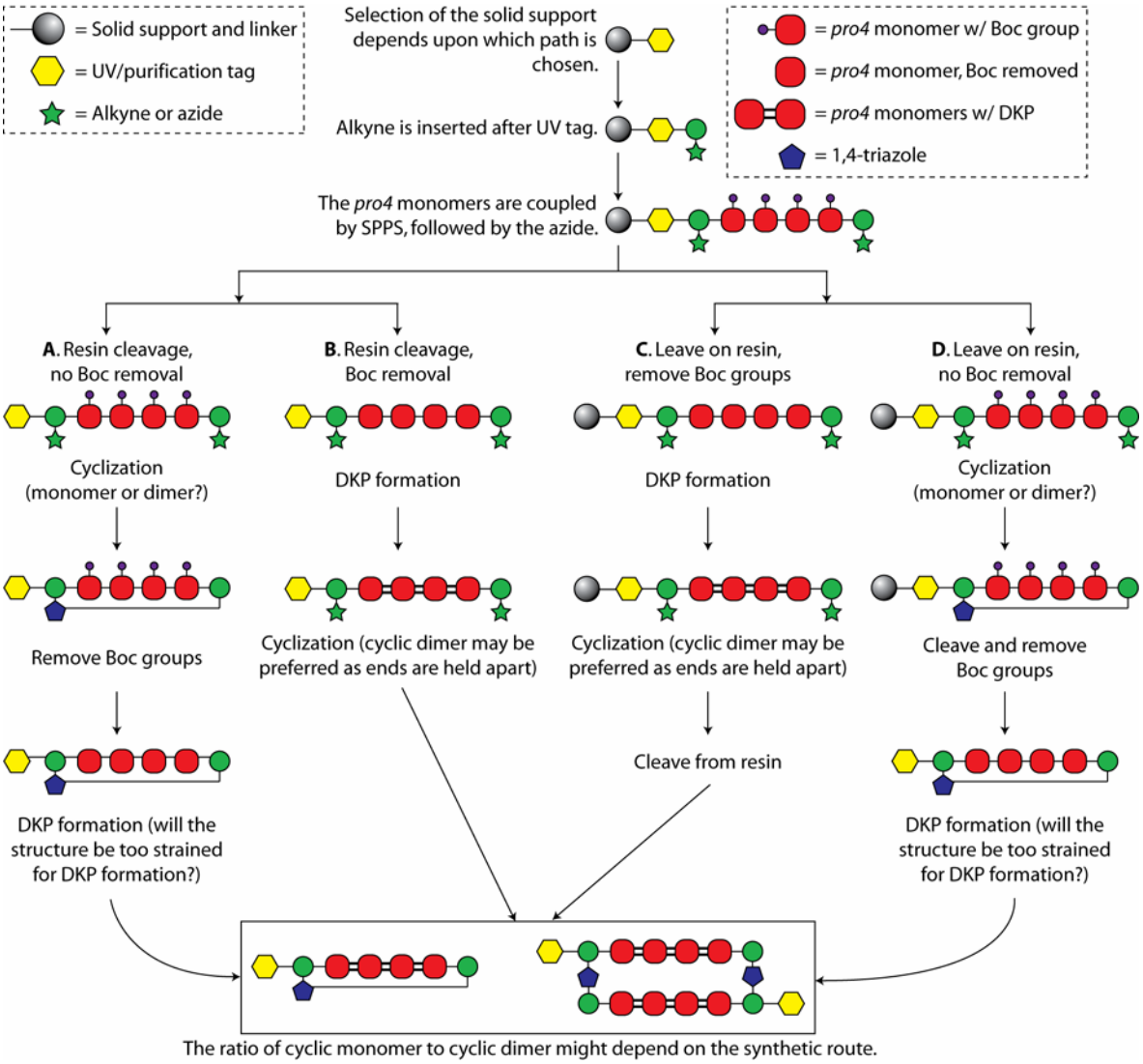

Figure 5-2: Diagram illustrating possible synthetic routes to *bis*-peptide macrocyclization

We chose to start with route **A** for several reasons. This is the most diagnostic approach; the reaction would be performed in solution, and could be monitored in real-time by HPLC-MS. In solution, it would be straightforward to change the monomer concentration, and if necessary, the reaction could be performed under very dilute conditions. On solid-phase, the concentration of the starting material is a function of resin loading, and cannot be manipulated to the same extent or as accurately as in solution. Ghadiri's cyclizations of side-chain protected peptides in acetonitrile[186] were high-yielding and were performed at room temperature; the same reaction conditions could be applied to the non-polar, Boc-protected open-form oligomers. Acetonitrile is

an excellent solvent for the reaction because it coordinates CuI, preventing oxidation by dissolved oxygen.[183]

5.2 AZIDE SYNTHESIS

Azides and terminal alkynes are stable to the conditions used for Fmoc-SPPS, as well as typical resin cleavage conditions, and have been introduced into peptides using a number of methods.[187,188] Propargylglycine is commercially available, and was the most convenient way to introduce the alkyne. We wanted to install the azide at the N-terminus of the oligomer on the side-chain of an amino acid. This would permit DKP formation between the azide-functionalized amino acid and the preceding *pro4* monomer, reducing the number of rotatable bonds between the azide and the oligomer, and converting the methyl ester (which slowly hydrolyzes under aqueous acidic conditions) to an amide. Fmoc-protected amino acids with a side-chain azide are not commercially available, so it was necessary to synthesize one.

The initial synthetic target was azide **81** (Fmoc-Dap-N_3, Figure 5-3), which we had originally intended to synthesize from Fmoc-serine (**82**).

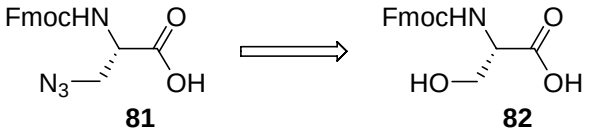

81 **82**

Figure 5-3: Fmoc-Dap-N_3 (**81**), and expected precursor Fmoc-serine (**82**)

The attempts to synthesize azide **81** from Fmoc-serine were unsuccessful (Scheme 5-5). The Weinreb amide[189] of Fmoc-serine was prepared. We tried to generate the mesylate from the Weinreb amide, then displace the mesylate by azide in DMF;[190] no product could be isolated. Similar results were obtained using Mitsunobu conditions[191] and TMS-N_3 as the nucleophile. We also tried to make the lactone from Fmoc-serine, and then open the heterocycle with NaN_3.[192,193] The recovered yield of **81** using this method was poor.

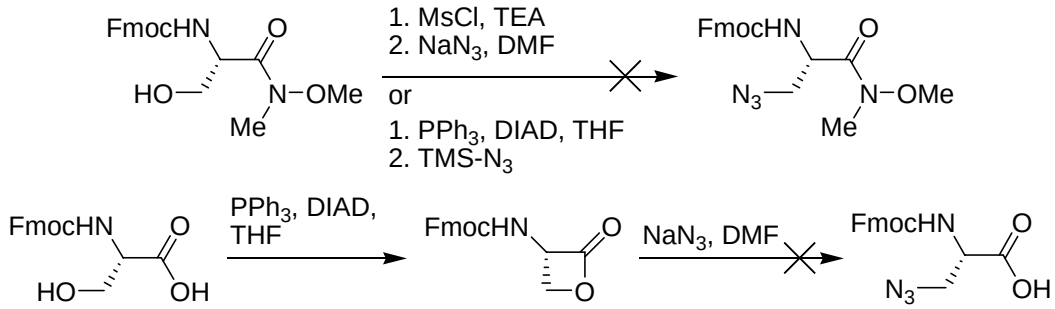

Scheme 5-5: Initial attempts to synthesize azide **81** from Fmoc-serine (**82**)

We obtained significantly better results using diazo transfer to Fmoc-protected diaminopropionic acid (**83**) with triflic azide[194] (Scheme 5-6) in the presence of a catalytic amount of Cu^{II} salt.[195] This method has been used extensively,[188,196,197] though not with Fmoc-protected amino acids. Triflic azide is explosive when concentrated,[194] but the reagent is prepared as a solution in dichloromethane, and added directly to reaction mixture. Clean conversion of **83** to azide **81** was achieved with good yield using this method.

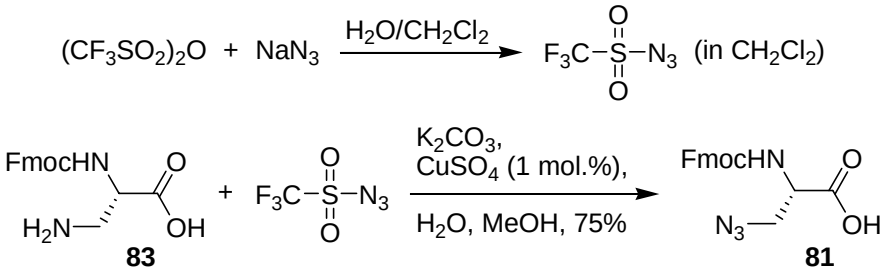

Scheme 5-6: Synthesis of azide **81** from Fmoc-diaminopropionic acid using triflic azide

With Fmoc-Dap-N_3 (**81**) and Fmoc-propargylglycine in hand, we tried to synthesize an alkyne/azide labeled *bis*-peptide oligomer. The "route **A**" approach to cyclization (Figure 5-2) requires that the oligomer be cleaved from the resin without removal of the Boc groups. 2-chlorotrityl chloride resin[198,199] was selected for oligomer synthesis. Peptides may be cleaved from this linker using very dilute TFA (1% TFA in CH_2Cl_2), which does not remove Boc groups.

The solid-phase syntheses of trimer and pentamer oligomers were performed as described in Scheme 5-7. Fmoc-(*S*)-propargylglycine was coupled to the resin in dichloroethane with DIPEA. After removing the Fmoc group from the propargylglycine, 3 or 5 Boc-*pro4*(2*S*,4*S*) monomers (**19**) were coupled sequentially to the propargylglycine with HATU. Finally, Fmoc-Dap-N_3 (**81**) was coupled to the resin. The final Fmoc deprotection was extended to allow complete DKP formation between the Dap-N_3 residue and the preceding *pro4*(2*S*,4*S*) monomer.

Analytical samples of both resins were then cleaved with 95% TFA. HPLC-MS analysis of the crude cleavage products indicated a single product from each resin that did not have the expected mass. Rather, the ESI mass spectra of the products were consistent with compounds **84** and **85** (Scheme 5-7); these appeared to have eliminated the azide anion.

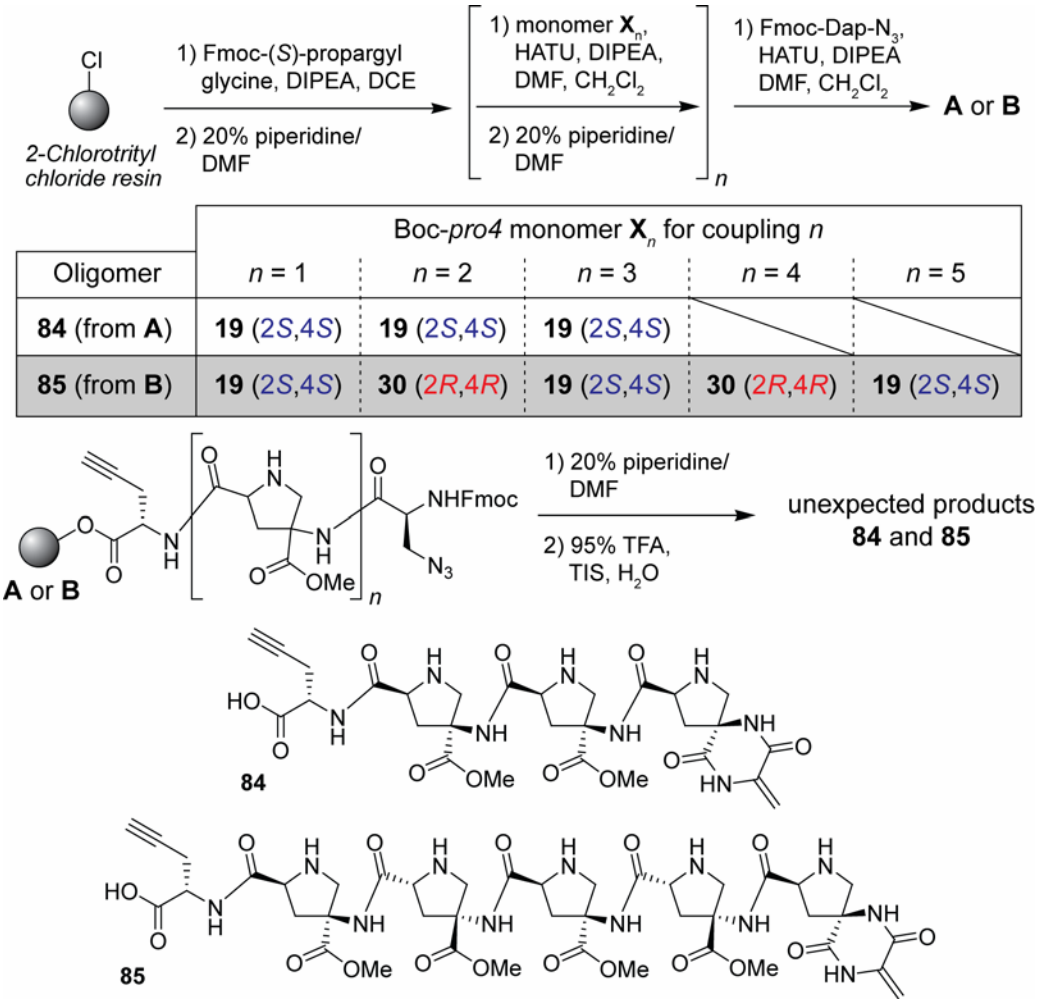

Oligomer	Boc-*pro4* monomer $\mathbf{X}_n$ for coupling *n*				
	n = 1	*n* = 2	*n* = 3	*n* = 4	*n* = 5
84 (from **A**)	**19** (2*S*,4*S*)	**19** (2*S*,4*S*)	**19** (2*S*,4*S*)		
85 (from **B**)	**19** (2*S*,4*S*)	**30** (2*R*,4*R*)	**19** (2*S*,4*S*)	**30** (2*R*,4*R*)	**19** (2*S*,4*S*)

Scheme 5-7: Synthesis of and proposed structure for **84** and **85**; these compounds suffered elimination of the azide anion during diketopiperazine closure (see below)

This result was unexpected; alkyl azides are stable to peptide coupling with DCC/HOBt[188] and HATU.[186] Fmoc-Dap-N_3 (**81**) has been used during Fmoc-SPPS and is stable to treatment with 20% piperidine/DMF.[200] Elimination may have occurred as illustrated in Figure 5-4. Removing the Fmoc group from Dap-N_3 initiated DKP formation between this residue and the preceding monomer. The α-proton of Dap, in the context of the DKP, is more acidic; piperidine could then abstract the proton, causing E2 elimination of the azide anion. This

result underscores the sensitivity of DKPs to basic conditions. Such elimination by loss of the azide anion usually requires a very strong base, such as DBU.[201]

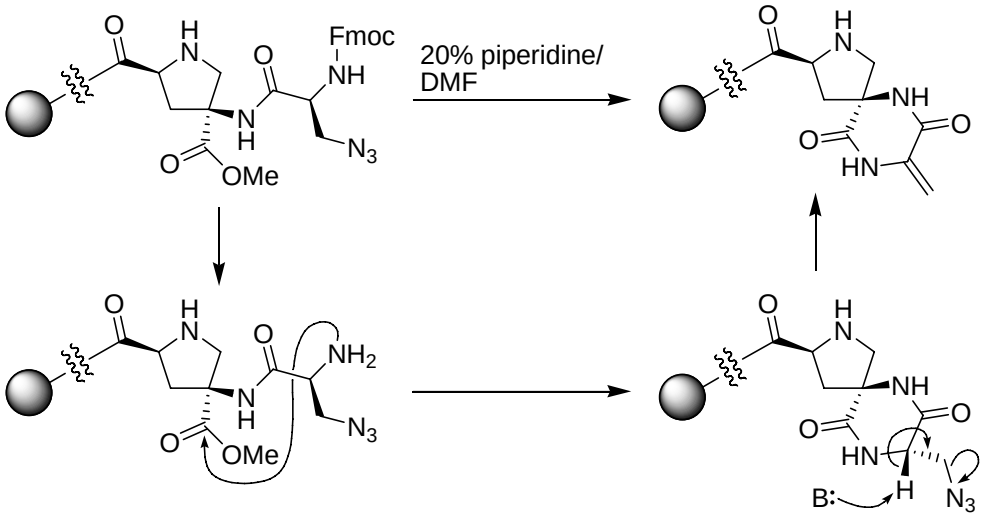

Figure 5-4: The mechanism likely responsible for the undesired azide elimination leading to **84** and **85**

To circumvent elimination, an analogous azide with an additional methylene group between the azide and α-proton (Scheme 5-8) was prepared. Commercially available *N*-α-Fmoc-*N*′-Boc-(*S*)-2,4-diaminobutanoic acid (**86**) was treated with TFA in CH_2Cl_2 to remove the Boc group from the side chain amine. The TFA salt **87** was subjected to the diazo-transfer conditions described for the synthesis of **81**, affording the desired azide **88** (Fmoc-Dab-N_3) in excellent yield. We found (see below) that the elimination reaction that occurred with Fmoc-Dap-N_3, **81**, did not occur with extended chain Fmoc-Dab-N_3, **88**.

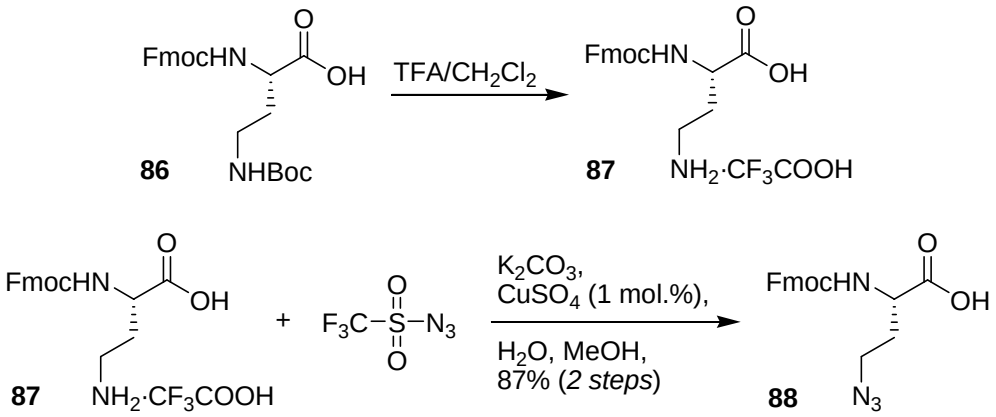

Scheme 5-8: Synthesis of azide **87**

5.3 MODEL SYSTEM 1

A trimer oligomer functionalized with propargylglycine, Dab-N_3, and naphthylalanine was synthesized (Scheme 5-9) as a model system for developing CuAAC reaction conditions. Fmoc-(*S*)-1-naphthylalanine, Fmoc-(*S*)-propargylglycine, three Boc-*pro4*(2*S*,4*S*) monomers (**19**) and Fmoc-Dab-N_3 (**88**) were coupled in sequence to 2-chlorotritylchloride resin. Cleavage with 1% TFA in CH_2Cl_2 afforded the desired product **89** in excellent purity and yield. **89** is non-polar, and soluble in acetonitrile.

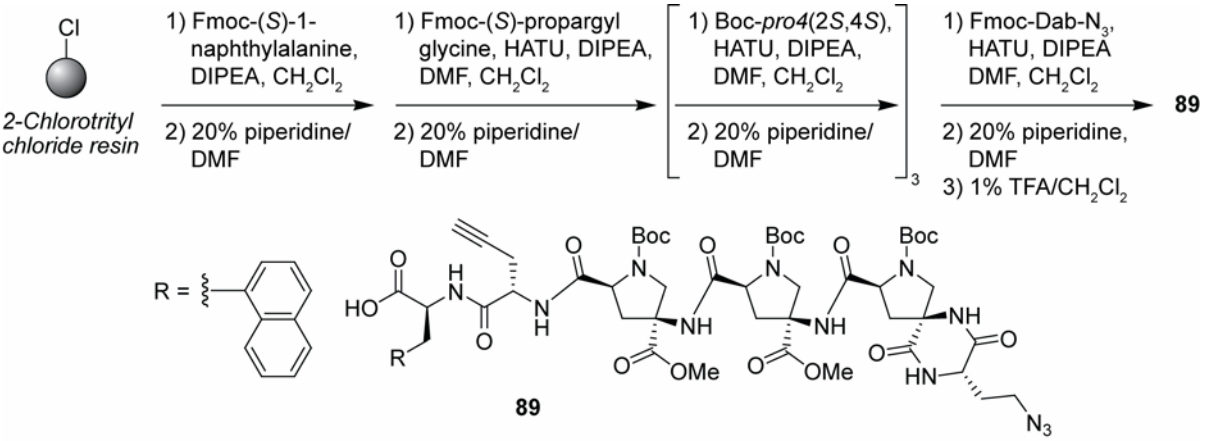

Scheme 5-9: Synthesis of **89**, model system for CuAAC macrocyclization

Ghadiri's conditions for CuAAC[186] were used for the first attempted cyclization with this model system. Compound **89** was dissolved in degassed acetonitrile; 2,6-lutidine and DIPEA were added to the solution, followed by CuI. Within 2 hours, HPLC-MS analysis indicated that the starting material **89** was being consumed, and three products, **90**, **91**, and **92** were forming (Figure 5-5). At 20 hours, the starting material had been entirely consumed. After the starting material had disappeared, subsequent HPLC analysis of the solution indicated no change over a period of days.

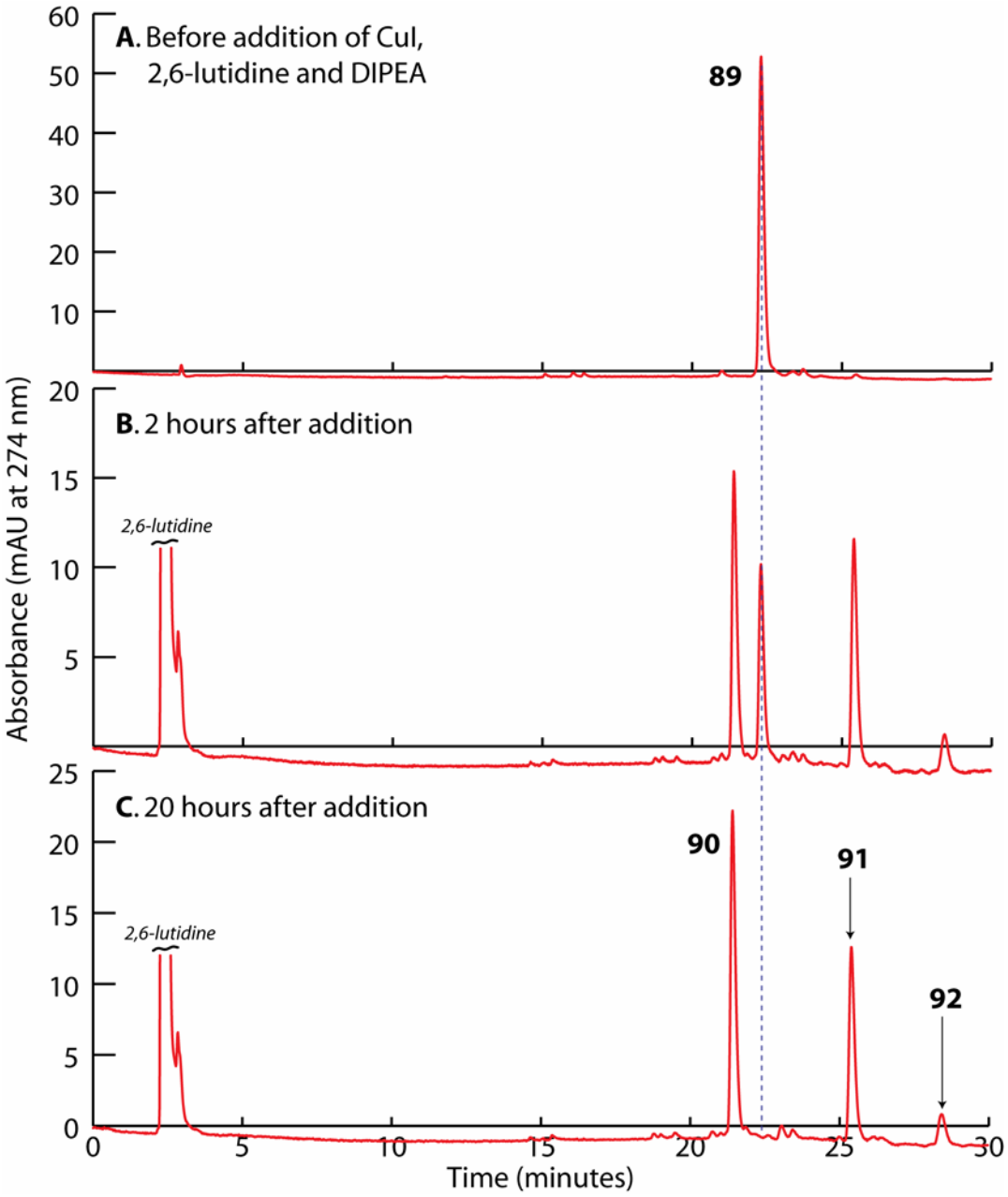

HPLC-MS: Column, Waters XTerra C_{18}, 4.6 × 150 mm; mobile phase, CH_3CN (0.05% HCOOH) / water (0.1% HCOOH), 5% to 95% CH_3CN over 30 min; flow rate, 0.80 mL/min; UV detection at 274 nm; t_R for **90**, 21.42 min; t_R for **89**, 22.30 min; t_R for **91**, 25.40 min; t_R for **92**, 28.43 min.

Figure 5-5: HPLC chromatograms that track the progress of the Cu^I catalyzed alkyne/azide cycloaddition of **89**. **A** (top): before addition of copper. **B** (middle): two hours after addition of copper. **C** (bottom): after reaction had stirred overnight.

Each of the three products has the characteristic absorption spectrum of naphthylalanine; this suggests that the starting material had been incorporated into each of these products. We tentatively assigned the structure of these products based upon the polarity of each compound.

We hypothesized that **90** (Figure 5-5, chromatogram **C**, peak at 21.42 min) was cyclic monomer; the cyclic monomer was expected to become more polar because it would have a triazole, but no additional hydrophobic groups (1,2,3-triazoles have very large dipole moments).[174] **91** (Figure 5-5, chromatogram **C**, peak at 25.40 min) was assigned as the cyclic dimer. The cyclic dimer has twice as many Boc and naphthyl groups as the starting material, so would likely be less polar than the starting material. By the same reasoning, **92** (Figure 5-5, chromatogram **C**, peak at 28.43 min) was cyclic trimer. We assumed that the products were cyclic oligomers, rather than linear oligomers, because there was no change in the concentration or distribution of the products once the starting material had been consumed.

The three products were easily separated by preparative HPLC, and the putative structure assignments were confirmed by detailed analysis of the electrospray mass spectrum of each compound. In the ESI mass spectrum of cyclic monomer **90** (spectrum **A**, Figure 5-6, top) the base *m/z* peak is 1215.4, which corresponds to $[M_{\text{cyclic monomer}} + H^+]$. A simulated mass spectrum[202] of **90** has a similar distribution of isotope peaks above the base peak (the peak ratio of M + 1 to M + 2 to M + 3, etc.). A small peak at *m/z* 2430.6 corresponds to $[2M_{\text{cyclic monomer}} + H^+]$; the ratio of the intensity of the base peak to this smaller peak is about 20:1.

In the ESI mass spectrum of cyclic dimer **91** (spectrum **B**, Figure 5-6, middle) the base peak is 1215.8, which corresponds to $[M_{\text{cyclic dimer}} + 2H^+]$; the distribution of isotope peaks around this *m/z* ratio is different from that observed with the cyclic monomer. The peak at 2430.6, $[M_{\text{cyclic dimer}} + H^+]$, is noticeably larger for the cyclic dimer than for the cyclic monomer; for the cyclic dimer, the ratio of the intensity of the base peak to this peak is about 5:1. The mass spectrum of **92** (spectrum **C**, Figure 5-6, bottom) provides strong evidence for the proposed structure. The base peak is 1823.4, an ion unique to the cyclic trimer. It corresponds with $[M_{\text{cyclic trimer}} + 2H^+]$.

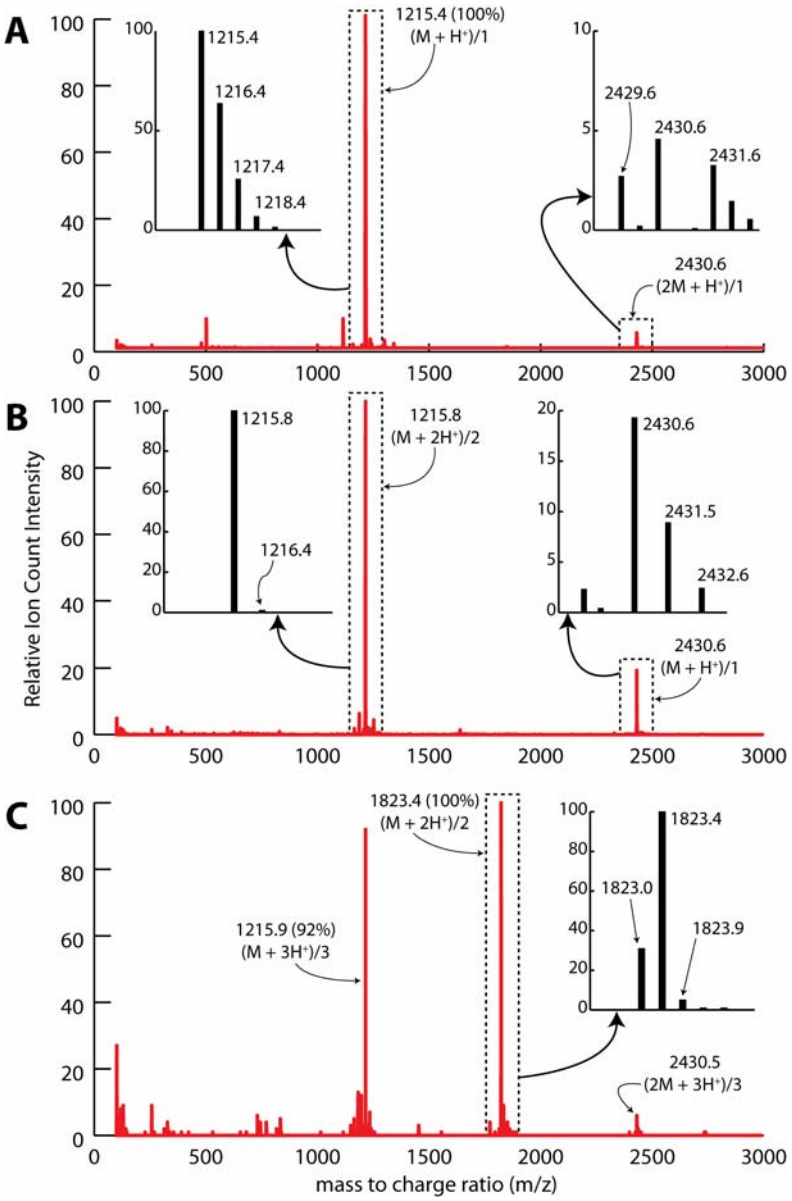

Figure 5-6: ESI mass spectra of the cyclic monomer **90** (**A**, top), cyclic dimer **91** (**B**, middle) and cyclic trimer **92** (**C**, bottom)

Having confirmed the identity of each product, we considered the yield and product distribution for the reaction; the analysis is summarized in Scheme 5-10. Based on the integrated areas under the peaks in the HPLC chromatogram, 76% of the alkyne/azide functionalized oligomer **89** was incorporated into the cyclic monomer, cyclic dimer, and cyclic trimer. The remaining 24% of the starting material may have been incorporated into trace amounts of higher order oligomers that were not detected by HPLC. The molar product distribution was 100:33:4 cyclic monomer / cyclic dimer / cyclic trimer.

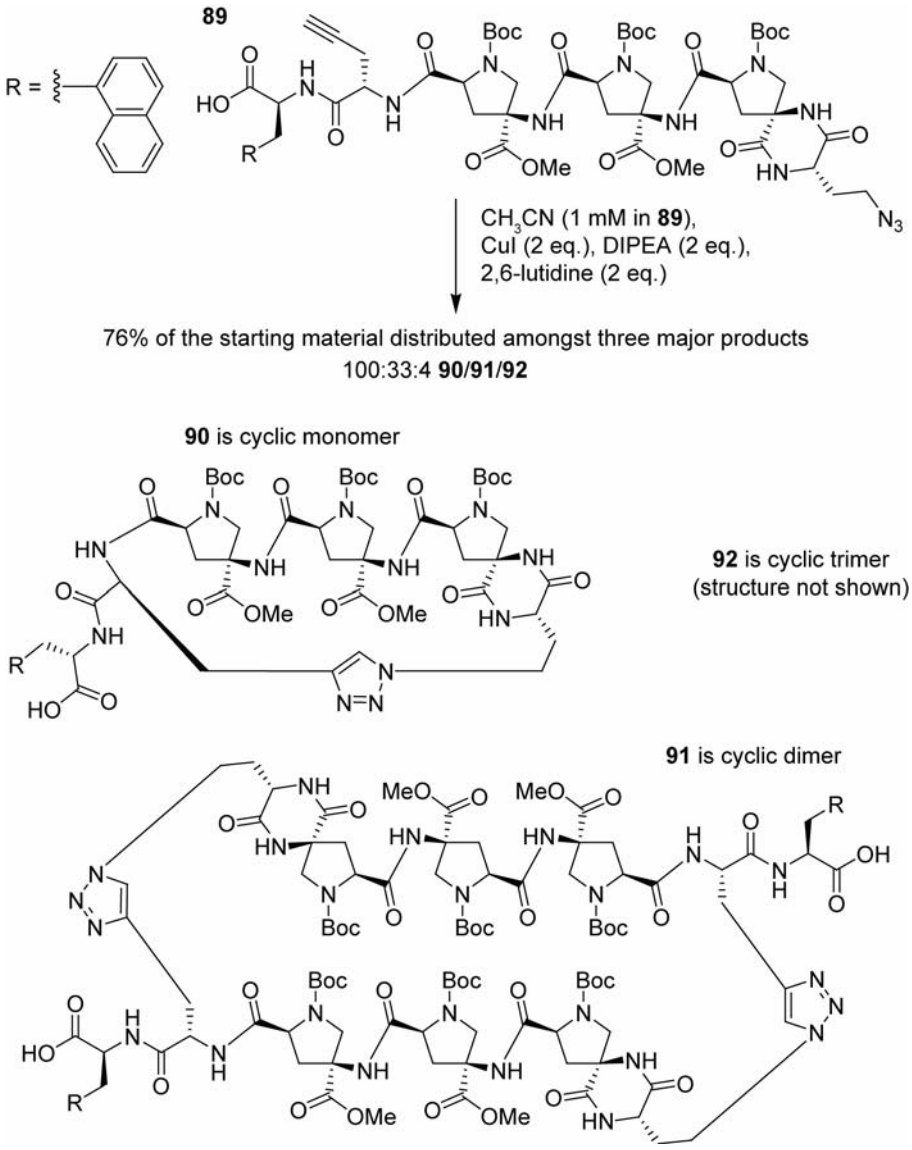

Scheme 5-10: The CuAAC macrocyclization of **89** in solution

To study the effects of macrocyclization on DKP closure, we performed the usual sequence of manipulations for *bis*-peptide preparation on the cyclic monomer **90**, cyclic dimer **91**, and cyclic trimer **92**. First, the purified samples of the three products were dissolved in TFA/CH_2Cl_2 to remove the Boc groups (Scheme 5-11). The products of Boc cleavage, **93** (from **90**), **94** (from **91**), and **95** (from **92**) were analyzed by HPLC-MS and found to be very clean.

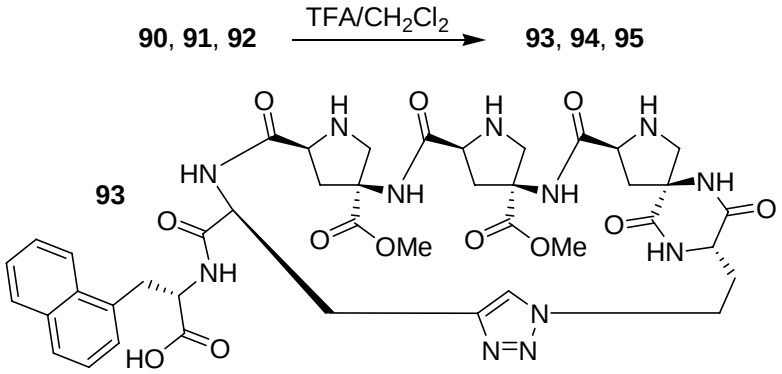

Scheme 5-11: Removing the Boc groups from **90**, **91**, and **92**, affording **93**, **94**, and **95**, respectively; the structure of **93** is illustrated

Removing the Boc groups exposes the ionizable secondary amines of the pyrrolidine rings; increasing the number of ionizable groups of macromolecules can improve the quality their ESI mass specta.[203] The intensity of the ESI mass spectra of the Boc-deprotected open-form cyclic monomer (**93**) and cyclic dimer (**94**) improved considerably after Boc removal. [M + $1H^+$], [M + $2H^+$], and [M + $3H^+$] mass peaks were identified for both compounds (Figure 5-7). The 610.7 [M + $3H^+$] *m/z* peak in the mass spectrum of **94** is characteristic of the cyclic dimer, and is not observed for the cyclic monomer. There was only a trace amount of Boc-deprotected cyclic trimer (**95**), and so this material was taken into the DKP closing reaction without preparing an analytical sample.

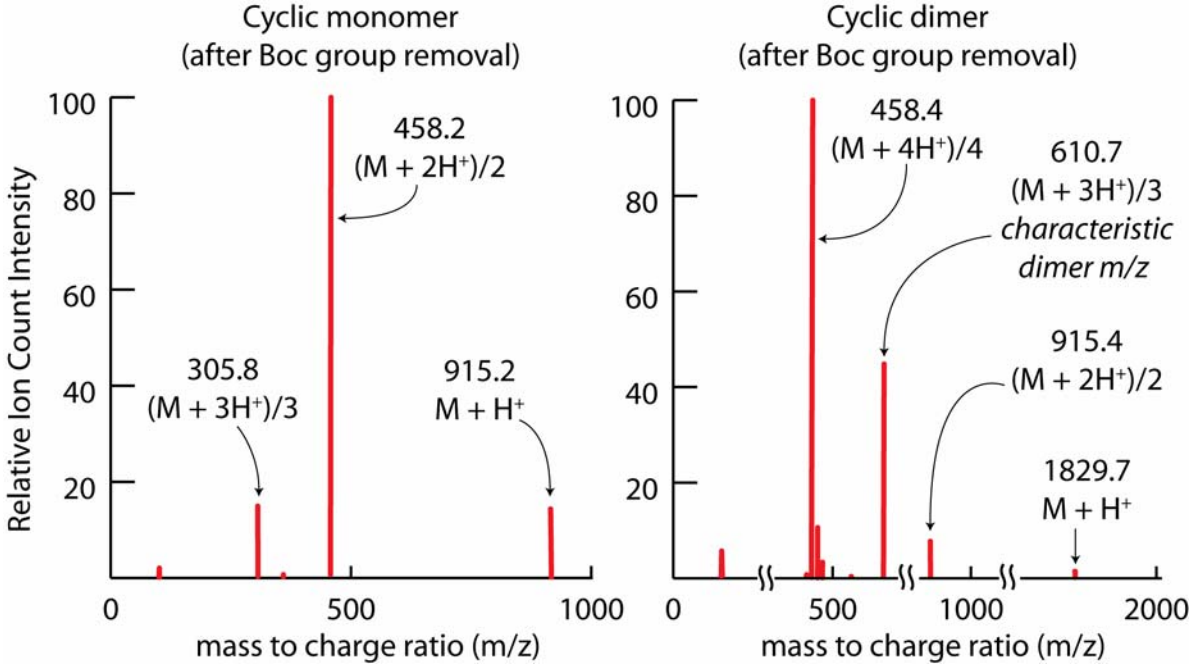

Figure 5-7: The ESI mass spectra of cyclic monomer **93** (left) and cyclic dimer **94** (right)

The Boc-deprotected macrocycles were dissolved in 20% piperidine/DMF, and the DKP closing reaction was monitored by HPLC-MS (Scheme 5-12). DKP closure for the open-form cyclic dimer was clean; **94** was converted to the expected product **97** within 12 hours (Scheme 5-12). There was trace evidence that complete DKP closure occurred in the cyclic trimer; though the absorbance signal in the HPLC chromatogram is barely above baseline, the ESI mass spectrum of what appears to be the major product is consistent with the expected product, **98** (see experimental details, Figure 5-16).

In less than 6 hours, the cyclic monomer **90** was converted to **96** (Scheme 5-12), which is not the desired product. In **96**, 2 of the 3 DKP rings have closed (the desired product has 3 closed DKP rings). **96** was incubated in the 20% piperidine/DMF solution for several days, but the HPLC chromatogram of the mixture did not change; DKP formation was stalled. The open-form Boc-deprotected cyclic monomer **90** is a relatively small macrocycle. In its preferred conformation, there may be a low-energy trajectory for the formation of one of the two DKP rings (*either* between monomer resides 1 and 2, *or* between residues 2 and 3); when this DKP ring closes, the macrocycle becomes even more constrained, perhaps locking the amide bond between the remaining two monomers resides into the *trans* conformation, preventing the closure of the final DKP ring.

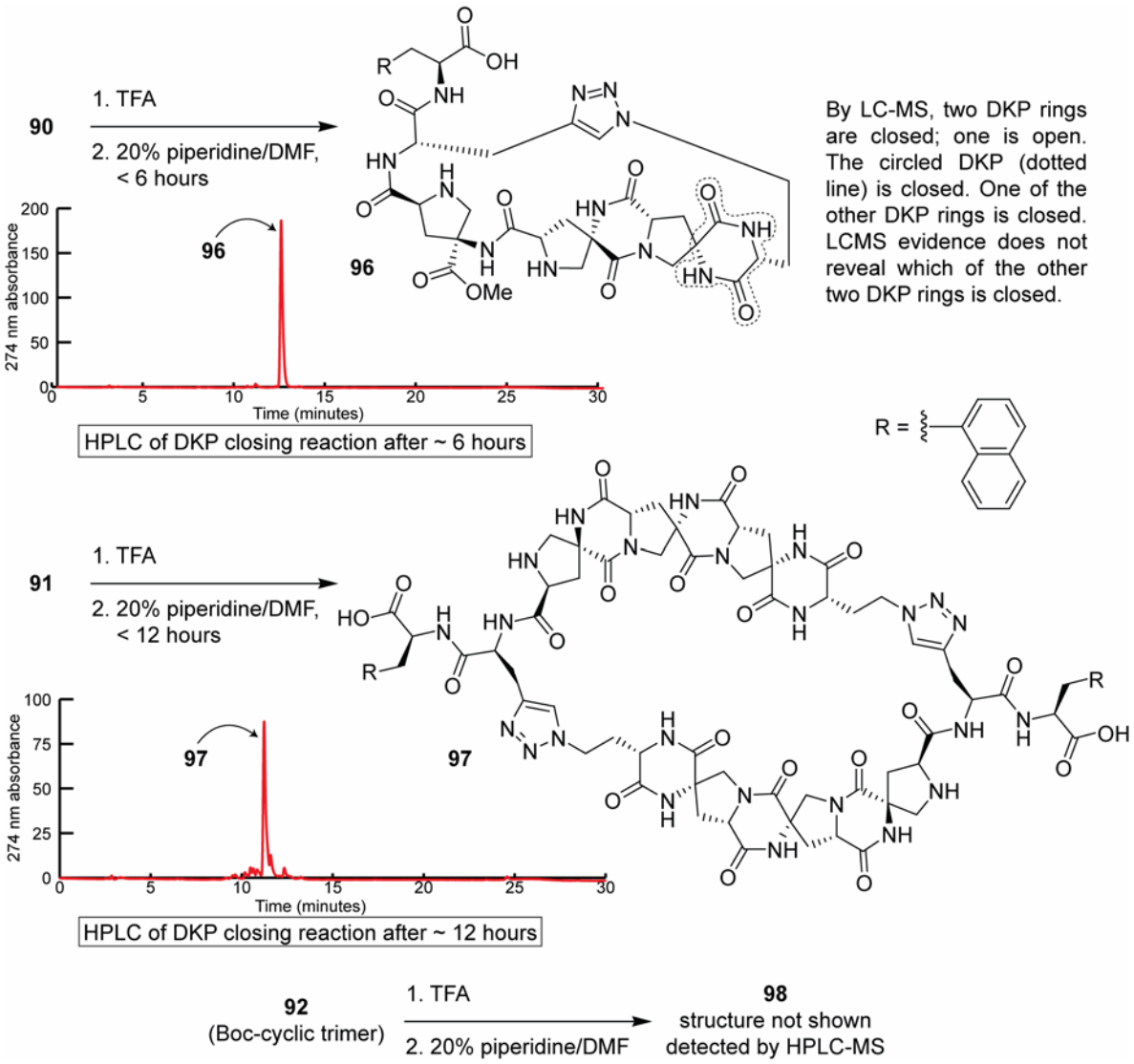

Scheme 5-12: DKP closing reaction for **90** and **91**; the inset HPLC chromatograms are of the crude DKP closing reaction in 20% piperidine/DMF at the times indicated. HPLC-MS: Column, Waters XTerra C18, 4.6 × 150 mm; mobile phase, CH_3CN (0.05% HCOOH) / water (0.1% HCOOH), 0% to 50% CH_3CN over 30 min; flow rate, 0.80 mL/min; UV detection at 274 nm.

5.4 EXPLORING OTHER CONDITIONS

The major product from the CuAAC macrocyclization reaction with model compound **89** was cyclic monomer **90**. DKP formation was incomplete for the cyclic monomer, likely because the macrocycle was too strained to permit every DKP ring to form. While the DKP closing reaction for the cyclic monomer stalled, complete DKP formation was achieved for the cyclic

dimer. Because it was possible to rigidify the cyclic dimer and obtain a well-defined product, it seemed like the more interesting macrocycle.

To determine if it was possible to increase selectivity for the cyclic dimer during macrocyclization, we explored the effects of oligomer and copper concentration on the product ratios (Table 5-1). Either 0.3 or 2.0 equivalents of CuI were added to the reaction, with either 1 mM or 5 mM oligomer concentration. At oligomer concentrations greater than 5 mM, a gelatinous precipitate would appear almost immediately in the reaction mixture, probably the result of oligomer polymerization.

The concentration of open-form oligomer **89** had a large effect upon the ratio of the three major products. Increasing the concentration of **89** did increase the ratio of cyclic dimer to cyclic monomer; unfortunately, this also increased the ratio of cyclic trimer to cyclic dimer. It was possible to increase the proportion of cyclic dimer relative to the cyclic monomer, but not the overall yield of cyclic dimer. Using sub-stoichiometric amounts of copper did not have a significant effect on yield or product distribution.

Table 5-1**:** Summary of the results obtained by performing the CuAAC macrocyclization of model compound **89** under different conditions

				Normalized molar product ratio		
Trial	**Equivalents of CuI**	**[89]**	**% Conversion to 3 products**	**Cyclic monomer (90)**	**Cyclic dimer (91)**	**Cyclic trimer (92)**
A	2	0.001 M	73%	100	34	7
B	0.3	0.005 M	85%	100	55	20
C	0.3	0.001 M	76%	100	46	6
D	2	0.005 M	78%	100	59	19

5.5 EFFECT OF OLIGOMER LENGTH UPON PRODUCT DISTRIBUTION

We also explored the effect of oligomer length on the product distribution obtained from CuAAC macrocyclization. A series of 7 oligomers were prepared (Scheme 5-13). These oligomers contain between 3 and 9 *pro4*(2*S*,4*S*) monomer residues; each oligomer is functionalized with an alkyne and azide. The methods used to synthesize these oligomers are similar to those used to prepare model oligomer **89** (Scheme 5-9).

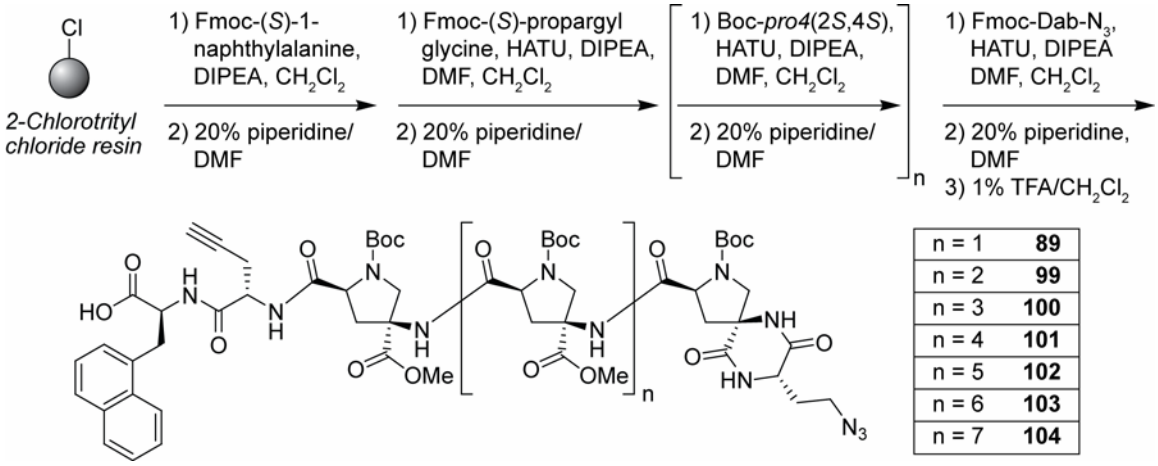

Scheme 5-13: Synthesis of the series of alkyne/azide functionalized oligomers

After cleaving each of the alkyne/azide functionalized oligomers from the 2-chlorotritylchloride resin, the products were purified, then subjected to the same CuAAC conditions used for the model system (2 equivalents CuI, 2 equivalents of DIPEA and 2,6-lutidine, 1 mM in ACN). The CuAAC reactions were monitored by HPLC-MS; the results of the macrocyclizations are summarized in Table 5-2. The macrocyclization yield was similar for each Boc-protected oligomer. As the length of the oligomers increased, the proportion of cyclic dimer decreased. Excluding the results from the 5-mer oligomer **100** and the 7-mer oligomer **102**, the ratio of cyclic dimer to cyclic monomer is nearly proportional to 1/n, n being the number of *pro4* monomer residues in the oligomer. The chances that the two ends of a Boc-protected open-form oligomer encounter one other must increase as the oligomers becomes longer. The increased proportion of cyclic dimer for the CuAAC macrocyclizations of **100** and **102** may be due to slightly higher oligomer concentration during the CuAAC reaction, caused by better than average cleavage yield or purification recovery.

Table 5-2: Product distribution and yields for the CuAAC macrocyclization for the alkyne/azide functionalized Boc-protected oligomers of varying length

Starting Material	Oligomer Length (*pro4* residues)	% yield	cyclic monomer	cyclic dimer	cyclic monomer / cyclic dimer
89	3	68%	**90**	**91**	100:34
99	4	65%	**105**	**106**	100:27
100	5	55%	**107**	**108**	100:50
101	6	66%	**109**	**110**	100:19
102	7	54%	**111**	**112**	100:25
103	8	61%	**113**	**114**	100:16
104	9	57%	**115**	**116**	100:11

The Boc groups were cleaved from all of the cyclized products as shown in Scheme 5-14. The products from Boc group cleavage were each dissolved in 20% piperidine/NMP, and the DKP closing reaction was monitored by HPLC.

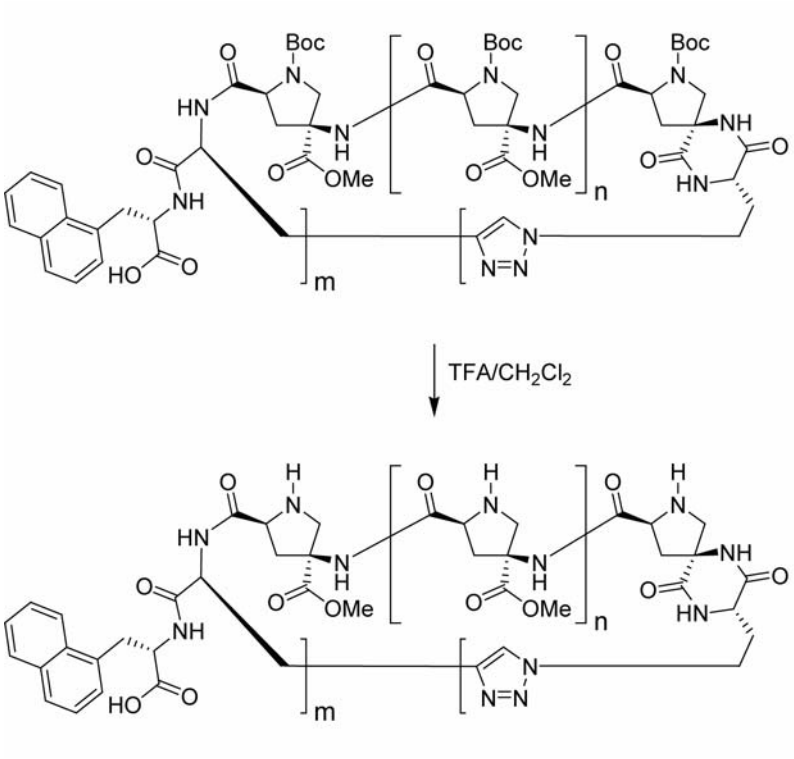

m = 1 cyclic monomers		m = 2 cyclic dimers	
n = 1	**90**	n = 1	**91**
n = 2	**105**	n = 2	**106**
n = 3	**107**	n = 3	**108**
n = 4	**109**	n = 4	**110**
n = 5	**111**	n = 5	**112**
n = 6	**113**	n = 6	**114**
n = 7	**115**	n = 7	**116**

m = 1 cyclic monomers		m = 2 cyclic dimers	
n = 1	**93**	n = 1	**94**
n = 2	**117**	n = 2	**118**
n = 3	**119**	n = 3	**120**
n = 4	**121**	n = 4	**122**
n = 5	**123**	n = 5	**124**
n = 6	**125**	n = 6	**126**
n = 7	**127**	n = 7	**128**

Scheme 5-14: Removing the Boc groups from the series of cyclic monomers and cyclic dimers

When the model system cyclic monomer **93** was dissolved in 20% piperidine, the reaction stalled after one DKP ring had closed. The cyclic monomers containing between 4 and 9 *pro4*(2*S*,4*S*) monomer resides behaved in a similar way during DKP formation. When dissolved in 20% piperidine/NMP, the open-form cyclic monomers were converted to mixtures of products; these products (by mass) had 1 or 2 DKP rings fewer than the expected product. After 24 hours, there was little change in the HPLC chromatograms of the reaction mixtures. DKP formation in the 7-mer cyclic monomer **123** is representative of the results obtained with the other cyclic monomers. Two HPLC chromatograms of this reaction are illustrated in Figure 5-8. After removing the Boc groups, the 7-mer cyclic monomer appears to be a single compound (Figure 5-8, top). After 48 hours in 20% piperidine/NMP, the 7-mer cyclic monomer had been converted into a mixture of products (Figure 5-8, bottom). The compounds with earlier retention time had masses consistent with oligomers that had closed 5 DKP rings; compounds which

eluted later had masses consistent with oligomers that had closed 6 DKP rings (7 DKP rings were expected to close).

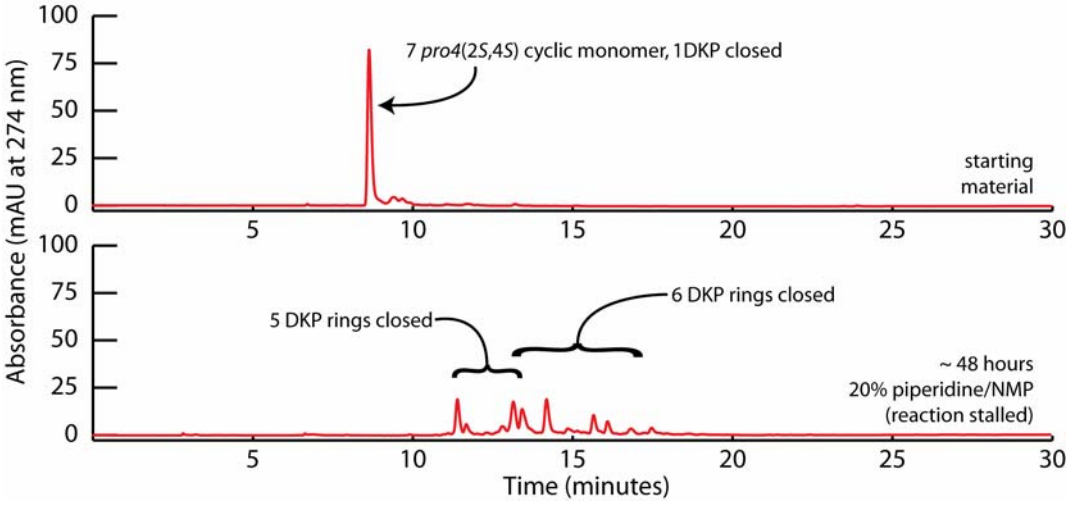

HPLC-MS: Column, Waters XTerra C_{18}, 4.6 × 150 mm; mobile phase, CH_3CN (0.05% HCOOH) / water (0.1% HCOOH), 0% to 50% CH_3CN over 30 min; flow rate, 0.80 mL/min; UV detection at 274 nm.

Figure 5-8: HPLC chromatograms of the DKP closing reaction for the 7-mer cyclic monomer **123**: starting material (top) and the DKP closing reaction after ~ 48 hours (bottom)

The products obtained when the cyclic monomers were dissolved in 20% piperidine/NMP are summarized in Table 5-3. In each case, it was possible to close one less than the expected number of DKP rings.

Table 5-3: A summary of the products obtained when each of the cyclic monomers in the series were dissolved in 20% piperidine/NMP (as determined by HPLC-MS)

Cyclic monomer	Oligomer Length (*pro4* residues)	Expected # of DKPs	Observations
93	3	3	Single product, 2 DKPs (compound **96**)
117	4	4	Products with 2 DKPs and 3 DKPs (mixture)
119	5	5	Some 3 DKPs, mostly 4 DKPs (mixture)
121	6	6	Some 4 DKPs, mostly 5 DKPs (mixture)
123	7	7	Some 5 DKPs, mostly 6 DKPs (mixture)
125	8	8	Some 6 DKPs, mostly 7 DKPs (mixture)
127	9	9	Trace of 7 DKPs, mostly 8 DKPs (mixture)

Conversion of the open-form 3-mer cyclic dimer **94** to the desired product **96** was clean. DKP formation for the open-form 4-mer and 5-mer cyclic dimers (**118** and **120**) was relatively clean; the *bis*-peptide cyclic dimers **129** and **130** were purified by preparative HPLC (Figure 5-9), and analyzed by HRMS. There was evidence of complete DKP closure for the longer cyclic dimers (6-mer through 9-mer open-form cyclic dimers). Unfortunately, substantial epimerization occurred while these samples were dissolved in 20% piperidine/NMP. The Boc-

deprotected open-form oligomers were dissolved in water in order to obtain samples for HPLC-MS analysis. The aqueous samples were concentrated by centrifugal evaporation (SpeedVac); the epimerization may have been caused by residual water content.

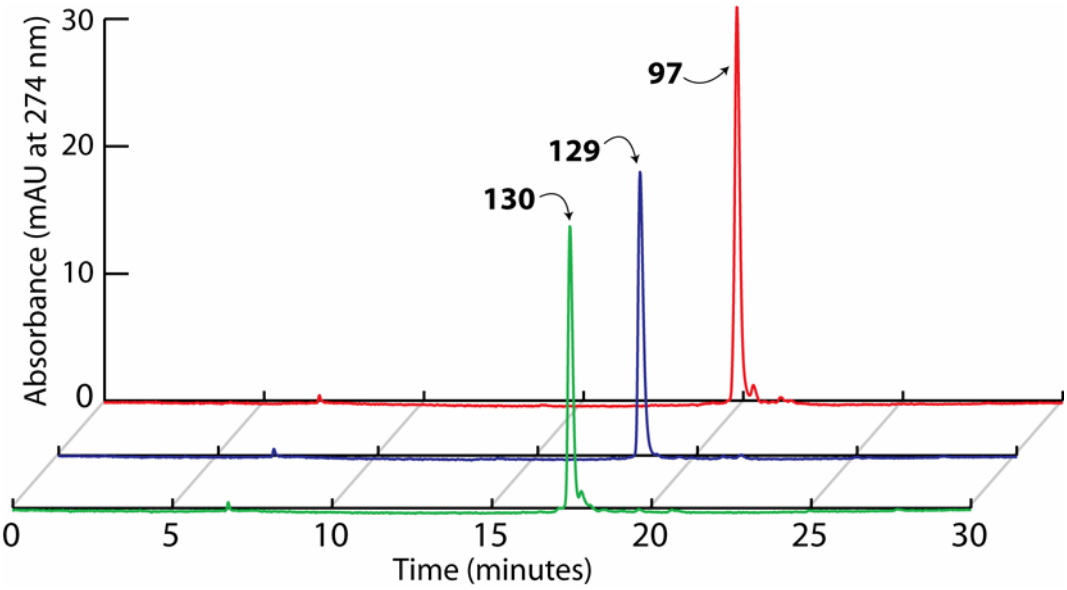

HPLC-MS: Column, Waters XTerra C_{18}, 4.6 × 150 mm; mobile phase, CH_3CN (0.05% HCOOH) / water (0.1% HCOOH), 0% to 50% CH_3CN over 30 min; flow rate, 0.80 mL/min; UV detection at 274 nm.

Figure 5-9: HPLC chromatograms of purified *bis*-peptide cyclic dimers: **97** (3-mer cyclic dimer), **129** (4-mer cyclic dimer), **130** (5-mer cyclic dimer)

5.6 ROD-HINGE-ROD MOTIF

The cyclic dimers generated in the model systems described above are large macrocycles. Nonetheless, the synthetic route favors cyclic monomers, which cannot undergo complete DKP closure. Although the dimers can be isolated and their *bis*-peptide oligomer components can be rigidified, these macrocycles are C_2 symmetric. To create cavities that are bio-mimetic, asymmetry is essential; asymmetry is intimately associated with biological sensing and molecular recognition.

The results from the model systems inspired us to pursue a different strategy: connecting two oligomers with a flexible hinge during solid-phase synthesis (Figure 5-10). This approach would exploit the cyclic monomer selectivity of the CuAAC macrocyclization reaction with lengthy Boc-protected oligomers. The expected major product was the cyclic monomer, which

would be composed of two *bis*-peptide oligomers connected through a 1,4-triazole and a flexible hinge. Once the DKP rings between the monomers have been closed, the macrocycle will resemble the cyclic dimers (or incompletely rigidified cyclic monomers). The linker should provide flexibility in the backbone, allowing complete rigidification of the *bis*-peptide oligomer segments.

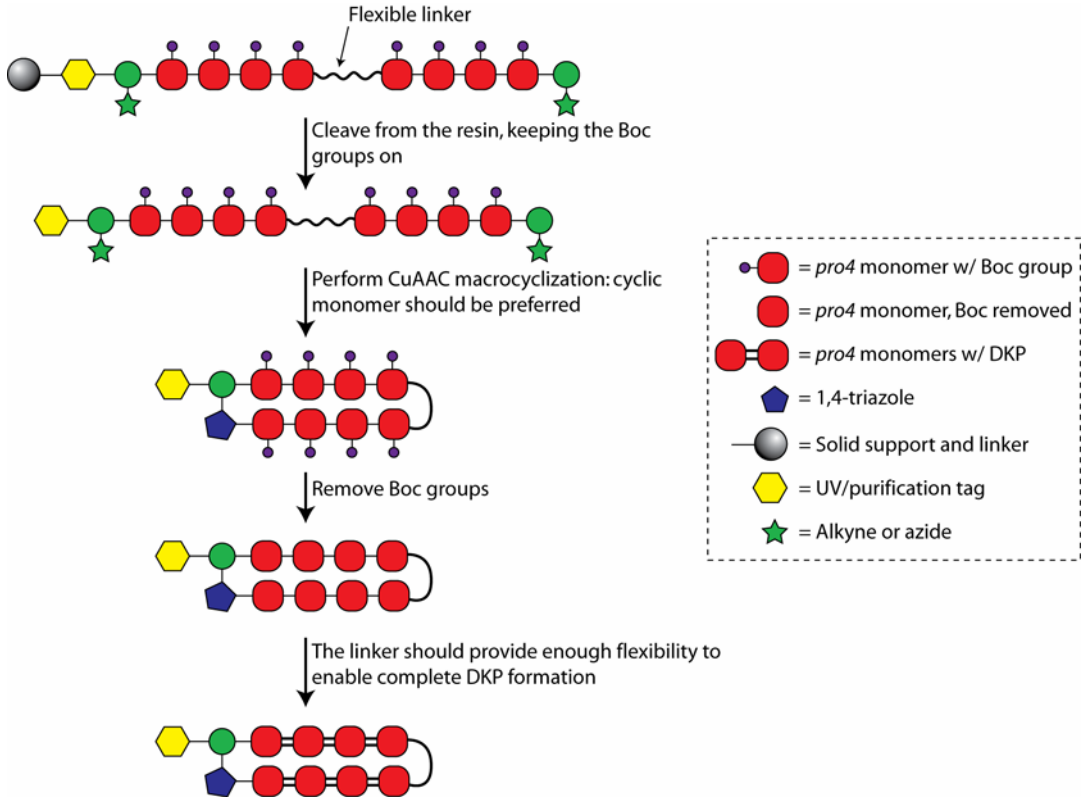

Figure 5-10: Schematic representation of a "rod-hinge-rod" approach toward asymmetrical *bis*-peptide oligomer based macrocycles

For the initial test of this strategy, we prepared **131**, the precursor of a "3-hinge-3" macrocycle (Scheme 5-15). The naphthylalanine, propargylglycine, and the first three Boc-*pro4*(2*S*,4*S*) monomers (**19**) were coupled to 2-chlorotritylchloride resin as described for the model system (above). The "hinge", *N*-Fmoc-*N*'-ivDde-(S)-diaminobutanoic acid (Fmoc-Dab-(ivDde)), was coupled to the third monomer using HATU. The Fmoc group was removed for an extended time to quantitatively close the DKP between the Dab and the preceding monomer. The ivDde group[204,205] was removed from the side chain amine of the residue using hydrazine; allyl alcohol was added to the reaction mixture to scavenge diimide, an impurity which accumulates in hydrazine solutions, and which could reduce the propargyl group.[206] Three

additional Boc-*pro4*(2*S*,4*S*) were coupled to the resin, followed by Fmoc-Dab-N_3 (**88**). **131** was isolated by resin cleavage with 1% TFA.

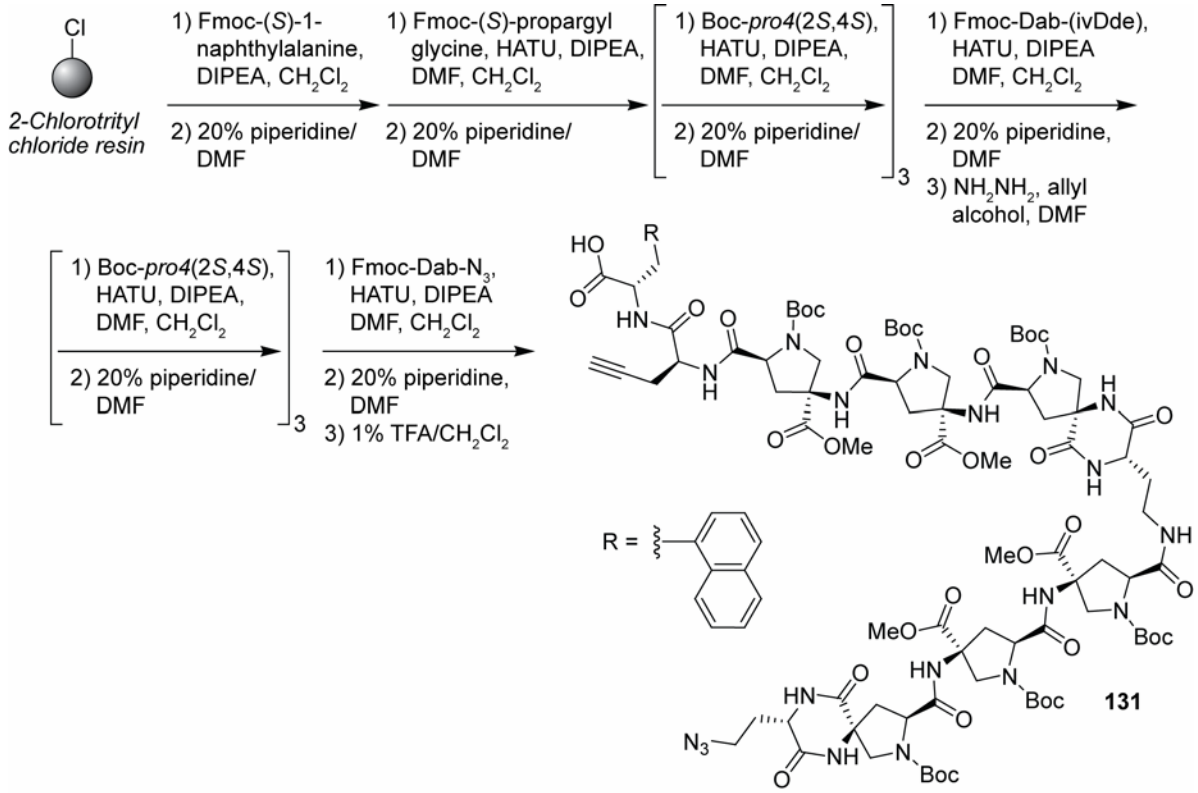

Scheme 5-15: Synthesis of **131**, the precursor of a "3-hinge-3" macrocycle

Because of the relationship between oligomer length and the cyclic monomer / cyclic dimer ratio during macrocyclization, **131** was expected to cyclize to the cyclic monomer under the CuAAC reaction conditions. The selectivity for the cyclic monomer was excellent; the ratio of cyclic monomer **132** to cyclic dimer **133** was 100:7 (Scheme 5-16). The combined yield of cyclic monomer and cyclic dimer was 89%. The Boc groups were removed using TFA, affording the Boc-deprotected open-form cyclic monomer, **134**.

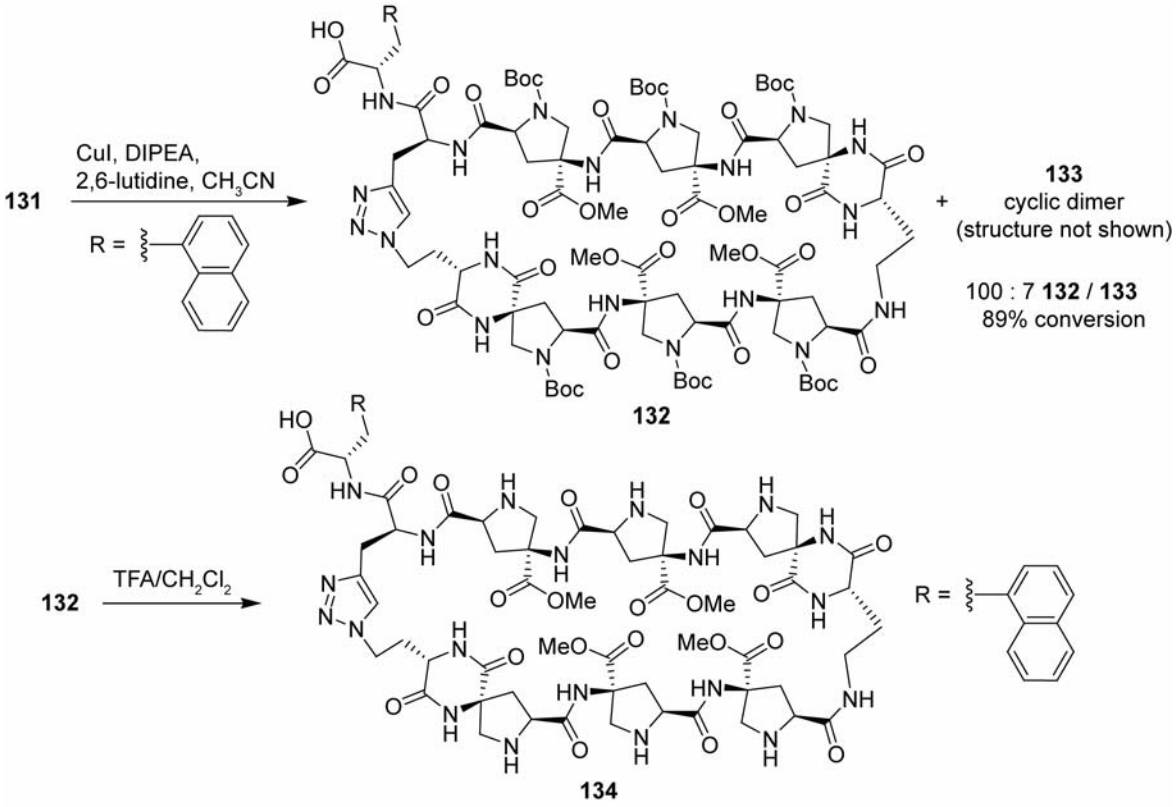

Scheme 5-16: CuAAC reaction of **131**, generating the major product, cyclic monomer **132**; the Boc groups were removed from **132**, forming **134.**

Finally, the Boc-deprotected open-form cyclic monomer was dissolved in 20% piperidine/NMP (Scheme 5-17); DKP occurred in the usual fashion. HPLC chromatograms of the crude reaction mixture for each step in the synthesis of **135** are illustrated in Figure 5-11.

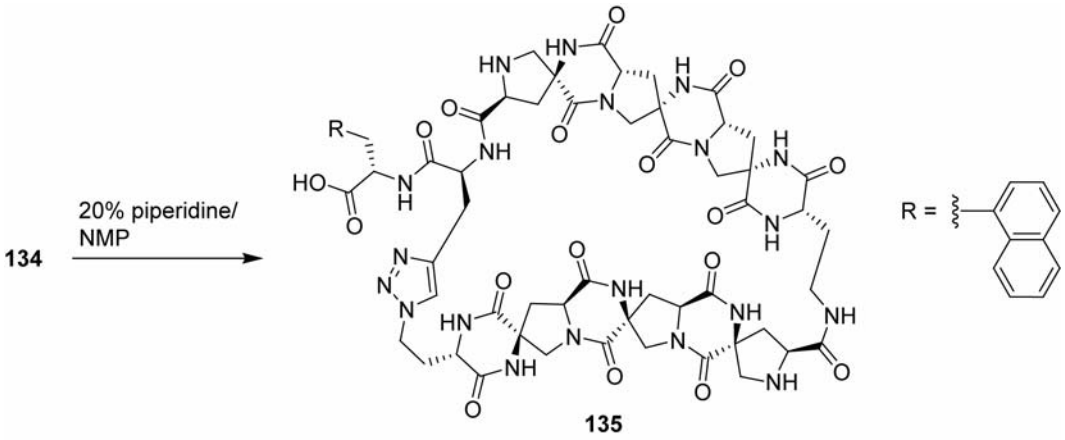

Scheme 5-17: DKP closure for the 3-hinge-3 macrocycle

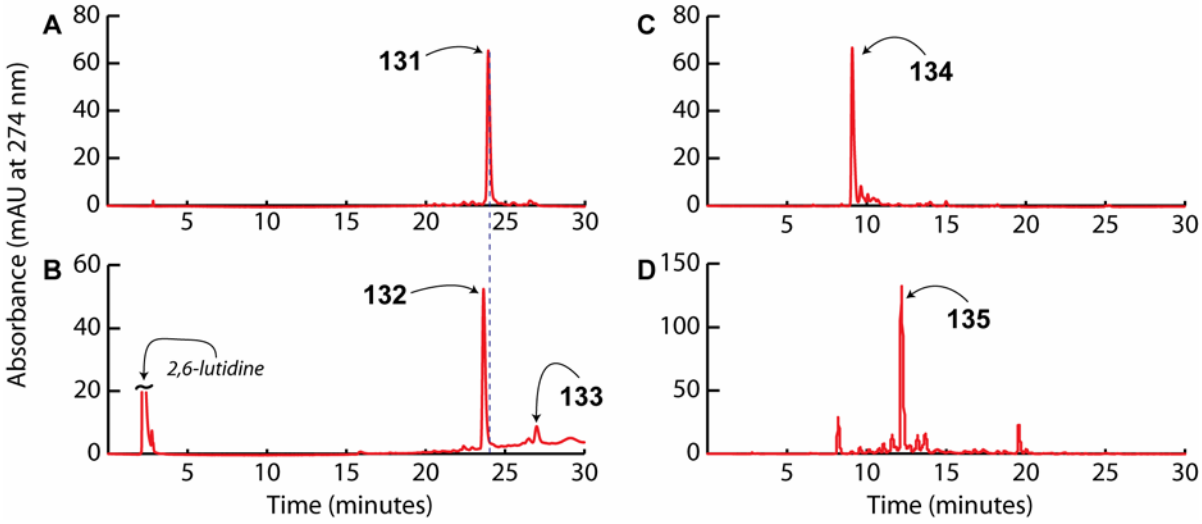

Figure 5-11: HPLC chromatograms of the intermediates and final product of the synthesis of the 3-hinge-3 cyclic *bis*-peptide oligomer: A (5% to 95% CH_3CN): **131** after resin cleavage, **B** (5 to 95% CH_3CN): **132** and **133** after the CuAAC reaction, **C** (0 to 50% CH_3CN): **134** after treating purified **132** with TFA, **D** (0 to 50% CH_3CN): the crude DKP closing reaction after ~ 24 hours

To test the generality of the "hinged" approach to *bis*-peptide macrocycles, a 6-hinge-6 macrocycle was prepared (6 *pro4*(2*S*,4*S*) monomers before and after the hinge). The complete synthesis of the 6-hinge-6 macrocycle **139** is illustrated in Scheme 5-18. **136** was synthesized on solid phase using the methods described for the synthesis of the 3-hinge-3 precursor **131**. Following resin cleavage, **136** was found to be contaminated by a small amount of a compound that resulted from incomplete coupling of the Fmoc-Dab-(ivDde) amino acid (Figure 5-12, HPLC chromatogram **A1**).

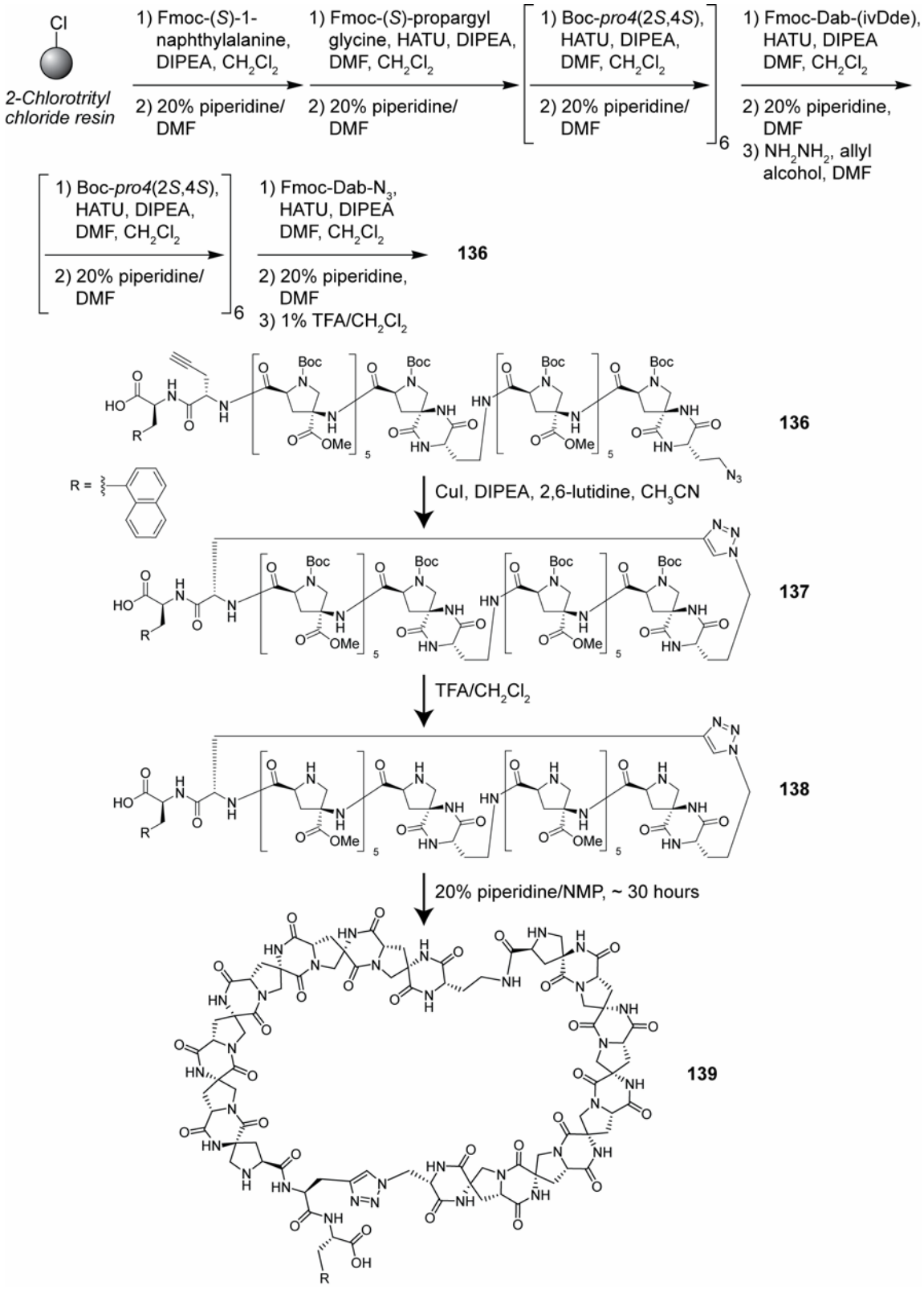

Scheme 5-18: Synthesis of the 6-hinge-6 cyclic monomer, **139**

After the resin cleavage product **136** was dissolved in the cycloaddition reaction solution (2 equivalents of CuI, DIPEA, and 2,6,-lutidine, ~ 1 mM in **136**), there was no apparent change in the HPLC chromatogram. As the number of Boc-*pro4* monomers increased, there was a corresponding decrease in the difference in retention time between the of the Boc-protected cyclic monomers and the starting material. This result was disappointing; unlike the previous CuAAC reactions, there was no immediate evidence that the starting material had undergone any chemical transformation.

Nonetheless, the ESI mass spectrum of the reaction mixture provides evidence for macrocyclization. In the ESI mass spectrum of the starting material **136**, there is a strong peak that corresponds to [M – 2Boc + $2H^+$] (Figure 5-16, ESI-MS **A2**). Following CuAAC, the intensity of this peak decreases. Also, the base peak in the mass spectrum becomes [M – Boc + $2H^+$] (Figure 5-16, ESI-MS **B2a**). There were similar differences between the ESI mass spectra of 3-hinge-3 precursor **131** and its cyclic monomer **132**.

To obtain addition proof that cyclization had occurred, a simple chemical test was performed to determine if the compound was functionalized with an azide. After removing the residual copper, a small amount of tris(2-carboxyethyl)phosphine (TCEP)[207] was added to a solution containing an analytical portion of the alleged cyclic monomer, **137**. TCEP is a strong, water-soluble reducing agent, typically used for the cleavage of disulfide bonds. Triazoles do not react with TCEP, but azides are rapidly reduced to amines; reduction elicits a change in the mass spectrum of compounds labeled with azides.[208] This test provides a means to distinguish between linear monomer and cyclic monomer. There was no change in the diagnostic ESI-MS peaks of **137** following treatment with TCEP (Figure 5-16, ESI-MS **B2b**). This suggests that the compound with the same retention time as **136** is not an azide; this also supports the proposed cyclization from **136** to **137**.

The residual copper was removed by adsorbing **137** upon C_{18} silica, washing the silica with water, and then eluting **137** with CH_3CN. Treatment of the concentrated eluent with TFA in dichloromethane afforded **138**, which has an exceptionally clean and characteristic ESI mass spectrum (Figure 5-12, ESI-MS **C2**) because of its numerous ionizable amines.

After Boc deprotection, crude **138** was dissolved in 20% piperidine/NMP. Within 12 hours (Figure 5-16, HPLC chromatogram **D1**) a single major product began to accumulate in solution. Considering the number of transformations that had been performed prior to DKP

formation, the major product of DKP closure, **139**, was remarkably clean, especially considering that none the intermediates had been rigorously purified (removal of the CuI from **137** on C_{18} silica was not performed with gradient elution). The product was isolated by preparative HPLC; HPLC-MS analysis of the purified product indicated that the mass of product **139** is consistent with the structure illustrated in Scheme 5-18 (Figure 5-16, HPLC chromatogram **E1** and ESI-MS **E2**).

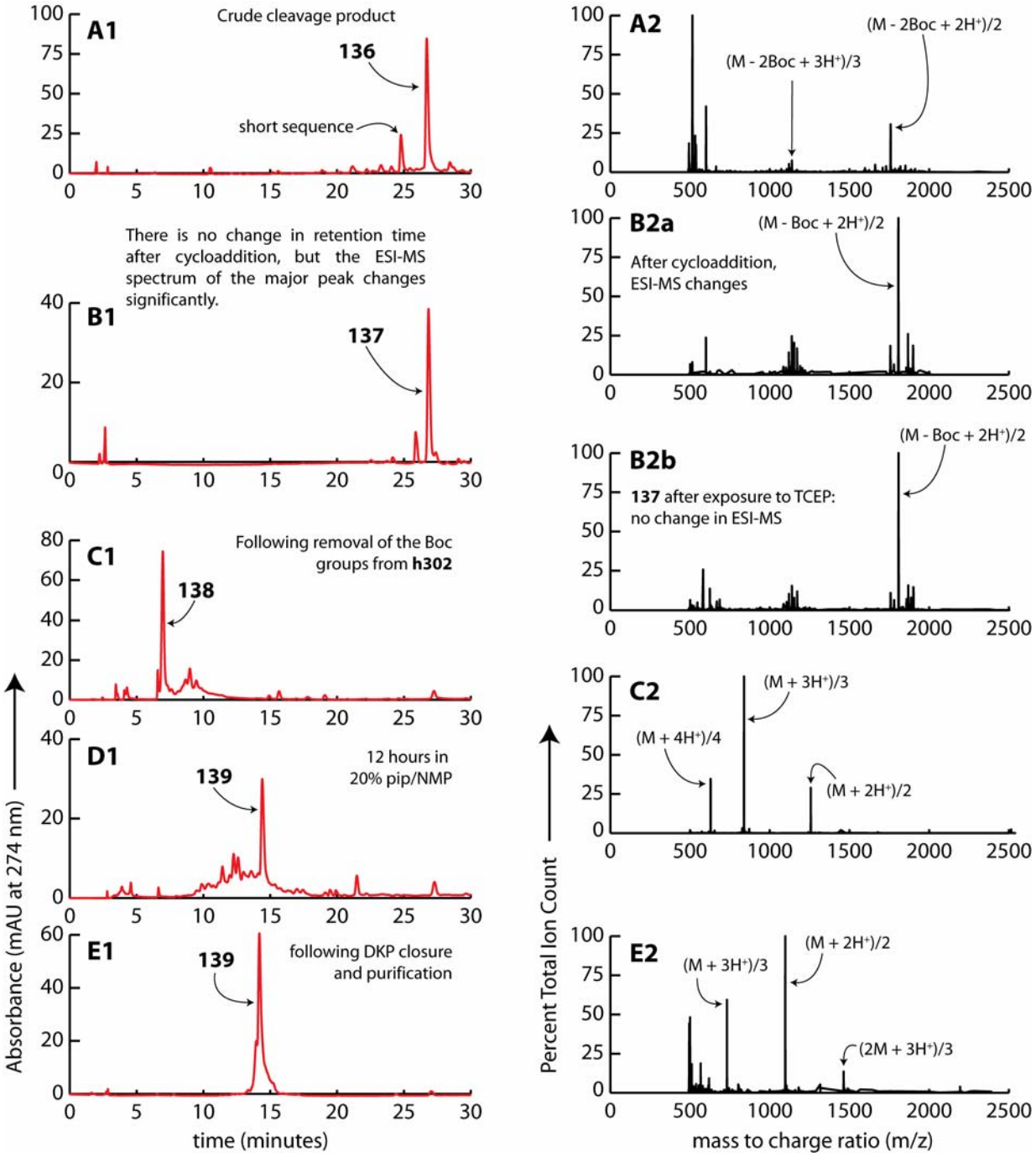

Figure 5-12: HPLC and ESI-MS analysis of the intermediates produced during the synthesis of **139**. **A1** (5% to 95% CH_3CN): HPLC of crude cleavage product **136**. **A2**: ESI-MS of **136**. B1 (5% to 95% CH_3CN): HPLC of **137**. **B2a**: ESI-MS of crude **137** before treatment with TCEP. **B2b**: ESI-MS of crude **137** after TCEP treatment. C1 (0% to 50% CH_3CN): **138**. **C2**: ESI-MS of crude **138**. **D1** (0% to 50% CH_3CN): DKP closing reaction at 12 hours. **E1** (0% to 50% CH_3CN): HPLC of purified **139**. **E2**: ESI-MS of **139**.

5.7 CONCLUSIONS

The CuAAC "click" reaction[209] has been used to create macrocycles from *bis*-peptide oligomers. The reaction was performed with the Boc-protected, open-form oligomers in acetonitrile. The macrocyclization reaction is very clean; the starting material was converted into recoverable macrocycles with good yields (> 70%). The reaction generates two major products; the cyclic monomer and cyclic dimer. In the model system (an alkyne/azide functionalized oligomer containing 3 Boc-*pro4* monomers) the cyclic monomer was the preferred product; selectivity for the cyclic monomer improved with increasing length of the open-form oligomers. This relationship was exploited for efficient preparation of "rod-hinge-rod" macrocycles. It was possible to rigidify the open-form *bis*-peptides in the context of the cyclic dimers and the rod-hinge-rod macrocycles; DKP formation was incomplete for the cyclic monomers without a hinge. These experiments have barely scratched the surface of using *bis*-peptide oligomers as building blocks for macromolecular construction.

5.7.1 Extending the rod-hinge-rod approach

The success of the approach toward the 3-hinge-3 and 6-hinge-6 macrocycles warrants further investigation; this method may be limited only by the practical constraints of SPPS. Introducing multiple hinges and *bis*-peptide oligomer subunits would allow access to macrocycles of tailored size and shape (Figure 5-13).

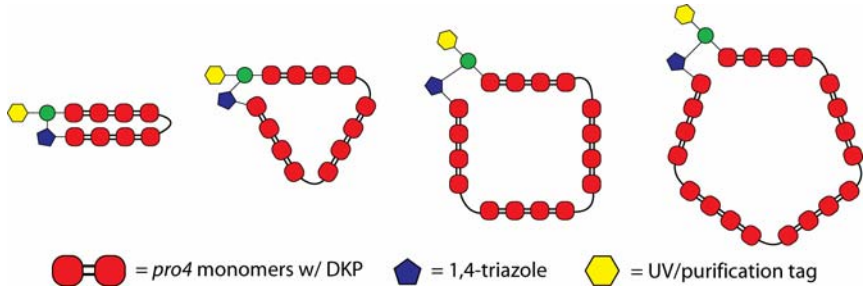

Figure 5-13: Incorporating multiple hinges and bis-peptide oligomer segments should allow control over the shape and size of the resulting macrocycles.

Consider Kimura's "helix-triangle" illustrated in Figure 5-14, which represents the state-of-the-art in large, covalently assembled, shaped macrocycles.[168] Three poly-aromatic amino

acids are used as the vertices of the triangle; assembly of the macrocycle is dictated by the 60° angle defined at each vertex. The sides of the helix triangle are rigid α-helical peptides. It is possible change the size of the triangle by increasing the length of the peptides. Creating different shapes, however, would be challenging; every shape would require molecules at the vertices which display co-planar functional groups in precise, geometric orientations. Certain shapes would likely be impossible (a heptagon, for instance). An almost limitless variety of macrocycle shapes and sizes could be synthesized using the rod-hinge-rod *bis*-peptide macrocyclization approach.

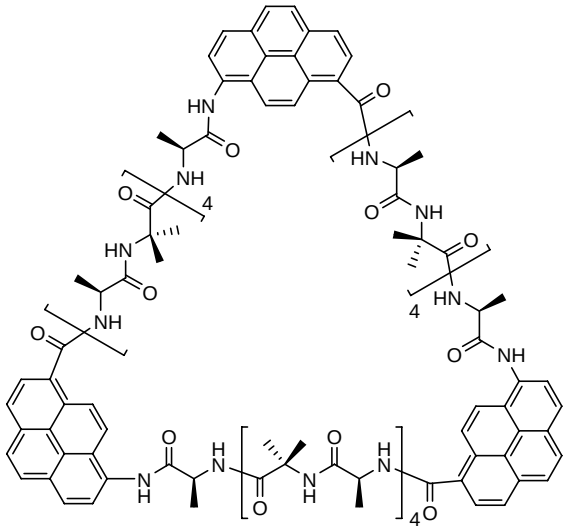

Figure 5-14: A "helix-triangle"[168]

5.7.2 Exploring solution and solid phase routes toward macrocyclization

Occasionally, exploring new *bis*-peptide chemistry on solid phase has led to intractable, inseparable mixtures following resin cleavage. It is difficult to identify the source of the problem in these cases; these circumstances usually require that the synthesis be repeated from the beginning. To avoid this situation, model CuAAC *bis*-peptide macrocyclization reactions were performed in solution. The progress of each reaction was monitored in (almost) real-time; products and side products were identified almost immediately.

Dealing with the residual copper in the product was irksome, and led to difficulties with NMR experiments and with purification. During the synthesis of the 6-hinge-6 oligomer, the crude CuAAC reaction was loaded onto a disposable C_{18} silica gel cartridge and washed

extensively with water; the desired product was eluted with acetonitrile. This method effectively removed residual copper from the product, but extensive product manipulation after resin cleavage leads to loss of material.

The CuAAC reaction of long, Boc-protected, open-form oligomers was extremely selective for the cyclic monomer. It might be possible to perform cyclization of the rod-hinge-rod oligomers on solid phase (see "Route **D**", Figure 5-2); the residual copper could be removed from the resin with chelating reagents, and the Boc groups could be removed upon resin cleavage, leaving only DKP formation. Resin loading is critically important for this approach. Selectivity for the cyclic monomer was possible under dilute conditions; when the CuAAC reaction was performed in more concentrated solutions, the proportion of cyclic dimer (and cyclic trimer) increased significantly. The reaction was performed at 1 mM concentration. The concentration of oligomer attached to 1% cross-linked polystyrene Rink Amide resin is considerably higher. The diffusion of the oligomers is inhibited because they are "anchored" to the solid support. Nonetheless, Rebek and Trend's study[210] on the interactions between short peptides anchored to solid support suggests that when the resin is solvated, peptides anchored to the resin can encounter and react with adjacent anchored peptides. Finn reported a dramatic example of tandem dimerization/macrocyclization between adjacent peptides on solid support using CuAAC.[187]

A number of questions remain about *bis*-peptide macrocyclization. The effect of macrocyclization upon the rigidity of the *bis*-peptides is unknown; bundling rod-like molecules can create macromolecules with increased rigidty.[2] It would also be interesting to develop conditions that caused macrocyclization after DKP closure; it is expected that the rigidified oligomers would undergo dimerization because the alkyne and azide are held apart. Sequences of alternating *pro4*(2*S*,4*S*) and *pro4*(2*R*,4*R*) monomers seem to impart curvature to *pro4* bis-peptides, but the exact amount of curvature is not known. If enough alternating monomers are incorporated into an oligomer, modeling suggests that the two ends of the *bis*-peptide will eventually meet. A series of alkyne-azide oligomers of increasing length could be synthesized, but with the alternating *pro4*(2*S*,4*S*)–*pro4* (2*R*,4*R*) motif (similar to the experiment described in section 0 above). DKP formation would be attempted before and after macrocyclization: such an experiment might provide good evidence about the degree of curvature imparted by this sequence motif. The CuAAC reaction could also be combined with other cyclization methods to

create 3-dimensional polyhedra from rigidified bis-peptide oligomers; these would be a spectacular demonstration of modular design and synthesis of nanoscale structures.

5.8 EXPERIMENTAL DETAILS

5.8.1 Fmoc-Dap-N_3 synthesis and incorporation into oligomers 84 and 85

(*S*)-3-Azido-2-(9*H*-fluoren-9-ylmethoxycarbonylamino)-propionic acid (Fmoc-Dap-N_3, 81) NaN_3 (597 mg, 9.19 mmol), water (1.6 mL) and CH_2Cl_2 (3.12 mL) were added to a conical vial containing a magnetic stir bar. The vial was immersed in an ice bath. Triflic anhydride (Tf_2O, 310 μL, 1.8 mmol, used as received from Acros) was added to the stirred reaction mixture very slowly by syringe. The mixture was stirred for 2 additional hours while warming to room temperature. The solution separated into two layers; the bottom organic layer was removed. The remaining aqueous layer was washed with CH_2Cl_2 (2 × ~ 1 mL). All of the CH_2Cl_2 layers were combined and washed with saturated aqueous K_2CO_3 (2 × 1 mL). The resulting solution of triflic azide (TfN_3) in CH_2Cl_2 was covered and set aside (CAUTION: TfN_3 is explosive when dry, and so the solution should not be concentrated, nor should the CH_2Cl_2 be allowed to evaporate). (*S*)-3-Amino-2-(9*H*-fluoren-9-ylmethoxycarbonylamino)-propionic acid (Fmoc-Dap, **83**, 300 mg, 0.92 mmol), potassium carbonate (190 mg, 1.4 mmol), and $CuSO_4 \cdot 5H_2O$ (2.3 mg, 9.2 μmol) were transferred to a 10 mL round bottom flask containing a magnetic stir bar. Methanol (4.7 mL) and water (3.1 mL) were added to the flask. The solution of TfN_3 in CH_2Cl_2 was added dropwise to the stirred reaction mixture, which became cloudy. By TLC (5:1 $CHCl_3$/MeOH), the starting material **83** (R_f = 0.1) was completely consumed within 1 hour; the product (**81**, R_f = 0.2) stained bright orange-yellow with anisaldehyde. The reaction mixture was distributed between EtOAc (50 mL) and pH 2 aqueous HCl (75 mL). After separating the two layers, the aqueous layer was extracted with additional EtOAc (3 × ~ 25 mL); the EtOAc layers were combined, washed with brine, dried over $MgSO_4$, filtered, then concentrated by rotary evaporation. The product was purified using gradient elution flash chromatography on silica ($CHCl_3$ (0.1% AcOH) to 10% MeOH/$CHCl_3$ (0.1% AcOH)). Fractions containing the product

were pooled and concentrated by rotary evaporation. Residual acetic acid was removed by repeatedly dissolving the product in 1:1 CH_2Cl_2/hexanes, then re-concentrating the solution. Solvent was removed overnight under reduced pressure affording **81** (244 mg, 69.2 mmol, 75.4%) as a white foam. The ^{1}H NMR spectrum of **81** was consistent with literature data.[200] ^{1}H NMR (300 MHz, $CDCl_3$): δ 7.78 (d, *J* = 7.5 Hz, 2H), 7.61 (d, *J* = 7.3 Hz, 2H), 7.42 (t, *J* = 7.2 Hz, 2H), 7.34 (t, *J* = 7.4 Hz, 2H), 5.61 (d, *J* = 7.9 Hz, 1H), 4.62 (m, 1H), 4.46 (d, *J* = 7.0 Hz, 2H), 4.25 (t, *J* = 6.7 Hz, 1H), 3.83 (m, 2H).

Compound 84: alkyne functionalized, 3-mer open-form oligomer (elimination product)
N-Fmoc-(*S*)-propargylglycine (22.1 mg, 66 μmol) and DIPEA (46 μL, 264 μmol) were dissolved in dichloroethane (330 μL); the solution was transferred into a 4 mL conical vial containing 15 mg of 2-chlorotritylchloride resin (1.1 mmol/gram loading) and a magnetic spin vane. The vial was capped, and the suspension was stirred under nitrogen for 5 hours. The resin was transferred to a solid phase reaction vessel, capped with methanol and DIPEA, and washed. The *N*-Fmoc group was removed from the propargylglycine with 20% piperidine/DMF, and the resin was washed thoroughly. **19**, **19**, **19**, and **81** were coupled sequentially to the resin with HATU (2 equiv of *N*-Fmoc protected amino acid, 2 equiv of HATU, 4 equiv of DIPEA, 0.2 M in 20% CH_2Cl_2 in DMF, 30 minute couplings). Every coupling was repeated an additional time to assure quantitative coupling, and following each coupling the resin was capped with 400:100:8 DMF/Ac_2O/DIPEA. The *N*-terminal Fmoc groups were removed by treatment with 20% piperidine/DMF for 40 minutes; Fmoc removal from **81** was extended to 2 hours, allowing the DKP to close. The resin was split into two portions. One half of the resin was treated with an 8:2:1 CH_3CN/DMSO/H_2O solution (231 μL) containing $CuSO_4 \cdot 5H_2O$ (0.6 mg, 2.3 μmol, 0.3 equiv relative to initial resin loading) and sodium ascorbate (1.5 mg, 7.7 μmol, 1 equiv relative to initial resin loading) overnight under argon. The Cu^I treated and untreated portions were washed thoroughly, and residual solvent was removed under reduced pressure. The products were cleaved from the resins using 95:2.5:2.5 TFA/TIS/H_2O. By HPLC-MS analysis, there was a single major product generated upon cleavage of both resin portions with identical retention times and ESI mass spectra. The mass spectra were consistent with the proposed structure of **84**. The yield of **84** from both resin portions was similar (based upon the relative area under the 220 nm absorbance peaks in their respective HPLC chromatograms).

HPLC-MS: column, Waters XTerra MS C_{18}, 4.6 × 150 mm; mobile phase, H_2O (0.l% HCOOH) / CH_3CN (0.05% HCOOH), 0% to 25% CH_3CN over 30 min; flow rate, 0.80 mL/min; UV detection at 220 nm; t_R for **84**, 3.92 min; ESI-MS *m/z* (ion) 660.6 (100%, M + H^+, expected 661.3), 331.0 (92%, [M +2H^+]/2, expected 331.1).

Compound 85: alkyne functionalized, 5-mer open-form oligomer (elimination product)
N-Fmoc-(*S*)-propargylglycine, **19**, **30**, **19**, **30**, **19**, and **81** were coupled sequentially to 15 mg of 2-chlorotritylchloride resin in the manner described for the synthesis of **84**. The resin was split into two portions; one half of the resin was treated with copper sulfate as described for **84**. Both the treated and untreated resin portions were washed thoroughly and residual solvent was removed under reduced pressure. The products were cleaved from the resins using 95:2.5:2.5 TFA/TIS/H_2O. By HPLC-MS analysis, there was a single major product generated upon cleavage of both resin portions with identical retention times and ESI mass spectra. The mass spectra were consistent with the proposed structure of **85**. The yield of **85** from both portions was very similar, based upon the relative HPLC chromatogram peak areas.
HPLC-MS: column, Waters XTerra MS C_{18}, 4.6 × 150 mm; mobile phase, H_2O (0.l% HCOOH) / CH_3CN (0.05% HCOOH), 0% to 25% CH_3CN over 30 min; flow rate, 0.80 mL/min; UV detection at 220 nm; t_R for **85**, 6.28 min; ESI-MS *m/z* (ion) 1000.4 (23%, M + H^+, expected 1001.4), 500.8 (100%, [M +2H^+]/2, expected 501.2).

5.8.2 Fmoc-Dab-N_3 and CuAAC model system 89

(*S*)-4-Azido-2-(9*H*-fluoren-9-yloxycarbonylamino)-butyric acid (Fmoc-Dab-N_3, 88)
NaN_3 (1.52 g, 23.4 mmol), water (4 mL) and CH_2Cl_2 (8.7 mL) were added to a 25 mL round bottom flask containing a magnetic stir bar. The flask was immersed in an ice bath. Tf_2O (790 μL, 4.68 mmol) was added to the stirred reaction mixture very slowly by syringe. The mixture was stirred for an additional 2 hours while warming to room temperature. The organic layer was removed, and the aqueous layer was washed with CH_2Cl_2 (2 ×). The portions of CH_2Cl_2 were combined and washed with saturated aqueous K_2CO_3 (2 ×). This TfN_3 solution was covered and set aside (see the caution above regarding TfN_3, which is explosive).

(*S*)-4-*tert*-Butoxycarbonylamino-2-(9*H*-fluoren-9-ylmethoxycarbonylamino)-butyric acid (**86**, 1000 mg, 2.34 mmol) was added to a 25 mL round bottom flask containing a magnetic stir bar, then dissolved in 1:1 TFA/CH_2Cl_2 (~ 12 mL). The reaction mixture was stirred until TLC analysis revealed that the starting material had been entirely consumed. The mixture was concentrated by rotary evaporation, and residual solvent was removed overnight under reduced pressure affording compound **87**, used without further purification.

Methanol (12 mL), water (8 mL) and a stir bar were added to the 25 mL round bottom flask containing **87**. Potassium carbonate (808 mg, 5.85 mmol) and $CuSO_4 \cdot 5H_2O$ (5.8 mg, 23.4 μmol) were transferred into the solution. The solution of TfN_3 in CH_2Cl_2 was added dropwise to the stirred reaction mixture, which became cloudy. The reaction mixture was concentrated, worked-up, and purified (as described for compound **81**), affording Fmoc-Dab-N_3 (**88**, 745 mg, 2.03 mmol, 87%) was a white foam. ^{1}H NMR (300 MHz, $CDCl_3$): δ 7.78 (d, *J* = 7.5 Hz, 2H), 7.60 (d, *J* = 7.2 Hz, 2H), 7.42 (t, *J* = 7.4 Hz, 2H), 7.33 (t, *J* = 7.4 Hz, 2H), 5.46 (d, *J* = 5.5 Hz, 1H), 4.59 – 4.46 (m, 3H), 4.24 (apparent t, *J* = 6.5 Hz, 1H), 3.43 (apparent t, *J* = 6.1 Hz, 2H), 2.20 (m, 1H), 2.03 (m, 1H); ^{13}C NMR (75.4 MHz, $CDCl_3$) mixture of rotamers δ 176.1 and 175.3, 156.8 and 156.0, 143.7 and 143.5, 141.3, 127.8 (CH), 127.1 (CH), 125.0 (CH), 120.0 (CH), 67.2 (CH_2), 51.6 (CH), 47.6 (CH_2), 47.1 (CH), 31.3 (CH_2); IR (neat film) 3306, 3066, 2929, 2102 (–N_3 stretch), 1720, 1524, 1478, 1450, 1337, 1250, 1154, 1104, 1059 cm^{-1}; $[\alpha]_D$ 21.5° (*c* 0.4, CH_3Cl); ES-MS *m/z* (relative intensity) 1121.5 (7%, 3M + Na^+), 909.3 (32%), 755.3 (48%, 2M + Na^+), 389.1 (100%, M + Na^+); HRESIQTOFMS calcd for $C_{19}H_{18}N_4O_4Na$ (M + Na^+) 389.1226, found 389.1227.

Compound 89: alkyne/azide functionalized Boc-protected open-form 3-mer oligomer

N-Fmoc-1-(*S*)-naphthylalanine (57.8 mg, 132 μmol), CH_2Cl_2 (660 μL) and DIPEA (92 μL, 527 μmol) were added to a 4 mL conical vial containing 2-chlorotritylchloride resin (30 mg, 1.1 mmol/gram substitution) and a magnetic spin vane. The vial was sealed and the reaction mixture was stirred for 3 hours. The resin was transferred into a SPPS reaction vessel, washed, and then capped using 17:2:1 CH_2Cl_2/MeOH/DIPEA. The *N*-Fmoc group was removed from the naphthylalanine using 20% piperidine/DMF for 40 minutes. *N*-Fmoc-(*S*)-propargylglycine, **19**,

19, **19**, and **88** were coupled sequentially to the resin with HATU as described above. The resin was stirred in 20% piperidine/DMF for 2 hours during the final Fmoc deprotection to ensure quantitative DKP formation between the last two residues. The resin was washed, and residual solvent was removed under reduced pressure.

The resin was re-swollen in CH_2Cl_2; the solvent was filtered away. Aliquots (~ 2 mL) of 1% TFA/CH_2Cl_2 were transferred to the resin, which immediately turned from pale yellow to maroon. The suspension was stirred with gentle argon bubbling for 2 minutes, and then the solution was siphoned from the resin into a receiving flask containing 20% pyridine/MeOH (4 mL). This procedure was repeated 10 times. The resin was washed with several portions of CH_2Cl_2 and MeOH; these were also transferred into the receiving flask. The solution was concentrated by centrifugal evaporation; hexanes and MeOH were added periodically to help remove residual solvent. One-half of the resulting fluffy powder was purified by chromatography on C_{18} silica (4 gram column, gradient elution from H_2O (0.1% HCOOH) to CH_3CN (0.05% HCOOH) over 14 column volumes). Fractions containing the desired product were pooled and concentrated by centrifugal evaporation, affording **89** (8.6 μmol, ~ 52% recovery relative initial resin loading, determined by HPLC calibration with naphthylalanine).

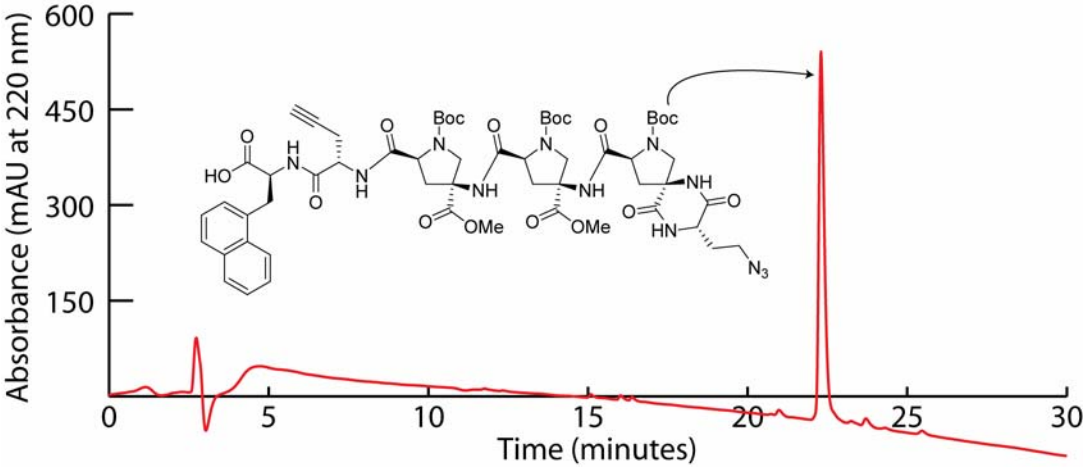

HPLC-MS: column, Waters XTerra MS C_{18}, 4.6 × 150 mm; mobile phase, H_2O (0.l% HCOOH) / CH_3CN (0.05% HCOOH), 5% to 95% CH_3CN over 30 min; flow rate, 0.80 mL/min; UV detection at 220 nm; t_R for **89**, 22.30 min; ESI-MS *m/z* (ion) 1115.3 (100%, M – Boc + H^+), 1215.4 (30%, M + H^+), 1283.4 (45%), 1300.4 (18%), 2330.6 (5%, 2M – Boc + H^+).

Figure 5-15: HPLC chromatogram of purified **89**

Compound 90, **Compound 91**, **Compound 92**: cyclic monomer, cyclic dimer and cyclic (respectively) from CuAAC reaction of Boc-protected oligomer **89**

Anhydrous CH_3CN was degassed by sparging with argon for 30 minutes. **89** (~ 8.6 μmol) was dissolved in the degassed CH_3CN (16.5 mL); the solution was transferred into a 25 mL round bottom flask containing a magnetic stir bar. DIPEA (5.7 μL, 33 μmol), 2,6-lutidine (3.8 μL, 33 μmol) and CuI (6.3 mg, 33 μmol) were added to the solution. The flask was sealed with a rubber stopper and the reaction mixture was stirred overnight. The solution was concentrated by centrifugal evaporation, and the three products (**90**, **91**, and **92**) were isolated by preparative HPLC (XTerra C_{18}, 10 × 100 mm; mobile phase, H_2O (0.l% HCOOH) / CH_3CN (0.05% HCOOH), 5% to 95% CH_3CN over 30 min; flow rate, 6.5 mL/min). By integrated area under peaks in the HPLC chromatogram of the reaction mixture, 76% of the starting material **89** was converted into one of the three major products, in the molar ratio 100:33:4 cyclic monomer **90** / cyclic dimer **91** / cyclic trimer **92**.

Compound 90:

HPLC-MS: column, Waters XTerra MS C_{18}, 4.6 × 150 mm; mobile phase, H_2O (0.l% HCOOH) / CH_3CN (0.05% HCOOH), 5% to 95% CH_3CN over 30 min; flow rate, 0.80 mL/min; UV detection at 220 nm; t_R for **90**, 21.42 min; ESI-MS *m/z* (ion) 1215.4 (100%, $M + H^+$), 2430.6 (5%, $2M + H^+$); HRESIQTOFMS calcd for $C_{57}H_{74}N_{12}O_{18}Na$ ($M + Na^+$) 1237.5142, found 1237.5171.

Compound 91:

HPLC-MS: column, Waters XTerra MS C_{18}, 4.6 × 150 mm; mobile phase, H_2O (0.l% HCOOH) / CH_3CN (0.05% HCOOH), 5% to 95% CH_3CN over 30 min; flow rate, 0.80 mL/min; UV detection at 220 nm; t_R for **91**, 25.40 min; ESI-MS *m/z* (ion) 1215.8 (100%, $[M + 2H^+]/2$), 2430.6 (20%, $M + H^+$); HRESIQTOFMS calcd for $C_{114}H_{148}N_{24}O_{36}Na$ ($M + Na^+$) 2452.0386, found 2451.9990.

Compound 92:

HPLC-MS: column, Waters XTerra MS C_{18}, 4.6 × 150 mm; mobile phase, H_2O (0.l% HCOOH) / CH_3CN (0.05% HCOOH), 5% to 95% CH_3CN over 30 min; flow rate, 0.80 mL/min; UV

detection at 220 nm; t_R for **92**, 28.41 min; ESI-MS *m/z* (ion) 1215.8 (65%, [M + $3H^+$]/3), 1823.4 (100%, [M + $2H^+$]/2), 2430.5 (7%, [2M + $3H^+$]/3); HRESIQTOFMS calcd for $C_{171}H_{222}N_{36}O_{54}Na_2$ / 2 ([M + $2Na^+$]/2) 1844.7759, found 1844.7683.

Compound 93, **Compound 94**, **Compound 95**: Boc-deprotected open-form cyclic monomer, cyclic dimer, and cyclic trimer (respectively)

The Boc-protected cyclic monomer **90**, cyclic dimer **91**, and cyclic trimer **92** were each dissolved in TFA (~ 4 mL). The solutions were mixed by swirling, allowed to stand for 1 hour, and then concentrated by centrifugal evaporation overnight. Analytical samples of **93** and **94** were prepared by dissolving a portion of the crude product in 1:1 CH_3CN/H_2O.

Compound 93:

HPLC-MS: column, Waters XTerra MS C_{18}, 4.6 × 150 mm; mobile phase, H_2O (0.l% HCOOH) / CH_3CN (0.05% HCOOH), 0% to 50% CH_3CN over 30 min; flow rate, 0.80 mL/min; UV detection at 220 nm; t_R for **93**, 12.81 min; ESI-MS *m/z* (ion) 915.2 (15% M + H^+), 458.2 (100%, [M + $2H^+$]/2); HRESIQTOFMS calcd for $C_{42}H_{51}N_{12}O_{12}$ (M + H^+) 915.3749, found 915.3744

Compound 94:

HPLC-MS: column, Waters XTerra MS C_{18}, 4.6 × 150 mm; mobile phase, H_2O (0.l% HCOOH) / CH_3CN (0.05% HCOOH), 0% to 50% CH_3CN over 30 min; flow rate, 0.80 mL/min; UV detection at 220 nm; t_R for **94**, 14.41 min; ESI-MS *m/z* (ion) 915.4 (8%, [M + $2H^+$]/2), 610.7 (43%, [M + $3H^+$]/3), 458.4 (100%, [M + $4H^+$]/4); HRESIQTOFMS calcd for $C_{84}H_{102}N_{24}O_{24}$ / 2 ([M + $2H^+$]/2) 915.3750, found 915.3774.

Compound 96, **Compound 97**, **Compound 98**: cyclic monomer, cyclic dimer, and cyclic trimer following DKP formation reaction

The residues containing Boc-deprotected cyclic monomer **93**, cyclic dimer **94**, and cyclic trimer **95** were each dissolved in 20% piperidine/DMF (1.25 mL) and transferred to HPLC vials. The progress of the DKP closing reactions were monitored by HPLC. After three days, each solution was added dropwise to stirred Et_2O; the resulting precipitates were pelleted by centrifugation. It was possible to isolate pellets containing **96** and **97**. These were dried, dissolved in 1:1

CH_3CN/H_2O, and found to be remarkably pure by analytical HPLC-MS; the samples were analyzed by HRMS. There was insufficient rigidified cyclic trimer **98** for HRMS analysis.

Compound 96:

HPLC-MS: column, Waters XTerra MS C_{18}, 4.6 × 150 mm; mobile phase, H_2O (0.l% HCOOH) / CH_3CN (0.05% HCOOH), 5% to 95% CH_3CN over 30 min; flow rate, 0.80 mL/min; UV detection at 220 nm; t_R for **96**, 12.29 min; ESI-MS *m/z* (ion) 883.2 (100%, M + H^+), 1766.4 (12%, 2M + H^+); HRESIQTOFMS calcd for $C_{41}H_{47}N_{12}O_{11}$ (M + H^+) 883.3487, found 883.3477.

Compound 97:

HPLC-MS: column, Waters XTerra MS C_{18}, 4.6 × 150 mm; mobile phase, H_2O (0.l% HCOOH) / CH_3CN (0.05% HCOOH), 5% to 95% CH_3CN over 30 min; flow rate, 0.80 mL/min; UV detection at 220 nm; t_R for **97**, 11.27 min; ESI-MS *m/z* (ion) 1702.3 (15%, M + H^+), 1277.0 ([3M + $4H^+$]/4), 1135.1 (20%, [2M + $3H^+$]/3), 851.2 (100%, [M + $2H^+$]/2), 568.0 (15%, [M + $3H^+$]/3); HRESIQTOFMS calcd for $C_{80}H_{85}N_{24}O_{20}$ (M + H^+) 1701.6372, found 1701.6433.

Compound 98: (not isolated: see the analytical HPLC of the crude DKP closure reaction mixture in Figure 5-16)

HPLC-MS: column, Waters XTerra MS C_{18}, 4.6 × 150 mm; mobile phase, H_2O (0.l% HCOOH) / CH_3CN (0.05% HCOOH), 5% to 95% CH_3CN over 30 min; flow rate, 0.80 mL/min; UV detection at 220 nm; t_R for **98**, 11.31 min; ESI-MS *m/z* (ion) 1276.6 (85%, [M + $2H^+$]/2), 851.0 (33%, [M + $3H^+$]/3).

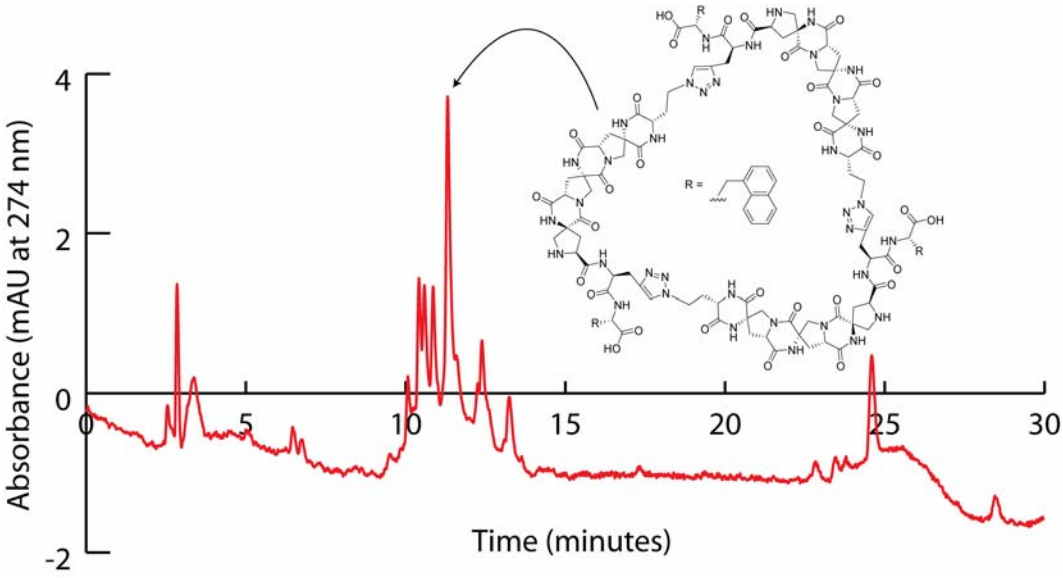

HPLC-MS: column, Waters XTerra MS C_{18}, 4.6 × 150 mm; mobile phase, H_2O (0.l% HCOOH) / CH_3CN (0.05% HCOOH), 5% to 95% CH_3CN over 30 min; flow rate, 0.80 mL/min.

Figure 5-16: HPLC chromatogram of crude **98** in 20% piperidine/DMF

5.8.3 Alkyne/azide functionalized oligomers of increasing length

N-Fmoc-1-(*S*)-naphthylalanine and *N*-Fmoc-(*S*)-propargylglycine were coupled sequentially to 2-chlorotritylchloride resin (100 mg, 1.1 mmol/gram substitution) using the methods described above. Boc-*pro4*(2*S*,4*S*) (**19**) was coupled to the resin with HATU, and the *N*-Fmoc group was removed from the monomer. ~ 10 mg of the resin was removed (based on initial resin weight; this was determined by suspending the resin in 10 mL of DMF, mixing the suspension thoroughly, and removing 1 mL of the suspension). The resin sample was transferred into a second SPPS vessel. Fmoc-(*S*)-Dab-N_3 (**88**) was coupled to the resin sample, and monomer **19** was coupled to the main batch. This procedure was repeated as described in Scheme 5-13. When SPPS was complete, the 7 resins were washed, and residual solvent was removed from each under reduced pressure. The products were cleaved from each resin using 1% TFA/CH_2Cl_2 as described above. The cleavage products were purified by flash chromatography on C_{18} silica (4 gram column, gradient elution over 14 column volumes from H_2O (0.1% HCOOH) to CH_3CN (0.05% HCOOH)). Fractions containing the desired products were concentrated by centrifugal evaporation. The yield of the cleavage reactions were typically around 70%. This was determined by HPLC analysis of the cycloaddition reactions before adding the CuI and 2,6-

lutidine; the HPLC calibration curve was generated by injecting various amounts of (*S*)-naphthylalanine under the same column conditions and flow rate.

Compound 99: alkyne/azide functionalized 4-mer oligomer (resin cleavage product)
HPLC-MS: column, Waters XTerra MS C_{18}, 4.6 × 150 mm; mobile phase, H_2O (0.l% HCOOH) / CH_3CN (0.05% HCOOH), 5% to 95% CH_3CN over 30 min, then 95% CH_3CN for 5 additional minutes); flow rate, 0.80 mL/min; UV detection at 220 nm; t_R for **99**, 23.37 min; ESI-MS *m/z* (ion) 1553.4 (7%), 1507.3 (10%), 1485.4 (25%, M + H^+), 1385.4 (100%, M – Boc + H^+); HRESIQTOFMS calcd for $C_{69}H_{92}N_{14}O_{23}Na$ (M + Na^+) 1507.6357, found 1507.6334.

Compound 100: alkyne/azide functionalized 5-mer oligomer (resin cleavage product)
HPLC-MS: column, Waters XTerra MS C_{18}, 4.6 × 150 mm; mobile phase, H_2O (0.l% HCOOH) / CH_3CN (0.05% HCOOH), 5% to 95% CH_3CN over 30 min, then 95% CH_3CN for 5 additional minutes); flow rate, 0.80 mL/min; UV detection at 220 nm; t_R for **100**, 23.31 min; ESI-MS *m/z* (ion) 1823.4 (7%), 1778.4 (12%), 1655.4 (100%, M – Boc + H^+); HRESIQTOFMS calcd for $C_{81}H_{110}N_{16}O_{28}Na$ (M + Na^+) 1777.7573, found 1777.7577.

Compound 101: alkyne/azide functionalized 6-mer oligomer (resin cleavage product)
HPLC-MS: column, Waters XTerra MS C_{18}, 4.6 × 150 mm; mobile phase, H_2O (0.l% HCOOH) / CH_3CN (0.05% HCOOH), 5% to 95% CH_3CN over 30 min, then 95% CH_3CN for 5 additional minutes); flow rate, 0.80 mL/min; UV detection at 220 nm; t_R for **101**, 24.95 min; ESI-MS *m/z* (ion) 1926.6 (100%, M – Boc + H^+), 913.2 (48%, [M – 2Boc + $2H^+$]/2), 885.2 (20%).

Compound 102: alkyne/azide functionalized 7-mer oligomer (resin cleavage product)
HPLC-MS: column, Waters XTerra MS C_{18}, 4.6 × 150 mm; mobile phase, H_2O (0.l% HCOOH) / CH_3CN (0.05% HCOOH), 5% to 95% CH_3CN over 30 min, then 95% CH_3CN for 5 additional minutes); flow rate, 0.80 mL/min; UV detection at 220 nm; t_R for **102**, 25.51 min; ESI-MS *m/z* (ion) 2196.4 (20%, M – Boc + H^+), 1048.4 (100%, [M – 2Boc + $2H^+$]/2).

Compound 103: alkyne/azide functionalized 8-mer oligomer (resin cleavage product)

HPLC-MS: column, Waters XTerra MS C_{18}, 4.6 × 150 mm; mobile phase, H_2O (0.l% HCOOH) / CH_3CN (0.05% HCOOH), 5% to 95% CH_3CN over 30 min, then 95% CH_3CN for 5 additional minutes); flow rate, 0.80 mL/min; UV detection at 220 nm; t_R for **103**, 26.01 min; ESI-MS *m/z* (ion) 1183.3 (100%, $[M - 2Boc + 2H^+]/2$).

Compound 104: alkyne/azide functionalized 9-mer oligomer (resin cleavage product)
HPLC-MS: column, Waters XTerra MS C_{18}, 4.6 × 150 mm; mobile phase, H_2O (0.l% HCOOH) / CH_3CN (0.05% HCOOH), 5% to 95% CH_3CN over 30 min, then 95% CH_3CN for 5 additional minutes); flow rate, 0.80 mL/min; UV detection at 220 nm; t_R for **104**, 26.47 min; ESI-MS *m/z* (ion) 1318.3 (100%, $[M - 2Boc + 2H^+]/2$).

General procedure for the CuAAC macrocyclizations of **99** through **104**:
Anhydrous CH_3CN was degassed by sparging with argon for 30 minutes. The resin cleavage product (the Boc-protected alkyne-azide functionalized oligomer) was dissolved in CH_3CN such that oligomer concentration was ~ 1 mM (estimated; based upon the theoretical yield from resin cleavage). The solution was transferred into a round bottom flask containing a magnetic stir bar. DIPEA (2 equivalents, relative to the theoretical cleavage yield), 2,6-lutidine (2 equivalents) and CuI (2 equivalents) were added to the solution. The flask was sealed with a rubber stopper, and the mixture was stirred overnight. The reaction mixture was concentrated by centrifugal evaporation, affording a bluish residue that was dissolved in 1:1 CH_3CN/H_2O. The cyclic monomer and cyclic dimer were isolated by preparative HPLC (XTerra C_{18}, 10 × 100 mm; mobile phase, H_2O (0.l% HCOOH) / CH_3CN (0.05% HCOOH), 5% to 95% CH_3CN over 30 min; flow rate, 6.5 mL/min). Fractions containing the desired products were concentrated.

Compound 105: Boc-protected 4-mer cyclic monomer
HPLC-MS: column, Waters XTerra MS C_{18}, 4.6 × 150 mm; mobile phase, H_2O (0.l% HCOOH) / CH_3CN (0.05% HCOOH), 5% to 95% CH_3CN over 30 min, then 95% CH_3CN for 5 additional minutes); flow rate, 0.80 mL/min; UV detection at 220 nm; t_R for **105**, 22.61 min; ESI-MS *m/z* (ion) 1485.4 (100%, $M + H^+$).

Compound 106: Boc-protected 4-mer cyclic dimer

HPLC-MS: column, Waters XTerra MS C_{18}, 4.6 × 150 mm; mobile phase, H_2O (0.l% HCOOH) / CH_3CN (0.05% HCOOH), 5% to 95% CH_3CN over 30 min, then 95% CH_3CN for 5 additional minutes); flow rate, 0.80 mL/min; UV detection at 220 nm; t_R for **106**, 26.91 min; ESI-MS *m/z* (ion) 1485.9 (72%, [M + 2H+]/2); HRESIQTOFMS calcd for $C_{69}H_{92}N_{14}O_{23}Na$ (M + Na^+) 1507.6357, found 1507.6339.

Compound 107: Boc-protected 5-mer cyclic monomer

HPLC-MS: column, Waters XTerra MS C_{18}, 4.6 × 150 mm; mobile phase, H_2O (0.l% HCOOH) / CH_3CN (0.05% HCOOH), 5% to 95% CH_3CN over 30 min, then 95% CH_3CN for 5 additional minutes); flow rate, 0.80 mL/min; UV detection at 220 nm; t_R for **107**, 23.65 min; ESI-MS *m/z* (ion) 1755.6 (100%, M + H^+), 828.6 (20%, M – Boc + H^+).

Compound 108: Boc-protected 5-mer cyclic dimer

HPLC-MS: column, Waters XTerra MS C_{18}, 4.6 × 150 mm; mobile phase, H_2O (0.l% HCOOH) / CH_3CN (0.05% HCOOH), 5% to 95% CH_3CN over 30 min, then 95% CH_3CN for 5 additional minutes); flow rate, 0.80 mL/min; UV detection at 220 nm; t_R for **108**, 28.48 min; ESI-MS *m/z* (ion) 1756.4 (10%, [M + $2H^+$]/2); HRESIQTOFMS calcd for $C_{81}H_{110}N_{16}NaO_{28}$ (M + Na^+) 1777.7573, found 1777.7533.

Compound 109: Boc-protected 6-mer cyclic monomer

HPLC-MS: column, Waters XTerra MS C_{18}, 4.6 × 150 mm; mobile phase, H_2O (0.l% HCOOH) / CH_3CN (0.05% HCOOH), 5% to 95% CH_3CN over 30 min, then 95% CH_3CN for 5 additional minutes); flow rate, 0.80 mL/min; UV detection at 220 nm; t_R for **109**, 24.47 min; ESI-MS *m/z* (ion) 2026.8 (100%, M + H^+), 963.8 (50%, M – Boc + H^+).

Compound 110: Boc-protected 6-mer cyclic dimer

HPLC-MS: column, Waters XTerra MS C_{18}, 4.6 × 150 mm; mobile phase, H_2O (0.l% HCOOH) / CH_3CN (0.05% HCOOH), 5% to 95% CH_3CN over 30 min, then 95% CH_3CN for 5 additional minutes); flow rate, 0.80 mL/min; UV detection at 220 nm; t_R for **110**, 28.52 min; ESI-MS *m/z* (ion) 2026.8 (15%, [M + $2H^+$]/2).

Compound 111: Boc-protected 7-mer cyclic monomer

HPLC-MS: column, Waters XTerra MS C_{18}, 4.6 × 150 mm; mobile phase, H_2O (0.l% HCOOH) / CH_3CN (0.05% HCOOH), 5% to 95% CH_3CN over 30 min, then 95% CH_3CN for 5 additional minutes); flow rate, 0.80 mL/min; UV detection at 220 nm; t_R for **111**, 25.35 min; ESI-MS *m/z* (ion) 2296.5 (100%, M + H^+), 1098.8 (60%, M – Boc + H^+).

Compound 112: Boc-protected 7-mer cyclic dimer

HPLC-MS: column, Waters XTerra MS C_{18}, 4.6 × 150 mm; mobile phase, H_2O (0.l% HCOOH) / CH_3CN (0.05% HCOOH), 5% to 95% CH_3CN over 30 min, then 95% CH_3CN for 5 additional minutes); flow rate, 0.80 mL/min; UV detection at 220 nm; t_R for **112**, 29.42 min; ESI-MS *m/z* (ion) 2296.3 (50%, [M + 2H^+]/2), 1497.7 (22%).

Compound 113: Boc-protected 8-mer cyclic monomer

HPLC-MS: column, Waters XTerra MS C_{18}, 4.6 × 150 mm; mobile phase, H_2O (0.l% HCOOH) / CH_3CN (0.05% HCOOH), 5% to 95% CH_3CN over 30 min, then 95% CH_3CN for 5 additional minutes); flow rate, 0.80 mL/min; UV detection at 220 nm; t_R for **113**, 25.93 min; ESI-MS *m/z* (ion) 2566.3 (20%, M + H^+), 1233.8 (100%, M – Boc + H^+).

Compound 114: Boc-protected 8-mer cyclic dimer

HPLC-MS: column, Waters XTerra MS C_{18}, 4.6 × 150 mm; mobile phase, H_2O (0.l% HCOOH) / CH_3CN (0.05% HCOOH), 5% to 95% CH_3CN over 30 min, then 95% CH_3CN for 5 additional minutes); flow rate, 0.80 mL/min; UV detection at 220 nm; t_R for **114**, 29.79 min; ESI-MS *m/z* (ion) 2566.6 (15%, [M + 2H^+]/2), 1677.5 (12%).

Compound 115: Boc-protected 9-mer cyclic monomer

HPLC-MS: column, Waters XTerra MS C_{18}, 4.6 × 150 mm; mobile phase, H_2O (0.l% HCOOH) / CH_3CN (0.05% HCOOH), 5% to 95% CH_3CN over 30 min, then 95% CH_3CN for 5 additional minutes); flow rate, 0.80 mL/min; UV detection at 220 nm; t_R for **115**, 26.48 min; ESI-MS *m/z* (ion) 2835.9 (5%, M + H^+), 1368.4 (100%, M – Boc + H^+).

Compound 116: Boc-protected 9-mer cyclic dimer

HPLC-MS: column, Waters XTerra MS C_{18}, 4.6 × 150 mm; mobile phase, H_2O (0.l% HCOOH) / CH_3CN (0.05% HCOOH), 5% to 95% CH_3CN over 30 min, then 95% CH_3CN for 5 additional minutes); flow rate, 0.80 mL/min; UV detection at 220 nm; t_R for **116**, 30.28 min; ESI-MS *m/z* (ion) 1857.6 (14%, $[M + 3H^+]/3$).

Removing the Boc groups from the series of cyclic monomers and dimers:
After purification of the cyclization products, each (**106** through **116**) was dissolved in 50% TFA/CH_2Cl_2. The solution was concentrated after ~ 30 minutes by centrifugal evaporation.

Compound 117: Boc-deprotected 4-mer cyclic monomer (open-form oligomer)
HPLC-MS: column, Waters XTerra MS C_{18}, 4.6 × 150 mm; mobile phase, H_2O (0.l% HCOOH) / CH_3CN (0.05% HCOOH), 0% to 50% CH_3CN over 30 min); flow rate, 0.80 mL/min; UV detection at 220 nm; t_R for **117**, 10.42 min; ESI-MS *m/z* (ion) 1085.2 (15%, $M + H^+$), 543.2 (90%, $[M + 2H^+]/2$), 362.6 (100%, $[M + 3H^+]/3$).

Compound 118: Boc-deprotected 4-mer cyclic dimer (open-form oligomer)
HPLC-MS: column, Waters XTerra MS C_{18}, 4.6 × 150 mm; mobile phase, H_2O (0.l% HCOOH) / CH_3CN (0.05% HCOOH), 0% to 50% CH_3CN over 30 min); flow rate, 0.80 mL/min; UV detection at 220 nm; t_R for **118**, 12.58 min; ESI-MS *m/z* (ion) 724.2 (8%, $[M + 3H^+]/3$), 543.3 (100%, $[M + 4H^+]/4$), 435.0 (13%, $[M + 5H^+]/5$).

Compound 119: Boc-deprotected 5-mer cyclic monomer (open-form oligomer)
HPLC-MS: column, Waters XTerra MS C_{18}, 4.6 × 150 mm; mobile phase, H_2O (0.l% HCOOH) / CH_3CN (0.05% HCOOH), 0% to 50% CH_3CN over 30 min); flow rate, 0.80 mL/min; UV detection at 220 nm; t_R for **119**, 10.03 min; ESI-MS *m/z* (ion) 1255.2 (3%, $M + H^+$), 628.3 (10%, $[M + 2H^+]/2$), 419.3 (100%, $[M + 3H^+]/3$).

Compound 120: Boc-deprotected 5-mer cyclic dimer (open-form oligomer)
HPLC-MS: column, Waters XTerra MS C_{18}, 4.6 × 150 mm; mobile phase, H_2O (0.l% HCOOH) / CH_3CN (0.05% HCOOH), 0% to 50% CH_3CN over 30 min); flow rate, 0.80 mL/min; UV

detection at 220 nm; t_R for **120**, 11.28 min; ESI-MS *m/z* (ion) 837.7 (7%, [M + $3H^+$]/3), 628.5 (55%, [M + $4H^+$]/4), 502.9 (100%, [M + $5H^+$]/5).

Compound 121: Boc-deprotected 6-mer cyclic monomer (open-form oligomer)
HPLC-MS: column, Waters XTerra MS C_{18}, 4.6 × 150 mm; mobile phase, H_2O (0.l% HCOOH) / CH_3CN (0.05% HCOOH), 0% to 50% CH_3CN over 30 min); flow rate, 0.80 mL/min; UV detection at 220 nm; t_R for **121**, 9.29 min; ESI-MS *m/z* (ion) 1425.2 (2%, M + H^+), 476.0 (100%, [M + $3H^+$]/3).

Compound 122: Boc-deprotected 6-mer cyclic dimer (open-form oligomer)
HPLC-MS: column, Waters XTerra MS C_{18}, 4.6 × 150 mm; mobile phase, H_2O (0.l% HCOOH) / CH_3CN (0.05% HCOOH), 0% to 50% CH_3CN over 30 min); flow rate, 0.80 mL/min; UV detection at 220 nm; t_R for **122**, 10.44 min; ESI-MS *m/z* (ion) 951.0 (5%, [M + $3H^+$]/3), 713.6 (25%, [M + $4H^+$]/4), 571.0 (100%, [M + $5H^+$]/5), 475.9 (15%, [M + $6H^+$]/6).

Compound 123: Boc-deprotected 7-mer cyclic monomer (open-form oligomer)
HPLC-MS: column, Waters XTerra MS C_{18}, 4.6 × 150 mm; mobile phase, H_2O (0.l% HCOOH) / CH_3CN (0.05% HCOOH), 0% to 50% CH_3CN over 30 min); flow rate, 0.80 mL/min; UV detection at 220 nm; t_R for **123**, 8.63 min; ESI-MS *m/z* (ion) 1595.3 (7%, M + H^+), 789.2 (23%, [M + $2H^+$]/2), 532.6 (100%, [M + $3H^+$]/3), 399.8 (65%, [M + $4H^+$]/4).

Compound 124: Boc-deprotected 7-mer cyclic dimer (open-form oligomer)
HPLC-MS: column, Waters XTerra MS C_{18}, 4.6 × 150 mm; mobile phase, H_2O (0.l% HCOOH) / CH_3CN (0.05% HCOOH), 0% to 50% CH_3CN over 30 min); flow rate, 0.80 mL/min; UV detection at 220 nm; t_R for **124**, 10.09 min; ESI-MS *m/z* (ion) 1595.8 (6%, [M + $2H^+$]/2), 1064.1 (8%, [M + $3H^+$]/3), 798.5 (43%, [M + $4H^+$]/4), 639.1 (100%, [M + $5H^+$]/5), 532.8 (40%, [M + $6H^+$]/6).

Compound 125: Boc-deprotected 8-mer cyclic monomer (open-form oligomer)
HPLC-MS: column, Waters XTerra MS C_{18}, 4.6 × 150 mm; mobile phase, H_2O (0.l% HCOOH) / CH_3CN (0.05% HCOOH), 0% to 50% CH_3CN over 30 min); flow rate, 0.80 mL/min; UV

detection at 220 nm; t_R for **125**, 8.27 min; ESI-MS *m/z* (ion) 1765.0 (5%, M + H^+), 883.3 (10%, [M + $2H^+$]/2), 589.4 (70%, [M + $3H^+$]/3), 442.4 (100%, [M + $4H^+$]/4).

Compound 126: Boc-deprotected 8-mer cyclic dimer (open-form oligomer)
HPLC-MS: column, Waters XTerra MS C_{18}, 4.6 × 150 mm; mobile phase, H_2O (0.l% HCOOH) / CH_3CN (0.05% HCOOH), 0% to 50% CH_3CN over 30 min); flow rate, 0.80 mL/min; UV detection at 220 nm; t_R for **126**, 9.76 min; ESI-MS *m/z* (ion) 883.6 (17%, [M + $4H^+$]/4), 707.2 (100%, [M + $5H^+$]/5), 589.5 (80%, [M + $6H^+$]/6), 505.5 (5%, [M + $7H^+$]/7).

Compound 127: Boc-deprotected 9-mer cyclic monomer (open-form oligomer)
HPLC-MS: column, Waters XTerra MS C_{18}, 4.6 × 150 mm; mobile phase, H_2O (0.l% HCOOH) / CH_3CN (0.05% HCOOH), 0% to 50% CH_3CN over 30 min); flow rate, 0.80 mL/min; UV detection at 220 nm; t_R for **127**, 8.04 min; ESI-MS *m/z* (ion) 968.2 (8%, [M + $2H^+$]/2), 646.1 (43%, [M + $3H^+$]/3), 485.0 (100%, [M + $4H^+$]/4).

Compound 128: Boc-deprotected 9-mer cyclic dimer (open-form oligomer)
HPLC-MS: column, Waters XTerra MS C_{18}, 4.6 × 150 mm; mobile phase, H_2O (0.l% HCOOH) / CH_3CN (0.05% HCOOH), 0% to 50% CH_3CN over 30 min); flow rate, 0.80 mL/min; UV detection at 220 nm; t_R for **128**, 9.52 min; ESI-MS *m/z* (ion) 968.7 (10%, [M + $4H^+$]/4), 775.2 (60%, [M + $5H^+$]/5), 646.2 (100%, [M + $6H^+$]/6), 554.1 (15%, [M + $7H^+$]/7).

After removing the Boc groups from the cyclic monomers and dimers, each was dissolved in anhydrous 20% piperidine/NMP (1.25 mL) and transferred into an HPLC vial. The DKP closing reactions were monitored by HPLC-MS. The cyclic monomers produced mixtures of incompletely closed products, whereas the cyclic dimers appeared to close completely. The rigidified cyclic dimer of the tetramer (**129**) and pentamer (**130**) oligomers were clean enough to purify by preparative HPLC and analyze by HRMS; there was extensive epimerization for the longer oligomers, and no major product of DKP formation was identified (probably due to water contamination; monitoring the DKP closure for the longer cyclic dimers was also complicated due to the incredibly small sample sizes). The analytical data for the rigidified cyclic dimer of

the trimer oligomer (**97**) is described above. The analytical data for the rigidified 4-mer and 5-mer cyclic dimers is provided here.

Compound 129: cyclic dimer of the tetramer oligomer, following DKP closure

HPLC-MS: column, Waters XTerra MS C_{18}, 4.6 × 150 mm; mobile phase, H_2O (0.l% HCOOH) / CH_3CN (0.05% HCOOH), 0% to 50% CH_3CN over 30 min); flow rate, 0.80 mL/min; UV detection at 220 nm; t_R for **129**, 18.20 min; ESI-MS *m/z* (ion) 989.2 (95%, $[M + 2H^+]/2$), 659.8 (100%, $[M + 3H^+]/3$); HRESIQTOFMS calcd for $C_{92}H_{98}N_{28}O_{24}$ / 2 ($[M + 2H^+]/2$) 988.3649, found 988.3644.

Compound 130: cyclic dimer of the pentamer oligomer, following DKP closure.

HPLC-MS: column, Waters XTerra MS C_{18}, 4.6 × 150 mm; mobile phase, H_2O (0.l% HCOOH) / CH_3CN (0.05% HCOOH), 0% to 50% CH_3CN over 30 min); flow rate, 0.80 mL/min; UV detection at 220 nm; t_R for **130**, 17.44 min; ESI-MS *m/z* (ion) 1127.7 (100%, $[M + 2H^+]/2$), 752.0 (22%, $[M + 3H^+]/3$), 564.3 (34%, $[M + 4H^+]/4$); HRESIQTOFMS calcd for $C_{104}H_{110}N_{32}O_{28}$ / 2 ($[M + 2H^+]/2$) 1127.4078, found 1127.4070.

5.8.4 Rod-hinge-rod motif

Compound 135: 3-hinge-3 *bis*-peptide cyclic monomer

N-Fmoc-1-(*S*)-naphthylalanine and *N*-Fmoc-(*S*)-propargylglycine were coupled sequentially to 2-chlorotritylchloride resin (30 mg, 1.1 mmol/gram substitution) using the methods described above. 3 Boc-*pro4*(2*S*,4*S*) monomers (**19**) were coupled to the resin sequentially with HATU. *N*-Fmoc-*N*'-ivDde-(*S*)-diaminobutanoic acid (Fmoc-Dab-(ivDde)) was coupled to the resin with HATU. The *N*-Fmoc group was removed using 20% piperidine/DMF; the deprotection was extended to 2 hours to ensure quantitative DKP formation. The resin was capped with acetic anhydride. The side-chain ivDde group was removed by soaking the resin in aliquots (2 mL) of a solution of hydrazine dihydrate and allyl alcohol in DMF (10 mL hydrazine dihydrate, 45 mL allyl alcohol, to 100 mL with DMF); the deprotection was monitored by measuring the UV absorbance of the deprotection solution at 280 nm. When no more chromophore was detected in the deprotection solution, the resin was washed thoroughly. 3 additional Boc-*pro4*(2*S*,4*S*)

monomers (**19**) were coupled to the resin using HATU, followed by Fmoc-(*S*)-Dab-N_3 (**88**). The Fmoc group was removed from the N-terminus by treatment with 20% piperidine/DMF for 2 hours (to ensure complete DKP formation between the last two residues). After washing and drying the resin, the desired product was obtained by treating the resin multiple times with a solution of 1% TFA in CH_2Cl_2, as described above. The cleavage product was purified by flash chromatography on C_{18} silica (4 gram column, gradient elution over 14 column volumes from H_2O (0.1% HCOOH) to CH_3CN (0.05% HCOOH)). Fractions containing the desired product were concentrated by centrifugal evaporation. The yield of **131**, based upon the initial resin loading, was approximately 65% (based upon HPLC analysis of the purified cleavage product).

131 (~ 21 μmol) was dissolved in degassed CH_3CN (33 mL) and transferred to a 50 mL round bottom flask containing a magnetic stir bar. DIPEA (11.5 μL, 66 μmol), 2,6-lutidine (7.6 μL, 66 μmol) and CuI (12.5 mg, 66 μmol) were added to the solution, and the flask was sealed with a rubber stopper. The mixture was stirred overnight, and analyzed the following morning by HPLC-MS. 89% of the starting material **131** had been converted to a mixture of cyclic monomer **132**, and cyclic dimer **133**; the monomer/dimer ratio was 100:7. Cyclic monomer **132** was isolated from the cyclic dimer **133** by flash chromatography on C_{18} silica (4 gram column, gradient elution over 14 column volumes from H_2O (0.1% HCOOH) to CH_3CN (0.05% HCOOH)).

All of the purified cyclic monomer **132** was dissolved in 50:50 TFA/CH_2Cl_2; after 30 minutes, the solution was concentrated by centrifugal evaporation (a large portion of the material was lost, likely due to bumping during concentration). Concentration afforded a residue that was determined to be **133** (cyclic monomer, open-form oligomer) by HPLC-MS. This residue was dissolved in 20% piperidine/NMP (4 mL) and the solution was transferred to a conical vial containing a magnetic spin vane; the solution was stirred for ~ 24 hours under nitrogen, and monitored by HPLC-MS. The product, **135** (3-hinge-3 *bis*-peptide cyclic monomer), was precipitated from ether, and purified by preparative HPLC. The fractions containing **135** were treated with neutralized Chelex Resin (Bio-Rad) to remove residual copper; unfortunately, the purified material was lost, probably because it bound to the resin.

Compound 131: 3-hinge-3 Boc-protected resin cleavage product

HPLC-MS: column, Waters XTerra MS C_{18}, 4.6 × 150 mm; mobile phase, H_2O (0.l% HCOOH) / CH_3CN (0.05% HCOOH), 5% to 95% CH_3CN over 30 min); flow rate, 0.80 mL/min; UV detection at 220 nm; t_R for **131**, 23.92 min; ESI-MS *m/z* (ion) 2180.5 (10%), 2093.4 (10%, M + H^+), 1993.6 (50%, M – Boc + H^+), 947.8 (100%, [M – 2Boc + $2H^+$]/2).

Compound 132: 3-hinge-3 cyclic monomer, Boc-protected open-form oligomer

HPLC-MS: column, Waters XTerra MS C_{18}, 4.6 × 150 mm; mobile phase, H_2O (0.l% HCOOH) / CH_3CN (0.05% HCOOH), 5% to 95% CH_3CN over 30 min, then 95% CH_3CN for 5 additional minutes); flow rate, 0.80 mL/min; UV detection at 220 nm; t_R for **132**, 23.65 min; ESI-MS *m/z* (ion) 2094.5 (100%, M + H^+), 997.2 (50%, [M – Boc + $2H^+$]/2).

Compound 134: 3-hinge-3 cyclic monomer, open-form oligomer

HPLC-MS: column, Waters XTerra MS C_{18}, 4.6 × 150 mm; mobile phase, H_2O (0.l% HCOOH) / CH_3CN (0.05% HCOOH), 0% to 50% CH_3CN over 30 min); flow rate, 0.80 mL/min; UV detection at 220 nm; t_R for **134**, 9.09 min; ESI-MS *m/z* (ion) 1493.2 (75%, M + H^+), 747.3 (100%, [M + $2H^+$]/2).

Compound 135: 3-hinge-3 *bis*-peptide cyclic monomer

HPLC-MS: column, Waters XTerra MS C_{18}, 4.6 × 150 mm; mobile phase, H_2O (0.l% HCOOH) / CH_3CN (0.05% HCOOH), 0% to 50% CH_3CN over 30 min); flow rate, 0.80 mL/min; UV detection at 220 nm; t_R for **135**, 12.19 min; ESI-MS *m/z* (ion) 1365.0 (100%, M + H^+), 683.3 (50%, [M + $2H^+$]/2), 456.2 (70%, [M + $3H^+$]/3).

Synthesis of 139: 6-hinge-6 *bis*-peptide cyclic monomer

N-Fmoc-1-(*S*)-naphthylalanine and *N*-Fmoc-(*S*)-propargylglycine were coupled sequentially to 2-chlorotritylchloride resin (25 mg, 1.1 mmol/gram substitution) using the methods described above. 6 Boc-*pro4*(2*S*,4*S*) monomers (**19**) and then *N*-Fmoc-*N*'-ivDde-(*S*)-diaminobutanoic acid (Fmoc-Dab-(ivDde)) were coupled sequentially to the resin as described. The *N*-Fmoc group from the Dab was removed (2 hours) with 20% piperidine, the resin was capped with acetic anhydride, and the ivDde group was removed with hydrazine (see details for the synthesis of 3-

hinge-3 *bis*-peptide cyclic monomer, **131**). 6 additional 3 Boc-*pro4*(2*S*,4*S*) monomers were coupled to the resin, followed by Fmoc-(*S*)-Dab-N_3 (**88**). The Fmoc group was removed, the resin was washed, and the desired product **136** (Boc-protected open-form oligomer prior to CuAAC macrocyclization) was cleaved from the resin with a solution of 1% TFA in CH_2Cl_2, as described above. The cleavage solution aliquots were combined and concentrated by rotary evaporation, and the residue was dissolved in EtOAc. This solution was transferred into a 125 mL separatory funnel and washed with pH 3.4 aqueous HCl (2 ×) and with brine (1 ×) to remove pyridine. The EtOAc solution was concentrated, affording a residue that was purified by preparative HPLC. The purified material was contaminated with some oligomer that ESI-MS suggested was the result of a partially failed coupling after installing the Dab hinge.

An analytical portion of the cleavage product (~ 1.5 μmol, by HPLC) was dissolved in CH_3CN (1.48 mL) and transferred into a conical vial containing a magnetic spin vane. CuI (0.5 mg, ~ 3 μmol), DIPEA (0.5 μL, ~ 3 μmol) and 2,6-lutidine (0.3 μL, ~ 3 μmol) were added to the solution. The vial was sealed with a rubber stopper, and the solution was stirred overnight. The solution was concentrated by rotary evaporation, dissolved in CH_3CN (500 μL) and transferred to the top of a short column containing 500 mg of C_{18} silica, pre-equilibrated with H_2O (0.1% HCOOH). The CH_3CN was evaporated under a stream of nitrogen. The column was flushed with 0.1% HCOOH/H_2O (12 ×) to remove copper, and then with CH_3CN (10 mL) to elute the desired product. A small portion (~ 300 μL) of the CH_3CN eluate was transferred into an HPLC vial. TCEP (~ 1 mg) was added to the solution; the vial was capped, then inverted several times to mix. This solution was analyzed by HPLC-MS to test for the presence of azide. The remaining CH_3CN eluate was concentrated by rotary evaporation affording crude **137**; the water washes were lyophilized and analyzed by HPLC to confirm that no product had been lost during the water wash.

Crude **137** was dissolved in 50% TFA/CH_2Cl_2 and stirred for 2 hours. The solvent was evaporated under a stream of nitrogen, and residual solvent was removed under reduced pressure overnight. An analytical sample of **138**, the product of Boc-cleavage, was dissolved in H_2O/ACN and analyzed by HPLC-MS. The remaining residue was dissolved in anhydrous 20% piperidine/NMP (800 μL); this solution was monitored by HPLC over the next 30 hours. The

solution was then purified by preparative HPLC; the desired fractions were concentrated by lyophilization. The resulting white powder was dissolved in 1:1 CH_3CN/H_2O, and was determined to be nearly pure **139** by HPLC-MS.

Compound 136: 6-hinge-6, Boc-protected resin cleavage product

HPLC-MS: column, Waters XTerra MS C_{18}, 4.6 × 150 mm; mobile phase, H_2O (0.l% HCOOH) / CH_3CN (0.05% HCOOH), 5% to 95% CH_3CN over 30 min, then 95% CH_3CN for 5 additional minutes); flow rate, 0.80 mL/min; UV detection at 220 nm; t_R for **136**, 26.72 min; ESI-MS *m/z* (ion) 1757.1 (36%, [M – 2Boc + $2H^+$]/2), 1139.2 (10%, [M – 3Boc + $3H^+$]/3), 600.3 (50%), 515.4 (100%).

Compound 137: 6-hinge-6 cyclic monomer, Boc-protected open-form oligomer

HPLC-MS: column, Waters XTerra MS C_{18}, 4.6 × 150 mm; mobile phase, H_2O (0.l% HCOOH) / CH_3CN (0.05% HCOOH), 5% to 95% CH_3CN over 30 min); flow rate, 0.80 mL/min; UV detection at 220 nm; t_R for **137**, 26.85 min; ESI-MS *m/z* (ion) 1899.4 (15%), 1867.1 (25%), 1806.9 (100%, [M – Boc + $2H^+$]/2), 1756.4 (15%), 1171.3 (15%), 1138.3 (21%), 1119.3 (12.5%), 599.9 (45%).

Compound 138: 6-hinge-6 cyclic monomer, open-form oligomer

HPLC-MS: column, Waters XTerra MS C_{18}, 4.6 × 150 mm; mobile phase, H_2O (0.l% HCOOH) / CH_3CN (0.05% HCOOH), 0% to 50% CH_3CN over 30 min); flow rate, 0.80 mL/min; UV detection at 220 nm; t_R for **138**, 6.96 min; ESI-MS *m/z* (ion) 1257.7 (30%, [M + $2H^+$]/2), 838.7 (100%, [M + $3H^+$]/3), 629.3 (23%, [M + $4H^+$]/4).

Compound 139: 6-hinge-6 *bis*-peptide cyclic monomer, all DKP rings closed

HPLC-MS: column, Waters XTerra MS C_{18}, 4.6 × 150 mm; mobile phase, H_2O (0.l% HCOOH) / CH_3CN (0.05% HCOOH), 0% to 50% CH_3CN over 30 min); flow rate, 0.80 mL/min; UV detection at 220 nm; t_R for **139**, 14.19 min; ESI-MS *m/z* (ion) 1464.3 (15%, [2M + $3H^+$]/3), 1097.6 (100%, [M + $2H^+$]/2), 731.8 (82%, [M + $3H^+$]/3).

APPENDIX A

REPRESENTATIVE 1D-NMR SPECTRA

The spectra illustrated in this appendix are representative 1D NMR spectra of the *pro4* monomers and their intermediates. For each pair of enantiomers, one spectra is shown.

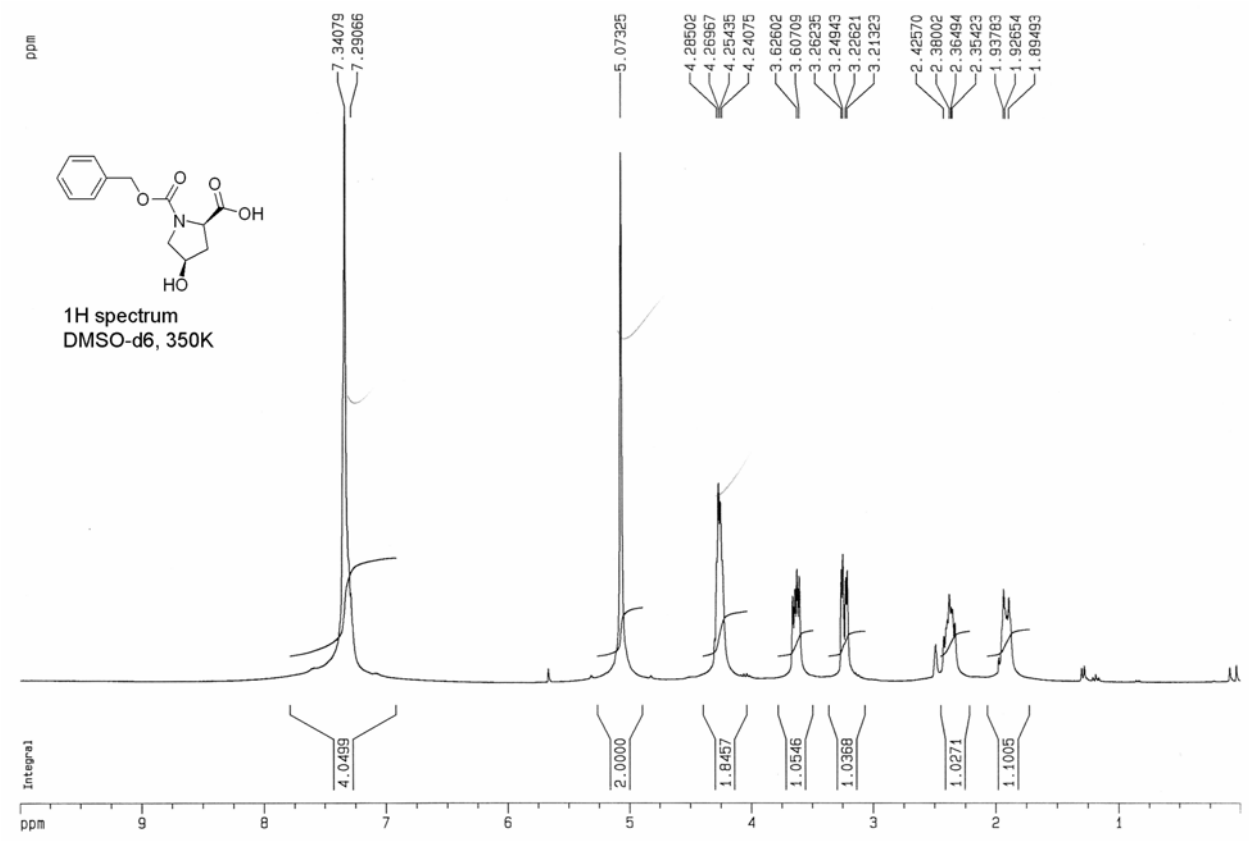

Supplemental Figure 1: ^{1}H NMR spectrum of **20**, 300 MHz, DMSO-d_6, 350 K

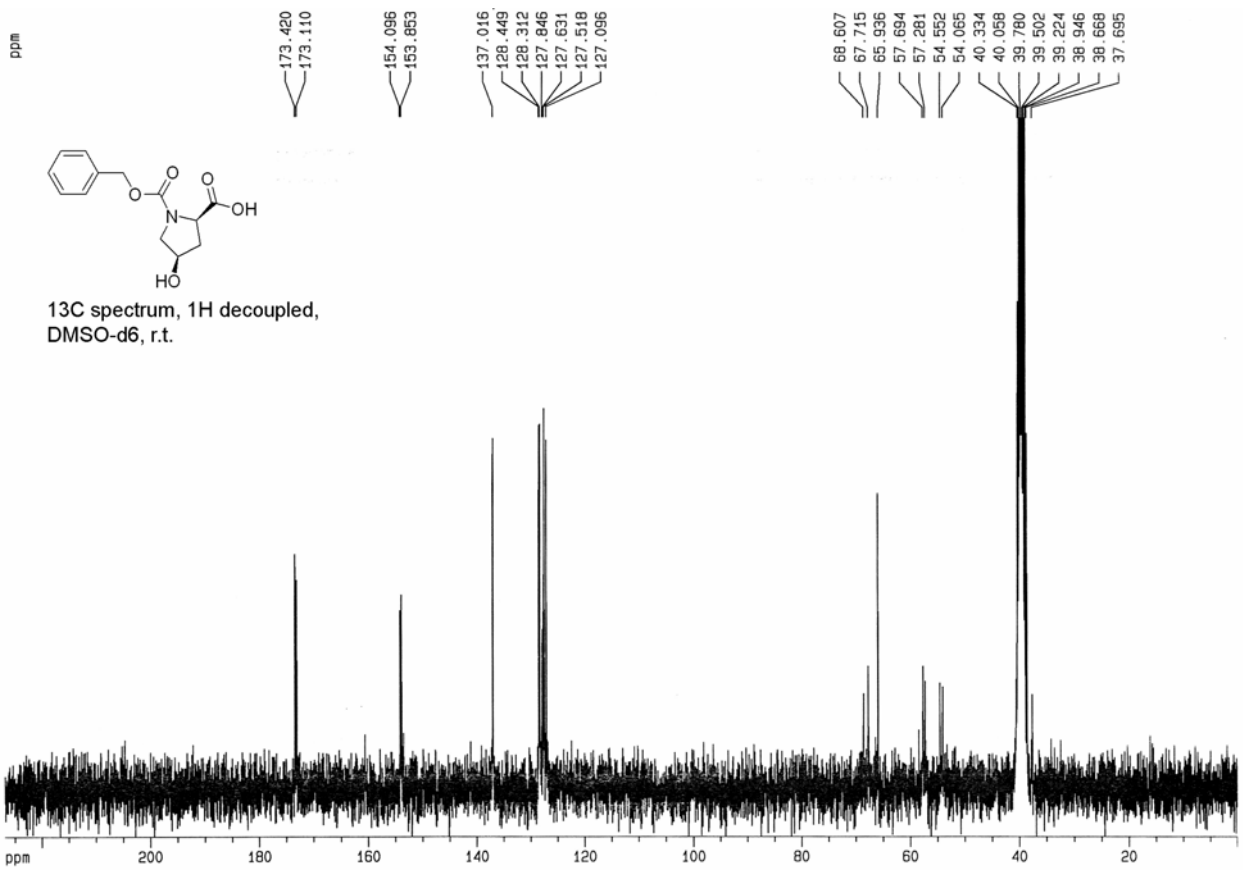

Supplemental Figure 2: ^{1}H decoupled ^{13}C spectrum of **20**, 75.4 MHz, DMSO-d_6

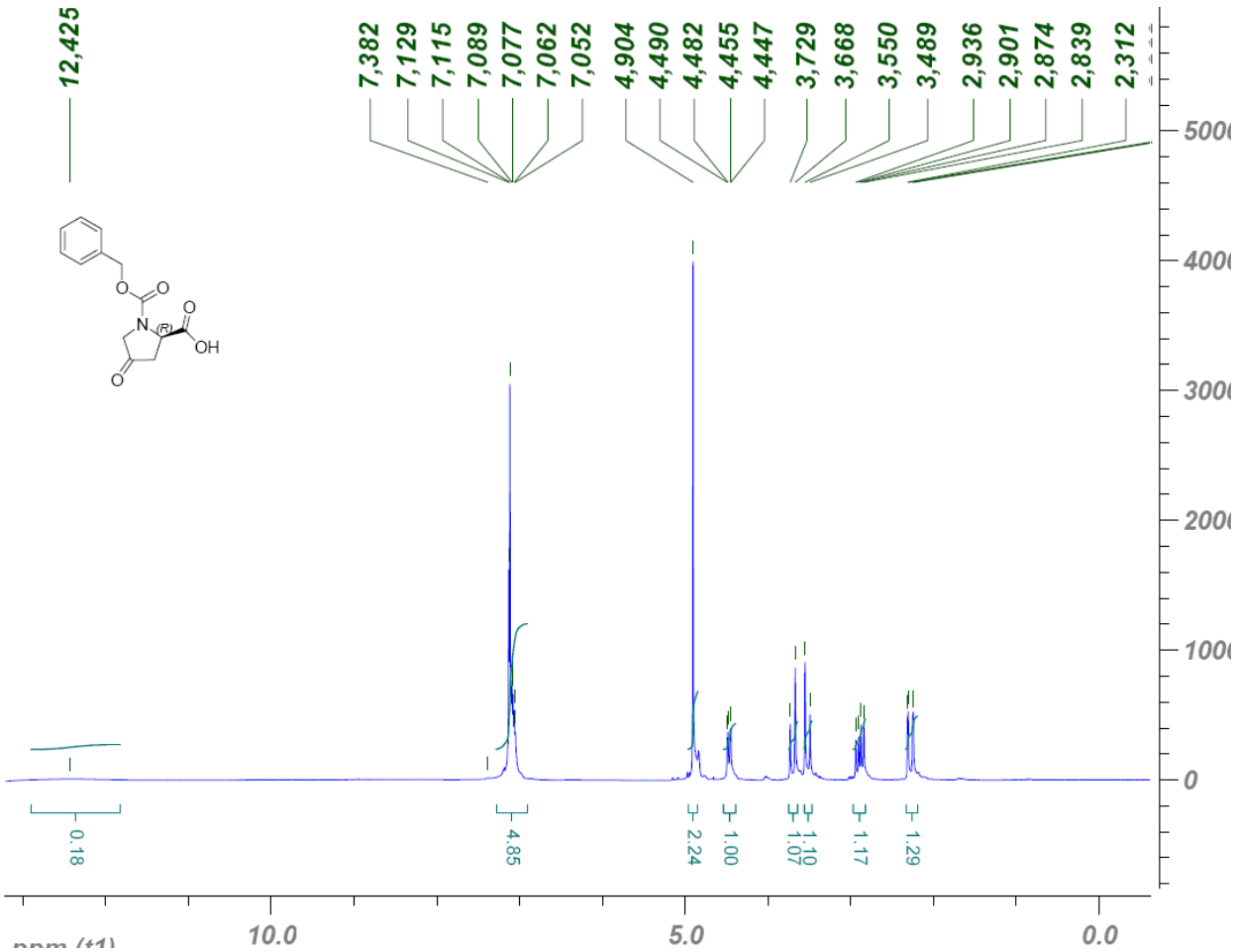

Supplemental Figure 3: ^{1}H NMR spectrum of **21**, 300 MHz, DMSO-d_6, 350 K

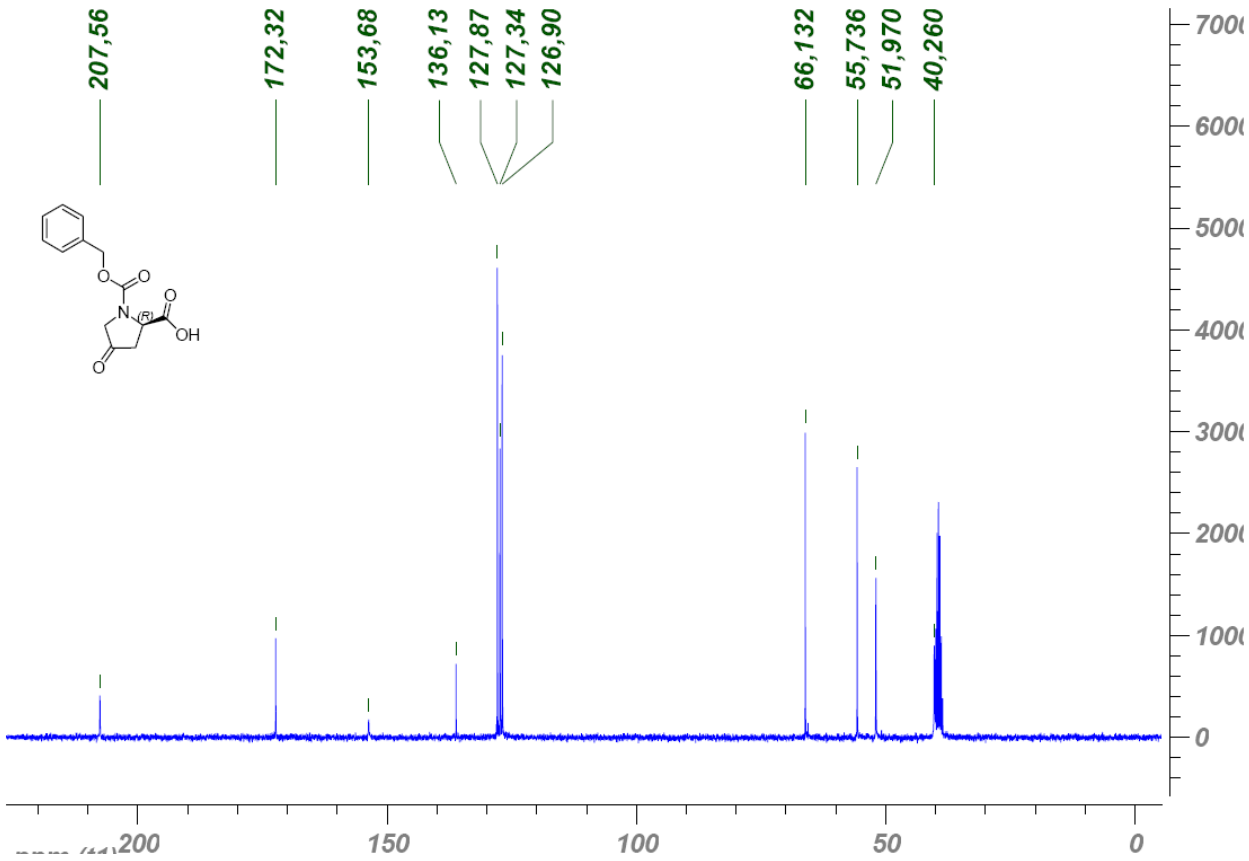

Supplemental Figure 4: ^{1}H decoupled ^{13}C spectrum of **21**, 75.4 MHz, DMSO-d_6, 350 K

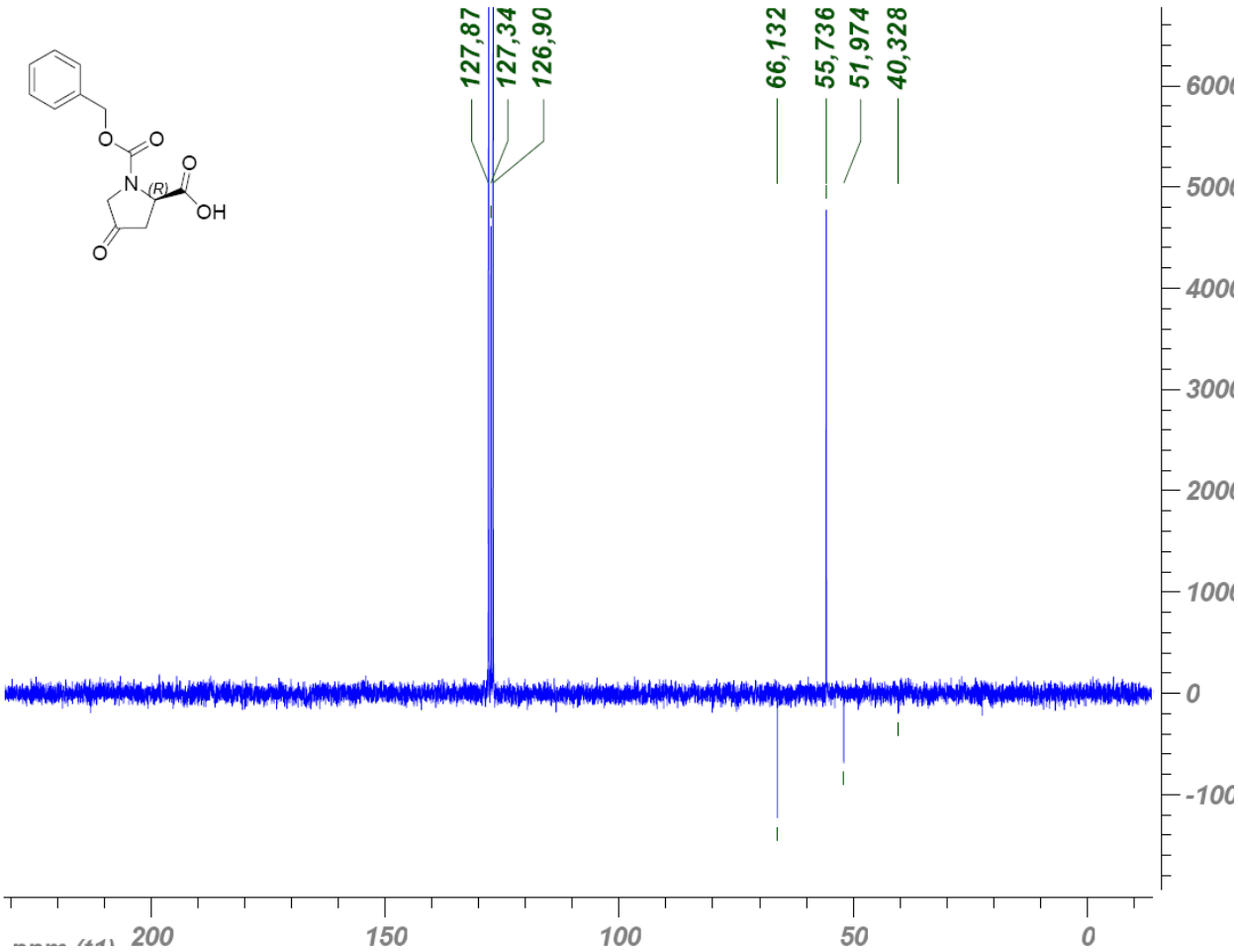

Supplemental Figure 5: dept135 spectrum of **21**, 75.4 MHz, DMSO-d_6, 350 K

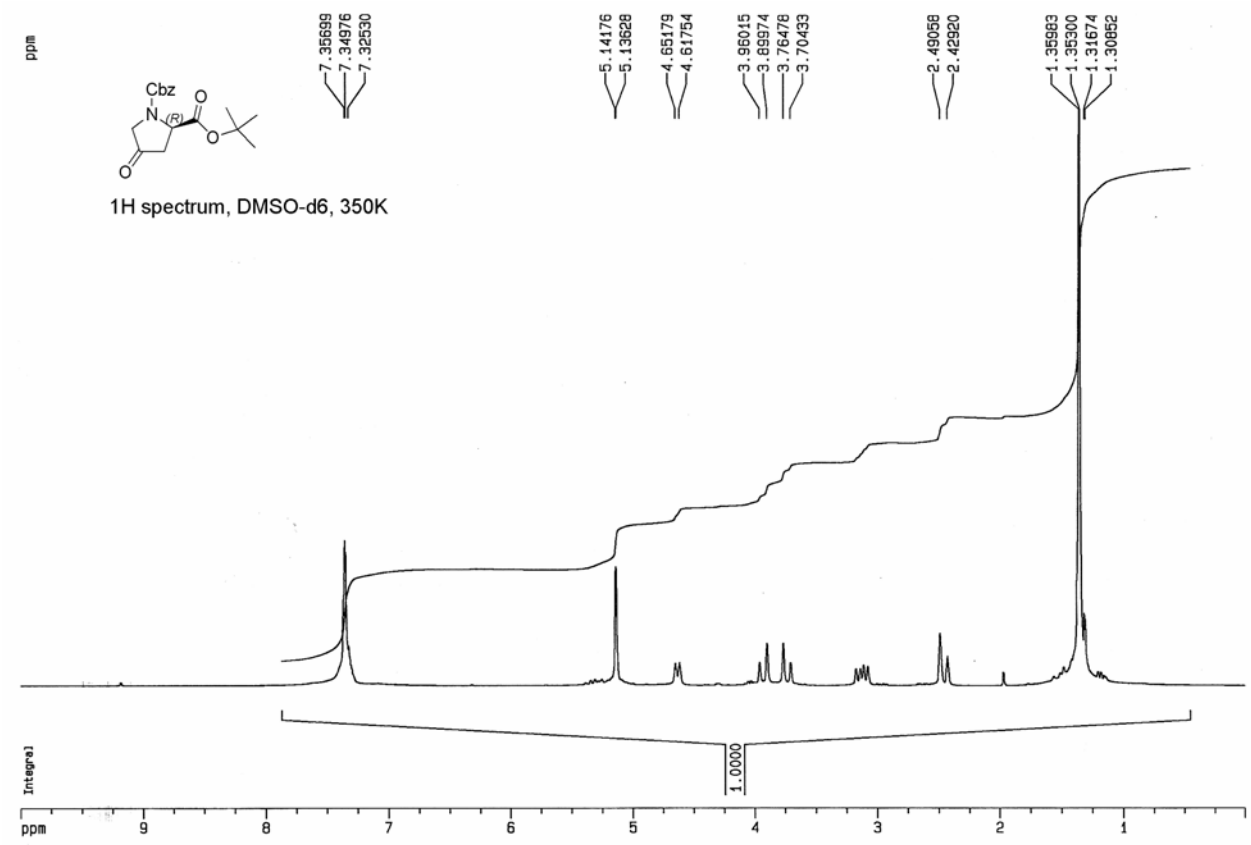

Supplemental Figure 6: ^{1}H spectrum of **22**, 300 MHz, DMSO-d_6, 350 K

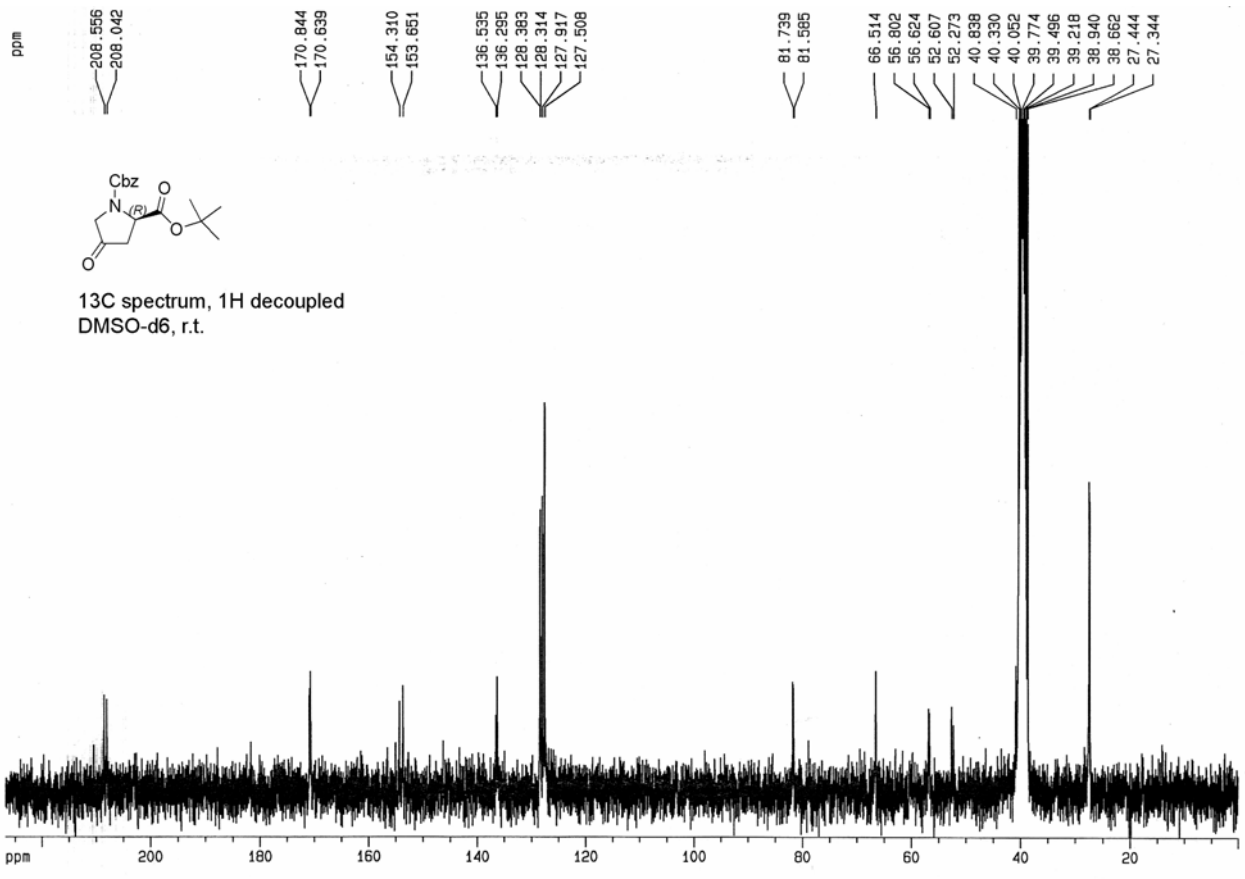

Supplemental Figure 7: ^{1}H decoupled ^{13}C spectrum of **22**, 75.4 MHz, DMSO-d_6

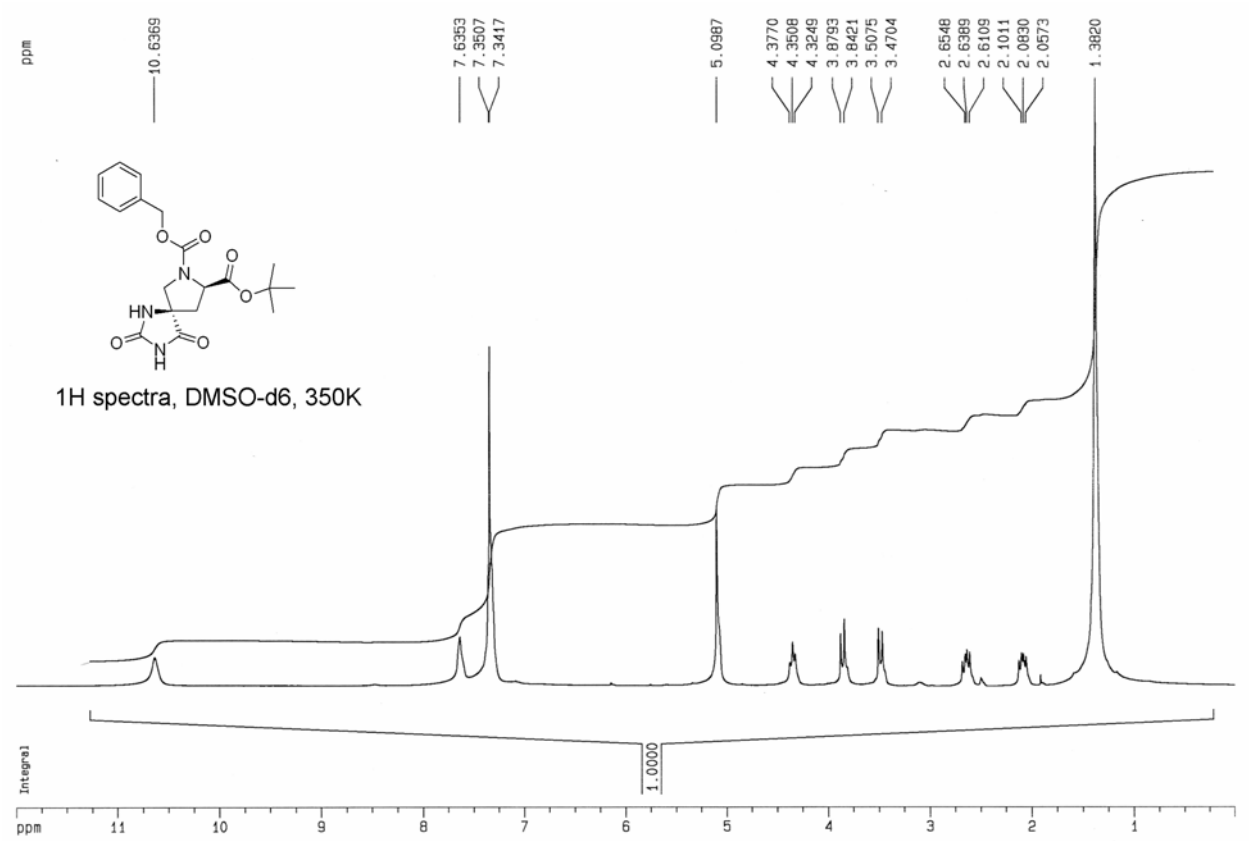

Supplemental Figure 8: ^{1}H NMR spectrum of **23**, 300 MHz, DMSO-d_6, 350 K

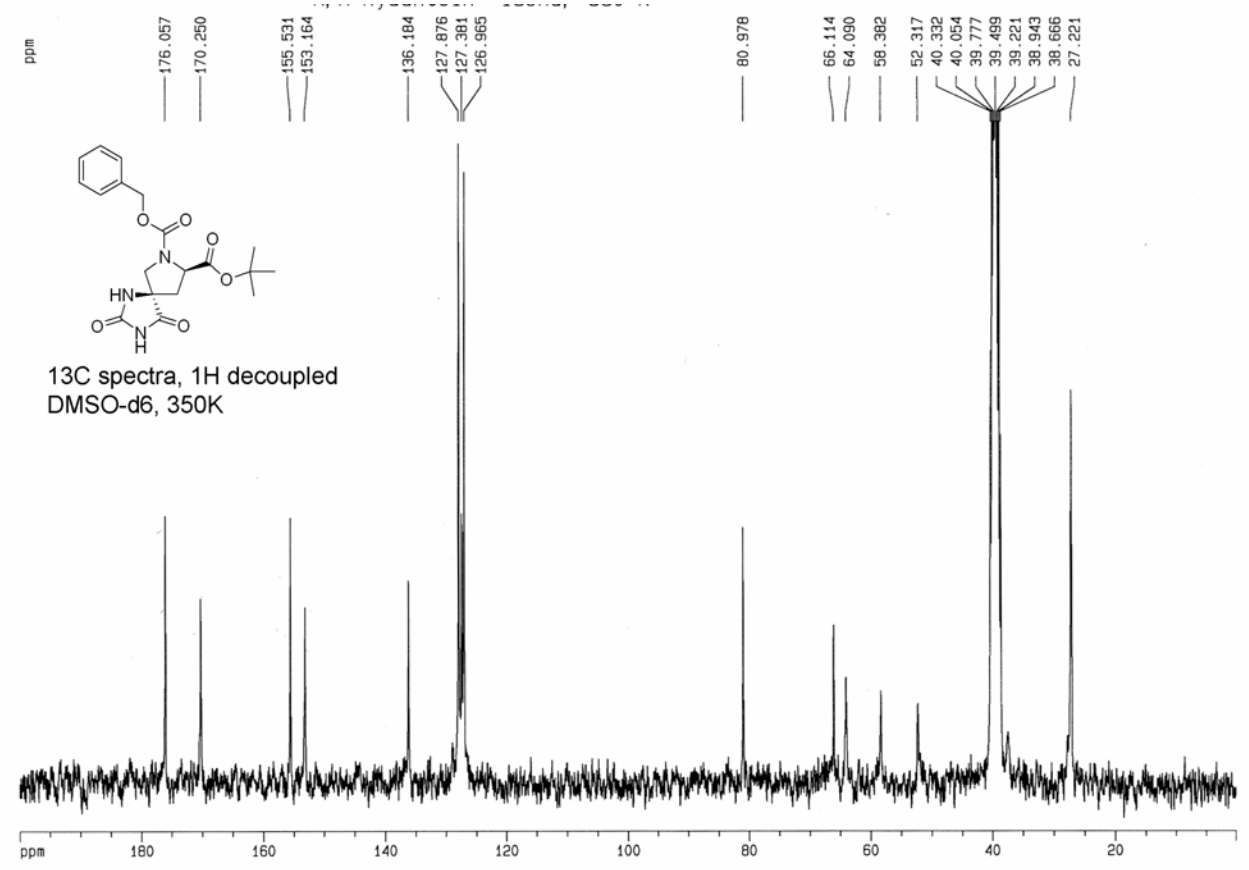

Supplemental Figure 9: ^{1}H decoupled ^{13}C NMR of **23**, 75.4 MHz, DMSO-d_6, 350 K

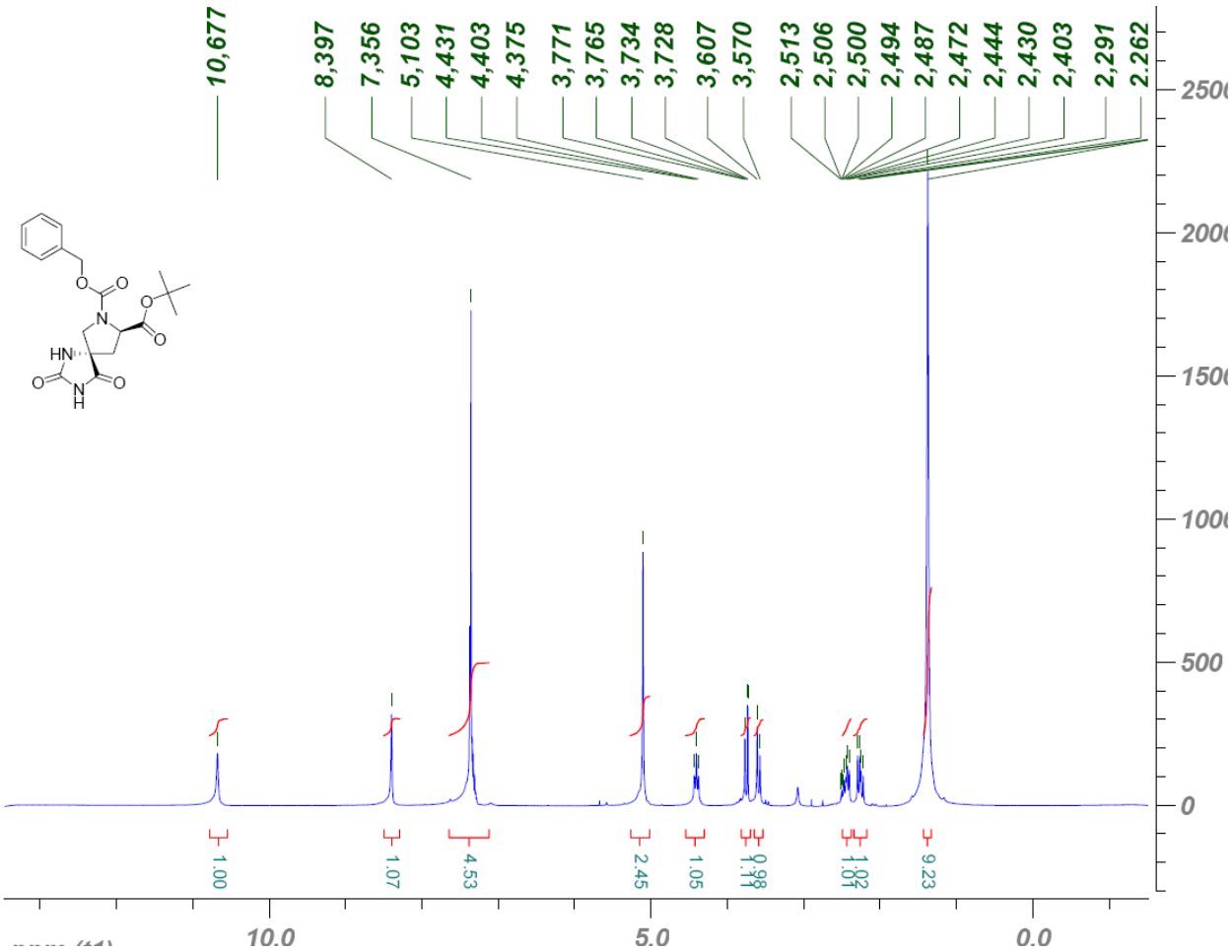

Supplemental Figure 10: ^{1}H NMR of **24**, 300 MHz, DMSO-d_6, 350 K

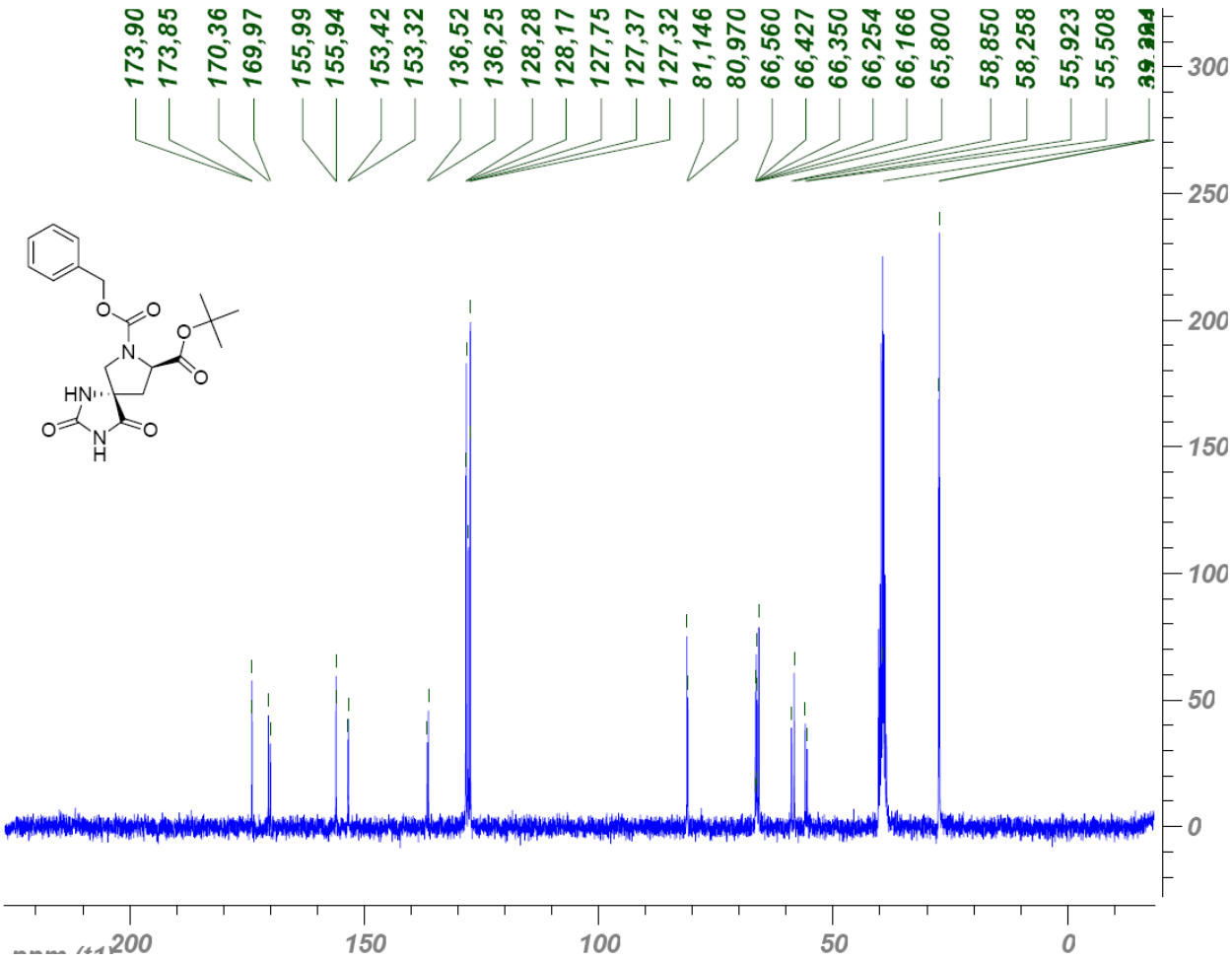

Supplemental Figure 11: ^{1}H decoupled ^{13}C spectrum of **24**, 75.4 MHz, DMSO-d_6

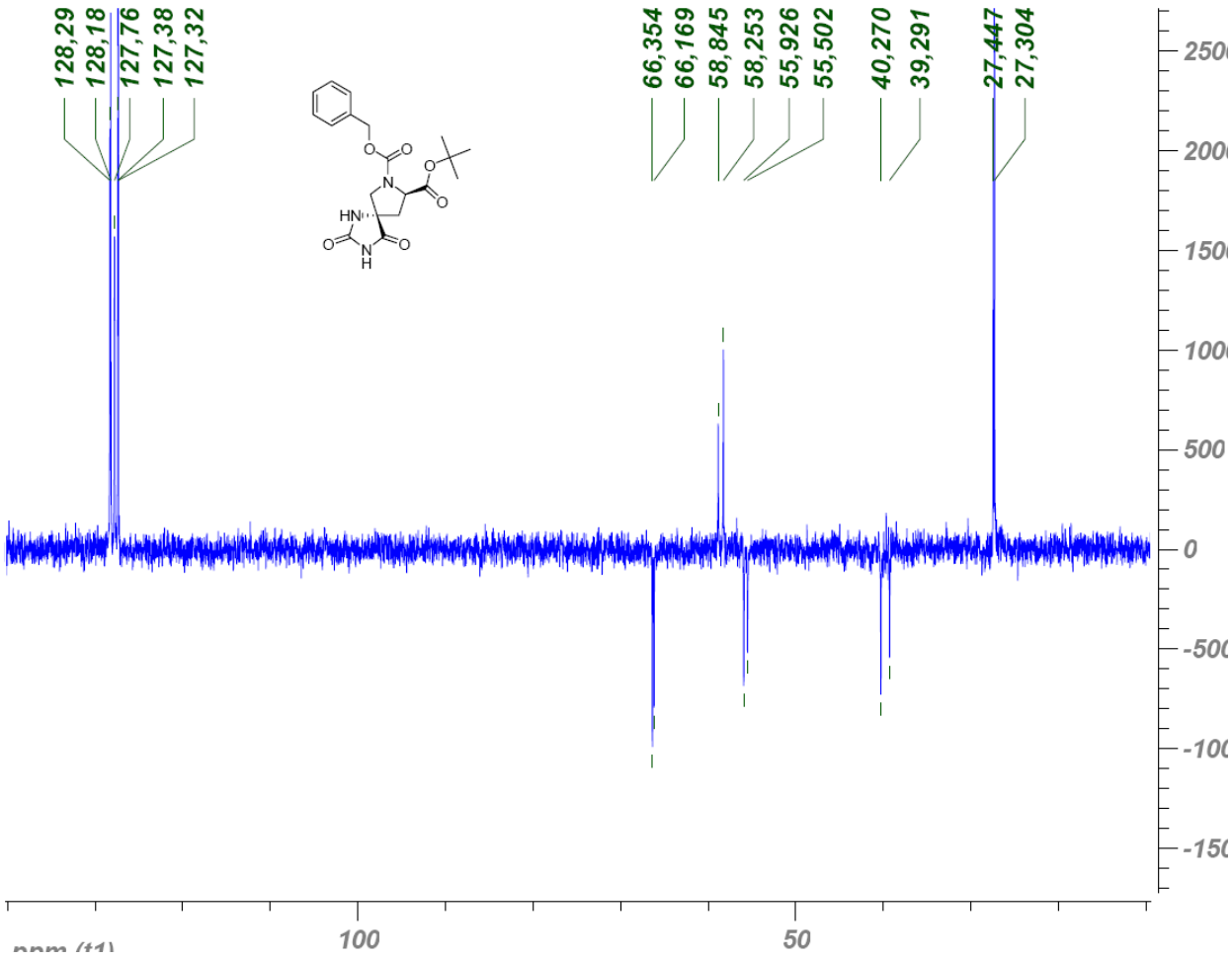

Supplemental Figure 12: dept135 spectrum of **24**, 75.4 MHz, DMSO-d_6

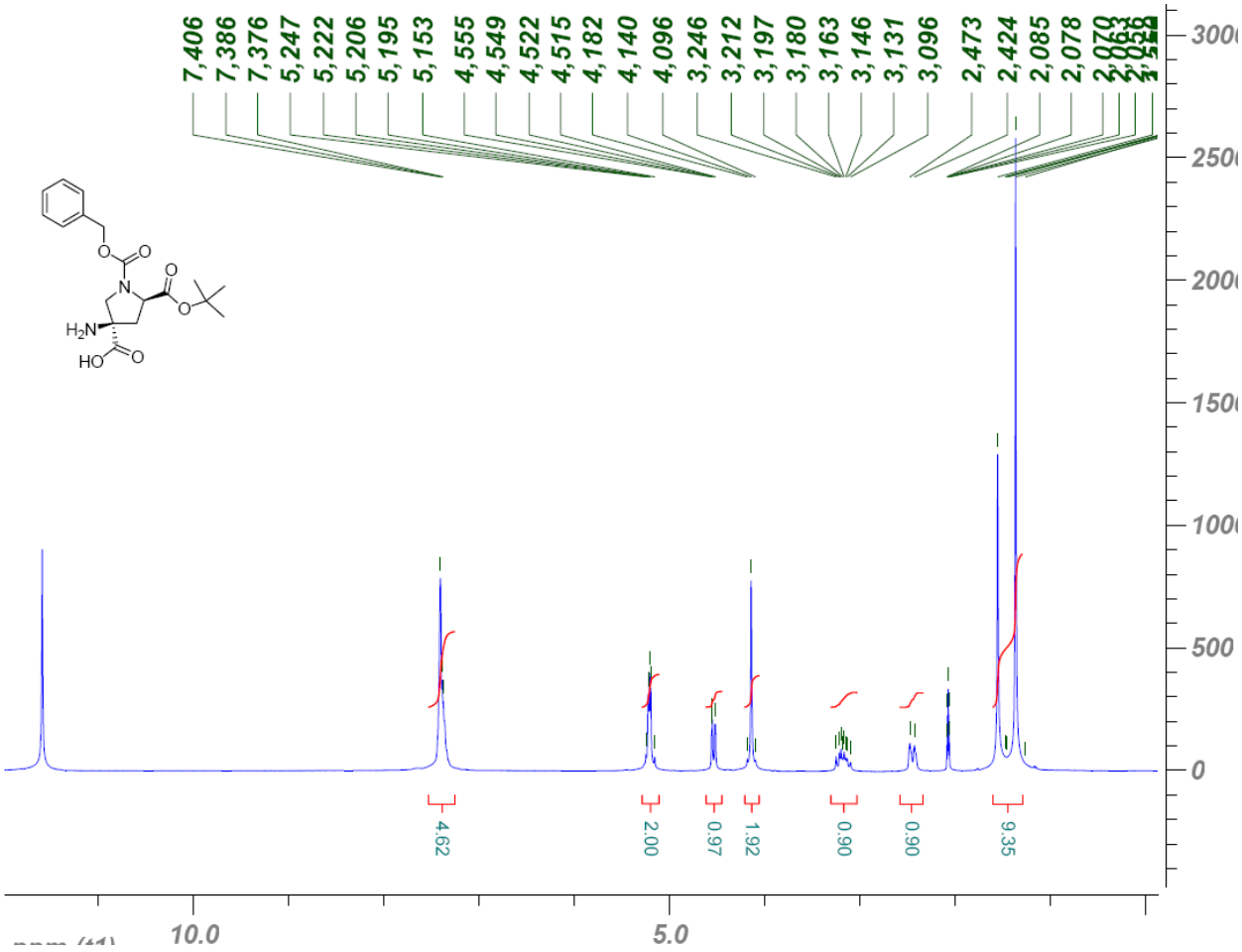

Supplemental Figure 13: ^{1}H NMR spectrum of **26**, 300 MHz, CD_3COOD

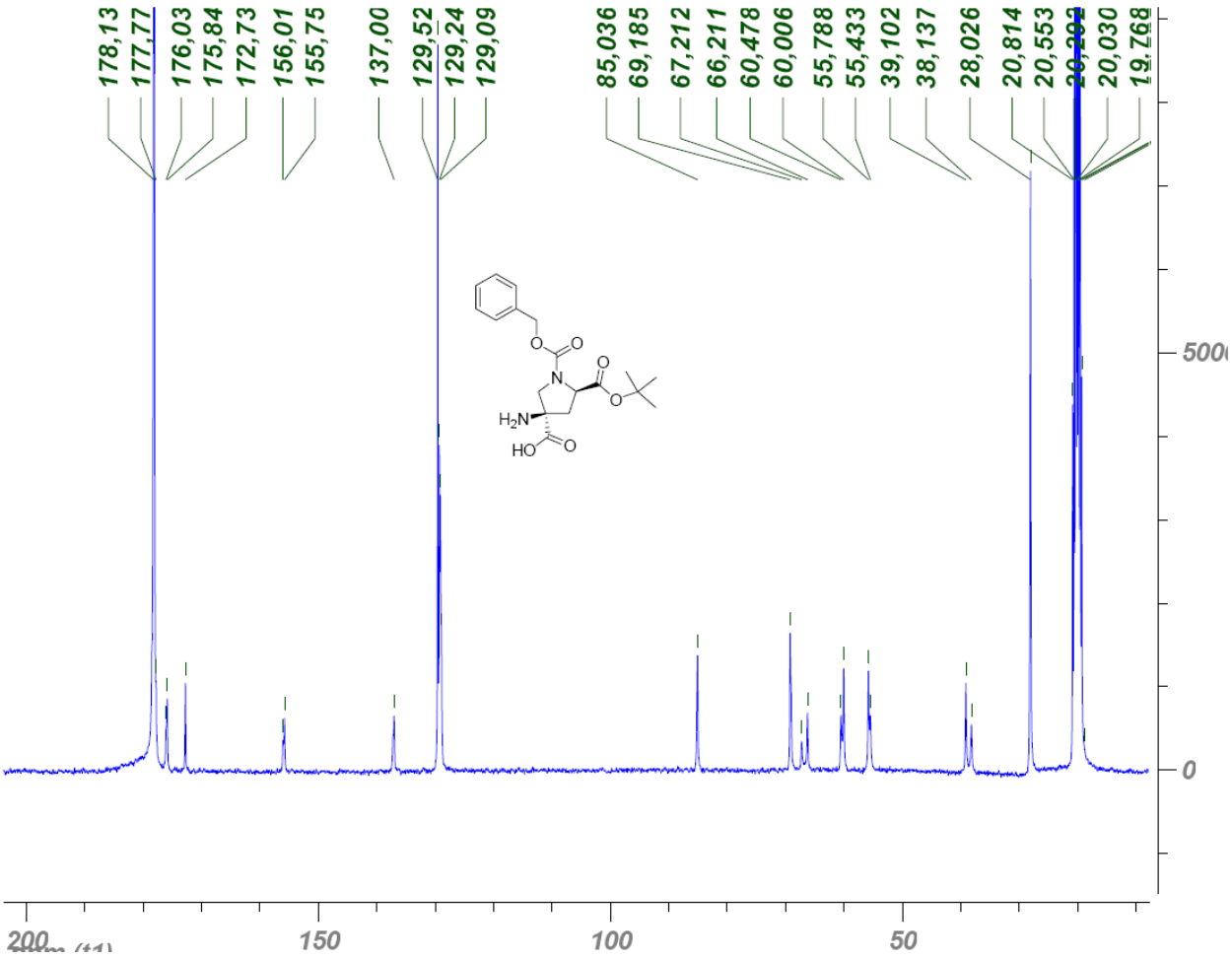

Supplemental Figure 14: ^{1}H decoupled ^{13}C spectrum of **26**, 75.4 MHz, CD_3COOD

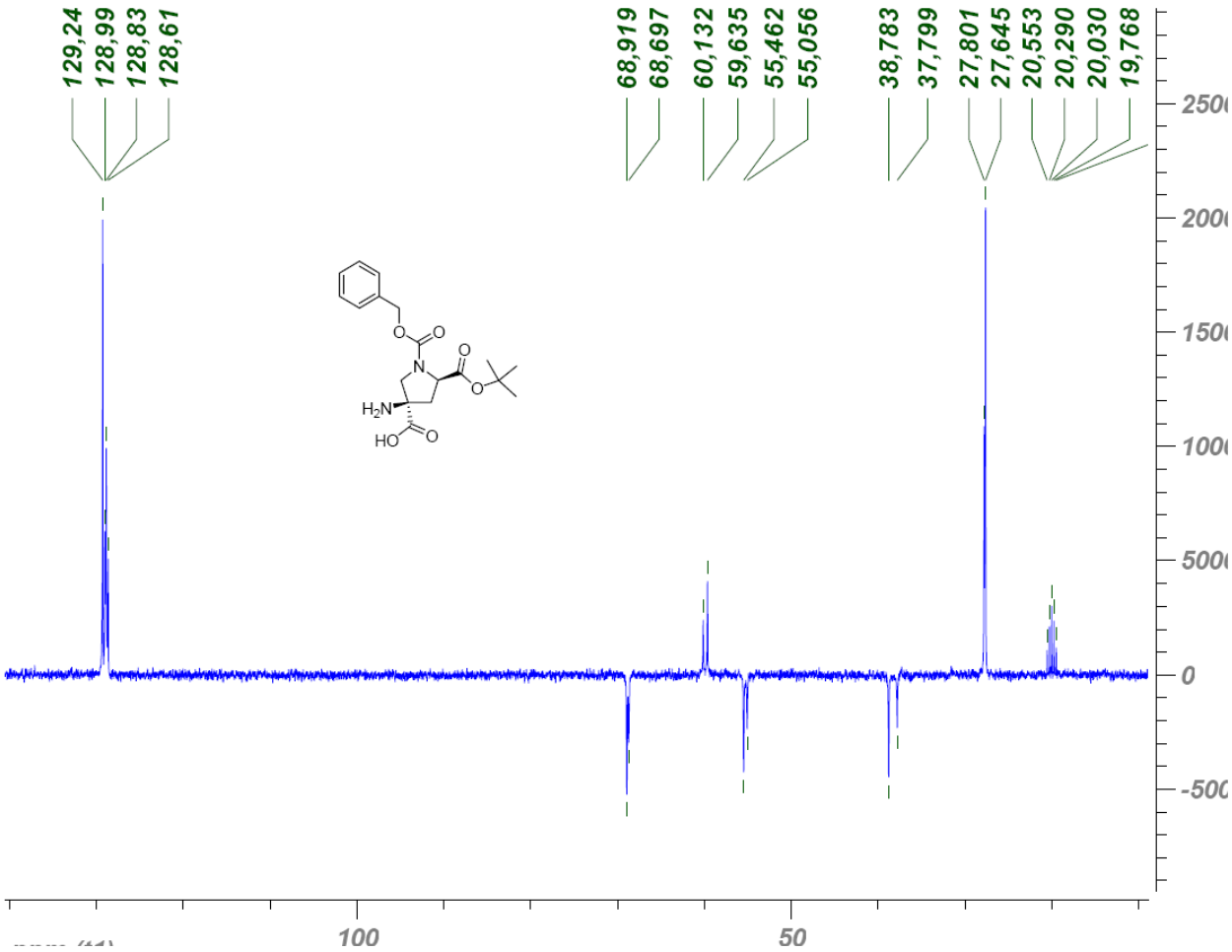

Supplemental Figure 15: dept135 spectrum of **26**, 75.4 MHz, CD_3COOD

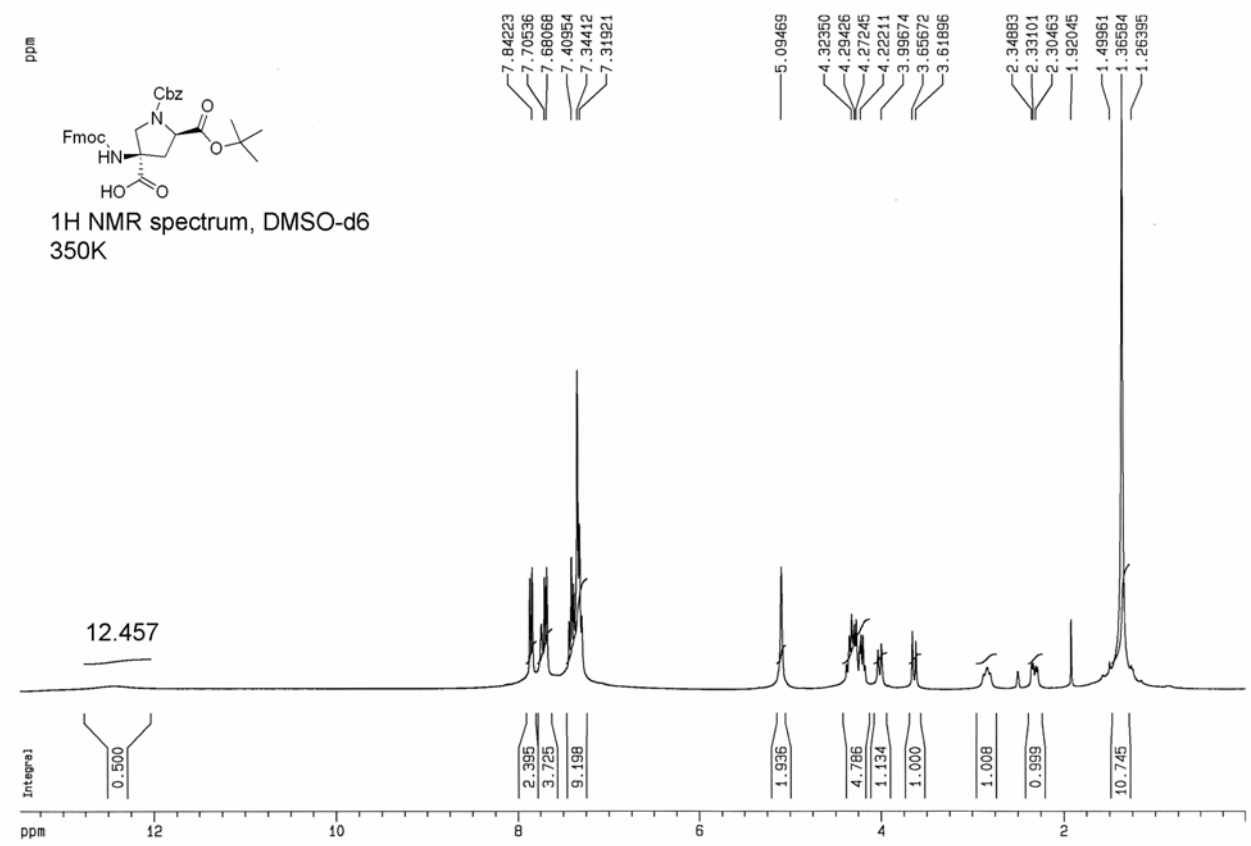

Supplemental Figure 16: ^{1}H NMR spectrum of **27**, 300 MHz, DMSO-d_6, 350 K

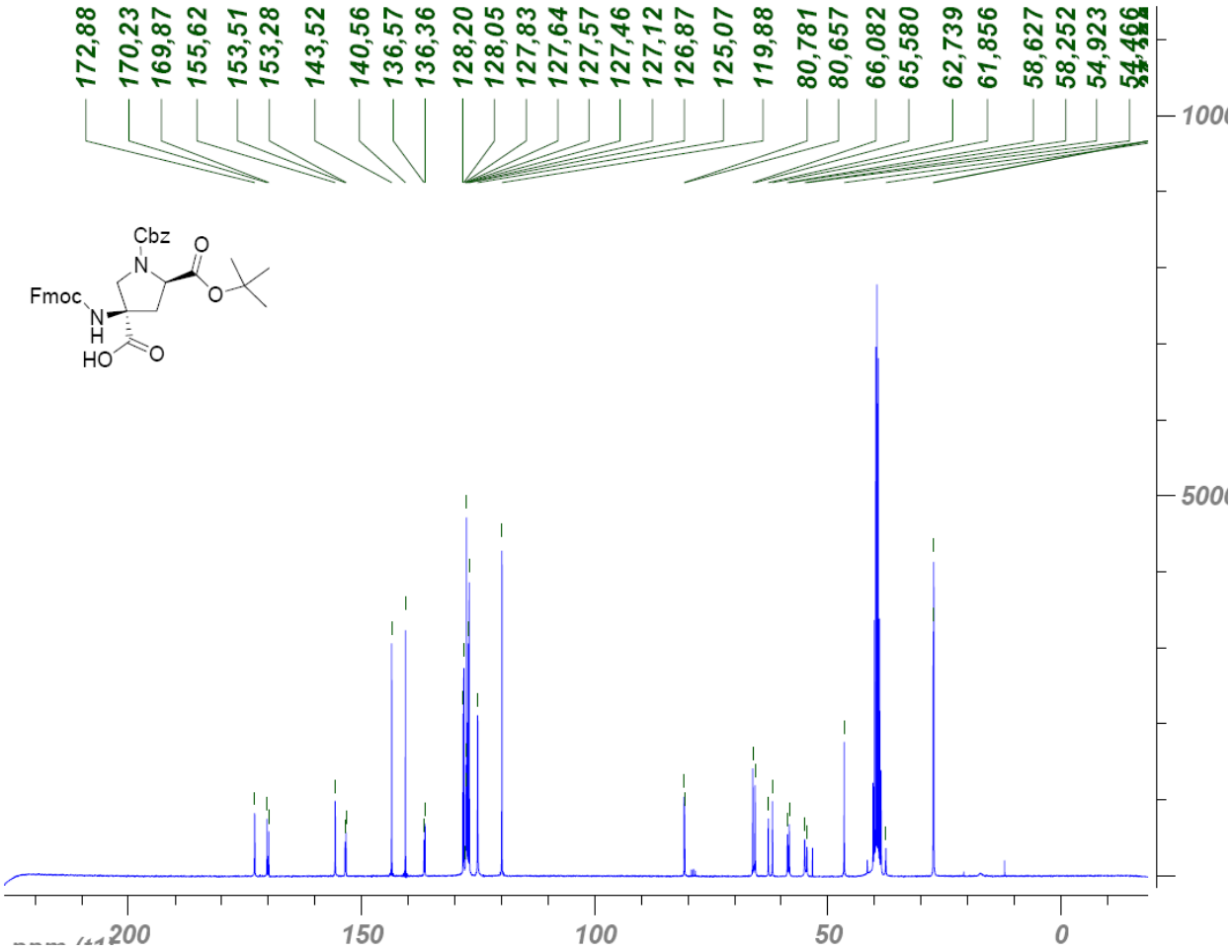

Supplemental Figure 17: ^{1}H decoupled ^{13}C spectrum of **27**, 75.4 MHz, DMSO-d_6

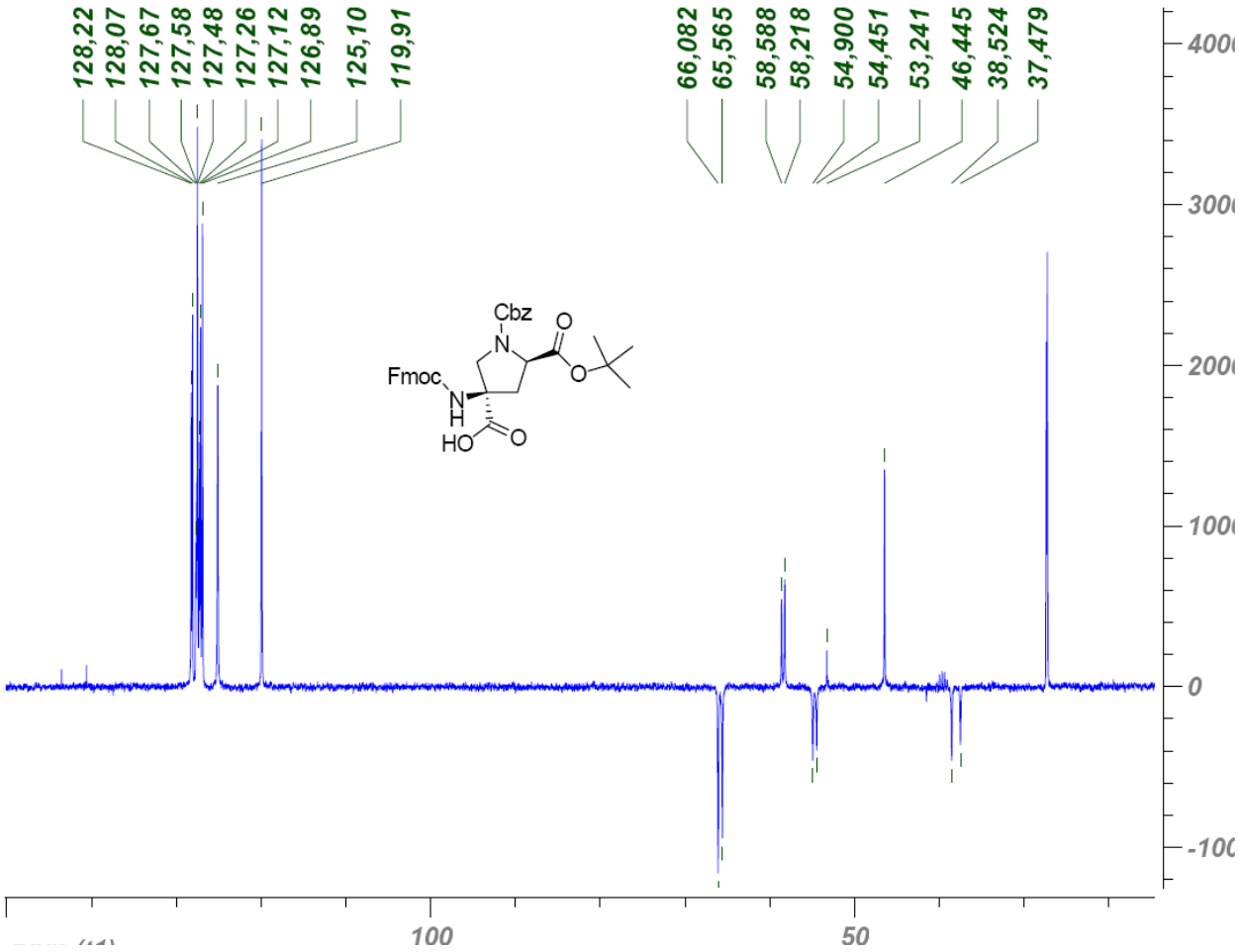

Supplemental Figure 18: dept135 spectrum of **27**, 75.4 MHz, DMSO-d_6

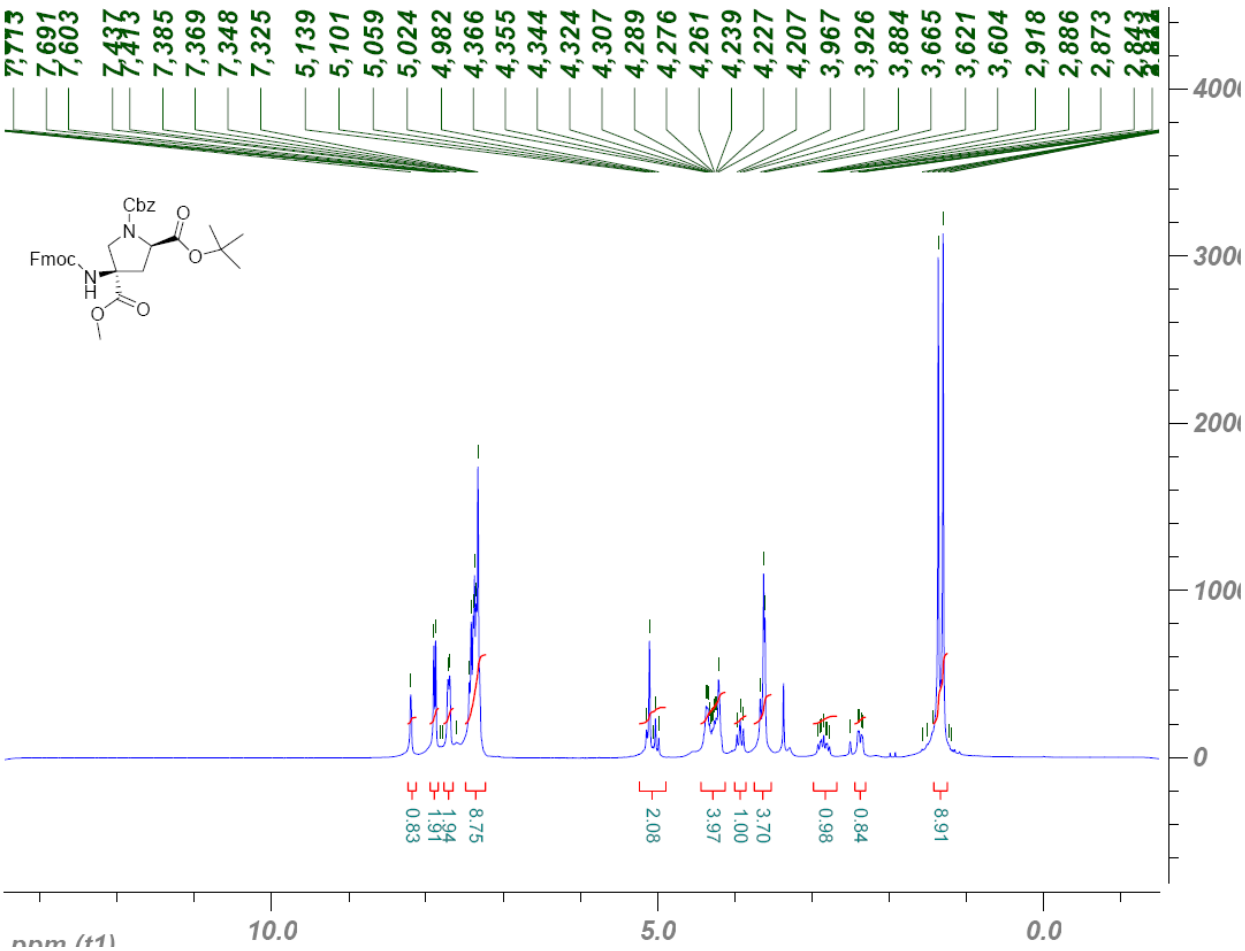

Supplemental Figure 19: ^{1}H NMR spectrum of **28**, 300 MHz, DMSO-d_6

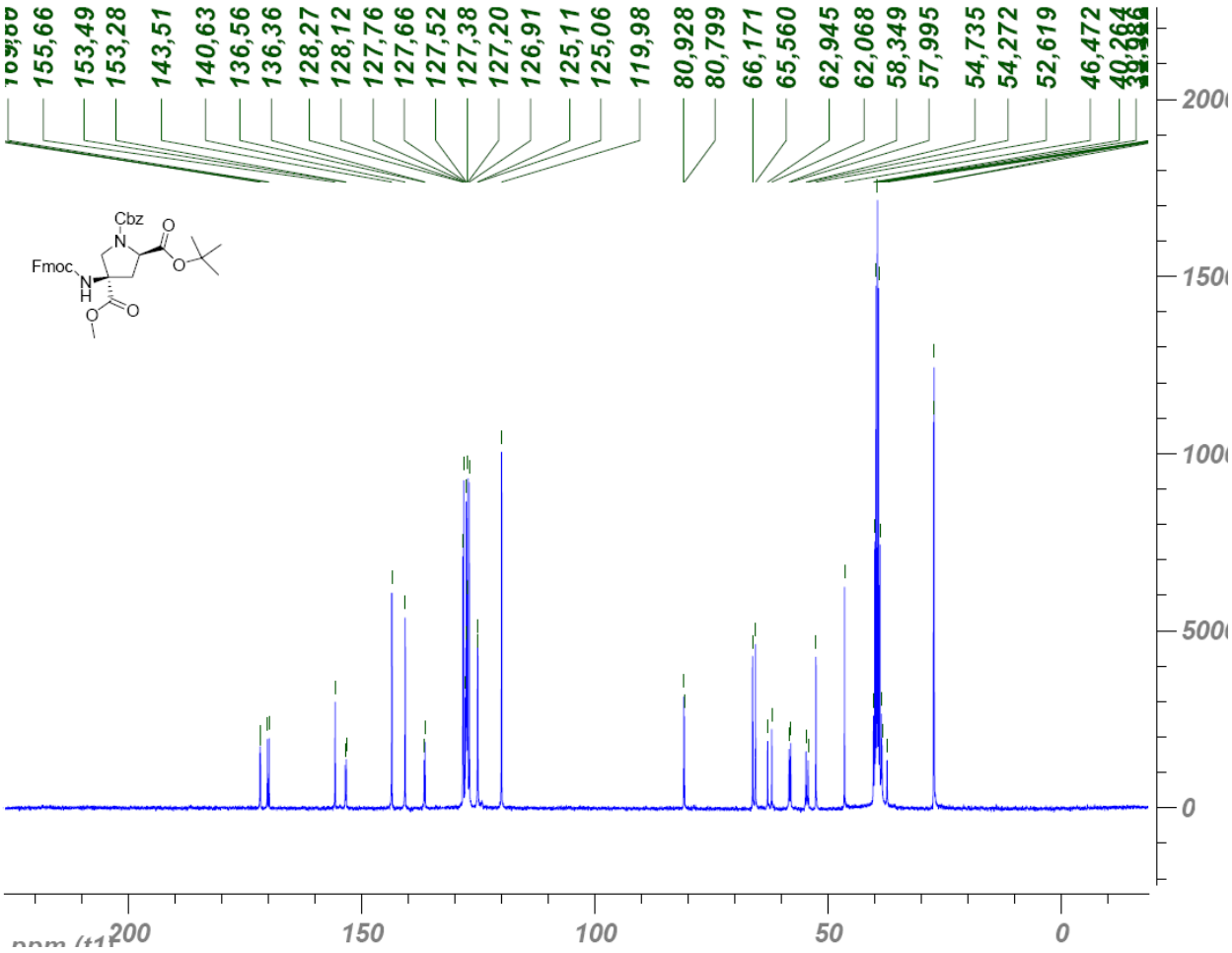

Supplemental Figure 20: ^{1}H decoupled ^{13}C spectrum of **28**, 75.4 MHz, DMSO-d_6

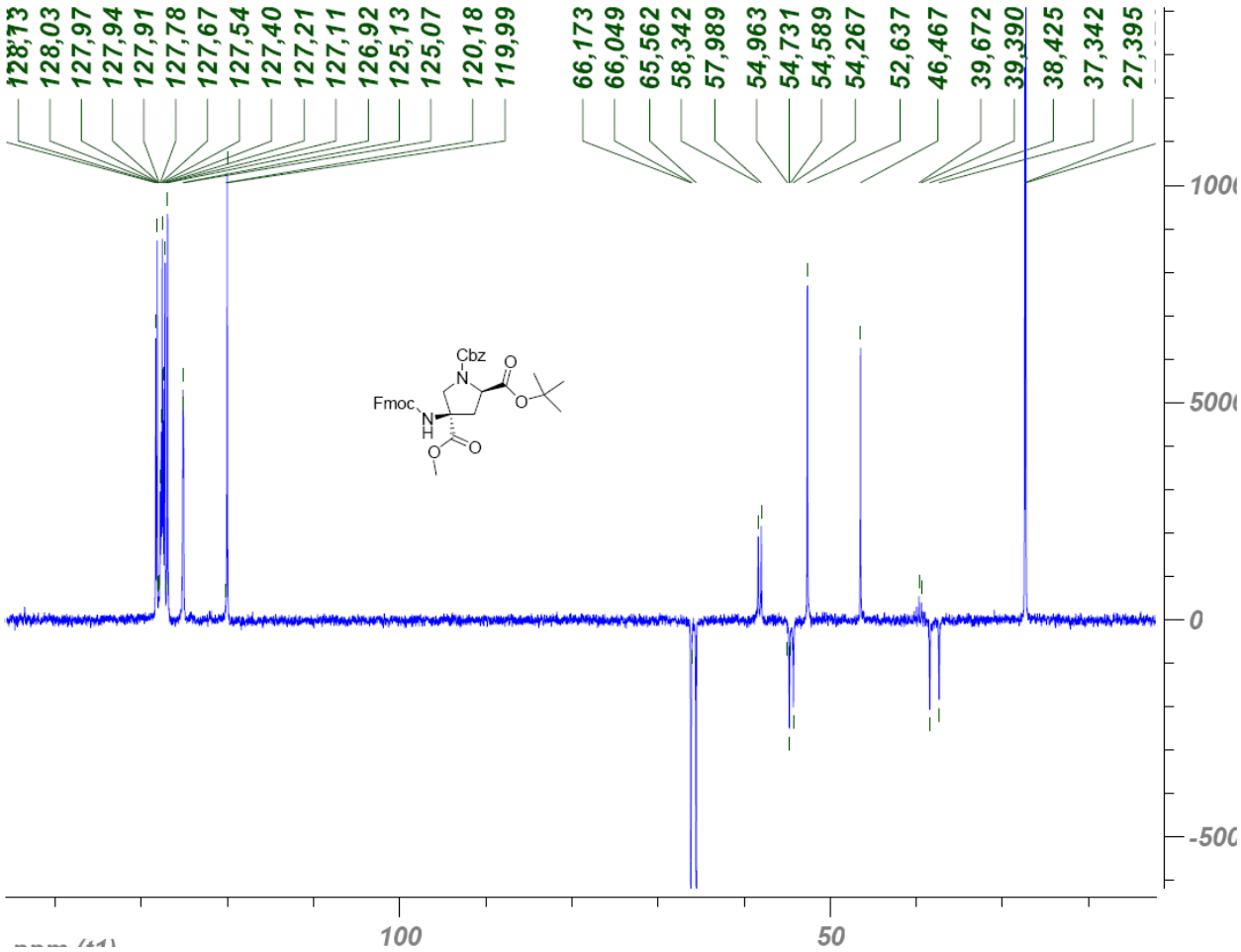

Supplemental Figure 21: dept135 spectrum of **28**, 75.4 MHz, DMSO-d_6

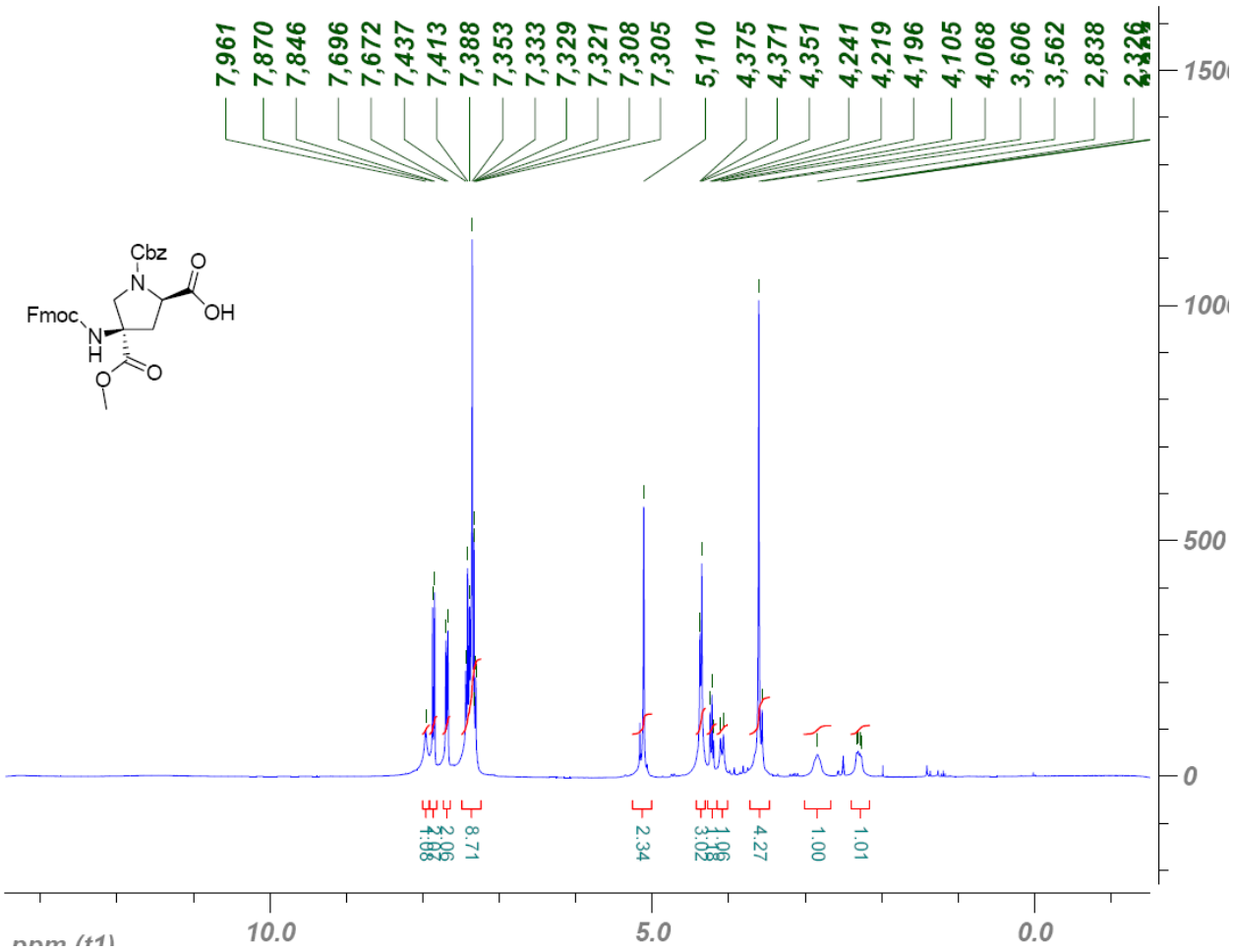

Supplemental Figure 22: ^{1}H NMR spectrum of **29**, 300 MHz, DMSO-d_6, 350 K

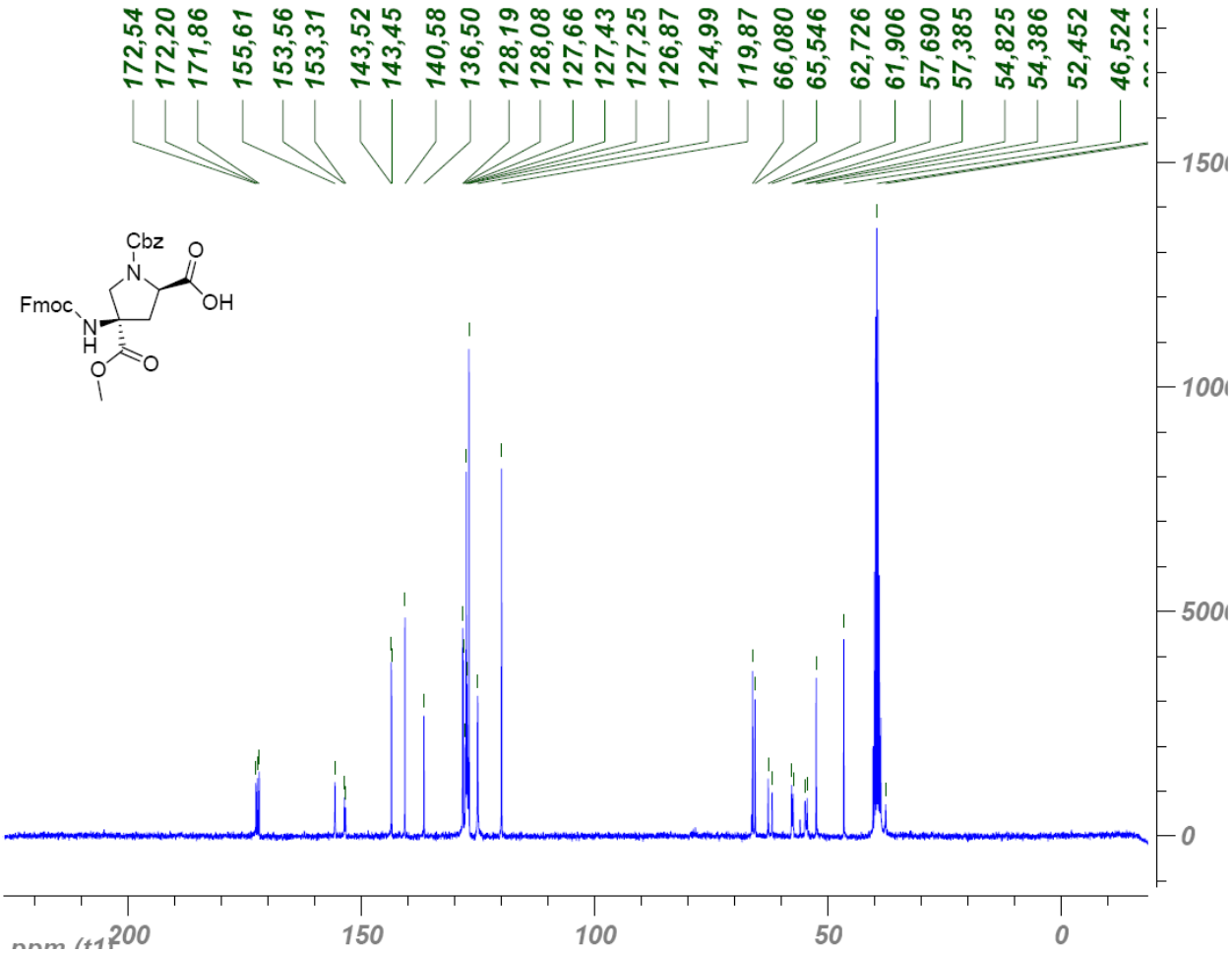

Supplemental Figure 23: ^{1}H decoupled ^{13}C spectrum of **29**, 75.4 MHz, DMSO-d_6

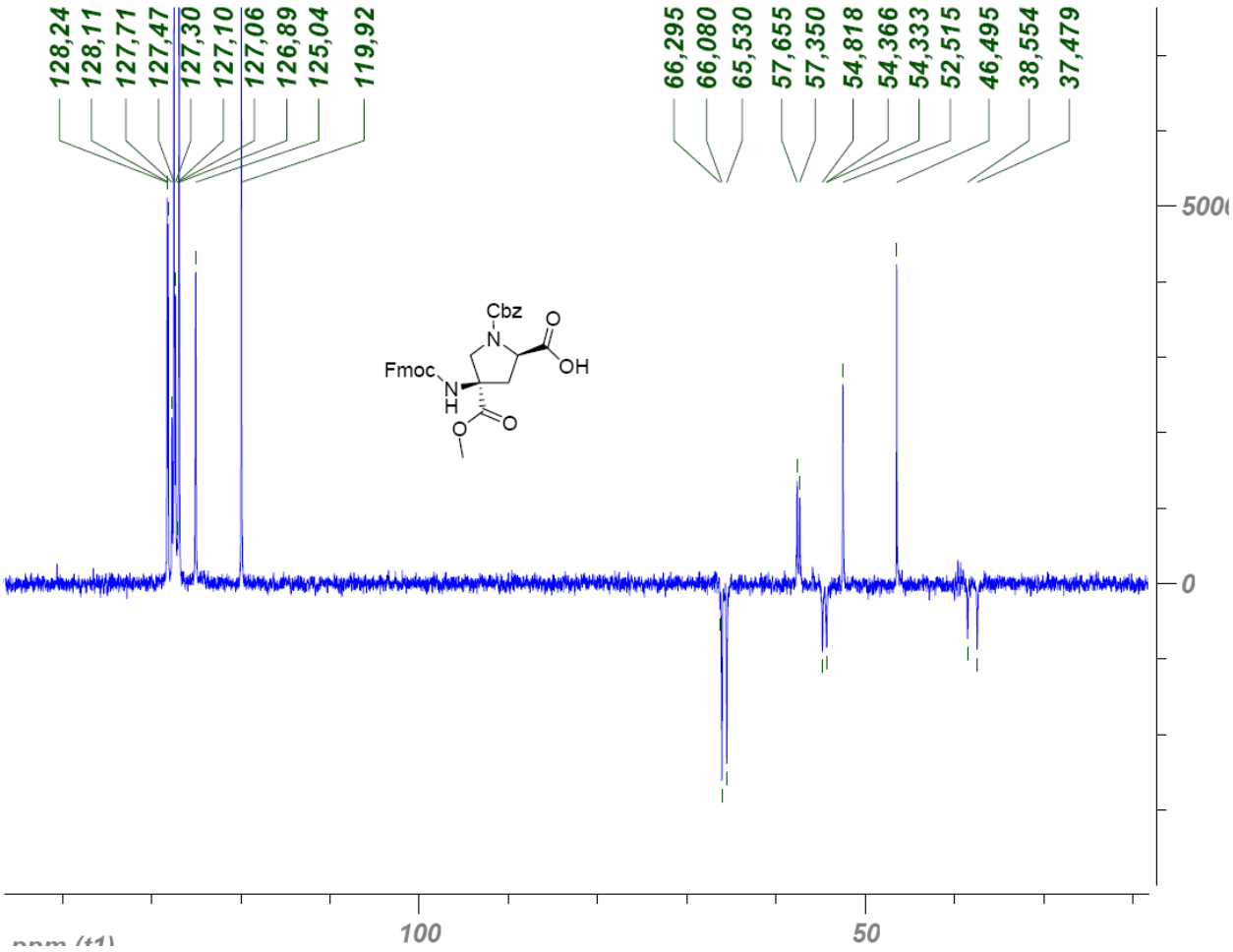

Supplemental Figure 24: dept 135 spectrum of **29**, 75.4 MHz, DMSO-d_6

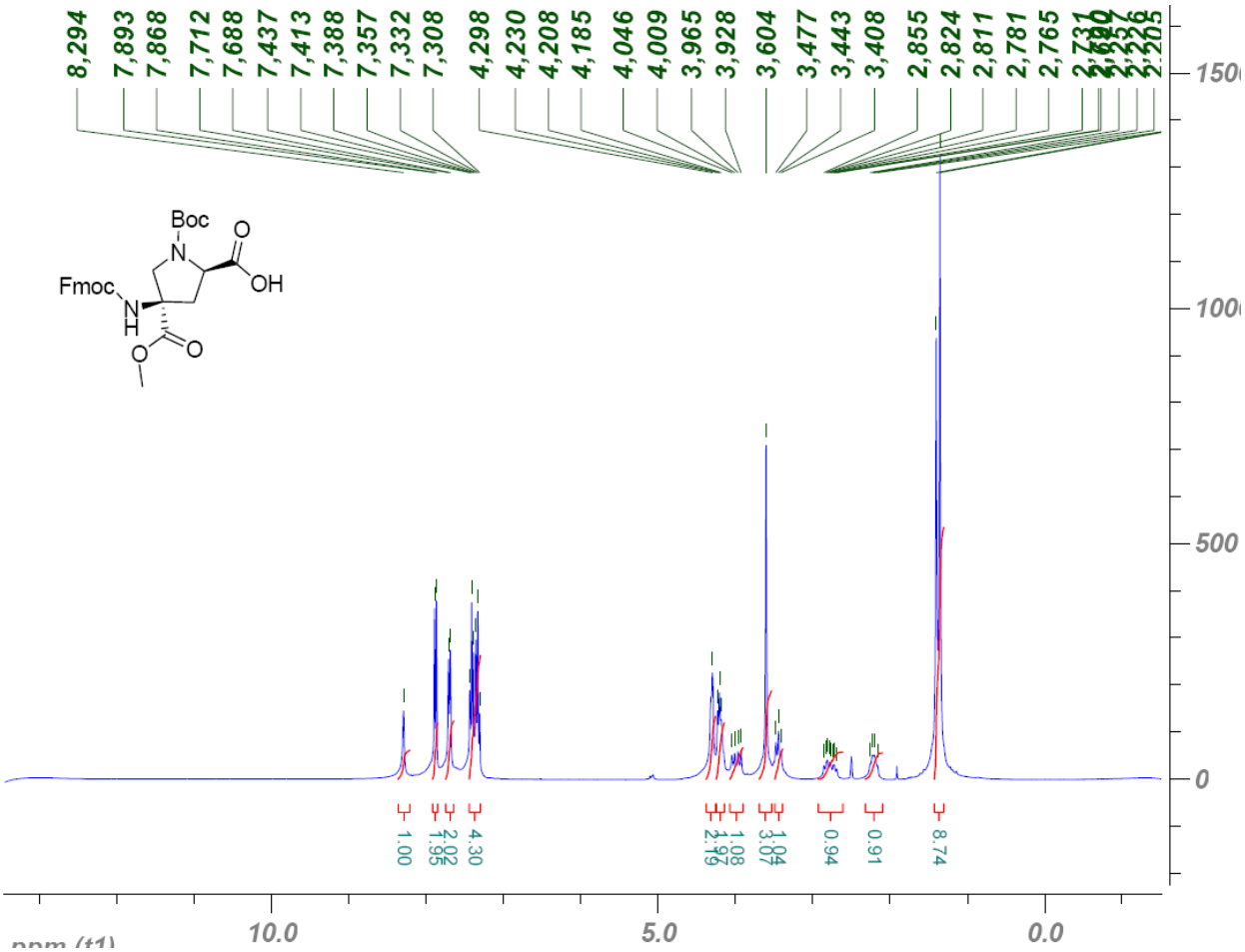

Supplemental Figure 25: ^{1}H NMR spectrum of **30**, 300 MHz, DMSO-d_6

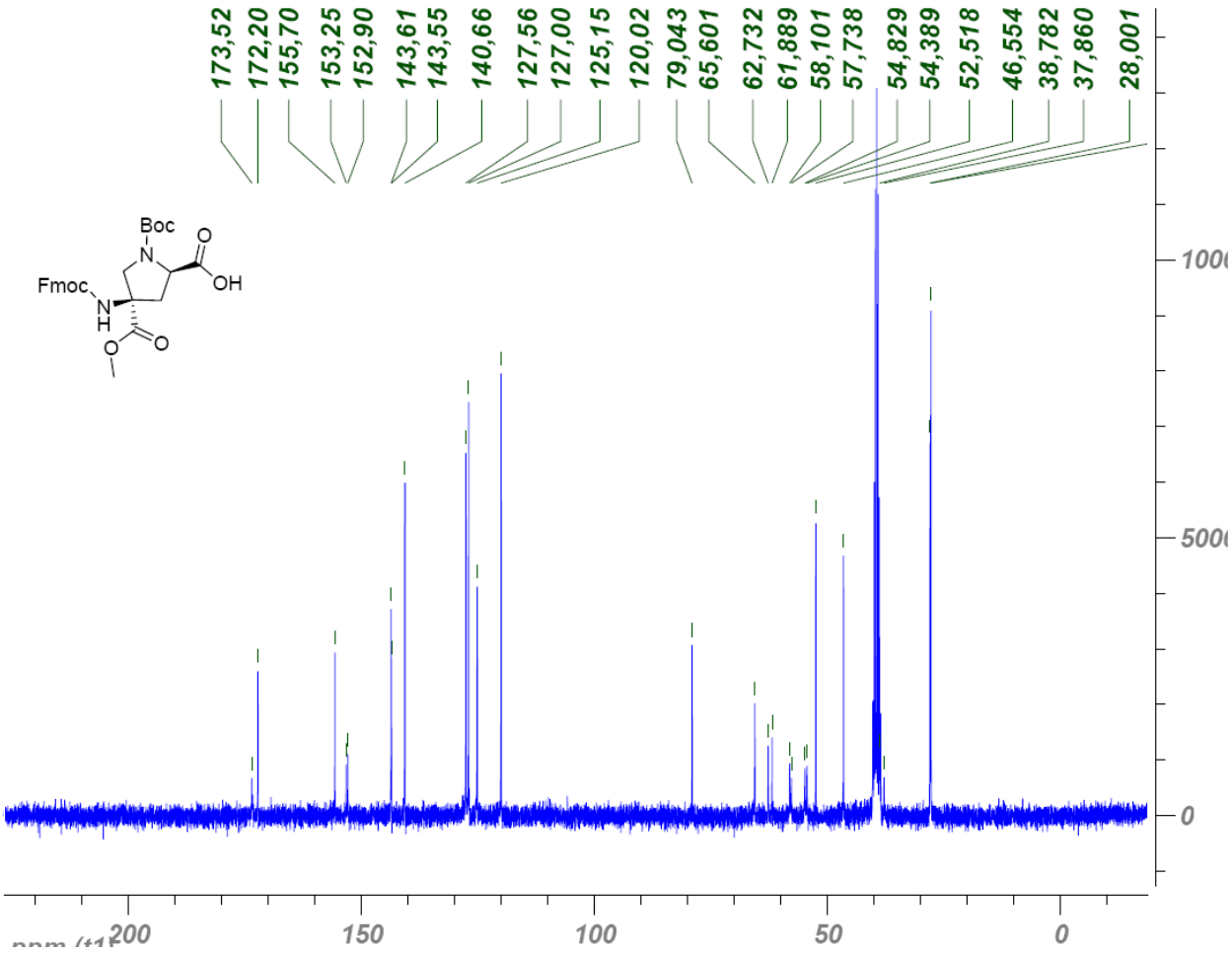

Supplemental Figure 26: ^{1}H decoupled ^{13}C spectrum of **30**, 75.4 MHz, DMSO-d_6

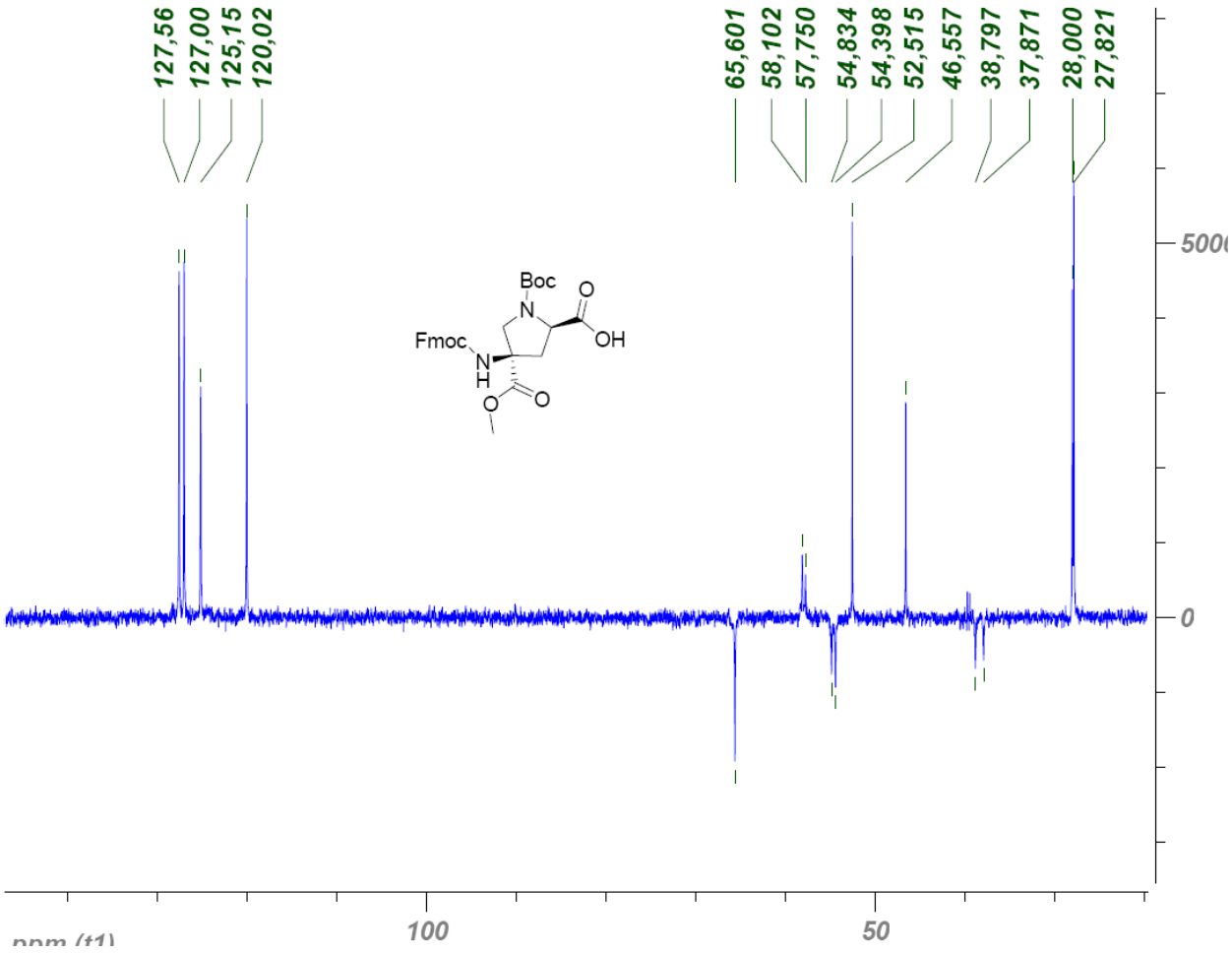

Supplemental Figure 27: dept 135 spectrum of **30**, 75.4 MHz, DMSO-d_6

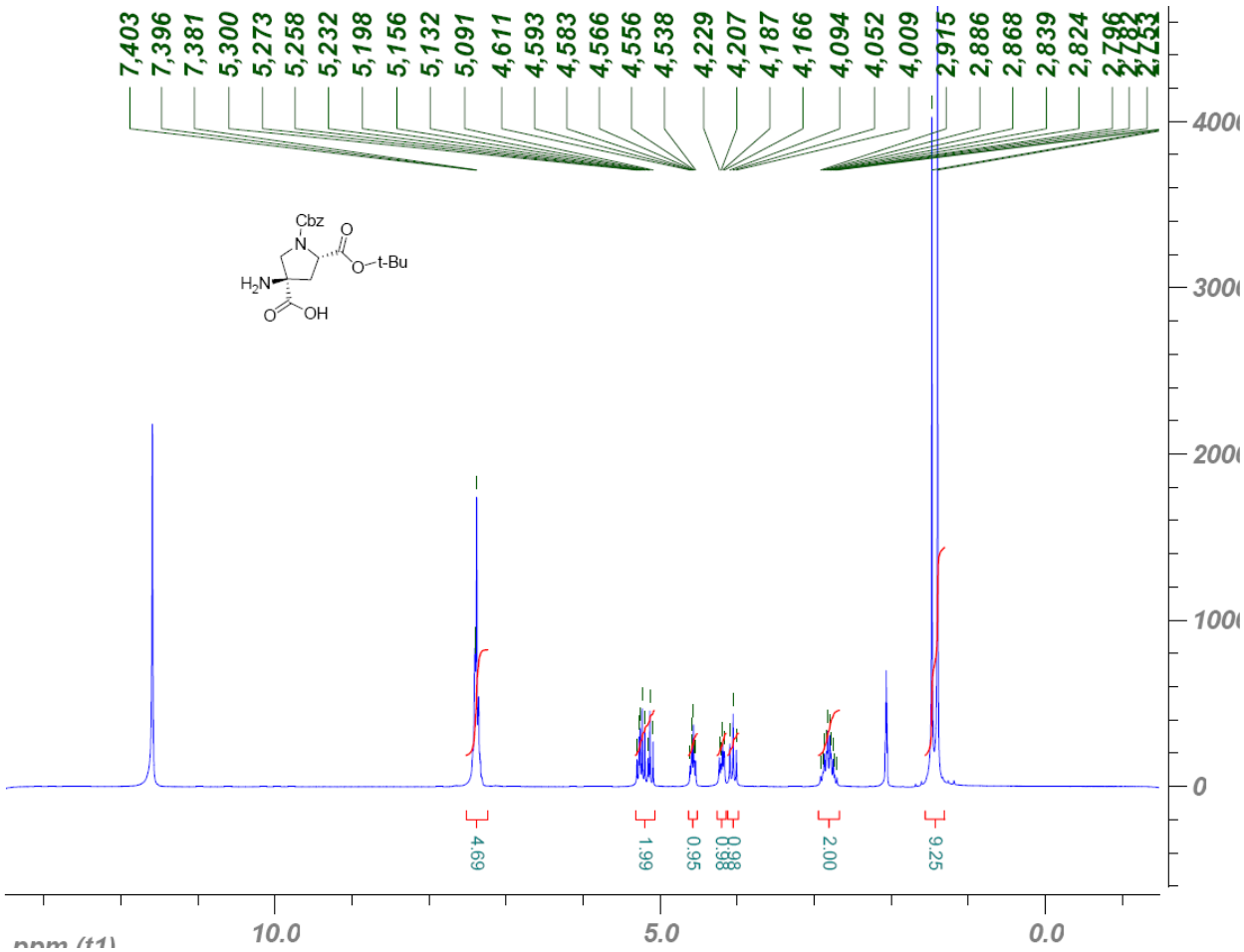

Supplemental Figure 28: ^{1}H NMR spectrum of **34**, 300 MHz, CD_3COOD

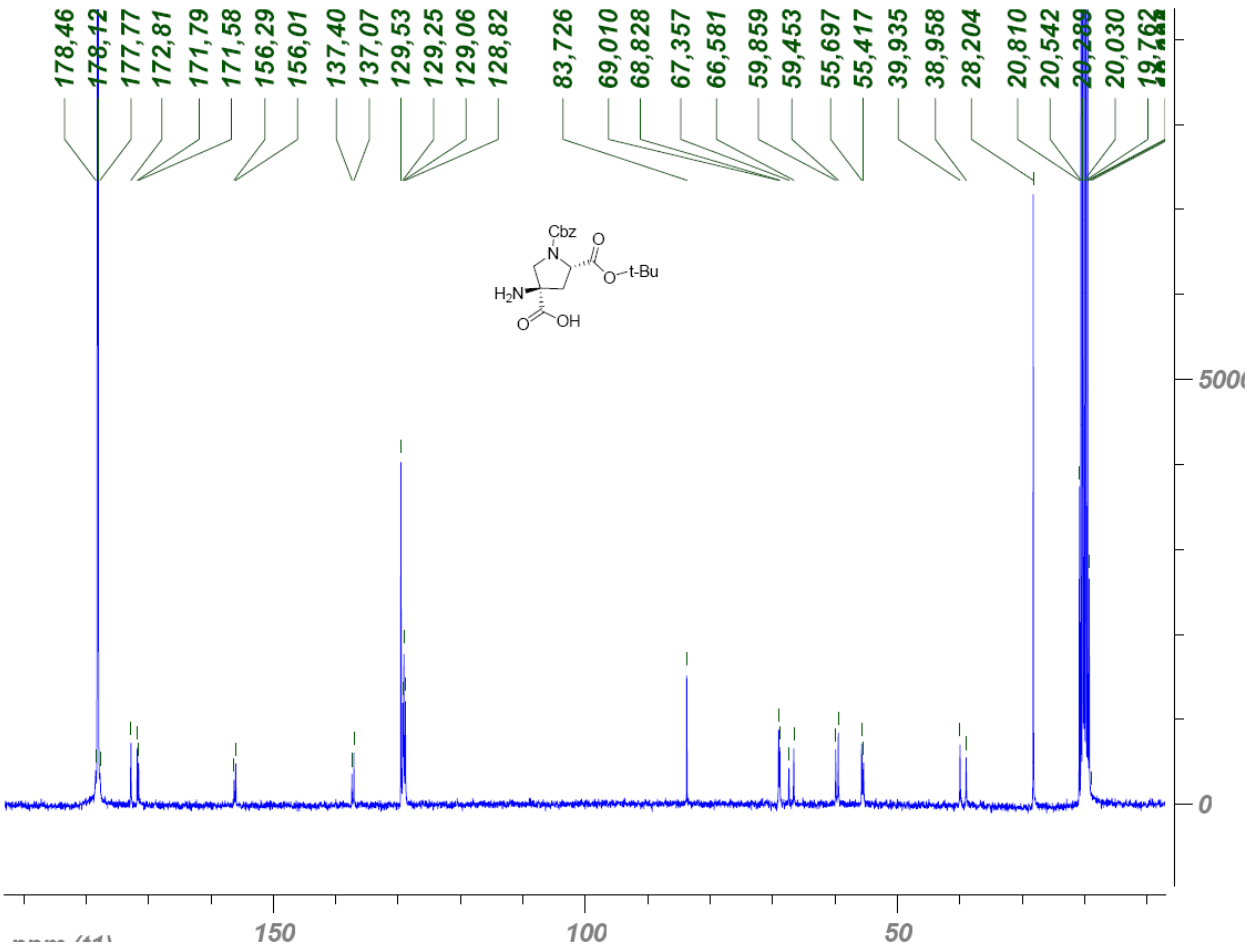

Supplemental Figure 29: ^{1}H decoupled ^{13}C spectrum of **34**, 75.4 MHz, CD_3COOD

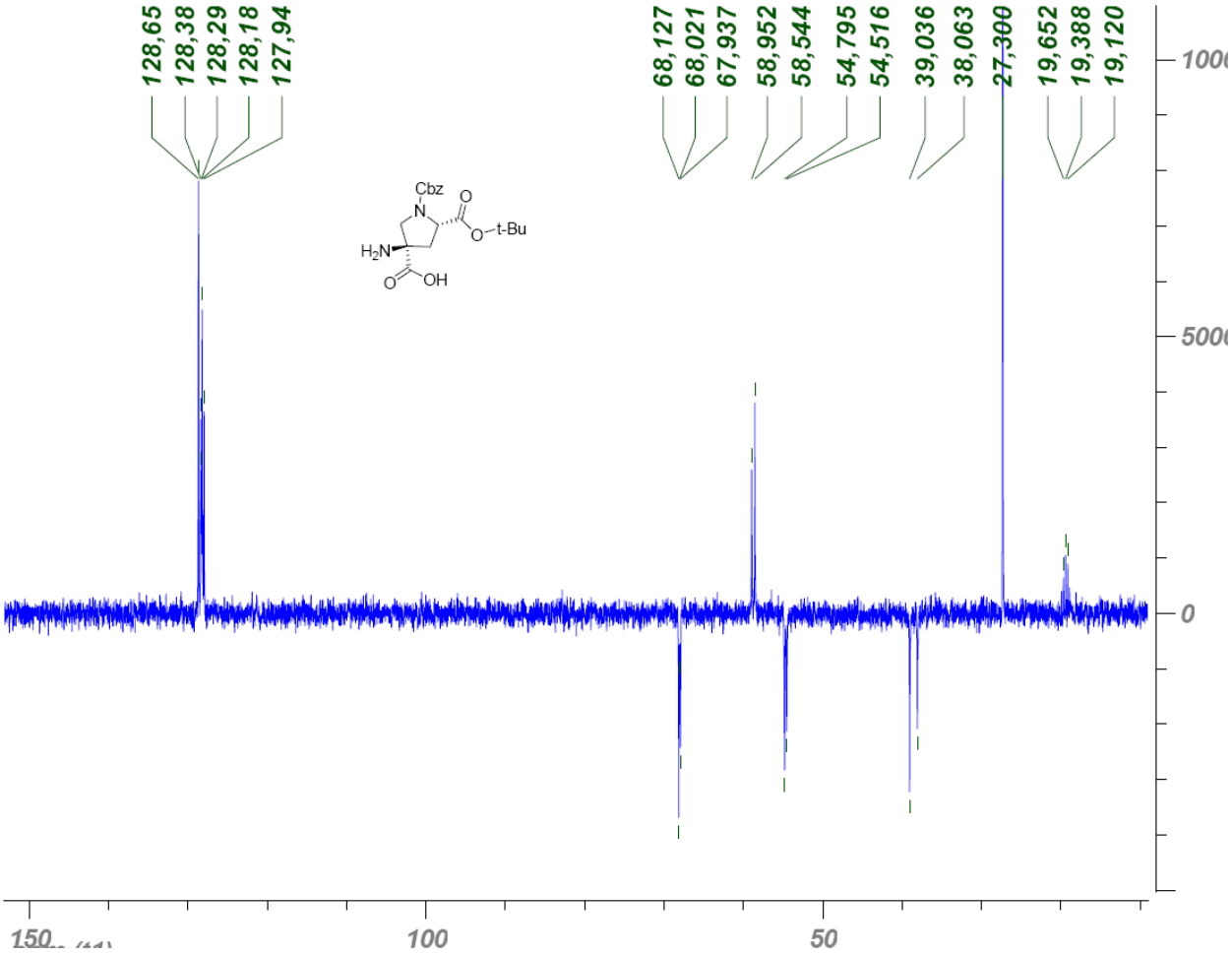

Supplemental Figure 30: dept135 spectrum of **34**, 75.4 MHz, CD_3COOD

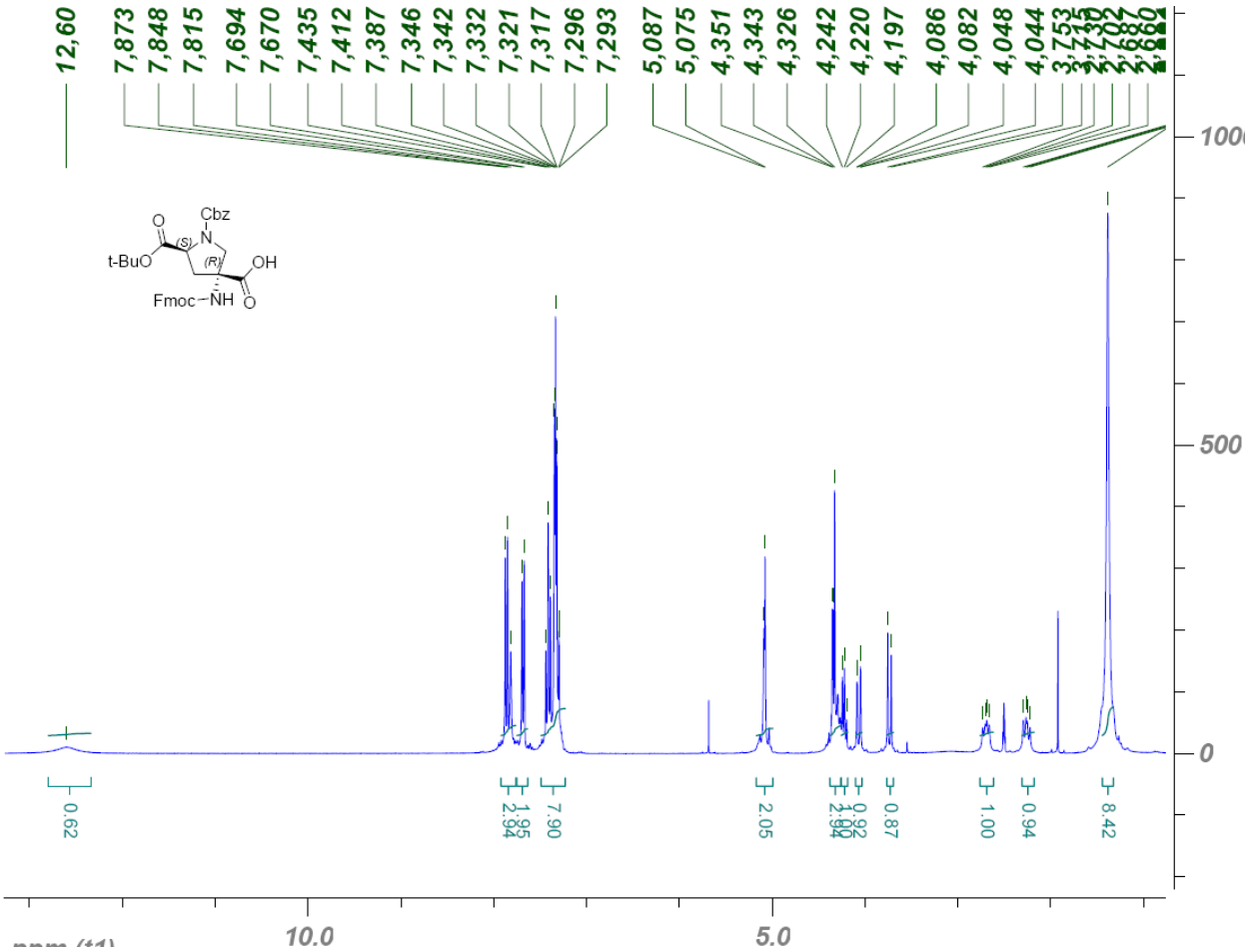

Supplemental Figure 31: ^{1}H NMR spectrum of **35**, 300 MHz, DMSO-d_6, 350 K

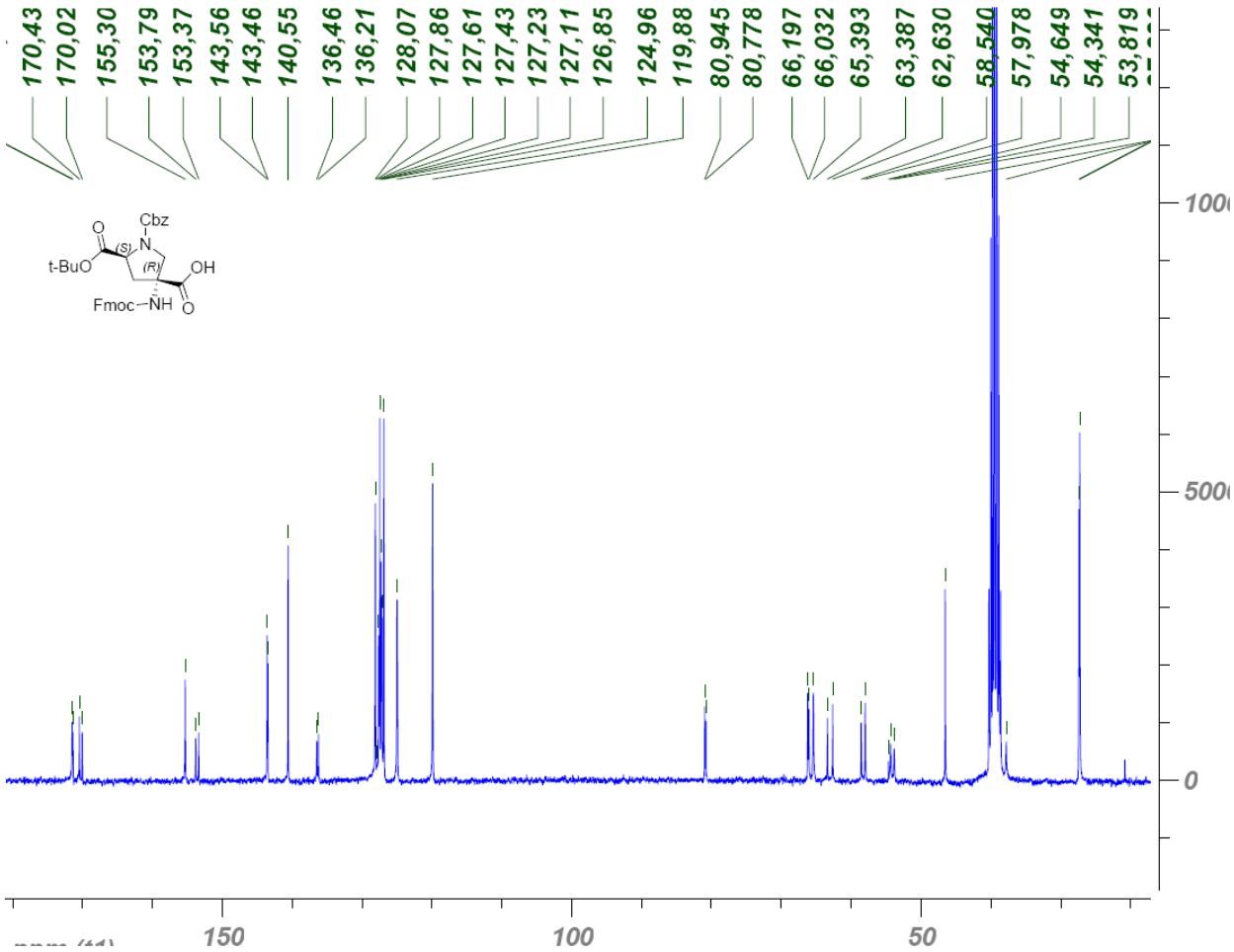

Supplemental Figure 32: ^{1}H decoupled ^{13}C spectrum of **35**, 75.4 MHz, DMSO-d_6

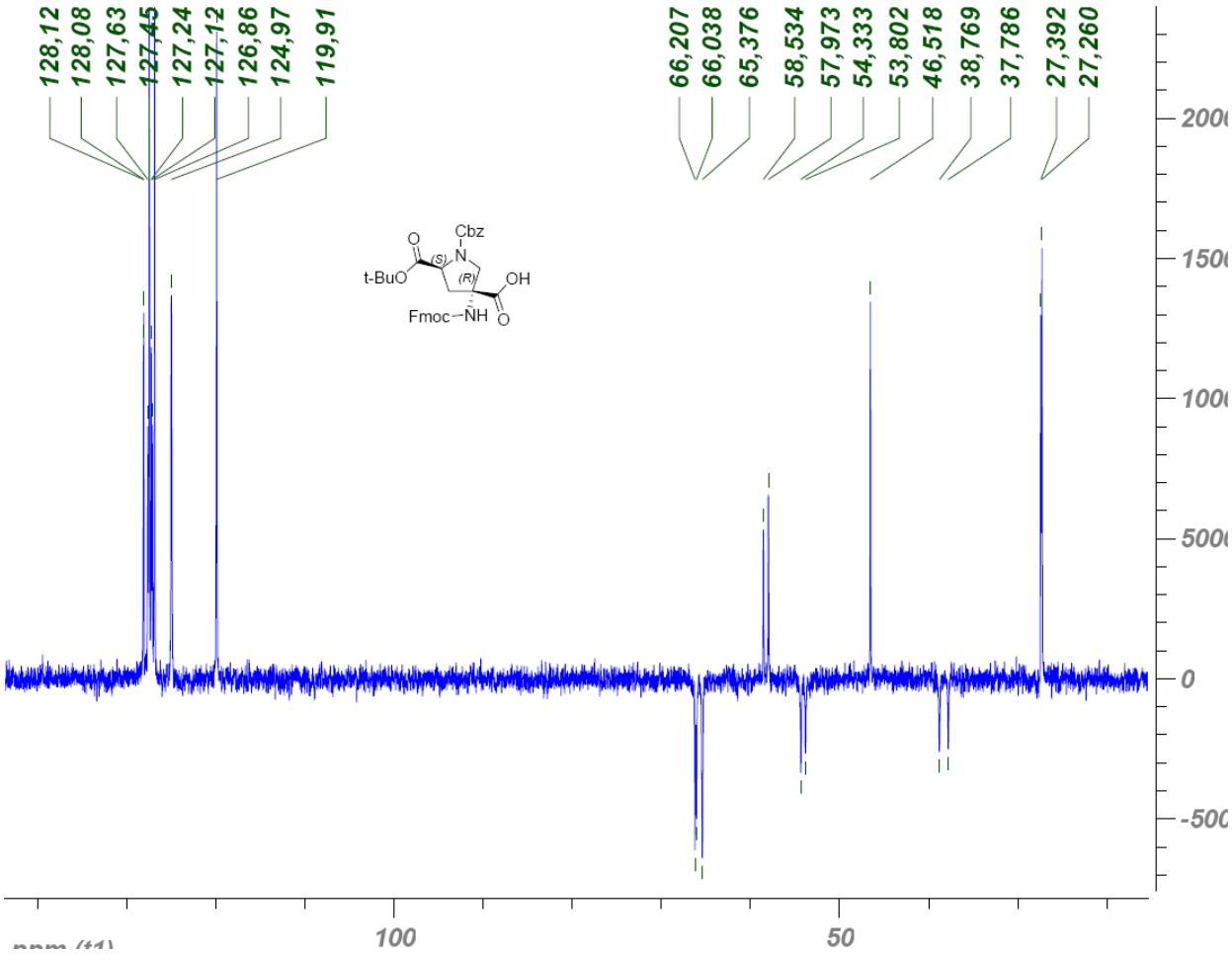

Supplemental Figure 33: dept135 spectrum of **35**, 75.4 MHz, DMSO-d_6

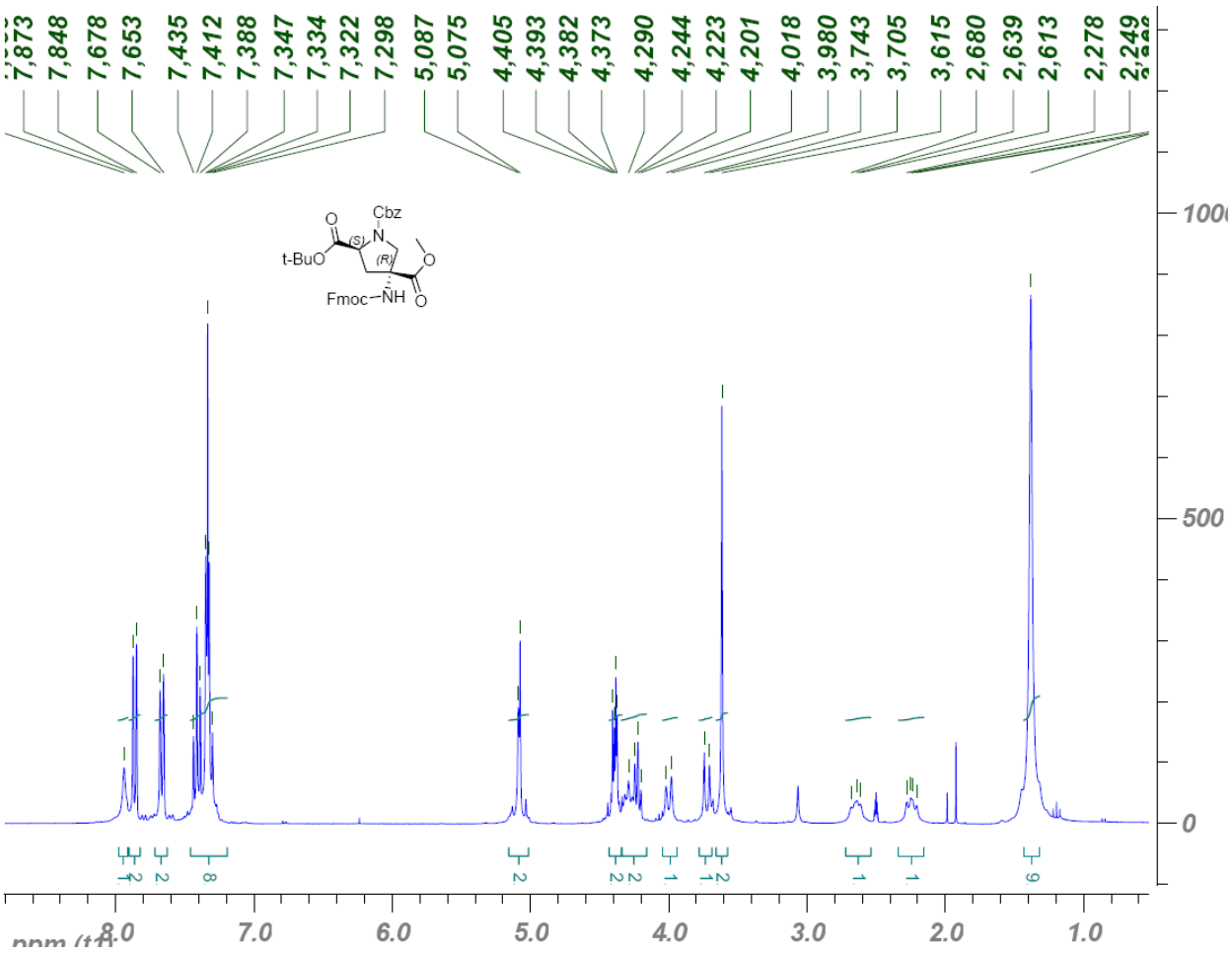

Supplemental Figure 34: ^{1}H NMR spectrum of **36**, 300 MHz, DMSO-d_6, 350 K

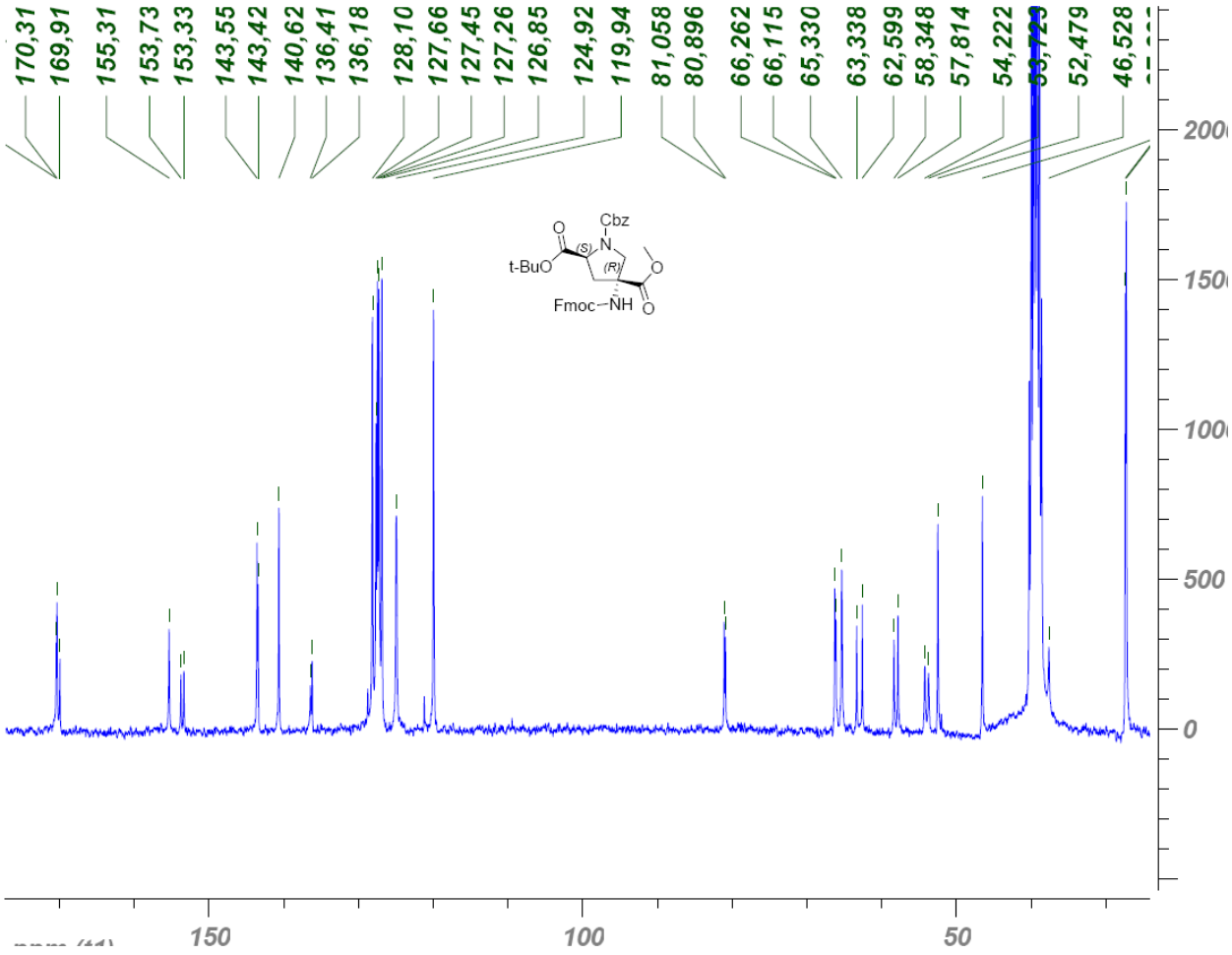

Supplemental Figure 35: ^{1}H decoupled ^{13}C spectrum of **36**, 75.4 MHz, DMSO-d_6

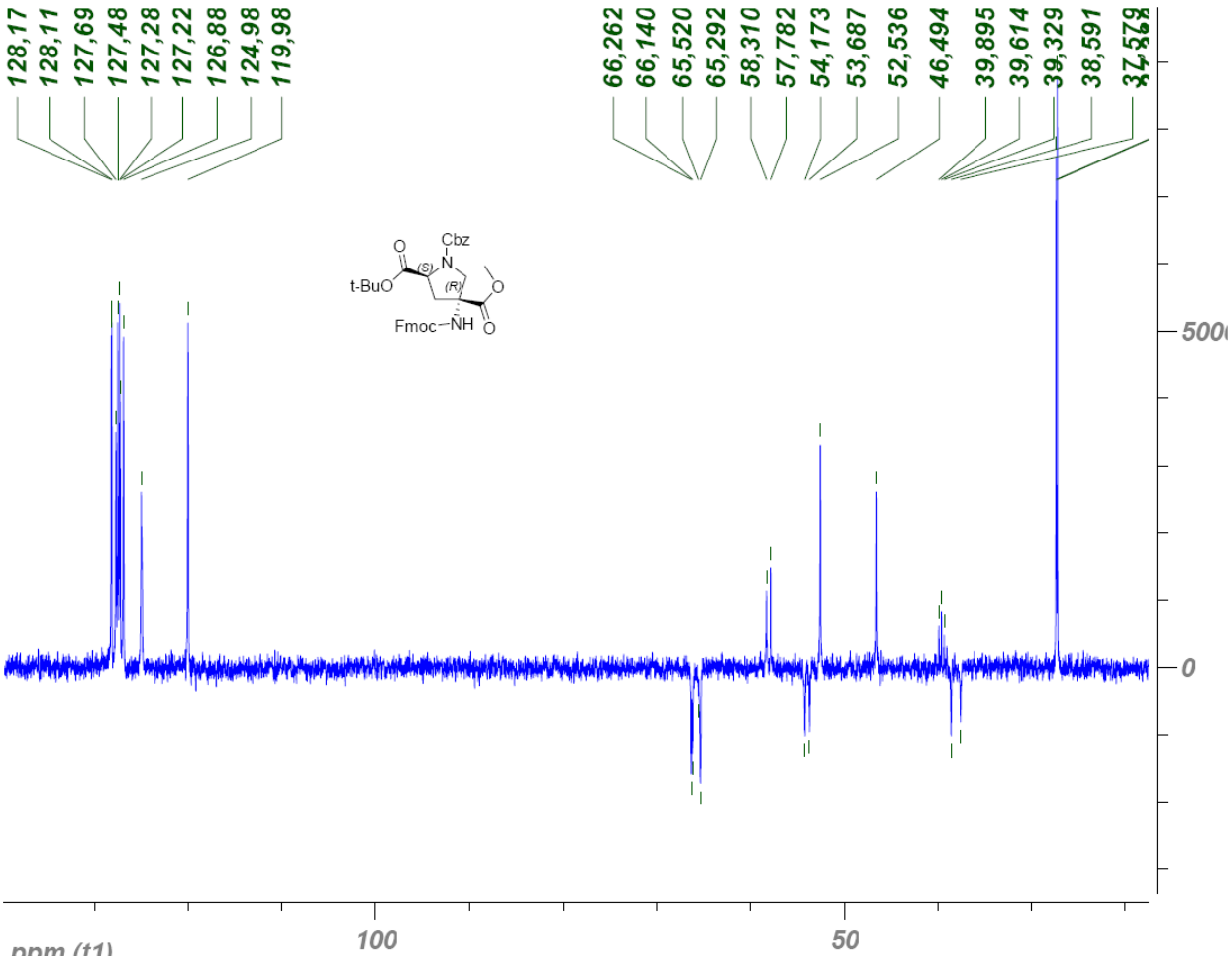

Supplemental Figure 36: dept135 spectrum of **36**, 75.4 MHz, DMSO-d_6

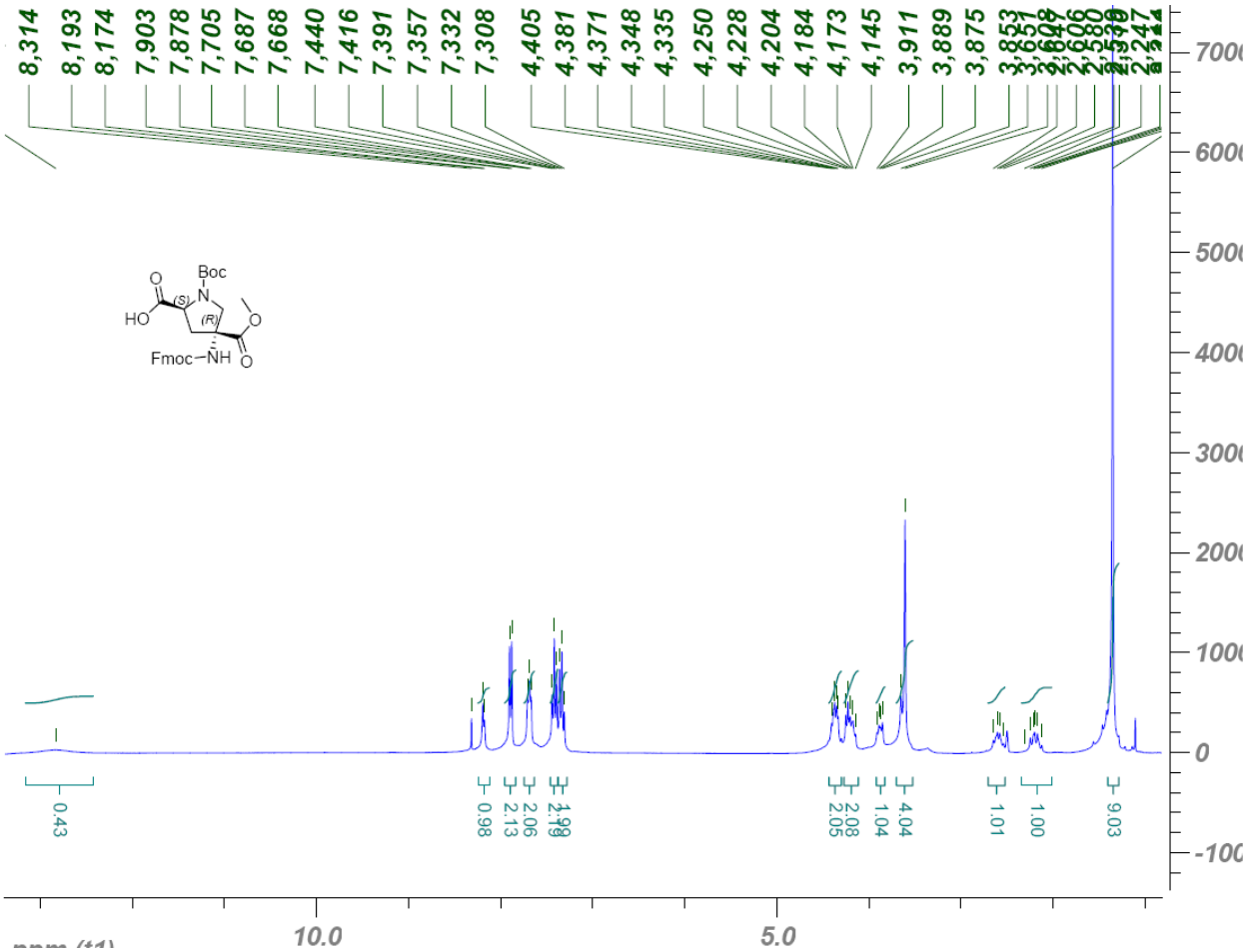

Supplemental Figure 37: ^{1}H NMR spectrum of **37**, 300 MHz, DMSO-d_6

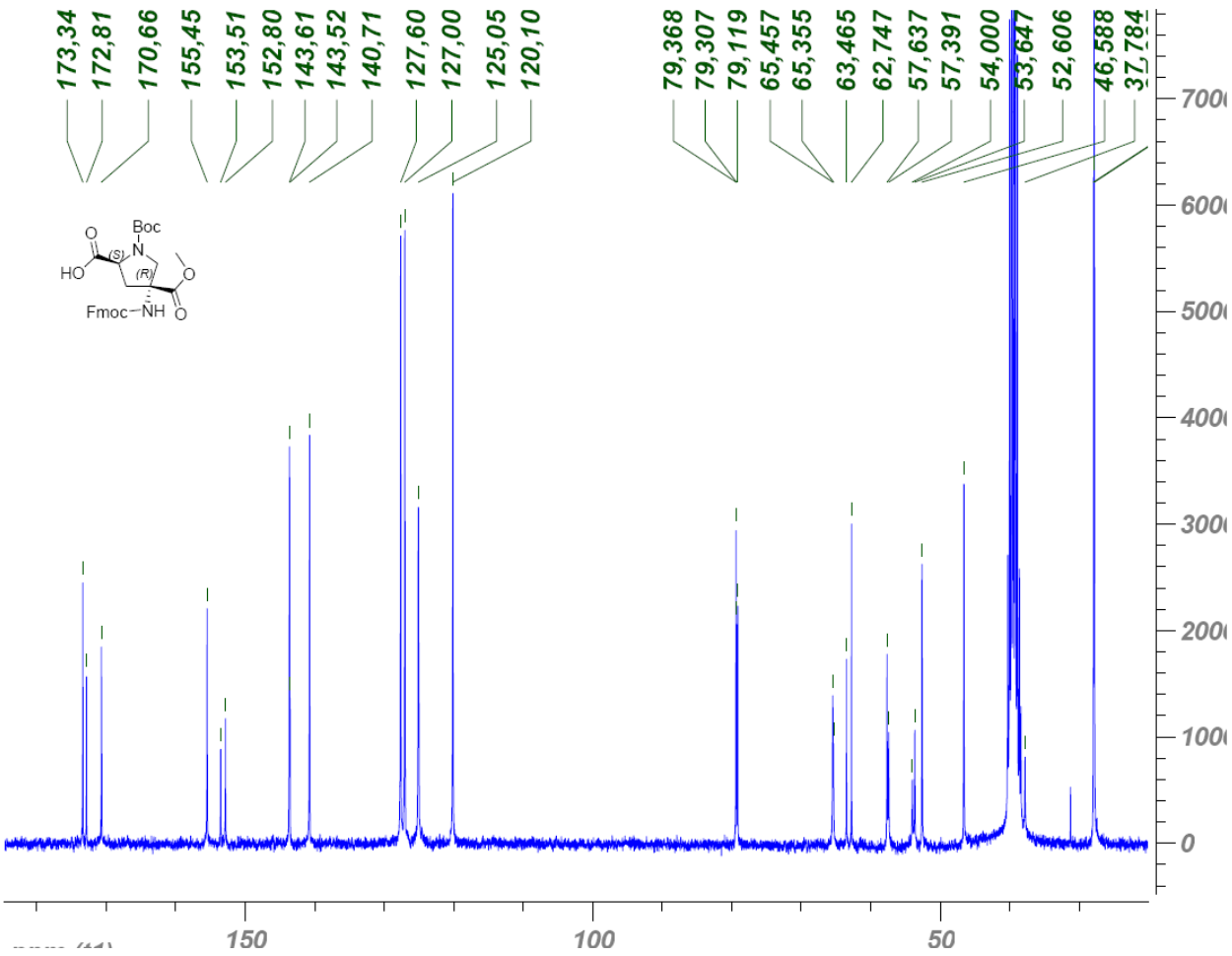

Supplemental Figure 38: ^{1}H decoupled ^{13}C spectrum of **37**, 75.4 MHz, DMSO-d_6

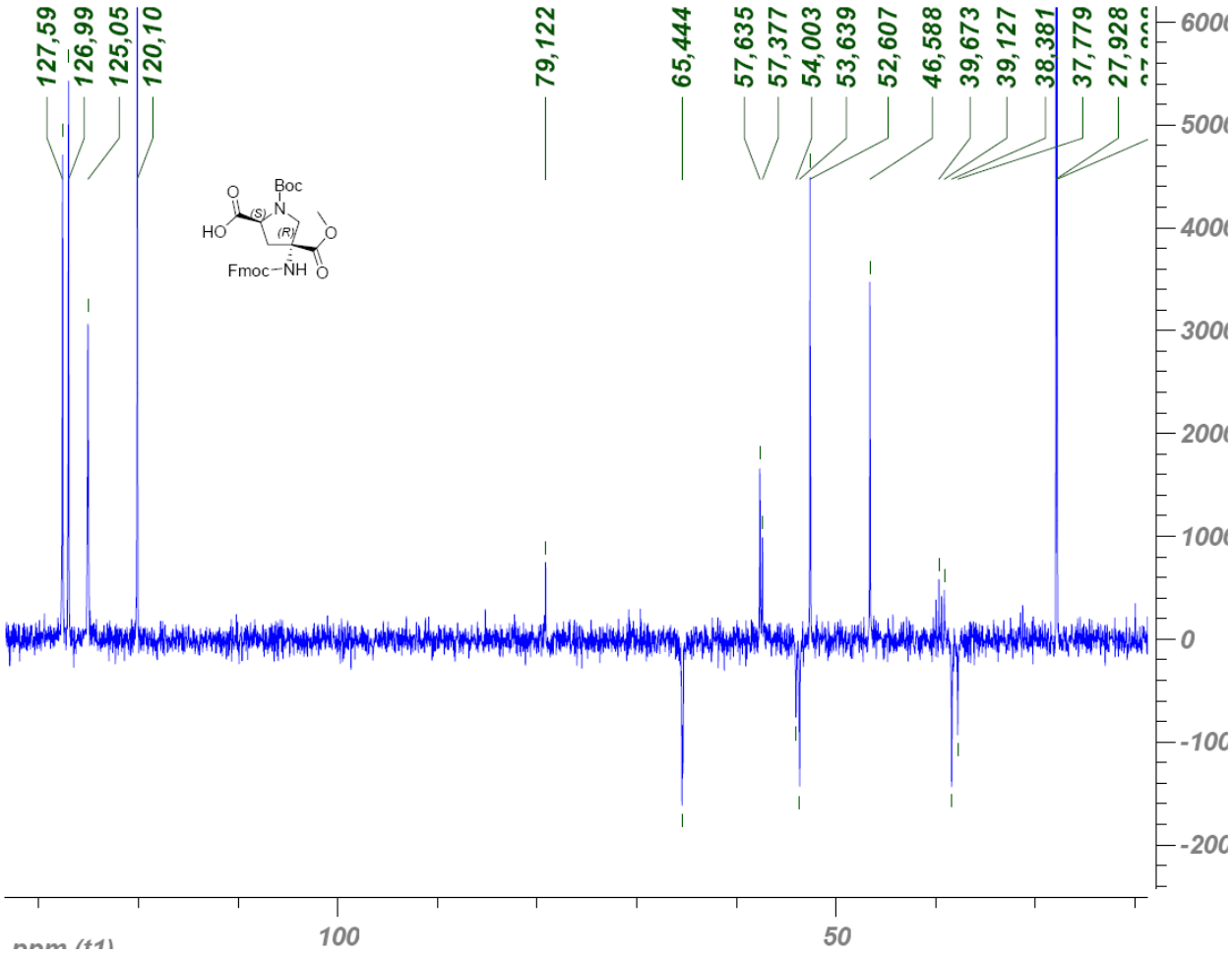

Supplemental Figure 39: dept135 spectrum of **37**, 75.4 MHz, DMSO-d_6

APPENDIX B

RESONANCE ASSIGNMENTS FOR TETRAMER OLIGOMERS

The NMR resonances derived from the 2D-NMR spectra of the tetramer oligomers are displayed in the following tables.

Group: the number corresponding to the place of the residue in the sequence
Heavy atom number: the numerical designation of the atoms in the structures shown in the text.
Atom: the first letter (C or H) designates the nucleus. The following letters are coded as follows;
A = alpha
B = beta
C = gamma
D = delta
AC = carbonyl carbon adjacent to alpha carbon
GC = carbonyl carbon adjacent to gamma carbon
N = amide nitrogen
Shift: chemical shift (on the δ scale)
#: number of cross-peaks in the COSY/ROESY/HMBC/HMQC spectra used to determine the resonance
StDev: the standard deviation of the mean chemical shift for each resonance

Supplemental Table 1: Nuclear resonance assignments of **57** based upon the 2D-NMR spectra

Group	Heavy Atom	Atom	Nuc	Shift	SDev	#
1		HB1	1H	2.86	0.004	7
1		HB2	1H	2.92	0.004	6
1	2	HA	1H	4.22	0.007	3
1	3	HN	1H	8.52	0.009	9
2	6	HB2	1H	1.48	0.018	10
2	6	HB1	1H	2.10	0.005	7
2	8	HD2	1H	3.00	0.006	6
2	8	HD1	1H	3.53	0.002	6
2	5	HA	1H	3.92	0.003	7
2	10	HN	1H	8.34	0.011	7
3	13	HB2	1H	1.88	0.006	8
3	13	HB1	1H	2.50	0.005	5
3	15	HD2	1H	3.37	0.003	6
3	15	HD1	1H	3.56	0.008	5
3	12	HA	1H	4.18	0.004	8
3	18	HN	1H	8.44	0.011	7
4	21	HB2	1H	2.03	0.008	8
4	21	HB1	1H	2.45	0.011	6
4	23	HD2	1H	3.34	0.005	5
4	23	HD1	1H	3.71	0.008	6
4	20	HA	1H	4.23	0.004	7
4	26	HN	1H	8.65	0.011	7
5	29	HB2	1H	2.13	0.006	5
5	29	HB1	1H	2.62	0.007	4
5	31	HD2	1H	3.69	0.003	2
5	28	HA	1H	4.54	0.013	6

Group	Heavy Atom	Atom	Nuc	Shift	SDev	#
1	2	CA	13C	55.4	0.010	3
1	1	CAC	13C	175.5	0.021	4
2	6	CB	13C	40.1	0.041	4
2	5	CA	13C	59.1	0.064	4
2	7	CG	13C	64.4	0.050	4
2	17	CGC	13C	166.0	0.049	5
2	4	CAC	13C	167.8	0.046	4
3	13	CB	13C	37.1	0.000	1
3	12	CA	13C	58.5	0.024	6
3	14	CG	13C	62.0	0.019	4
3	25	CGC	13C	167.4	0.025	4
3	11	CAC	13C	170.1	0.030	3
4	20	CA	13C	57.5	0.051	5
4	22	CG	13C	62.5	0.021	5
4	33	CGC	13C	166.9	0.015	4
4	19	CAC	13C	170.2	0.028	4
5	29	CB	13C	37.0	0.023	2
5	28	CA	13C	52.9	0.131	2
5	30	CG	13C	60.4	0.008	3
5	27	CAC	13C	169.6	0.071	2

Supplemental Table 2: Crosspeaks on the ROESY spectrum of **57**

Resonance 1	Shift	Resonance 2	Shift	Integrated Volume
01HB1	2.85	HN	8.52	3.39E+06
01HB2	2.91	HN	8.52	1.89E+06
02HA	3.92	01HN	8.52	1.24E+07
02HB1	2.11	01HN	8.52	1.57E+06
02HB1	2.11	03HA	4.18	6.72E+06
02HB2	1.48	01HN	8.52	1.37E+06
02HB2	1.48	HD2	2.99	2.17E+07
02HB2	1.48	HN	8.33	2.94E+06
02HD1	3.53	HA	3.91	4.18E+06
02HD2	3.00	HN	8.33	1.10E+07
03HA	4.18	02HN	8.33	8.61E+05
03HB2	1.88	HD2	3.36	6.10E+06
03HB2	1.88	HN	8.43	1.53E+07
03HD1	3.55	HA	4.17	4.42E+06
03HD1	3.56	04HA	4.23	1.25E+07
03HD2	3.37	HN	8.43	4.13E+06
03HD2	3.37	04HA	4.23	4.49E+06
04HA	4.23	03HN	8.43	1.30E+06
04HB1	2.48	05HA	4.56	1.01E+08
04HB2	2.02	HD2	3.35	8.88E+06
04HB2	2.03	HN	8.64	3.88E+06
04HD1	3.70	HA	4.23	6.47E+06
04HD2	3.34	HN	8.64	1.56E+07
05HA	4.54	04HN	8.64	4.51E+05
05HB2	2.14	HD2	3.69	4.01E+06

Supplemental Table 3: Nuclear resonance assignments of **58** based upon the 2D-NMR spectra

Group	Heavy Atom	Atom	Nuc	Shift	SDev	#	Group	Heavy Atom	Atom	Nuc	Shift	SDev	#
1		HB1	1H	2.779	0.013	8	1		CB	13C	36.8	0.019	3
1		HB2	1H	2.837	0.012	5	1	2	CA	13C	55.0	0.043	5
1	2	HA	1H	4.24	0.01	10	1	1	CAC	13C	175.0	0.049	4
1	3	HN	1H	8.601	0.002	9	2	6	CB	13C	38.0	0.051	5
2	6	HB2	1H	1.69	0.004	9	2	8	CD	13C	52.9	0.023	4
2	6	HB1	1H	2.648	0.005	7	2	5	CA	13C	59.1	0.008	4
2	8	HD2	1H	3.071	0.005	9	2	7	CG	13C	63.8	0.016	6
2	8	HD1	1H	3.356	0.003	8	2	17	CGC	13C	165.0	0.014	5
2	5	HA	1H	4.187	0.007	8	2	4	CAC	13C	167.9	0.029	5
2	10	HN	1H	8.28	0.001	8	3	13	CB	13C	36.9	0.026	2
3	13	HB2	1H	1.864	0.012	10	3	15	CD	13C	55.0	0.000	1
3	13	HB1	1H	2.491	0.004	5	3	12	CA	13C	57.9	0.050	2
3	15	HD2	1H	3.402	0.012	7	3	14	CG	13C	61.6	0.081	3
3	15	HD1	1H	3.487	0.006	3	3	25	CGC	13C	166.7	0.019	3
3	12	HA	1H	4.401	0.003	7	3	11	CAC	13C	169.7	0.019	3
3	18	HN	1H	8.428	0.001	8	4	21	CB	13C	37.3	0.029	2
4	21	HB2	1H	1.91	0.009	9	4	23	CD	13C	55.1	0.000	1
4	21	HB1	1H	2.533	0.004	5	4	20	CA	13C	57.7	0.099	3
4	23	HD2	1H	3.456	0.008	4	4	22	CG	13C	61.7	0.094	4
4	23	HD1	1H	3.52	0.006	3	4	33	CGC	13C	166.6	0.067	3
4	20	HA	1H	4.479	0.007	6	4	19	CAC	13C	169.9	0.019	3
4	26	HN	1H	8.542	0	9	5	29	CB	13C	36.4	0.000	1
5	29	HB2	1H	2.083	0.012	8	5	31	CD	13C	52.1	0.000	1
5	29	HB1	1H	2.575	0.001	6	5	28	CA	13C	56.9	0.012	4
5	36	HME	1H	3.447	0	1	5	30	CG	13C	59.8	0.006	3
5	31	HD1	1H	3.646	0.003	4	5	27	CAC	13C	168.7	0.036	3
5	28	HA	1H	4.453	0.006	7	5	34	CGC	13C	169.6	0.015	4
5	37	HN	1H	8.575	0	1							

Supplemental Table 4: Crosspeaks on the ROESY spectrum of **58**

Resonance 1	Shift	Resonance 2	Shift	Integrated Volume
01H1	7.31	HN	8.60	2.15E+06
01H3	7.00	HN	8.60	1.76E+06
01HA	4.24	H1	7.31	1.22E+07
01HA	4.24	H3	6.99	3.55E+07
01HA	4.24	H4	7.40	2.39E+07
01HB1	2.80	H1	7.31	3.42E+07
01HB1	2.80	H3	6.98	4.31E+07
01HB1	2.79	HN	8.60	1.51E+07
02HB1	2.64	01HN	8.60	3.24E+06
02HB2	1.68	HD2	3.07	4.78E+07
02HB2	1.69	HN	8.28	2.18E+07
02HD1	3.35	HA	4.18	8.53E+06
02HD1	3.35	03HA	4.40	2.22E+07
02HD2	3.07	HN	8.28	5.99E+06
02HD2	3.07	03HA	4.40	1.14E+07
03HA	4.41	02HN	8.28	2.03E+06
03HB2	1.85	HD2	3.39	1.10E+07
03HB2	1.87	HN	8.43	2.24E+07
03HD1	3.49	HA	4.40	
03HD1	3.49	04HA	4.49	
03HD2	3.40	HB2	1.88	6.41E+07
03HD2	3.40	HN	8.43	5.45E+06
03HD2	3.40	04HA	4.47	
04HA	4.47	03HN	8.43	3.83E+06
04HB2	1.90	HN	8.54	2.18E+07
04HD1	3.52	HN	8.54	1.51E+06
04HD1	3.52	05HA	4.46	
04HD2	3.47	HB2	1.91	2.11E+08
04HD2	3.45	HN	8.54	5.85E+06
04HD2	3.46	05HA	4.46	
05HA	4.46	04HN	8.54	1.86E+06
05HB2	2.06	HN	8.58	2.58E+06
05HD1	3.64	HA	4.45	2.28E+07

Supplemental Table 5: Nuclear resonance assignments of **61** based upon the 2D-NMR spectra

Group	Atom	Heavy Atom #	Nuc	Shift	SDev	#	Group	Atom	Heavy Atom #	Nuc	Shift	SDev	#
2	CA	3	13C	58.73	0.033	4	1	H2NA	1	1H	8.04	0.003	4
2	CAC	2	13C	169.68	0.037	5	1	H2NB	1	1H	7.59	0.002	3
2	CB	4	13C	39.49	0.056	2	2	HA	3	1H	4.64	0.009	8
2	CD	6	13C	50.68	0.002	3	2	HB1	4	1H	3.11	0.012	8
2	CG	5	13C	64.26	0.006	4	2	HB2	4	1H	2.51	0.017	5
2	CGC	15	13C	165.64	0.058	4	2	HD1	6	1H	4.10	0.015	8
3	CA	10	13C	57.04	0.041	4	2	HD2	6	1H	3.57	0.012	6
3	CAC	9	13C	169.61	0.01	3	2	HN	8	1H	8.92	0.004	7
3	CB	11	13C	38.71	0.049	3	3	HA	10	1H	4.85	0.015	7
3	CD	13	13C	53.40	0.008	2	3	HB1	11	1H	2.74	0.008	9
3	CG	12	13C	61.83	0.017	4	3	HB2	11	1H	2.58	0.011	4
3	CGC	23	13C	165.32	0.014	4	3	HD1	13	1H	3.64	0.011	7
4	CA	18	13C	56.61	0.026	4	3	HD2	13	1H	4.48	0.011	6
4	CAC	17	13C	170.09	0.012	3	3	HN	16	1H	9.18	0.006	8
4	CB	19	13C	35.65	0.038	3	4	HA	18	1H	4.87	0.011	6
4	CD	21	13C	54.19	0	1	4	HB1	19	1H	2.49	0.012	6
4	CG	20	13C	61.08	0.036	5	4	HB2	19	1H	3.06	0.008	8
4	CGC	31	13C	166.04	0.047	4	4	HD1	21	1H	3.52	0.006	8
5	CA	26	13C	57.60	0.02	6	4	HD2	21	1H	4.34	0.006	7
5	CAC	25	13C	169.57	0.101	3	4	HN	24	1H	8.82	0.005	7
5	CB	27	13C	39.73	0.007	2	5	HA	26	1H	4.51	0.016	9
5	CD	29	13C	55.37	0.017	2	5	HB1	27	1H	1.03	0.019	9
5	CG	28	13C	59.84	0.026	5	5	HB2	27	1H	1.50	0.013	9
5	CGC	28	13C			0	5	HD1	29	1H	3.83	0.012	8
6	C1	38	13C	125.79	0	1	5	HD2	29	1H	3.60	0.015	5
6	C2	39	13C	131.55	0.01	2	5	HN	32	1H	8.86	0.004	3
6	C3	40	13C	115.56	0.005	2	6	H2	39	1H	7.10	0.014	7
6	C4	41	13C	155.12	0.01	2	6	H2'	39	1H	7.12	0.001	3
6	CA	34	13C	55.81	0.005	3	6	H3	40	1H	6.92	0.015	6
6	CAC	33	13C	168.54	0.021	2	6	H3'	40	1H	6.94	0	1
6	CB	37	13C	37.85	0.038	2	6	HA	34	1H	4.47	0.002	4
							6	HB1	37	1H	3.25	0.016	4
							6	HB2	37	1H	2.97	0.012	6
							6	HN	35	1H	8.87	0.004	4

Supplemental Table 6: Nuclear resonance assignments of **62** based upon the 2D-NMR spectra

Group	Atom	Heavy Atom #	Nuc	Shift	SDev	#	Group	Atom	Heavy Atom #	Nuc	Shift	SDev	#
2	CA	3	13C	59.34	0.026	6	1	H2NA	1	1H	8.18	0.015	2
2	CAC	2	13C	170.25	0.01	5	1	H2NB	1	1H	7.89	0.297	4
2	CB	4	13C	37.78	0.009	5	2	HA	3	1H	4.78	0.005	8
2	CD	6	13C	52.89	0.01	2	2	HB1	4	1H	3.06	0.378	10
2	CG	5	13C	64.06	0.013	6	2	HB2	4	1H	2.40	0.279	10
2	CGC	15	13C	165.38	0.014	5	2	HD1	6	1H	3.91	0.087	9
3	CA	10	13C	57.11	0.036	6	2	HD2	6	1H	3.70	0.089	8
3	CAC	9	13C	169.70	0.008	2	2	HN	8	1H	8.87	0.02	7
3	CB	11	13C	38.55	0	1	3	HA	10	1H	4.80	0.01	9
3	CD	13	13C	53.41	0.01	3	3	HB1	11	1H	2.74	0.004	9
3	CG	12	13C	62.26	0.021	4	3	HB2	11	1H	2.59	0.003	7
3	CGC	23	13C	165.55	0.023	4	3	HD1	13	1H	3.64	0.01	8
4	CA	18	13C	57.19	0.013	3	3	HD2	13	1H	4.50	0.006	8
4	CAC	17	13C	169.75	0.055	4	3	HN	16	1H	9.18	0.02	10
4	CB	19	13C	38.70	0.03	2	4	HA	18	1H	4.82	0.007	7
4	CD	21	13C	53.81	0.002	3	4	HB1	19	1H	2.67	0.006	11
4	CG	20	13C	62.37	0.007	4	4	HB2	19	1H	2.49	0.005	9
4	CGC	31	13C	165.11	0.018	4	4	HD1	21	1H	3.59	0.005	5
5	CA	26	13C	57.70	0.027	6	4	HD2	21	1H	4.41	0.003	7
5	CAC	25	13C	169.62	0.154	7	4	HN	24	1H	9.10	0.021	10
5	CB	27	13C	39.56	0.004	3	5	HA	26	1H	4.55	0.005	10
5	CD	29	13C	55.50	0.008	2	5	HB1	27	1H	1.05	0.007	9
5	CG	28	13C	59.85	0.028	5	5	HB2	27	1H	1.51	0.003	11
5	CGC	28	13C			0	5	HD1	29	1H	3.89	0.007	9
6	C1	38	13C	125.81	0.012	3	5	HD2	29	1H	3.62	0.004	10
6	C2	39	13C	131.58	0.016	3	5	HN	32	1H	8.83	0.018	6
6	C3	40	13C	115.56	0	1	6	H2	39	1H	7.09	0.006	10
6	C4	41	13C	155.12	0.014	2	6	H2'	39	1H	7.09	0.002	2
6	CA	34	13C	55.86	0.039	3	6	H3	40	1H	6.91	0.006	5
6	CAC	33	13C	168.60	0.016	3	6	H3'	40	1H	6.90	0	1
6	CB	37	13C	37.85	0.013	2	6	HA	34	1H	4.47	0.006	6
							6	HB1	37	1H	3.16	0.133	7
							6	HB2	37	1H	2.99	0.087	9
							6	HN	35	1H	8.86	0.025	7

Supplemental Table 7: Nuclear resonance assignments for **63** based upon the 2D-NMR spectra

Group	Atom	Heavy Atom #	Nuc	Shift	SDev	#	Group	Atom	Heavy Atom #	Nuc	Shift	SDev	#
2	CA	3	13C	59.37	0.047	5	1	H2NA	1	1H	7.57	0.001	2
2	CAC	2	13C	170.36	0.016	5	1	H2NB	1	1H	8.13	0.016	3
2	CB	4	13C	38.00	0.041	5	2	HA	3	1H	4.74	0.008	10
2	CD	6	13C	52.98	0.054	3	2	HB1	4	1H	3.16	0.002	10
2	CG	5	13C	63.84	0.019	5	2	HB2	4	1H	2.28	0.004	11
2	CGC	15	13C	165.33	0.025	5	2	HD1	6	1H	3.91	0.006	12
3	CA	10	13C	56.64	0.037	4	2	HD2	6	1H	3.64	0.008	13
3	CAC	9	13C	170.05	0.032	4	2	HN	8	1H	8.80	0.019	10
3	CB	11	13C	35.92	0.05	6	3	HA	10	1H	4.81	0.008	15
3	CD	13	13C	54.17	0.031	3	3	HB1	11	1H	2.51	0.003	11
3	CG	12	13C	61.21	0.028	5	3	HB2	11	1H	3.05	0.005	10
3	CGC	23	13C	166.36	0.034	5	3	HD1	13	1H	3.57	0.006	14
4	CA	18	13C	58.10	0.053	5	3	HD2	13	1H	4.39	0.006	8
4	CAC	17	13C	168.73	0	1	3	HN	16	1H	8.91	0.018	10
4	CB	19	13C	36.98	0.069	5	4	HA	18	1H	4.92	0.012	5
4	CD	21	13C	55.06	0.075	3	4	HB1	19	1H	2.95	0.004	10
4	CG	20	13C	61.31	0.02	5	4	HB2	19	1H	2.34	0.005	10
4	CGC	31	13C	166.79	0.035	5	4	HD1	21	1H	3.91	0.012	10
5	CA	26	13C	56.60	0.028	4	4	HD2	21	1H	3.81	0.007	12
5	CAC	25	13C	166.85	0.015	2	4	HN	24	1H	8.73	0.019	8
5	CB	27	13C	38.99	0.01	2	5	HA	26	1H	4.48	0.009	10
5	CD	29	13C	55.62	0.077	4	5	HB1	27	1H	1.23	0.007	14
5	CG	28	13C	59.21	0.03	6	5	HB2	27	1H	1.61	0.007	12
5	CGC	28	13C	169.60	0.084	6	5	HD1	29	1H	3.29	0.005	10
6	C1	38	13C	125.77	0.025	3	5	HD2	29	1H	4.29	0.004	9
6	C2	39	13C	131.65	0.018	3	5	HN	32	1H	8.84	0.018	9
6	C3	40	13C	115.66	0	1	6	H2	39	1H	7.07	0.004	11
6	C4	41	13C	155.11	0.013	2	6	H2'	39	1H	7.06	0.002	2
6	CA	34	13C	55.89	0.069	3	6	H3	40	1H	6.90	0.006	7
6	CAC	33	13C			0	6	H3'	40	1H			
6	CB	37	13C	37.96	0.019	3	6	HA	34	1H	4.47	0.004	7
							6	HB1	37	1H	3.23	0.005	9
							6	HB2	37	1H	2.95	0.007	10
							6	HN	35	1H	8.70	0.022	8

Supplemental Table 8: ROESY crosspeaks for **61**, **62**, and **63**

61				**62**				**63**			
Assignment	w1	w2	Volume	Assignment	w1	w2	Volume	Assignment	w1	w2	Volume
2HA-1H2NA	4.65	8.04	1.57E+06	2HA-1H2NA	4.78	8.16	5.11E+06	2HA-1H2NB	4.74	8.12	4.34E+06
2HA-1H2NB	4.65	7.60	4.31E+04	2HB1-HD1	3.25	3.94	1.39E+06	2HB1-1H2NB	3.16	8.12	7.37E+05
2HB1-1H2NA	3.13	8.03	5.08E+05	2HB2-HD2	2.30	3.67	3.41E+06	2HB2-HN	2.29	8.79	2.63E+06
2HB1-HD1	3.12	4.14	2.93E+05	2HB2-HN	2.30	8.84	6.00E+06	2HD1-HA	3.90	4.72	2.25E+06
2HB1-3HA	3.14	4.85	1.90E+06	2HD1-3HA	3.94	4.78	1.37E+07	2HD1-HB1	3.90	3.16	1.16E+06
2HB2-1H2NA	2.52	8.04	1.01E+05	2HD2-HN	3.67	8.84	2.23E+06	2HD1-3HA	3.92	4.81	6.94E+06
2HB2-HD2	2.52	3.59	1.60E+06	3HA-HN	4.80	9.15	3.16E+06	2HD2-HA	3.63	4.74	1.05E+06
2HB2-HN	2.52	8.91	7.20E+05	3HB1-HD1	2.75	3.64	1.23E+06	2HD2-HB2	3.66	2.28	2.45E+06
2HD1-HA	4.12	4.65	6.14E+05	3HB1-HN	2.74	9.16	9.56E+05	2HD2-HN	3.63	8.78	2.18E+06
2HD2-HN	3.59	8.92	1.81E+06	3HB2-HD2	2.59	4.49	5.33E+06	2HD2-3HA	3.64	4.81	1.52E+06
3HA-HN	4.87	9.17	9.96E+05	3HD1-HA	3.66	4.78	8.99E+06	3HA-HN	4.81	8.89	1.32E+06
3HB1-HD1	2.75	3.67	2.42E+05	3HD1-HN	3.64	9.15	7.80E+06	3HB1-HN	2.52	8.89	3.79E+06
3HB1-HN	2.75	9.17	3.32E+05	4HA-HN	4.82	9.07	2.50E+06	3HD1-HA	3.57	4.80	2.92E+06
3HB2-HD2	2.59	4.50	1.32E+06	4HB1-HD1	2.67	3.59	1.03E+06	3HD1-HB1	3.56	2.51	2.49E+06
3HD1-HA	3.64	4.87	8.36E+05	4HB1-HN	2.67	9.07	5.14E+05	3HD1-HN	3.56	8.90	2.53E+06
3HD1-HN	3.65	9.17	2.66E+06	4HB1-5HA	2.66	4.55	1.32E+07	3HD2-HB2	4.40	3.04	1.60E+06
4HA-HN	4.88	8.81	4.26E+05	4HB2-HD2	2.49	4.40	4.85E+06	4HA-3HD1	4.91	3.57	2.53E+05
4HB1-HD1	2.51	3.52	8.49E+05	4HB2-5HA	2.50	4.55	1.28E+06	4HA-3HD2	4.90	4.38	2.17E+06
4HB1-HN	2.51	8.81	2.70E+06	4HD1-HA	3.58	4.82	4.24E+06	4HB2-HN	2.33	8.71	3.43E+06
4HB2-HD2	3.08	4.35	4.72E+05	4HD1-HN	3.59	9.08	7.80E+06	4HD1-HB1	3.91	2.95	8.70E+05
4HD1-HA	3.52	4.89	7.28E+05	5HB1-HD1	1.05	3.89	8.23E+05	4HD1-5HA	3.90	4.46	9.24E+06
4HD1-HN	3.52	8.81	1.01E+06	5HB1-6H2'	1.06	7.09	2.84E+06	4HD2-HB2	3.82	2.34	1.65E+06
4HD1-5HA	3.52	4.53	6.43E+05	5HB1-6H3'	1.06	6.90	3.43E+06	4HD2-HN	3.81	8.72	2.21E+06
4HD2-5HA	4.35	4.53	2.60E+06	5HB2-HD2	1.51	3.62	3.32E+06	4HD2-5HA	3.81	4.49	5.58E+06
5HA-6H2'	4.50	7.12	5.79E+05	5HB2-HN	1.50	8.81	2.05E+06	5HA-HN	4.47	8.83	8.83E+05
5HB1-HD1	1.05	3.86	1.45E+05	5HB2-6H2	1.51	7.09	1.47E+06	5HB1-HD1	1.24	3.29	1.83E+06
5HB1-6H2'	1.06	7.12	4.57E+05	5HB2-6H3	1.51	6.90	2.18E+06	5HB1-HN	1.23	8.84	5.76E+05
5HB1-6H3'	1.06	6.94	3.20E+05	5HD1-HA	3.88	4.55	4.64E+06	5HB1-6H2'	1.24	7.06	1.62E+06
5HB2-HD2	1.52	3.62	5.67E+05	5HD2-HN	3.62	8.81	4.53E+06	5HB1-6H3	1.25	6.89	2.62E+06
5HB2-HN	1.51	8.86	9.93E+05	6H2-HN	7.09	8.82	2.75E+06	5HB2-HD2	1.60	4.29	2.45E+06
5HB2-6H2	1.51	7.13	2.35E+05	6HB1-H2'	3.25	7.09	1.36E+07	5HB2-6H2	1.61	7.06	2.41E+06
5HB2-6H3	1.51	6.95	1.94E+05	6HB2-H2	2.96	7.09	1.24E+07	5HB2-6H3	1.62	6.89	3.20E+06
5HD1-HA	3.84	4.53	1.52E+06	6HB2-HN	2.96	8.82	5.53E+06	5HD1-HN	3.30	8.83	1.84E+06
5HD2-HN	3.62	8.85	2.42E+06					6H2-HN	7.06	8.68	2.22E+06
6HB1-H2'	3.28	7.12	4.00E+06					6HA-HN	4.46	8.68	7.99E+06
6HB2-5HN	2.98	8.86	1.83E+06					6HB1-H2'	3.24	7.05	1.30E+07
6HB2-H2	2.99	7.12	2.75E+06					6HB2-H2	2.95	7.05	6.11E+06
								6HB2-HN	2.94	8.69	9.75E+05

APPENDIX C

2D-NMR SPECTRA

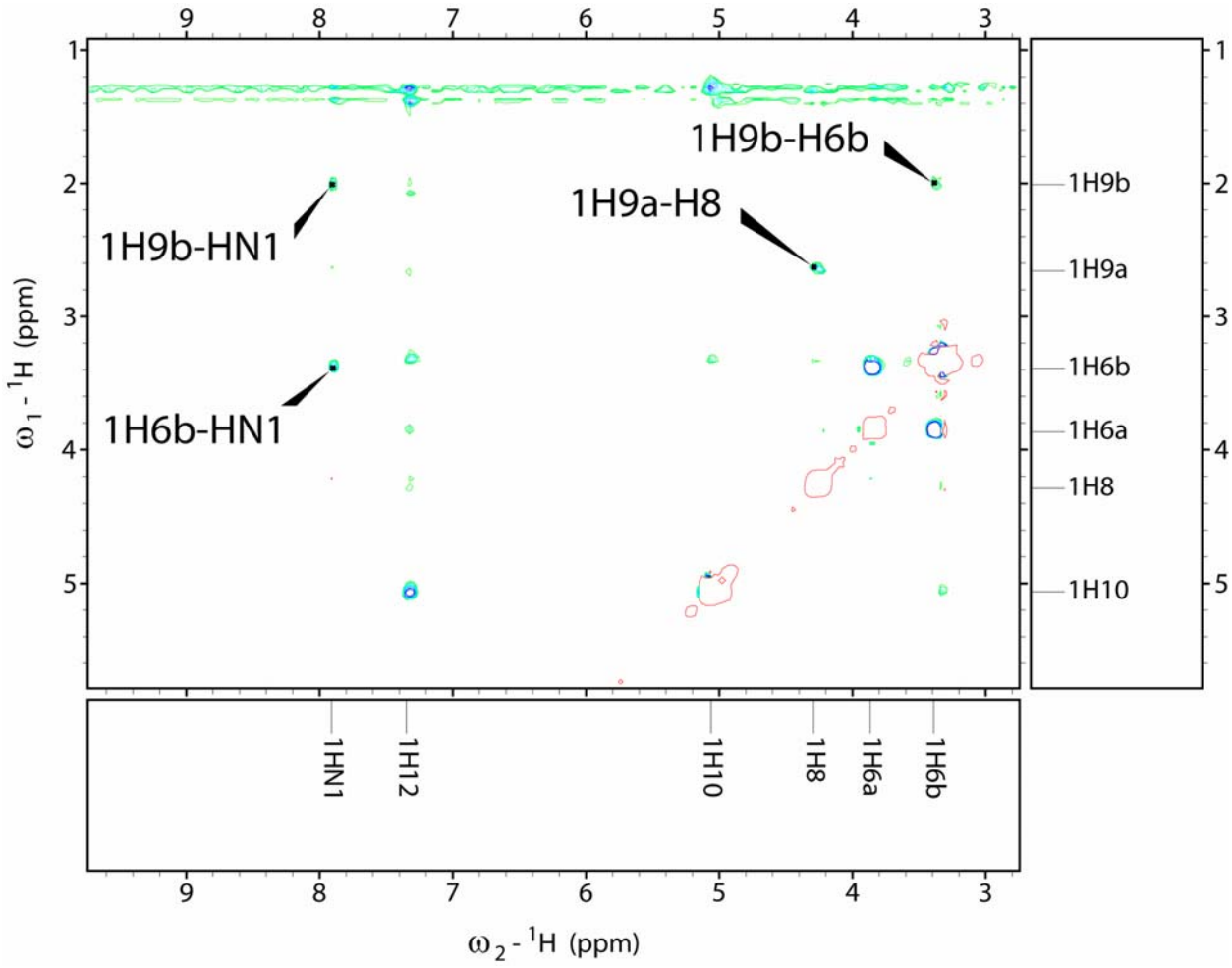

Supplemental Figure 40. 500 MHz NOESY spectrum of **12**, DMSO-d_6

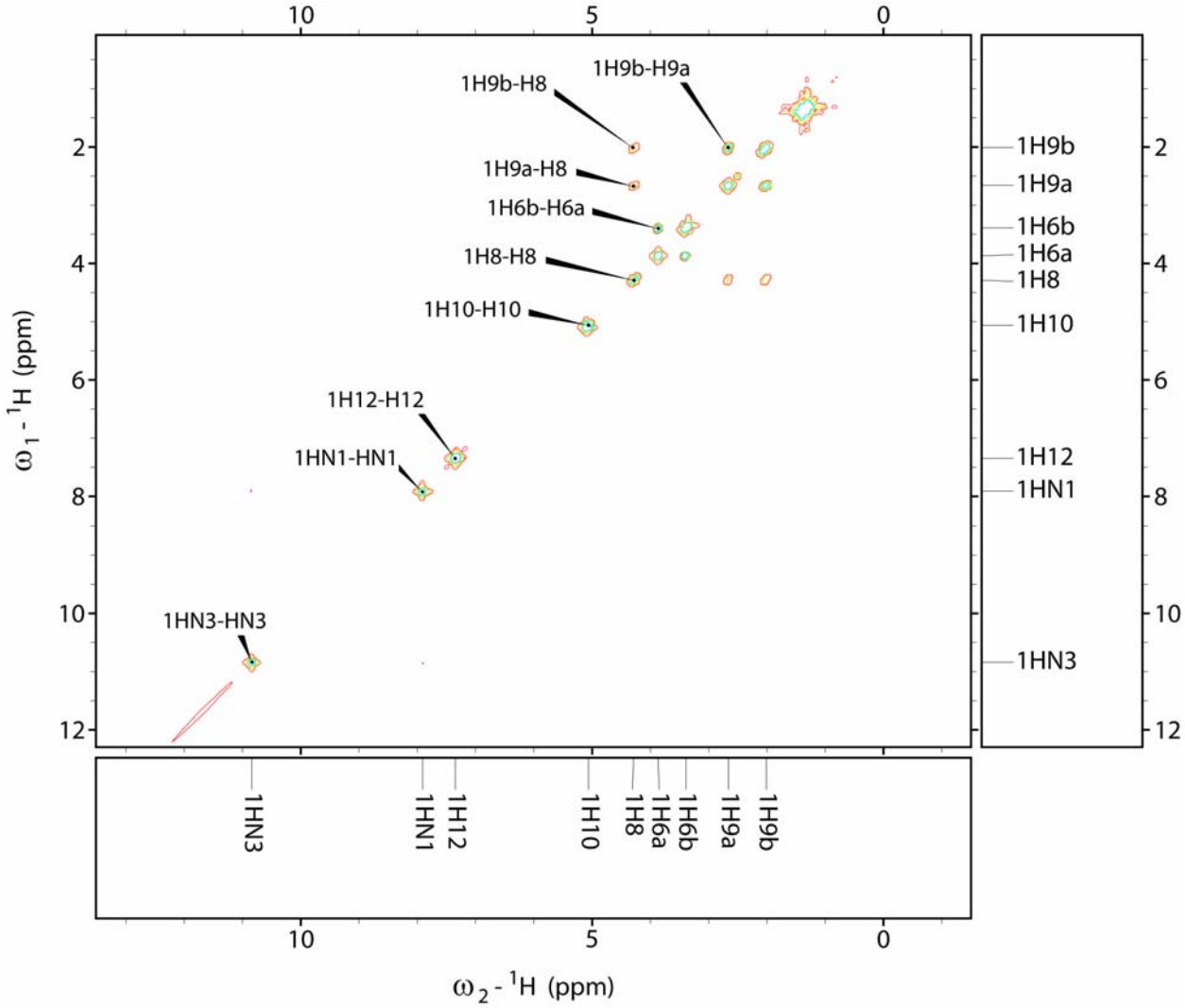

Supplemental Figure 41. 500 MHz COSY spectrum of **12**, DMSO-d_6

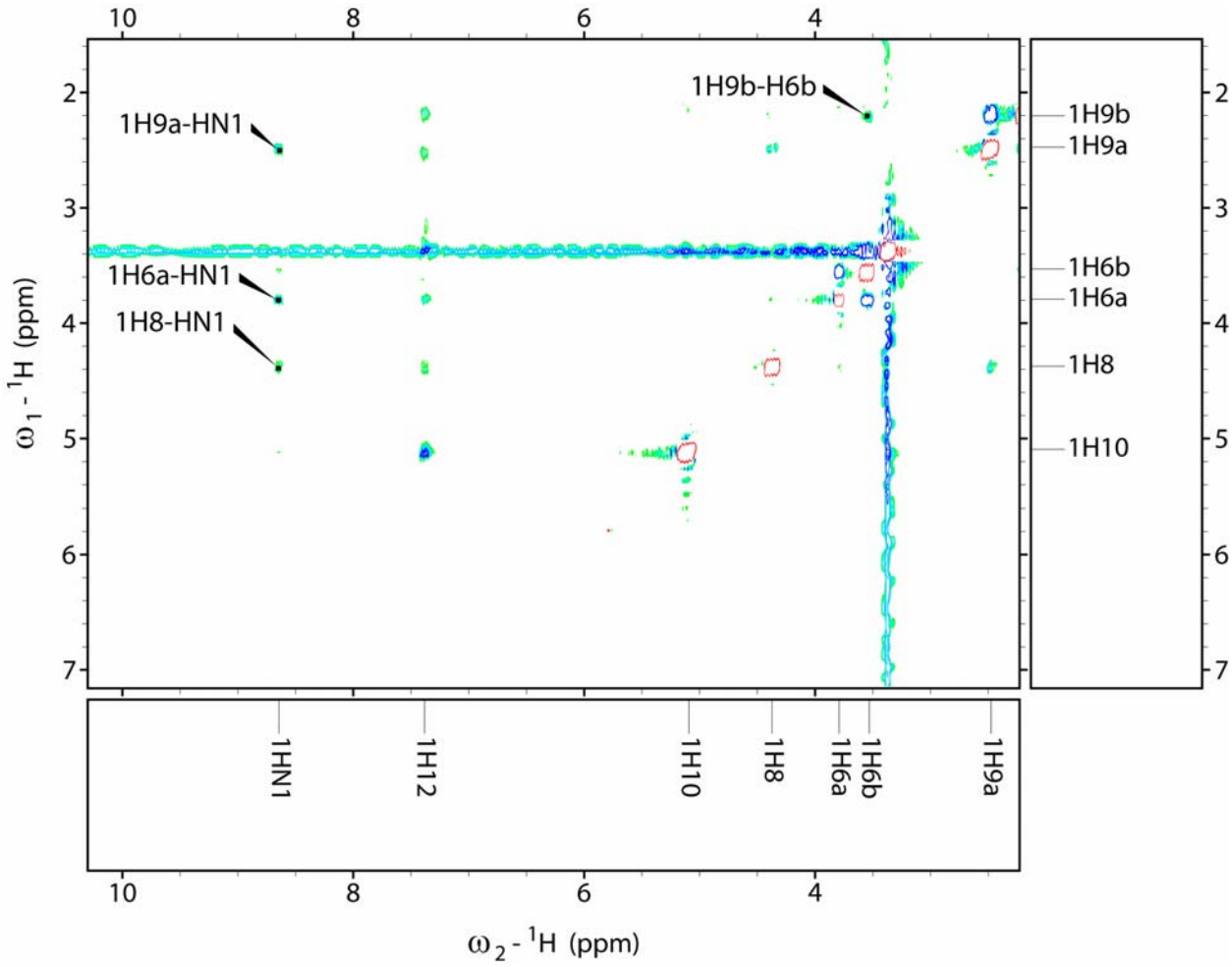

Supplemental Figure 42: 500 MHz NOESY spectrum of **13**, DMSO-d_6

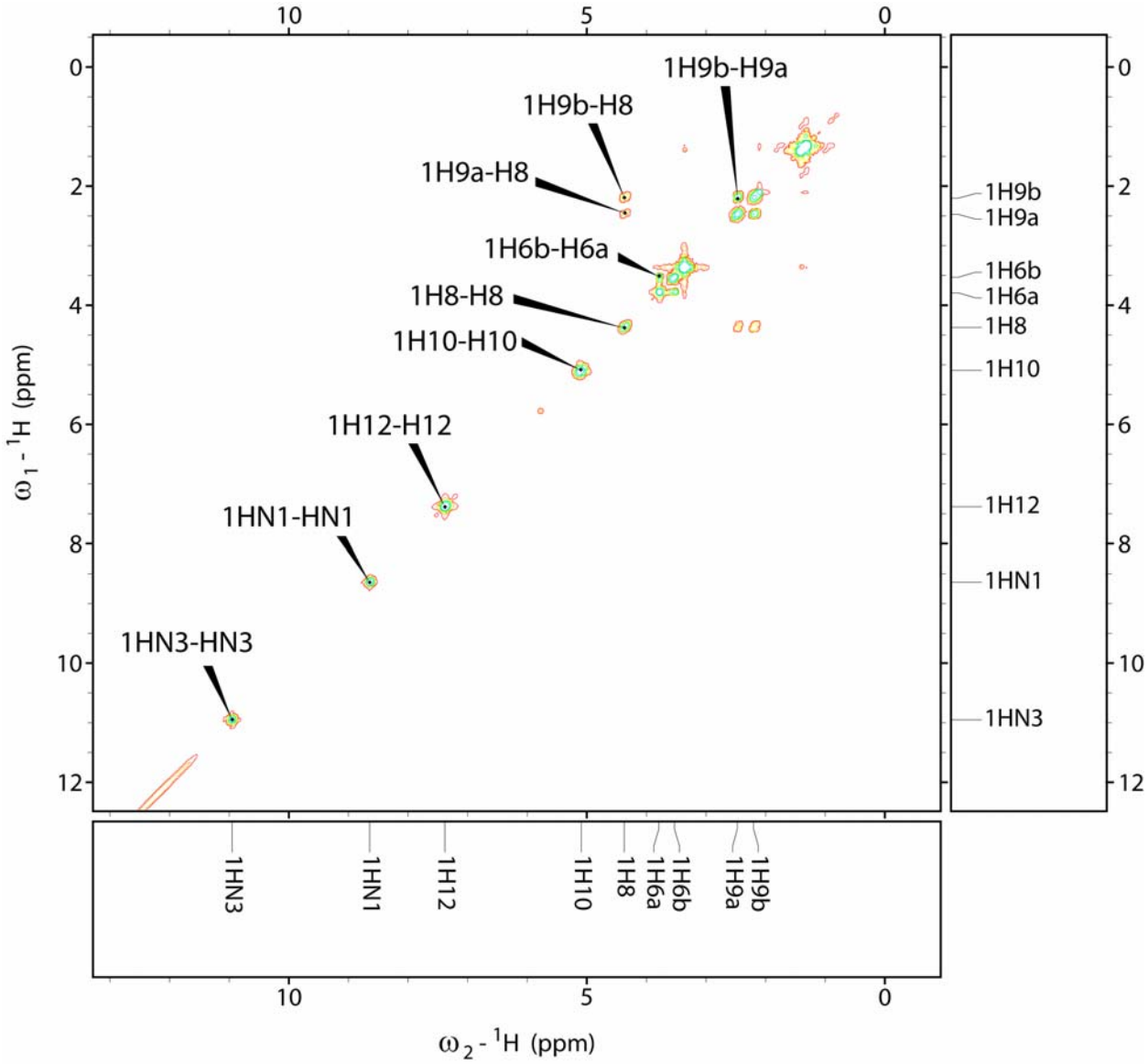

Supplemental Figure 43. 500 MHz COSY spectrum of **13**, DMSO-d_6

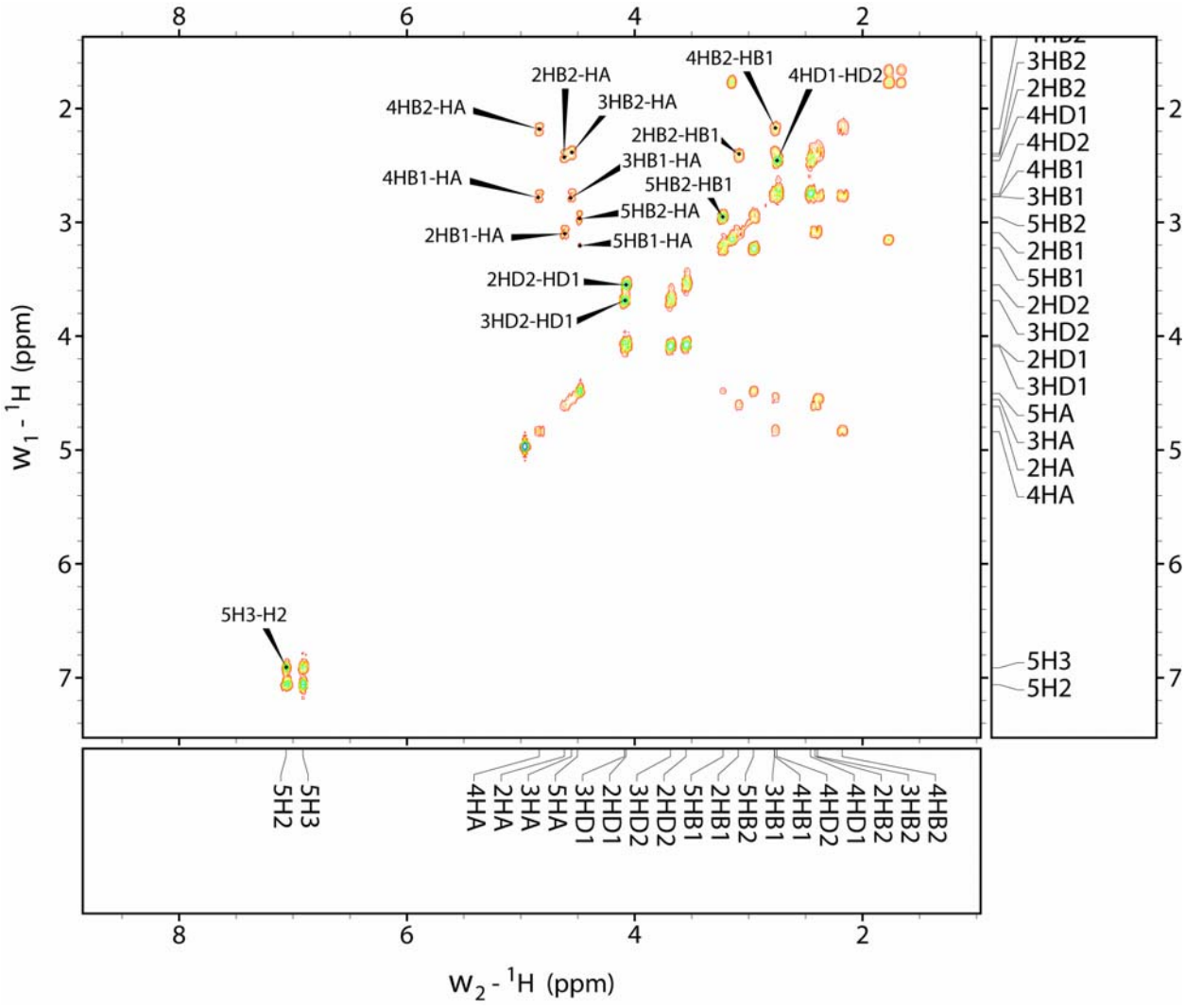

Supplemental Figure 44. 500 MHz COSY spectrum of **44**, 10 °C, D_2O

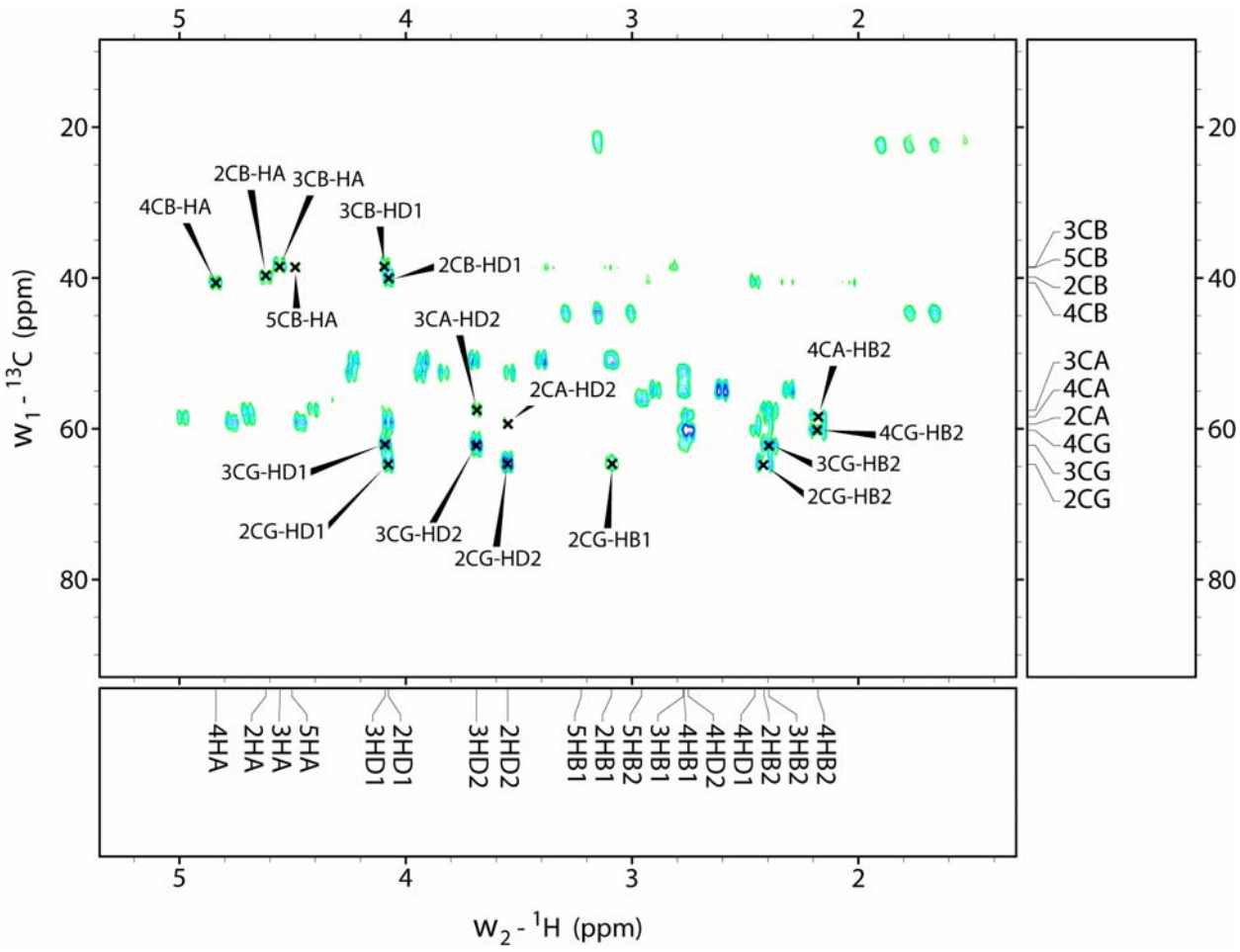

Supplemental Figure 45. 500 MHz HMBC spectrum (expansion 1 of 2) of **44**, 10 °C, D_2O

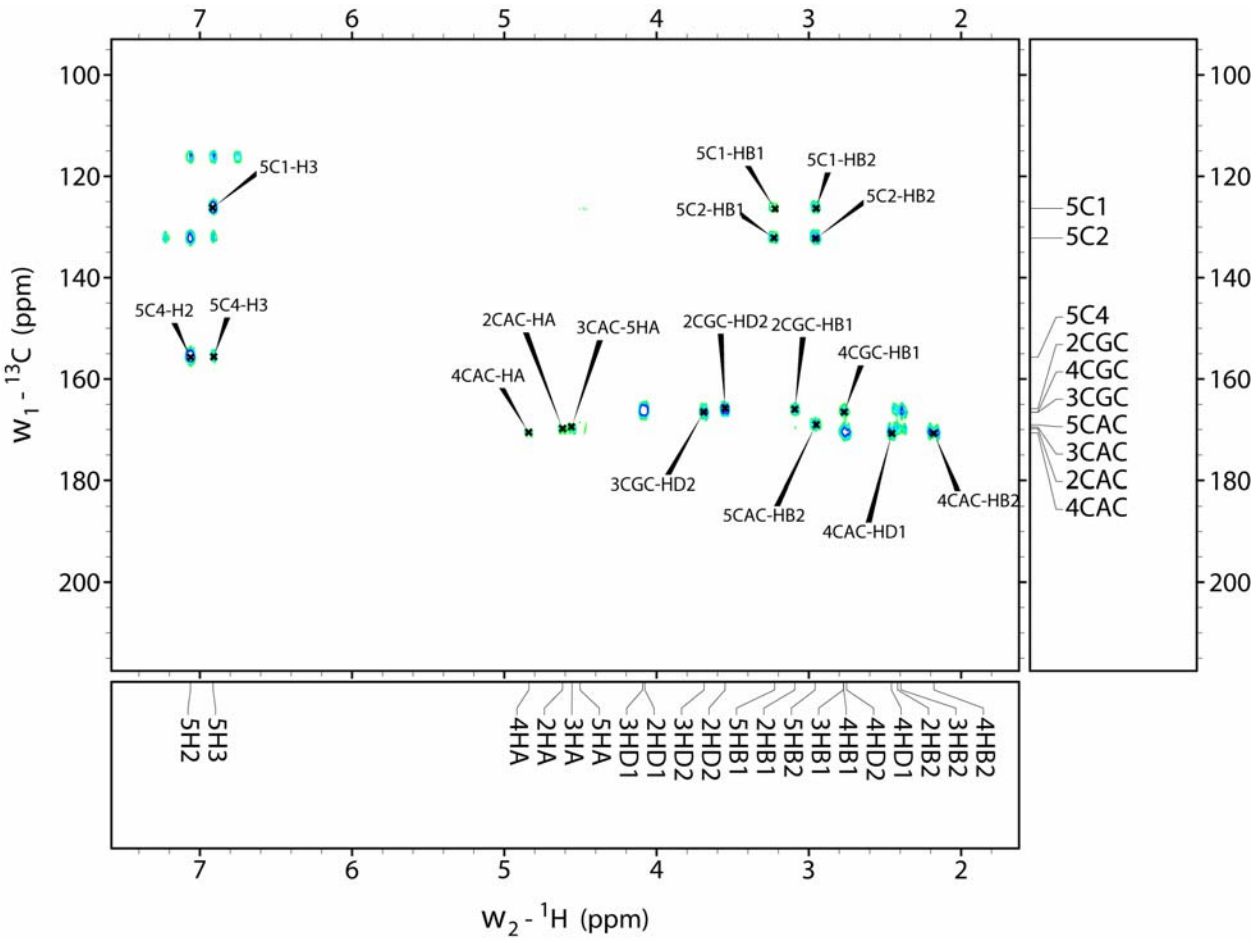

Supplemental Figure 46. 500 MHz HMBC spectrum (expansion 2 of 2) of **44**, 10 °C, D_2O

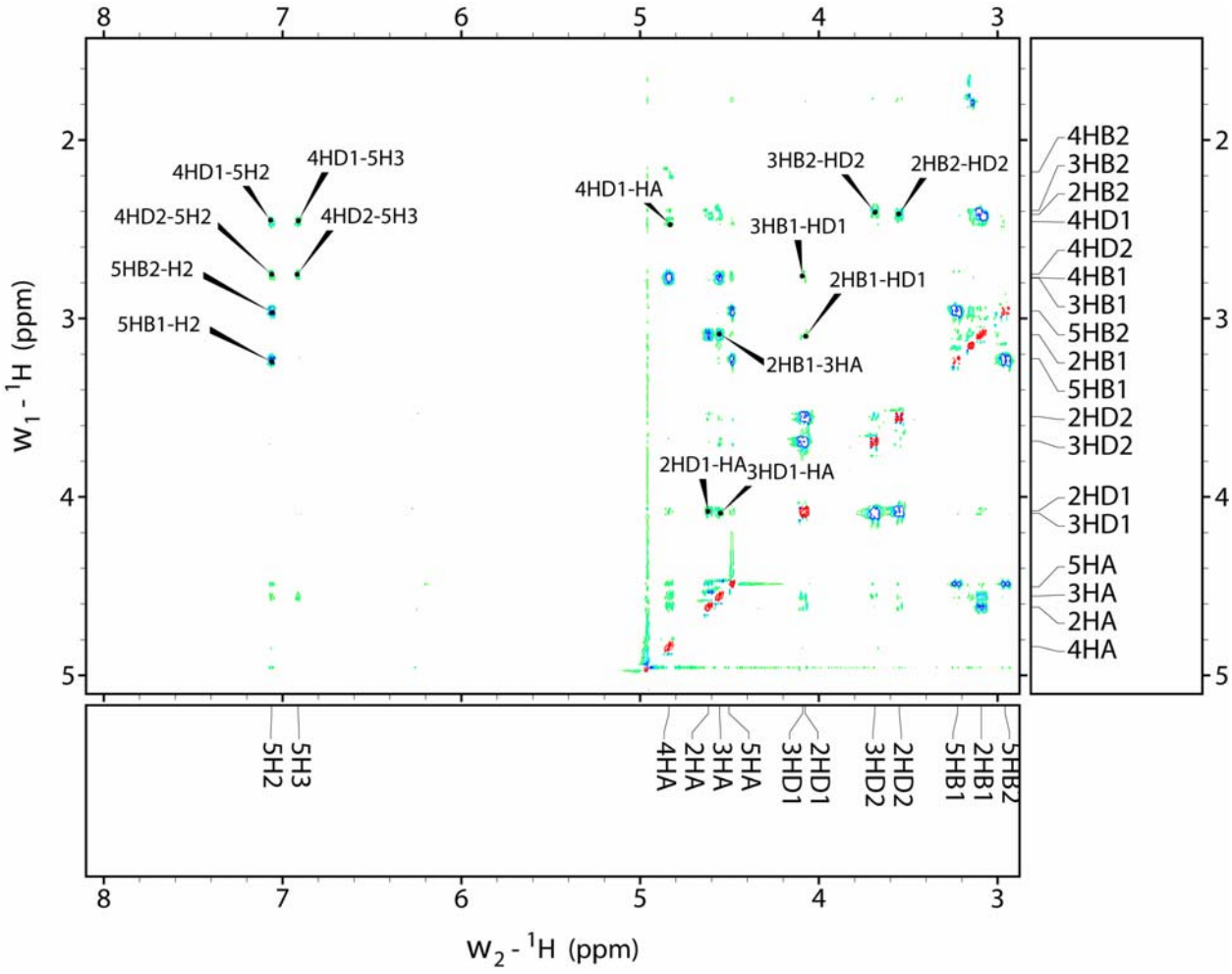

Supplemental Figure 47. 500 MHz ROESY spectrum of **44**, 10 °C, D_2O

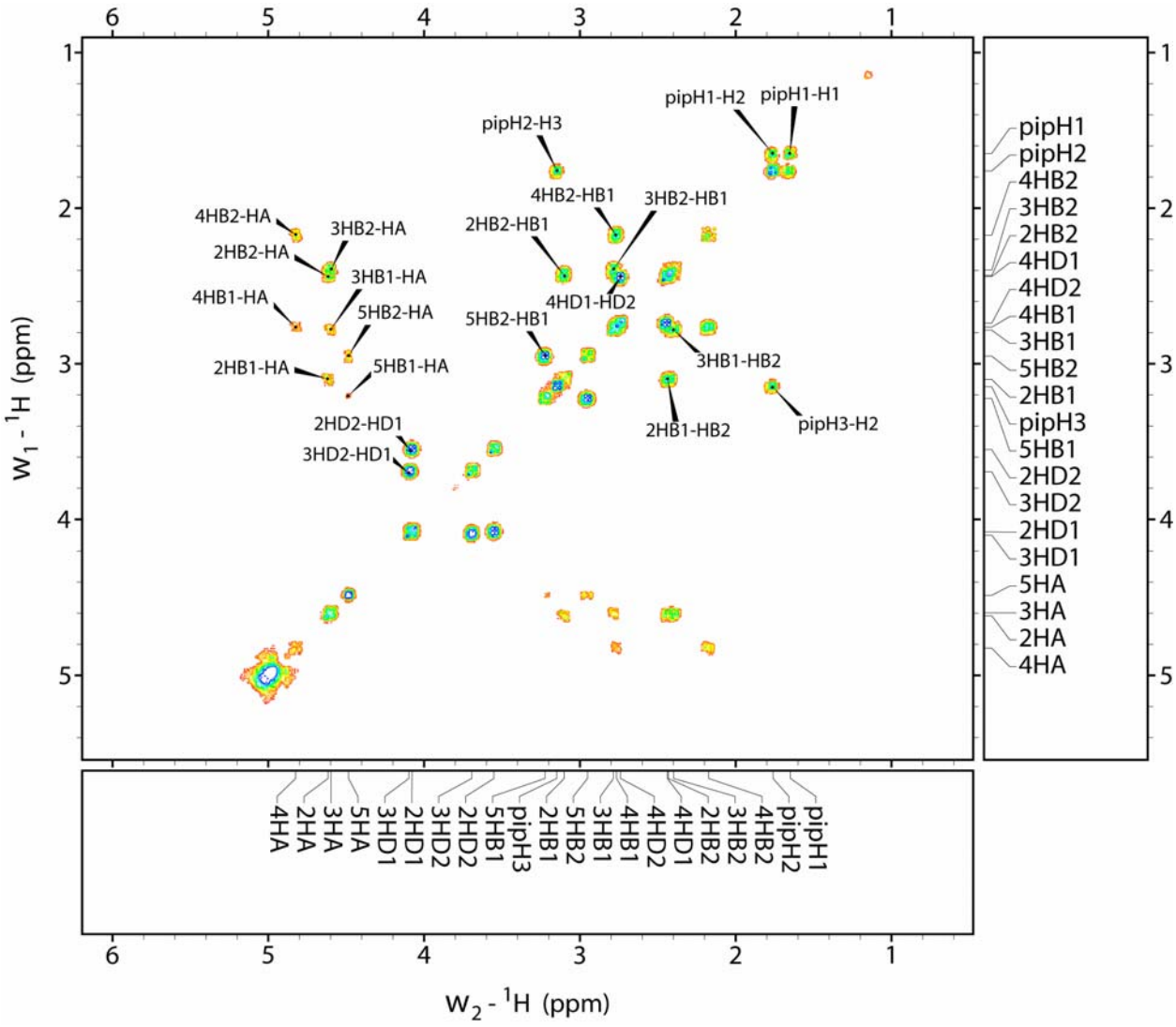

Supplemental Figure 48. 500 MHz COSY spectrum of **44**, 10 °C, 10% D_2O/H_2O, pH ~ 0

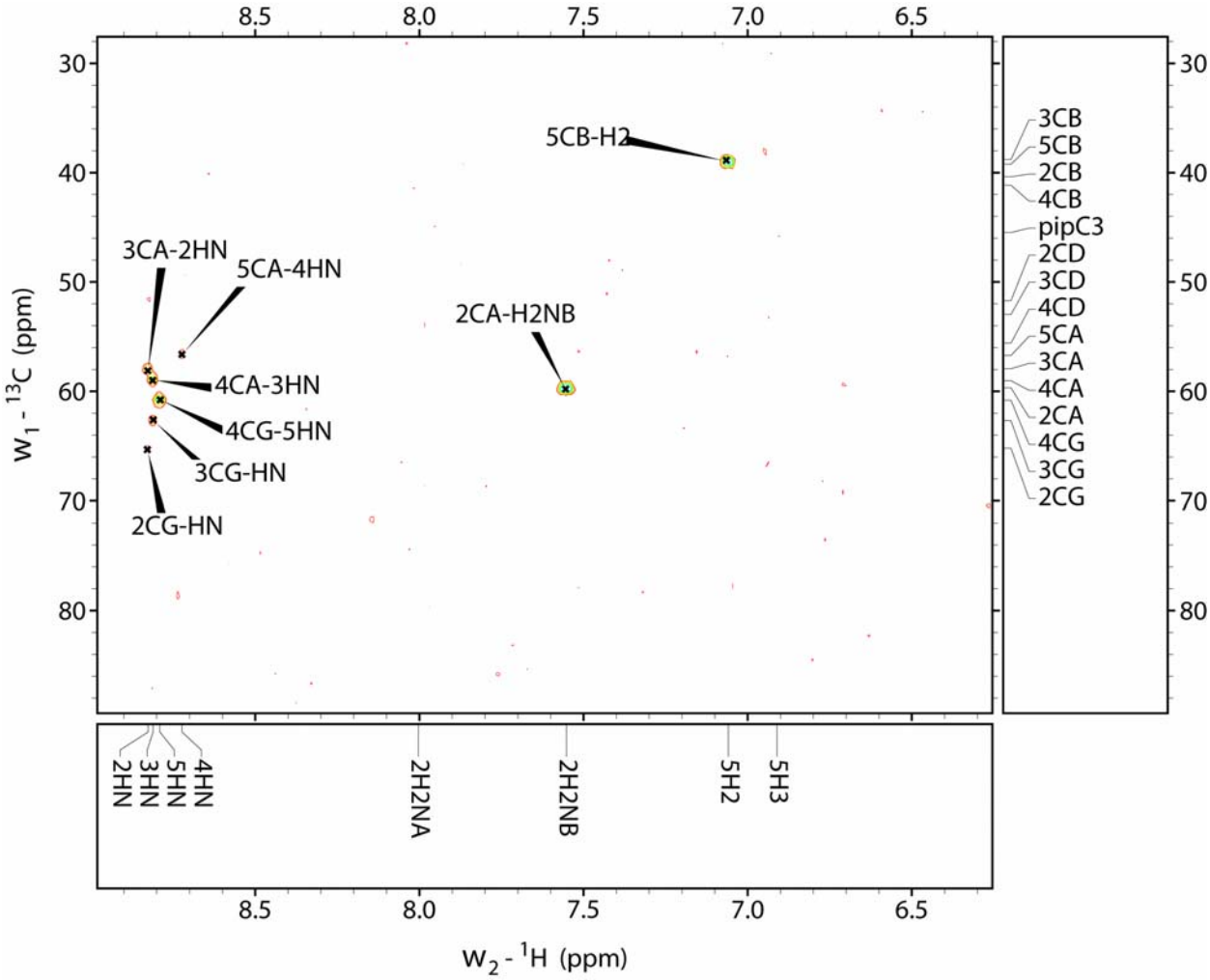

Supplemental Figure 49. 500 MHz HMBC spectrum (expansion 1 of 4) of **44**, 10 °C, 10% D_2O/H_2O, pH ~ 0

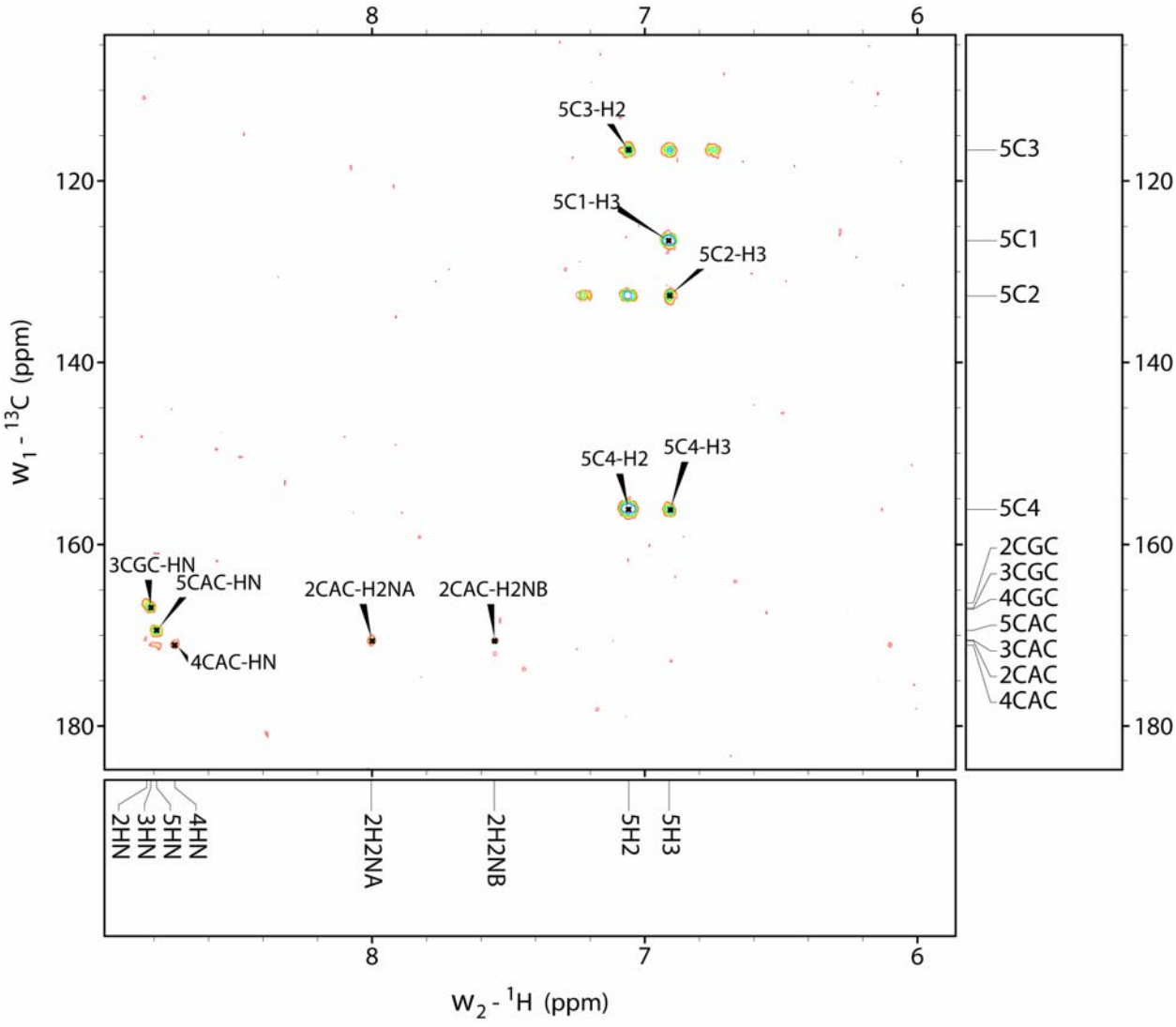

Supplemental Figure 50. 500 MHz HMBC spectrum (expansion 2 of 4) of **44**, 10 °C, 10% D_2O/H_2O, pH ~ 0

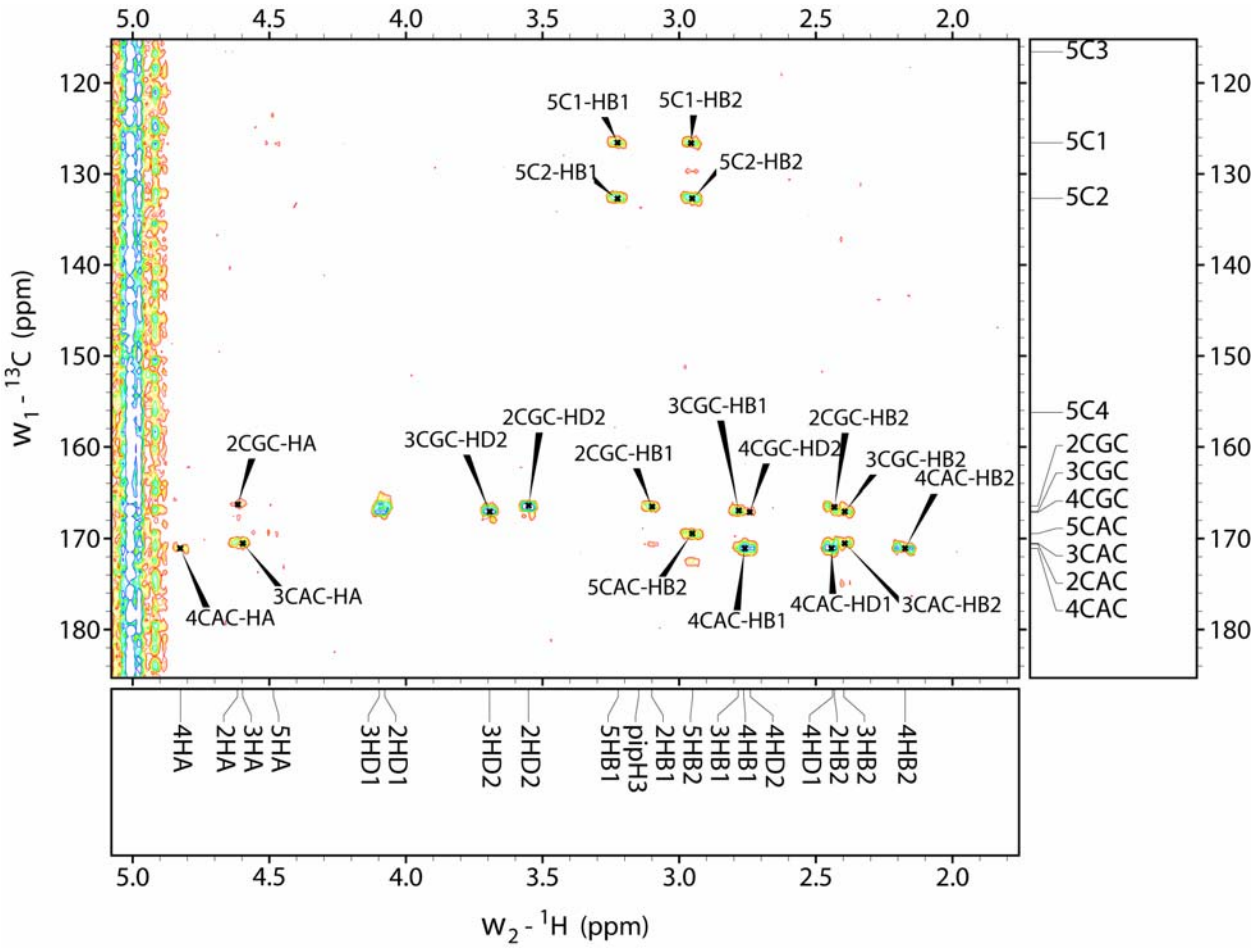

Supplemental Figure 51. 500 MHz HMBC spectrum (expansion 3 of 4) of **44**, 10 °C, 10% D_2O/H_2O, pH ~ 0

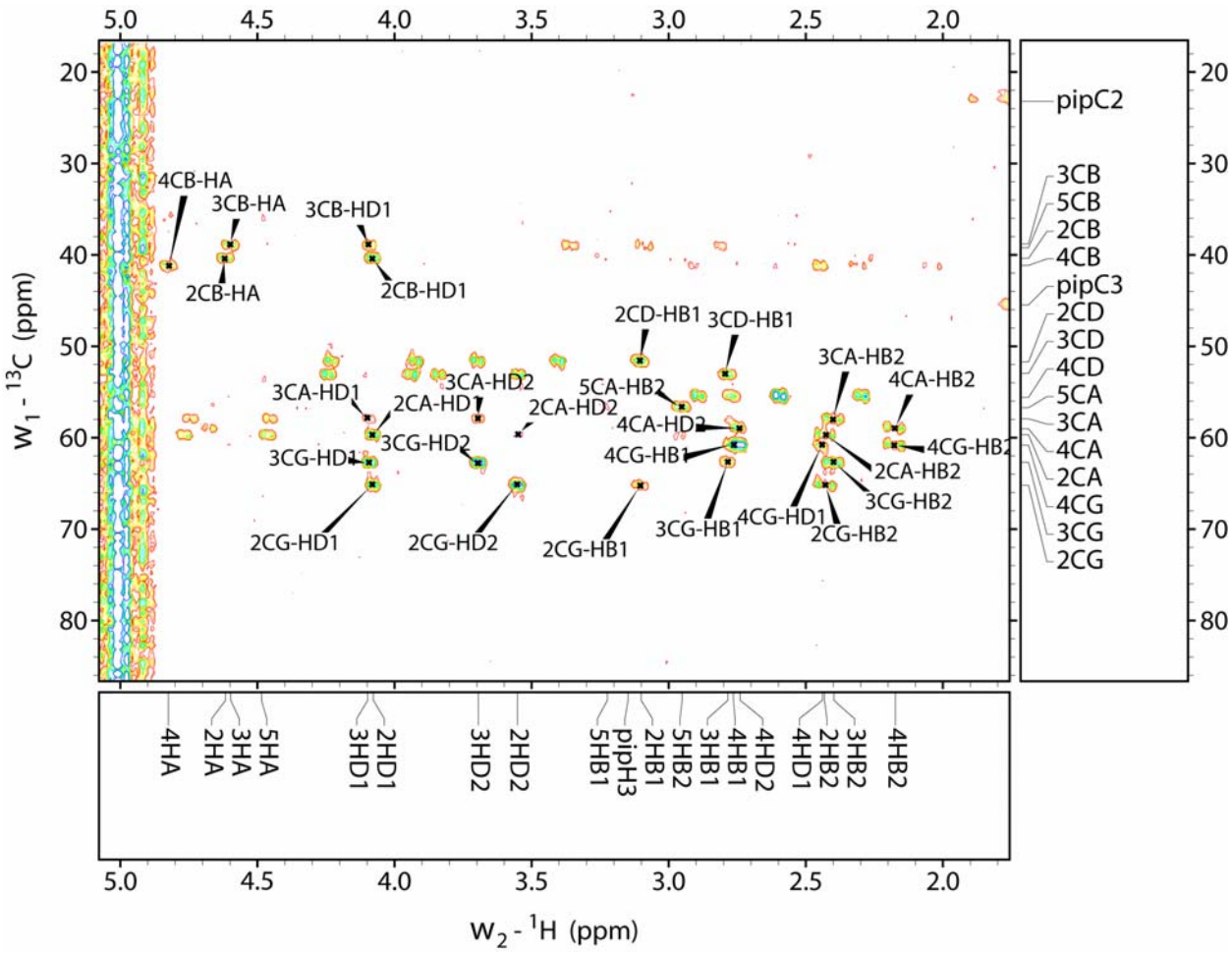

Supplemental Figure 52. 500 MHz HMBC spectrum (expansion 4 of 4) of **44**, 10 °C, 10% D_2O/H_2O, pH ~ 0

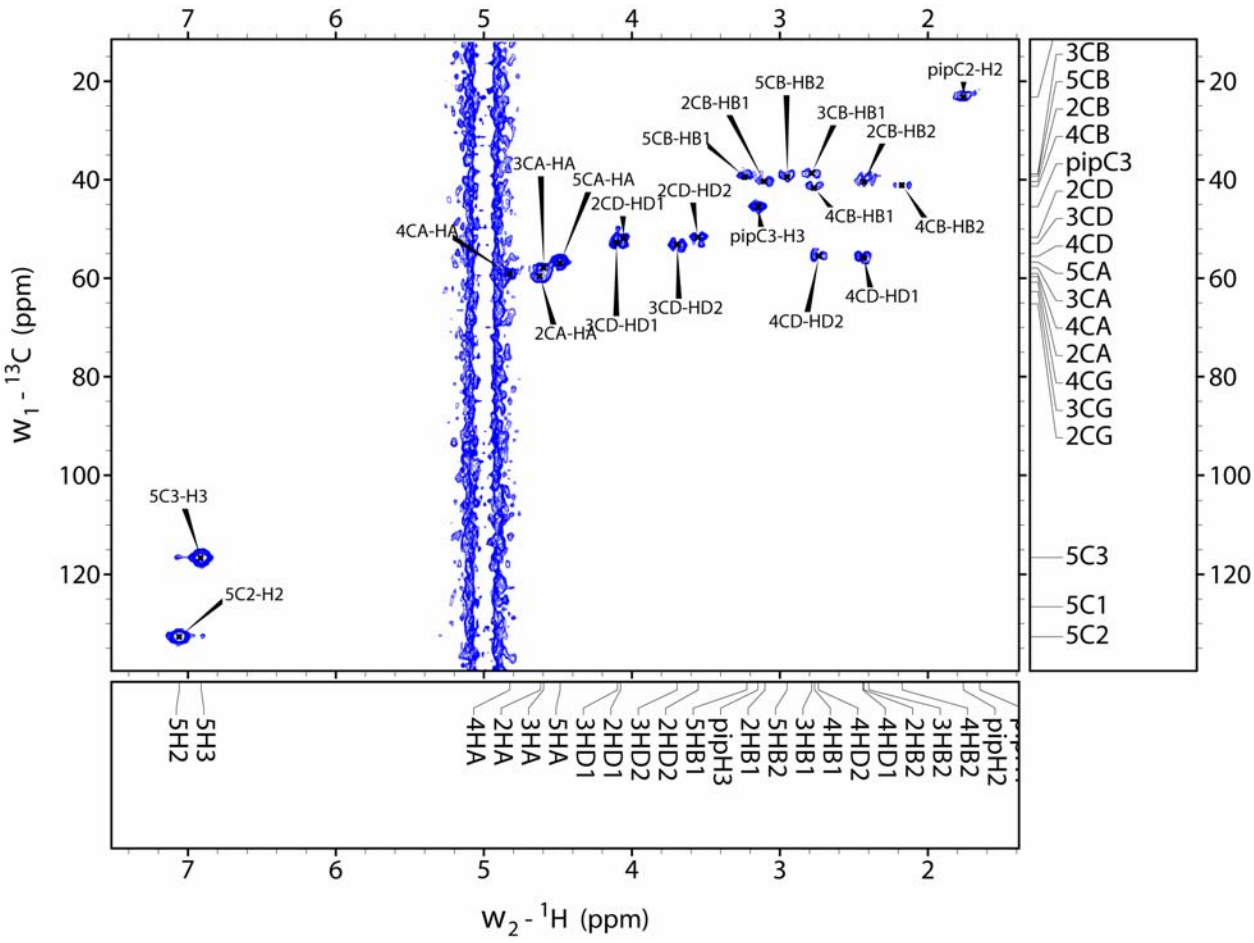

Supplemental Figure 53. 500 MHz HMQC spectrum of **44**, 10 °C, 10% D_2O/H_2O, pH ~ 0

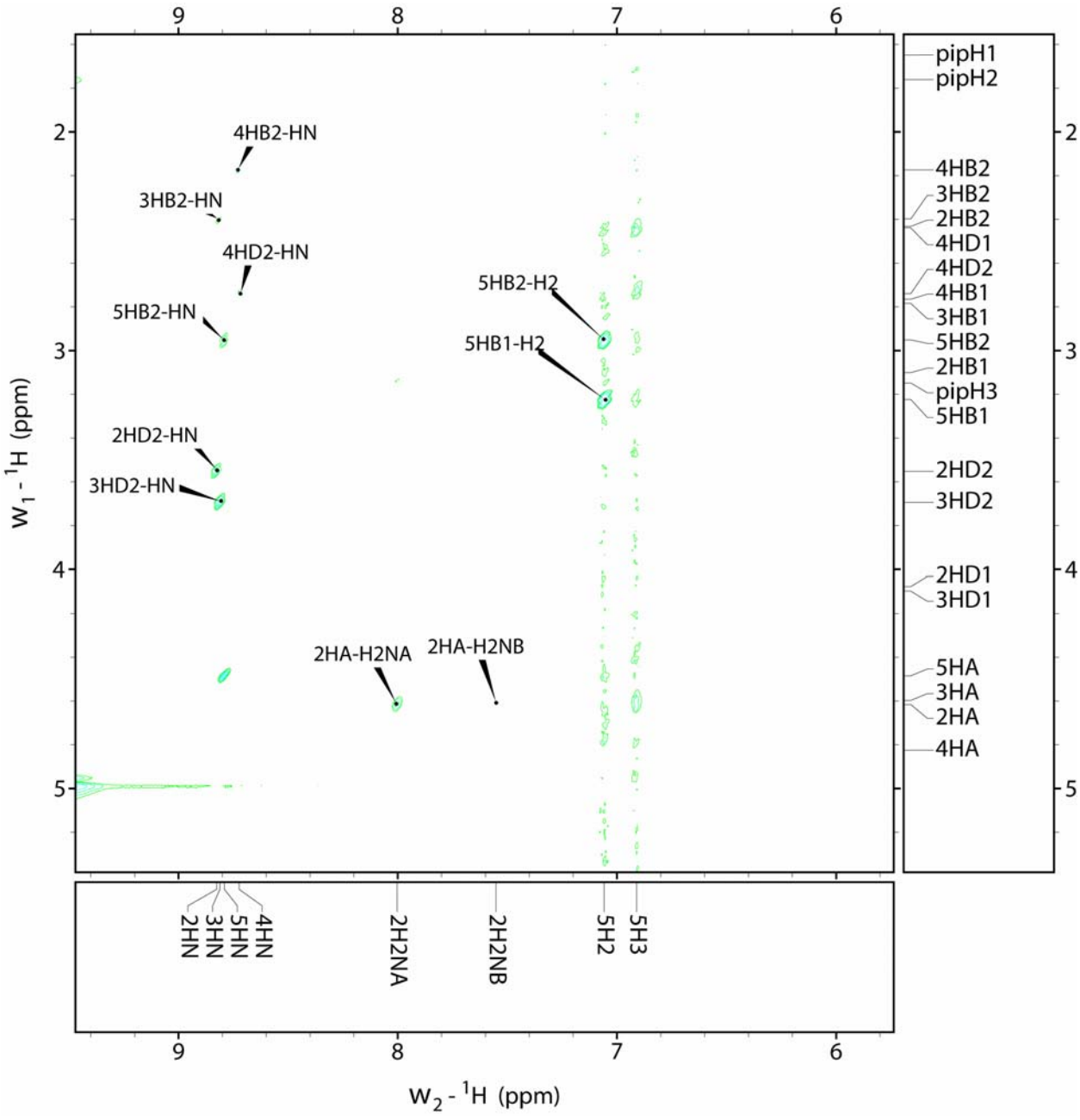

Supplemental Figure 54. 500 MHz ROESY spectrum of **44**, 10 °C, 10% D_2O/H_2O, pH ~ 0

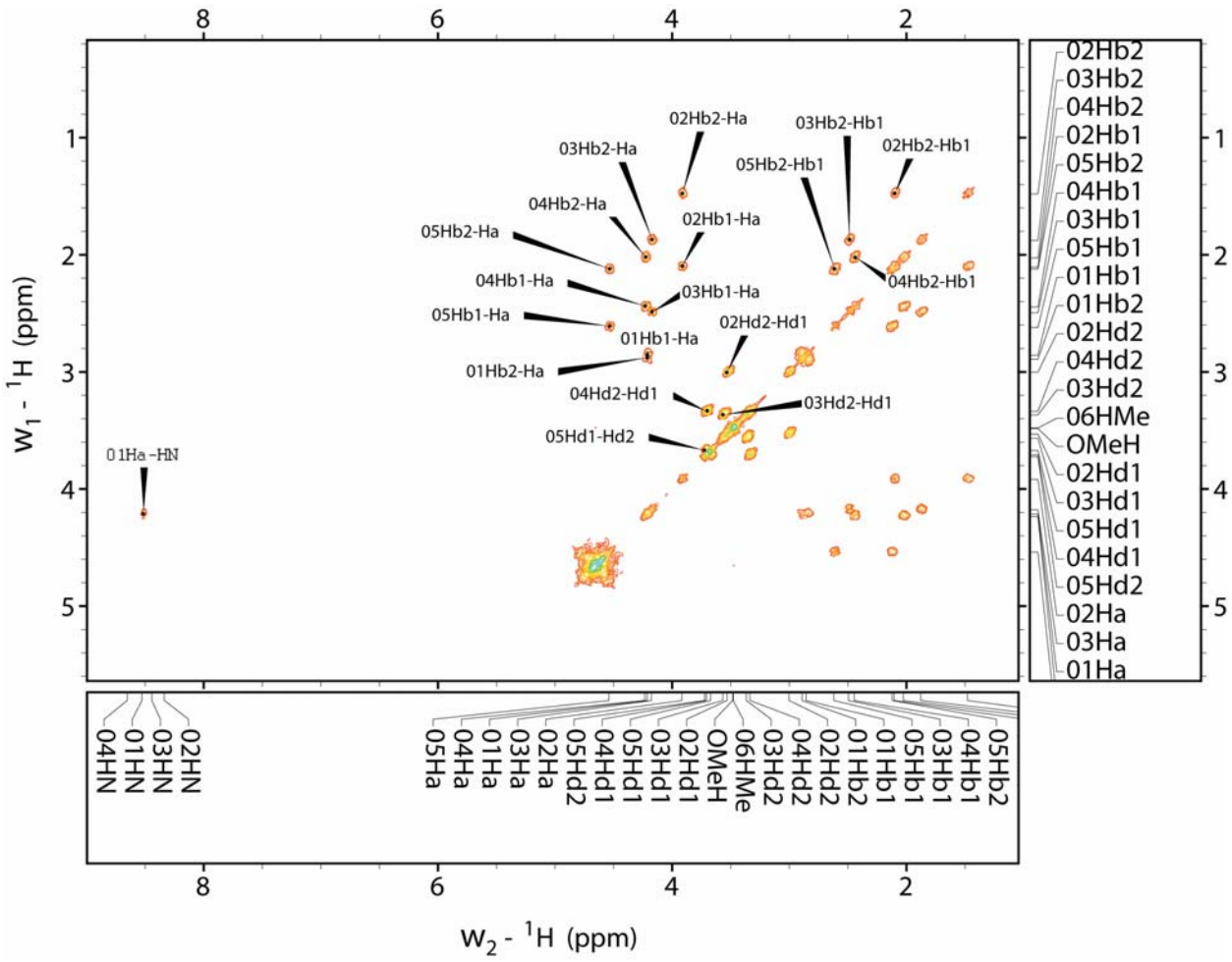

Supplemental Figure 55. 500 MHz COSY spectrum of compound **57**, 2 °C, 9:1 H_2O/D_2O with 0.025 M ND_4COOD:CD_3COOD buffer (pH 4-5)

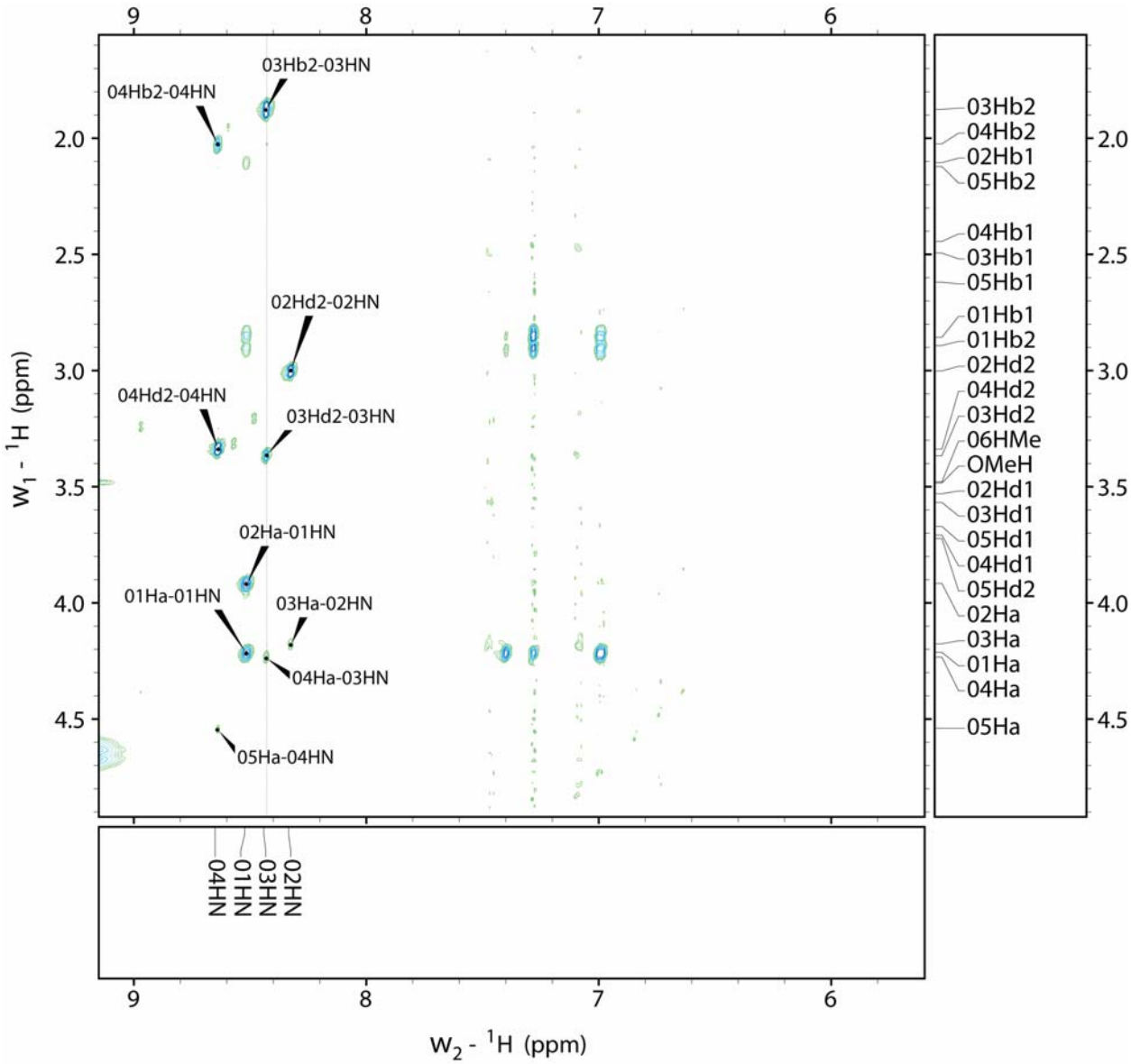

Supplemental Figure 56. 500 MHz ROESY spectrum (expansion 1 of 2) of compound **57**, 2 °C, 9:1 H_2O/D_2O with 0.025 M ND_4COOD:CD_3COOD buffer (pH 4-5)

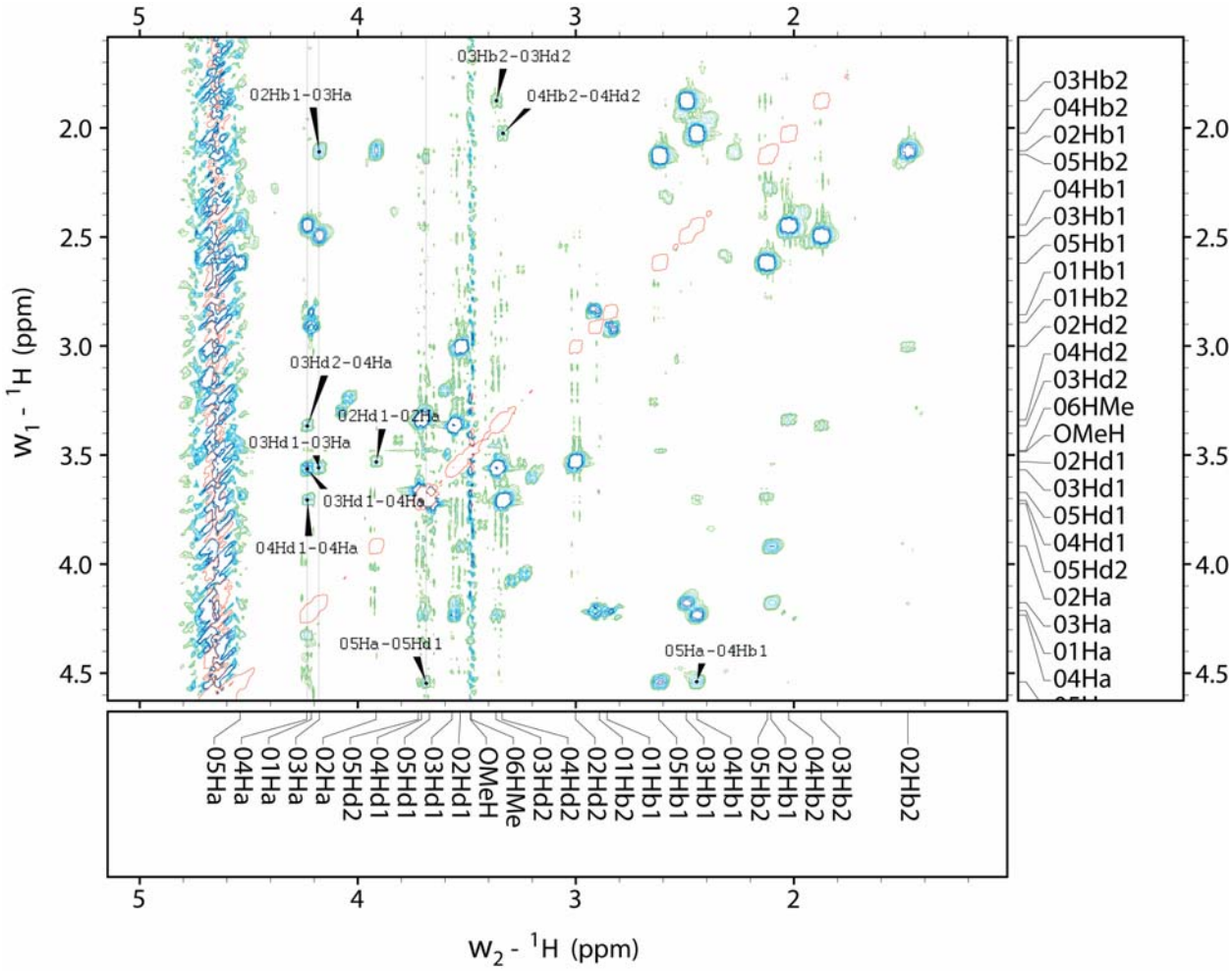

Supplemental Figure 57. 500 MHz ROESY spectrum (expansion 2 of 2) of compound **57**, 2 °C, 9:1 H_2O/D_2O with 0.025 M ND_4COOD:CD_3COOD buffer (pH 4-5)

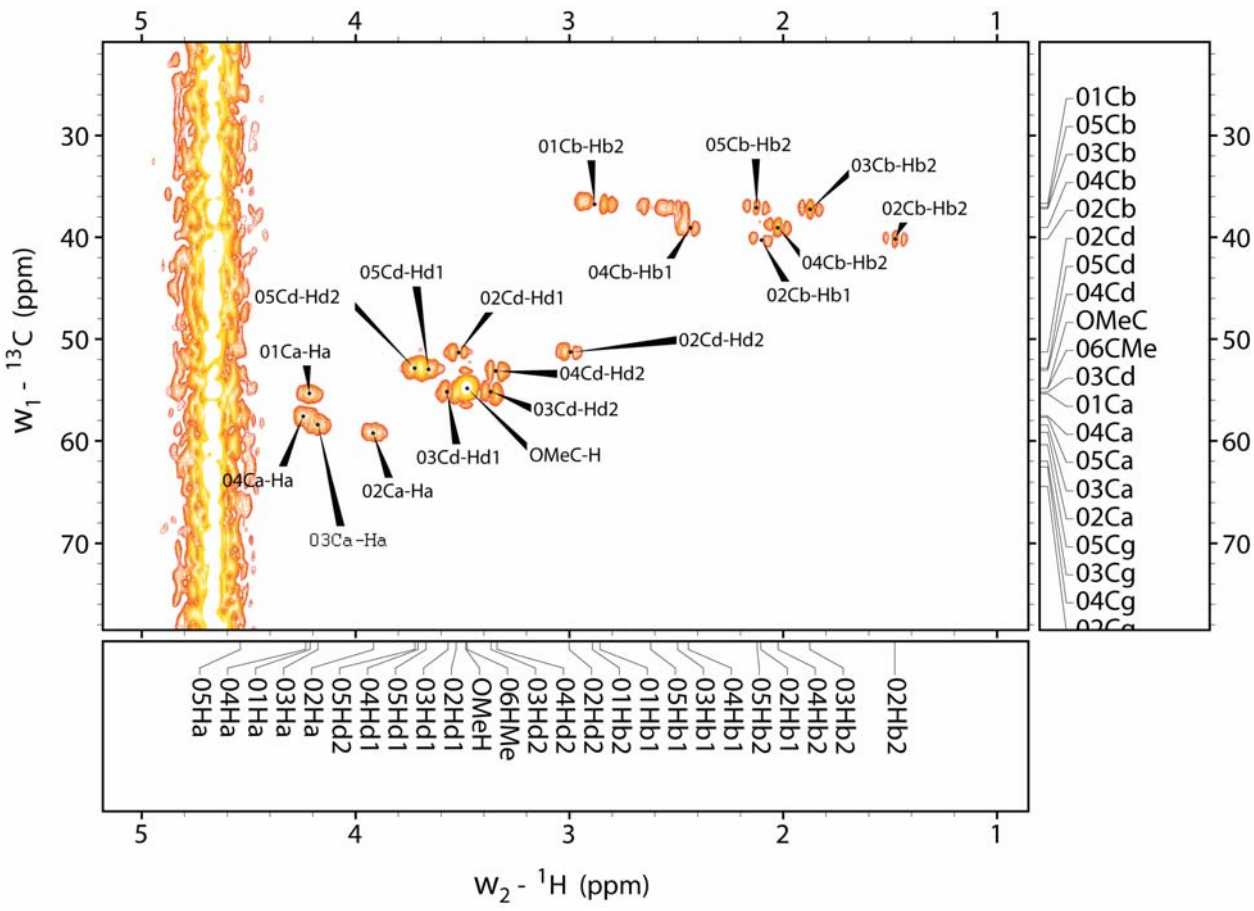

Supplemental Figure 58. 500 MHz HMQC spectrum of compound **57**, 2 °C, 9:1 H_2O/D_2O with 0.025 M ND_4COOD:CD_3COOD buffer (pH 4-5)

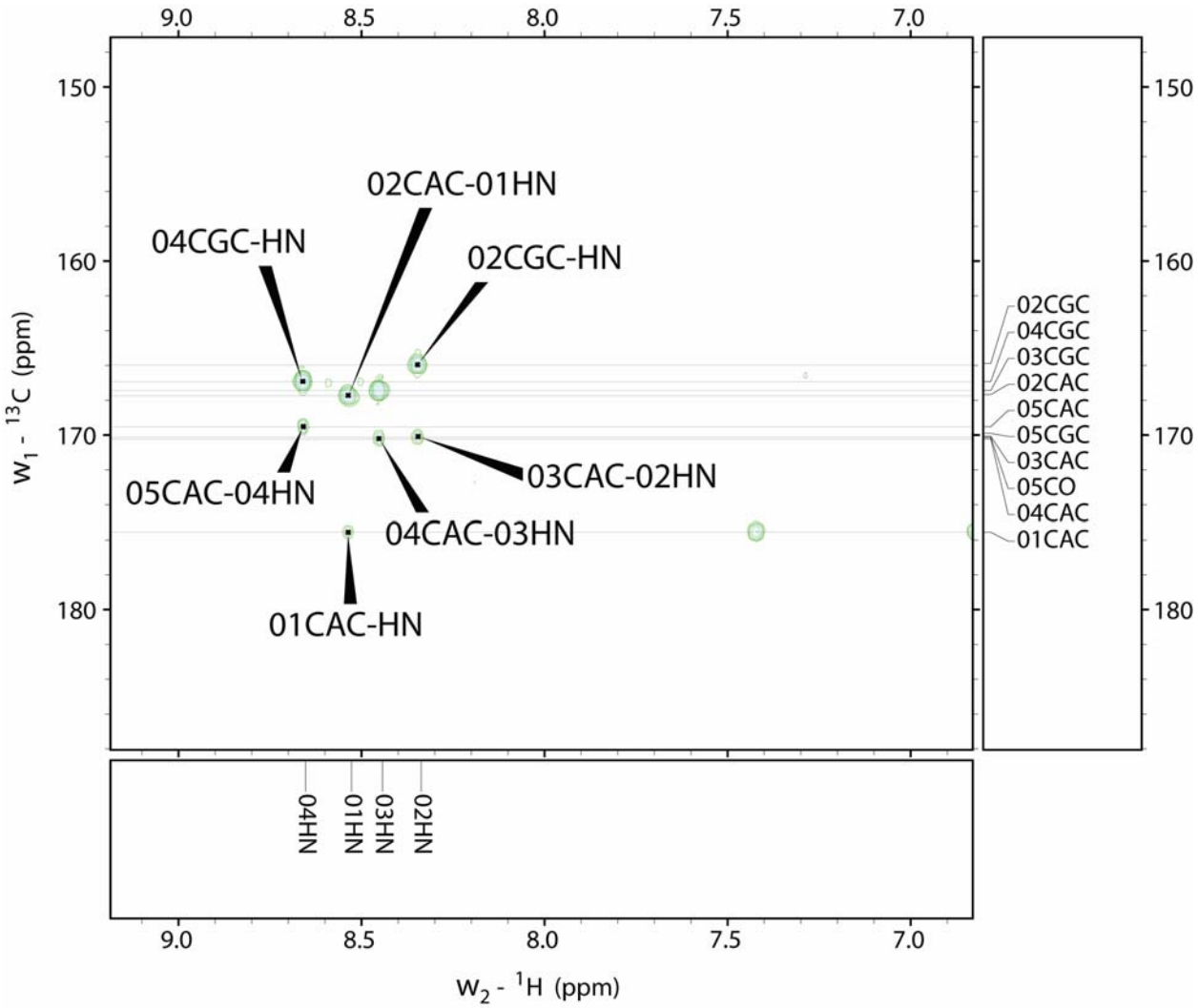

Supplemental Figure 59. 500 MHz HMBC spectrum (expansion 1 of 4) of compound **57**, 2 °C, 9:1 H_2O/D_2O with 0.025 M ND_4COOD:CD_3COOD buffer (pH 4-5)

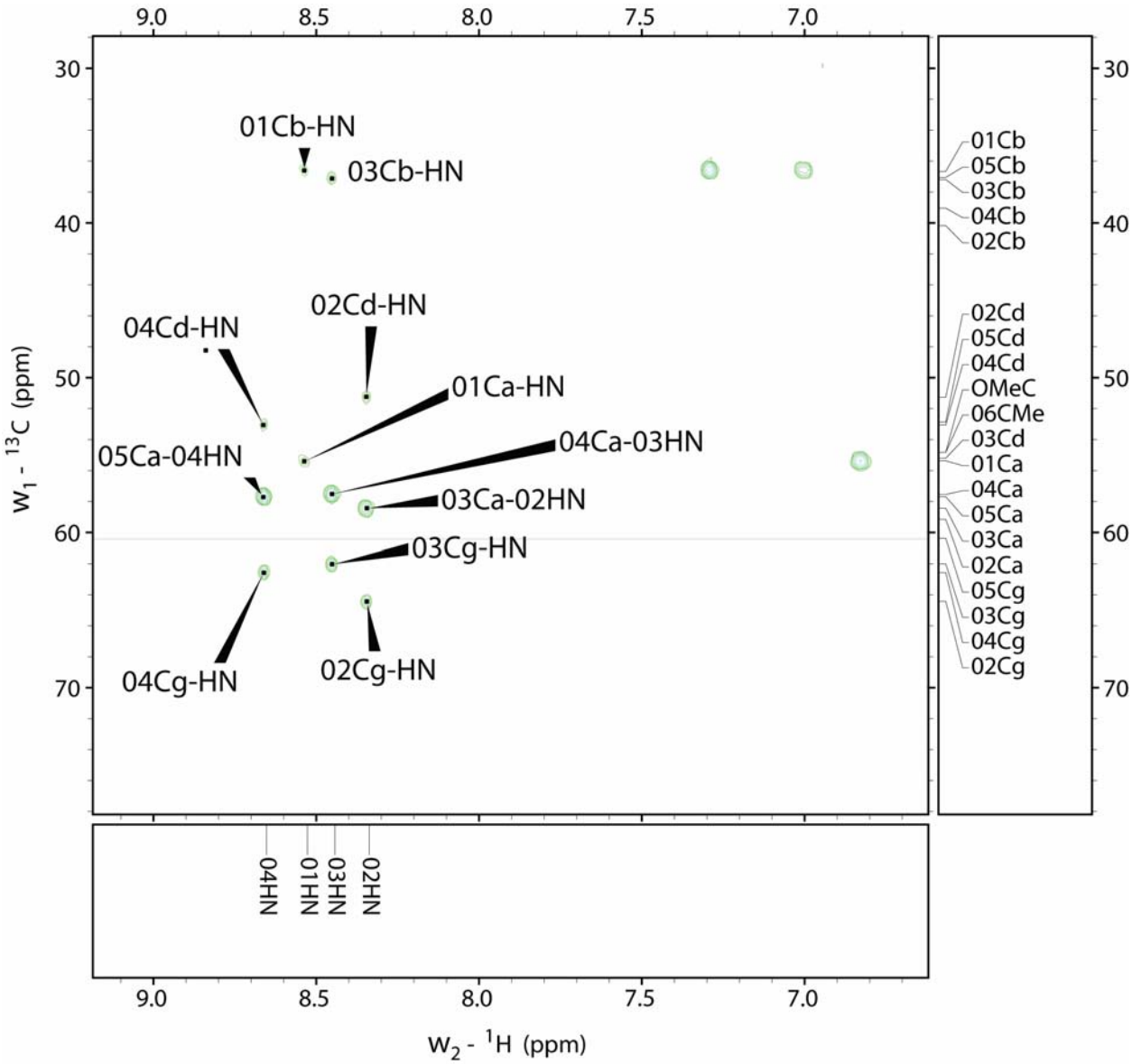

Supplemental Figure 60. 500 MHz HMBC spectrum (expansion 2 of 4) of compound **57**, 2 °C, 9:1 H_2O/D_2O with 0.025 M ND_4COOD:CD_3COOD buffer (pH 4-5)

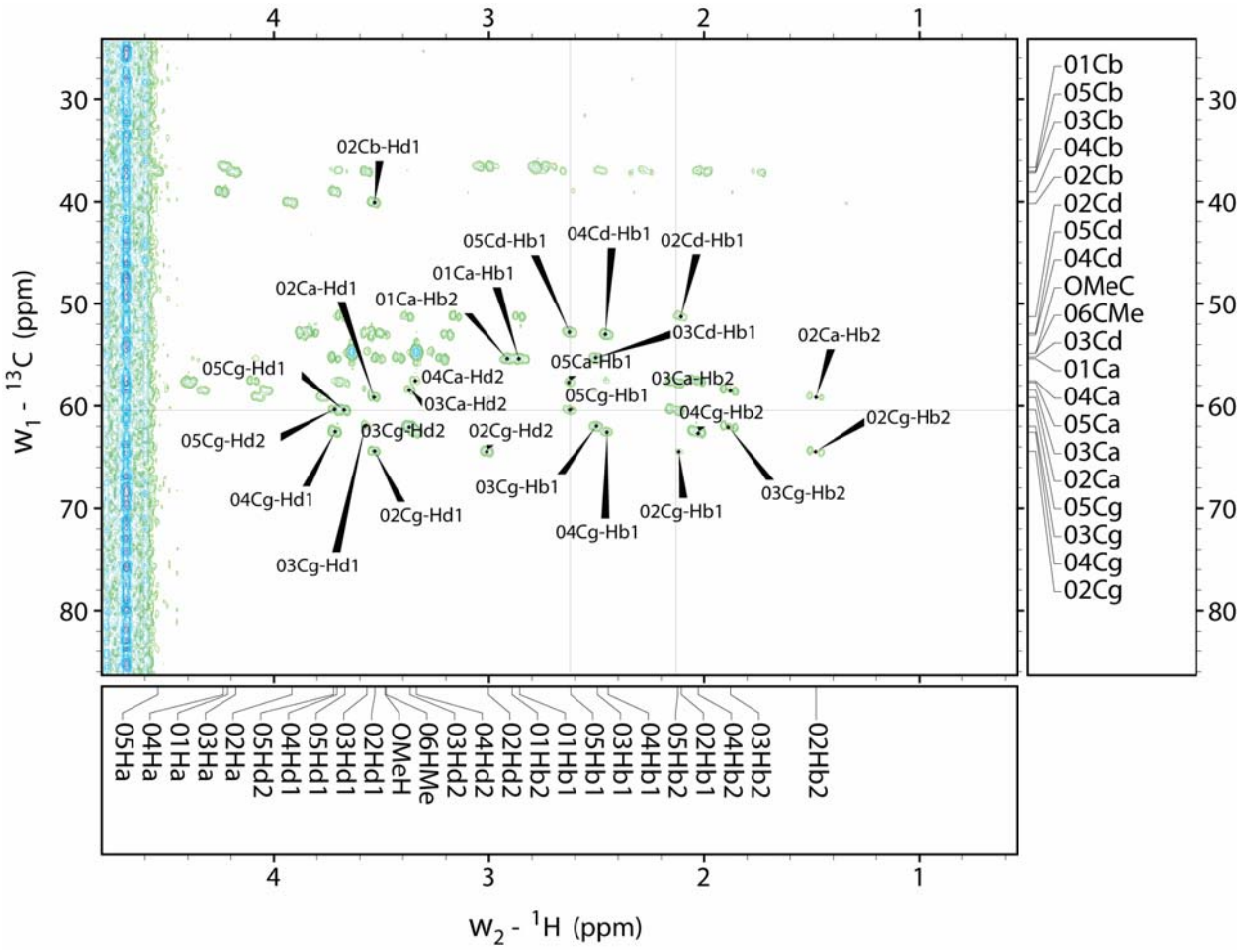

Supplemental Figure 61. 500 MHz HMBC spectrum (expansion 3 of 4) of compound **57**, 2 °C, 9:1 H_2O/D_2O with 0.025 M ND_4COOD:CD_3COOD buffer (pH 4-5)

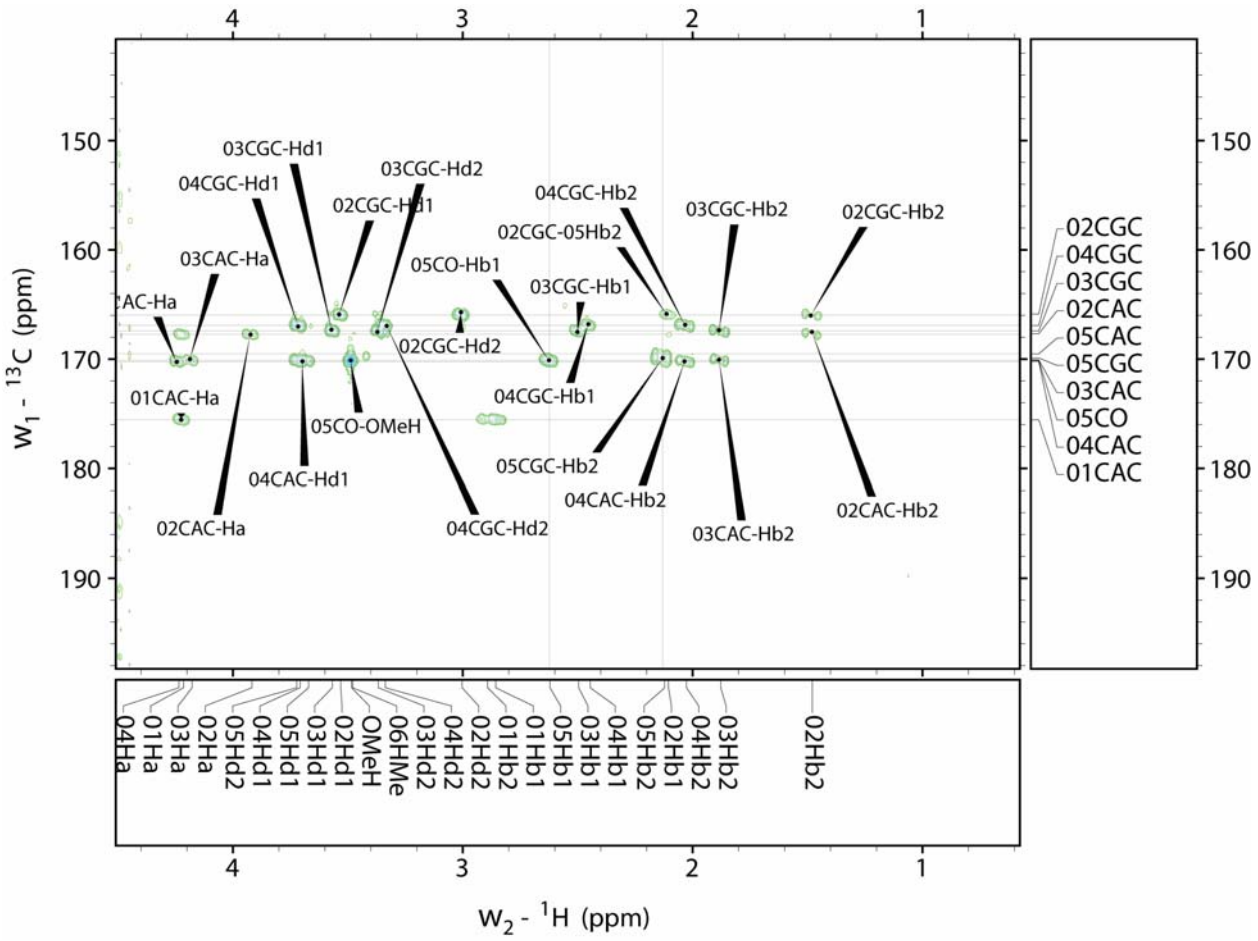

Supplemental Figure 62. 500 MHz HMBC spectrum (expansion 4 of 4) of compound **57**, 2 °C, 9:1 H_2O/D_2O with 0.025 M ND_4COOD:CD_3COOD buffer (pH 4-5)

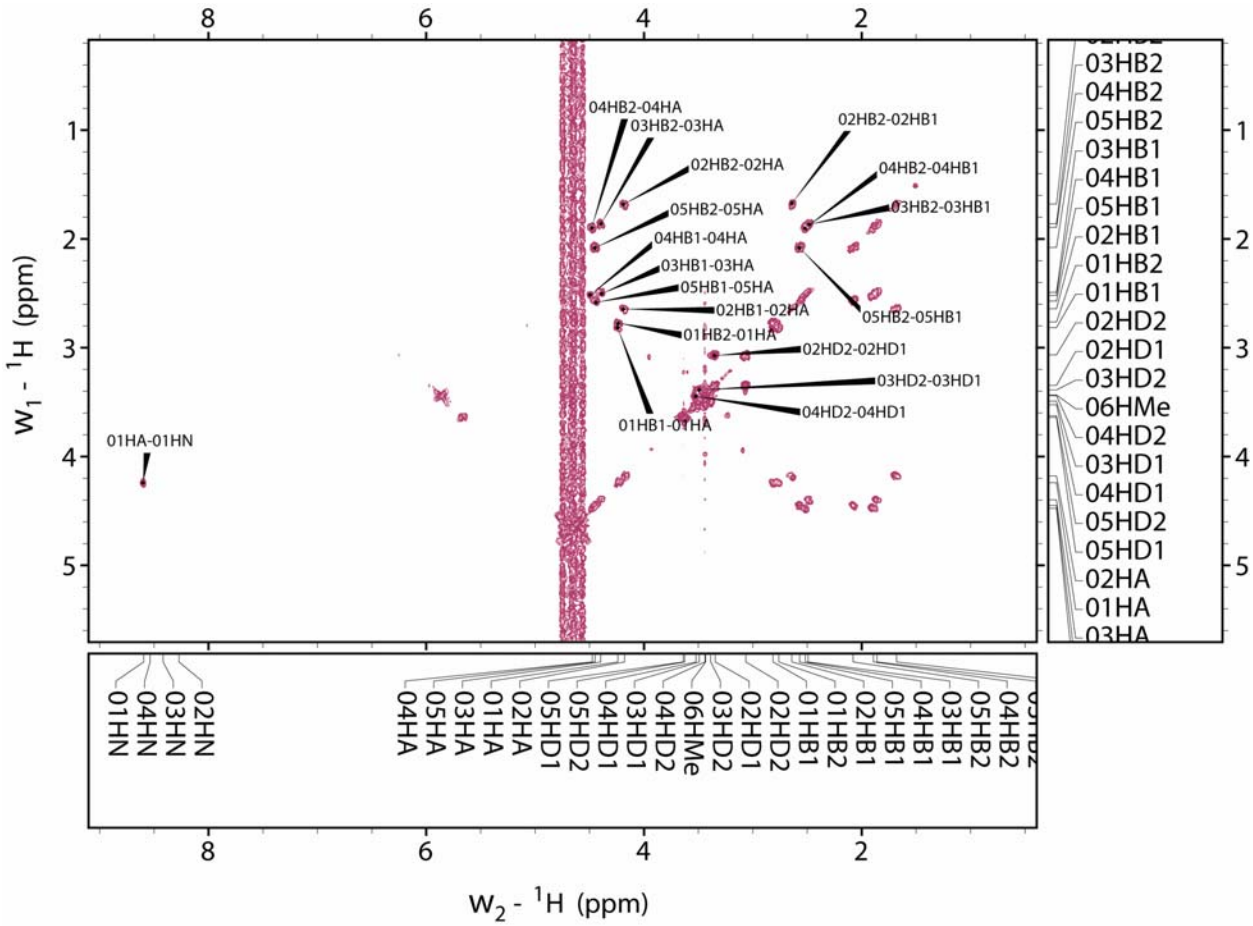

Supplemental Figure 63. 500 MHz COSY spectrum of compound **58**, 2 °C, 9:1 H_2O/D_2O with 0.025 M ND_4COOD:CD_3COOD buffer (pH 4-5)

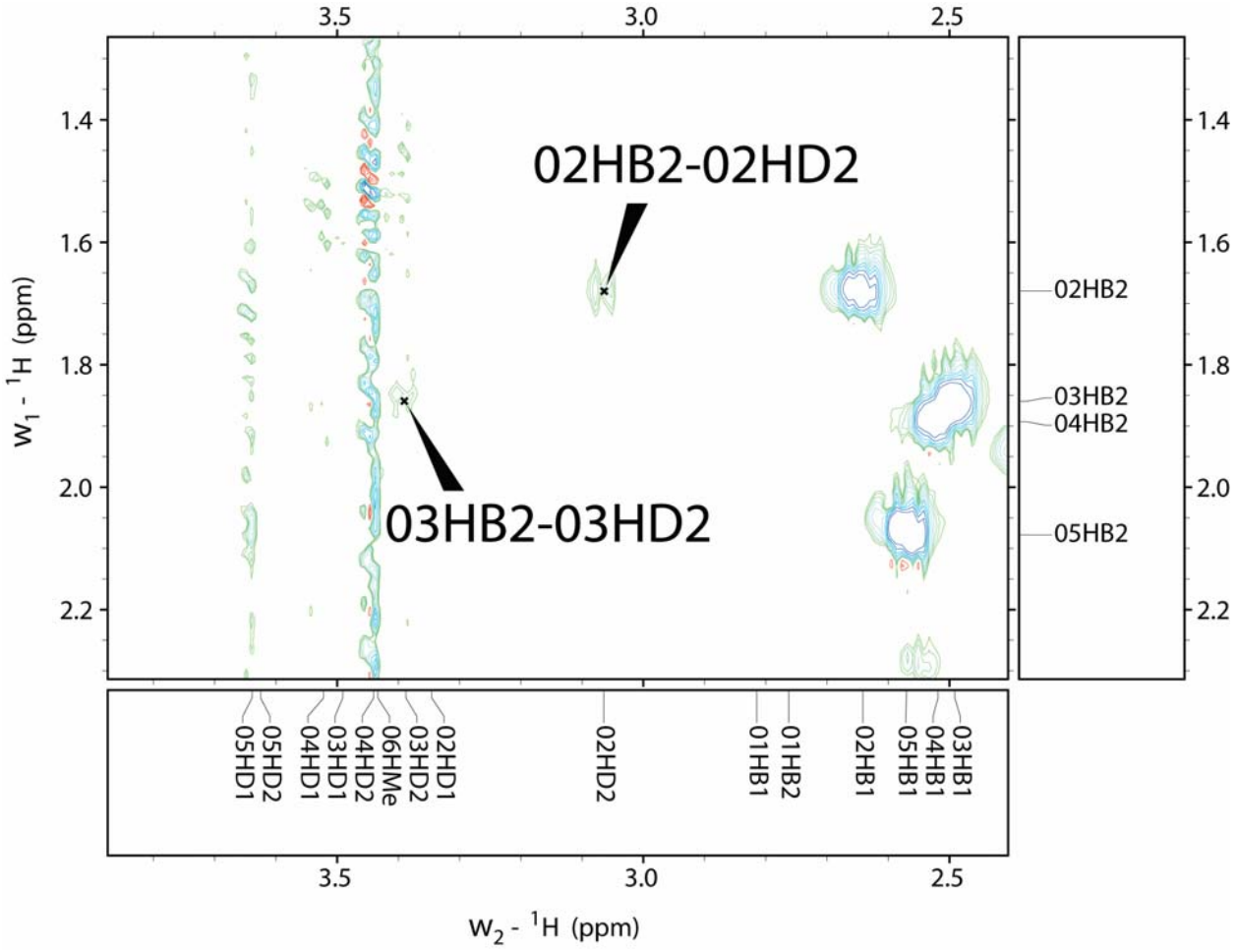

Supplemental Figure 64. 500 MHz ROESY spectrum (expansion 1 of 3) of compound **58**, 2 °C, 9:1 H_2O/D_2O with 0.025 M ND_4COOD:CD_3COOD buffer (pH 4-5)

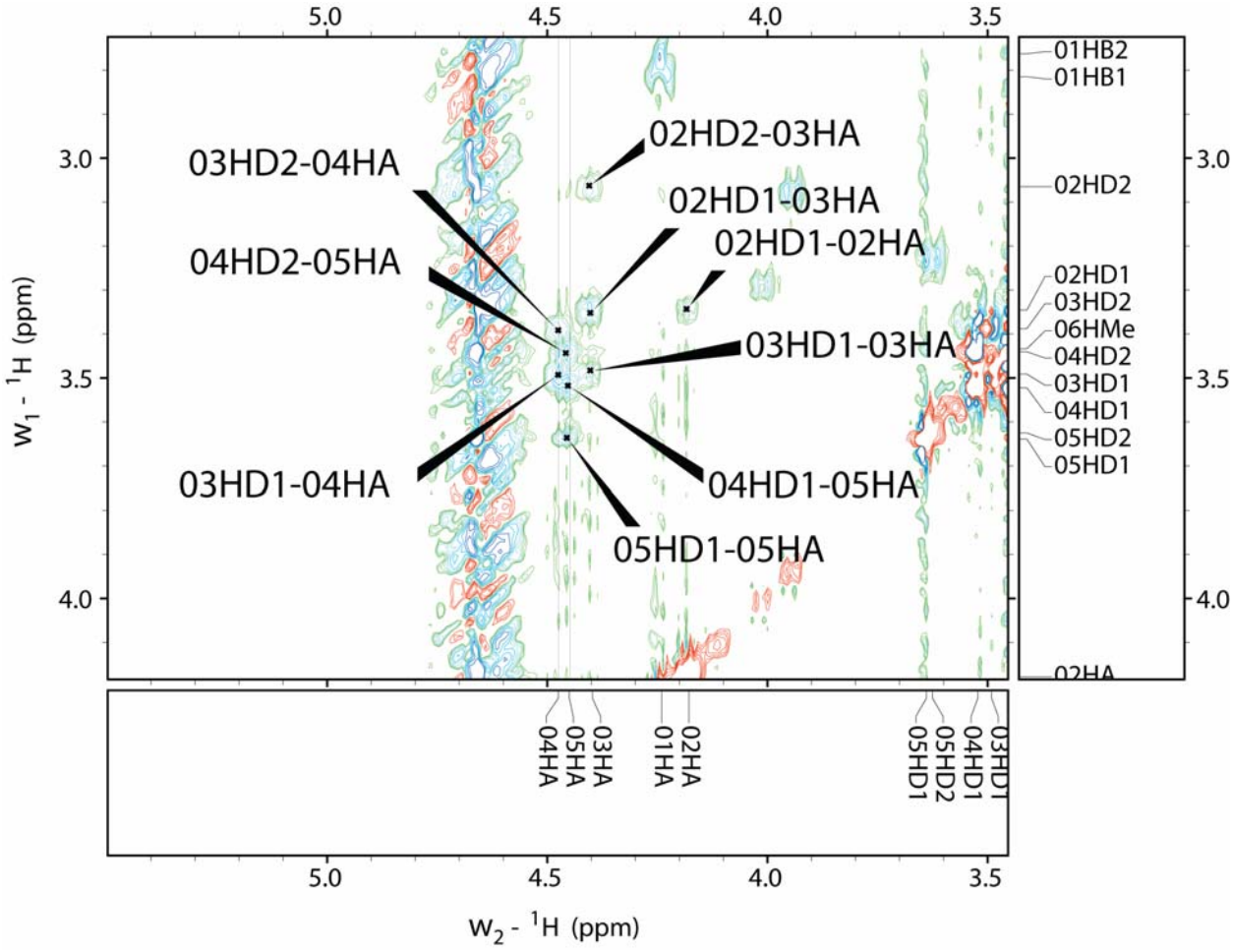

Supplemental Figure 65. 500 MHz ROESY spectrum (expansion 2 of 3) of compound **58**, 2 °C, 9:1 H_2O/D_2O with 0.025 M ND_4COOD:CD_3COOD buffer (pH 4-5)

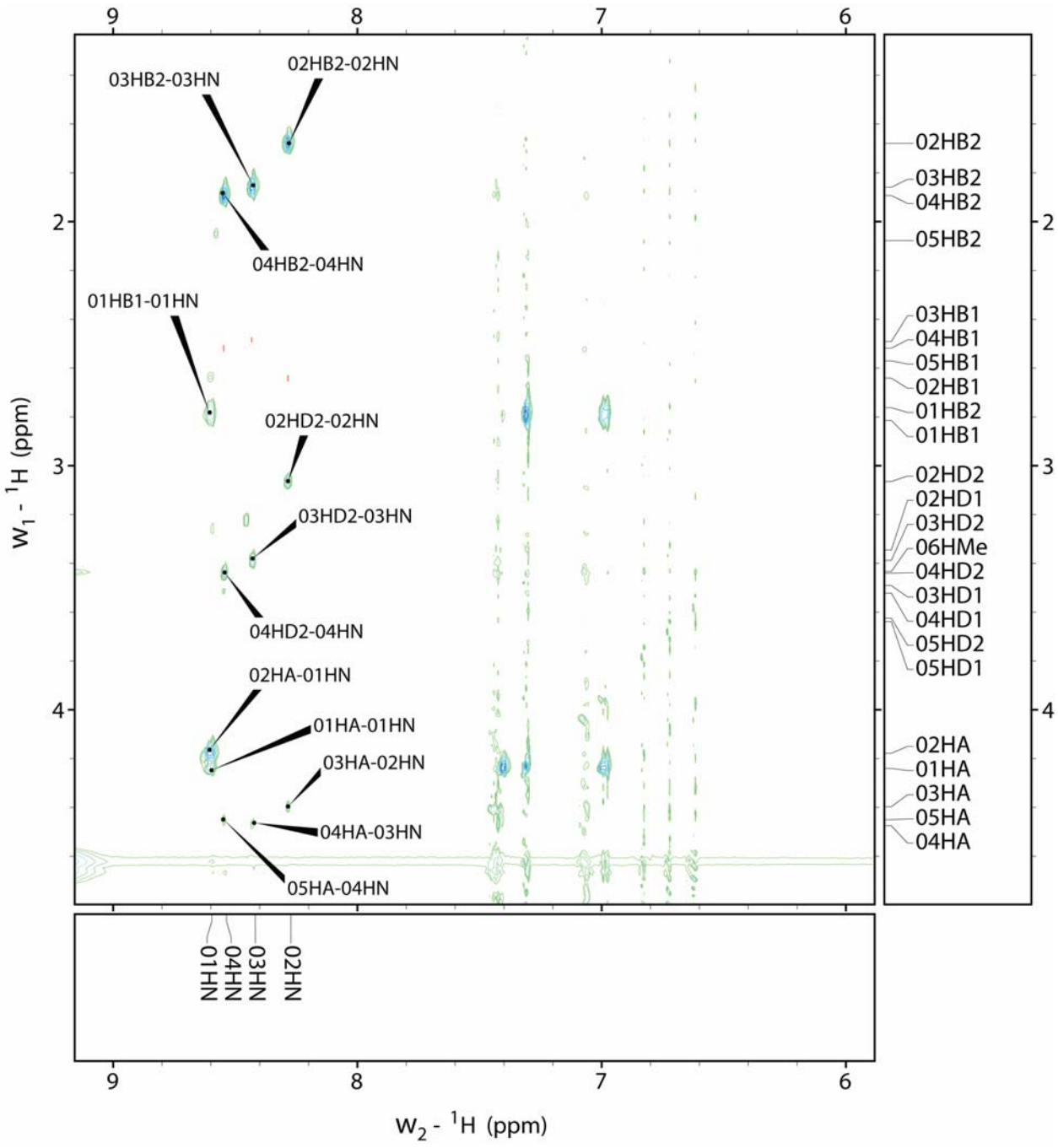

Supplemental Figure 66. 500 MHz ROESY spectrum (expansion 3 of 3) of compound **58**, 2 °C, 9:1 H_2O/D_2O with 0.025 M ND_4COOD:CD_3COOD buffer (pH 4-5)

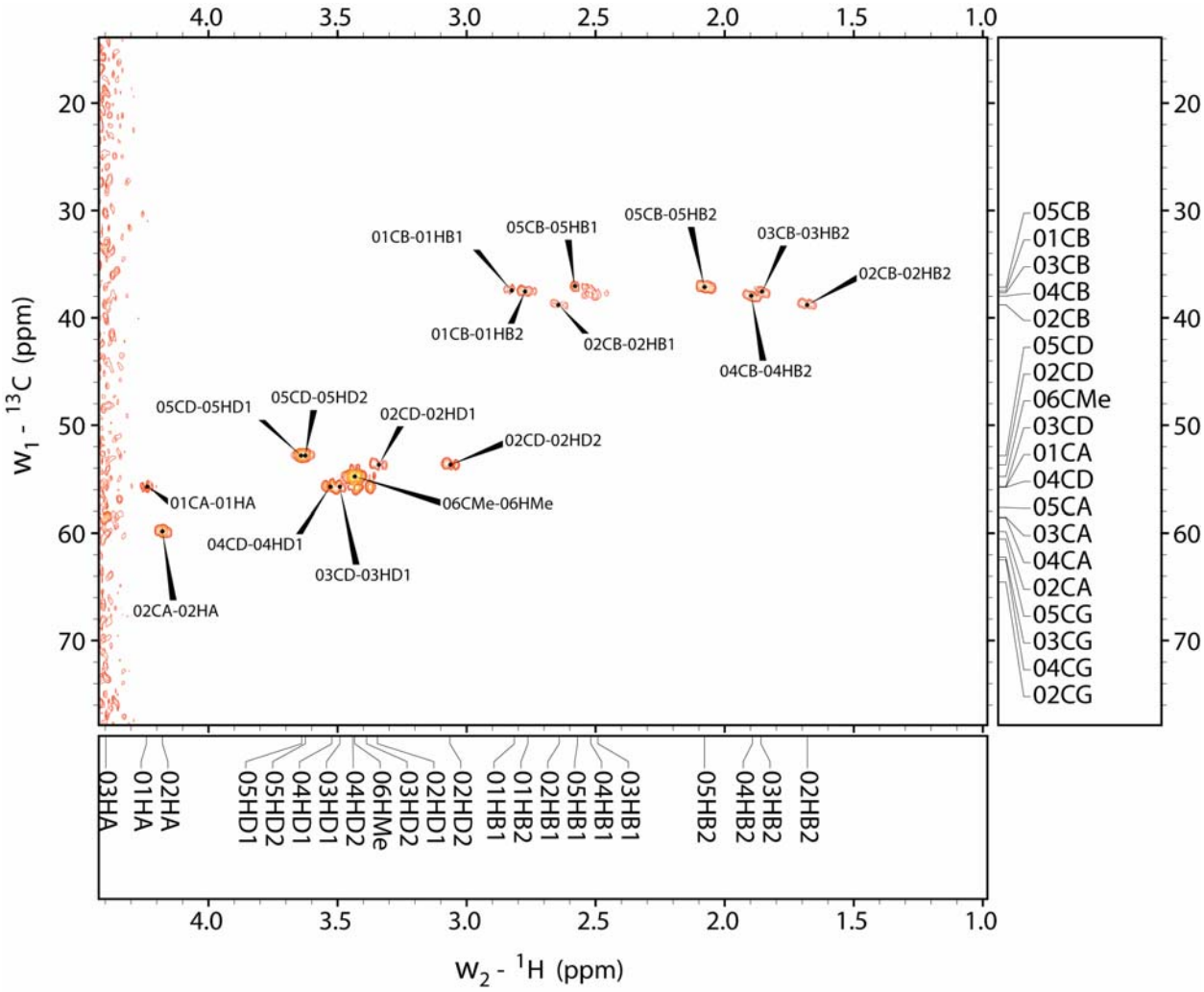

Supplemental Figure 67. 500 MHz HMQC spectrum of compound **58**, 2 °C, 9:1 H_2O/D_2O with 0.025 M ND_4COOD:CD_3COOD buffer (pH 4-5)

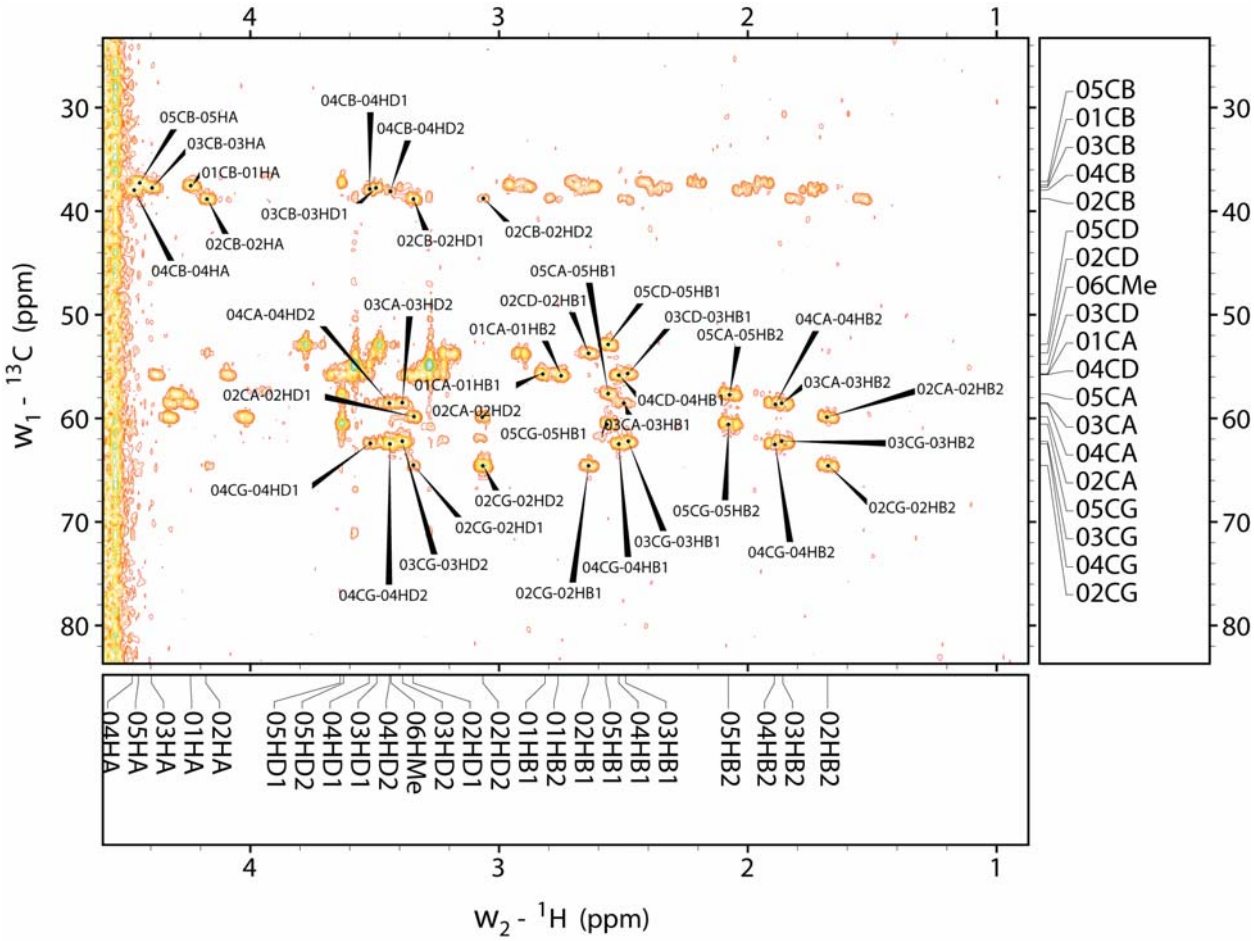

Supplemental Figure 68. 500 MHz HMBC spectrum (expansion 1 of 4) of compound **58**, 2 °C, 9:1 H_2O/D_2O with 0.025 M ND_4COOD:CD_3COOD buffer (pH 4-5)

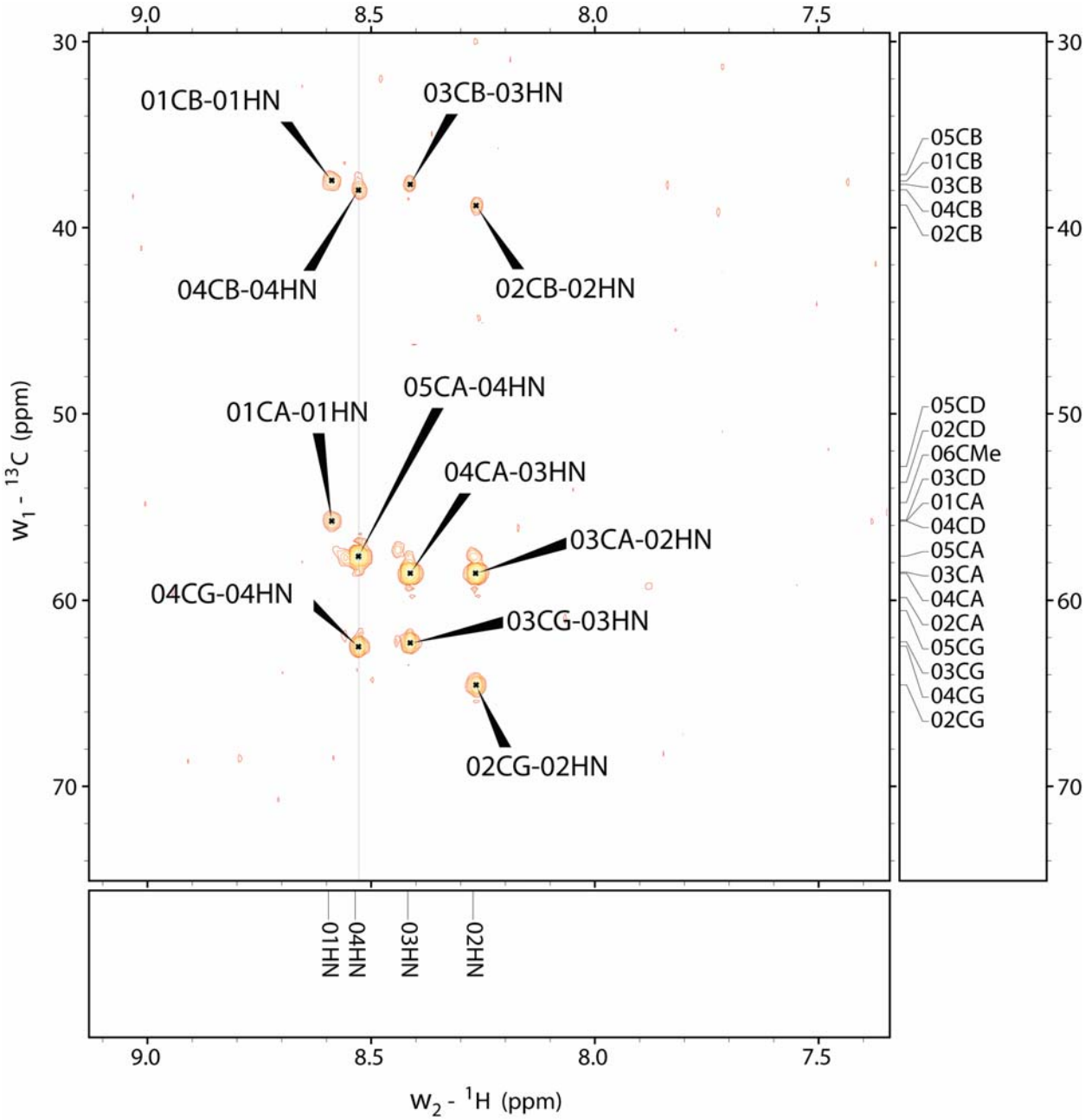

Supplemental Figure 69. 500 MHz HMBC spectrum (expansion 2 of 4) of compound **58**, 2 °C, 9:1 H_2O/D_2O with 0.025 M ND_4COOD:CD_3COOD buffer (pH 4-5)

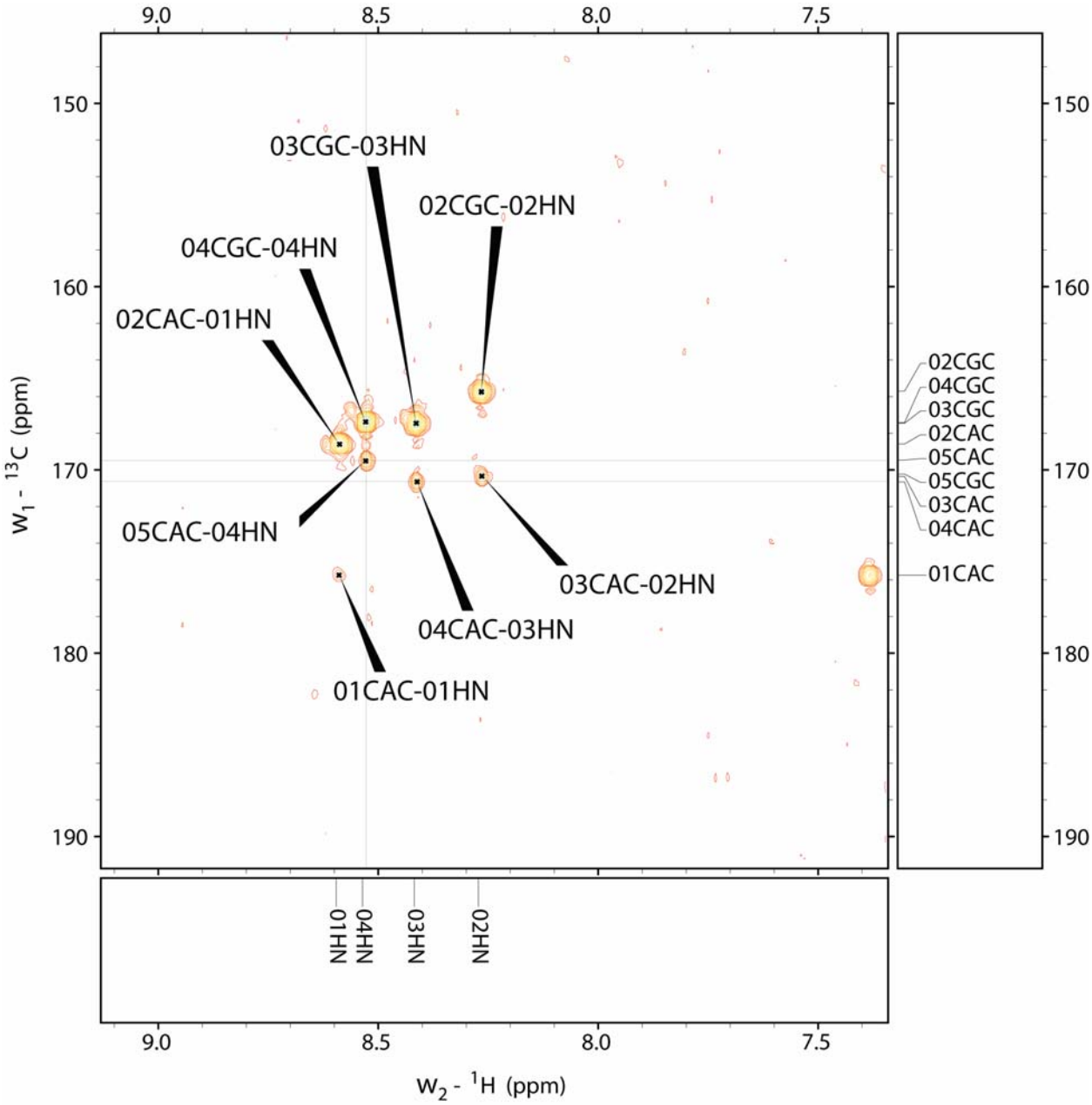

Supplemental Figure 70. 500 MHz HMBC spectrum (expansion 3 of 4) of compound **58**, 2 °C, 9:1 H_2O/D_2O with 0.025 M ND_4COOD:CD_3COOD buffer (pH 4-5)

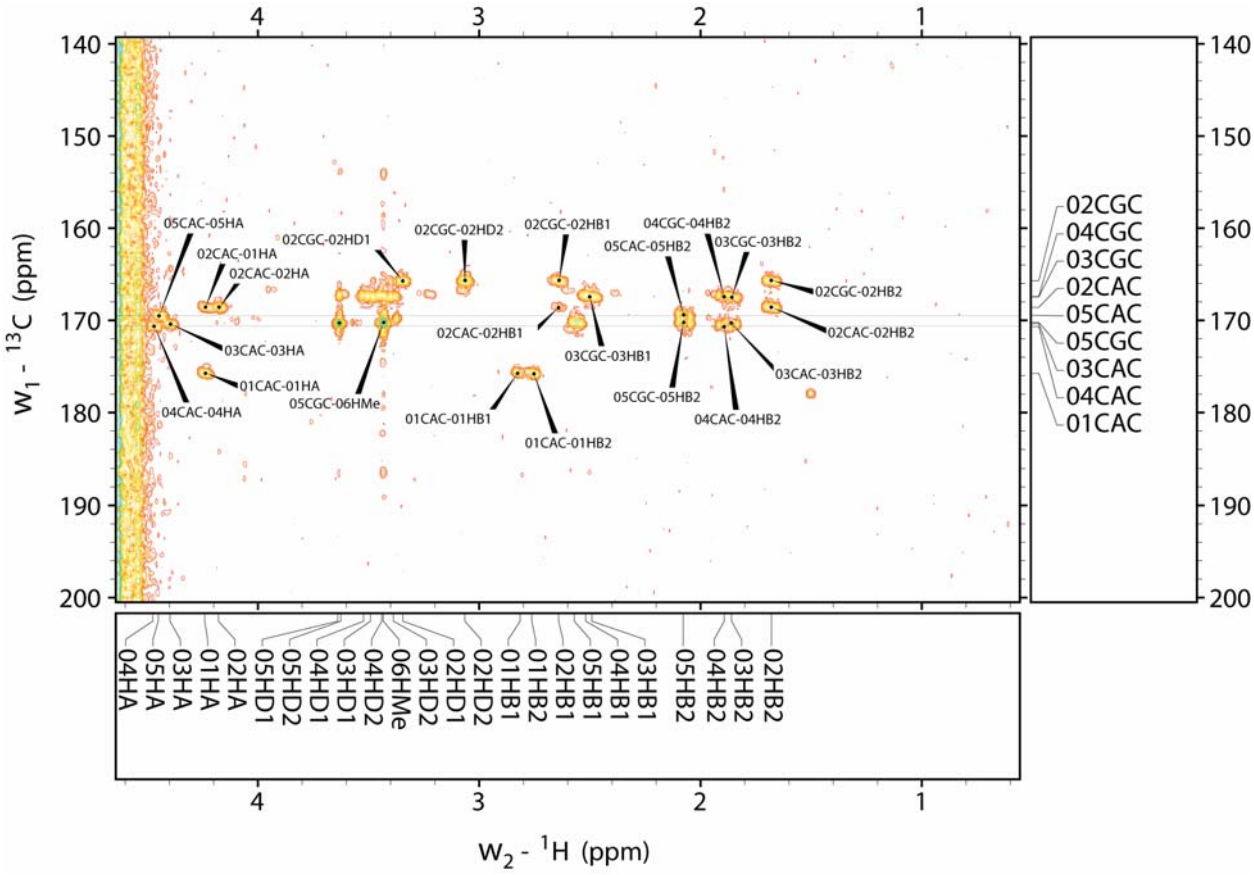

Supplemental Figure 71. 500 MHz HMBC spectrum (expansion 4 of 4) of compound **58**, 2 °C, 9:1 H_2O/D_2O with 0.025 M ND_4COOD:CD_3COOD buffer (pH 4-5)

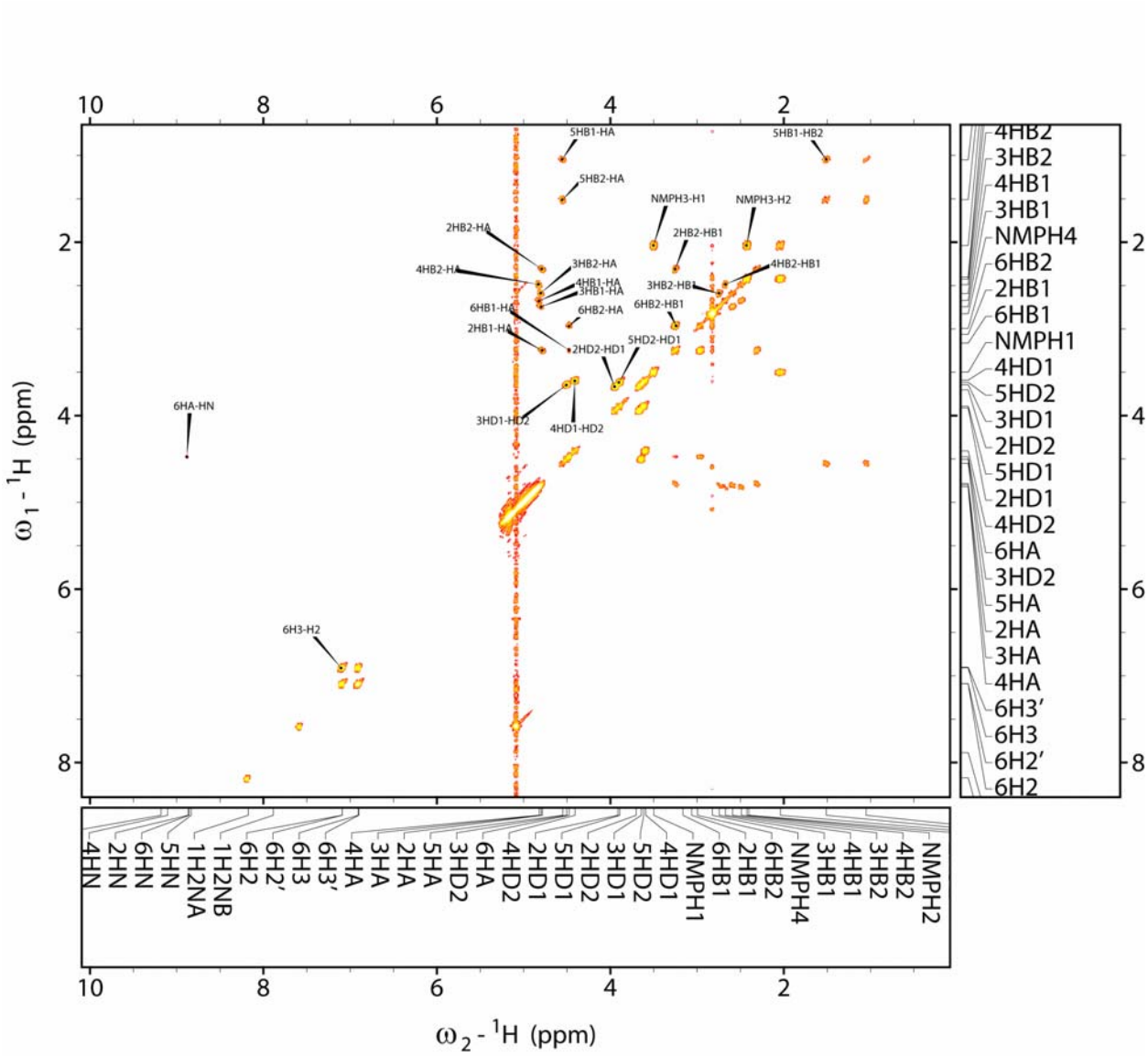

Supplemental Figure 72. Oligomer **61**, 500 MHz COSY spectrum

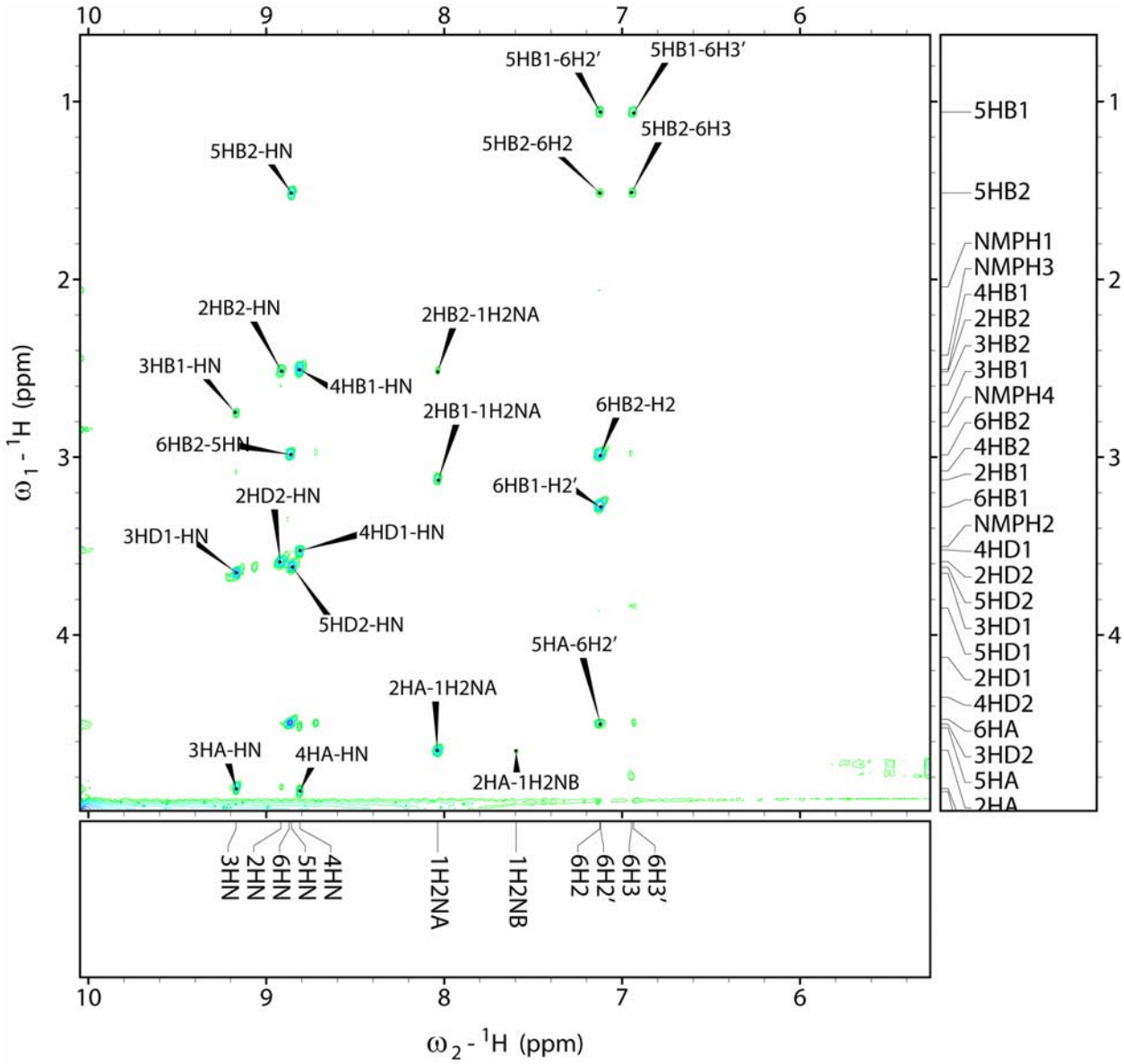

Supplemental Figure 73: Oligomer **61**, 600 MHz ROESY spectrum (1 of 2)

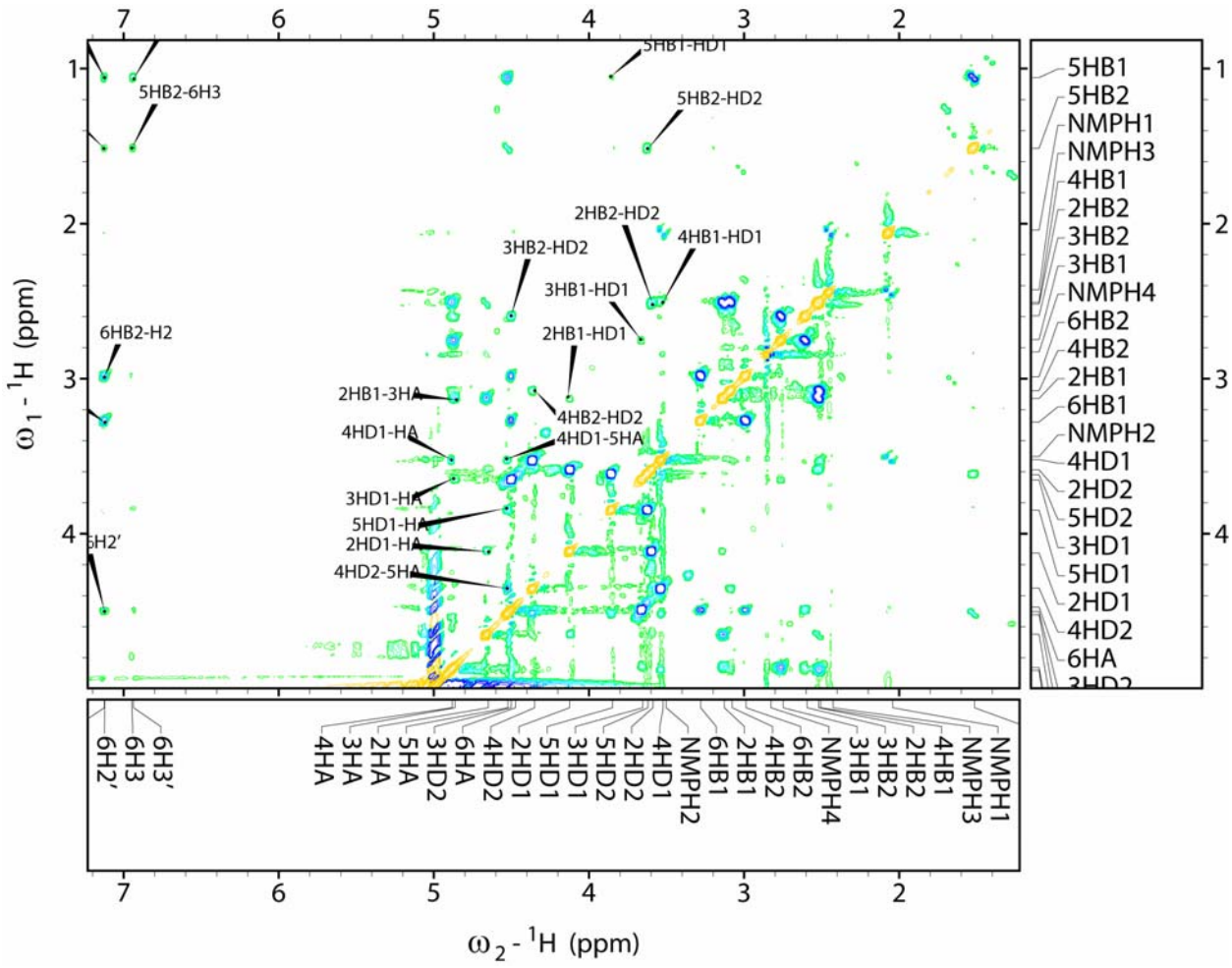

Supplemental Figure 74: Oligomer **61**, 600 MHz ROESY spectrum (2 of 2)

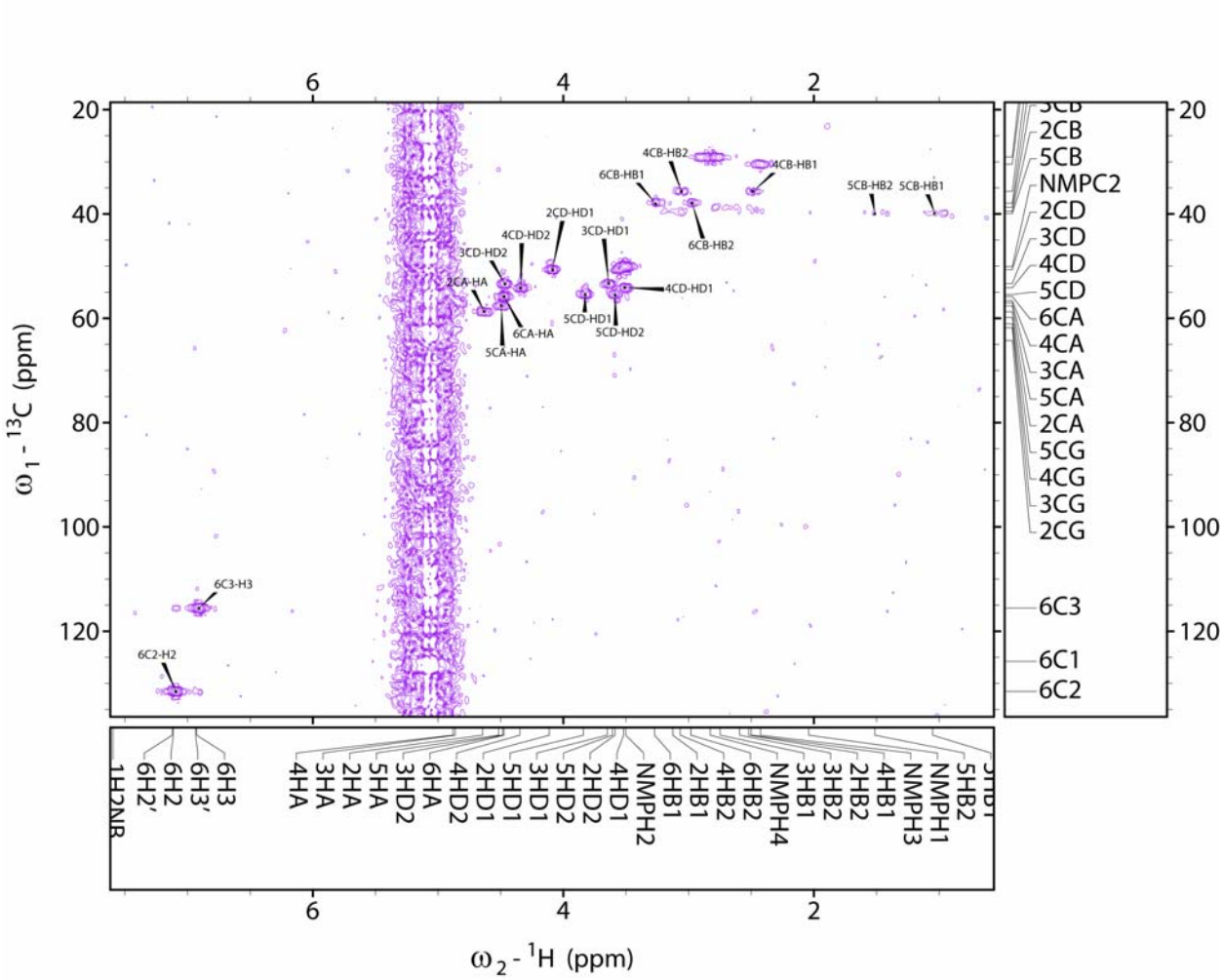

Supplemental Figure 75: Oligomer **61**, 500 MHz HMQC spectrum

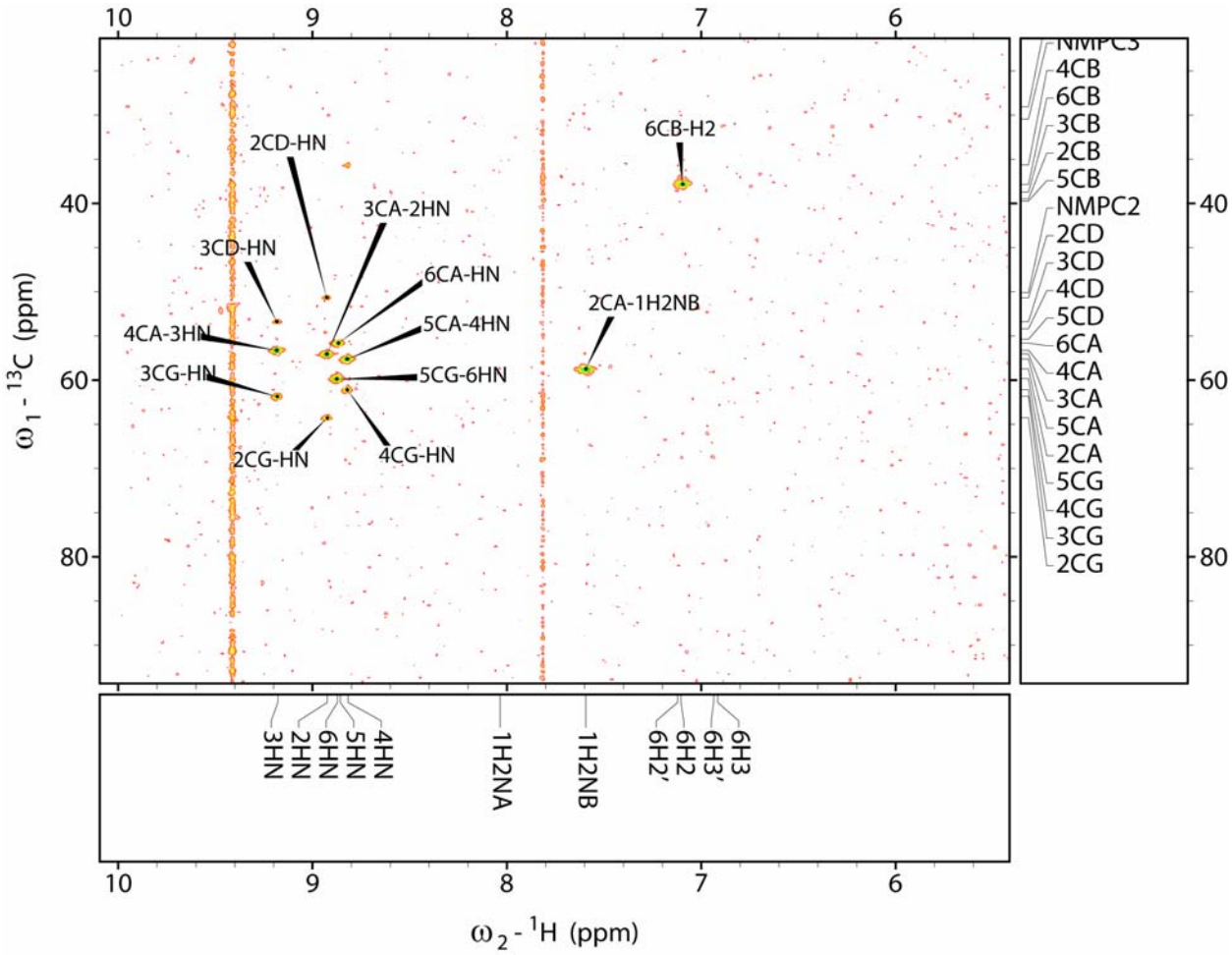

Supplemental Figure 76. Oligomer **61**, 500 MHz HMBC spectrum (1 of 4)

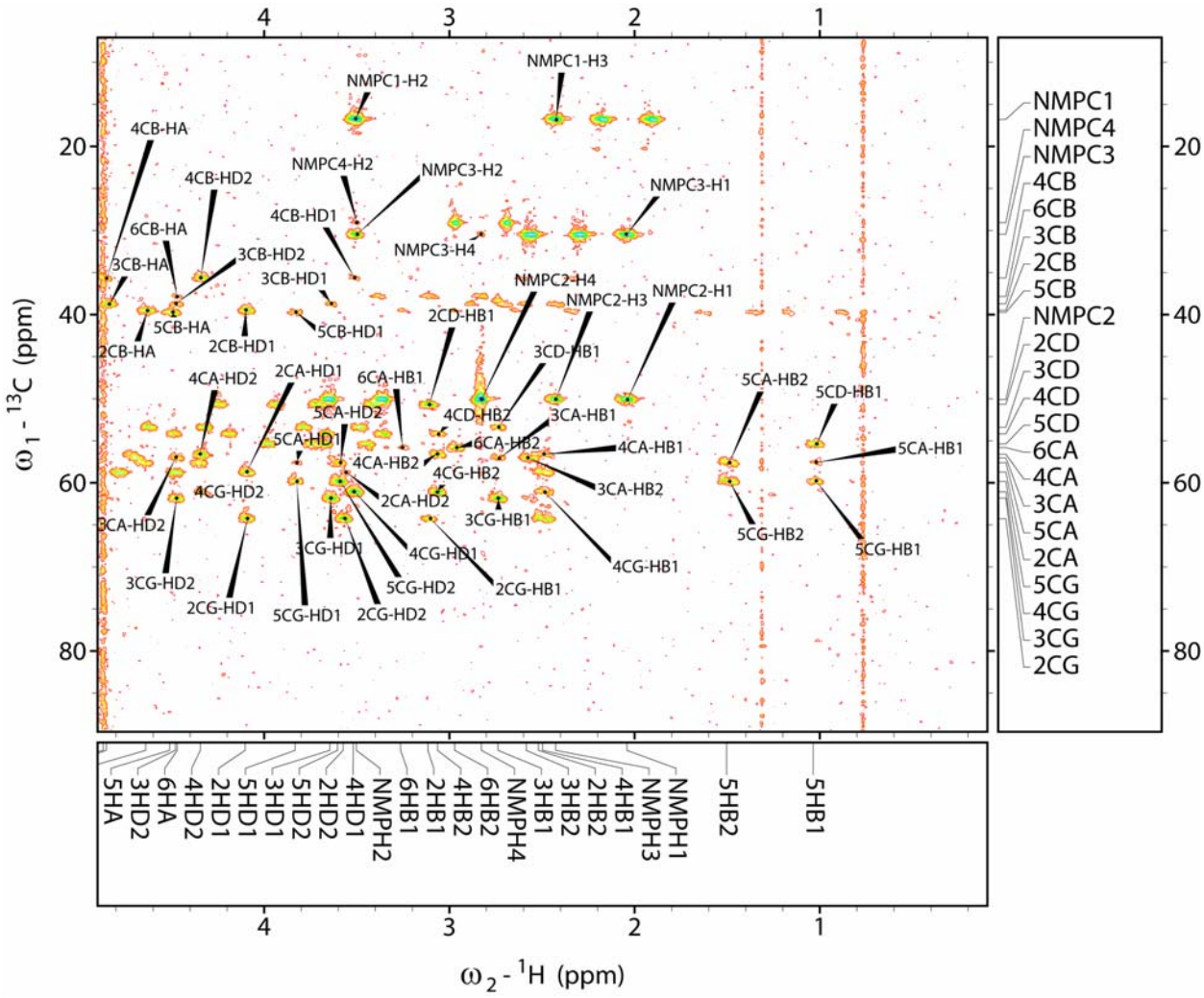

Supplemental Figure 77. Oligomer **61**, 500 MHz HMBC spectrum (2 of 4)

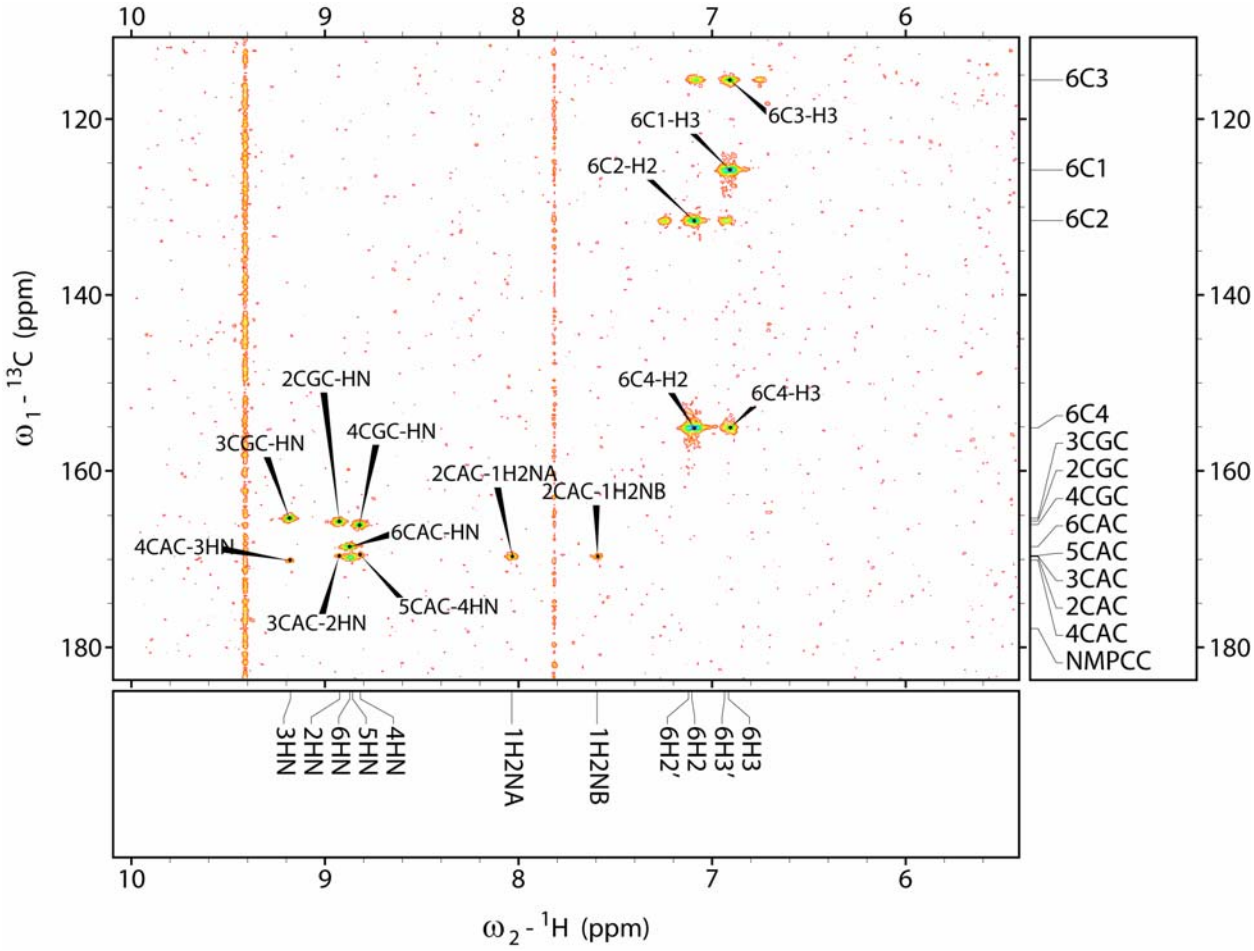

Supplemental Figure 78: Oligomer **61**, 500 MHz HMBC spectrum (3 of 4)

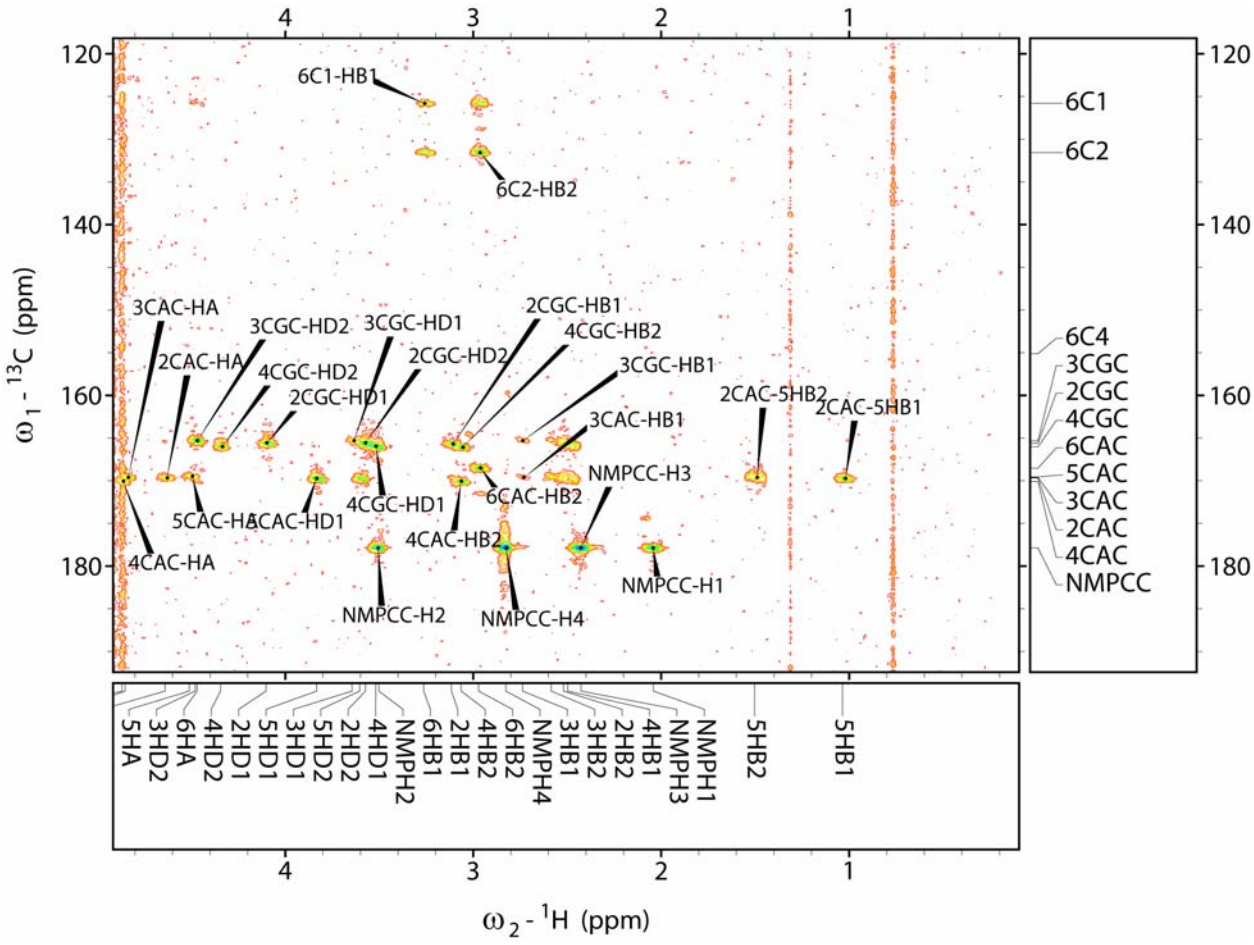

Supplemental Figure 79: Oligomer **61**, 500 MHz HMBC spectrum (4 of 4)

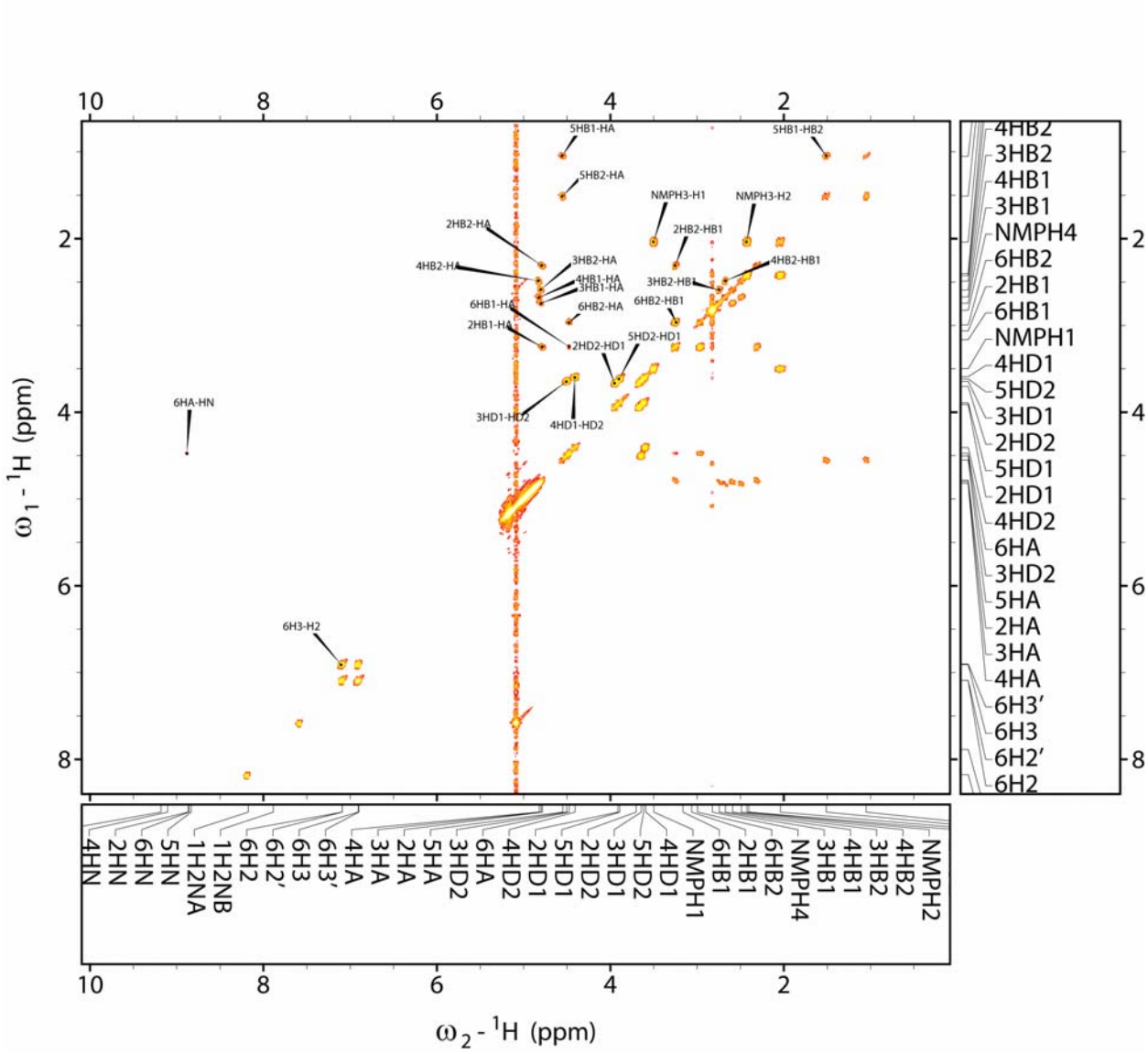

Supplemental Figure 80. Oligomer **62**, 500 MHz COSY spectrum

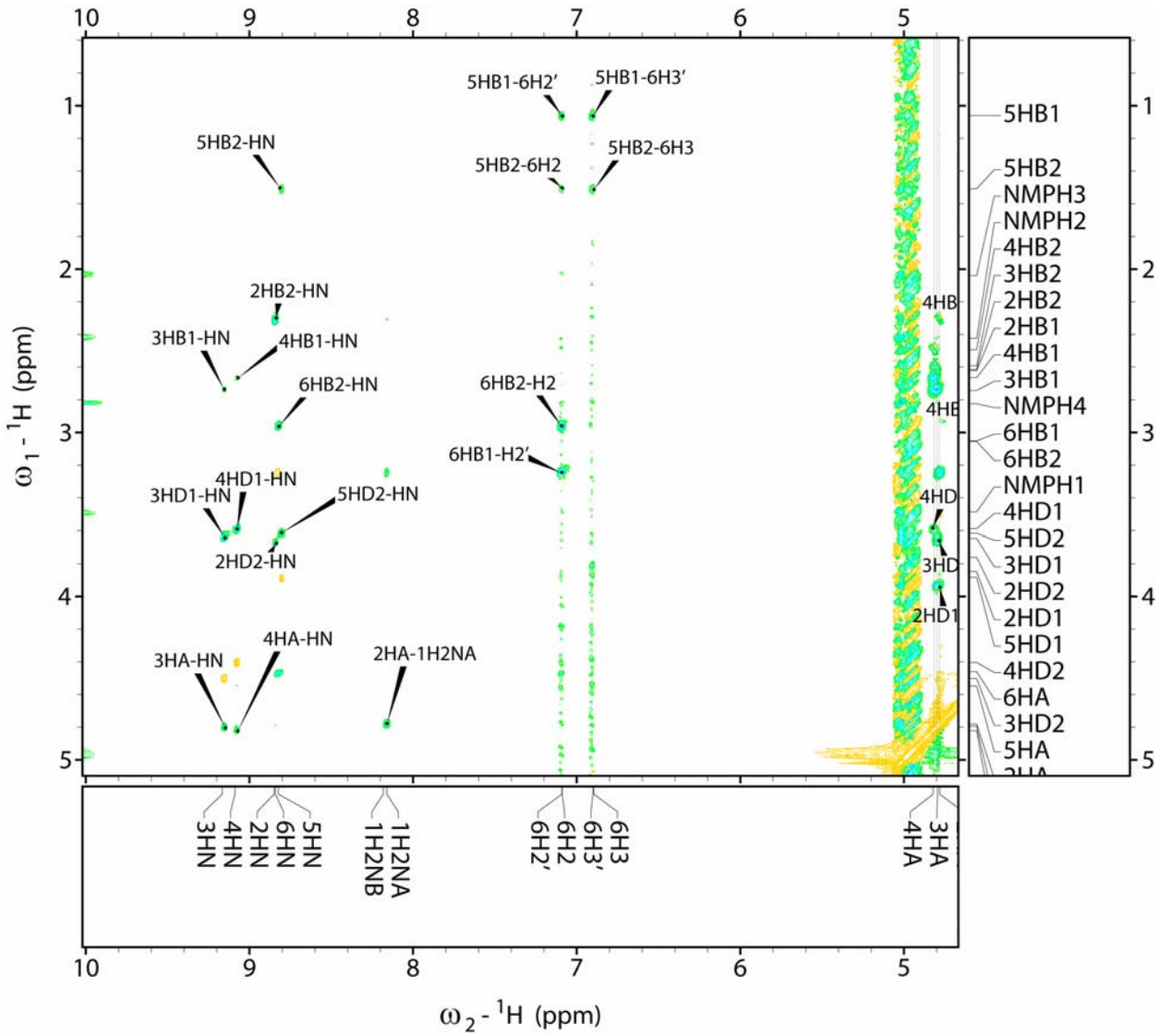

Supplemental Figure 81. Oligomer **62**, 600 MHz ROESY spectrum (1 of 2)

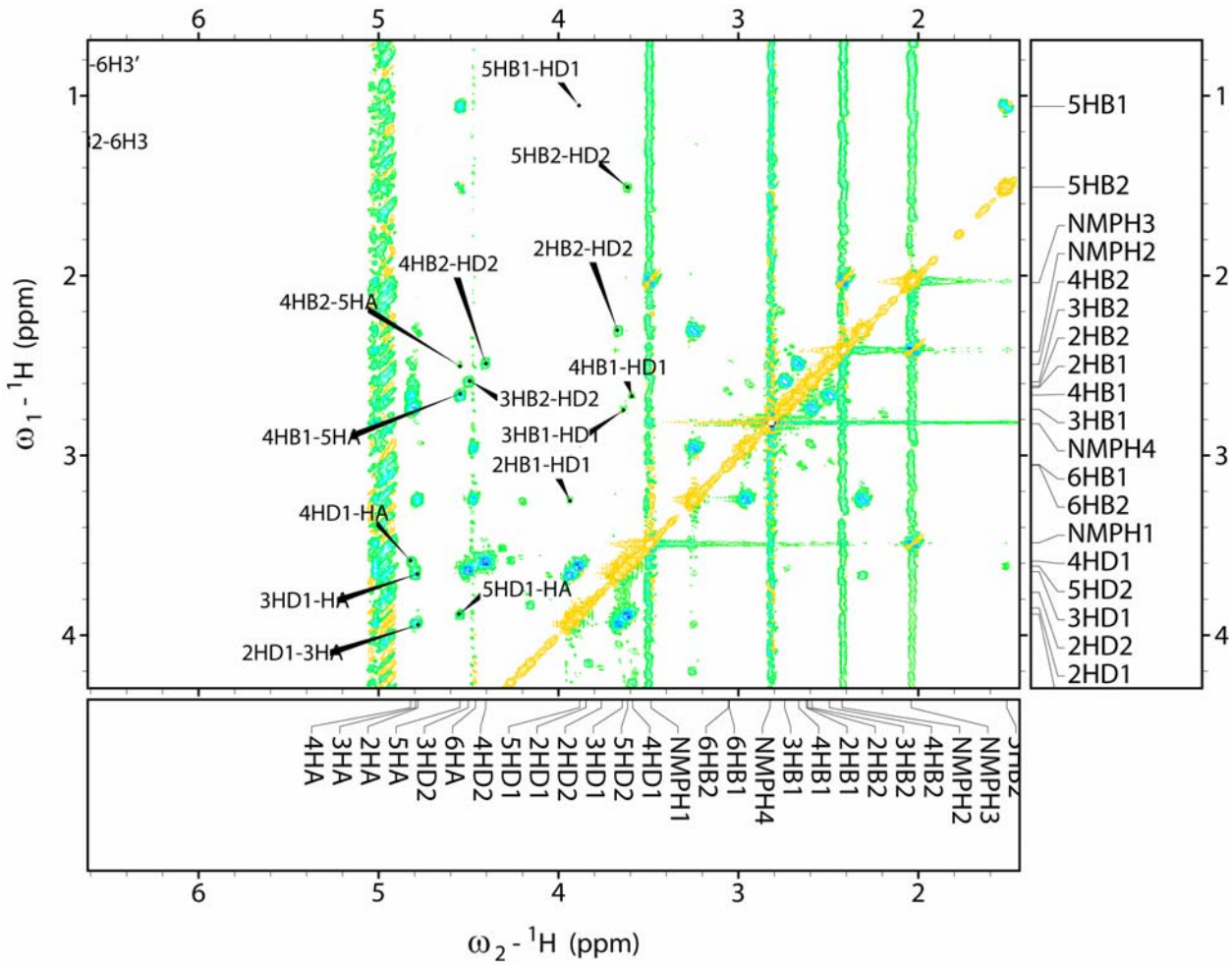

Supplemental Figure 82: Oligomer **62**, 600 MHz ROESY spectrum (2 of 2)

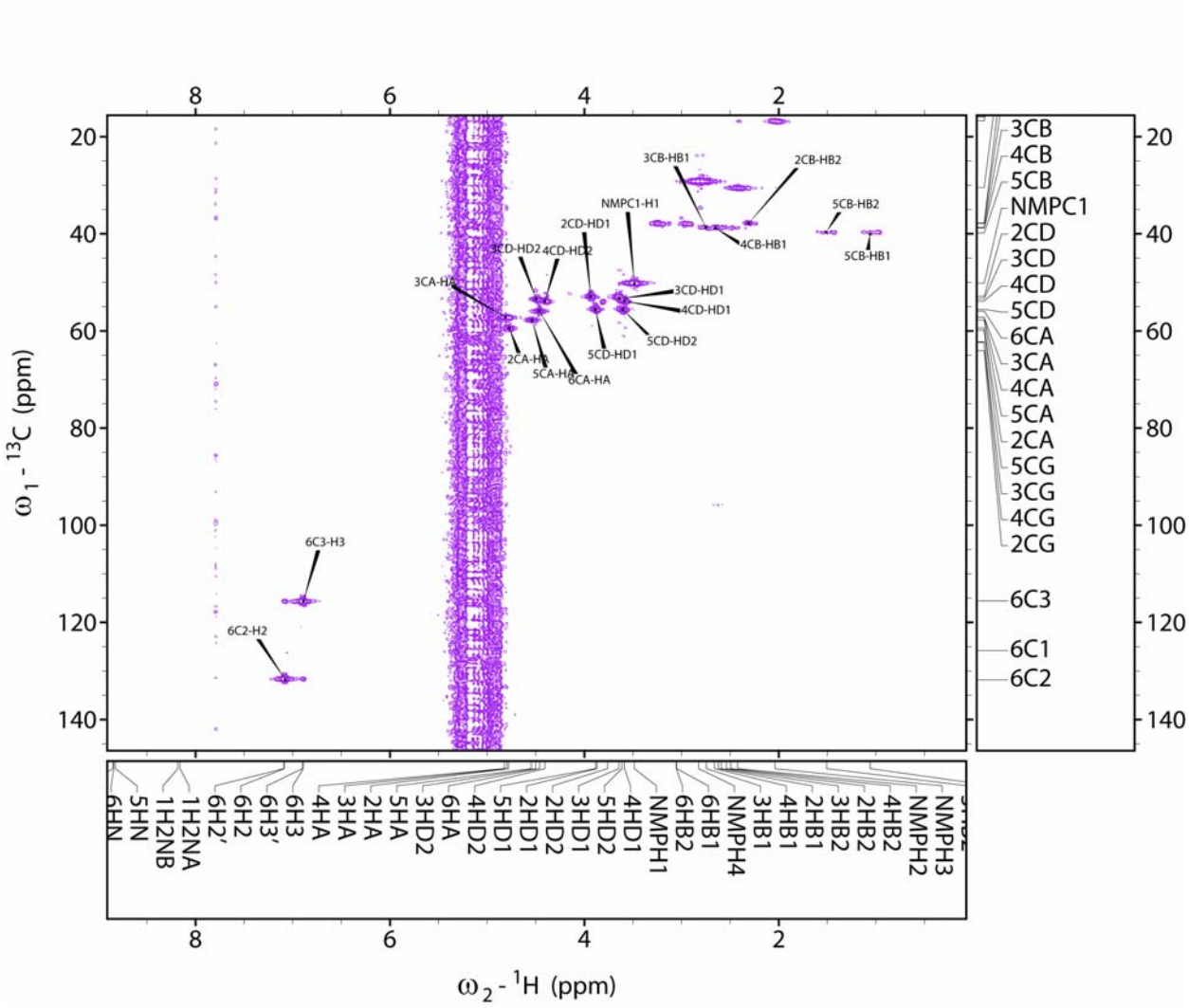

Supplemental Figure 83: Oligomer **62**, 500 MHz HMQC spectrum

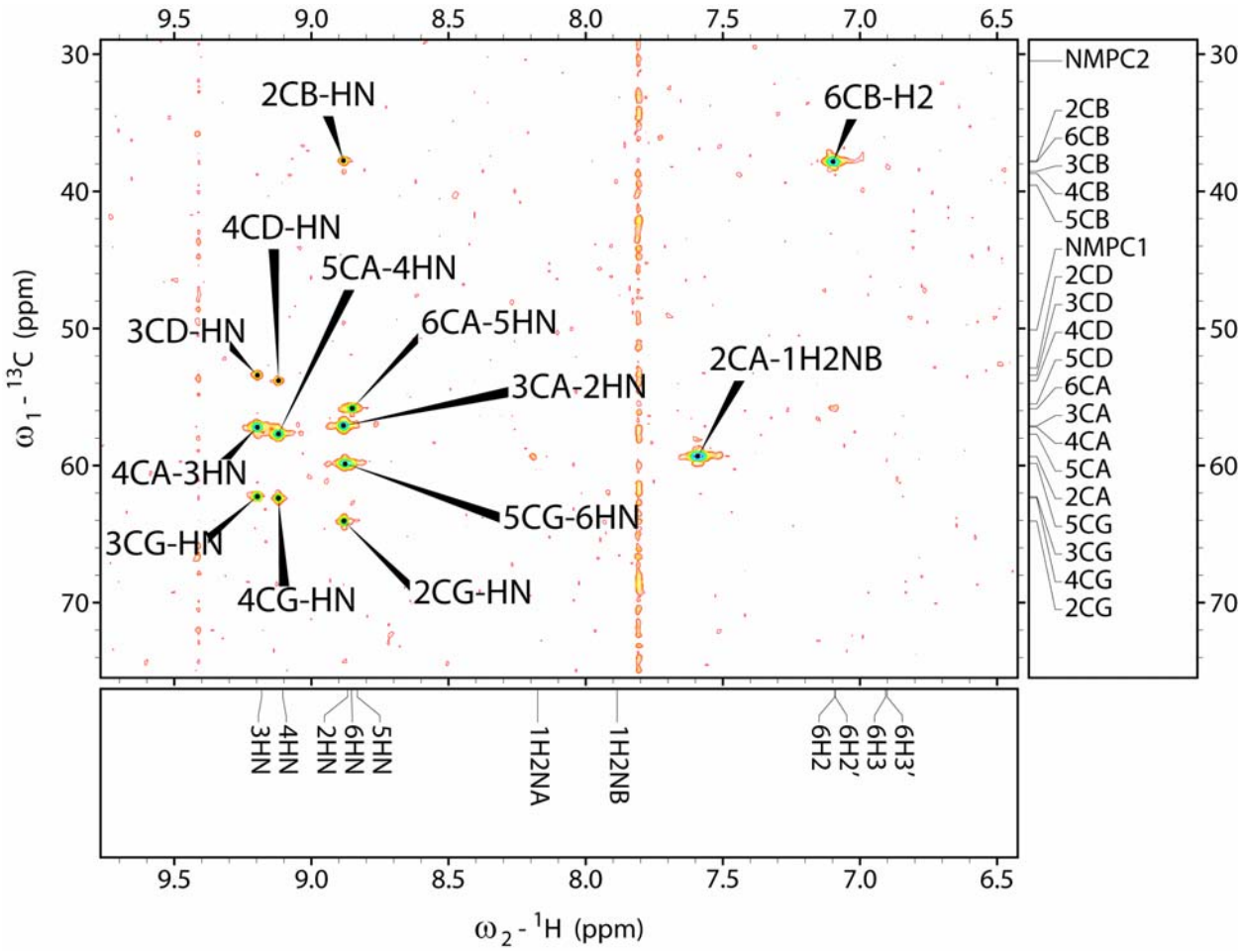

Supplemental Figure 84. Oligomer **62**, 500 MHz HMBC spectrum (1 of 4)

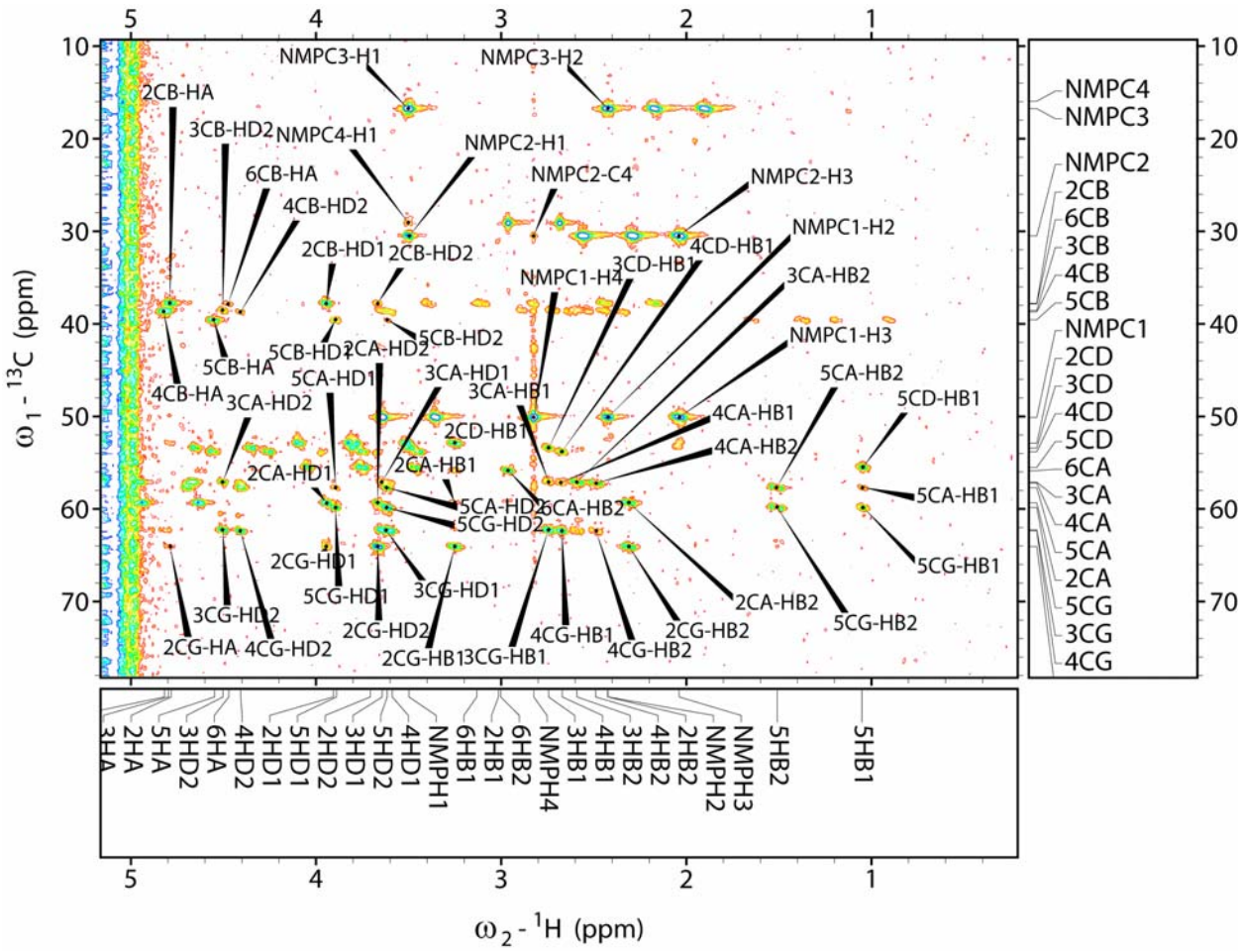

Supplemental Figure 85. Oligomer **62**, 500 MHz HMBC spectrum (2 of 4)

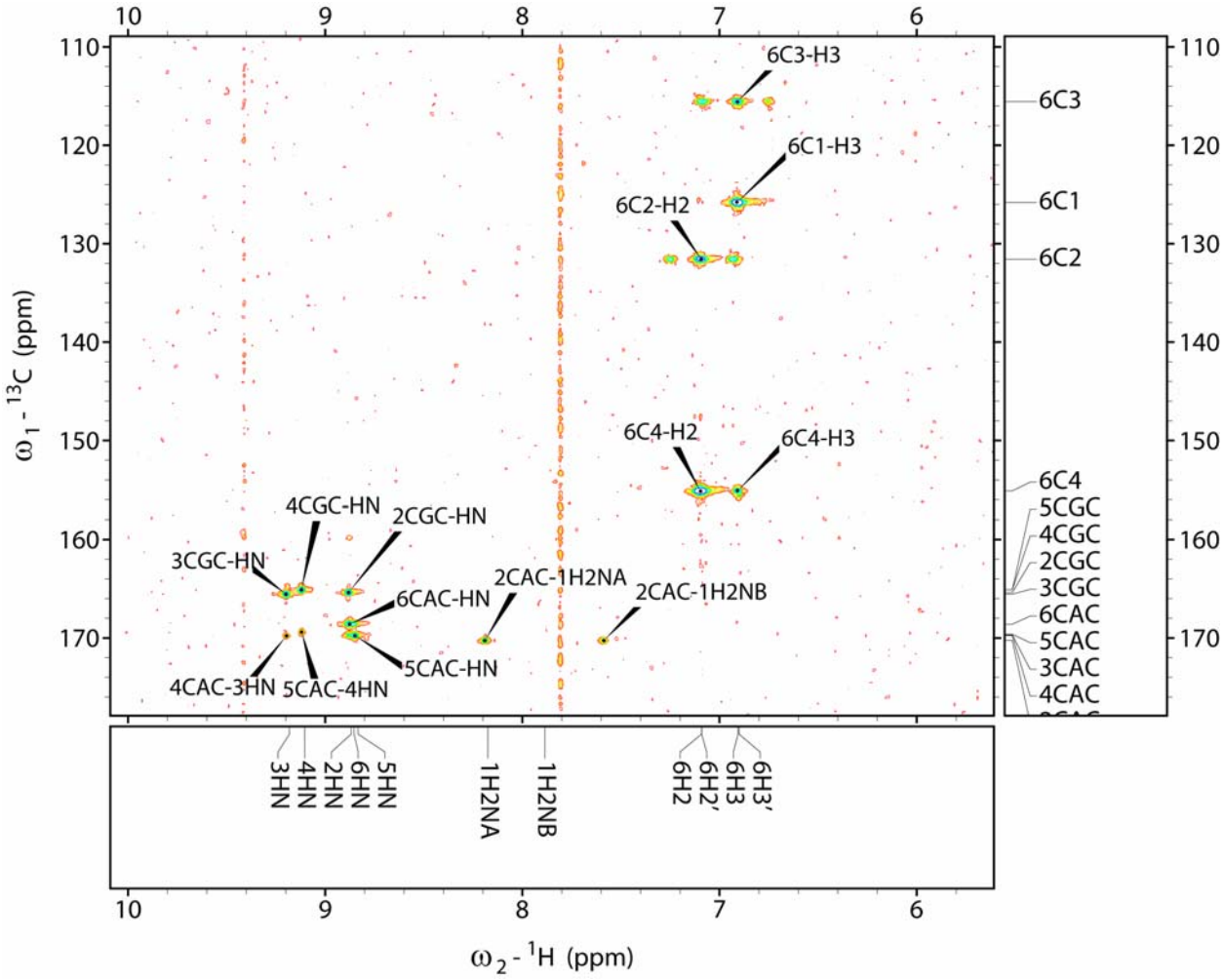

Supplemental Figure 86. Oligomer **62**, 500 MHz HMBC spectrum (3 of 4)

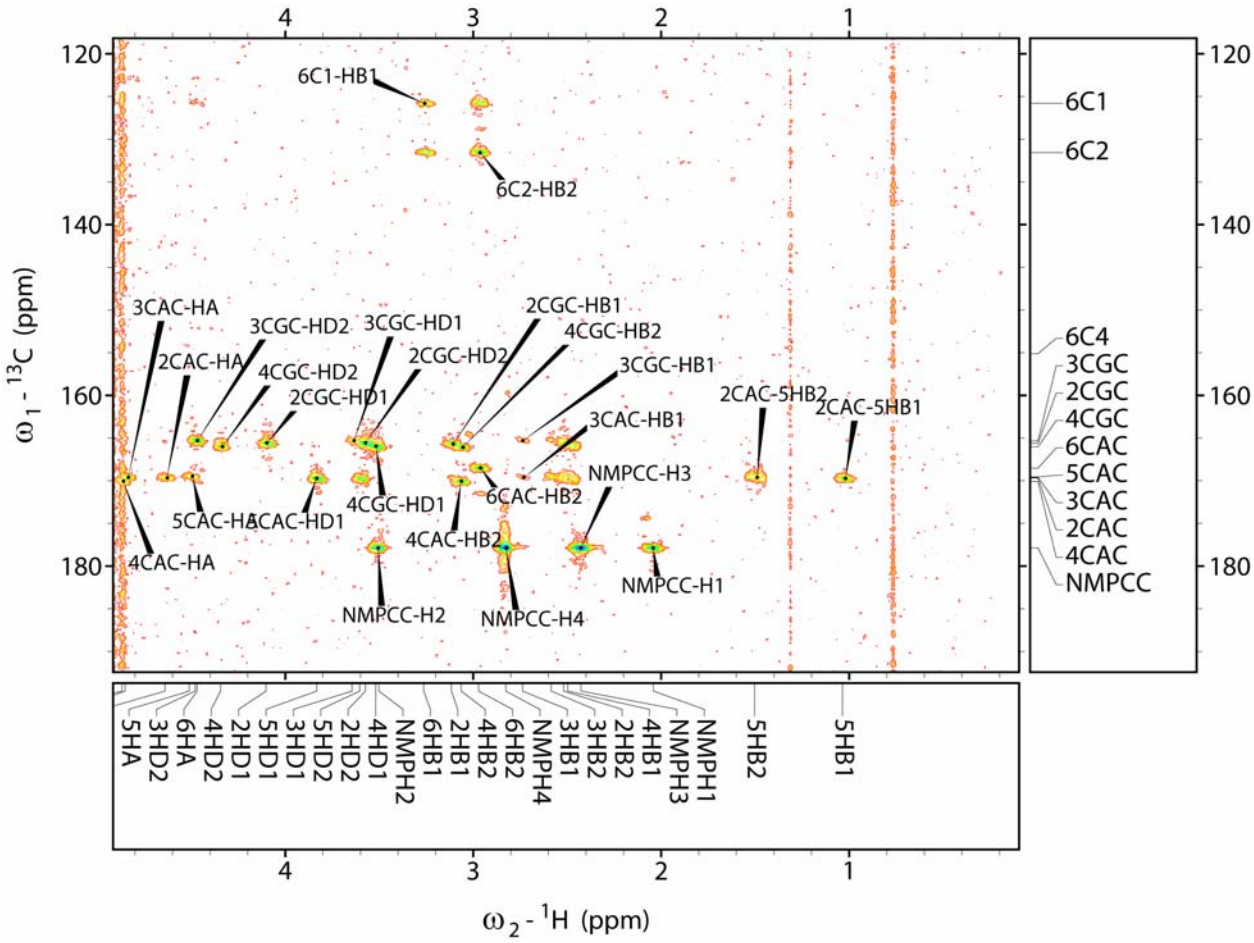

Supplemental Figure 87. Oligomer **62**, 500 MHz HMBC spectrum (4 of 4)

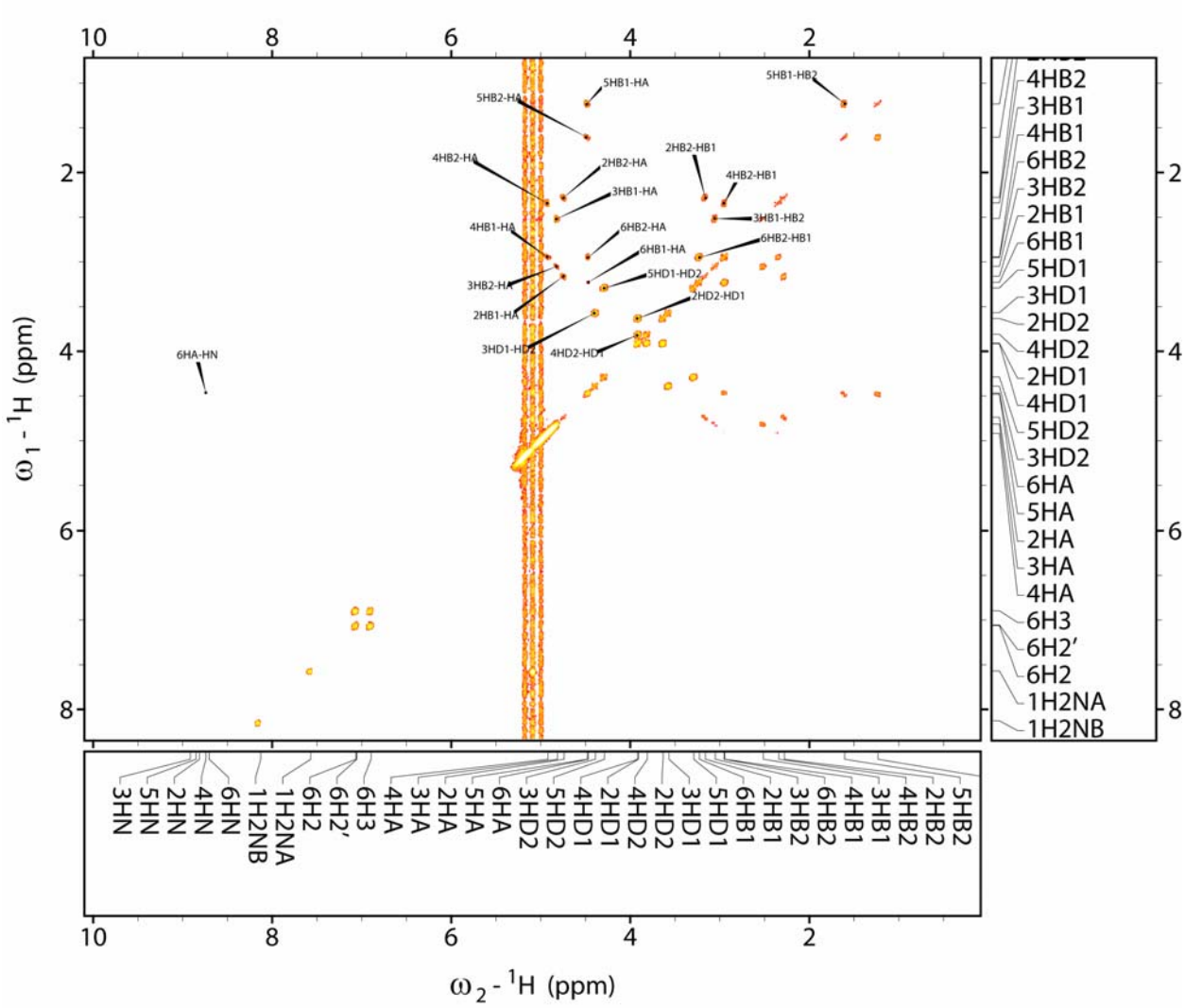

Supplemental Figure 88. Oligomer **63**, 500 MHz COSY spectrum

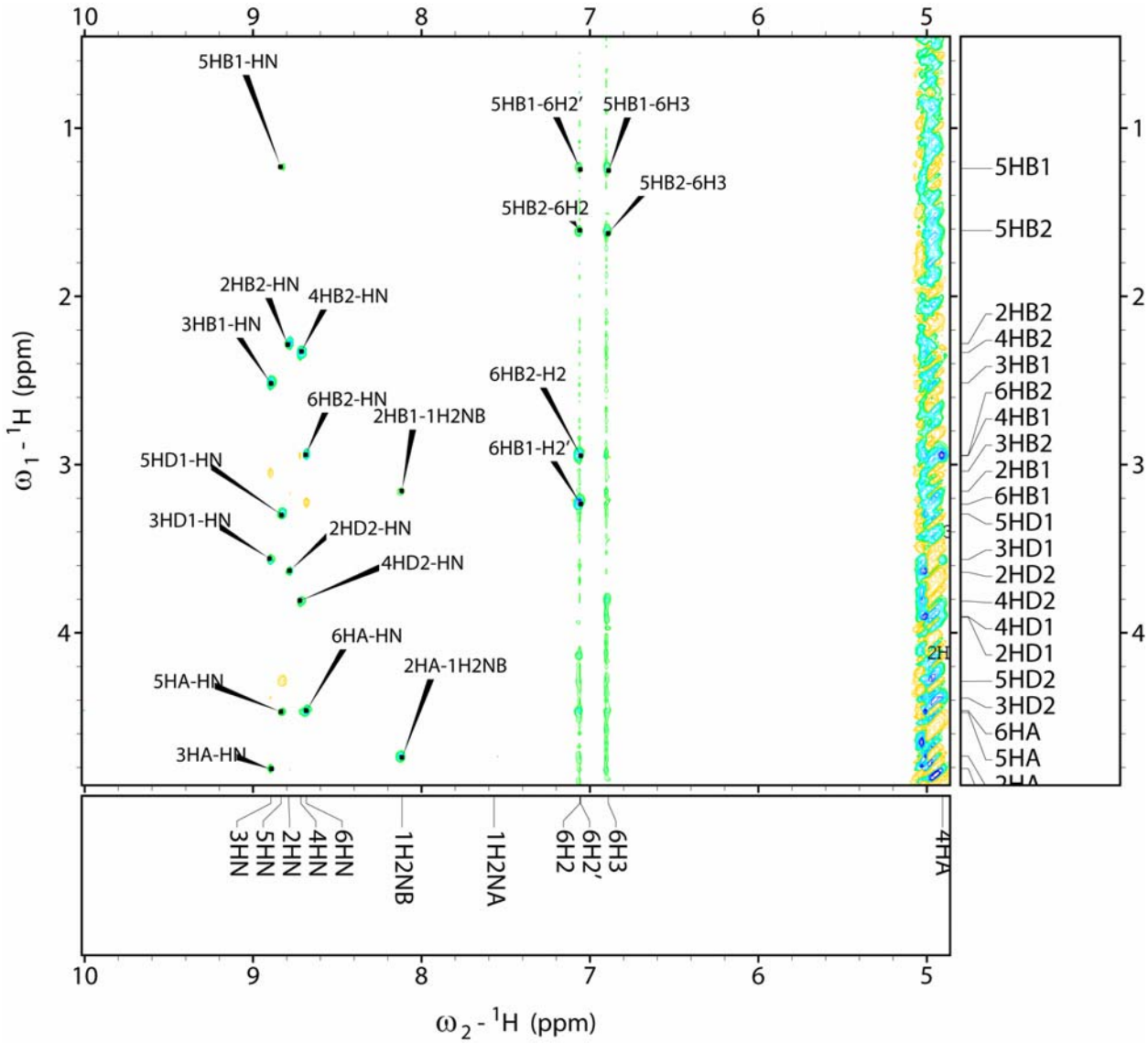

Supplemental Figure 89. Oligomer **63**, 600 MHz ROESY spectrum (1 of 2)

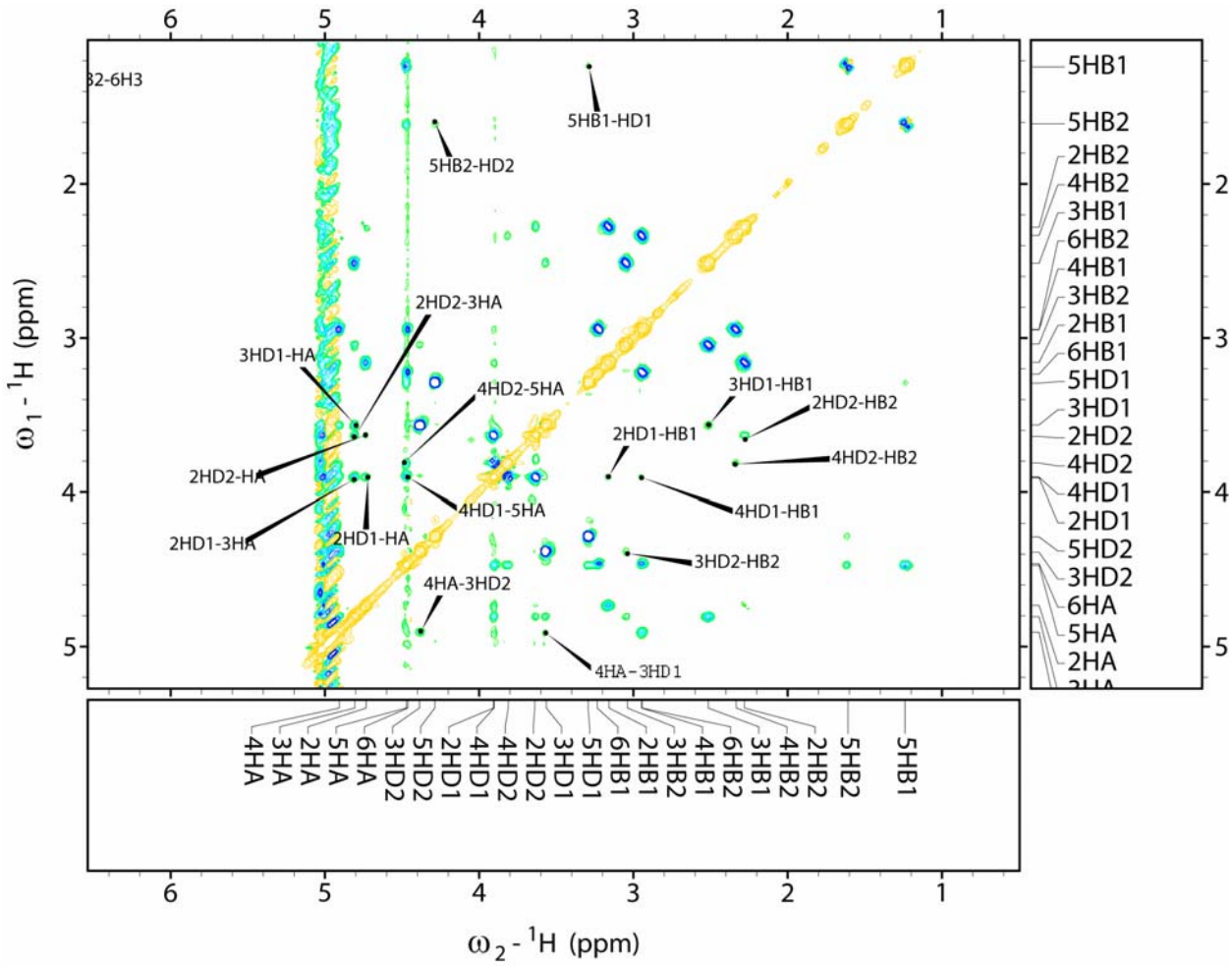

Supplemental Figure 90. Oligomer **63**, 600 MHz ROESY spectrum (2 of 2)

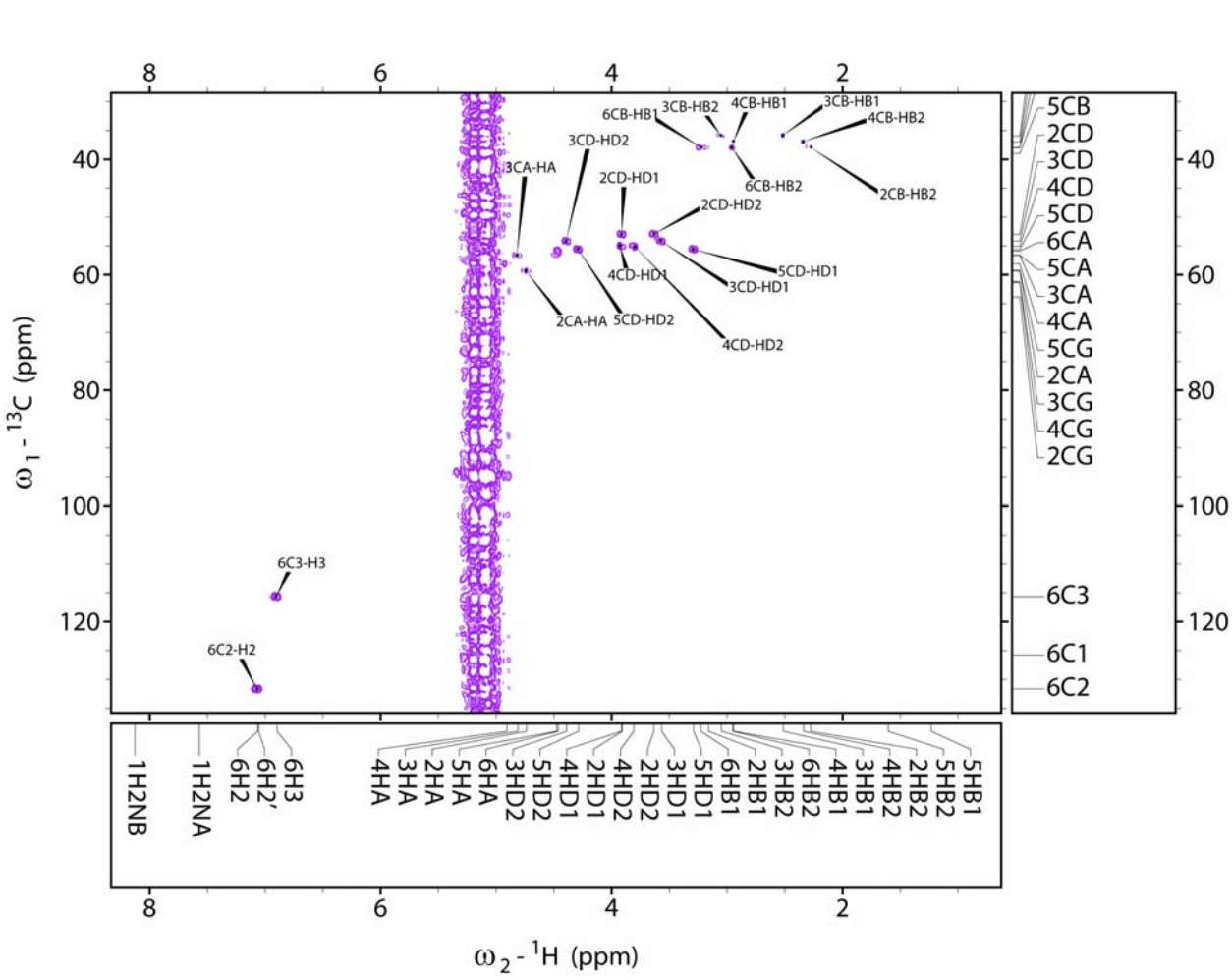

Supplemental Figure 91. Oligomer **63**, 500 MHz HMQC spectrum

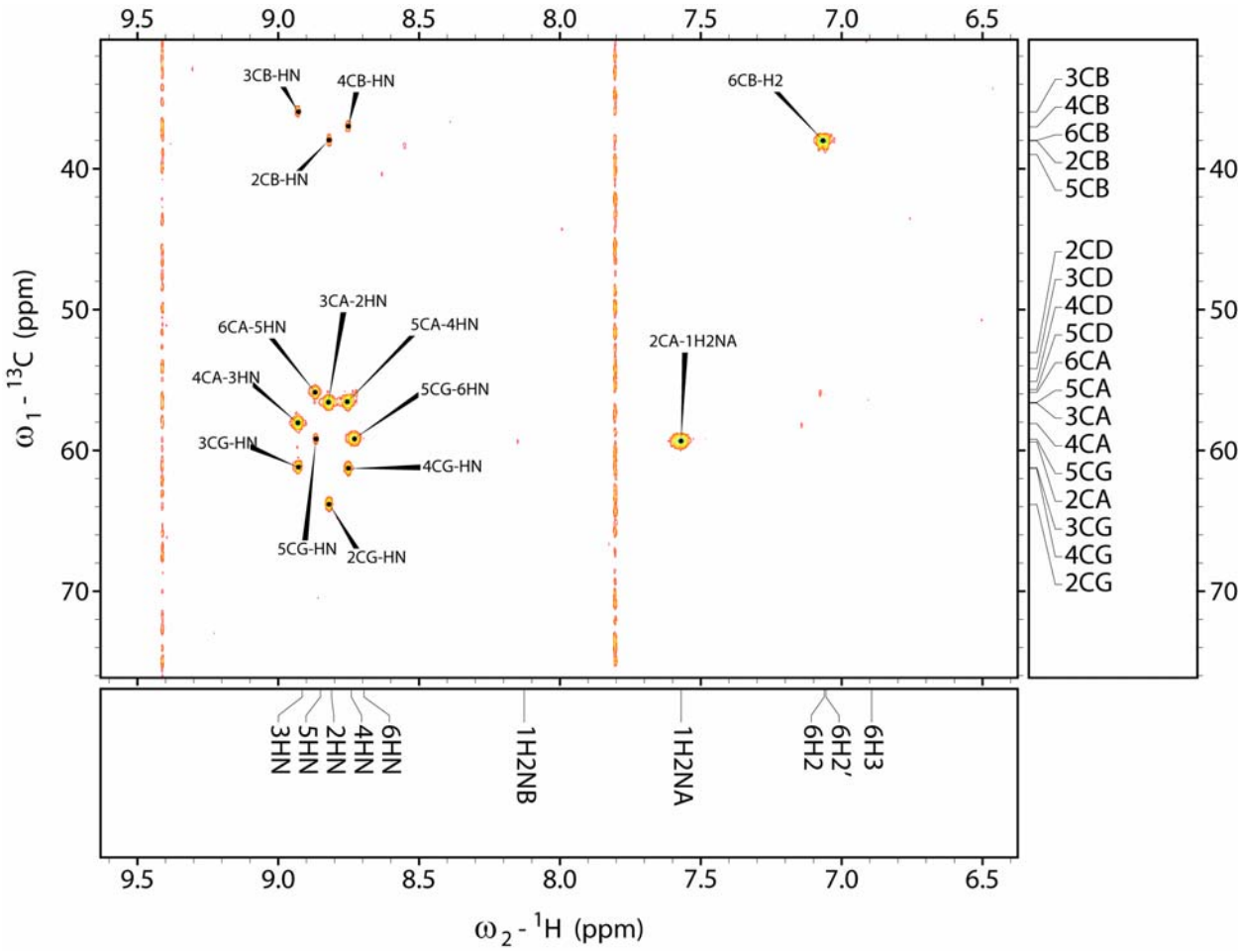

Supplemental Figure 92. Oligomer **63**, 500 MHz HMBC spectrum (1 of 4)

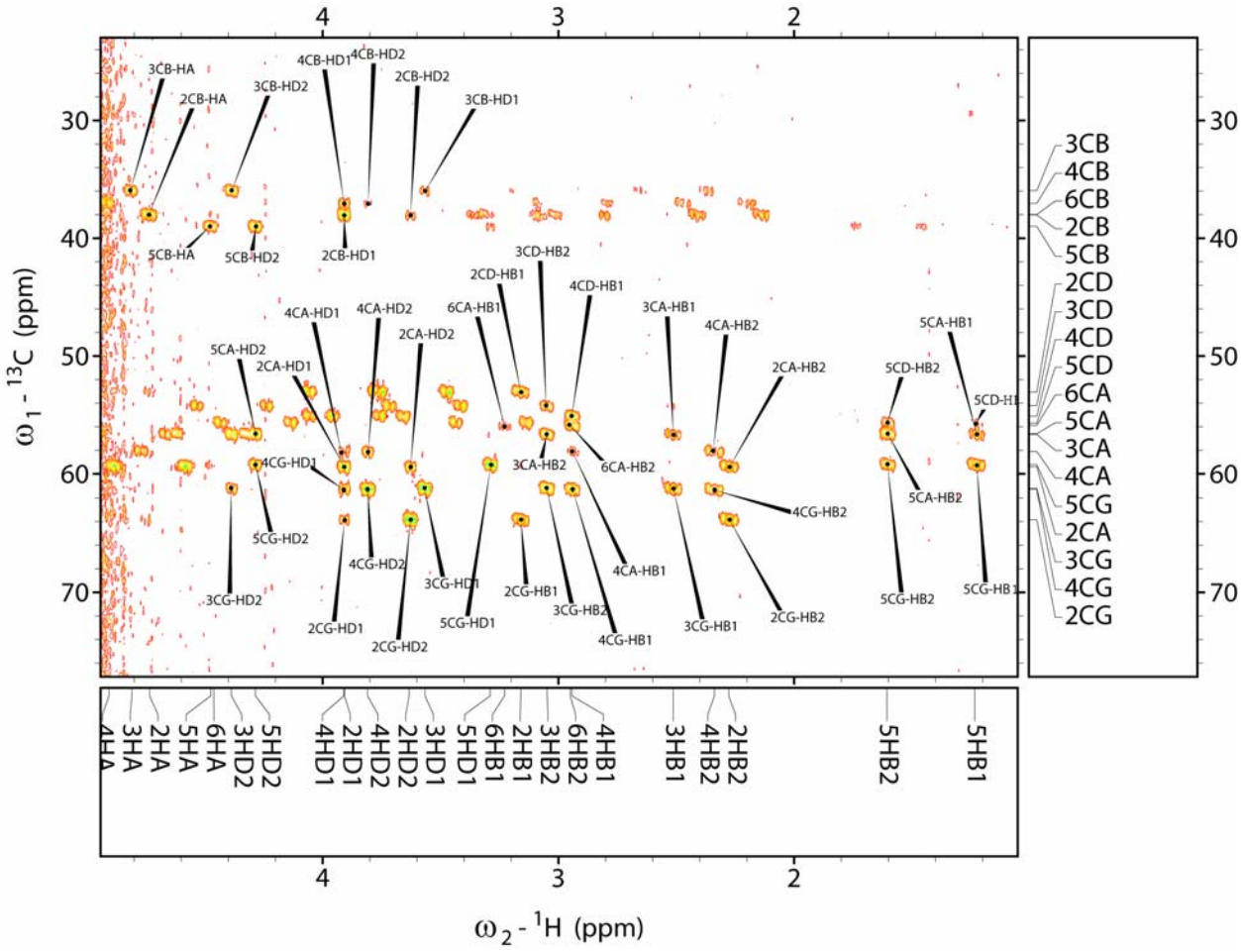

Supplemental Figure 93. Oligomer **63**, 500 MHz HMBC spectrum (2 of 4)

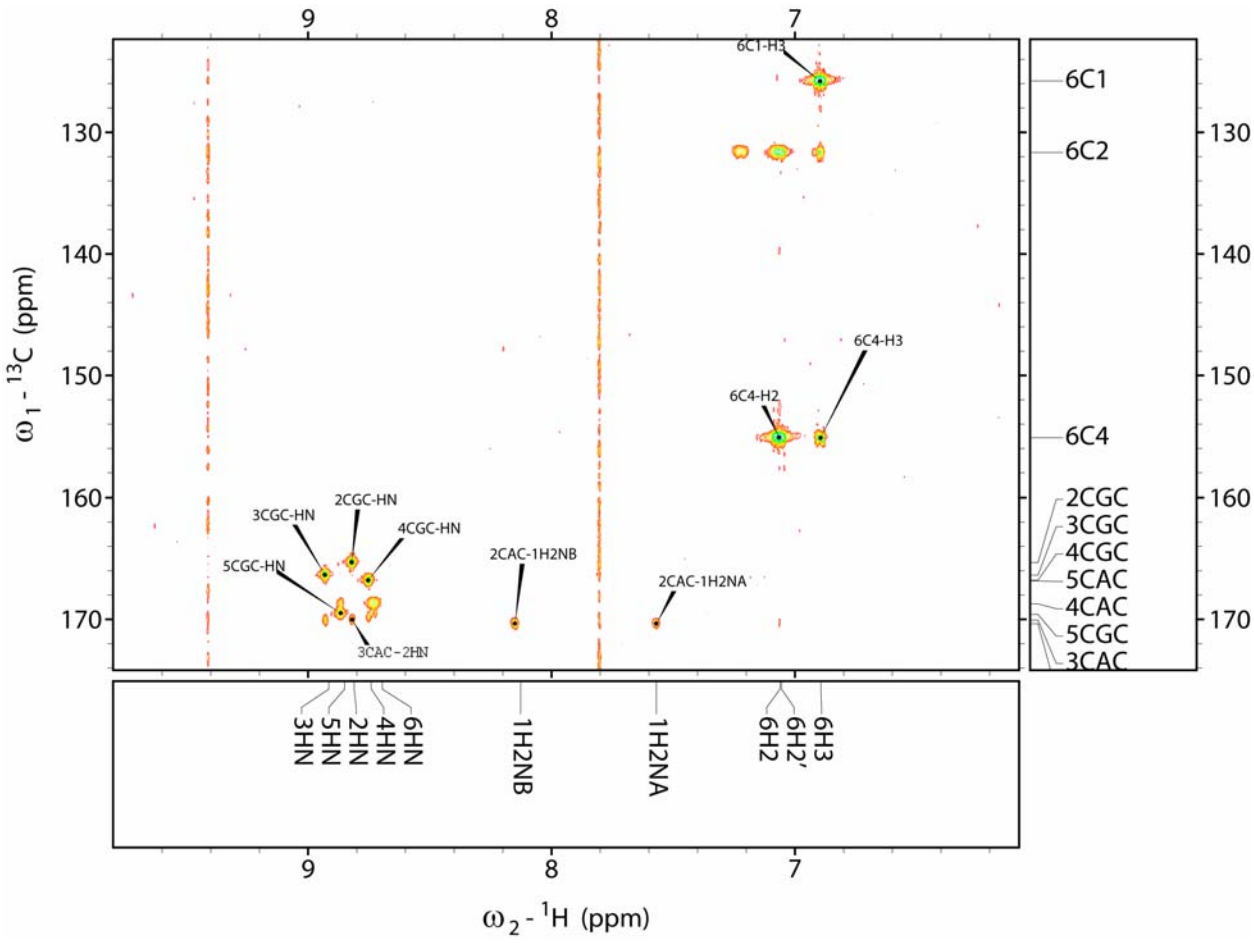

Supplemental Figure 94. Oligomer **63**, 500 MHz HMBC spectrum (3 of 4)

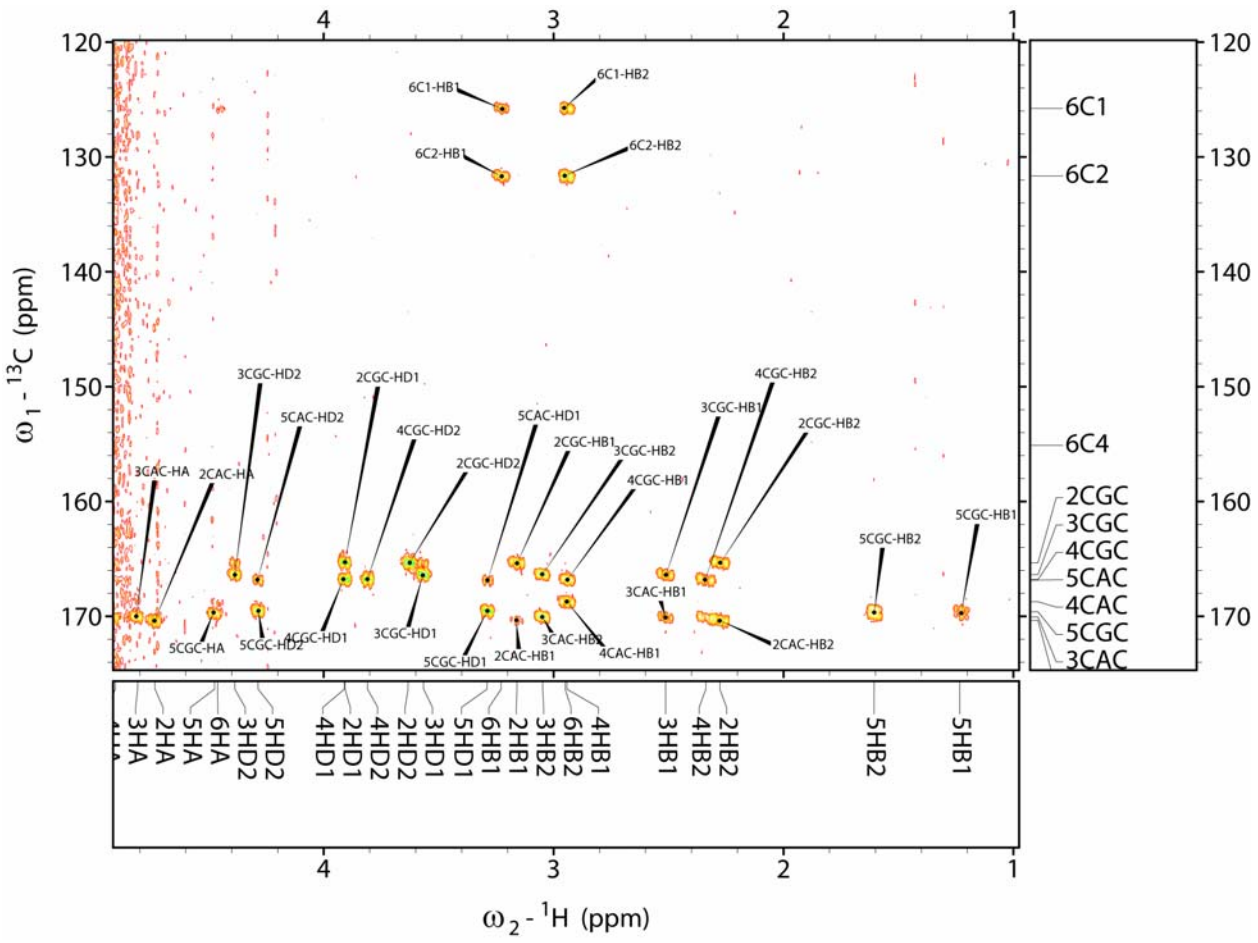

Supplemental Figure 95. Oligomer **63**, 500 MHz HMBC spectrum (4 of 4)

APPENDIX D

SCHEMATIC OF MANUAL SPPS APPARATUS

The schematic diagram on the following page illustrates the type of solid-phase reaction apparatus constructed for the SPPS reactions described above. The commercial source and part number for all components are indicated.

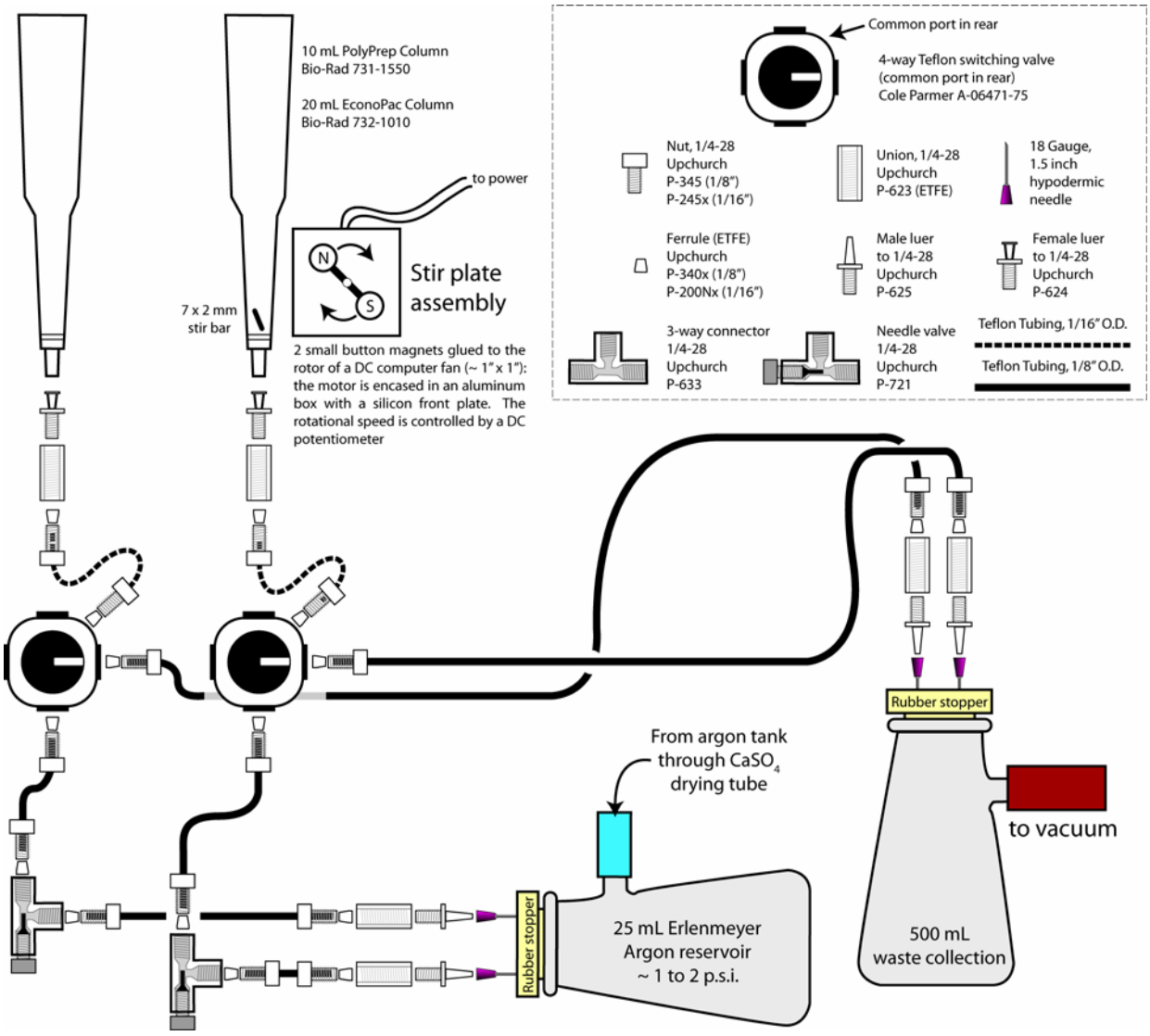

Supplemental Figure 96: A schematic diagram illustrating the construction of the reactors for solid-phase peptide synthesis

BIBLIOGRAPHY

(1) Gellman, S. H. Foldamers: A Manifesto. *Acc. Chem. Res.* **1998,** *31*, 173-180.

(2) Schwab, P. F. H.; Levin, M. D.; Michl, J. Molecular rods. 1. Simple axial rods. *Chem. Rev.* **1999,** *99*, (7), 1863-1933.

(3) Kohnke, F. H.; Mathias, J. P.; Stoddart, J. F. Structure-Directed Synthesis of New Organic Materials. *Angew. Chem. Int. Ed.* **1989,** *28*, 1103-1110.

(4) Merkle, R. C. Molecular building blocks and development strategies for molecular nanotechnology. *Nanotechnology* **2000,** *11*, (2), 89-99.

(5) Breslow, R. Biomimetic Chemistry and Artificial Enzymes: Catalysis by Design. *Acc. Chem. Res.* **1995,** *28*, (3), 146-153.

(6) Lehn, J.-M. Toward complex matter: Supramolecular chemistry and self-organization. *Proc. Natl. Acad. Sci. U.S.A.* **2002,** *99*, (8), 4763-4768.

(7) Lin, Y.-Y.; Risk, M.; Ray, S. M.; Engen, D. V.; Clardy, J.; Golik, J.; James, J. C.; Nakanishi, K. Isolation and Structure of Brevetoxin B from the "Red Tide" Dinoflagellate *Ptychodiscus brevis* (*Gymnodinium breve*). *J. Am. Chem. Soc.* **1981,** *103*, 6773-6775.

(8) Nicolaou, K. C.; Rutjes, F. P. J. T.; Theodorakis, E. A.; Tiebes, J.; Sato, M.; Untersteller, E. Total Synthesis of Brevetoxin B. 2. Completion. *J. Am. Chem. Soc.* **1995,** *117*, 1173-1174.

(9) Nicolaou, K. C.; Duggan, M. E.; Hwang, C.-K. New Synthetic Technology for the Construction of Oxocenes. *J. Am. Chem. Soc.* **1986,** *108*, 2468-2469.

(10) Nicolaou, K. C.; Sorensen, E. J., *Classics in Total Synthesis*. Wiley-VCH: Weinheim, 1996.

(11) Cantrill, S. J.; Pease, A. R.; Stoddart, J. F. A Molecular Meccano Kit. *J. Chem. Soc., Dalton Trans.* **2000,** *21*, 3715-3734.

(12) Moore, J. S. Shape-Persistent Molecular Architectures of Nanoscale Dimension. *Acc. Chem. Res.* **1997,** *30*, 402-413.

(13) Gupta, S.; Das, B. C.; Schafmeister, C. E. Synthesis of a pipecolic acid-based bis-amino acid and its assembly into a spiro ladder oligomer. *Org. Lett.* **2005,** *7*, (14), 2861-2864.

(14) Habay, S. A.; Schafmeister, C. E. Synthesis of a bis-amino acid that creates a sharp turn. *Org. Lett.* **2004,** *6*, (19), 3369-3371.

(15) Levins, C. G.; Schafmeister, C. E. The synthesis of functionalized nanoscale molecular rods of defined length. *J. Am. Chem. Soc.* **2003,** *125*, (16), 4702-4703.

(16) Ashton, P. R.; Brown, G. R.; Isaacs, N. S.; Giuffrida, D.; Kohnke, F. H.; Mathias, J. P.; Slawin, A. M. Z.; Smith, D. R.; Stoddart, J. F.; Williams, D. J. Molecular LEGO. 1. Substrate-Directed Synthesis via Stereoregular Diels-Alder Oligomerizations. *J. Am. Chem. Soc.* **1992,** *114*, 6330-6353.

(17) Bolon, D. N.; Mayo, S. L. Enzyme-like proteins by computational design. *Proc. Natl. Acad. Sci. U.S.A.* **2001,** *98*, (25), 14272-14279.

(18) Wilken, J.; Kent, S. B. H. Chemical protein synthesis. *Curr. Opin. Biotech.* **1998,** *9*, 412-426.

(19) Winkler, J. R.; Gray, H. B. Protein Folding. *Acc. Chem. Res.* **1998,** *31*, 698.

(20) Yue, K.; Dill, K. A. Forces of tertiary structural organization in globular proteins. *Proc. Natl. Acad. Sci. U.S.A.* **1995,** *92*, 146-150.

(21) Anfinsen, C. B. Principles that Govern the Folding of Protein Chains. *Science (Washington, D.C.)* **1973,** *181*, (4096), 223-230.

(22) Dill, K. A.; Chan, H. S. From Levinthal to pathways to funnels. *Nat. Struct. Biol.* **1997,** *4*, (1), 10-19.

(23) Levinthal, C. Are There Pathways for Protein Folding? *J. Chim. Phys. Phys.-Chem. Biol.* **1968,** *65*, (1), 44.

(24) Bolon, D. N.; Voight, C. A.; Mayo, S. L. *De novo* design of biocatalysts. *Curr. Opin. Struct. Biol* **2002,** *6*, 125-129.

(25) Penning, T. M.; Jez, J. M. Enzyme Redesign. *Chem. Rev.* **2001,** *101*, 3027-3046.

(26) Schafmeister, C. E.; LaPorte, S. L.; Miercke, L. J. W.; Stroud, R. M. A designed four helix bundle protein with native-like structure. *Nat. Struct. Biol.* **1997,** *4*, (12), 1039-1046.

(27) Dahiyat, B. I.; Mayo, S. L. De Novo Protein Design: Fully Automated Sequence Selection. *Science (Washington, D.C.)* **1997,** *278*, 82-87.

(28) DeGrado, W. F.; Summa, C. M.; Pavone, V.; Nastri, F.; Lombardi, A. De Novo Design and Structural Characterization of Proteins and Metalloproteins. *Annu. Rev. Biochem.* **1999,** *68*, 779-819.

(29) Hagihara, M.; Anthony, N. J.; Stout, T. J.; Clardy, J.; Schreiber, S. L. Vinylogous Polypeptides: An Alternative Peptide Backbone. *J. Am. Chem. Soc.* **1992,** *114*, (16), 6568-6570.

(30) Hill, D. J.; Mio, M. J.; Prince, R. B.; Hughes, T. S.; Moore, J. S. A Field Guide to Foldamers. *Chem. Rev.* **2001,** *101*, (12), 3893-4011.

(31) Seebach, D.; Matthews, J. L. β-Peptides: a surprise at every turn. *Chem. Commun.* **1997,** *1997*, 2015-2022.

(32) Cheng, R. P.; Gellman, S. H.; DeGrado, W. F. β-Peptides: From Structure to Function. *Chem. Rev.* **2001,** *101*, 3219-3232.

(33) Abele, S.; Seebach, D. Preparation of Achiral and of Enantiopure Geminally Disubstituted β-Amino Acids for β-Peptide Synthesis. *Eur. J. Org. Chem.* **2000,** *2000*, (1), 1-15.

(34) Webb, T. H.; Wilcox, C. S. Enantioselective and diastereoselective molecular recognition of neutral molecules. *Chem. Soc. Rev.* **1993,** *22*, (6), 383-95.

(35) Huck, B. R.; Fisk, J. D.; Guzei, I. A.; Carlson, H. A.; Gellman, S. H. Secondary Structural Preferences of 2,2-Disubstituted Pyrrolidine-4-carboxylic Acid Oligomers: b-Peptide Foldamers that Cannot Form Internal Hydrogen Bonds. *J. Am. Chem. Soc.* **2003,** *125*, (30), 9035-9037.

(36) Murray, J. K.; Gellman, S. H. Application of Microwave Irradiation to the Synthesis of 14-Helical beta-Peptides. *Org. Lett.* **2005,** *7*, (8), 1517-1520.

(37) Park, J.-S.; Lee, H.-S.; Lai, J. R.; Kim, B. M.; Gellman, S. H. Accommodation of alpha-Substituted Residues in the beta-Peptide 12-helix: Expanding the Range of Substitution Patterns Available to a Foldamer Scaffold. *J. Am. Chem. Soc.* **2003,** *125*, (28), 8539-8545.

(38) Hayen, A.; Schmitt, M. A.; Ngassa, F. N.; Thomasson, K. A.; Gellman, S. H. Two Helical Conformations from a Single Foldamer Backbone: "Split Personality" in Short alpha/beta-peptides. *Angew. Chem. Int. Ed.* **2004,** *43*, (4), 505-510.

(39) Porter, E. A.; Wang, X.; Schmitt, M. A.; Gellman, S. H. Synthesis and 12-Helical Secondary Structure of β-Peptides Containing (2*R*,3*R*)-Aminoproline. *Org. Lett.* **2002,** *4*, (19), 3317-3319.

(40) Cho, C. Y.; Moran, E. J.; Cherry, S. R.; Stephens, J. C.; Fodor, S. P. A.; Adams, C. L.; Sundaram, A.; Jacobs, J. W.; Schultz, P. G. An Unnatural Biopolymer. *Science (Washington, D.C.)* **1993,** *261*, (5126), 1303-1305.

(41) Semetey, V.; Moustakas, D.; Whitesides, G. M. Synthesis and Conformational Study of Water-Soluble, Rigid, Rodlike Oliopiperidines. *Angew. Chem. Int. Ed.* **2006,** *45*, (4), 588-591.

(42) Gong, B.; Zeng, H.; Zhu, J.; Yuan, L.; Han, Y.; Cheng, S.; Furukawa, M.; Parra, R. D.; Kovalevsky, A. Y.; Mills, J. L.; Skrzypczak-Jankun, E.; Martinovic, S.; Smith, R. D.; Zheng, C.; Szyperski, T.; Zeng, X. C. Creating nanocavities of tunable sizes: Hollow helices. *Proc. Natl. Acad. Sci. U.S.A.* **2002,** *99*, (18), 11583-11588.

(43) Nielsen, P. E. Peptide Nucleic Acid. A Molecule with Two Identities. *Acc. Chem. Res.* **1999,** *32*, (7), 624-630.

(44) Watson, R. M.; Skorik, Y. A.; Patra, G. K.; Achim, C. Influence of Metal Coordination on the Mismatch Tolerance of Ligand-Modified PNA Duplexes. *J. Am. Chem. Soc.* **2005,** *127*, (42), 14628-14639.

(45) Hill, D. J.; Moore, J. S. Helicogenicity of solvents in the conformational equilibrium of oligo(m-phenylene ethynylene)s: Implications for foldamer research. *Proc. Natl. Acad. Sci. U.S.A.* **2002,** *99*, (8), 5053-5057.

(46) Zhang, W.; Brombosz, S. M.; Mendoza, J. L.; Moore, J. S. A high-yield, one-step synthesis of o-phenylene ethynylene cyclic trimer via precipitation-driven alkyne metathesis. *J. Org. Chem.* **2005,** *70*, (24), 10198-10201.

(47) Schwab, P. F. H.; Noll, B. C.; Michl, J. Synthesis and Structure of Trigonal and Tetragonal Connectors for a "Tinkertoy" Construction Set. *J. Org. Chem.* **2002,** *67*, 5476-5485.

(48) Magnera, T. F.; Peslherbe, L. M.; Körblová, E.; Michl, J. The organometallic "Molecular Tinkertoy" approach to planar grid polymers. *J. Organomet. Chem.* **1997,** *548*, 83-89.

(49) Kaszynski, P.; Friedli, A. C.; Michl, J. Toward a Molecular-Size "Tinkertoy" Construction Set. Preparation of Terminally Functionalized [*n*]Staffanes from [1.1.1]Propellane. *J. Am. Chem. Soc.* **1992,** *114*, 601-620.

(50) Tanatani, A.; Hughes, T. S.; Moore, J. S. Foldamers as Dynamic Receptors: Probing the Mechanism of Molecular Association between Helical Oligomers and Rodlike Ligands. *Angew. Chem. Int. Ed.* **2001,** *41*, (2), 325-328.

(51) Arora, P. S.; Ansari, A. Z.; Best, T. P.; Ptashne, M.; Dervan, P. B. Design of Artificial Transcriptional Activators with Rigid Poly-L-Proline Linkers. *J. Am. Chem. Soc.* **2002,** *124*, (44), 13067-13071.

(52) Stryer, L.; Haugland, R. P. Energy transfer: a spectroscopic ruler. *Proc. Natl. Acad. Sci. U.S.A.* **1967,** *58*, (2), 719-726.

(53) Lakowicz, J. R.; Gryczynski, I.; Wiczk, W.; Laczko, G.; Prendergast, F. C.; Johnson, M. L. Conformational distributions of melittin in water/methanol mixtures from frequency-domain measurements of nonradiative energy transfer. *Biophysical Chemistry* **1990,** *36*, (2), 99-115.

(54) Paar, J. M.; Harris, N. T.; Holowka, D.; Baird, B. Bivalent Ligands with Rigid Double-Stranded DNA Spacers Reveal Structural Constraints on Signaling by FcεRI. *J. Immunol.* **2002,** *169*, (2), 856-864.

(55) Whitesides, G. M.; Mammen, M.; Choi, S.-K. Polyvalent Interactions in Biological Systems: Implications for Design and Use of Multivalent Ligands and Inhibitors. *Angew. Chem. Int. Ed.* **1998,** *37*, (2754-2794).

(56) Sakai, N.; Mareda, J.; Matile, S. Rigid-Rod Molecules in Biomembrane Models: From Hydrogen-Bonded Chains to Synthetic Multifunctional Pores. *Acc. Chem. Res.* **2005,** *38*, (2), 79-87.

(57) Merrifield, R. B. Solid Phase Peptide Synthesis. I. The Synthesis of a Tetrapeptide. *J. Am. Chem. Soc.* **1963,** *85*, 2149-2154.

(58) Atherton, E.; Fox, H.; Harkiss, D.; Logan, C. J.; Sheppard, R. C.; Williams, B. J. A mild procedure for solid phase peptide synthesis: use of fluorenylmethoxycarbonylamino-acids. *Chem. Commun.* **1978**, (13), 537-9.

(59) Atherton, E.; Sheppard, R. C., *Solid Phase Peptide Synthesis*. IRL: Oxford, 1989.

(60) Gisin, B. F.; Merrifield, R. B. Carboxyl-Catalyzed Intramolecular Aminolysis. A Side Reaction in Solid-Phase Peptide Synthesis. *J. Am. Chem. Soc.* **1972,** *94*, (9), 3102-3106.

(61) Capasso, S.; Mazzarella, L. Activation of diketopiperazine formation by alkylammonium carboxylate salts and aprotic dipolar protophobic solvents. *Peptides* **1998,** *19*, (2), 389-391.

(62) Giralt, E.; Eritja, R.; Pedroso, E. Diketopiperazine formation in acetamido- and nitrobenzamido-bridged polymeric supports. *Tetrahedron Lett.* **1981,** *22*, (38), 3779-82.

(63) Fischer, P. M. Diketopiperazines in peptide and combinatorial chemistry. *J. Pept. Sci.* **2003,** *9*, (1), 9-35.

(64) Dinsmore, C. J.; Beshore, D. C. Recent Advances in the Synthesis of Diketopiperazines. *Tetrahedron* **2002,** *58*, 3297-3312.

(65) Bada, J. L.; Gaines, S. M. Aspartame Decomposition and Epimerization in the Diketopiperazine and Dipeptide Products as a Function of pH and Temperature. *J. Org. Chem.* **1988,** *54*, 2757-2764.

(66) Bada, J. L.; Steinberg, S. M. Peptide Decomposition in the Neutral pH Region via the Formation of Diketopiperazines. *J. Org. Chem.* **1983,** *48*, 2295-2298.

(67) Schafmeister, C. E. Unpublished results. **2001**.

(68) Haas, W. L.; Krumkalns, E. V.; Gerzon, K. Adamantyloxycarbonyl, a New Blocking Group. Preparation of 1-Adamantyl Chloroformate. *J. Am. Chem. Soc.* **1966,** *88*, (9), 1988-1992.

(69) Wenschuh, H.; Carpino, L. A.; Beyermann, M.; Krause, E.; Brudel, M.; Winter, R.; Schümann, M.; Bienert, M. Fmoc Amino Acid Fluorides: Convenient Reagents for the Solid-Phase Assembly of Peptides Incorporating Sterically Hindered Residues. *J. Org. Chem.* **1994,** *59*, 3275-3280.

(70) Based upon the Acros 2006-2007 catalog: trans-4-hydroxy-L-proline is $1.59 / gram.

(71) Remuzon, P. Trans-4-hydroxy-L-proline, a useful and versatile chiral starting block. *Tetrahedron* **1996,** *52*, (44), 13803-13835.

(72) Bucherer, H. T.; Fischbeck, H. Hexahydrodiphenylamine and its Derivatives. *J. Prakt. Chem.* **1934,** *140*, 69-89.

(73) Bucherer, H. T.; Steiner, W. Syntheses of Hydantoins. I. Reactions of α-Oxy and α-Amino Nitriles. *J. Prakt. Chem.* **1934,** *140*, 129-150.

(74) Carpino, L. A.; Han, G. Y. 9-Fluorenylmethoxycarbonyl function, a new base-sensitive amino-protecting group. *J. Am. Chem. Soc.* **1970,** *92*, (19), 5748-9.

(75) Merrifield, R. B. Solid-phase peptide synthesis. III. An improved synthesis of bradykinin. *Biochemistry* **1964,** *3*, (9), 1385-9.

(76) Fukuyama, T.; Cheung, M.; Jow, C.-K.; Hidai, Y.; Kan, T. 2,4-Dinitrobenzenesulfonamides: a simple and practical method for the preparation of a variety of secondary amines and diamines. *Tetrahedron Lett.* **1997,** *38*, (33), 5831-5834.

(77) Miller, S. C.; Scanlan, T. S. Site-Selective N-Methylation of Peptides on Solid Support. *J. Am. Chem. Soc.* **1997,** *119*, 2301-2302.

(78) Miller, S. C.; Scanlan, T. S. oNBS-SPPS: A New Method for Solid-Phase Peptide Synthesis. *J. Am. Chem. Soc.* **1998,** *120*, (11), 2690-2691.

(79) Carpino, L. A.; Chao, H. G.; Beyermann, M.; Bienert, M. ((9-Fluorenylmethyl)oxy)carbonyl Amino Acid Chlorides in Sold-Phase Peptide Synthesis. *J. Org. Chem.* **1991,** *56*, 2635-2642.

(80) Meisenheimer, J. Reactions of aromatic nitro structures. *Liebigs Ann. Chem.* **1902,** *323*, 205-226.

(81) Schotten, C. *Ber. Dtsch. Chem. Ges.* **1884,** *17*, 2544.

(82) Natchus, M. G.; Cheng, M.; De, B.; Almstead, N. G.; Pikul, S.; Dowty, M. E.; Dietsch, C. R.; Dunaway, C. M.; Gu, F.; Hsieh, L. C.; Janusz, M. J.; Taiwo, Y. O. Design, Synthesis, and Biological Evaluation of Matrix Metalloproteinase Inhibitors Derived from a Modified Proline Scaffold. *J. Med. Chem.* **1999,** *42*, 5426-5436.

(83) Bolin, D. R.; Sytwu, I.-I.; Humiec, F.; Meienhofer, J. Preparation of Oligiomer-Free N^{α}-Fmoc and N^{α}-Urethane Amino Acids. *Int. J. Pept. Protein Res.* **1989,** *33*, 353-359.

(84) Barlos, K.; Papaioannou, D.; Theodoropoulos, D. Efficient "One-Pot" Synthesis of *N*-Trityl Amino Acids. *J. Org. Chem.* **1982,** *47*, 1324-1326.

(85) Arrieta, A.; Palomo, C. Reagents and Synthetic Methods; 19. Synthesis of *N*-(*N*-Aryl- or *N*-Alkylaminocarbonyl)-amino Acids by Addition of *N*,*O*-Bis[trimethylsilyl]amino Acids to Isocyanates. *Synthesis* **1982**, (12), 1050-1052.

(86) Wenschuh, H.; Carpino, L. A.; Beyermann, M.; Winter, R.; Bienert, M.; Ionescu, D. Fmoc Amino Acid Fluorides in Peptide Synthesis - Extension of the Method to Extremely Hindered Amino Acids. *Tetrahedron Lett.* **1996,** *37*, (31), 5483-5486.

(87) Carpino, L. A.; Ionescu, D.; El-Faham, A.; Beyermann, M.; Henklein, P.; Hanay, C.; Wenschuh, H.; Bienert, M. Complex Polyfluoride Additives in Fmoc-Amino Acid Fluoride Coupling Processes. Enhanced Reactivity and Avoidance of Stereomutation. *Org. Lett.* **2003,** *5*, (7), 975-977.

(88) Hudlický, M., *ACS Monograph 186: Oxidations in Organic Chemistry*. American Chemical Society: Washington, D.C., 1990; p 273.

(89) Armstrong, A.; Brackenridge, I.; Jackson, R. F. W.; Kirk, J. M. A new method for the preparation of tertiary butyl ethers and esters. *Tetrahedron Lett.* **1988,** *29*, (20), 2483-2486.

(90) Takeda, K.; Akiyama, A.; Nakamura, H.; Takizawa, S.; Mizuno, Y.; Takayanagi, H.; Harigaya, Y. Dicarbonates: Convenient 4-Dimethylaminopyridine Catalyzed Esterification Reagents. *Synthesis* **1994,** *10*, 1063-1066.

(91) Anderson, G. W.; Callahan, F. M. *t*-Butyl Esters of Amino Acids and Peptides and their Use in Peptide Synthesis. *J. Am. Chem. Soc.* **1960,** *82*, 3359.

(92) Trost, B. M. The atom economy: a search for synthetic efficiency. *Science (Washington, D.C.)* **1991,** *254*, (5037), 1471-7.

(93) Ware, E. The Chemistry of the Hydantoins. *Chem. Rev.* **1950,** *46*, (3), 403-470.

(94) Bergmann, M.; Zervas, L. A general process for the synthesis of peptides. *Chem. Ber.* **1932,** *65B*, 1192-1201.

(95) Yajima, H.; Fujii, N.; Ogawa, H.; Kawatani, H. Trifluoromethanesulfonic acid, as a deprotecting reagent in peptide chemistry. *Chem. Commun.* **1974**, (3), 107-8.

(96) Patchett, A. A.; Witkop, B. Studies on Hydroxyproline. *J. Am. Chem. Soc.* **1957,** *79*, 185-192.

(97) Dieter, L. Selective Oxidation of Organic Compounds - Sustainable Catalytic Reactions with Oxygen and without Transition Metals? *Angew. Chem. Int. Ed.* **2006,** *45*, (20), 3206-3210.

(98) Swern, D.; Mancuso, A. J.; Huang, S.-L. Oxidation of Long-Chain and Related Alcohols to Carbonyls by Dimethyl Sulfoxide "Activated" by Oxalyl Chloride. *J. Org. Chem.* **1978,** *43*, (12), 2480-2482.

(99) Dess, D. B.; Martin, J. C. A useful 12-I-5 triacetoxyperiodinane (the Dess-Martin periodinane) for the selective oxidation of primary or secondary alcohols and a variety of related 12-I-5 species. *J. Am. Chem. Soc.* **1991,** *113*, 7277.

(100) Levins, C. G.; Schafmeister, C. E. The synthesis of curved and linear structures from a minimal set of monomers. *J. Org. Chem.* **2005,** *70*, (22), 9002-9008.

(101) Chubb, F. L.; Edward, J. T.; Wong, S. C. Simplex Optimization of Yields in the Bucherer-Bergs Reaction. *J. Org. Chem.* **1980,** *45*, 2315-2320.

(102) *MOE*, version 2005.06; Chemical Computing Group: Montreal, 2005.

(103) Tanaka, K.-i.; Sawanishi, H. Asymmetric Syntheses of All Four Isomers of 4-Amino-4-carboxyproline: Novel Conformationally Restricted Glutamic Acid Analogues. *Tetrahedron: Asymmetry* **1995,** *6*, (7), 1641-1656.

(104) Edward, J. T.; Jitrangsri, C. Stereochemistry of the Bucherer-Bergs and Strecker Reactions of 4-*tert*-Butylcyclohexanone. *Can. J. Chem.* **1975,** *53*, 3339-3350.

(105) Hammond, G. S. A Correlation of Reaction Rates. *J. Am. Chem. Soc.* **1955,** *77*, (2), 334-358.

(106) Seeman, J. I. Effect of conformational change on reactivity in organic chemistry. Evaluations, applications, and extensions of Curtin-Hammett Winstein-Holness kinetics. *Chem. Rev.* **1983,** *83*, (2), 83-134.

(107) May, O.; Verseck, S.; Bommarius, A.; Drauz, K. Development of Dynamic Kinetic Resolution Processes for Biocatalytic Production of Natural and Nonnatural L-Amino Acids. *Org. Process Res. Dev.* **2002,** *6*, (4), 452-457.

(108) Gokhale, D. V.; Bastawde, K. B.; Patil, S. G.; Kalkote, U. R.; Joshi, R. R.; Joshi, R. A.; Ravindranathan, T.; Gaikwad, B. G.; Jogdand, V. V.; Nene, S. Chemoenzymatic Synthesis of D(-)Phenylglycine Using Hydantoinase of *Pseudomonas Desmolyticum* Resting Cells. *Enzyme Microb. Technol.* **1996,** *18*, 353-357.

(109) Rebek, J., Jr.; Kubik, S.; Meissner, R. S. Synthesis of α,α-Dialkylated Amino Acids with Adenine or Thymine Residues. A New Mild and Facile Hydrolysis of Hydantoins. *Tetrahedron Lett.* **1994,** *35*, (36), 6635-6638.

(110) Grieco, P. A.; Flynn, D. L.; Zelle, R. E. A Mild Two-Step Method for the Hydrolysis/Methanolysis of Secondary Amides and Lactams. *J. Org. Chem.* **1983,** *48*, 2424-2426.

(111) Hammarström, L. G. J.; Fu, Y.; Vail, S.; Hammer, R. P.; McLaughlin, M. L. A convenient preparation of an orthogonally protected C^{α},C^{α}-disubstituted amino acid analog of lysine: 1-tert-butyloxycarbonyl-4-((9-fluorenylmethyloxycarbonyl)amino)-piperidine-4-carboxylic acid. *Org. Synth.* **2005,** *81*, 213-224.

(112) Shioiri, T.; Aoyama, T.; Mori, S. Trimethylsilyldiazomethane. *Org. Synth.* **1990,** *68*, 1.

(113) Sakaitani, M.; Hori, K.; Ohfune, Y. One-Pot Conversion of N-Benzyloxtcarbonyl Group Into N-tert-Butoxycarbonyl Group. *Tetrahedron Lett.* **1988,** *29*, (24), 2983-2984.

(114) Robinson, D. S.; Greenstein, J. P. Stereoisomers of Hydroxyproline. *J. Biol. Chem.* **1952,** *195*, 383-388.

(115) Lowe, G.; Vilaivan, T. Amino Acids Bearing Nucleobases for the Synthesis of Novel Peptide Nucleic Acids. *J. Chem. Soc., Perkin Trans. 1* **1997**, (4), 539-546.

(116) Carter, H. E.; Stevens, C. M. Azlactones. II. Azlactone formation in glacial and in aqueous acetic acid and preparation of benzoyl-a-aminocrotonic acid azlactone II. *J. Biol. Chem.* **1940,** *133*, 117-28.

(117) Levins, C. G.; Brown, Z. Z.; Schafmeister, C. E. Maximizing the stereochemical diversity of spiro-ladder oligomers. *Org. Lett.* **2006,** *8*, (13), 2807-10.

(118) Pornsuwan, S.; Bird, G.; Schafmeister, C. E.; Saxena, S. Flexibility and Lengths of Bis-peptide Nanostructures by Electron Spin Resonance. *J. Am. Chem. Soc.* **2006,** *128*, (12), 3876-3877.

(119) Gupta, S.; Macala, M.; Schafmeister, C. E. The synthesis of structurally diverse *bis*-peptide oligomers. *J. Org. Chem.* **2006**, manuscript accepted (8/2006).

(120) Frackenpohl, J.; Arvidsson, P. I.; Schreiber, J. V.; Seebach, D. The Outstanding Biological Stability of β- and γ-Peptides toward Proteolytic Enzymes: An In Vitro Investigation with Fifteen Peptidases. *ChemBioChem* **2001,** *2*, (6), 445-455.

(121) Rink, H. Solid-Phase Synthesis of Protected Peptide Fragments using a Trialkoxy-Diphenyl-Methylester Resin. *Tetrahedron Lett.* **1987,** *28*, (33), 3787-3790.

(122) Bernatowicz, M. S.; Daniels, S. B.; Köster, H. A Comparison of Acid Labile Linkage Agents for the Synthesis of Peptide C-Terminal Amides. *Tetrahedron Lett.* **1989,** *30*, (35), 4645-4648.

(123) Fields, G. B.; Noble, R. L. Solid phase peptide synthesis utilizing 9-fluorenylmethoxycarbonyl amino acids. *Int. J. Pept. Protein Res.* **1990,** *35*, 161-214.

(124) Kaiser, E.; Colescott, R. L.; Bossinger, C. D.; Cook, P. I. Color test for detection of free terminal amino groups in the solid-phase synthesis of peptides. *Anal. Biochem.* **1970,** *34*, (2), 595.

(125) Carpino, L. A.; Imazumi, H.; El-Faham, A.; Ferrer, F. J.; Zhang, C.; Lee, Y.; Foxman, B. M.; Henklein, P.; Hanay, C.; Mugge, C.; Wenschuh, H.; Klose, J.; Beyermann, M.; Bienert, M. The uronium/guanidinium peptide coupling reagents: finally the true uronium salts. *Angew. Chem. Int. Ed.* **2002,** *41*, (3), 441-445.

(126) Carpino, L. A. 1-Hydroxy-7-azabenzotriazole. An Efficient Peptide Coupling Additive. *J. Am. Chem. Soc.* **1993,** *115*, 4397-4398.

(127) Albericio, F.; Bofill, J. M.; El-Faham, A.; Kates, S. A. Use of Oniom Salt-Based Coupling Reagents in Peptide Synthesis. *J. Org. Chem.* **1998,** *63*, 9678-9683.

(128) Carpino, L. A.; El-Faham, A.; Albericio, F. Racemization Studies During Solid-Phase Peptide Synthesis Using Azabenzotriazole-Based Coupling Reagents. *Tetrahedron Lett.* **1994,** *35*, (15), 2279-2282.

(129) Li, P.; Xu, J. C. The development of highly efficient onium-type peptide coupling reagents based upon rational molecular design. *J. Peptide Res.* **2001,** *58*, 129-139.

(130) Carpino, L. A.; Imazumi, H.; Foxman, B. M.; Vela, M. J.; Henklein, P.; El-Faham, A.; Klose, J.; Bienert, M. Comparison of the Effects of 5- and 6-HOAt on Model Peptide Coupling Reactions Relative to the Cases for the 4- and 7-Isomers. *Org. Lett.* **2000,** *2*, (15), 2253-2256.

(131) Carpino, L. A.; El-Faham, A. Tetramethylfluoroformamidinium Hexafluorophosphate: A Rapid-Acting Coupling Reagent for Solution and Solid Phase Peptide Synthesis. *J. Am. Chem. Soc.* **1995,** *117*, 5401-5402.

(132) Carpino, L. A.; Beyermann, M.; Wenschuh, H.; Bienert, M. Peptide Synthesis via Amino Acid Halides. *Acc. Chem. Res.* **1996,** *29*, 268-274.

(133) Pedroso, E.; Grandas, A.; Heras, X. d. l.; Eritja, R.; Giralt, E. Diketopiperazine formation in solid phase peptide synthesis using p-alkoxybenzyl ester resins and fmoc-amino acids. *Tetrahedron Lett.* **1986,** *27*, (6), 743-746.

(134) Pearson, D. A.; Blanchette, M.; Baker, M. L.; Guindon, C. A. Trialkylsilanes as Scavengers for the Trifluoroacetic Acid Deblocking of Protecting Groups in Peptide Synthesis. *Tetrahedron Lett.* **1989,** *30*, (21), 2739-2742.

(135) Muzart, J.; Hénin, F.; Létinois, S. Nitriles under Palladium-Catalyzed Hydrogenation Conditions as Substitutes for Aldehydes in the Reaction with 1,2-Amino Alcohols: Formation of 1,3-Oxazolidines and Reductive *N*-Alkylation. *Tetrahedron Lett.* **1997,** *38*, (41), 7187-7190.

(136) Filira, F.; Biondi, L.; Gobbo, M.; Rocchi, R. N-alkylation of amino acids during hydrogenolytic deprotection. *Tetrahedron Lett.* **1991,** *32*, (50), 7463.

(137) Mazaleyrat, J.-P.; Xie, J.; Wakselman, M. Selective Hydrogenolysis of the Benzyloxycarbonyl Protecting Group of N^{ε}-Lysine in Cyclopeptides Containing A

Benzylic Phenyl Ether Function. Evidence for N^{ε}-Methylated Lysine Side Products. *Tetrahedron Lett.* **1992,** *33*, (30), 4301-4302.

(138) Cornell, W. D.; Cieplak, P.; Bayly, C. I.; Gould, I. R.; Merz, K., M., Jr.; Ferguson, D. M.; Spellmeyer, D. C.; Fox, T.; Caldwell, J. W.; Kollman, P. A. A Second Generation Force Field for the Simulation of Proteins, Nucleic Acids, and Organic Molecules. *J. Am. Chem. Soc.* **1995,** *117*, (19), 5179-5197.

(139) Webb, L. E.; Lin, C.-F. Conformations of cyclic dipeptides. Structure of cyclo-glycyl-L-tyrosyl (L-3-(4-hydroxybenzyl)-2,5-piperazinedione). *J. Am. Chem. Soc.* **1971,** *93*, (15), 3818-3819.

(140) Karle, I. L. Crystal structure and conformation of the cyclic dipeptide cyclo-L-prolyl-L-leucyl. *J. Am. Chem. Soc.* **1972,** *94*, (1), 81-84.

(141) Karle, I. L.; Ottenheym, H. C. J.; Witkop, B. Conformation and synthesis of diketopiperazines. 3,4-Dehydroproline anhydride. *J. Am. Chem. Soc.* **1974,** *96*, (2), 539-43.

(142) Smith, G. G.; Evans, R. C.; Baum, R. Neighboring Residue Effects: Evidence for Intramolecular Assistance to Racemization of Epimerization of Dipeptide Residues. *J. Am. Chem. Soc.* **1986,** *108*, 7327-7332.

(143) Gund, P.; Veber, D. F. On the Ease of Base-Catalyzed Epimerization of N-Methylated Peptides and Diketopiperazines. *J. Am. Chem. Soc.* **1979,** *101*, (7), 1885-1887.

(144) Dugave, C.; Demange, L. Cis-trans isomerization of organic molecules and biomolecules: implications and applications. *Chem. Rev.* **2003,** *103*, (7), 2475-532.

(145) Grathwohl, C.; Wuthrich, K. NMR Studies of the Rates of Proline *Cis-Trans* Isomerization in Oligopeptides. *Biopolymers* **1981,** *20*, 2623-2633.

(146) Mulliken, R. S. Conjugation and hyperconjugation: a survey with emphasis on isovalent hyperconjugation. *Tetrahedron* **1959,** *5*, (2-3), 253.

(147) Kolthoff, I. M. Acid-Base Equilibria in Dipolar Aprotic Solvents. *Anal. Chem.* **1992,** *46*, (13), 1992-2003.

(148) Vrasidas, I.; André, S.; Valentini, P.; Böck, C.; Lensch, M.; Kaltner, H.; Liskamp, R. M. J.; Gabius, H. J.; Pieters, R. J. Rigidified multivalent lactose molecules and their interactions with mammalian galectins; a route to selective inhibitors. *Org. Biomol. Chem.* **2003,** *1*, (5), 803-810.

(149) Peter, C.; Rueping, M.; Worner, H.; Jaun, B.; Seebach, D.; van Gunsteren, W. Molecular dynamics simulations of small peptides: can one derive conformational preferences from ROESY spectra? *Chem.-Eur. J.* **2003,** *9*, (23), 5838-5849.

(150) Weiner, S. J.; Kollman, P. A.; Case, D. A.; Singh, U. C.; Ghio, C.; Alagona, G.; Profeta, S.; Weiner, P. A new force field for molecular mechanical simulation of nucleic acids and proteins. *J. Am. Chem. Soc.* **1984,** *106*, (3), 765-784.

(151) Goddard, T. D.; Kneller, D. G. *Sparky 3*, version 3.111; University of California, San Francisco: San Francisco, 2004.

(152) van Gunsteren, W. F.; Bakowies, D.; Baron, R.; Chandrasekhar, I.; Christen, M.; Daura, X.; Gee, P.; Geerke, D. P.; Glättli, A.; Hünenberger, P. H.; Kastenholz, M. A.; Oostenbrink, C.; Schenk, M.; Trzesniak, D.; van der Vegt, N. F. A.; Yu, H. B. Biomolecular Modeling: Goals, Problems, Perspectives. *Angew. Chem. Int. Ed.* **2006,** *45*, (25), 4064-4092.

(153) Haas, E.; Wilchek, M.; Katchalski-Katzir, E.; Steinberg, I. Z. Distribution of End-To-End Distances of Oligopeptides in Solution as Estimated by Energy Transfer. *Proc. Natl. Acad. Sci. U.S.A.* **1975,** *72*, (5), 1807-1811.

(154) Selvin, P. R. The renaissance of fluorescence resonance energy transfer. *Nat. Struct. Biol.* **2000,** *7*, (9), 730-734.

(155) Anslyn, E. V.; Dougherty, D. A., *Modern Physical Organic Chemistry*. University Science Books: Sausalito, 2004; p 1095.

(156) Förster, T. Intermolecular energy transference and fluorescence. *Ann. Physik.* **1948,** *2*, 55-75.

(157) Stryer, L. Fluorescence energy transfer as a spectroscopic ruler. *Annu. Rev. Biochem.* **1978,** *47*, 819-46.

(158) Wu, P.; Brand, L. Resonance Energy Transfer: Methods and Applications. *Anal. Biochem.* **1994,** *218*, 1-13.

(159) Beythien, J.; White, P. Abstracts of Poster Section C; Abstracts of Poster Section D; Abstracts of Poster Section E. *Peptide Sci.* **2003,** *71*, (3), 337-414.

(160) Albericio, F.; Kneib-Cordonier, N.; Biancalana, S.; Gera, L.; Masada, R. I.; Hudson, D.; Barany, G. Preparation and application of the 5-(4-(9-fluorenylmethyloxycarbonyl)aminomethyl-3,5-dimethoxyphenoxy)-valeric acid (PAL) handle for the solid-phase synthesis of C-terminal peptide amides under mild conditions. *J. Org. Chem.* **1990,** *55*, (12), 3730-3743.

(161) Förster, T. Transfer mechanisms of electronic excitation. *Discuss. Faraday Soc.* **1959,** *No. 27*, 7-17.

(162) Schuler, B.; Lipman, E. A.; Steinbach, P. J.; Kumke, M.; Eaton, W. A. Polyproline and the "spectroscopic ruler" revisited with single-molecule fluorescence. *Proc. Natl. Acad. Sci. U.S.A.* **2005,** *102*, (8), 2754-2759.

(163) Davies, J. S. The cyclization of peptides and depsipeptides. *J. Pept. Sci.* **2003,** *9*, (8), 471-501.

(164) Wessjohann, L. A.; Ruijter, E.; Garcia-Rivera, D.; Brandt, W. What can a chemist learn from nature's macrocycles? A brief, conceptual view. *Molecular Diversity* **2005,** *9*, (1), 171-186.

(165) Wessjohann, L. A.; Voigt, B.; Rivera, D. G. Diversity oriented one-pot synthesis of complex macrocycles: Very large steroid-peptoid hybrids from multiple multicomponent reactions including bifunctional building blocks. *Angew. Chem. Int. Ed.* **2005,** *44*, (30), 4785-4790.

(166) Fujita, M.; Tominaga, M.; Hori, A.; Therrien, B. Coordination Assemblies from a Pd(II)-Cornered Square Complex. *Acc. Chem. Res.* **2005,** *38*, (4), 369-378.

(167) Menozzi, E.; Busi, M.; Massera, C.; Ugozzoli, F.; Zuccaccia, D.; Macchioni, A.; Dalcanale, E. Metal-Directed Self-Assembly of Cavitand Frameworks. *J. Org. Chem.* **2006,** *71*, (7), 2617-2624.

(168) Yoshida, K.; Kawamura, S.-I.; Morita, T.; Kimura, S. Helix Triangle: Unique Peptide-Based Molecular Architecture. *J. Am. Chem. Soc.* **2006,** *128*, (24), 8034-8041.

(169) Wiskur, S.; Ait-Haddou, H.; Anslyn, E.; Lavigne, J. Teaching Old Indicators New Tricks. *Acc. Chem. Res.* **2001,** *34*, (12), 963-972.

(170) Czarnik, A. W. Desparately Seeking Sensors. *Chem. Biol.* **1995,** *2*, 423-428.

(171) Breslow, R.; Dong, S. D. Biomimetic Reactions Catalyzed by Cyclodextrins and Their Derivatives. *Chem. Rev.* **1998,** *98*, (5), 1997-2012.

(172) Huisgen, R. 1,3-Dipolar Cycloadditions: Past and Future. *Angew. Chem. Int. Ed.* **1963,** *2*, (10), 565-632.

(173) Bock, V. D.; Hiemstra, H.; Maarseveen, J. H. v. Cu^{I}-Catalyzed Alkyne-Azide "Click" Cycloadditions from a Mechanistic and Synthetic Perspective. *Eur. J. Org. Chem.* **2006,** *2006*, (1), 51-68.

(174) Kolb, H. C.; Sharpless, K. B. The growing impact of click chemistry on drug discovery. *Drug Discovery Today* **2003,** *8*, (24), 1128-1137.

(175) Franke, R.; Doll, C.; Eichler, J. Peptide ligation through click chemistry for the generation of assembled and scaffolded peptides. *Tetrahedron Lett.* **2005,** *46*, (26), 4479-4482.

(176) Rostovtsev, V. V.; Green, L. G.; Fokin, V. V.; Sharpless, K. B. A Stepwise Huisgen Cycloaddition Process: Copper(I)-Catalyzed Regioselective "Ligation" of Azides and Terminal Alkynes. *Angew. Chem. Int. Ed.* **2002,** *41*, (14), 2596-2599.

(177) Tornøe, C. W.; Christensen, C.; Meldal, M. Peptidotriazoles on Solid Phase: [1,2,3]-Triazoles by Regiospecific Copper(I)-Catalyzed 1,3-Dipolar Cycloadditions of Terminal Alkynes to Azides. *J. Org. Chem.* **2002,** *67*, 3057-3064.

(178) Wang, Q.; Chan, T. R.; Hilgraf, R.; Fokin, V. V.; Sharpless, K. B.; Finn, M. G. Bioconjugation by copper(I)-catalyzed azide-alkyne [3+2] cycloaddition. *J. Am. Chem. Soc.* **2003,** *125*, (11), 3192-3193.

(179) Bodine, K. D.; Gin, D. Y.; Gin, M. S. Synthesis of Readily Modifiable Cyclodextrin Analogues via Cyclodimerization of an Alkynyl-Azido Trisaccharide. *J. Am. Chem. Soc.* **2004,** *126*, (6), 1638-1639.

(180) Wu, P.; Malkoch, M.; Hunt, J. N.; Vestberg, R.; Kaltgrad, E.; Finn, M. G.; Fokin, V. V.; Sharpless, K. B.; Hawker, C. J. Multivalent, bifunctional dendrimers prepared by click chemistry. *Chem. Commun.* **2005**, (46), 5775-5777.

(181) Jang, H.; Fafarman, A.; Holub, J. M.; Kirshenbaum, K. Click to Fit: Versatile Polyvalent Display on a Peptidomimetic Scaffold. *Org. Lett.* **2005,** *7*, (10), 1951-1954.

(182) Perez-Balderas, F.; Ortega-Munoz, M.; Morales-Sanfrutos, J.; Hernandez-Mateo, F.; Calvo-Flores, F. G.; Calvo-Asin, J. A.; Isac-Garcia, J.; Santoyo-Gonzalez, F. Multivalent Neoglycoconjugates by Regiospecific Cycloaddition of Alkynes and Azides Using Organic-Soluble Copper Catalysts. *Org. Lett.* **2003,** *5*, (11), 1951-1954.

(183) Billing, J. F.; Nilsson, U. J. C_2 Symmetric Macrocyclic Carbohydrate/Amino Acid Hybrids through Copper(I)-Catalyzed Formation of 1,2,3-Triazoles. *Journal of Organic Chemistry.* **2005,** *70*, (12), 4847-4850.

(184) Angell, Y.; Burgess, K. Ring Closure to β-Turn Mimics via Copper-Catalyzed Azide/Alkyne Cycloadditions. *J. Org. Chem.* **2005,** *70*, (23), 9595-9598.

(185) Bock, V. D.; Perciaccante, R.; Jansen, T. P.; Hiemstra, H.; van Maarseveen, J. H. Click Chemistry as a Route to Cyclic Tetrapeptide Analogues: Synthesis of *cyclo*-[Pro-Val-psi(triazole)-Pro-Tyr]. *Org. Lett.* **2006,** *8*, (5), 919-922.

(186) van Maarseveen, J. H.; Horne, W. S.; Ghadiri, M. R. Efficient route to C-2 symmetric heterocyclic backbone modified cyclic peptides. *Org. Lett.* **2005,** *7*, (20), 4503-4506.

(187) Punna, S.; Kuzelka, J.; Wang, Q.; Finn, M. G. Head-to-tail peptide cyclodimerization by copper-catalyzed azide-alkyne cycloaddition. *Angew. Chem. Int. Ed.* **2005,** *44*, (15), 2215-2220.

(188) Lundquist IV, J. T.; Pelletier, J. C. Improved Solid-Phase Peptide Synthesis Method Utilizing α−Azide-Protecting Amino Acids. *Org. Lett.* **2001,** *3*, (5), 781-783.

(189) Weinreb, S. M.; Nahm, S. N-Methoxy-N-Methylamides as Effective Acylating Agents. *Tetrahedron Lett.* **1981,** *22*, (39), 3815-3818.

(190) Panda, G.; Rao, V., N. A Short Synthetic Approach to Chiral Azido Derivatives. *Synlett* **2004**, (4), 714-716.

(191) Mitsunobu, O. The use of diethyl azodicarboxylate and triphenylphosphine in synthesis and transformation of natural products. *Synthesis* **1981**, (1), 1-28.

(192) Arnold, L. D.; Kalantar, T. H.; Vederas, J. C. Conversion of serine to stereochemically pure b-substituted a-amino acids via b-lactones. *J. Am. Chem. Soc.* **1985,** *107*, (24), 7105-9.

(193) Arnold, L. D.; May, R. G.; Vederas, J. C. Synthesis of optically pure a-amino acids via salts of a-amino-b-propiolactone. *J. Am. Chem. Soc.* **1988,** *110*, (7), 2237-41.

(194) Cavender, C. J.; Shiner, V. J., Jr. Trifluoromethanesulfonyl azide. Its reaction with alkyl amines to form alkyl azides. *J. Org. Chem.* **1972,** *37*, (22), 3567-9.

(195) L'Abbé, G. Decomposition and Addition Reactions of Organic Azides. *Chem. Rev.* **1969,** *69*, (3), 345-63.

(196) Link, A. J.; Vink, M. K. S.; Tirrell, D. A. Presentation and Detection of Azide Functionality in Bacterial Cell Surface Proteins. *J. Am. Chem. Soc.* **2004,** *126*, 10598-10602.

(197) Alper, P. B.; Hung, S.-C.; Wong, C.-H. Metal Catalyzed Diazo Transfer for the Synthesis of Azides From Amines. *Tetrahedron Lett.* **1996,** *37*, (34), 6029-6032.

(198) Barlos, K.; Gatos, D.; Schäfer, W. Synthesis of Prothymosin α (ProTα) - a Protein Consisting of 109 Amino Acid Residues. *Angew. Chem., Int. Ed. Eng.* **1991,** *30*, (5), 590-593.

(199) Barlos, K.; Gatos, D.; Kallitsis, J.; Papaphotiu, G.; Sotiriu, P.; Wenqing, Y.; Schafer, W. Darstellung geschutzter peptid-fragmente unter einsatz substituierter triphenylmethyl-harze. *Tetrahedron Lett.* **1989,** *30*, (30), 3943-3926.

(200) Roice, M.; Johannsen, I.; Meldal, M. High Capacity Poly(ethylene glycol) Based Amino Polymers for Peptide and Organic Synthesis. *QSAR & Combinatorial Science* **2004,** *23*, (8), 662-673.

(201) Alves, M. J.; Gilchrist, T. L. Generation and Diels-Alder reactions of t-butyl 2H-azirine-3-carboxylate. *Tetrahedron Lett.* **1998,** *39*, (41), 7579-7582.

(202) *ChemDraw Ultra*, version 8.0; CambridgeSoft Corporation: Cambridge, 2003.

(203) Dawson, P. E.; Kent, S. B. H. Synthesis of Native Proteins by Chemical Ligation. *Annu. Rev. Biochem.* **2000,** *69*, 923-960.

(204) Chhabra, S. R.; Hothi, B.; Evans, D. J.; White, P. D.; Bycroft, B. W.; Chan, W. C. An appraisal of new variants of Dde amine protecting group for solid phase peptide synthesis. *Tetrahedron Lett.* **1998,** *39*, (12), 1603-1606.

(205) Bycroft, B. W.; Chan, W. C.; Chharbra, S. R.; Hone, N. D. A novel lysine-protecting procedure for continuous flow solid phase synthesis of branched peptides. *Chem. Commun.* **1993**, (9), 778-9.

(206) Rohwedder, B.; Mutti, Y.; Dumy, P.; Mutter, M. Hydrazinolysis of Dde: complete orthogonality with Aloc protecting groups. *Tetrahedron Lett.* **1998,** *39*, (10), 1175-1178.

(207) Burns, J. A.; Butler, J. C.; Moran, J.; Whitesides, G. M. Selective Reduction of Disulfides by Tris(2-carboxyethyl)phosphine. *J. Org. Chem.* **1991,** *56*, 2648-2650.

(208) Saxon, E.; Bertozzi, C. R. Cell Surface Engineering by a Modified Staudinger Reaction. *Science (Washington, D.C.)* **2000,** *287*, (5460), 2007-2010.

(209) Kolb, H. C.; Finn, M. G.; Sharpless, K. B. Click chemistry: diverse chemical function from a few good reactions. *Angew. Chem. Int. Ed.* **2001,** *40*, (11), 2004-2021.

(210) Rebek, J., Jr.; Trend, J. E. On the rate of Site-Site Interactions in Functionalized Polystyrenes. *J. Am. Chem. Soc.* **1979,** *101*, (3), 737-737.